L. Van Hoe · D. Vanbeckevoort
K. Mermuys · W. Van Steenbergen

MR Cholangio-pancreatography

Atlas with Cross-Sectional Imaging Correlation

Springer

L. Van Hoe · D. Vanbeckevoort
K. Mermuys · W. Van Steenbergen

MR Cholangiopancreatography

L. Van Hoe · D. Vanbeckevoort
K. Mermuys · W. Van Steenbergen

MR Cholangio-pancreatography

Atlas with Cross-Sectional Imaging Correlation

With 197 Illustrations in 749 Parts

Springer

Lieven Van Hoe, MD, PhD
Staff Radiologist
Department of Radiology
OLV Hospital
9300 Aalst
Belgium

Koen Mermuys, MD
Department of Radiology
University Hospital K. U. Leuven
Herestraat 49
3000 Leuven
Belgium

Dirk Vanbeckevoort, MD
Clinical Supervisor
Department of Radiology
University Hospital K. U. Leuven
Herestraat 49
3000 Leuven
Belgium

Werner Van Steenbergen, MD, PhD
Professor
Department of Hepatology
University Hospital K. U. Leuven
Herestraat 49
3000 Leuven
Belgium

ISBN-10 3-540-22269-3 Springer Berlin Heidelberg New York
ISBN-13 978-3-540-22269-9 Springer Berlin Heidelberg New York

Library of Congress Control Number: 2005934304

Springer is a part of Springer Science + Business Media

springeronline.com

Printed in Germany

Editor: Dr. Ute Heilmann
Desk editor: Wilma McHugh
Production: Elke Beul-Göhringer
Cover design: Estudio Calamar, F. Steinen-Broo, Pau/Girona, Spain
Typesetting and reproduction of the figures: AM-productions GmbH, Wiesloch

Printed on acid-free paper

24/3151/beu-göh 5 4 3 2 1 0

The more our knowledge increases,
the more our ignorance unfolds.

John F. Kennedy

Preface to the Second Edition

When we started preparing the first edition of this book in 1998, MR cholangiopancreatography (MRCP) was a newly developed technique successful only on high-end MRI machines equipped with strong gradients. Now, in 2005, most MRI units are capable of providing high quality images of the upper abdomen, and the technique has found its way into clinical practice.

In comparison with the first edition of the book, the basic structure remains unchanged. Many examples have been added and older images have been replaced by new ones. Some new concepts and references have been added where needed.

It only remains to express the hope that the current edition will prove of value to all involved with the interpretation of upper abdominal MRI and MRCP.

October 2005 Lieven Van Hoe

Foreword to the First Edition

Since its clinical introduction, already many years ago now, the advance of MRI has not been stopped or slowed down by technical limitations. On the contrary, technical improvements have constantly triggered the further spread of MRI into new clinical domains.

Though initially introduced as a new "cross-sectional" imaging modality, it soon became obvious that MRI could also produce "continuity" images, comparable to conventional X-ray techniques. With MRI, continuity images can either be calculated from cross-sectional data or obtained directly by using volumetric projective acquisition schemes. MR angiography (MRA) is typically calculated from tomographic images using a maximum-intensity projection algorithm, whereas magnetic resonance cholangiopancreatography (MRCP) is often obtained with projective acquisition sequences. The two approaches each have various advantages, but they are also subject to specific limitations and artifacts.

Continuity information is extremely useful in the interpretation of the pathology of smaller tubular structures. Particularly if it can be obtained directly without the intermediate step of tomography, this information constitutes one of the advantages of MRI over ultrasonography and computed tomography (CT).

MRCP is often considered as a noninvasive alternative to diagnostic endoscopic retrograde cholangiopancreatograhy (ERCP) because it does not necessitate contrast medium injection, irradiation, or endoscopic manipulation. However, MRCP is obtained under totally different conditions, showing images of the ducts in "physiologic" or "pathophysiologic" conditions, in contrast to ERCP, which is obtained under nonphysiologic conditions, i. e., positive injection pressure. These differences become particularly obvious in the presence of obstrucitve lesions. In addition, MR images differ not only in terms of spatial and time resolution, but also fundamentally in the physics involved in the imaging process. Diagnostic features such as calcification or air can therefore be missed on MRCP.

The authors of this textbook have aimed to provide the interested reader with a comprehensive overview of all the issues involved in the acquisition and interpretation of MRI of the biliary and pancreatic ducts, not only from the point of view of the radiologist but also from that of the endoscopist and gastroenterologist. The chapters and text are arranged accordingly, providing key facts in terms of disease and MRI. A large spectrum of diseases is illustrated, and relevant references have been included.

We hope that this volume will be a successful stimulant for an even greater spread of MRI in abdominal radiology.

Guy Marchal

Preface to the First Edition

It was our aim to place at the disposal of radiologists and clinicians an atlas of Magnetic Resonance Cholangio Pancreatography (MRCP). From more than 1200 patients studied with this technique, we tried to assemble representative images of a large variety of diseases.

There is no doubt that the availability of MR systems equipped with high-power gradients opens new perspectives in the evaluation of abdominal diseases. While the non-invasive nature of MRI remains a crucial advantage over other techniques, the introduction of "snapshot" sequences providing images free of motion artifact in all patients, including those unable to cooperate, has triggered a more widespread use of this modality. A unique characteristic of state-of-the art MRI is its unrivaled capability for *integrated* abdominal imaging. Classic T1- and T2-weighted *cross-sectional* imaging, *projective* cholangiography, *dynamic* evaluation of contrast enhancement patterns or muscular contractility, *functional* imaging by assessing the uptake and excretion of specific contrast media, MR *angiography*, …all these techniques can be used within one session if required. It is likely, therefore, that MRI/MRCP will become an effective and cost-effective "one-stop shopping" diagnostic modality in a number of patients with suspected pancreatobiliary disease.

This book has some characteristics that should be stressed. First of all, it has been conceived as an atlas – teaching file. The format was designed so that the interested reader can "walk through" a large spectrum of pancreatobiliary abnormalities within a relatively short period of time. Besides diseases confined to the biliary or pancreatic ducts, other conditions that may cause secondary ductal abnormalities, that have the potential to mimic ductal disease clinically, or that may be discovered incidentally during an "MRCP" study are also discussed. Most of the 200 separate topics consist of a short description of the entity under consideration, a summary of MRI/MRCP features, and a few representative images. Unlike classical teaching files, the book has rigourously been structured. With the exception of the first chapter on technique, each of the five other chapters that cover the intra- and extrahepatic bile ducts, gallbladder and cystic duct, Vaterian sphincter complex, and pancreatic ducts, has been subdivided in normal anatomy and variants, benign diseases, traumatic and postoperative conditions, and malignant disorders. Hopefully, this organization will be beneficial for those faced with specific problems or questions. In order to further enhance the practical usefulness of the work, important issues such as pitfalls, specific problems in differential dignosis, and clues to a specific diagnosis have been indicated by a special symbol !.

We hope that the readers of this book will enjoy it like we did enjoy its preparation.

Lieven Van Hoe, Dirk Vanbeckevoort,
Werner Van Steenbergen
Leuven, 1998

Contents

MRCP Technique

Intrahepatic Bile Ducts

Extrahepatic Bile Duct

Gallbladder and Cystic Duct

Abbreviations

CBD	Common Bile Duct
CT	Computed Tomography
DD	Differential Diagnosis
EPI	Echo Planar Imaging
ERCP	Endoscopic Retrograde Cholangio-Pancreatography
EUS	Endoscopic Sonography
FSE	Fast Spin Echo
GE	Gradient Echo
HASTE	Half-Fourier Single-Shot Turbo Spin Echo
HCC	Hepatocellular Carcinoma
IV	Intravenous
MEN	Multiple Endocrine Neoplasia
MIP	Maximum Intensity Projection
MP	Magnetization Prepared
MR	Magnetic Resonance
MRA	Magnetic Resonance Angiography
MRCP	Magnetic Resonance Cholangio-Pancretography
MRI	Magnetic Resonance Imaging
PTC	Percutaneous Transhepatic Cholangiography
RARE	Rapid Acquisition with Relaxation Enhancement
RES	Reticulo Endothelial System
SE	Spin Echo
SI	Signal Intensity
T	Tesla
TE	Echo Time
TR	Repetition Time
TSE	Turbo Spin Echo
US	Sonography
VSC	Vaterian Sphincter Complex

I Introduction: Basic Principles of Magnetic Resonance Imaging

1 Magnetic Field, Radio Frequency Pulses, and Resonance

Magnetic resonance imaging (MRI) does not use X-rays to produce images. MRI relies on the fact that hydrogen nuclei (protons) behave like small magnets. When placed in an external magnetic field, the protons align along the direction of the field. In clinical magnetic resonance (MR) systems, the strength of the magnetic field varies between 0.2 and 2 T, which is much higher than the earth's magnetic field (0.6×10^{-4} T). The net result of the specific orientation of the billions of protons is a macroscopic magnetization vector that is aligned with the field. The external magnetic field is oriented parallel to the longitudinal body axis of the patient (z-axis).

The alignment of the protons can be perturbed by a pulse of external electromagnetic energy (excitation). This energy pulse is called a radio frequency (RF) pulse. Excitation can only occur if the radio frequency pulse has a frequency similar to the "natural" frequency of the protons themselves. This transfer of energy is called *resonance*. The angle over which the magnetization vector is tilted away from the z-axis is called the *flip angle*. In conventional MRI, a 90° flip angle is used and the magnetization vector is tilted from the z-axis to the transverse (xy) plane (Fig. I.1). In technical terms, longitudinal magnetization is changed into transverse magnetization. After perturbation, the spins return to their equilibrium state (Fig. I.1, right). This return to equilibrium is called *relaxation*.

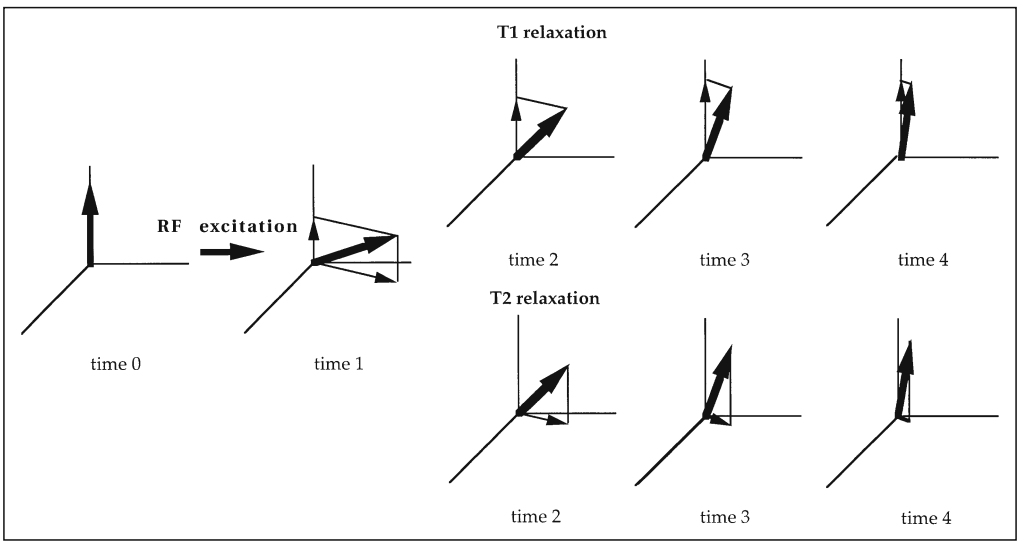

Fig. I.1. T1 and T2 relaxation in MRI. After an excitation pulse (radio frequency pulse), the magnetization vector (*thick arrow*) is flipped towards the axial plane. During relaxation, the longitudinal magnetization gradually recovers (T1 relaxation), while the transverse magnetization gradually disappears (T2 relaxation). The T1 and T2 relaxation times are tissue specific and form the basis of image contrast in MRI

2 T1- and T2-Weighted Images

Relaxation is characterized by *relaxation times*, which are specific for each biological tissue. Two different components of relaxation can be distinguished (Fig. I.1). *T1 relaxation* reflects the gradual recovery of the longitudinal magnetization (longitudinal relaxation), while *T2 relaxation* reflects the loss of transverse magnetization (transverse relaxation). Both T1 and T2 relaxation times are tissue-dependent parameters; the differences between relaxation times of various tissues is the source of contrast in MRI.

In order to obtain an MR signal (or echo), the transverse magnetization is measured shortly after the radio frequency pulse. The time interval between the radio frequency pulse and the measurement of the echo is called the *echo time* (TE). The echo time, together with the *repetition time* (TR, i.e. the time interval between two consecutive 90° pulses), determines which type of MR image is created. A *T1-weighted image* is one in which the intensity contrast between any two tissues in an image is due mainly to the T1 relaxation properties of the tissues. Similarly, a *T2-weighted image* is one in which the intensity contrast between any two tissues is due mainly to their T2 relaxation properties. To produce a T1-weighted image, short TE and TR values are used (typical values: TR ≤500 ms; TE ≤20 ms). Use of long TE and TR values results in the creation of a T2-weighted image (typical values: TR >1500 ms; TE >40 ms). T1- and T2-weighted images can be distinguished by considering the signal intensity (SI) of water or water-containing structures (e.g., cerebrospinal fluid): as a general rule, water has a low signal intensity on T1-weighted images (i.e., it is rendered black), while it has a high signal intensity on T2-weighted images (i.e., it is rendered white).

3 Imaging Times in "Classical" Magnetic Resonance Imaging

The classical technique for obtaining MR images is called *spin echo*. In this technique, a 90° radio frequency pulse is followed by a 180° pulse (the purpose of adding a 180° pulse is to avoid signal loss caused by local inhomogeneity in the magnetic field). After each 90° (and 180°) pulse, an echo is measured. Each echo is used to fill a single horizontal line in a raw data matrix called *k-space* (Fig. I.2). The process is then repeated by applying a second 90° pulse and so on. Once all lines of the raw data matrix have been filled, sufficient information is available to calculate an image.

An important constraint in spin echo MRI is that, in order to allow for recovery of the longitudinal magnetization after a 90° pulse, TR values should be sufficiently long. Because of this, and because many (typically ± 256) consecutive 90° pulses have to be applied to fill all the lines in k-space, spin echo MRI is a rather slow technique that cannot be used for imaging during breathholding. In order to reduce the total examination time, adjacent slices are excited and measured during the spin relaxation of the first slice, i.e., before the next 90° pulse is applied. This procedure is repeated for the acquisition of all necessary k-space lines. If this technique (known as multislice MRI) is applied, the total examination time (i.e., the time required to examine a predefined number of slices) roughly corresponds to the time required to examine a single slice. Typical acquisition times required to obtain high-quality T1- and T2-weighted images of the upper abdomen with spin echo MRI are 2–3 and 8–10 min, respectively.

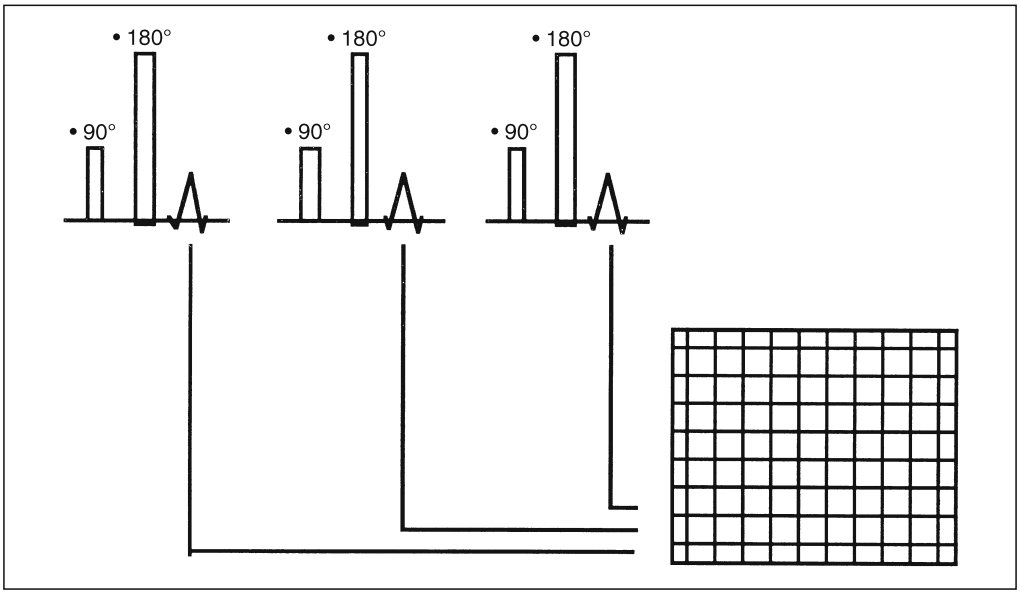

Fig. I.2. Data collection in spin echo MRI. One horizontal line of the raw data matrix (k-space) is filled after each 90° excitation pulse. The scan time is determined by the length of the TR (i.e., the time interval between two consecutive 90° pulses), and by the total number of lines to be filled. Since both TR and the number of 90° pulses should be sufficiently large (typical values: TR 0.5 s; number of 90° pulses, 256) to obtain images with acceptable quality, spin echo MRI is a rather slow technique

4 Fast and Ultrafast Magnetic Resonance Imaging

While it was initially believed that rapid MRI would be impossible, several solutions were proposed in the mid-1980s. Two major independent approaches to reduce acquisition times in MRI are (1) the generation of multiple echoes after a single excitation pulse and (2) the replacement of the classical 90° excitation pulse by lower flip angles.

If multiple echoes are generated after a single 90° excitation pulse, each of these echoes fills a horizontal line in the raw data matrix and thus contributes to the image (Fig. I.3). If all the information required to calculate an image is obtained after one single 90° pulse, the technique is referred to as *rapid acquisition with relaxation enhancement* (RARE) (see #5). In order to allow "snapshot" imaging, the number of echoes is reduced and half-Fourier reconstruction is used (see #1). If several 90° pulses are used, the technique is called *fast spin echo* (FSE) or *turbo spin echo* (TSE). RARE, half-Fourier acquisition single-shot turbo spin echo (HASTE), and fast spin echo are usually applied to provide T2-weighted images (see 1–8).

Replacement of the classical 90° flip angle by lower flip angles is used in a fast technique called *gradient echo MRI*. The rationale of using lower flip angles is that a (nonlinear) relationship exists between the flip angle and the lowest possible value for TR: the lower the flip angle, the lower the lowest possible value for TR and the lower the examination time. In clinical practice, gradient echo images are commonly used to provide T1-weighted images. Due to recent technical improvements, acquisition times per slice can be reduced to less than 1 s (snapshot gradient echo, see #9).

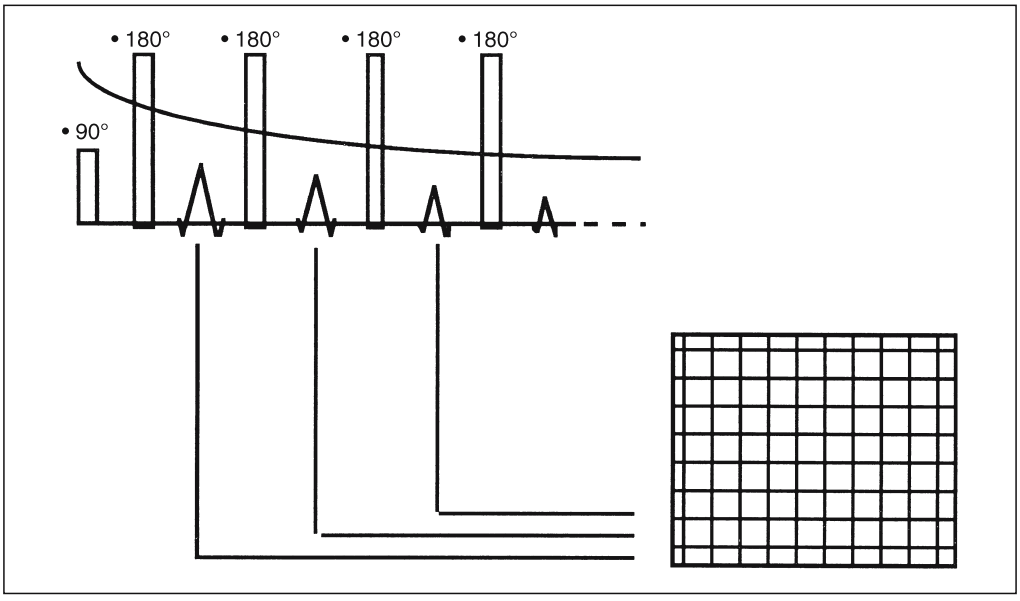

Fig. I.3. Data collection in RARE (turbo spin echo, fast spin echo). Unlike in spin echo, more than one echo (*inverse V*) is obtained after one single 90° pulse; each echo is used to fill one horizontal line of k-space. The larger the number of echoes after a single 90° pulse, the shorter the scan time. Each echo has a decreasing amplitude, which is represented here by the downward slope of the curve

5 Contraindications for Magnetic Resonance Imaging

In order to avoid acute hazards, patients referred to the MRI department should be questioned for traumatic and surgical antecedents. *Absolute contraindications for MRI* include the following:

- Electronically, magnetically, and mechanically activated implants, e.g., cardiac pacemakers
- Ferromagnetic implants, particularly some types of intracranial aneurysm clips and some types of heart valves (lists of MR-compatible implants should be consulted in each case)
- Intraocular metallic foreign bodies

Pregnancy is not considered as an absolute contraindication. As yet, there are no known biological effects of MRI on fetuses. It might be prudent, however, to exclude pregnant women during the first 3 months of pregnancy.

Suggested Reading

Hashemi RH, Bradley WG (1997) MRI. The basics. Williams & Wilkins, Baltimore

Horowitz A (1995) MRI physics for radiologists. A visual approach. Springer, Berlin Heidelberg New York

Lufkin RB (1990) The MRI manual. Year Book Medical, Chicago

Westbrook C, Kaut C (1993) MRI in practice. Blackwell Scientific, Oxford

MRCP Technique

1 Technique

1.1 Magnetic Resonance Sequences

#1 Overview of Imaging Protocol

For practical purposes, our standard protocol for pancreaticobiliary MRI and MRCP using the Siemens platform (1.5-T Symphony or Sonata) is given below.

Phased array body coil and rectangular FOV are used. No specific preparation is required. No drugs or oral contrast media are given for routine studies.

1. Coronal free breathing T2-weighted HASTE (TR infinite, TE 60 ms, 5-mm slices, 1-mm gap, matrix 256×230, acquisition time ± 400 ms/slice, no fat saturation).
   Purpose: characterisation of focal parenchymal lesions, visualisation of fluid-containing structures, general anatomical overview.
2. Same sequence as in (1) but with TE = 360 ms. Alternatively, if the double-echo HASTE sequence is available, both sets of images may be obtained using one single acquisition.
   Purpose: characterisation of focal parenchymal lesions, detection of small amounts of fluid, evaluation of biliary and pancreatic ducts.
3. Same sequence as in (1) but images obtained in the axial plane.
4. Same sequence as in (2) but images obtained in the axial plane.
5. Axial free-breathing magnetisation prepared gradient echo (turboFLASH) (TR 7 ms, TE 4.3 ms, 5-mm slices, 1-mm gap, matrix 192×256, acquisition time ± 700 ms/slice). Alternatively, a spoiled gradient echo sequence may be used during breath-holding. No fat saturation. Care should be taken to optimise T1 contrast.
   Purpose: detection of hepatic and pancreatic tumors, evaluation of extrapancreatic spread of pancreatic neoplasms, lesion characterisation (together with T2-weighted images).
6. Breath-hold single-slice MR cholangiography using the RARE sequence (TR 2800, TE 1100, acquisition time ± 3 s; matrix 256×256, 3-cm slice). Imaging should be repeated during consecutive breath-holding episodes using different slice position and/or orientation in order to obtain visualisation of the entire biliary and pancreatic ductal system. Also, in the case of suspected biliary obstruction, kinematic imaging can be performed by repeating the acquisition without changing the parameters for slice position and slice orientation (see Fig. 3).
   Later in the book, images obtained with this sequence are referred to as projective MR images (see # 5).
   Purpose: overview images of biliary and pancreatic ducts.

   Optional (according to clinical information and/or findings at non-contrast imaging):
7. Coronal breath-hold multislice 3D VIBE T1-weighted gradient echo before IV contrast administration, and in the pancreatic and portal venous phases (± 30 and 70 s after initiation of contrast injection, respectively) (TR 4.8, TE 1.6, acquisition time ± 20 s, 3.5-mm partitions, matrix 384×512). Fat saturation is used to optimise contrast.
   Purpose: differentiation of pancreatic neoplasm from surrounding pancreatitis, characterisation of focal lesions, detection of hypervascular lesions, assessment of vascular anatomy.

These sequences provide complementary information. Together, and with experience, they allow accurate diagnosis of most conditions encountered in the clinical setting. The complementarity of the different types of images is illustrated in Fig. 1 a–d (diagnosis and staging of pancreatic cancer) and Fig. 1 e–k (characterisation of pancreatic mass).

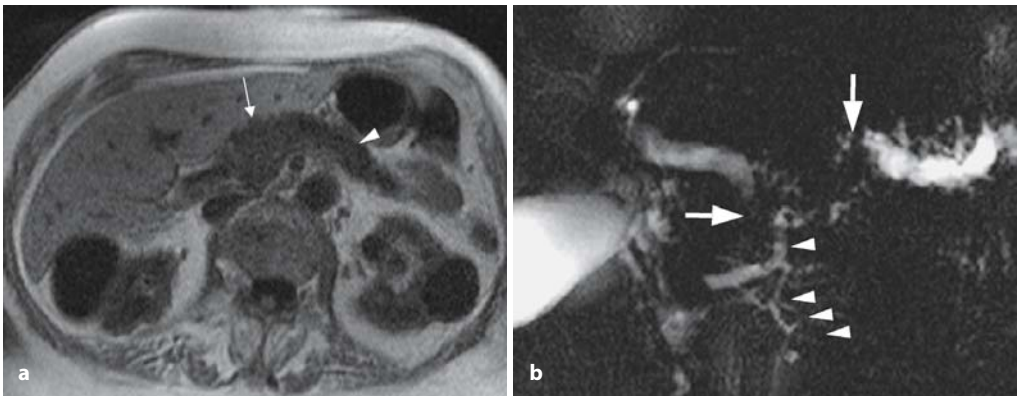

Fig. 1 a–c. Patient with obstructive jaundice. **a** T1-weighted, non-fat-suppressed snapshot image. Although the image is noisy, the contrast is excellent, and the image has a high diagnostic value. The pancreas has a diffusely low signal intensity (*arrow*), which is aspecific. Atrophy of pancreatic tail is also observed (*arrowhead*). Projective cholangiographic (RARE) image (**b**) shows dilatation of biliary duct and proximal pancreatic duct with severe stenosis of distal biliary and pancreatic ducts (*arrows*). Note dilated side branch in pancreatic head (*arrowheads*). Contrast-enhanced VIBE image (**c**) shows hypointense lesion in pancreatic neck (*arrow*) with dilatation of proximal pancreatic duct. Note enhancement of pancreatic parenchyma in the body/tail (*arrowhead*). Based on these findings, the diagnosis of adenocarcinoma with retro-obstructive pancreatitis and biliary invasion can be made. In another patient with pancreatic carcinoma, coronal HASTE image (**d**) shows intraperitoneal free fluid (*arrow*) and omental cake (*arrowheads*): peritoneal/omental metastatic disease. **e–k** Patient presenting with weight loss and dorsal back pain. **e** ERCP image shows long and severe stenosis of pancreatic duct (*arrow*). Because of these findings, pancreatic cancer is the first diagnosis. Cross-sectional T2-weighted image (**f**) shows marked atrophy of pancreatic parenchyma in the tail (*arrow*), associated ductal dilatation, and a mass-like lesion in the pancreatic neck (*arrowheads*) (all supportive of the presumed diagnosis of malignancy). Heavily T2-weighted image and projective MRCP (**g, h**) show absence of penetrating main pancreatic duct, again a suspect finding. There is possibly some focal narrowing of the distal common bile duct (*arrowhead* in **h**), a finding that can also be observed at ERCP. Snapshot T1-weighted image (**i**) surprisingly reveals high signal intensity of the process causing the ductal narrowing (*arrow*). Such a finding is surprising in this context because it virtually excludes adenocarcinoma. Note that this crucial finding is not well seen on the fat-suppressed T1-weighted VIBE image, where the lesion is grey (*arrow*), just like the remaining parenchyma in the tail (**j**). Dynamic contrast-enhanced imaging reveals contrast uptake of the lesion, which is another argument against carcinoma (carcinomas present as "black holes" on dynamic contrast-enhanced VIBE images). Based on integration of all these pieces of information and on experience with the relative value of the different findings, chronic pancreatitis with "pseudotumor" was proposed as first diagnosis. Surgery was not performed. The diagnosis was confirmed by follow-up (unchanged appearance at 2-year interval)

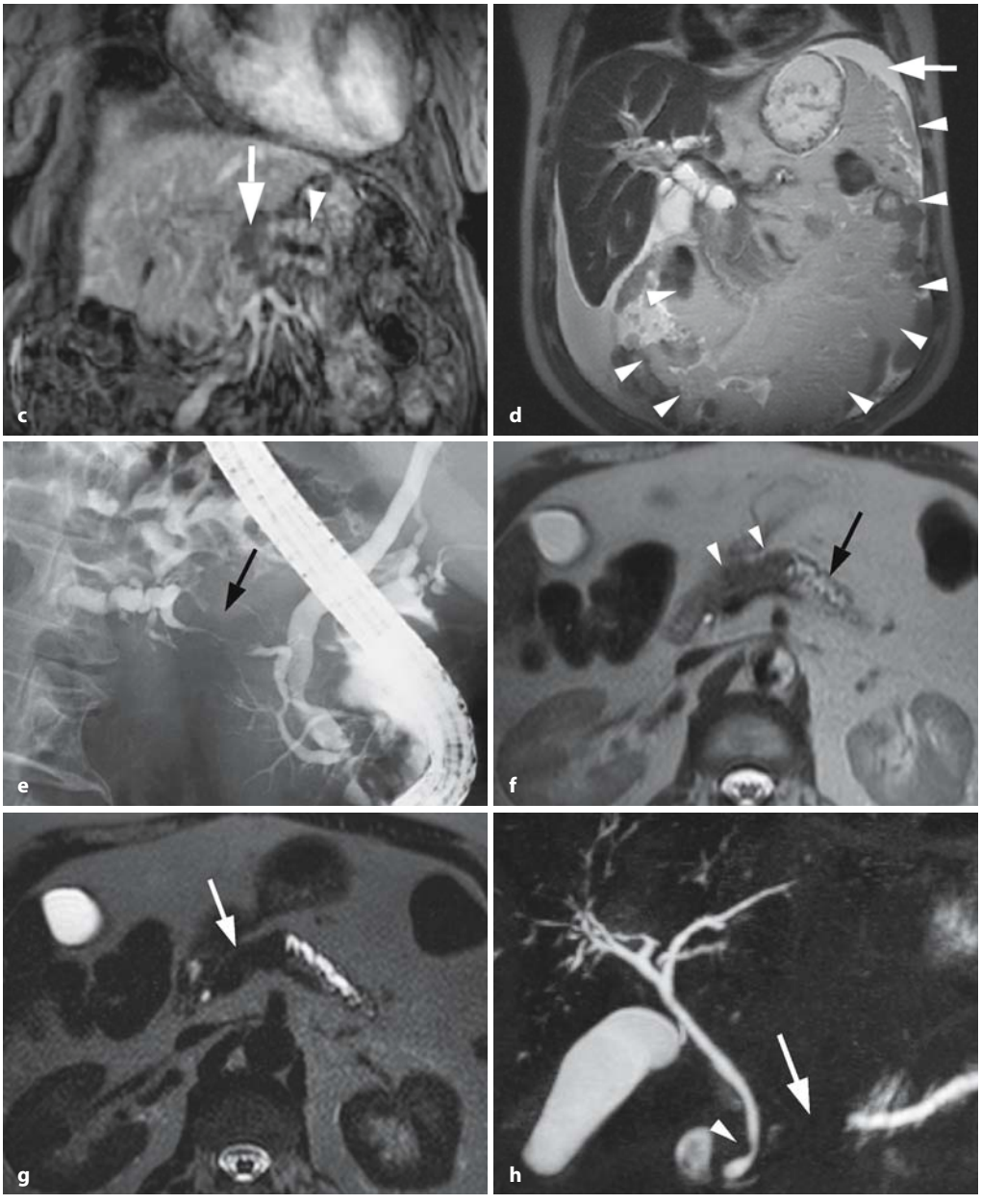

Fig. 1 a–k. (*continued*)

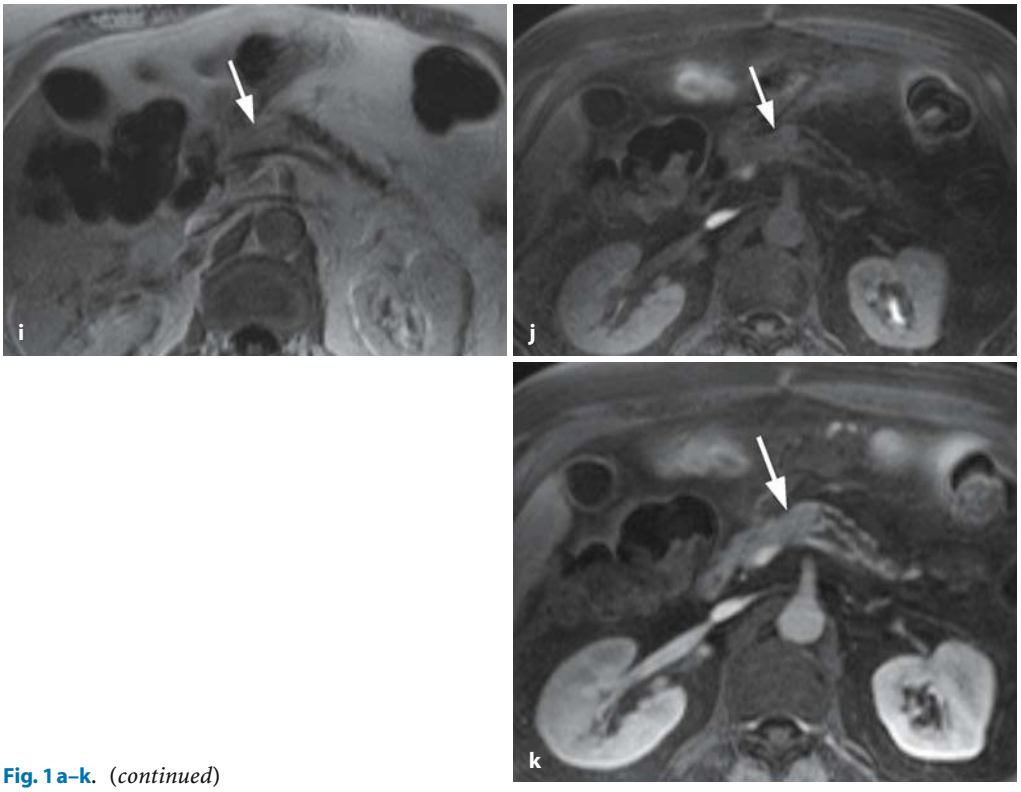

Fig. 1 a–k. (*continued*)

References

Fayad LM, Kowalski T, Mitchell DG (2003) MR cholangiopancreatography: evaluation of common pancreatic diseases. Radiol Clin North Am 41: 97–114

Fulcher AS, Turner MA (2002) MR cholangiopancreatography. Radiol Clin North Am 40: 1363–1376

Hundt W, Petsch R, Scheidler J et al. (2002) Clinical evaluation of further-developed MRCP sequences in comparison with standard MRCP sequences. Eur Radiol 12: 1768–1777

Kim MJ, Mitchell DG, Ito K et al. (2000) Biliary dilatation: differentiation of benign from malignant causes – value of adding conventional MR imaging to MR cholangiopancreatography. Radiology 214: 173–181

Lopez Hanninen E, Amthauer H, Hosten N et al. (2002) Prospective evaluation of pancreatic tumors: accuracy of MR imaging with MR cholangiopancreatography and MR angiography. Radiology 224: 34–41

Ly JN, Miller FH (2002) MR imaging of the pancreas: a practical approach. Radiol Clin North Am 40: 1289–1306

Van Hoe L, Mermuys K, Vanhoenacker P (2004) MRCP pitfalls. Abdom Imaging 29: 360–387

#2 Snapshot T2-Weighted MRI

KEY FACTS

- "Snapshot" MRI: acquisition of individual slices in less than 1 s
- Advantages:
  - Short examination times
  - Image quality independent of patient cooperation
- Commonly used sequences:
  - Echo planar imaging (EPI) (see # 8)
  - Half-Fourier acquisition single-shot turbo spin echo (HASTE) = half-Fourier rapid acquisition with relaxation enhancement (RARE; acquisition time per slice, ±400 ms) (Kiefer et al. 1994; Van Hoe et al. 1996)
- Technical realization of HASTE (Fig. 2a; Kiefer et al. 1994; Van Hoe et al. 1996):
  - Generation of multiple echoes after a single 90° excitation pulse
  - Each echo fills a horizontal line in k-space
  - Approximately 56 % of k-space is filled, starting from a few lines above the center of k-space to the bottom
  - Half-Fourier reconstruction is used
- Advantages of HASTE:
  - General advantages of snapshot imaging (see above)
  - Images nearly unaffected by specific artifacts (magnetic susceptibility, chemical shift)
- Disadvantages of HASTE:
  - Intrinsic limitations in signal-to-noise ratio and spatial resolution
  - Inconsistent signal intensity of blood vessels: a typical "flow void" is seen only in case of high blood velocity
- Clinical applications:
  - Excellent technique for cross-sectional T2-weighted MRI
  - Can also be used to obtain cholangiographic images (Morrin et al. 2000)

References

Morrin MM, Farrell RJ, McEntee G et al. (2000) MR cholangiopancreatography of pancreaticobiliary diseases: comparison of single-shot RARE and multislice HASTE sequences. Clin Radiol 55 : 866 – 873

Kiefer B, Grässner J, Hausman R (1994) Image acquisition in a second with half-Fourier acquisition single-shot turbo spin echo. J Magn Reson Imaging (P) Suppl: 86 – 87

Tang Y, Yamashita Y, Arakawa A et al. (2000) Pancreaticobiliary ductal system: value of half-Fourier rapid acquisition with relaxation enhancement MR cholangiopancreatography for postoperative evaluation. Radiology 215 : 81 – 88

Van Epps K, Regan F (1999) MR cholangiopancreatography using HASTE sequences. Clin Radiol 54 : 588 – 594

Van Hoe L, Bosmans H, Aerts P, Baert AL, Fevery J, Kiefer B, Marchal G (1996) Focal liver lesions: fast T2-weighted MR imaging with half-Fourier rapid acquisition with relaxation enhancement. Radiology 201: 817 – 823

Vitellas KM, El-Dieb A, Vaswani KK, et al. (2002) Using contrast-enhanced MR cholangiography with IV mangafodipir trisodium (Teslascan) to evaluate bile duct leaks after cholecystectomy: a prospective study of 11 patients. AJR Am J Roentgenol 179 : 409 – 416

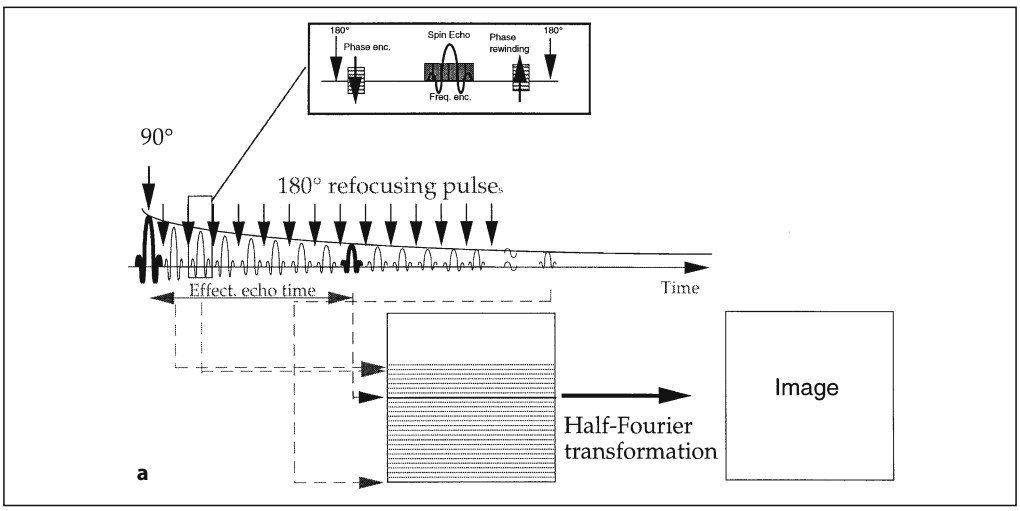

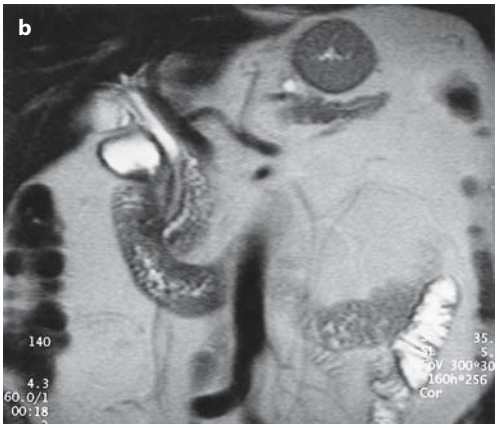

Fig. 2. **a** The HASTE pulse sequence. The 90° radio frequency excitation pulse is followed by a long series of spin echoes. The interval between successive echoes is as short as possible. Phase encoding, 180° refocusing pulse, frequency encoding, and phase rewinding are performed within a window of about 4 ms. The k-space is filled from eight lines above the center to the bottom. The effective TE of the image is defined as the time between the radio frequency excitation pulse and the acquisition of the line of the center of k-space. **b** Coronal T2-weighted image obtained with HASTE. The bile duct, pancreatic duct, and the fluid within the lumen of the duodenum and small bowel are markedly hyperintense. Solid organs and bowel walls have relatively low signal intensity. Fat has intermediate to high signal intensity. Flowing blood and air have very low signal intensity. Note the absence of artifacts related to motion and susceptibility and the good delineation of the contours of the stomach, pancreas, duodenum, and colon

#3 Snapshot T2-Weighted MRI: Double-Echo Technique

KEY FACTS

- Modification of the HASTE technique (see #2)
- Two images are calculated per anatomical slice position
- Image characteristics:
  - First image: moderately T2-weighted
  - Second image: heavily T2-weighted
- Acquisition time per slice: ± 700 ms
- Technical realization (see Fig. 3a; Bosmans et al. 1997a, b):
  - Each excitation pulse is followed by a long echo train
  - The first part of the echo train is used to construct an image with short TE (e.g., 60 ms)
  - The second part of the echo train is used to construct an image with long TE (e.g., 350 ms)
- Theoretical advantages:
  - Excellent visualization of fluid-containing structures and lesions on images with long TE
- Clinical applications:
  - *Characterization* of focal liver lesions (Bosmans et al. 1997a; Table 3.1)
  - *Detection* of acute pancreatitis, acute cholecystitis, biliary fistulas, subtle anomalies of bile ducts, and pancreatic ducts (Fig. 3b, c)
  - *Differentiation* between acute and chronic cholecystitis (see #104)
  - Part of routine imaging protocol at our institution
- *Note:* Unless specifically indicated, all T2-weighted MR images shown in the book are obtained using this sequence
- *Note:* as an alternative, two separate acquisitions with short and long TE can be obtained (see #1)

References

Bosmans H, Gryspeerdt S, Van Hoe L, Van Oostende S, De Jaegere T, Kiefer B, Baert AL, Marchal G (1997a) Preliminary experience with a new double echo half-Fourier single-shot turbo spin echo acquisition in the characterisation of liver lesions. MAGMA 5:79–84

Bosmans H, Van Hoe L, Gryspeerdt S, Kiefer B, Van Steenbergen W, Baert AL, Marchal G (1997b) Technical note. Single-shot T2-weighted MR imaging of the upper abdomen: preliminary experience with the double echo HASTE technique. AJR Am J Roentgenol 169:1291–1293

Pawluk RS, Borrello JA, Brown JJ, McFarland EG, Mirowitz SA, Tsao LY (2000) A prospective assessment of breath-hold fast spin echo and inversion recovery fast spin echo techniques for detection and characterization of focal hepatic lesions. Magn Reson Imaging 18:543–551

Table 3.1. Characterization of focal liver lesions

	Signal intensity (relative to normal liver)	
	First echo (TE 60 ms)	Second echo (TE 250–350 ms)
Cyst	Hyperintense ++/+++	Hyperintense ++++
Hemangioma	Hyperintense ++	Hyperintense +
Solid lesion	Hyperintense +/++	Isointense[a]

[a] Lesions containing cystic components or necrosis may be *partially* hyperintense.

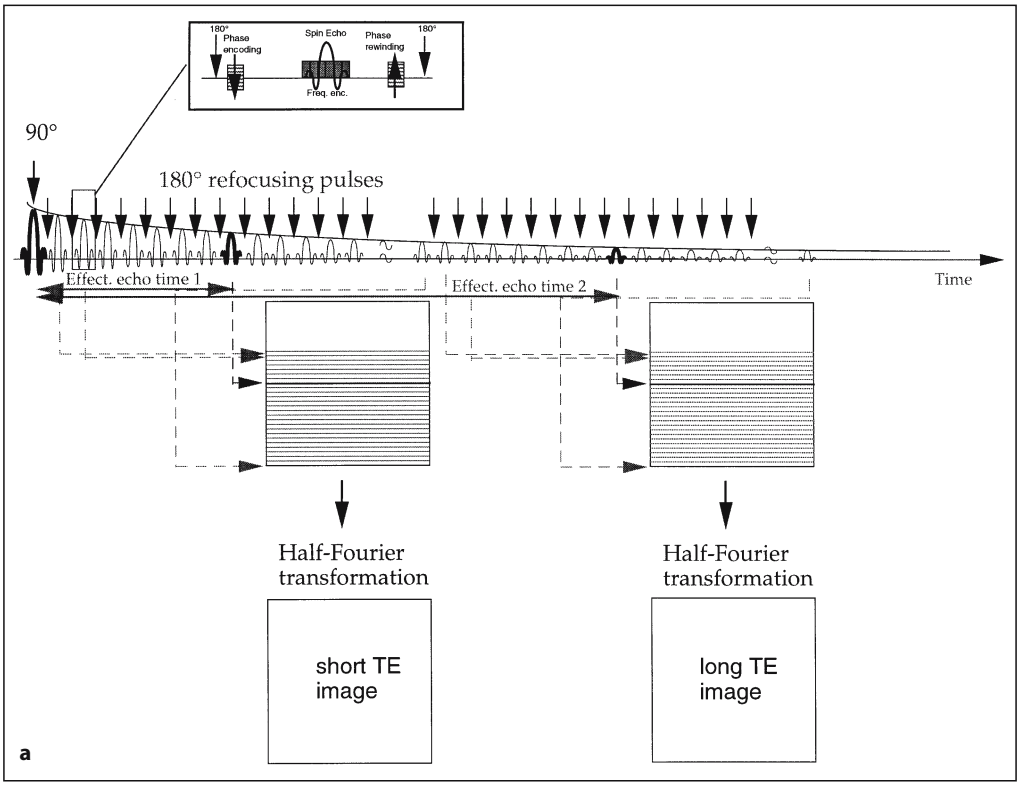

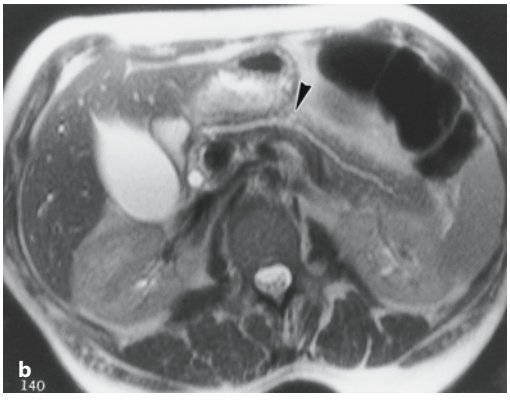

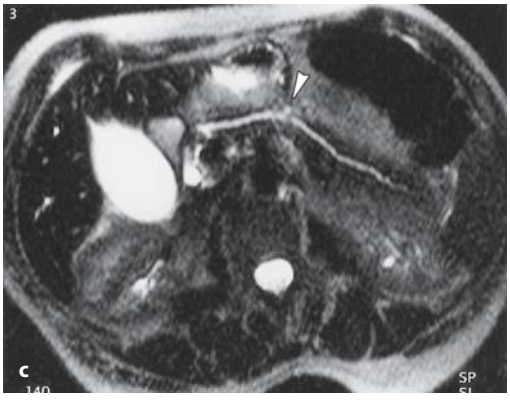

Fig. 3. **a** The double-echo HASTE pulse sequence. A 90° radio frequency excitation pulse is followed by a very long echo train. Two k-spaces are filled successively and transformed into an image with a half-Fourier reconstruction technique. The effective TE of the resulting images is the time between the radio frequency pulse and the acquisition of the echo attributed to the center of the first and second k-space, respectively. **b, c** Corresponding "double-echo" HASTE images with **b** a TE of 60 ms and **c** a TE of 439 ms showing a slightly dilated pancreatic duct with a small pseudocyst (or dilated side branch) in the pancreatic body (*arrowheads*). The pseudocyst is better seen in **c**. Note that in **b** the signal intensity of fat and fluid is comparable. In **c**, fluid really stands out

#4 Snapshot T2-Weighted MRI: Is Fat Suppression Required?

KEY FACTS

- Use of fat suppression improves the quality of spin echo MR images of the upper abdomen (Lu et al. 1994)
- Advantages of fat suppression in spin echo MRI (Lu et al. 1994):
  - Reduction of image noise, mainly because fat signal does not contribute to motion-related phase-encoding artifacts
  - Improved conspicuity of focal liver lesions, particularly in the case of fatty liver
- In snapshot T2-weighted MRI, the advantages of fat suppression are questionable (Bosmans et al. 1997):
  - Motion-related artifacts are virtually absent (see # 2)
  - Use of fat suppression significantly decreases the conspicuity of the contours of several extrahepatic structures (e. g., bile duct, gastric wall, pancreas, retroperitoneal vessels; Fig. 4)
  - The double-echo technique offers effective fat suppression while highlighting fluid (long TE)

References

Bosmans H, Van Hoe L, Gryspeerdt S et al. (1997) Technical note. Single-shot T2-weighted MR imaging of the upper abdomen: preliminary experience with the double echo HASTE technique. AJR Am J Roentgenol 169 : 1291 – 1293

Lu DS, Saini S, Hahn PF et al. (1994) T2-weighted MR imaging of the upper part of the abdomen: should fat suppression be used routinely? AJR Am J Roentgenol 162 : 1095 – 1100

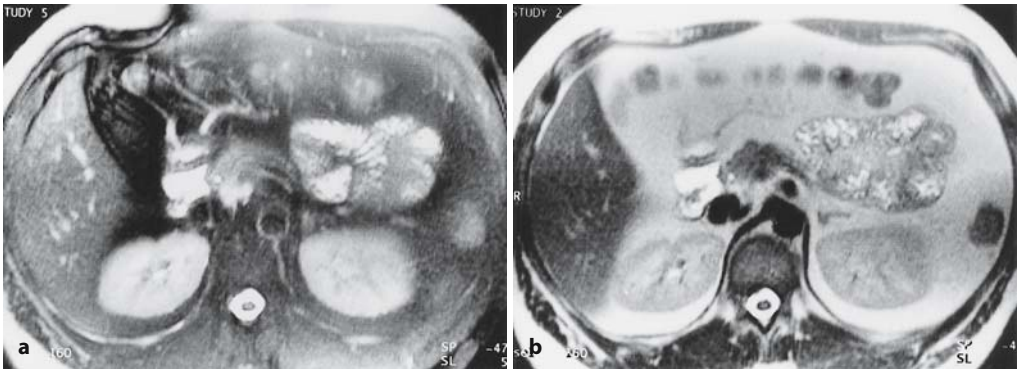

Fig. 4 a, b. Corresponding images **a** with and **b** without fat suppression. Note better visualization of the contours of the pancreas, colon, and adrenals in **b**

#5 "Projective" Cholangiography

KEY FACTS

- Principle:
  - A projection image is obtained through the structure of interest with a relatively large slice thickness (2–10 cm)
  - One voxel dimension is significantly larger than the other two dimensions
  - In order to obtain sufficiently high contrast, the signal obtained from the structure of interest (e.g., bile ducts) should be much higher than the signal of background tissue
- Sequence commonly used: RARE (Laubenberger et al. 1995; Matos et al. 1997; Van Hoe et al. 2004)
- Image characteristics of RARE:
  - Only structures/lesions containing pure water are displayed
- Technical realization of RARE (Fig. 5a):
  - All echoes are obtained after a single excitation pulse
  - A very long echo train is used (usually ± 250 echoes)
  - The resulting image has an extremely long effective TE (e.g., 1100 ms)
- Acquisition time: ± 3–5 s (breathholding required)
- Advantages:
  - Excellent display of bile duct and/or pancreatic ducts on one image (Fig. 5b)
  - Relatively high in-plane resolution
- *Note:* Unless specifically indicated, all projective cholangiographic MR images shown in the book are obtained using this technique

References

Laubenberger J, Büchert M, Schneider B, Blum B, Hennig J, Langer M (1995) Breath-hold projection magnetic resonance cholangio-pancreaticography (MRCP): a new method for the examination of the bile and pancreatic ducts. Magn Reson Med 33 : 18–23

Matos C, Metens T, Devière J et al. (1997) Pancreatic duct: morphologic and functional evaluation with dynamic MR pancreatography after secretin stimulation. Radiology 203 : 435–441

Keogan MT, Edelman RR (2001) Technologic advances in abdominal MR imaging. Radiology 220 : 310–320

Van Hoe L, Mermuys K, Vanhoenacker P (2004) MRCP pitfalls. Abdom Imaging 29 : 360–387

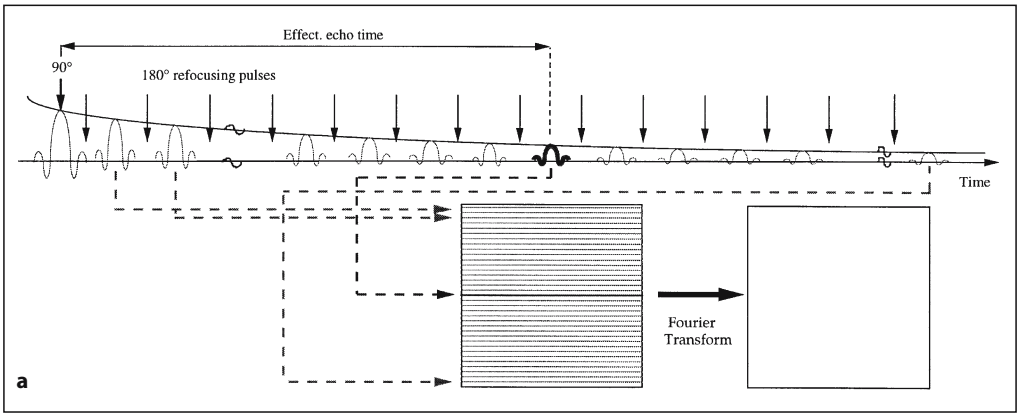

Fig. 5. **a** RARE acquisition is a single-shot technique in which a 90° radio frequency excitation pulse is followed by an extremely long echo train. The k-space is completely filled, with the center of k-space acquired half way along the acquisition. The effective TE can be as long as 1100 ms. **b** RARE image obtained in a patient with papillary stenosis after cholecystectomy, showing entire common bile duct, pancreatic duct, and cystic duct remnant. A 3-cm slice thickness was used

#6 "Projective" Cholangiography: Limitations

KEY FACTS

- Image quality dependent on patient cooperation (breathholding required) (Fig. 6 a, b)
- Suboptimal visualization of bile duct and/or pancreatic ducts in the case of elevation of signal intensity of background tissue (presence of free water or edema), e. g.:
  - Acute pancreatitis with peripancreatic exudate
  - Liver transplant with hilar biloma/hematoma
  - Ascites (Fig. 6 c, d)
- Suboptimal visualization of intraluminal structures/lesions that are *not* surrounded by fluid, e. g.:
  - Stone impacted in the distal common bile duct or cystic duct
  - Blood clots, sludge, or necrotic debris filling a large part of the bile duct (see also # 23)
- Medical interaction required during image acquisition
  - Selection of slice position depending on the clinical question and findings on cross-sectional images (see # 11)

References

Laubenberger J, Büchert M, Schneider B, Blum B, Hennig J, Langer M (1995) Breath-hold projection magnetic resonance cholangio-pancreaticography (MRCP): a new method for the examination of the bile and pancreatic ducts. Magn Reson Med 33 : 18 – 23

Matos C, Metens T, Devière J et al. (1997) Pancreatic duct: morphologic and functional evaluation with dynamic MR pancreatography after secretin stimulation. Radiology 203 : 435 – 41

Van Hoe L, Mermuys K, Vanhoenacker P (2004) MRCP pitfalls. Abdom Imaging 29 : 360 – 387

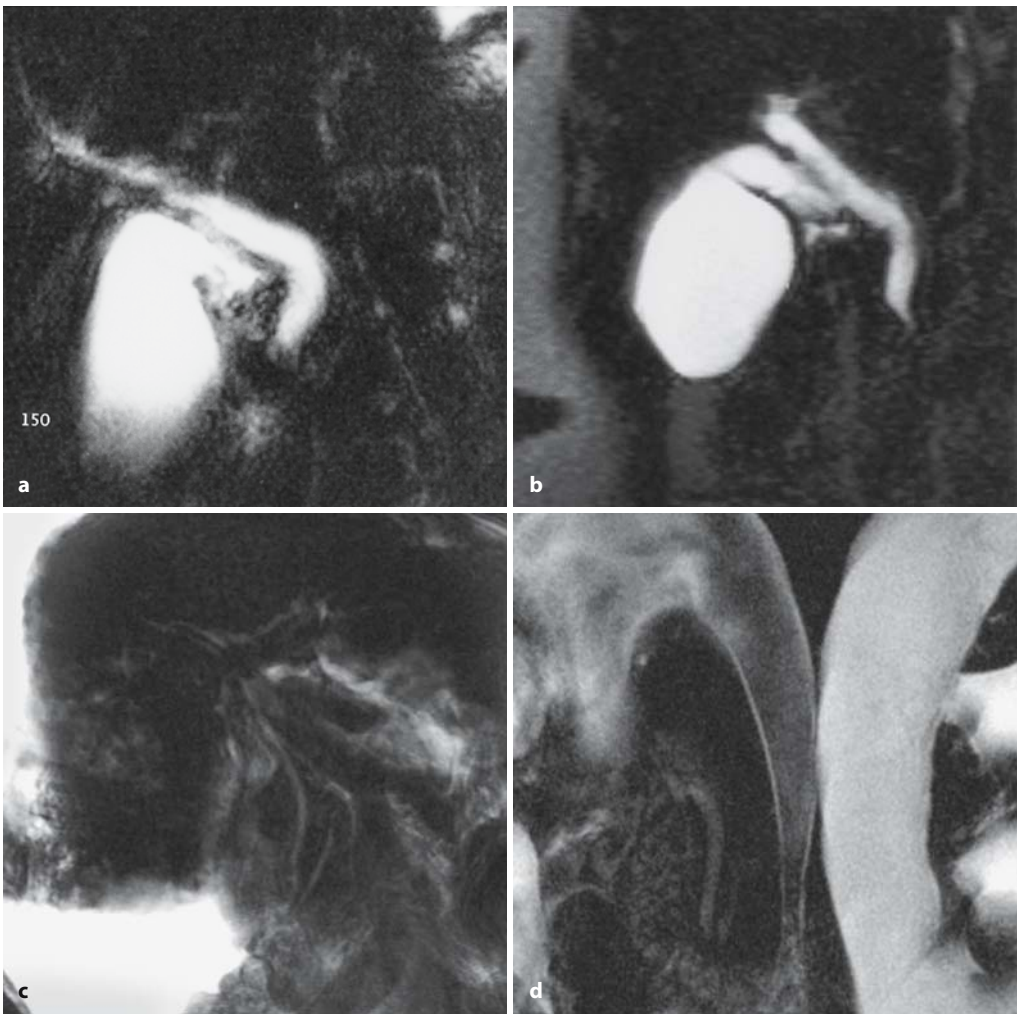

Fig. 6 a,b. Elderly patient. **a** The quality of the projective (RARE) image is severely degraded by respiratory artifact. Choledocholithiasis cannot be ruled out. **b** Heavily T2-weighted snapshot (HASTE) image adequately showing the anatomy of the distal common bile duct; no stone. **c** Projective image severely degraded by the presence of ascites. Adequate interpretation is not possible. **d** Projective image severely degraded by the presence of ascites and wrap-around artifact

#7 An Alternative Approach: Calculation of Maximum-Intensity Projection Images

KEY FACTS

- Maximum-intensity projection (MIP): postprocessing technique that calculates projective images from a stack of cross-sectional images
- Principle (Laub 1990):
  - Mathematical rays are projected in the desired viewing direction through a stack of reconstructed sections.
  - The density of each pixel in the resulting image is the maximum intensity encountered along the ray as it traverses the volume
- Advantages over RARE:
  - If used in combination with snapshot techniques for T2-weighted MRI, image quality is less dependent on patient cooperation
  - If used in combination with a three-dimensional acquisition technique, high-resolution projective images can be calculated a posteriori in any desired viewing direction
- Disadvantages compared with RARE:
  - Time required for postprocessing
  - Elevation of background intensity caused by the algorithm, leading to lower levels of contrast and a less sharp delineation of small biliary and pancreatic ducts (Fig. 7)
  - If used in combination with a two-dimensional sequence, high-resolution images can be calculated in one viewing direction only
- Applications:
  - Tends to be replaced by direct RARE projective cholangiography (Bearcroft and Lomas 1997)
  - Maximum-intensity projection processing of heavily T2-weighted HASTE images can be used as an alternative to RARE projective cholangiography in patients unable to cooperate

References

Bearcroft P, Lomas D (1997) Magnetic resonance cholangiopancreatography. Gut 41:135–137

Laub G (1990) Displays for MR angiography. Magn Reson Med 14:222–229

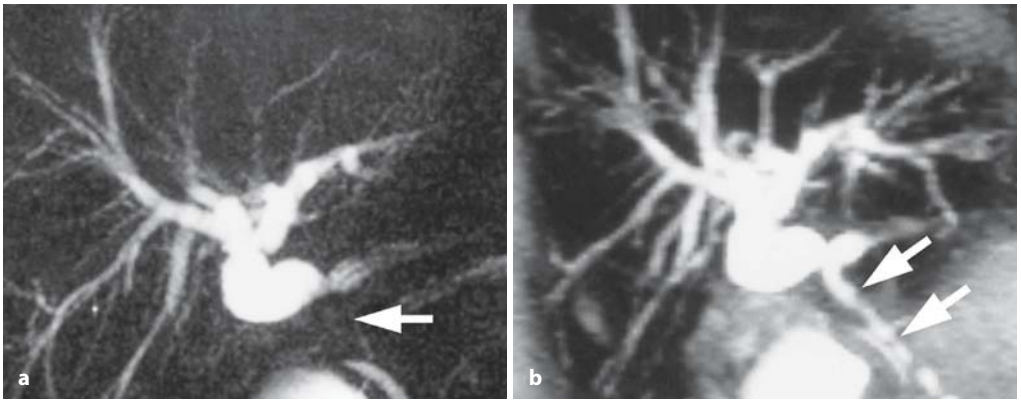

Fig. 7 a, b. Limitations of MIP images. Patient with jaundice after gallbladder surgery. Projective (RARE) image with 3-cm slice thickness (**a**) compared with MIP image obtained after postprocessing of a series of thin slices (**b**). Both images show intrahepatic biliary dilatation. The single-slice MRCP image clearly shows occlusion of the common hepatic duct (*arrow*). This diagnosis is missed on the MIP image because an intrahepatic bile duct superimposes on the common hepatic duct (*arrows*)

#8 Other Techniques for Obtaining T2-Weighted Images

KEY FACTS

Techniques that have been used to obtain T2-weighted MR images in pancreatobiliary MRI can be classified as follows:

Spin Echo Versus Gradient Echo Techniques

Spin Echo Techniques

- Use a 180° radio frequency pulse for rephasing
- Provide images relatively unaffected by magnetic field inhomogenities and magnetic susceptibility
- Examples: spin echo, fast spin echo (FSE) or turbo spin echo (TSE), RARE (see #5), and HASTE (see #2)

Gradient Echo Techniques

- Use gradients instead of 180° radio frequency pulses. Consequently, images are more susceptible to different types of artifacts (Fig. 8)
- Examples: steady state free precession (SSFP) gradient echo (e.g., FISP) (Morimoto et al. 1992), and echo planar imaging

Breathhold Versus Non-breathhold Techniques Versus Snapshot Techniques

Breathhold Techniques

- Advantages: reduction of artifacts caused by respiration
- Disadvantages: intrinsic limitations in signal-to-noise ratio and spatial resolution
- Examples: breathhold fast spin echo, RARE

Non-breathhold Techniques

- Advantages: possible to obtain multiple averages with a high signal-to-noise ratio and spatial resolution
- Disadvantages: speed, respiratory artifacts
- Examples: spin echo, all three-dimensional techniques

Snapshot Techniques

- See #2

Two- Versus Three-Dimensional Techniques

Two-Dimensional Techniques

- Advantages: shorter imaging time
- Disadvantages: limited resolution in the third dimension (slice thickness)
- Examples: two-dimensional fast spin echo, RARE

Three-Dimensional Techniques

- Advantages: high resolution in all three dimensions
- Disadvantages: long acquisition times
- Examples: three-dimensional steady state free precession (Morimoto et al. 1992), three-dimensional fast spin echo (Barish et al. 1995)

References

Barish MA, Yucel EK, Soto JA, Chuttani R, Ferruci JT (1995) MR cholangiopancreatography: efficacity of a three-dimensional turbo spin-echo technique. AJR Am J Roentgenol 165:295–300

Morimoto K, Shimoi M, Shirakawa T et al. (1992) Biliary obstruction: evaluation with three-dimensional MR cholangiography. Radiology 183:578–80

Reinhold C, Bret P (1996) MR cholangiopancreatography. Abdom Imaging 21:105–116

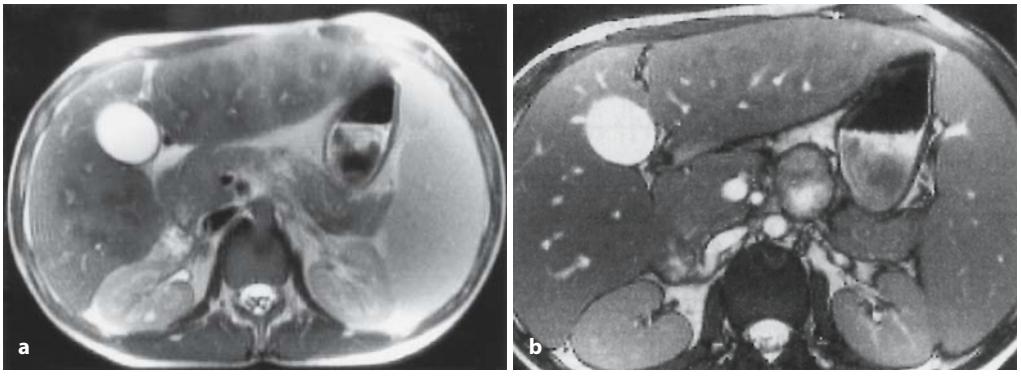

Fig. 8 a, b. T 2-weighted images obtained with **a** HASTE and **b** fast imaging with steadystate precession. Note black borders of all abdominal organs in **b**, related to intravoxel dephasing. The hepatic abnormalities (peribiliary fibrosis in patient with primary sclerosing cholangitis) are more clearly seen in **a**

#9 T1-Weighted MRI: Non-fat-suppressed Magnetizationprepared Snapshot Gradient Echo

KEY FACTS

- Abbreviation: MP snapshot GE T1
- Synonyms: snapshot fast low-angle shot (snapshot FLASH), turbo FLASH
- Acquisition time per slice: ± 700 ms
- Principle and technical realization (Fig. 9a; Haase 1990; Holsinger-Bampton et al. 1991):
  - Application of multiple small flip angle excitation pulses
  - Generation of one echo after each excitation pulse
  - Short TR (e.g., 7 ms)
  - Use of an inversion recovery pulse for contrast preparation
- Theoretical advantages:
  - Good T1 contrast (excellent detection of hepatic and pancreatic neoplasms)
  - Image quality independent of patient motion
- Limitations:
  - Not applicable for fat-suppressed T1-weighted imaging
  - Sensitive to susceptibility artifact (no 180° refocusing pulses)
- Clinical use: part of our standard protocol for routine upper abdominal imaging together with the double-echo HASTE sequence
- Alternatively, a breath-hold T1-weighted sequence can be used

References

Haase A (1990) Snapshot FLASH MRI. Applications to T1,T2 and chemical shift imaging. Magn Reson Med 13:77–89

Holsinger-Bampton AE, Riederer SJ, Campeau NG, Ehman RL, Johnson CD (1991) T1-weighted snapshot gradient-echo MR imaging of the abdomen. Radiology 181:25–32

Keogan MT, Edelman RR (2001) Technologic advances in abdominal MR imaging. Radiology 220:310–320

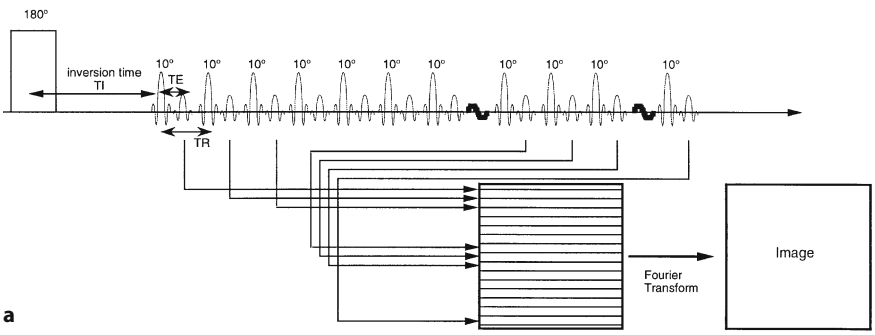

a

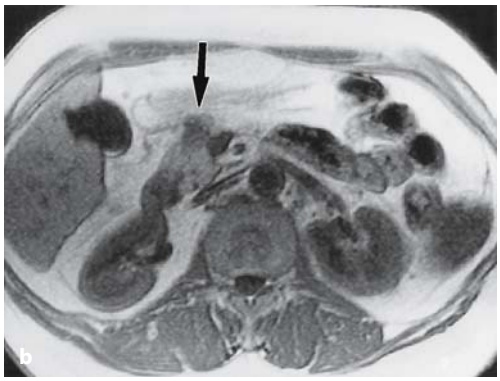

Fig. 9. a Magnetization-prepared snapshot gradient echo. This technique is basically an ultrafast gradient echo acquisition that uses a small flip angle and short TR. An 180° inversion recovery pulse prepares the magnetization of the spins prior to the acquisition. The inversion time is chosen so that adequate T1 contrast is obtained. **b** Magnetization-prepared snapshot gradient echo T1-weighted image showing liver and pancreatic head as relatively hyperintense. A small tumor is shown as a hypointense lesion in the pancreatic neck (*arrow*). Although this sequence does not offer spectacular contrast, it is very sensitive in the detection of hepatic and pancreatic tumors

#10 T1-Weighted MRI: Use of Fat Suppression

KEY FACTS

- For unenhanced T1-weighted imaging use of fat suppression is not recommended (decreased liver-to-spleen contrast)
- For dynamic contrast-enhanced imaging, fat-suppressed images are routinely obtained
- Out-of-phase images can be useful for confirmation of fatty infiltration

References

Keogan MT, Edelman RR (2001) Technologic advances in abdominal MR imaging. Radiology 220 : 310 – 320

Semelka SR, Asher SM (1993) MR imaging of the pancreas. Radiology 188 : 593 – 602

Rofsky, NM, Lee VS, Laub G, et al. (1999) Abdominal MR imaging with a volumetric interpolated breath-hold examination. Radiology 212 : 876 – 884

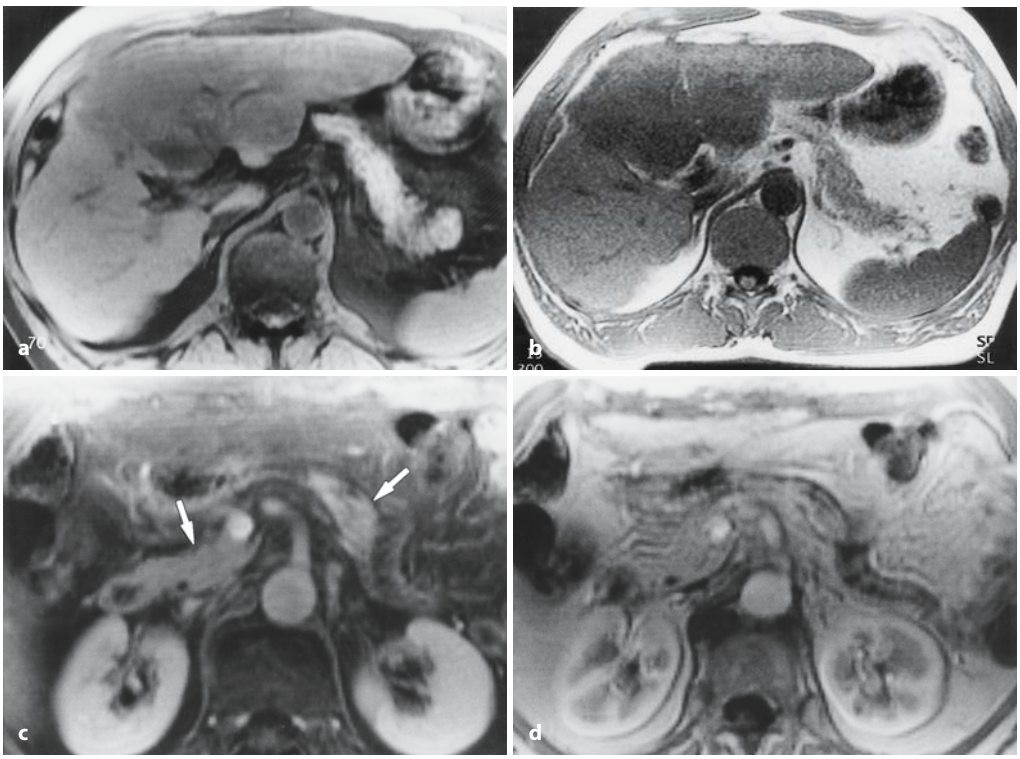

Fig. 10 a, b. T1-weighted MR images **a** with and **b** without fat suppression. Both images adequately show the normal pancreas and the large liver tumor. Note inversion of intensity of normal pancreas versus surrounding fat when **b** is compared to **a**. **c, d** Different patient. Contrast-enhanced images obtained **c** with and **d** without fat suppression. Part of the pancreatic head and body are clearly seen in **d** (*arrows*). In **d**, the pancreatic parenchyma and the surrounding retroperitoneal fat are nearly isointense

1.2 Practical Setup of an MRCP Study

#11 Selection of Slice Location for Projective MRCP

METHOD (FIG. 11)

- Cross-sectional T2-weighted MR images are obtained first
- Projective imaging is obtained in the plane determined by the position of the structures of interest (e.g., bile duct, pancreatic duct) as seen on the cross-sectional images
- Superimpositions of bowel contents can be eliminated by varying the slice orientation and adjusting the slice thickness
- Several (up to ten to 15) views should usually be obtained in order to obtain all the relevant information
- *Note:* The selection of the optimal section planes for projective MRCP requires a preliminary study of cross-sectional images. Preferably, both axial and coronal images (e.g., snapshot T1 and double-echo snapshot T2) should be routinely obtained and analyzed. One could call this approach "real-time interactive MRCP".

References

Laubenberger J, Büchert M, Schneider B, Blum B, Hennig J, Langer M (1995) Breath-hold projection magnetic resonance cholangio-pancreaticography (MRCP): a new method for the examination of the bile and pancreatic ducts. Magn Reson Med 33:18–23

Van Hoe L, Gryspeerdt S, Vanbeckevoort D et al. (1998) Normal Vaterian sphincter complex: evaluation of morphology and contractility with dynamic single-shot MR cholangiography. AJR 170:1497–1500

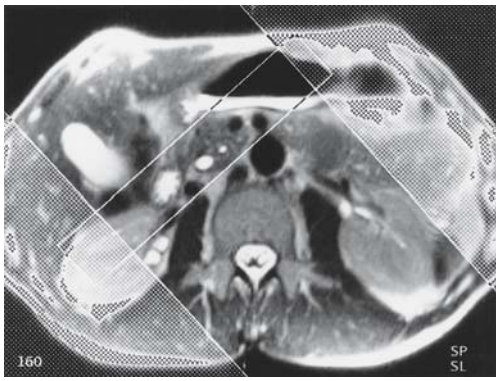

Fig. 11. Axial cross-sectional T2-weighted MR image used to select the optimal section plane for projective MRCP. Saturation bands are used to avoid infolding

#12 Selection of Slice Thickness

KEY FACTS

- Cross-sectional techniques: slice thickness usually 5–7 mm, representing an optimal compromise between:
  - Signal-to-noise ratio (increases as the slice thickness increases)
  - Contrast resolution (decreases as the slice thickness increases)
- *Note:* Snapshot T2-weighted images are preferentially obtained in an interleaved fashion, i.e., two separate series of images are obtained with an intersection gap equal to the slice thickness (to reduce artifact related to cross talk; Bosmans et al. 1997)
- Projective MRI:
  - Use of a slice thickness of 3 cm constitutes a good compromise between examination volume and contrast resolution (Fig. 12)
  - A slice thickness of 2 cm may be optimal for particular studies (e.g., vaterian sphincter complex, ductal anatomy in children)
  - A larger slice thickness (up to 12 cm) may be selected to obtain "overview" images; however, small structures and lesions may become invisible

References

Bosmans H, Van Hoe L, Gryspeerdt S, Kiefer B, Van Steenbergen W, Baert AL, Marchal G (1997) Technical note. Single-shot T2-weighted MR imaging of the upper abdomen: preliminary experience with the double echo HASTE technique. AJR Am J Roentgenol 169 : 1291 – 1293

Laubenberger J, Büchert M, Schneider B, Blum B, Hennig J, Langer M (1995) Breath-hold projection magnetic resonance cholangio-pancreaticography (MRCP): a new method for the examination of the bile and pancreatic ducts. Magn Reson Med 33 : 18 – 23

Reuther G, Kiefer B, Tuchmann A (1996) Cholangiography before biliary surgery: single-shot MR cholangiography versus intravenous cholangiography. Radiology 198 : 561 – 566

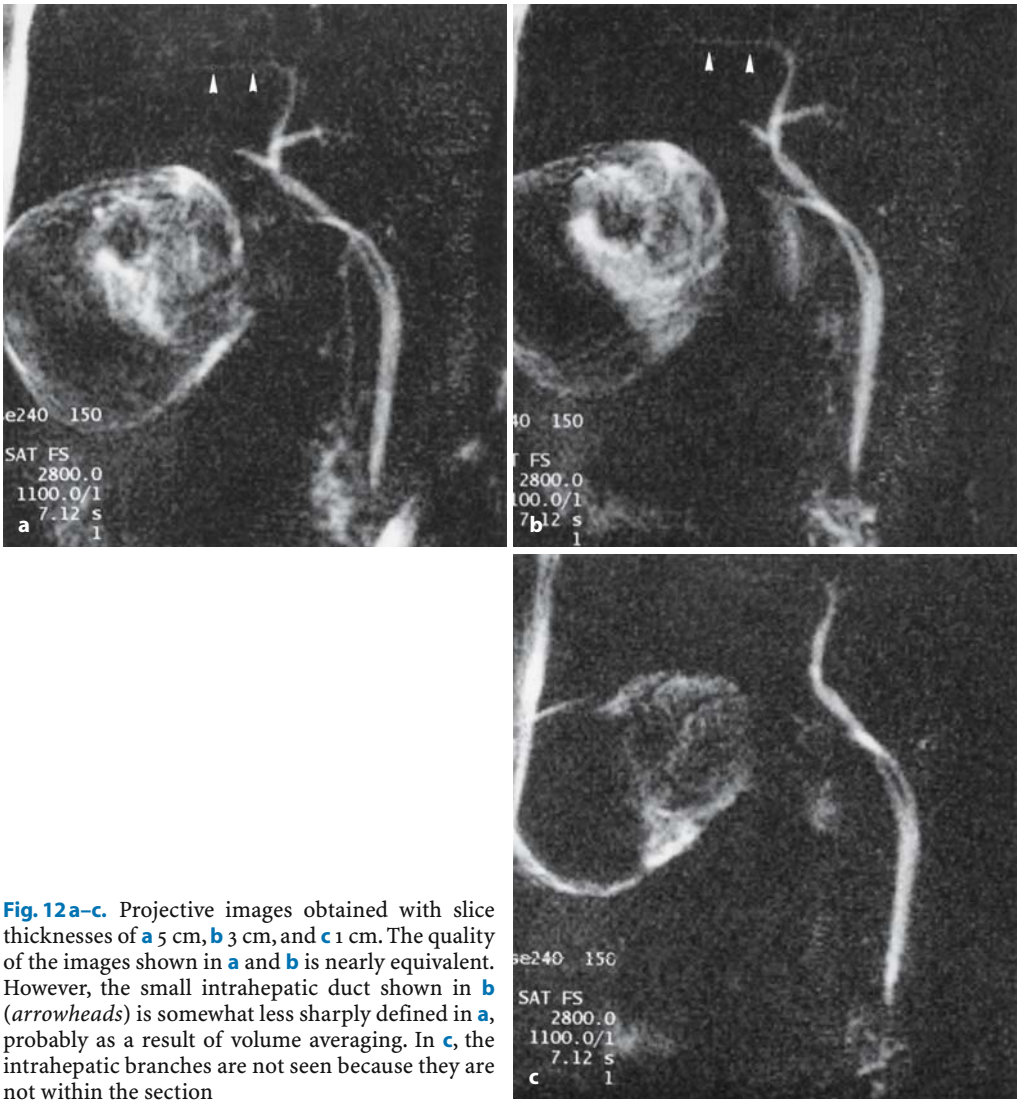

Fig. 12 a–c. Projective images obtained with slice thicknesses of **a** 5 cm, **b** 3 cm, and **c** 1 cm. The quality of the images shown in **a** and **b** is nearly equivalent. However, the small intrahepatic duct shown in **b** (*arrowheads*) is somewhat less sharply defined in **a**, probably as a result of volume averaging. In **c**, the intrahepatic branches are not seen because they are not within the section

#13 Dynamic Evaluation of the Vaterian Sphincter Complex

KEY FACTS

- Rationale (see also # 120):
  - A normal sphincter contracts approximately four times per min
  - On MR images, the appearance of the vaterian sphincter complex varies: during contraction, it is not visualized (no fluid in lumen); during relaxation, it is seen as a thin, fluid-containing structure
  - Dynamic imaging of the vaterian sphincter complex allows both anatomy and contractility to be evaluated
- Technique (Van Hoe et al. 1998):
  - Localization of the distalmost portions of the common bile duct and pancreatic duct on cross-sectional images
  - Selection of optimal slice position and orientation (showing the distal parts of the common bile duct and pancreatic duct; see # 11)
  - Repetitive imaging of the same section during consecutive (up to 20) episodes of breathholding

References

Van Hoe L, Gryspeerdt S, Vanbeckevoort D et al. (1998) Normal Vaterian sphincter complex: evaluation of morphology and contractility with dynamic single-shot MR cholangiography. AJR 170 : 1497 – 1500

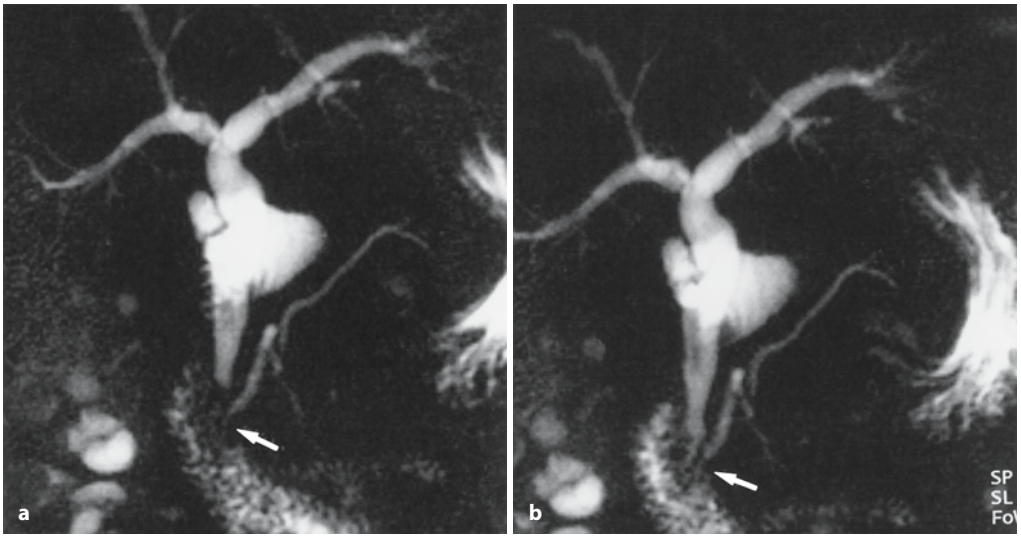

Fig. 13 a, b. Two images from a dynamic study of the vaterian sphincter complex, obtained at the same location at an interval of ± 10 s. Note that the distal (intramural) parts of the common bile duct and pancreatic duct are not visible in **a** (image obtained during contraction of the sphincter), while they are clearly visible in **b** (*arrows*). For further details, see # 120

1.3 Use of Contrast Media and Drugs

#14 Oral Contrast Media

KEY FACTS

T1-Weighted MRI

Positive Contrast Media

- Examples: manganese or gadolinium compounds
- Advantages: improved distention of stomach, duodenum and jejunum, improved evaluation of mural and intraluminal abnormalities
- Potential applications: evaluation of mucosal and mural abnormalities, assessment of contractility, etc. (Geitung and Gjesdal 1997)

T2-Weighted MRI

Positive Contrast Media

- Examples: tap water
- Advantages: improved distention of stomach, duodenum, jejunum
- Applications: prerequisite for adequate evaluation of bilioenteric anastomoses (Pavone et al. 1997); also useful in the evaluation of ampullary tumors and tumors of pancreatic head

Negative Contrast Media

- Examples: iron-containing oral suspension
- Advantages: elimination of overlapping fluid-containing organs
- Applications: evaluation of pancreatic fluid outflow (Matos et al. 1997)
- Limitations: exact length and location of the vaterian sphincter complex more difficult to evaluate

Note: We only administer oral contrast media in a minority of patients (see indications for use of tap water). Patients do not fast prior to MR study

References

Chan JH, Tsui EY, Yuen MK et al. (2000) Gadopentetate dimeglumine as an oral negative gastrointestinal contrast agent for MRCP. Abdom Imaging 25 : 405 – 408

Geitung JT, Gjesdal KI (1997) Dynamic imaging of the gastric ventricle using MRI. MAGMA 5 [Suppl] : 39

Matos C, Metens T, Devière J et al. (1997) Pancreatic duct: morphologic and functional evaluation with dynamic MR pancreatography after secretin stimulation. Radiology 203 : 435 – 441

Papanikolaou N, Karantanas A, Maris T et al. (2000) MR cholangiopancreatography before and after oral blueberry juice administration. J Comput Assist Tomogr 24 : 229 – 234

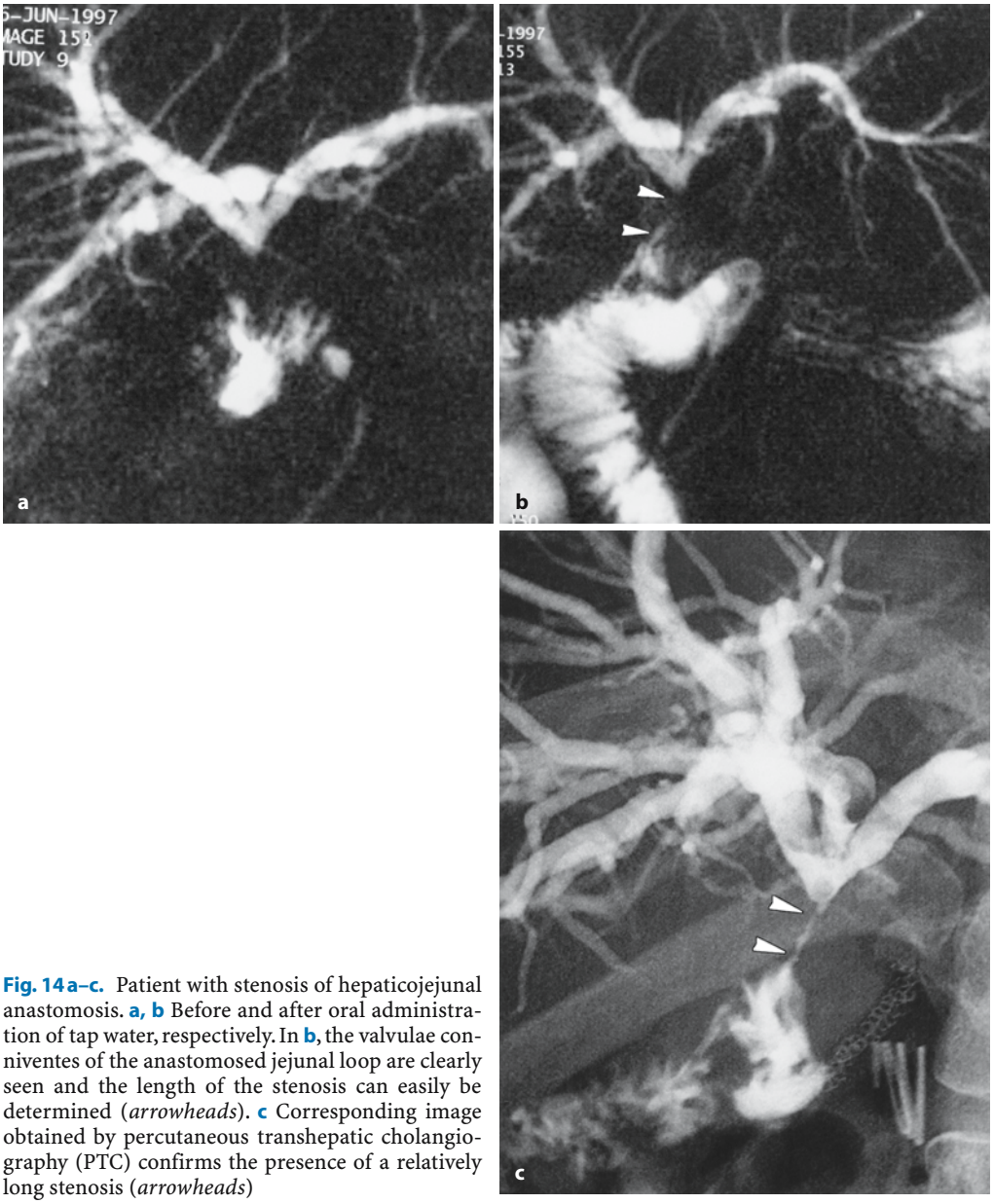

Fig. 14 a–c. Patient with stenosis of hepaticojejunal anastomosis. **a, b** Before and after oral administration of tap water, respectively. In **b**, the valvulae conniventes of the anastomosed jejunal loop are clearly seen and the length of the stenosis can easily be determined (*arrowheads*). **c** Corresponding image obtained by percutaneous transhepatic cholangiography (PTC) confirms the presence of a relatively long stenosis (*arrowheads*)

#15 Nonspecific Intravenous Contrast Media (1): Parenchymal Organs and Lymph Nodes

KEY FACTS

- Type: gadolinium chelates
- May be used routinely or in function of clinical information and/or findings at non-contrast imaging (see # 1)
- Formal indications
  - Characterization of focal liver lesions displaying indeterminate features on double-echo HASTE (± 10 % – 20 % of lesions)
  - Evaluation of pancreatic perfusion (detection of necrotizing pancreatitis; see # 155)
  - Detection of pancreatic carcinoma in patients with associated pancreatitis (see # 194; Gabata et al. 1994)
  - Detection/staging of endocrine pancreatic tumors (see # 177, # 197)
  - Preoperative evaluation of pancreatic tumors (e. g., detection of lymph nodes; Fig. 15 a, b; see also # 16)
- *Note:* Many abnormalities are clearly displayed on non-contrast-enhanced images (Fig. 15 c, d). Moreover, some tumors (particularly endocrine pancreatic tumors) may temporarily become less conspicuous or even invisible after administration of intravenous contrast agents (see # 177, # 197).
- Timing: biphasic imaging at 15 and 45 seconds or later after arrival of contrast material in the abdominal aorta is a practical method for acquisition of high-quality dynamic T1-weighted MR images of pancreatic parenchyma (Kanematusu et al. 2000)
- For dynamic imaging, a fat-saturated volumetric interpolated breath-hold (VIBE) sequence is preferred (Rofsky et al. 1999)

References

Gabata T, Matsui O, Kadoya M et al. (1994) Small pancreatic adenocarcinomas: efficacy of MR imaging with fat suppression and gadolinium enhancement. Radiology 193 : 683 – 688

Hamm B, Mahfouz A-E, Taupitz M et al. (1997) Liver metastases: improved detection with dynamic gadolinium-enhanced MR imaging? Radiology 202 : 677 – 682

Kanematsu M, Shiratori Y, Hoshi H, et al. (2000) Pancreas and peripancreatic vessels: effect of imaging delay on gadolinium enhancement at dynamic gradient-recalled-echo MR imaging. Radiology 215 : 95 – 102

Rofsky, NM, Lee VS, Laub G, et al. (1999) Abdominal MR imaging with a volumetric interpolated breath-hold examination. Radiology 212 : 876 – 884

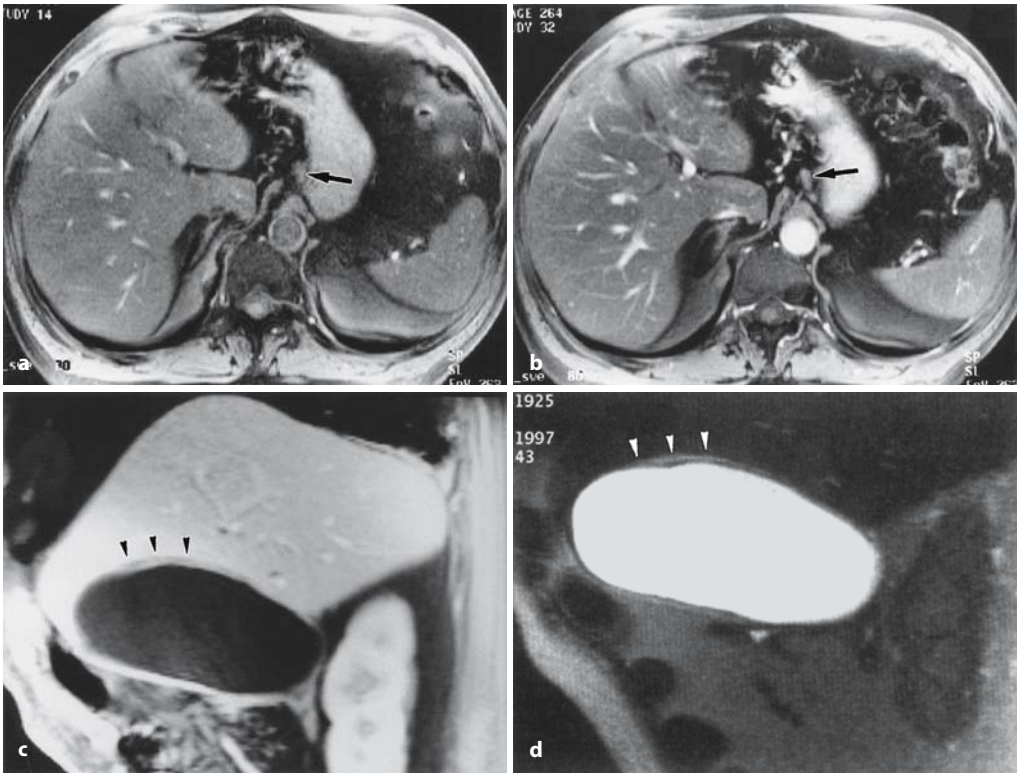

Fig. 15 a–d. Patient with pancreatic cancer and enlarged lymph nodes. **a** Non-contrast-enhanced and **b** contrast-enhanced fat-suppressed T1-weighted images. Slightly enlarged lymph node is better seen in **b** (*arrows*). **c, d** Patient with acute cholecystitis. **c** Contrast-enhanced T1-weighted image obtained in the sagittal plane showing thin hypoenhancing zone between gallbladder wall and liver (*arrowheads*), corresponding to fluid. **d** Heavily T2-weighted snapshot image also nicely shows the small amount of fluid

#16 Nonspecific Intravenous Contrast Media (2): Vascular "Roadmapping"

KEY FACTS

- Breathhold three-dimensional contrast-enhanced MRI/MRA has emerged as a highly promising method for the evaluation of abdominal vascular disease (Prince et al. 1995)
- Using high-power gradient systems, the arteries of the entire upper abdomen can be imaged during one single breathhold (Earls et al. 1997)
- Critical elements of successful MRA examination (Earls et al. 1997; Prince et al. 1995):
  - Timing examination (test dose)
  - Patient coaching with or without oxygen administration
  - Fast injection of contrast medium
  - Optimization of voxel size in function of vessel size
- Indications:
  - Preoperative evaluation of (suspected) pancreatic cancer ("all-in-one" approach; see Fig. 191 c, d; Gaa et al. 1997)
  - Detection of anatomic variants prior to pancreatic or hepatobiliary surgery (Fig. 16)
  - Clinical suspicion of pseudoaneurysm, arteriovenous fistula, arterial occlusion
  - Suspicion of venous involvement in patients with neoplastic disease (e.g., hepatocellular carcinoma)
- In practice, vascular roadmapping and dynamic contrast-enhanced parenchymal imaging can be combined by using VIBE or similar sequences (Rofsky et al. 1999, Keogan et al. 2000)

References

Earls JP, Rofsky NM, DeCorato DR, Krinsky GA, Weinreb JC (1997) Breath-hold single-dose gadolinium-enhanced three-dimensional MR aortography: usefulness of a timing examination and an MR power injector. Radiology 202: 268–273

Gaa J, Wendl K, Trede M, Georgi M (1997) New concepts in MR imaging of pancreatic carcinoma: the all-in-one approach. In: Oudkerk M, Edelman R (eds) High-power gradient MR-imaging. Blackwell Science, Berlin, pp 425–430

Keogan MT, Edelman RR (2001) Technologic advances in abdominal MR imaging. Radiology 220: 310–320

Prince MR, Narasimham DL, Stanley JC, Chenevert TL, Williams DM, Marx MV, Cho KJ (1995) Breath-hold gadolinium-enhanced MR angiography of the abdominal aorta and its major branches. Radiology 197: 785–792

Rofsky, NM, Lee VS, Laub G, et al. (1999) Abdominal MR imaging with a volumetric interpolated breath-hold examination. Radiology 212: 876–884

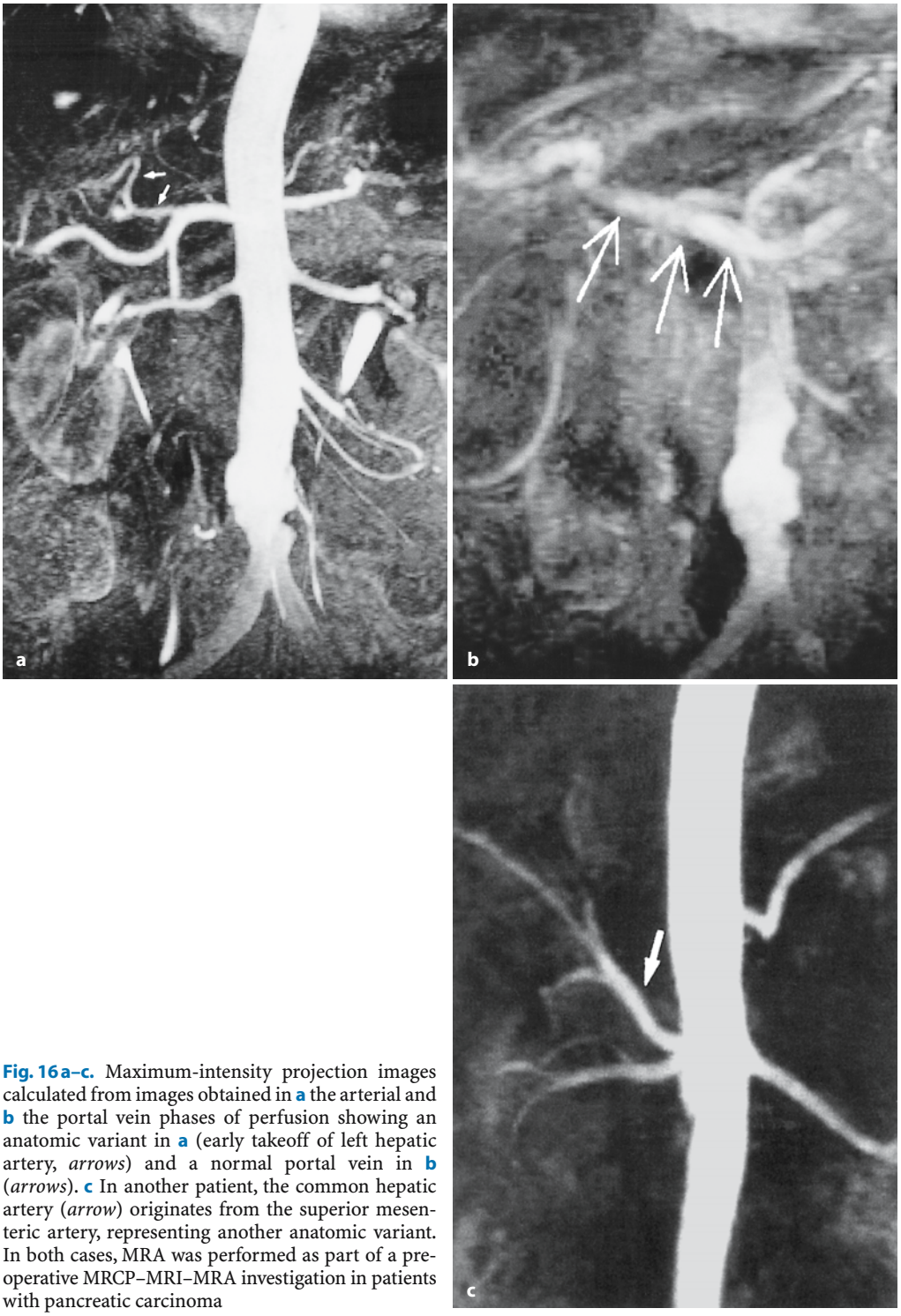

Fig. 16 a–c. Maximum-intensity projection images calculated from images obtained in **a** the arterial and **b** the portal vein phases of perfusion showing an anatomic variant in **a** (early takeoff of left hepatic artery, *arrows*) and a normal portal vein in **b** (*arrows*). **c** In another patient, the common hepatic artery (*arrow*) originates from the superior mesenteric artery, representing another anatomic variant. In both cases, MRA was performed as part of a preoperative MRCP–MRI–MRA investigation in patients with pancreatic carcinoma

#17 Specific Intravenous Contrast Media (1): Hepatocyte-Directed Agents

KEY FACTS

- Molecules with large lipophilic component
- Uptake by hepatocytes and excretion in bile; sometimes uptake in other parenchymal organs (see below)
- Influence on tissue contrast: increase in signal intensity on T1-weighted images (paramagnetic agents)
- Examples (Van Beers et al. 1997):
  - Manganese-dipyridoxyl diphosphate (manganese-DPDP; uptake also in pancreas and adrenals)
  - Gd-ethoxybenzyl-diethylenetriaminopentoacetic acid (Gd-EOB-DTPA)
  - Gd-benzyloxyproprionic-tetraacetic acid (Gd-BOPTA)
- Main advantage:
  - Improved visualization of secondary hepatic tumors (e.g., metastases of pancreatic carcinoma) (Fig. 17a, c)
  - Evalution of bile duct integrity (Vitellas et al. 2002, Fayad et al. 2005)
- Other advantages/potential applications:
  - Evaluation of biliary excretory function (the biliary excretion fraction of Gd-EOB-DTPA, for instance, is 50%) (Fig. 17e)
  - Detection of pancreatic tumors (manganese-DPDP; Gehl et al. 1991; Kettritz et al. 1996) (Fig. 17b, d)

References

Fayad LM, Kamel IR, Mitchell DG, Bluemke DA (2005) Functional MR cholangiography: diagnosis of functional abnormalities of the gallbladder and biliary tree. Am. J. Roentgenol 184 : 1563 – 1571

Gehl HB, Vorwerk D, Klose KC, Guenther RW (1991) Pancreatic enhancement after low-dose infusion of Mn-DPDP. Radiology 180 : 337 – 339

Kettritz U, Warshauer D, Brown E, Schlund J, Eisenberg L, Semelka R (1996) Enhancement of the normal pancreas: comparison of manganese-DPDP and gadolinium chelate. Eur Radiol 6 : 14 – 18

Van Beers B, Gallez B, Pringot J (1997) Contrast-enhanced MR imaging of the liver. Radiology 203 : 297 – 306

Vitellas KM, El-Dieb A, Vaswani KK, et al. (2002) Using contrast-enhanced MR cholangiography with IV mangafodipir trisodium (Teslascan) to evaluate bile duct leaks after cholecystectomy: a prospective study of 11 patients. AJR Am J Roentgenol 179 : 409 – 416

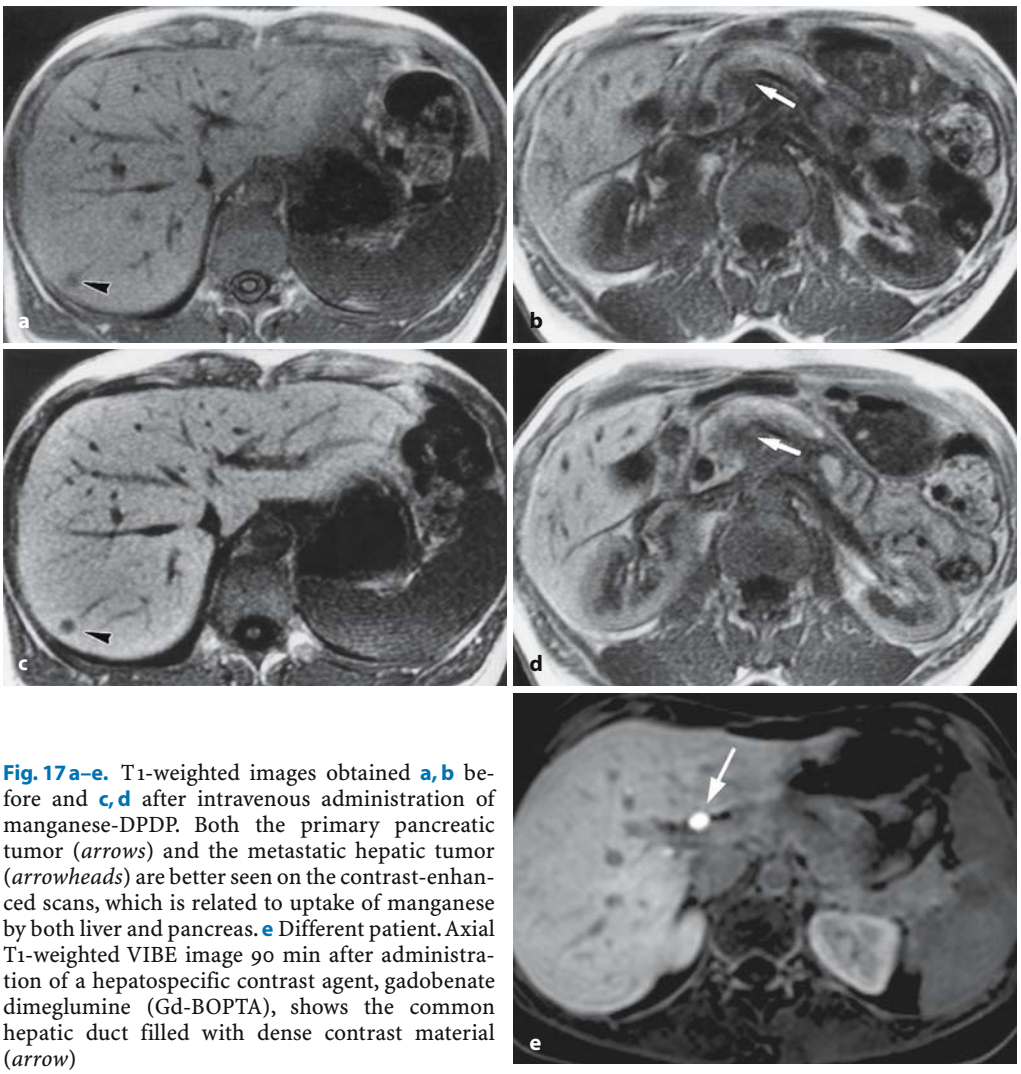

Fig. 17 a–e. T1-weighted images obtained **a, b** before and **c, d** after intravenous administration of manganese-DPDP. Both the primary pancreatic tumor (*arrows*) and the metastatic hepatic tumor (*arrowheads*) are better seen on the contrast-enhanced scans, which is related to uptake of manganese by both liver and pancreas. **e** Different patient. Axial T1-weighted VIBE image 90 min after administration of a hepatospecific contrast agent, gadobenate dimeglumine (Gd-BOPTA), shows the common hepatic duct filled with dense contrast material (*arrow*)

#18 Specific Intravenous Contrast Media (2): Reticuloendothelial Agents

KEY FACTS

- Iron-containing particles
- Specific uptake by elements of the reticuloendothelial system in liver, spleen, bone marrow, and lymph nodes
- Influence on contrast of superparamagnetic agents: cause dephasing and focal signal loss, mainly on T2-weighted images (the effect on T1-weighted images is variable)

Small Iron Oxide Particles

- 80% uptake by hepatic Kupffer cells
- Improve the detection of hepatic metastases (Fig. 18; Senéterre et al. 1996)
- Useful for characterization of primary liver tumors (uptake by focal nodular hyperplasia and adenoma; Vogl et al. 1996)

Ultrasmall particles

- Accumulation mainly in bone marrow and lymph nodes
- Blood pool contrast agent
- Potential application: characterization of (enlarged) lymph nodes (Anzai et al. 1994; Rogers et al. 1994)

References

Anzai Y, Blackwell KE, Hirschowitz SL et al. (1994) Initial clinical experience with dextran-coated superparamagnetic iron oxide for detection of lymph node metastases in patients with head and neck cancer. Radiology 192 : 709 – 715

Rogers JM, Lewis J, Josephson L (1994) Visualization of superior mesenteric lymph nodes by the combined oral and intravenous administration of the ultrasmall superparamagnetic iron oxide AMI 227. Magn Reson Imaging 12 : 1161 – 1165

Senéterre E, Taourel P, Bouvier Y et al. (1996) Detection of hepatic metastases: ferumoxides-enhanced MR imaging versus unenhanced MR imaging and CT during arterial portography. Radiology 200 : 785 – 792

Vogl TJ, Hammerstingl R, Schwarz W et al. (1996) Superparamagnetic iron oxide-enhanced versus gadolinium-enhanced MR imaging for differential diagnosis of focal liver lesions. Radiology 198 : 881 – 887

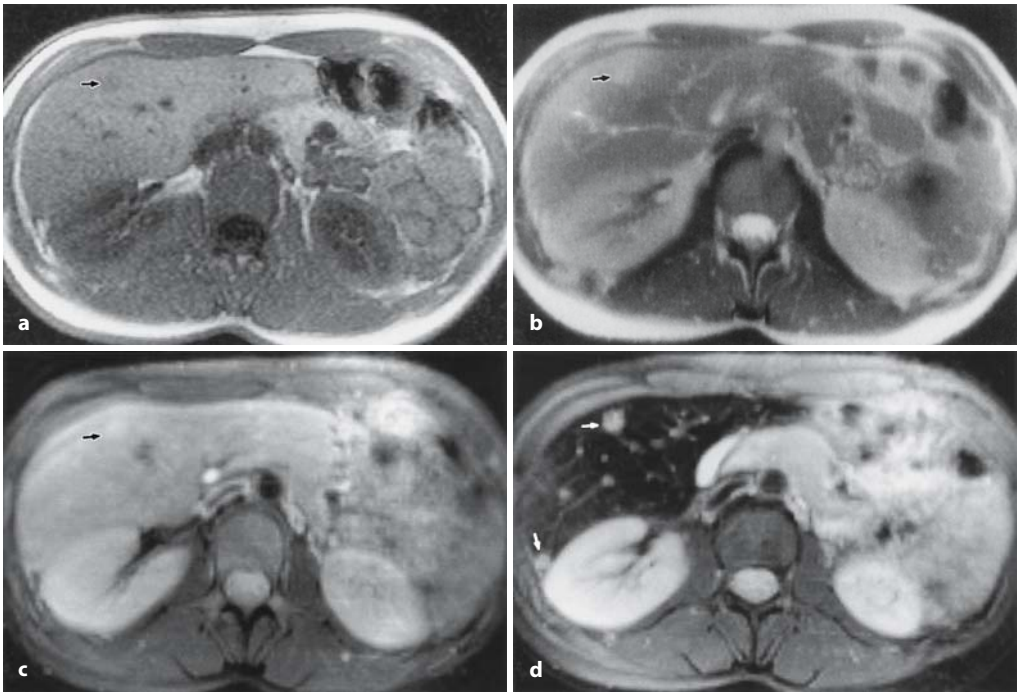

Fig. 18 a–d. Patient with hepatic metastases of cholangiocarcinoma. **a, b** T1- and T2-weighted snapshot images and **c** T2-weighted fat-suppressed fast spin echo image, all obtained before administration of contrast agent. **d** T2-weighted fat-suppressed fast spin echo image obtained after administration of small iron oxide particles. Note the much better visibility of two small metastases (*arrows*) in **d**, which is explained by signal loss of normal liver tissue (uptake by Kupffer cells)

#19 Drugs Stimulating Excretory Function

KEY FACTS

Pancreatic Ducts: Secretin

- Stimulates the secretion of fluid and bicarbonate by the exocrine pancreas
- Potential applications (Matos et al. 1997; Warschaw et al. 1985):
  - Assessment of the anatomy of the pancreatic duct (Fig. 19)
  - Evaluation of pancreatic excretory function
  - Detection of pancreatic outlet obstruction (e.g., papillary obstruction; see #127)
  - Demonstration of pancreatico-biliary reflux
- Limitations:
  - Does not allow visualization of *normal* side branches

Biliary Tree: Cholecystokinin

- Cholecystokinin produces:
  - Powerful contraction of the gallbladder
  - Decreased resistance of the sphincter of Oddi
  - Increased hepatic secretion of bile
- Can be used in conjunction with imaging studies (Krishnamurthy and Krishnamurthy (1996) to detect ampullary obstruction (e.g., dysfunction of vaterian sphincter complex)
- A similar effect can be obtained by administration of a fatty meal (results in endogenous release of cholecystokinin; Darweesh et al. 1988)

References

Czako L, Endes J, Takacs T et al. (2001) Evaluation of pancreatic exocrine function by secretin-enhanced magnetic resonance cholangiopancreatography. Pancreas 23 : 323 – 328

Darweesh R, Dodds W, Hogan W et al. (1988) Efficacy of quantitative hepatobiliary scintigraphy and fatty-meal sonography for evaluating patients with suspected partial common duct obstruction. Gastroenterology 94 : 779 – 786

Hosoki T, Hasuike Y, Takeda Y et al. (2004) Visualization of pancreaticobiliary reflux in anomalous pancreaticobiliary junction by secretin-stimulated dynamic magnetic resonance cholangiopancreatography. Acta Radiol 45 : 375 – 382

Hellerhoff KJ, Helmberger H, Rösch T, et al. (2002) Dynamic MR pancreatography after secretin administration: image quality and diagnostic accuracy. AJR Am J Roentgenol 179 : 121 – 129

Krishnamurthy S, Krishnamurthy G (1996) Cholecystokin and morphine pharmacological intervention during 99mTc-HIDA cholescintigraphy: a rational approach. Semin Nucl Med 26 : 16 – 24

Matos C, Metens T, Devière J et al. (1997) Pancreatic duct: morphologic and functional evaluation with dynamic MR pancreatography after secretin stimulation. Radiology 203 : 435 – 441

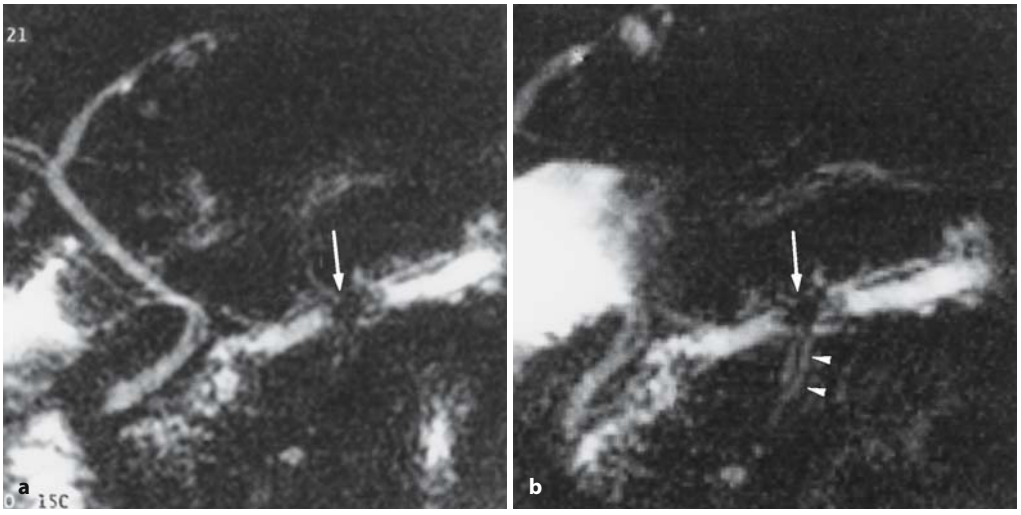

Fig. 19 a, b. Images obtained **a** before and **b** after administration of secretin in a patient with chronic pancreatitis. Both images show signs of chronic pancreatitis and a large intraductal stone (*arrows*). In **b**, the degree of filling of the distal pancreatic duct is slightly improved and some additional side branches are shown (*arrowheads*)

#20 Spasmolytic Drugs (1): Buscopan

KEY FACTS

- Active component: butylhyoscin
- Spasmolytic drug causing relaxation of smooth muscles in the gastrointestinal tract, pancreatobiliary tract, urogenital tract, and gallbladder (Forssmann and Singer 1994)
- Half-life after intravenous injection: ± 15 min
- Possible indications:
  - Evaluation of stomach, duodenum, ampullary region, pancreatic head
  - Contracted gallbladder: differentiation of organic abnormalities (e.g., chronic cholecystitis) and functional spasm (Fig. 20)

References

Chopra K, Westaby D, Murray-Lyon I (1996) Why use buscopan during diagnostic upper gastrointestinal endoscopy? Gut 38 : 473

Forssmann K, Singer MV (1994) Akute Cholezystitis – konservative Therapie. Schweiz Rundsch Med Prax 83 : 877 – 879

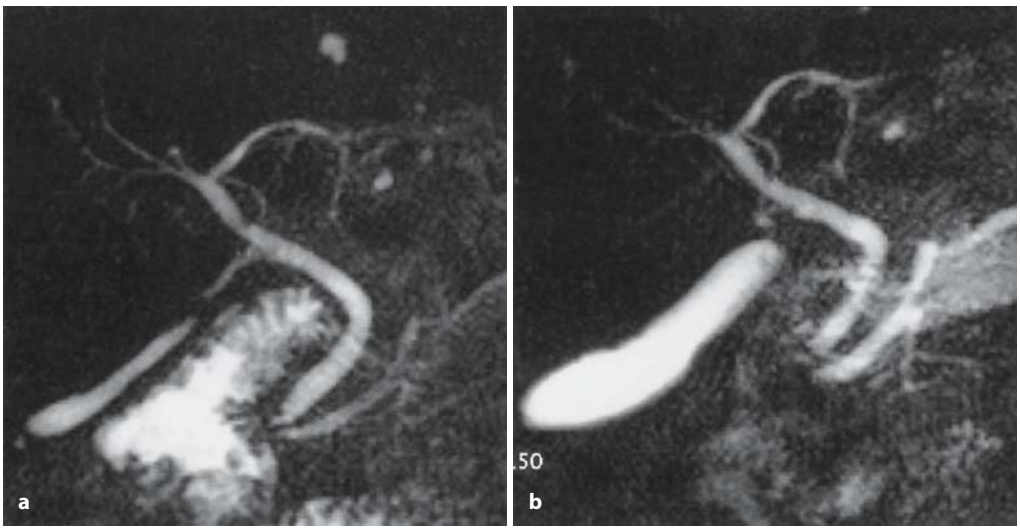

Fig. 20 a, b. Projective images obtained **a** before and **b** after intravenous administration of Buscopan. Note significantly increased size of the gallbladder in **b**, suggesting (normal) smooth muscle relaxation

#21 Spasmolytic Drugs (2): Glucagon

KEY FACTS

- Smooth muscle spasmolytic agent
- Relatively short half-life (a few minutes)
- Effects:
  - Effective inhibitor of the baseline pressure of the vaterian sphincter (Staritz 1988)
  - Effective inhibitor of motility and tonicity of the esophagus, stomach, duodenum, and colon
  - Increases the amount of fluid in the duodenum (Fig. 21)
- Applications:
  - Evaluation of stomach, duodenum, ampullary region, and pancreatic head
  - Potentially useful in the evaluation of the distal common bile duct and vaterian sphincter complex (hypotonic cholangiography; Ferruci et al. 1976; Dalal et al. 2004)

References

Dalal PU, Howlett DC, Sallomi DF et al. (2004) Does intravenous glucagon improve common bile duct visualisation during magnetic resonance cholangiopancreatography? Results in 42 patients. Eur J Radiol 49 : 258 – 261

Ferruci J, Wittenberg J, Stone L, Dreyfuss J (1976) Hypotonic cholangiography with glucagon. Radiology 118 : 466 – 467

Staritz M (1988) Pharmacology of the sphincter of Oddi. Endoscopy 20 : 171 – 174

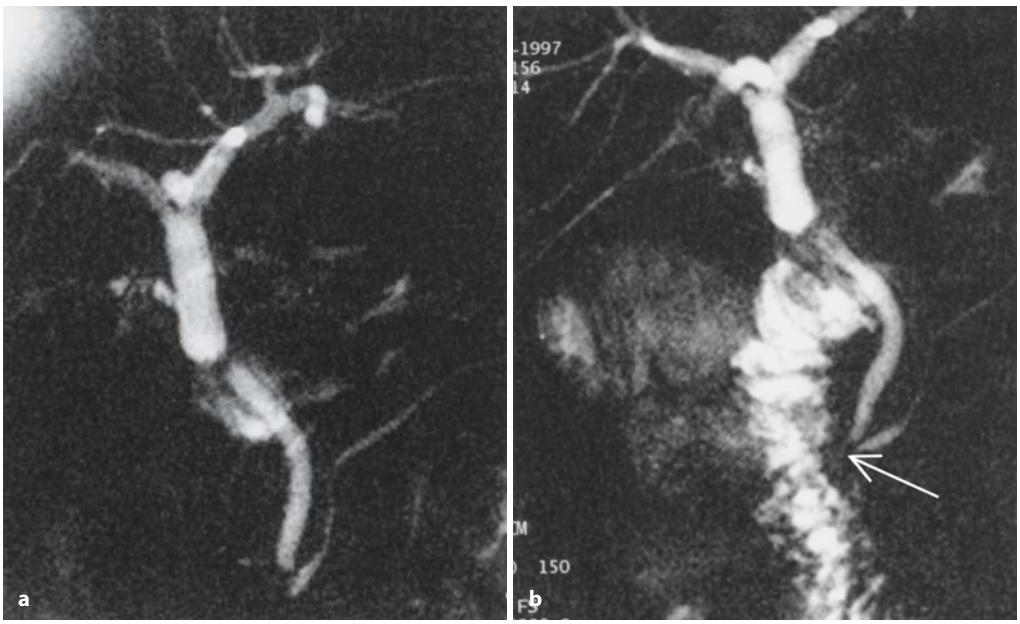

Fig. 21 a, b. Patient who underwent hepatic transplantation. Images obtained **a** before and **b** after intravenous administration of glucagon. Note the significantly increased amount of fluid in the duodenum in **b**, which is a common finding. The arrow in **b** shows the intramural portion of the common bile duct. Note that no oral contrast medium was given

1.4 Comparison with Other Techniques

#22 MRCP Compared with ERCP (1): Limitations of ERCP

KEY FACTS

- The limitations of endoscopic retrograde cholangiopancreatography (ERCP) can be summarized as follows:
  - Invasive nature (complication rate between 4.6 % and 12 %, depending on the type of procedure, e. g., diagnostic, manometry, sphincterotomy; Cotton and Chong 1995)
  - Highly operator dependent
  - Unsuccessful cannulation of the common bile duct or pancreatic ducts in 3 % – 9 % of cases (failure rate of MRCP, 1 % – 4 %)
  - Sedation usually required
  - No direct information on extraductal abnormalities (Fig. 22 a – e)
  - No opacification of ducts proximal to a complete obstruction (Fig. 22 f – h)
  - Less accurate MRCP for detection of intrahepatic stones (Kim et al. 2002)
  - Less accurate than MRCP for characterization of pancreatic duct stenoses

References

Cotton P, Chong W. Complications of ERCP and therapy. In: Silvis S, Rohrmann C, Ansel H (eds) Endoscopic retrograde cholangiopancreatography. Igaku-Shoin, New York, pp 446 – 469

Kim JH, Kim MJ, Park SI et al. (2002) Using kinematic MR cholangiopancreatography to evaluate biliary dilatation. AJR Am J Roentgenol. 178 : 909 – 914

Reinhold C, Bret PM (1996) Current status of MR cholangiopancreatography. AJR Am J Roentgenol 166 : 1285 – 1295

Soto JA, Yucel EK, Barish MA, Chuttani R, Ferruci JT (1996) MR cholangiography after unsuccessful or incomplete ERCP. Radiology 199 : 91 – 98

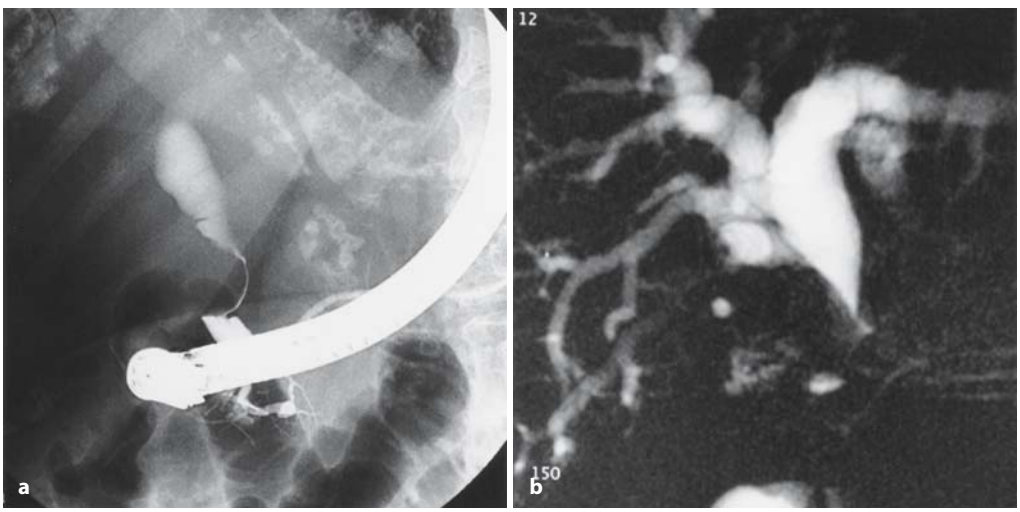

Fig. 22 a–e. ERCP image (**a**) showing smooth extrinsic compression on distal common bile duct, suggesting Mirizzi syndrome. **b** Projective MR image confirms gradual narrowing of the common bile duct.

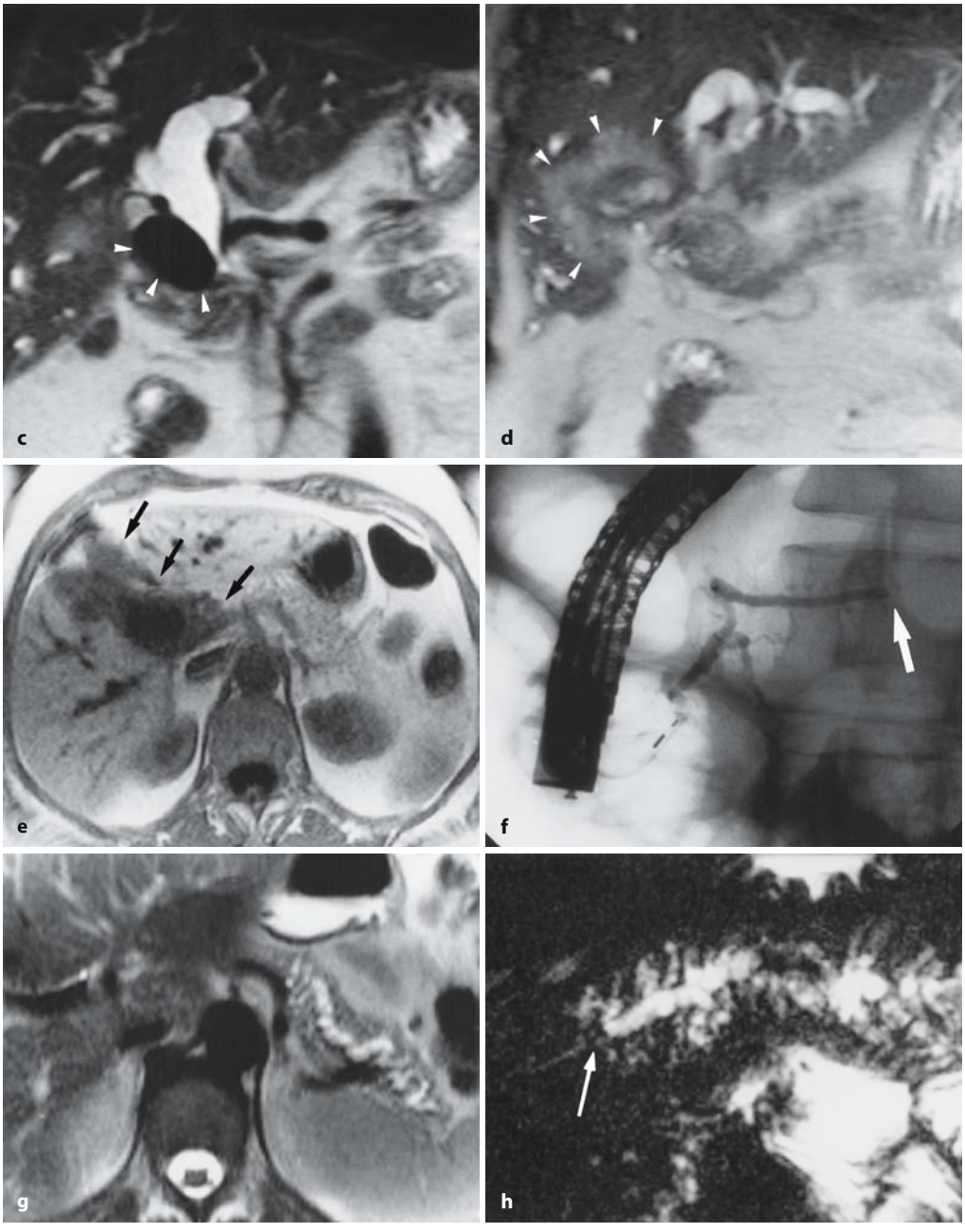

Fig. 22. c, d Cross-sectional T2-weighted images obtained in the coronal plane showing large stone impacted in the cystic duct (*arrowheads* in **c**), thus confirming the initial diagnosis, and a soft tissue mass centered on the gallbladder and invading the liver parenchyma (*arrowheads* in **d**). **e** Axial T1-weighted image also shows large soft tissue mass in the liver hilum, surrounding the stone (*arrows*). Final diagnosis: Mirizzi syndrome associated with gallbladder carcinoma (see also #71). **f–h** Other patient. ERCP image (**f**) showing obstruction of pancreatic duct (*arrow*): possibly a stone or a tumor. **g** Cross-sectional axial T2-weighted image showing dilation of the pancreatic duct in the pancreatic tail. **h** Projective MR image confirms the dilation and shows its cause: a small intraductal stone (*arrow*)

#23 MRCP Compared with ERCP (2): Limitations of MRCP

KEY FACTS

- The disadvantages of MRCP can be summarized as follows:
  - Artifacts related to the presence of surgical clips, metallic stents (see #57), and pneumobilia (see #67)
  - More limited spatial resolution (this is *not* the most important limitation)
  - Ducts are examined in their physiologic state (in ERCP, ducts are distended due to filling); this may lead to both under- and overestimation of stenoses (Figs. 23, 27c, d, 179) and to poor visualization of intraductal lesions (Figs. 23, 125d)
  - The normally high signal intensity (and consequently the conspicuity) of biliary ducts on T2-weighted images may be lost in the case of hemobilia, casting of necrotic debris, etc.
  - Superimposition of fluid-containing structures (e.g., cysts, exudates) may prevent adequate visualization of biliary and pancreatic ducts and may degrade the quality of projective images (see Fig. 35)
  - *Currently* not suited for guidance of interventional procedures or biopsy

References

Reinhold C, Bret PM (1996) Current status of MR cholangiopancreatography. AJR Am J Roentgenol 166:1285–1295

Van Hoe L, Mermuys K, Vanhoenacker P (2004) MRCP pitfalls. Abdom Imaging 29:360–387

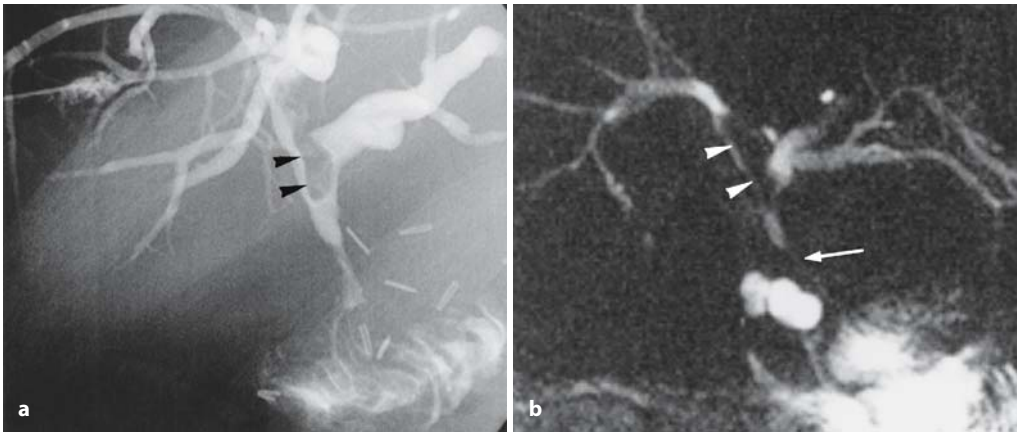

Fig. 23 a, b. Patient who underwent hepatojejunostomy. **a** PTC image showing stenosis at anastomosis and presence of an intrabiliary structure (*arrowheads*), perhaps a blood clot or sludge. **b** Projective MR image overestimates the severity of the stenosis (*arrow*). Moreover, the intraductal filling defect (*arrowheads*) is less conspicuous because it is not completely surrounded by fluid. This case typically illustrates the disadvantage of imaging the biliary tree in its physiologic state

#24 MRCP Compared with Ultrasonography

KEY FACTS

Transabdominal Ultrasonography

- Advantages of MRCP:
  - Higher sensitivity in the detection of common bile duct stones (reported values for sensitivity: ultrasonography, 13 % – 75 %; MRI, > 90 %; Guibaud et al. 1995; O'Conner et al. 1986)
  - More constant visualization of biliary, pancreatic, and retroperitoneal abnormalities
  - Better characterization of focal liver lesions
- Limitations:
  - Cost
  - Availability

Endoscopic and Intraductal Ultrasonography

- Relative value largely dependent on equipment/experience
- Theoretical advantages of MRCP:
  - Less invasive
  - Much larger field of view
  - More powerfull tool for tissue characterization
  - More versatile and comprehensive technique
- Theoretical limitations of MRCP:
  - Spatial resolution

References

Guibaud L, Bret P, Reinhold C, Atri M, Barkun AL (1995) Bile duct obstruction and choledocholithiasis: diagnosis with MR cholangiography. Radiology 197 : 109 – 115

O'Conner HJ, Hamilton I, Ellis WR, Watters J, Lintott DJ, Axon AT (1986) Ultrasound detection of choledocholithiasis: prospective comparison with ERCP in the postcholecystectomy patient. Gastrointest Radiol 11 : 161 – 164

Rosch T, Lightdale CJ, Botet JF et al. (1992) Localization of pancreatic endocrine tumors by endoscopic ultrasonography. N Engl J Med 326 : 1721 – 1726

Zerbey AL, Lee MJ, Brugge WR, Mueller PR (1996) Endoscopic sonography of the upper gastrointestinal tract and pancreas. AJR Am J Roentgenol 166 : 45 – 50

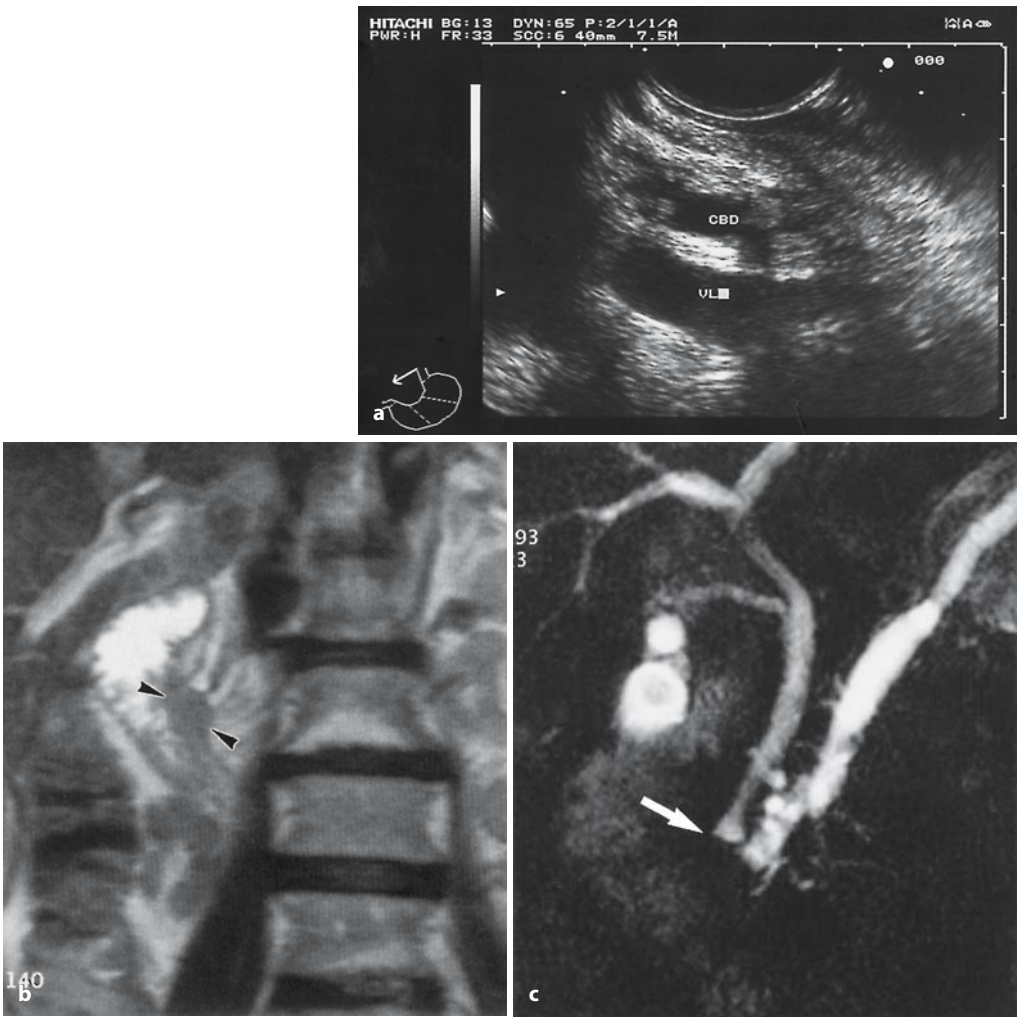

Fig. 24. **a** In this patient, endoscopic sonography showed no abnormalities (*VL*, splenic vein; *CBD*, common bile duct). Axial T1- and T2-weighted MR images also revealed no focal lesions. **b** However, the coronal T2-weighted image suggests the presence of a small mass in the papillary area (*arrowheads*). **c** Projective MR image showing abrupt narrowing of the common bile duct and pancreatic duct (*arrow*), together with some dilated side branches. This case illustrates the advantages of a comprehensive MR approach: projective and cross-sectional MR images clearly provide complementary information

#25 MRCP Compared with Multislice Computed Tomography

KEY FACTS

- General advantages of MRI:
  - Absence of ionizing radiation
  - Higher intrinsic soft tissue contrast (Fig. 25)
  - Possible to obtain projective (e.g., cholangiographic) images in any desired plane
  - Direct multiplanar imaging capability
- General advantages of CT:
  - Spatial resolution (pixel size typically four to eight times smaller in CT)
  - Physical basis and artifact behavior easier to understand
  - Cost
  - Larger examination volume: possible to investigate the entire abdomen or even thorax and abdomen in one session
  - Better visualization of calcifications (see Fig. 47)
- Value in clinical practice:
  - In most institutions multislice CT is the first imaging modality in patients referred for evaluation of upper abdominal disease
  - MRC/MRCP commonly used for problem solving and for specific indications

References

Cahir JG, Freeman AH, Courtney HM (2004) Multislice CT of the abdomen. Br J Radiol 77 Spec No 1: S64–73

Ichikawa T, Haradome H, Hachiya J et al. (1997) Pancreatic ductal adenocarcinoma: preoperative assessment with helical CT versus dynamic MR imaging. Radiology 202: 655–662

Semelka RC, Kelekis NL, Molina PL, Sharp TJ, Calvo B (1996) Pancreatic masses with inconclusive findings on spiral CT: is there a role for MRI? J Magn Reson Imaging 6: 585–588

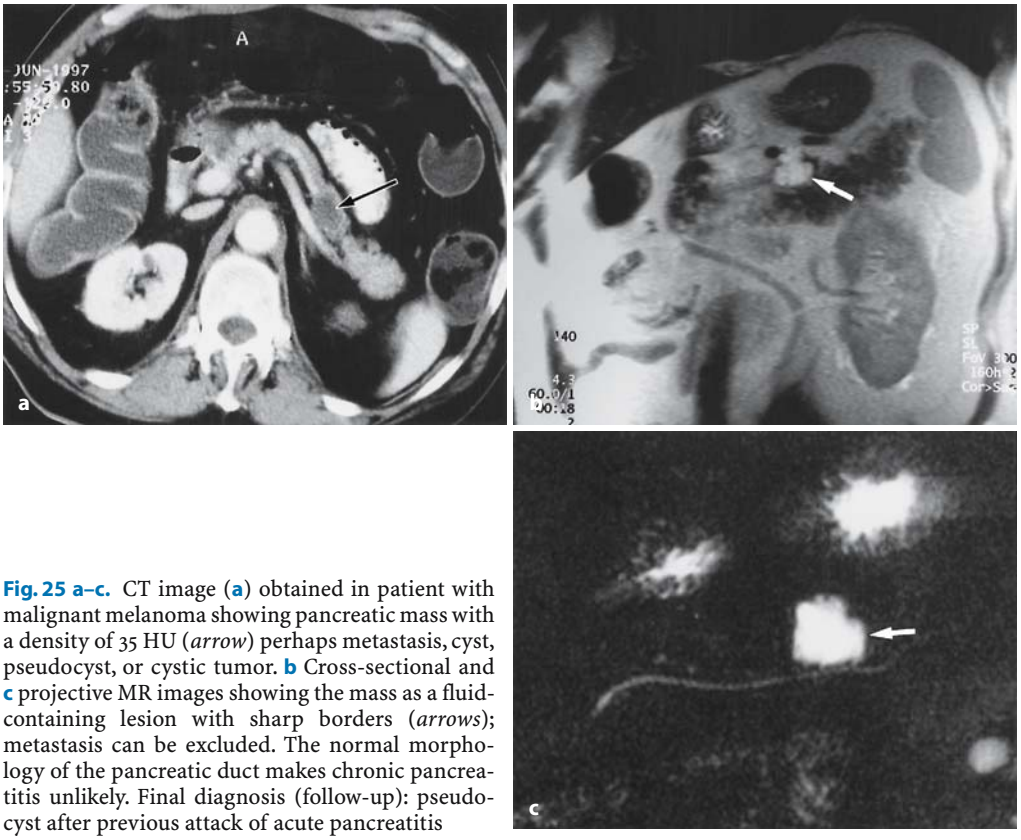

Fig. 25 a–c. CT image (**a**) obtained in patient with malignant melanoma showing pancreatic mass with a density of 35 HU (*arrow*) perhaps metastasis, cyst, pseudocyst, or cystic tumor. **b** Cross-sectional and **c** projective MR images showing the mass as a fluid-containing lesion with sharp borders (*arrows*); metastasis can be excluded. The normal morphology of the pancreatic duct makes chronic pancreatitis unlikely. Final diagnosis (follow-up): pseudocyst after previous attack of acute pancreatitis

Intrahepatic Bile Ducts

2 Intrahepatic Bile Ducts

2.1 Normal Anatomy and Variants

#26 Normal Anatomy

KEY FACTS: ANATOMY

- The bile ducts generally follow the internal hepatic segmental anatomy (Fig. 26 a). However, marked variation in the branching pattern is common
- Major branches:
  - Right hepatic duct, dividing into the posterior right hepatic duct (dorsocaudal course) and the anterior right hepatic duct (ventrocranial course)
  - Left hepatic duct (more anterior in position)
- Segmental branches:
  - From the posterior right hepatic duct: right posterior superior duct (serves segment VII) and right posterior inferior duct (segment VI)
  - From the anterior right hepatic duct: right anterior superior duct (segment VIII) and right anterior inferior duct (segment V)
  - The ductal branches that serve segments I–IV stem directly from the left hepatic duct
- Projective MRCP nearly invariably shows the right and left hepatic ducts and their major branches (Reinhold and Bret 1996; Fig. 26 b)
- Heavily T2-weighted cross-sectional images also show smaller branches throughout the liver parenchyma (complete absence of bile ducts in a lobe or segment is abnormal)
- The degree of visualization of small and/or peripheral branches depends on the following:
  - Technical parameters (e.g., projective versus cross-sectional, choice of slice thickness)
  - Patient-related parameters (age, constitution)

References

Dodd GD III (1993) An American's guide to Couinaud's numbering system. AJR Am J Roentgenol 574–575

Reinhold C, Bret PM (1996) Current status of MR cholangiopancreatography. AJR Am J Roentgenol 166:1285–1295

Taylor AJ, Bohorfoush AG (1997) Interpretation of ERCP. Lippincott-Raven, Philadelphia, p 62

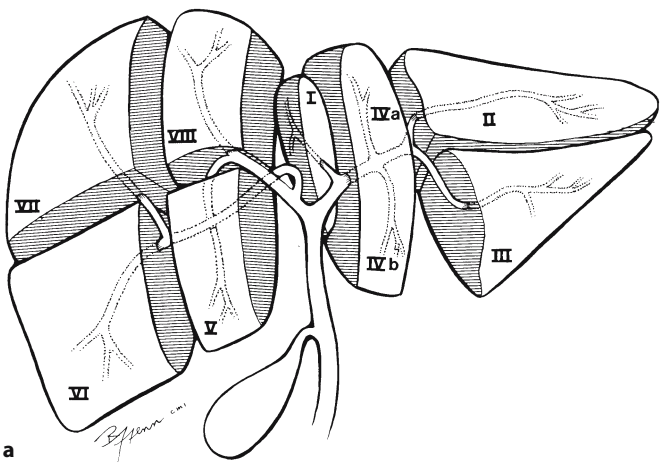

a

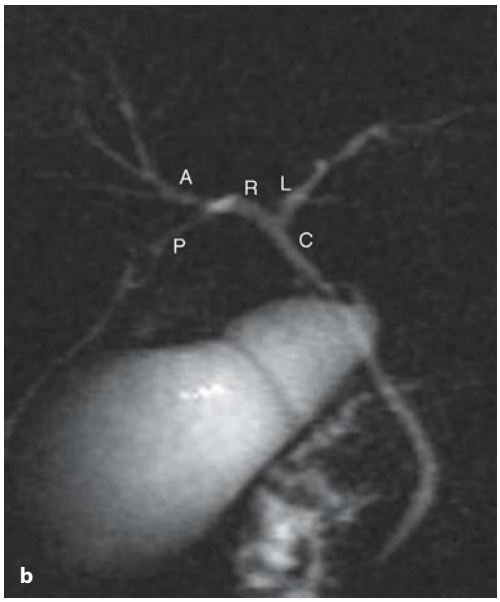

b

Fig. 26. **a** The intrahepatic biliary tree and its relation to the hepatic segments. Note that the distal portions of the right and left hepatic duct travel outside the liver substance before they join to form the common hepatic duct. The right posterior hepatic duct serves segments VI and VII and runs in a more horizontal direction than the right anterior duct. (Reprinted with permission from Taylor and Bohorfoush 1997) **b** Projective image obtained in a young asymptomatic patient showing the common hepatic duct (*C*) and right (*R*) and left (*L*) hepatic duct as well as the posterior (*P*) and anterior (*A*) right hepatic ducts

#27 Variant Anatomy (1): Variable Junction of the Posterior Right Hepatic Duct

Related topic: #52 (after cholecystectomy: stricture/transection of aberrant bile duct)

KEY FACTS: ANATOMY

- Aberrant bile ducts occur in 14%–28% of the population (Sussman et al. 1986)
- The most common anomaly is a failure of fusion of the anterior and posterior right segmental ducts. In the majority of cases, the right posterior segmental duct joins the left hepatic duct (Fig. 27 a, b; see also Fig. 63). This appears as a trifurcation if the right posterior duct joins the left hepatic duct near the confluence with the right anterior duct
- In 2%–3% of the population, the right posterior hepatic duct drains into the common hepatic duct, cystic duct, gallbladder, common bile duct, or even duodenum (Fig. 27 a, c)
- Clinical significance: risk of operative bile duct injury, particularly during (laparoscopic) cholecystectomy (see #52)

References

Russell E, Yrizzary KM, Montalvo BM et al. (1990) Left hepatic duct anatomy: implications. Radiology 174 : 353–356

Sussman SK, Hall FM, Elboim CM (1986) Radiographic assessment of anomalous bile ducts. Gastrointest Radiol 11 : 269–272

Taourel P, Bret P, Reinhold C, Barkum AN, Atri M (1996) Anatomic variants of the biliary tree: diagnosis with MRCP. Radiology 199 : 521–527

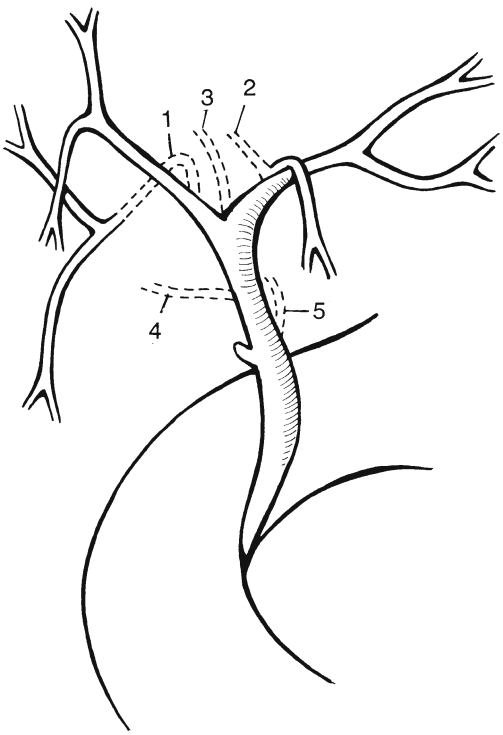

Fig. 27. a Variations in the drainage pattern of the right posterior hepatic duct: drainage into right anterior duct (*1*), left hepatic duct (*2*), bifurcation (*3*), lateral side of common hepatic duct (*4*), and medial side of common hepatic duct (*5*). (Reprinted with permission from Russell et al. 1990)

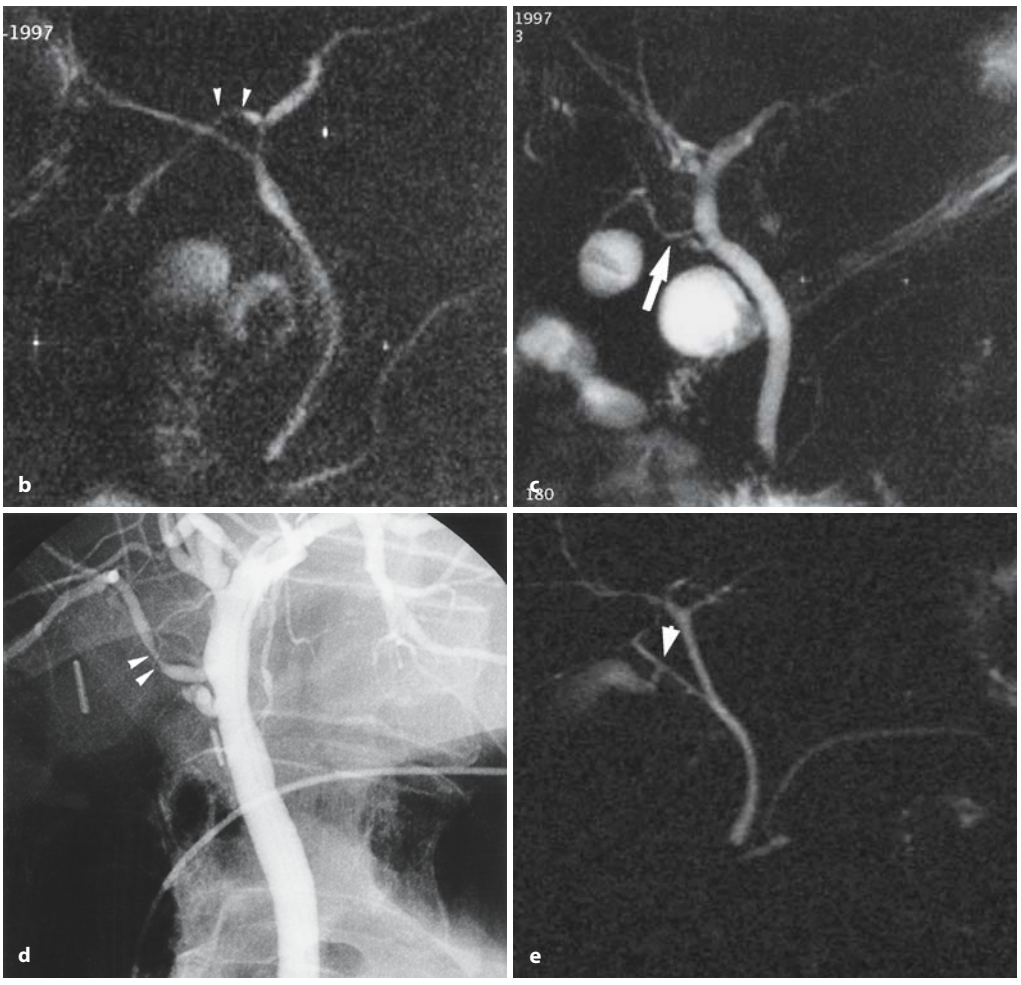

Fig. 27. b Projective image showing drainage of the right posterior segmental duct into the left hepatic duct (*arrowheads*). **c, d** In another patient, projective MR image (**c**) showing aberrant right posterior duct draining into the common hepatic duct in close proximity to the cystic duct (*arrow*). **d** Corresponding ERCP image confirms the presence of an aberrant right posterior hepatic duct. Moreover, it shows a short stenosis of this duct (*arrowheads*), probably related to trauma during cholecystectomy. Note that this stenosis is not well seen in **c** (see #23). **e** Different patient. Projective MR (RARE) image showing aberrant right posterior segmental duct; the cystic duct appears to drain in this duct (*arrow*)

#28 Variant Anatomy (2): Other Variations

KEY FACTS: ANATOMY

- Many other variations in anatomy and branching pattern exist, including the following:
  - Quadrifurcation of the right or main hepatic duct (Fig. 28 a, b)
  - Cystohepatic duct: intrahepatic ducts draining into the gallbladder (Fig. 28 c)
  - Subvesicle ducts (also called Luschka ducts, found in 35 % of autopsy cases): tiny ducts (< 2 mm in size) beginning in the wall of the gallbladder but not communicating with the lumen
  - Unusually large right or left segmental branches

References

Schulte S (1995) Embryology and congenital anomalies of the bile and pancreatic ducts. In: Silvis S, Rohrmann C, Ansel H (eds) Endoscopic retrograde cholangiopancreatography. Igaku-Shoin, New York, pp 114–126

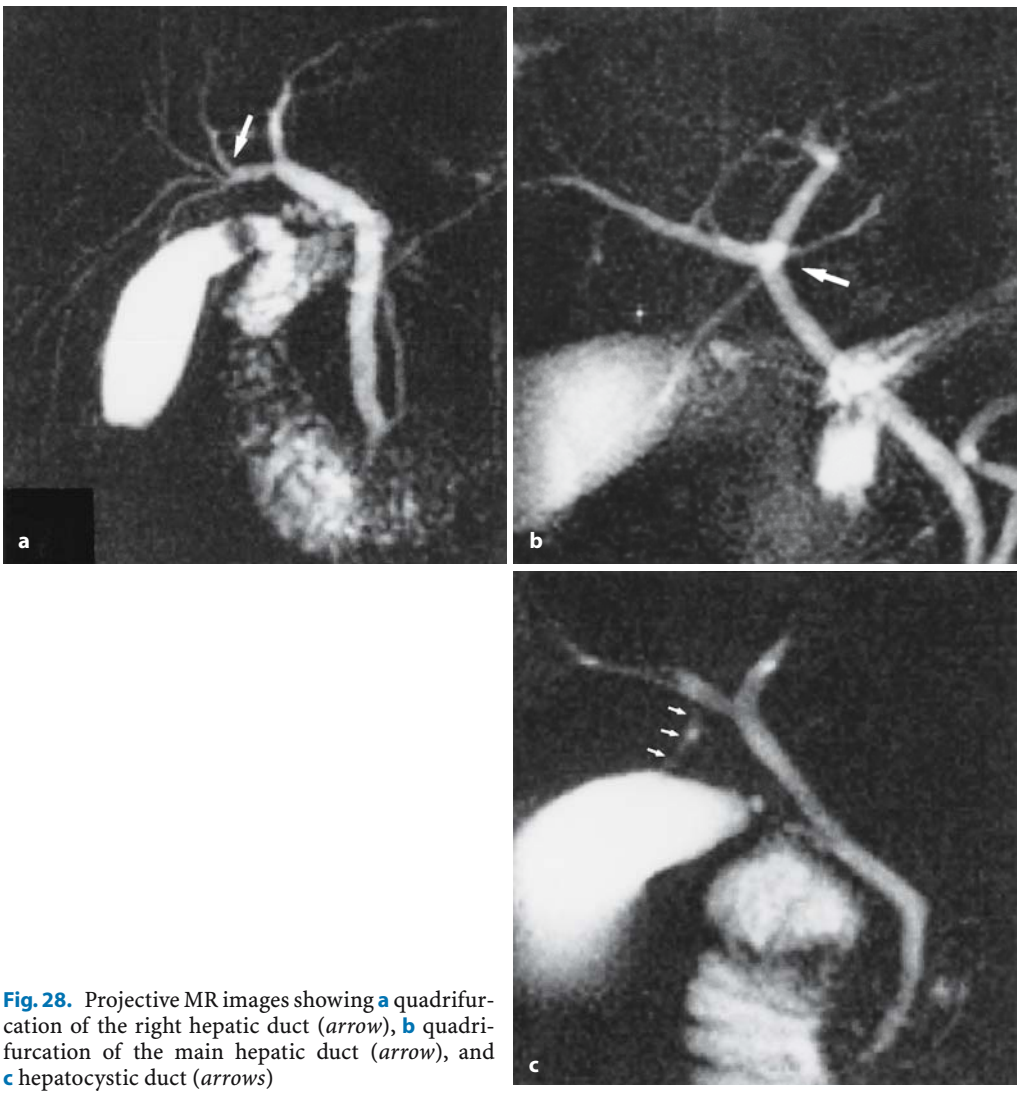

Fig. 28. Projective MR images showing **a** quadrifurcation of the right hepatic duct (*arrow*), **b** quadrifurcation of the main hepatic duct (*arrow*), and **c** hepatocystic duct (*arrows*)

#29 Postoperative Anatomy: After Hepat(ic)ojejunostomy

Related topics: #49 (after hepaticojejunostomy: anastomotic stricture), #56 (recurrent tumor after hepaticojejunostomy), #66 (postoperative anatomy: after the Whipple procedure)

KEY FACTS: TECHNIQUE

- Hepat(ic)ojejunostomy: subtype of bilioenteric anastomoses
- Indications: neoplasms located in the liver hilum or common hepatic duct, benign strictures of common hepatic duct, etc.
- Terminology (Karakousis and Douglass 1977):
  - *Hepatojejunostomy* in the strict sense of the term: anastomosis between the liver hilum and jejunum (operation performed when individual ducts can not be anastomosed to the jejunum)
  - *Hepaticojejunostomy*: duct-to-mucosa anastomosis with main hepatic duct or with left and/or right hepatic duct
  - *Intrahepatic cholangiojejunostomy*: anastomosis with more peripheral bile duct
- Common reasons for investigating the patency of bilioenteric anastomoses: fever, abnormal liver function, jaundice
- Complications: anastomotic stricture, cholangitis, biliary stones, recurrent tumor (see #49, 56)

KEY FACTS: MRI

- MR cholangiography shows the size of intrahepatic bile ducts and dimensions of anastomosis (Fig. 29; Pavone et al. 1997)
- MR criteria for a normal anastomosis:
  - The anastomosis should be visible (i.e., filled with fluid) but should not necessarily have the same diameter as the proximal bile duct
  - No significant intrahepatic bile duct dilation
- *Note:* Administration of oral contrast medium (e.g., tap water) and spasmolytic agent (see #14) required

References

Karakousis CP, Douglass HO (1977) Hilar hepatojejunostomy in resection of carcinoma of the main hepatic duct junction. Surg Gynecol Obstet 145 : 245 – 248

Bengmark S, Ekberg H, Evander A, Klofver-Stahl B, Tranberg KG (1988) Major liver resection for hilar cholangiocarcinoma. Ann Surg 207 : 120 – 125

Pavone P, Laghi A, Catalano C et al. (1997) MR cholangiography in the examination of patients with biliary-enteric anastomoses. AJR Am J Roentgenol 169 : 807 – 811

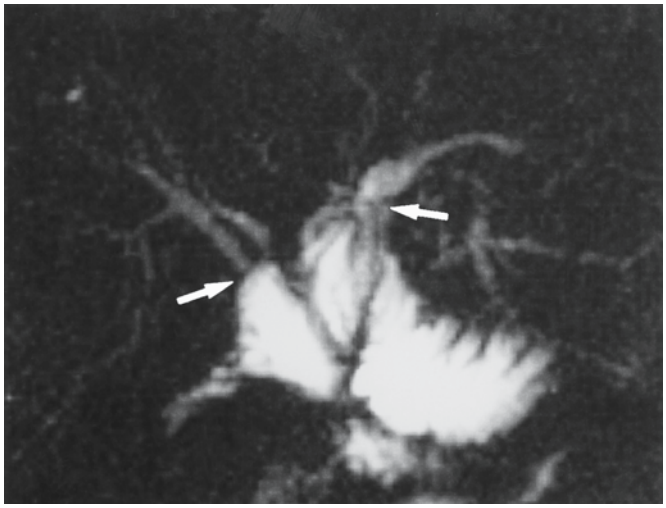

Fig. 29. Patient who underwent resection of the common hepatic duct and separate left and right hepaticojejunostomy. Both anastomoses are well seen on this projective image (*arrows*)

2.2 Benign Nontraumatic Abnormalities

#30 Developmental Abnormalities (1): Caroli's Disease

Related topics: #68 (choledochal cyst), #126 (choledochocele)

KEY FACTS: DISEASE

- Communicating cavernous ectasia of intrahepatic ducts with multiple nonobstructive saccular dilations
- Rare, autosomal recessive inheritance
- Age of presentation: children and second/third decade
- Corresponds to type V bile ducts cysts (Table 30a, b; De Wilde et al. 1991):
- Associations:
  - Developmental hepatic fibrosis (Caroli's *syndrome*)
  - Choledochal cyst
  - Polycystic kidney disease
- Symptoms: usually cramplike abdominal pain
- Complications:
  - Stone formation (34%) (typically pigmented stones)
  - Bile stasis with recurrent cholangitis
  - Abscess
  - Sepsis
  - Cholangiocarcinoma (7%)
  - Portal hypertension (in Caroli's syndrome)

KEY FACTS: MRI

- Projective and cross-sectional images:
  - Several to multiple saccular dilations of intrahepatic ducts, varying in size (Fig. 30)
  - Usually diffuse distribution
- Cross-sectional images:
  - Typical feature: portal radicles completely surrounded by dilated bile ducts (*central dot sign*; Choi et al. 1990) (Fig. 30d)
- Differential diagnosis:
  - Multiple liver cysts. This may be difficult on MRCP (unlike ERCP, MRCP cannot prove or exclude the connection between "cysts" and bile ducts with certainty). The diagnosis can be made in most cases, however, by tracing the course of the bile ducts on contiguous cross-sectional images
  - Bacterial cholangitis (see #40)
  - Oriental cholangitis (see #46)
  - Primary sclerosing cholangitis (see #41–44; dilation usually less pronounced)

References

Choi BI, Yeon KM, Kim SH, Han MC (1990) Caroli disease: central dot sign in CT. Radiology 174: 161–163

De Wilde VG, Elewaut AG, De Vos MP, Hendrix RF, Barbier FE (1991) Choledochal cysts in the adult. Endoscopy 23: 4–7

Levy AD, Rohrmann CA J., Murakata LA et al. (2002) Caroli's disease: radiologic spectrum with pathologic correlation. AJR Am J Roentgenol 179: 1053–1057

Table 30.1a. Classification of bile duct cysts

Type	(%)	Findings	Type	(%)	Findings
I	50–80	Choledochal cyst (see #68)	IV	18–43	Multiple areas of cystic dilation
II	2	Diverticula	V	4–13	Intrahepatic ducts (e.g., Caroli's disease)
III	1–6	Choledochocele (see #126)			

Table 30.1b. Graphic presentation of bile duct cysts (reprinted with permission from De Wilde et al. 1991)

Type	Description	Type	Description
I	Solitary fusiform extrahepatic	IVa	Fusiform and intrahepatic cysts
II	Extrahepatic supraduodenal diverticulum	IVb	Multiple extrahepatic cysts
III	Intraduodenal diverticulum; choledochocele	V	Multiple intrahepatic cysts; Caroli's Disease

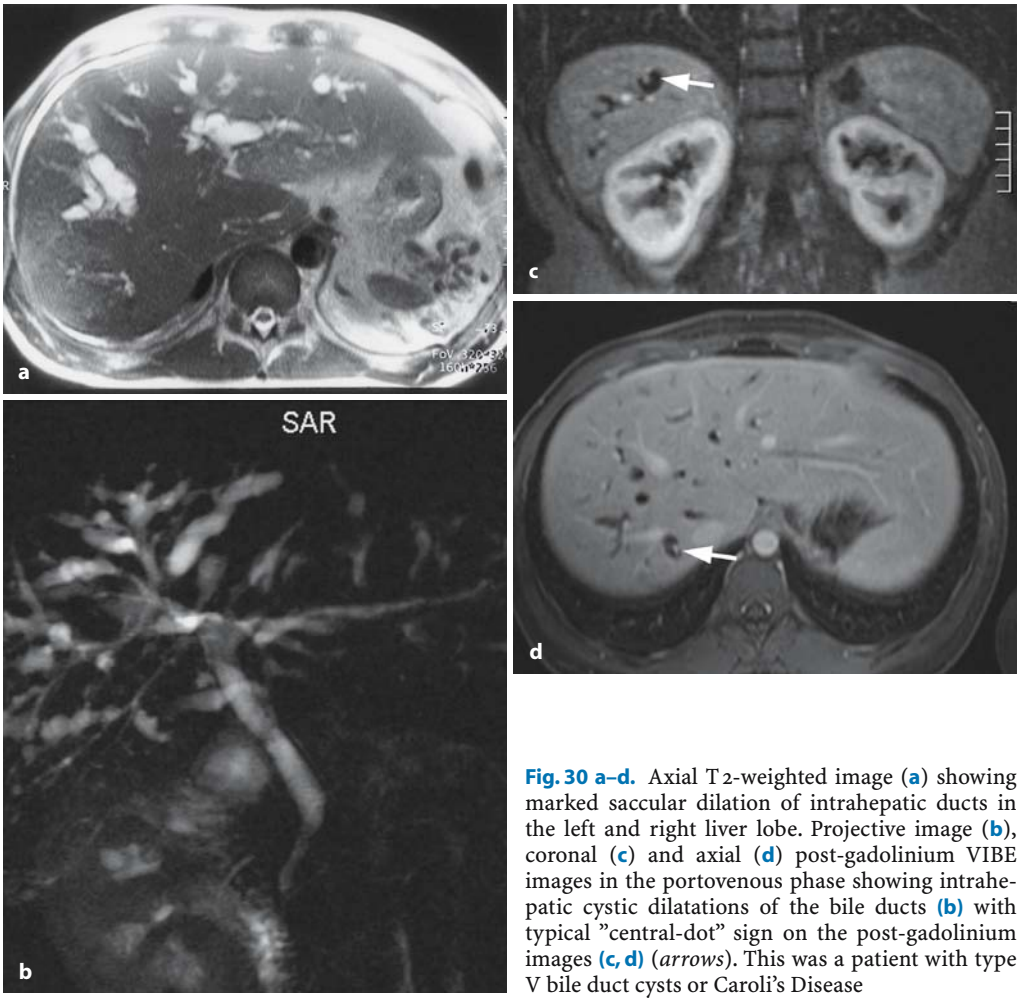

Fig. 30 a–d. Axial T2-weighted image (**a**) showing marked saccular dilation of intrahepatic ducts in the left and right liver lobe. Projective image (**b**), coronal (**c**) and axial (**d**) post-gadolinium VIBE images in the portovenous phase showing intrahepatic cystic dilatations of the bile ducts **(b)** with typical "central-dot" sign on the post-gadolinium images **(c, d)** (*arrows*). This was a patient with type V bile duct cysts or Caroli's Disease

#31 Developmental Abnormalities (2): Hepatic Cysts

Related topic: #171 (simple true cyst of the pancreas)

KEY FACTS: DISEASE

- Fluid-containing lesions lined by an epithelial layer
- Common
- Types:
  - Solitary liver cyst
  - Liver cysts in autosomal dominant polycystic kidney disease (ADPKD; most patients with ADPKD have hepatic cysts)
- Symptoms:
  - Solitary liver cyst: usually asymptomatic
  - Liver cysts in ADPKD: sometimes vague right upper quadrant pain
- Complications (rare in solitary liver cyst):
  - Infection
  - Hemorrhage
  - Bile duct obstruction

KEY FACTS: MRI

- Sharply marginated lesions with a signal intensity typical of fluid
- Easily differentiated from hemangiomas and other lesions on heavily T2-weighted images (Bosmans et al. 1997; see #2)
- Septa may be present
- No connection with biliary tree
- Differential diagnosis (other fluid-containing lesions):
  - Biloma: history, evolution, shape, relation to bile ducts
  - Abscess: thick wall; irregular contours
  - Cystic/necrotic metastases: irregular contours, peripheral soft tissue component on moderately T2-weighted MR images, rim enhancement (see #193)
  - Caroli's disease (see #30)
  - Hydatid cyst (see #47)
  - Biliary cystadenoma: thick irregular wall, papillary projections
  - Bile duct hamartomas (Fig. 31b, c)

References

Bosmans H, Gryspeerdt S, Van Hoe L et al. (1997) Preliminary experience with a new double echo half-Fourier single-shot turbo spin echo acquisition in the characterisation of liver lesions. MAGMA 5:79–84

Levine E, Cook L, Grantham JJ (1985) Liver cysts in autosomal-dominant polycystic kidney disease: clinical and computed tomographic study. AJR Am J Roentgenol 145:229–233

Mortelé KJ, Ros PR (2001) Cystic focal liver lesions in the adult: differential CT and MR imaging features. Radiographics 21:895–910

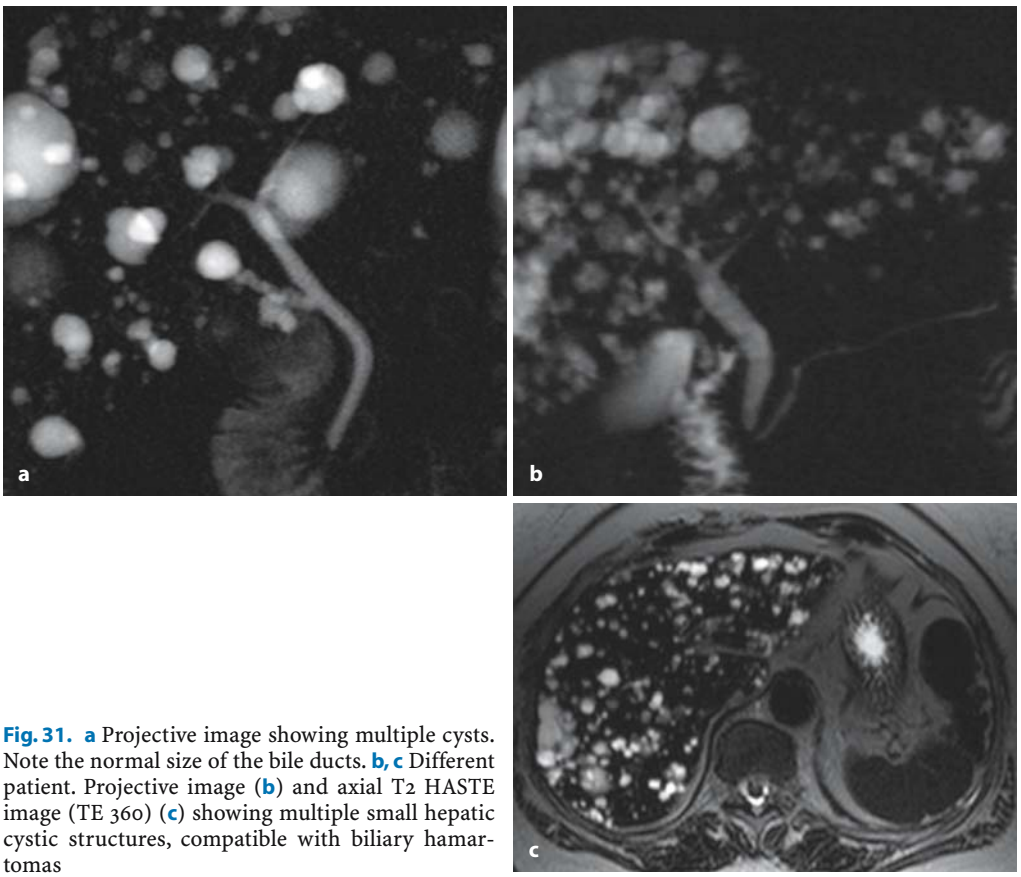

Fig. 31. **a** Projective image showing multiple cysts. Note the normal size of the bile ducts. **b, c** Different patient. Projective image (**b**) and axial T2 HASTE image (TE 360) (**c**) showing multiple small hepatic cystic structures, compatible with biliary hamartomas

#32 Morphologic Description of Biliary Abnormalities in Parenchymal Liver Disease

KEY FACTS

- Use of appropriate terminology is a prerequisite for accurate reporting. Some commonly used terms are the following (Fig. 32):
  - *Pruning:* diminished arborization (implies that peripheral branches are obstructed or obliterated)
  - *Crowding:* decreased distance between structures (usually implies focal or diffuse loss of liver volume)
  - *Encasement:* narrowing caused by circular compression by mural or extrinsic process
  - *Splaying:* spreading apart (suggests parenchymal edema or a space-occupying lesion)

References

Rohrmann C, Silverstein F, Templeton F (1997) Intrahepatic conditions of the biliary tree. In: Stewart E, Vennes J, Geenen J (eds) Atlas of endoscopic retrograde cholangiopancreatography. Mosby, St Louis, pp 236 – 271

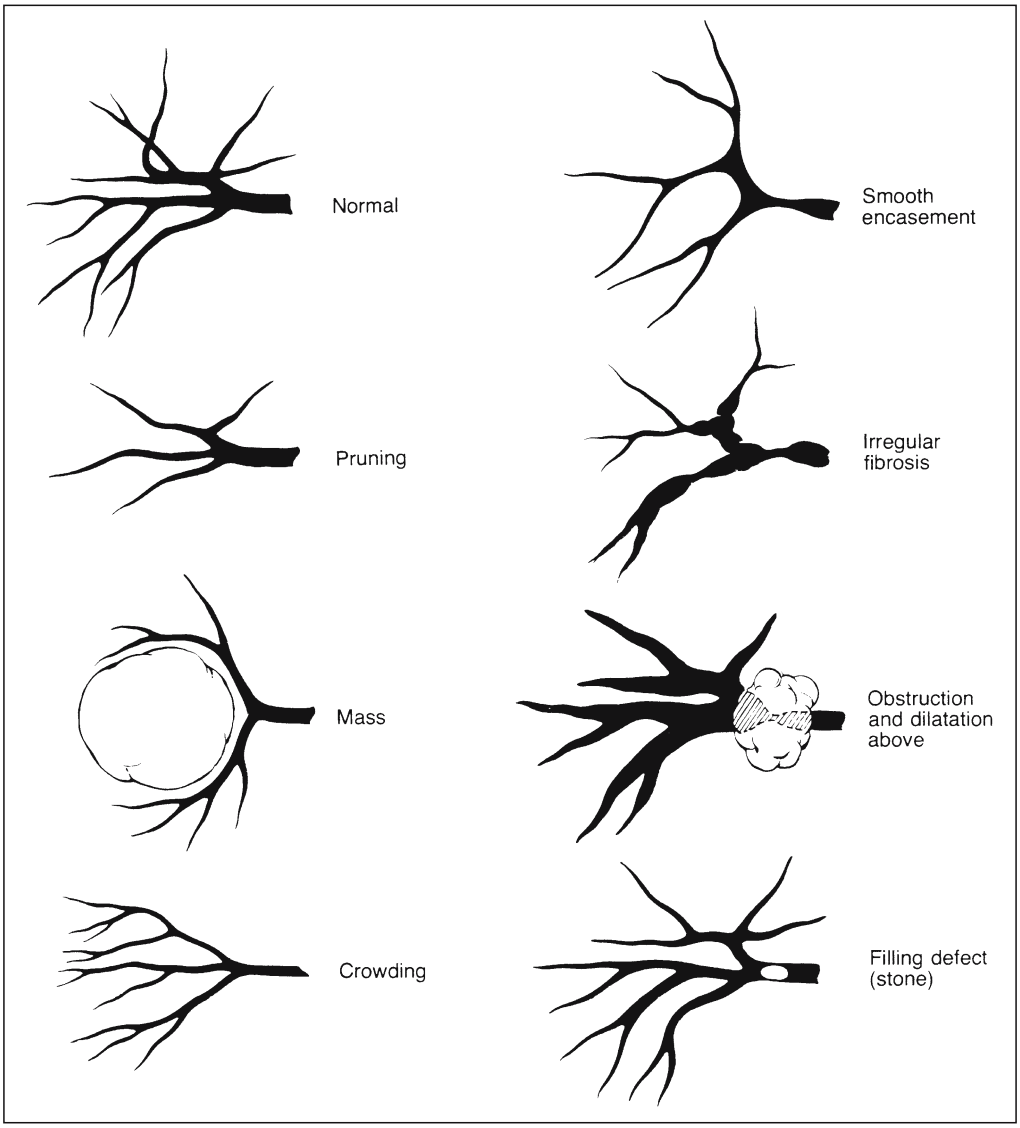

Fig. 32. Intrahepatic ducts as they might appear when affected by various pathologic processes. (Reprinted with permission from Stewart et al. 1977)

#33 Bile Duct Lithiasis

Related topic: #72–74 (stones in the common bile duct)

KEY FACTS: DISEASE

- Incidence:
  - Intrahepatic bile duct lithiasis is rare as a solitary abnormality
  - Common complication of other diseases (see below)
- Predisposing and associated disease:
  - Chronic biliary obstruction with or without cholangitis (see #40)
  - Biliary ascariasis
  - Caroli's disease (see #30)
  - Oriental cholangitis (see #46)
  - Primary sclerosing cholangitis (see #44)
- Symptoms: none or signs of cholangitis/obstruction
- Complications: cholangitis, liver abscess, fistula formation

KEY FACTS: MRI

- Stones are easily diagnosed as well-defined intraluminal structures with low signal intensity on T1- and T2-weighted images
- Differential diagnosis with aerobilia:
  - Small amounts of air in intrahepatic ducts usually not clearly seen at MRI
  - If significant aerobilia is present, a fluid–air level may be present (see #67)
  - Differentiation may be impossible unless X-ray or CT correlation is obtained

References

Kim JH, Kim MJ, Park SI et al. (2002) Using kinematic MR cholangiopancreatography to evaluate biliary dilatation. AJR Am J Roentgenol. 178: 909–914

Menu Y, Lorphelin JM, Scherrer A, Grenier P, Nahum H (1985) Sonographic and computed tomographic evaluation of intrahepatic calculi. AJR Am J Roentgenol 145: 579–583

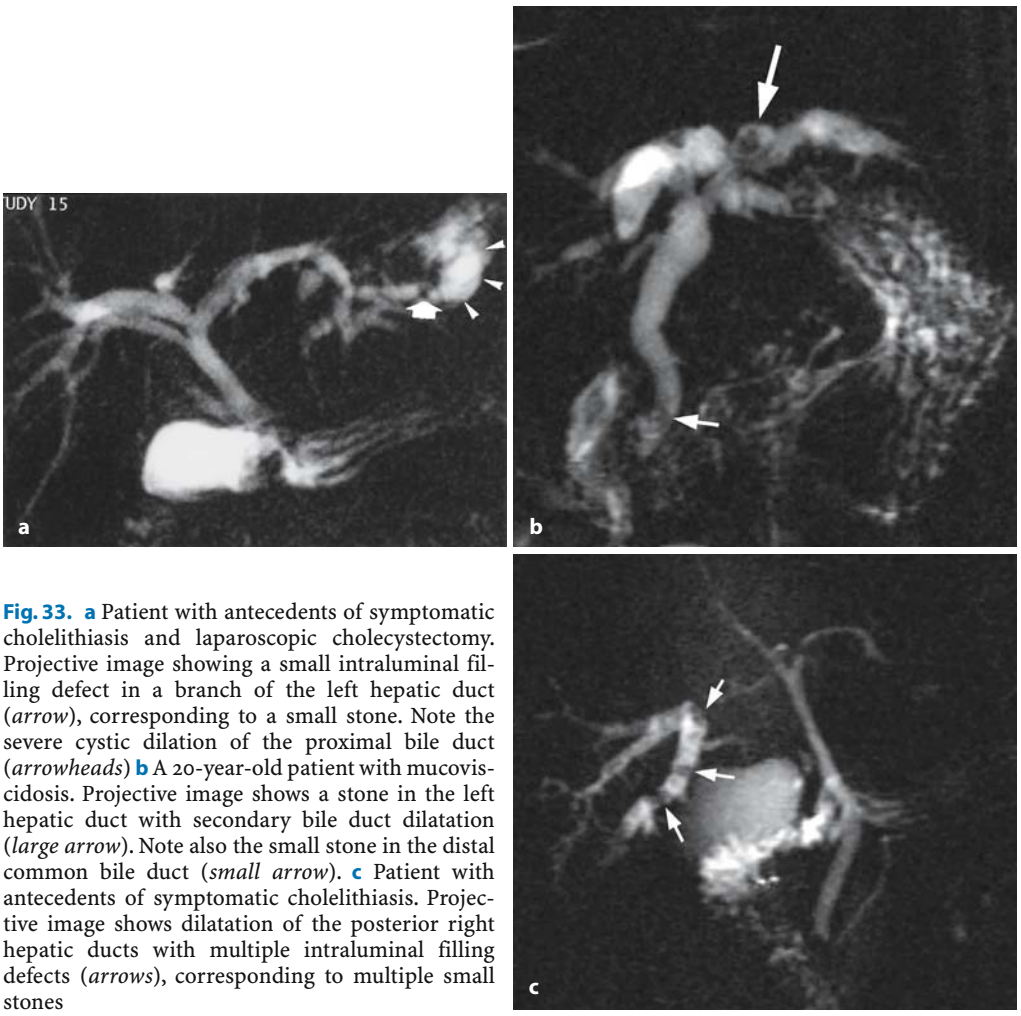

Fig. 33. **a** Patient with antecedents of symptomatic cholelithiasis and laparoscopic cholecystectomy. Projective image showing a small intraluminal filling defect in a branch of the left hepatic duct (*arrow*), corresponding to a small stone. Note the severe cystic dilation of the proximal bile duct (*arrowheads*) **b** A 20-year-old patient with mucoviscidosis. Projective image shows a stone in the left hepatic duct with secondary bile duct dilatation (*large arrow*). Note also the small stone in the distal common bile duct (*small arrow*). **c** Patient with antecedents of symptomatic cholelithiasis. Projective image shows dilatation of the posterior right hepatic ducts with multiple intraluminal filling defects (*arrows*), corresponding to multiple small stones

#34 Acute Hepatitis

KEY FACTS: DISEASE

- Acute inflammation of liver parenchyma
- Pathology: diffuse inflammation with centrilobular necrosis, portal infiltration by lymphocytes, and reactive changes in Kupffer cells
- Causes:
  - Viral (hepatitis A – E, G)
  - Bacterial
  - Fungal
  - Toxic agents and drugs
- Symptoms:
  - Fatigue, anorexia, nausea, vomiting
  - Jaundice usually appears 1 – 2 weeks after the onset of symptoms
- Complications:
  - Massive hepatic necrosis (primarily seen in hepatitis B, D, and E)
  - Chronic hepatitis (> 6 months; particularly hepatitis B – D)
  - Cirrhosis (viral hepatitis, alcoholic hepatitis; see # 36, 37)
  - Hepatocellular carcinoma (hepatitis B and C, alcoholic hepatitis; see # 58, 59)

KEY FACTS: MRI

- Cholangiographic images: edema of liver parenchyma may cause separation (splaying) and diffuse narrowing of the bile ducts (Fig. 34 a–c; Rohrmann et al. 1977)
- Cross-sectional images:
  - Hepatomegaly
  - Gallbladder wall thickening (see # 111) (Fig. 34 d)
  - Periportal cuffing (Itoh et al. 1992)
- *Note:* Ultrasonography may be more specific than MRI by showing abnormally bright portal venule walls (seen in 60 % of cases; Needleman et al. 1986)
- Differential diagnosis:
  - Infiltrative diseases (amyloidosis, sarcoidosis, infiltrating tumor)
  - Other causes of diffuse hepatocellular edema (e. g., alcohol)
  - Severe steatosis (# 35)

References

Itoh H, Sakai T, Takahashi N et al. (1992) Periportal high intensity on T 2-weighted MR images in acute viral hepatitis. J Comp Assist Tomogr 16 : 564 – 567

Needleman L, Kurtz AB, Rifkin MD, Cooper HS, Pasto ME, Goldberg BB (1986) Sonography of diffuse benign liver disease: accuracy of pattern recognition and grading. AJR Am J Roentgenol 146 : 1011 – 1015

Rohrmann CA, Ansel HJ, Ayoola EA, Silvis SE, Vennes JA (1977) Endoscopic retrograde intrahepatic cholangiogram: radiographic findings in intrahepatic disease. AJR Am J Roentgenol 128 : 45 – 52

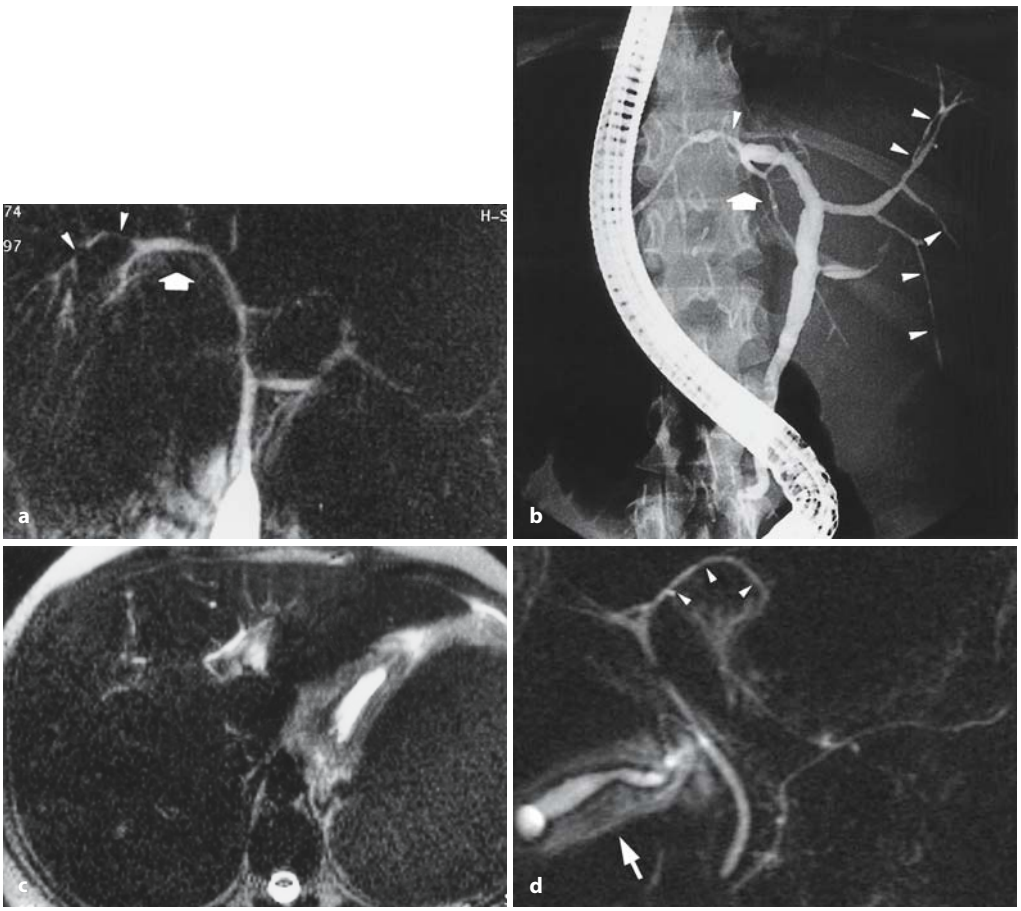

Fig. 34 a–c. **a** Projective MR image and **b** ERCP obtained in 23-year-old woman, both showing splaying and displacement of the central intrahepatic ducts (*arrows*) and narrowing of the more peripheral ducts (*arrowheads*), probably secondary to hepatocellular edema. The ducts in the right lobe are not clearly seen in **a** because they are not within the section **c**. Same patient. Heavily T2-weighted axial cross-sectional image showing marked paucity of bile ducts in the right liver lobe. Biopsy revealed acute hepatitis. **d** Projective image (different patient) in acute hepatitis due to graft-versus-host disease, showing splaying and displacement of the intrahepatic ducts (*arrowheads*) and reactive thickening of the gallbladder wall (*arrow*)

Note: In **a** and **b**, the right side of the image corresponds to the right side of the patient

#35 Fatty Metamorphosis (Steatosis)

KEY FACTS: DISEASE

- Histology: hepatocytes with large cytoplasmic fat vacuoles
- Causes:
  - Metabolic disorder (diabetes, obesity, corticosteroids)
  - Hepatotoxins (e.g., alcohol, chemotherapy)
- Types:
  - Diffuse fatty infiltration
  - Focal fatty infiltration (predominantly periportal and subcapsular)
- Association: focal fatty infiltration in the posterior edge of the quadrate lobe may be associated with aberrant gastric venous drainage (Kawamori et al. 1996)

KEY FACTS: MRI

Diffuse Fatty Infiltration (Fig. 35 a–d)

- Cross-sectional images:
  - Sometimes no abnormalities (MRI less sensitive than ultrasonography and CT)
  - Hepatomegaly
  - Hyperintensity on T1-weighted images (not always present)
  - Variable signal intensity on T2-weighted images, depending on the type of sequence used (fat is rendered bright on fast spin echo and HASTE sequences unless fat suppression is applied)
- Projective images:
  - Stretching and splaying of the intrahepatic biliary tree may eventually be seen

Focal Fatty Infiltration (Fig. 35 e–l)

- Focal lesion, usually with sharp borders
- Undisplaced course of vessels
- No bulging of liver contour
- Specific diagnosis can be made by comparing images obtained:
  - With and without fat suppression
  - "In phase" and "out of phase" (Mitchell et al. 1991)
- May be inhomogeneous (Fig. 35 k, l)

Focal Sparing (Fig. 35 m, n)

- Non-steatotic areas in otherwise steatotic liver

References

Kawamori Y, Matsui O, Takahashi S, Kadoya M, Takashima T, Miyayama S (1996) Focal hepatic fatty infiltration in the posterior edge of the medial segment associated with aberrant gastric venous drainage: CT, US, and MR findings. J Comp Assist Tomogr 20 : 356 – 359

Mitchell DG, Kim I, Chang TS et al. (1991) Fatty liver. Chemical shift phase-difference and suppression magnetic resonance imaging techniques in animals, phantoms, and humans. Invest Radiol 26 : 1041 – 1052

Van Steenbergen W, Lanckmans S (1995) Liver disturbances in obesity and diabetes mellitus. Int J Obesity 19 [Suppl 3] : 27 – 36

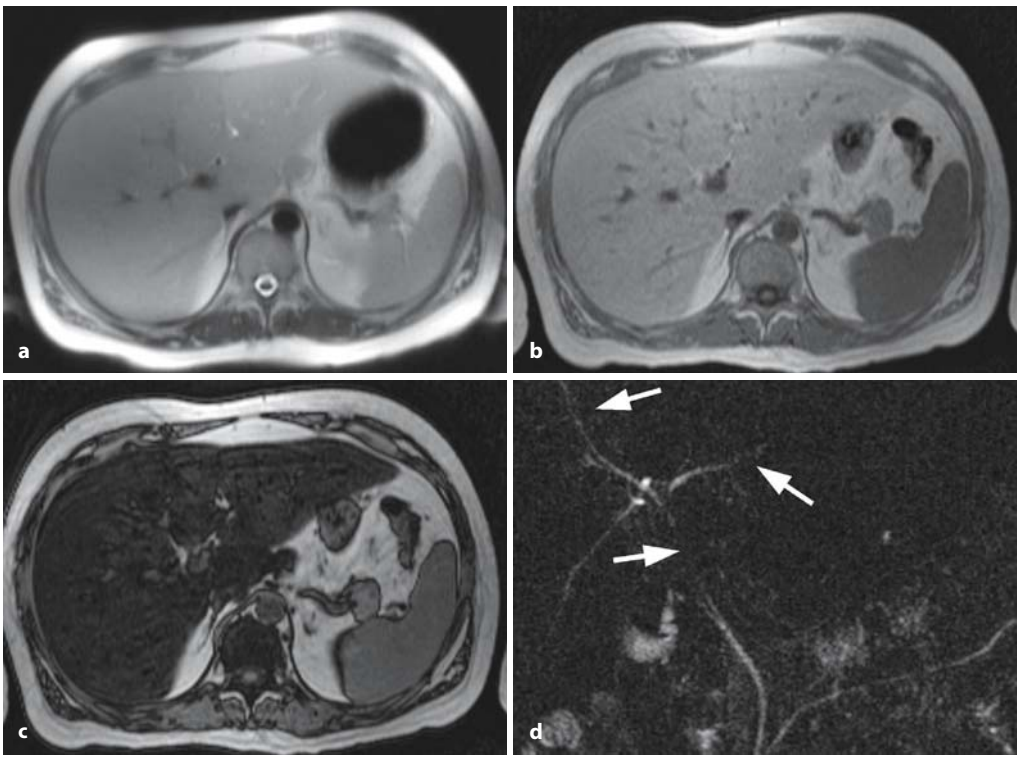

Fig. 35 a–d. Diffuse steatosis and mild hepatomegaly. **a** Axial T2-weighted HASTE image (TE, 60 msec) showing high signal intensity of the hepatic parenchyma (the liver and spleen are nearly isointense), which can be explained by the markedly increased hepatic fat content. **b, c** T1-weighted images in phase and out of phase showing a dramatic drop of the signal intensity of the liver on the "out of phase" image due to the diffuse steatosis. **d** projective image showing the narrowing and paucity of the intrahepatic bile ducts (arrows)

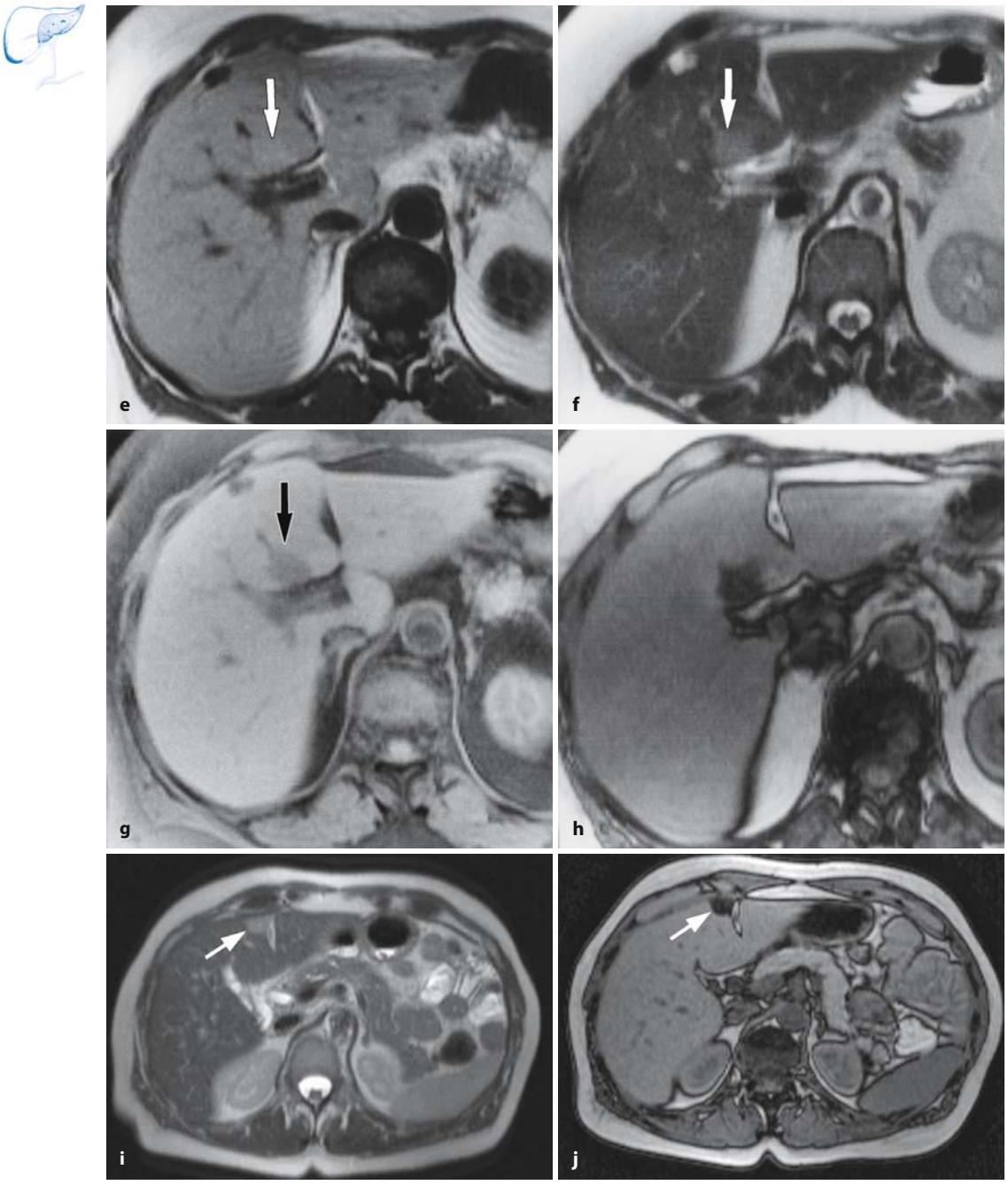

Fig. 35 e–j. **e** Axial T1- and **f** T2-weighted images showing area of discrete hyperintensity posteriorly in the quadrate lobe (*arrows*) **g** Frequency-selective fat-suppressed T1-weighted image and **h** T1-weighted image "out of phase" showing the lesion as hypointense, thus confirming the diagnosis of focal fatty infiltration. Axial T2-weighted HASTE image (TE 60) (**i**) and T1-weighted image "out of phase" (**j**) showing a small area of focal fatty infiltration adjacent to the falciform ligament (*arrow*). This area is hyperintense on the T2-weighted image and shows a loss of signal on the T1-weighted "out of phase" image.

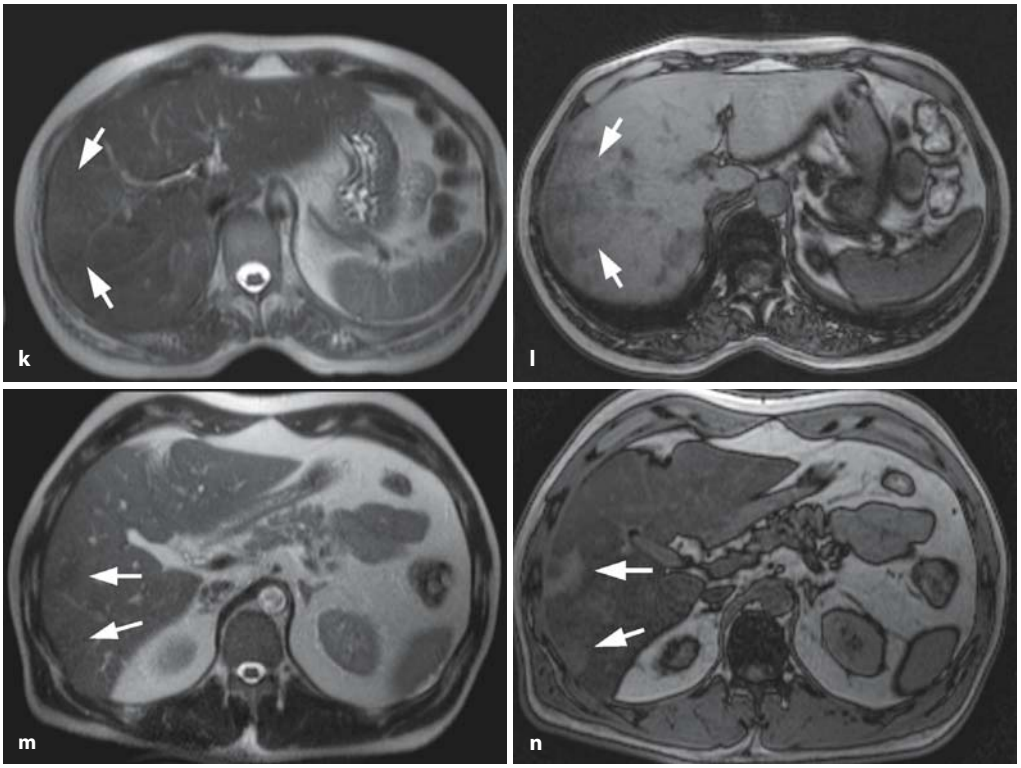

Fig. 35 k–n. Axial T2-weighted HASTE image (TE 60) (**k**) and T1-weighted image "out of phase" (**l**) showing an area of inhomogeneous steatosis in the right lobe of the liver. Note that the areas with increased fat content show a subtle increase in signal intensity on the T2-weighted HASTE image, and a marked drop in signal on the T1-weighted image out of phase (arrows). **m, n** Different patient. Axial T2-weighted HASTE image (TE 60) (**m**) and T1-weighted image "out of phase" (**n**) showing two small areas of focal sparing in de right lobe in a otherwise steatotic liver. Note that the signal intensity of the non-steatotic parenchyma is low on the T2-weighted HASTE image and high on the out-of-phase T1-weighted image (*arrows*)

#36 Cirrhosis, Ductal Changes

Related topics: #38 (primary biliary cirrhosis), #58, 59 (hepatocellular carcinoma)

KEY FACTS: DISEASE

- Chronic liver disease characterized by diffuse parenchymal destruction, fibrosis, and nodular regeneration, with abnormal reconstruction of preexisting lobular architecture
- Etiology:
  - Toxic agents: alcohol (most common cause in the West, 60 % – 70 %), drugs, iron (hemochromatosis, 5 %), copper (Wilson's disease)
  - Inflammation (viral; 10 %)
  - Biliary obstruction (e.g., cystic fibrosis, primary biliary cirrhosis)
  - Other causes (vascular, nutritional, hereditary)
- Symptoms: fatigue, weight loss, …
- Complications:
  - Ascites
  - Portal hypertension with or without esophageal varices
  - Hepatic encephalopathy
  - Development of hepatocellular carcinoma (cirrhosis is the main risk factor)

KEY FACTS: MRI

- Early changes: subtle scattered ductal narrowing, pruning
- Changes occurring in patients with more advanced disease (Fig. 36):
  - Ductal tortuosity and crowding (fibrosis, micronodular disease)
  - Focal stenoses
  - Displacement (large areas of regeneration)
- *Note:* Cholangiographic findings are usually nonspecific

References

Altman C, Fabre M, Adrien C et al. (1995) Cholangiographic features in fibrosis and cirrhosis of the liver. Radiological-pathological correlation. Dig Dis Sci 40 : 2128 – 2133

Legge DA, Carlson HC, Ludwig J (1971) Cholangiographic findings in diseases of the liver: a postmortem study. AJR Am J Roentgenol 113 : 34 – 40

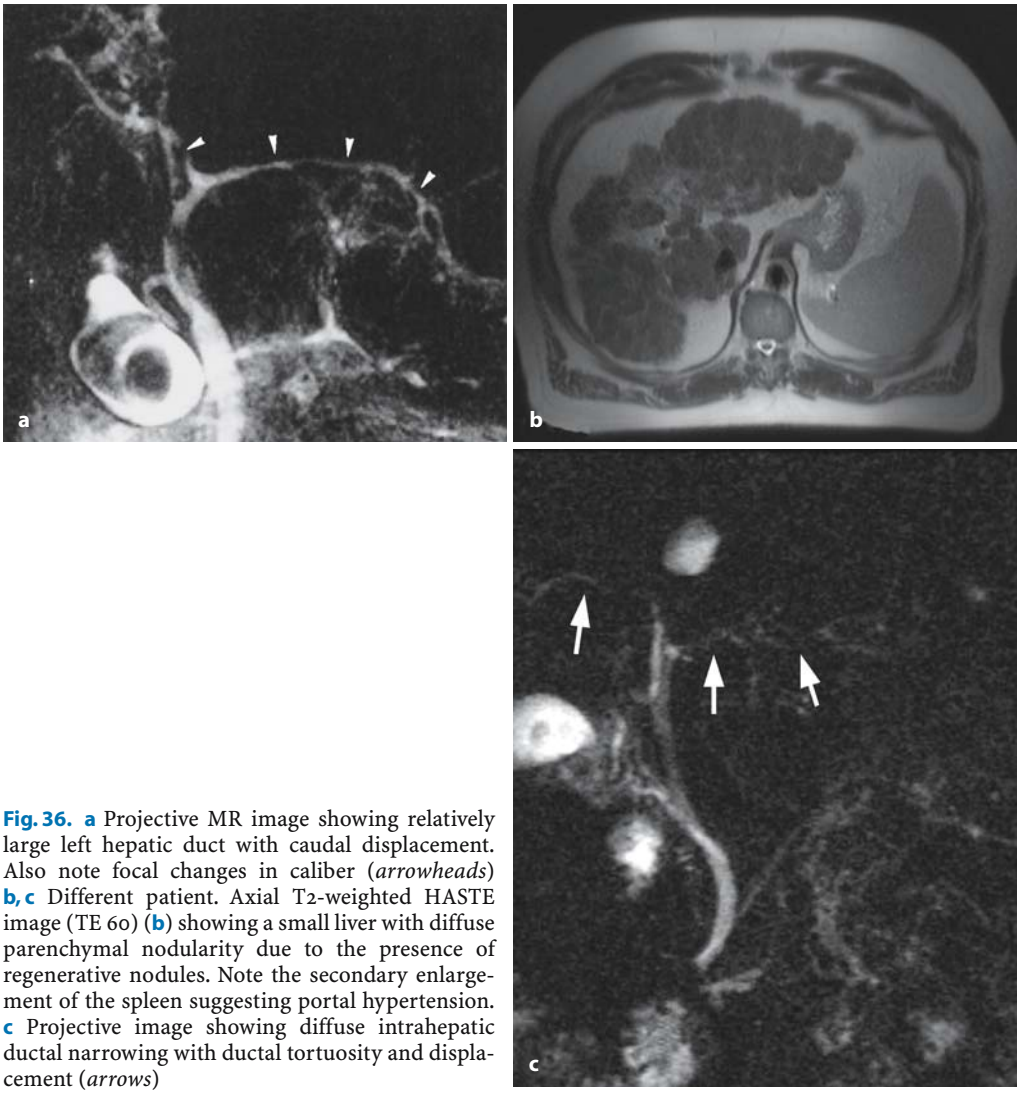

Fig. 36. **a** Projective MR image showing relatively large left hepatic duct with caudal displacement. Also note focal changes in caliber (*arrowheads*) **b, c** Different patient. Axial T2-weighted HASTE image (TE 60) (**b**) showing a small liver with diffuse parenchymal nodularity due to the presence of regenerative nodules. Note the secondary enlargement of the spleen suggesting portal hypertension. **c** Projective image showing diffuse intrahepatic ductal narrowing with ductal tortuosity and displacement (*arrows*)

#37 Cirrhosis, Parenchymal Changes

Related topics: #38 (primary biliary cirrhosis), #58, 59 (hepatocellular carcinoma)

KEY FACTS: TYPICAL MR FEATURES

- Volume loss (Fig. 37)
  - Segmental, usually quadrate lobe and/or right lobe
  - Global (less common)
- Caudate lobe hypertrophy (ratio caudate lobe to right lobe greater than 0.65 on transverse images; most sensitive in patients with post-hepatitis B cirrhosis)
- Periportal cuffing (see #48):
  - Presence of fluid, probably lymphedema, around the portal vein tributaries
  - Differential diagnosis with biliary dilation: typical location on both sides of venous branches
- Other common findings on cross-sectional images:
  - Prominence of fissures and porta hepatis
  - Surface nodularity
  - Signs of portal hypertension (venous collaterals)
  - Ascites
  - Enlarged hilar lymph nodes
  - Thickening of the gallbladder wall (see #111)
- Differential diagnosis: Budd-Chiari syndrome (obstruction of hepatic vein outflow), which also causes enlargement of the caudate lobe

References

Harbin WP, Robert NJ, Ferruci JT (1980) Diagnosis of cirrhosis based on regional changes in hepatic morphology: a radiological and pathological analysis. Radiology 135 : 273 – 283

Lafortune M, Matricardi M, Denys A, Favret M, Déry R, Pomier-Layrargues G (1998) Segment 4 (the quadrate lobe): a barometer of cirrhotic liver disease at US. Radiology 206 : 157 – 160

Wang TF, Hwang SJ, Lee EY et al. (1997) Gallbladder wall thickening in patients with liver cirrhosis. J Gastroenterol Hepatol 12 : 445 – 449

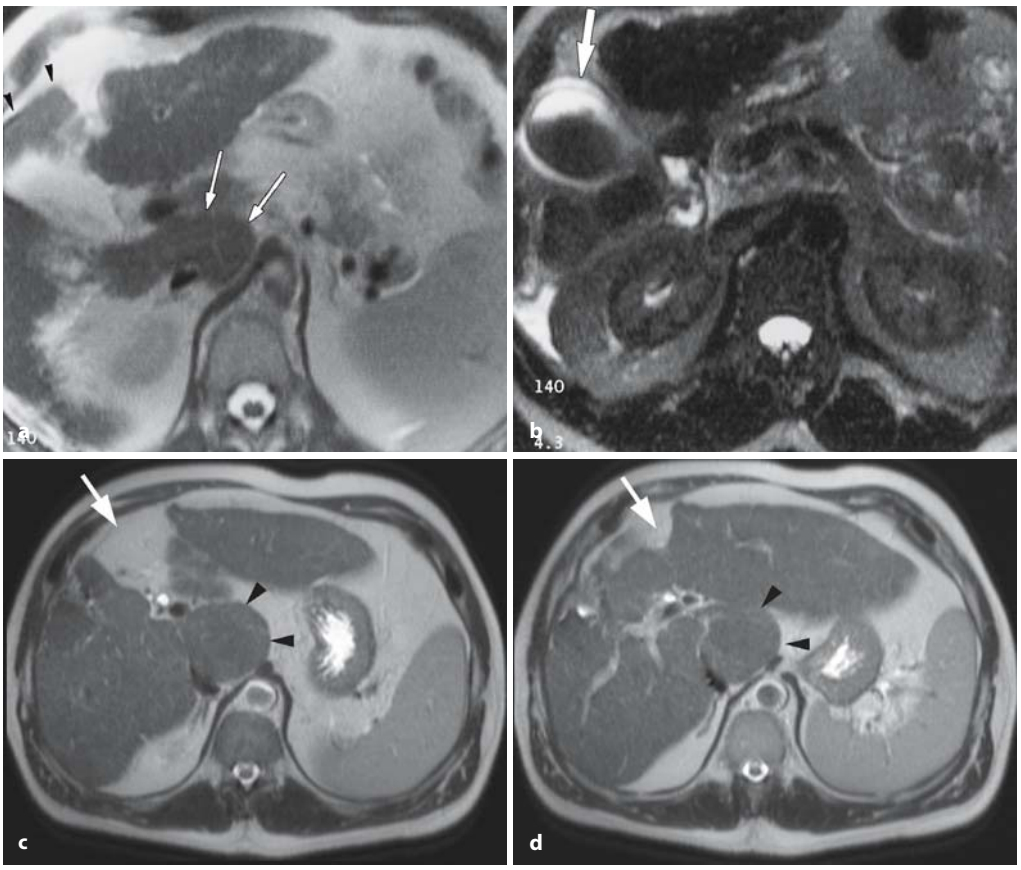

Fig. 37 a, b. **a** Moderately and **b** heavily T2-weighted images showing irregular contours of hepatic parenchyma, relative atrophy of the quadrate lobe (*arrowheads* in **a**), hypertrophy of the caudate lobe (*arrows* in **a**), reactive thickening of the gallbladder wall (*arrow* in **b**), and ascites **c, d** Different patient. Axial T2-weighted HASTE images (TE 60) showing marked volume loss of segment IV (*arrow*) together with hypertrophy of the caudate lobe (*arrowheads*) and (to a lesser degree) segment II and III

#38 Primary Biliary Cirrhosis

Related topics: #36, 37 (cirrhosis)

KEY FACTS: DISEASE

- Progressive destructive cholangitis of interlobar and septal bile ducts with inflammatory cellular infiltrate, portal fibrosis, nodular regeneration, and shrinkage of hepatic parenchyma
- Presenting age: 35 – 55 years
- Ratio of women to men: 9 : 1
- Etiology: immune response disorder
- Associated diseases: rheumatoid arthritis, Sjögren's syndrome, Hashimoto's thyroiditis, dermatomyositis, systemic lupus erythematosus
- Clinical signs: fatigue, pruritus, keratoconjunctivitis sicca, hyperpigmentation
- Tests for antimitochondrial antibodies usually positive (> 90 %)
- Differential diagnosis with primary sclerosing cholangitis (see #41): sex distribution, associated diseases, cholangiographic findings (see below)
- Complications: hepatocellular carcinoma, liver insufficiency

KEY FACTS: MRI

- Early stage: no abnormalities
- Advanced disease (Fig. 38):
  - "Tree in winter" appearance: diffuse narrowing or even disappearance (vanishing) of small ducts
  - Signs of cirrhosis (tortuosity, narrowing, caliber variation, segmental changes)
- Differential diagnosis with primary sclerosing cholangitis
  - Bile duct deformities less common
  - Disease initially more limited to small ducts
  - No extrahepatic disease
  - No diverticular outpouchings

References

Blachar A, Federle MP, Brancatelli G (2001) Primary biliary cirrhosis: clinical, pathologic, and helical CT findings in 53 patients. Radiology 220 : 329

Wiesner RH, LaRusso NF, Ludwig J, Dickson ER (1985) Comparison of the clinicopathologic features of primary sclerosing cholangitis and primary biliary cirrhosis. Gastroenterology 88 : 108 – 114

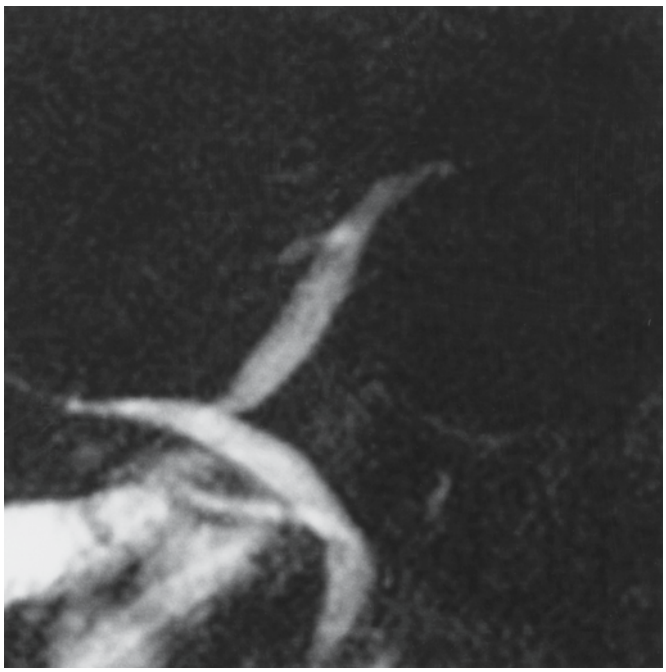

Fig. 38. Projective MR image showing marked discrepancy between the (normal) extrahepatic duct and main right and left hepatic ducts on one hand and the (nearly invisible) more distal branches on the other hand ("pruning")

#39 Vanishing Bile Duct Disease: Differential Diagnosis

KEY FACTS: CAUSES/ASSOCIATED DISEASES (SHERLOCK 1987; DESMET 1992)

- Immunologically based liver diseases:
  - Primary biliary cirrhosis (see #38)
  - Graft-versus-host disease
  - Chronic liver transplant rejection
  - AIDS cholangiopathy
- Sarcoidosis, amyloidosis
- Primary sclerosing cholangitis (see #41–44)
- Bacterial cholangitis (see #40)
- Hepatic artery occlusion with ischemia
- Chemical cholangitis (intra-arterial chemotherapy)
- Developmental disorders (intrahepatic atresia, cystic fibrosis)
- Acute hepatitis (see #34)
- Severe steatosis (see #35)

KEY FACTS: MRI

- Regional or diffuse invisibility of intrahepatic bile ducts (Fig. 39)

References

Desmet VJ (1992) Vanishing bile duct disorders. Prog Liver Dis 10: 89–121

Sherlock S (1987) The syndrome of disappearing intrahepatic bile ducts. Lancet 29: 493–496

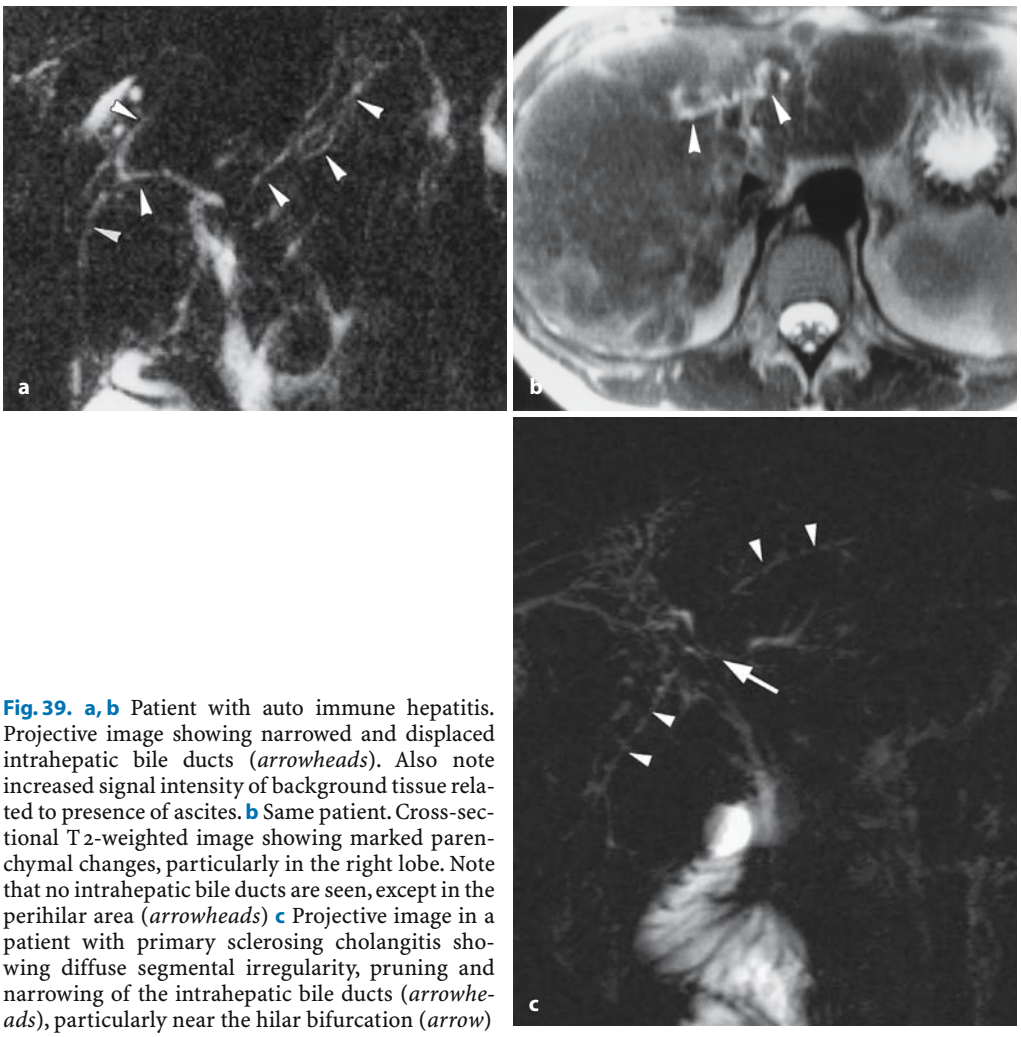

Fig. 39. a, b Patient with auto immune hepatitis. Projective image showing narrowed and displaced intrahepatic bile ducts (*arrowheads*). Also note increased signal intensity of background tissue related to presence of ascites. **b** Same patient. Cross-sectional T 2-weighted image showing marked parenchymal changes, particularly in the right lobe. Note that no intrahepatic bile ducts are seen, except in the perihilar area (*arrowheads*) **c** Projective image in a patient with primary sclerosing cholangitis showing diffuse segmental irregularity, pruning and narrowing of the intrahepatic bile ducts (*arrowheads*), particularly near the hilar bifurcation (*arrow*)

#40 Bacterial Cholangitis

Related topic: #75 (extrahepatic bile duct, bacterial cholangitis)

KEY FACTS: DISEASE

- Bacterial infection of biliary tree
- Synonyms: ascending cholangitis, pyogenic cholangitis, acute cholangitis, obstructive cholangitis
- Organisms: *Escherichia coli* > *Klebsiella* > *Pseudomonas*
- Underlying cause: nearly always obstructive lesion of biliary tree
  - Malignant
    (e.g., ampullary carcinoma)
  - Benign
    (e.g., stricture of surgical anastomosis, calculi)
- Symptoms: fever, chills, jaundice
- Complications:
  hepatic abscess, septicemia, shock
- Prognosis:
  100 % mortality without treatment

KEY FACTS: MRI

- Early changes: dilation (may be the only finding)
- Advanced disease:
  - Mucosal irregularities
  - Intraluminal filling defects (stones, sludge, inflammatory debris)
  - Intrahepatic abscess, typically communicating with the bile ducts (Fig. 40)
- Differential diagnosis: oriental cholangitis (see #46)
- *Note:* The primary task of MRCP is not to detect signs of cholangitis, but to detect the underlying obstructive lesion

References

Bader TR, Braga L, Beavers KL, Semelka RC (2001) MR imaging findings of infectious cholangitis. Magn Reson Imaging 19 : 781 – 788

Mathieu D, Vasile N, Fagniez PL, Segui S, Grably D, Larde D (1985) Dynamic CT features of hepatic abscesses. Radiology 154 : 749 – 752

Mendez RJ, Schiebler ML, Outwater EK, Kressel HV (1994) Hepatic abscesses: MR imaging findings. Radiology 190 : 431 – 436

Taylor AJ, Bohorfoush AG (1997) Inflammation of the biliary tract. In: Taylor AJ, Bohorfoush AG (eds) Interpretation of ERCP. Lippincott-Raven, Philadelphia, pp 77 – 125

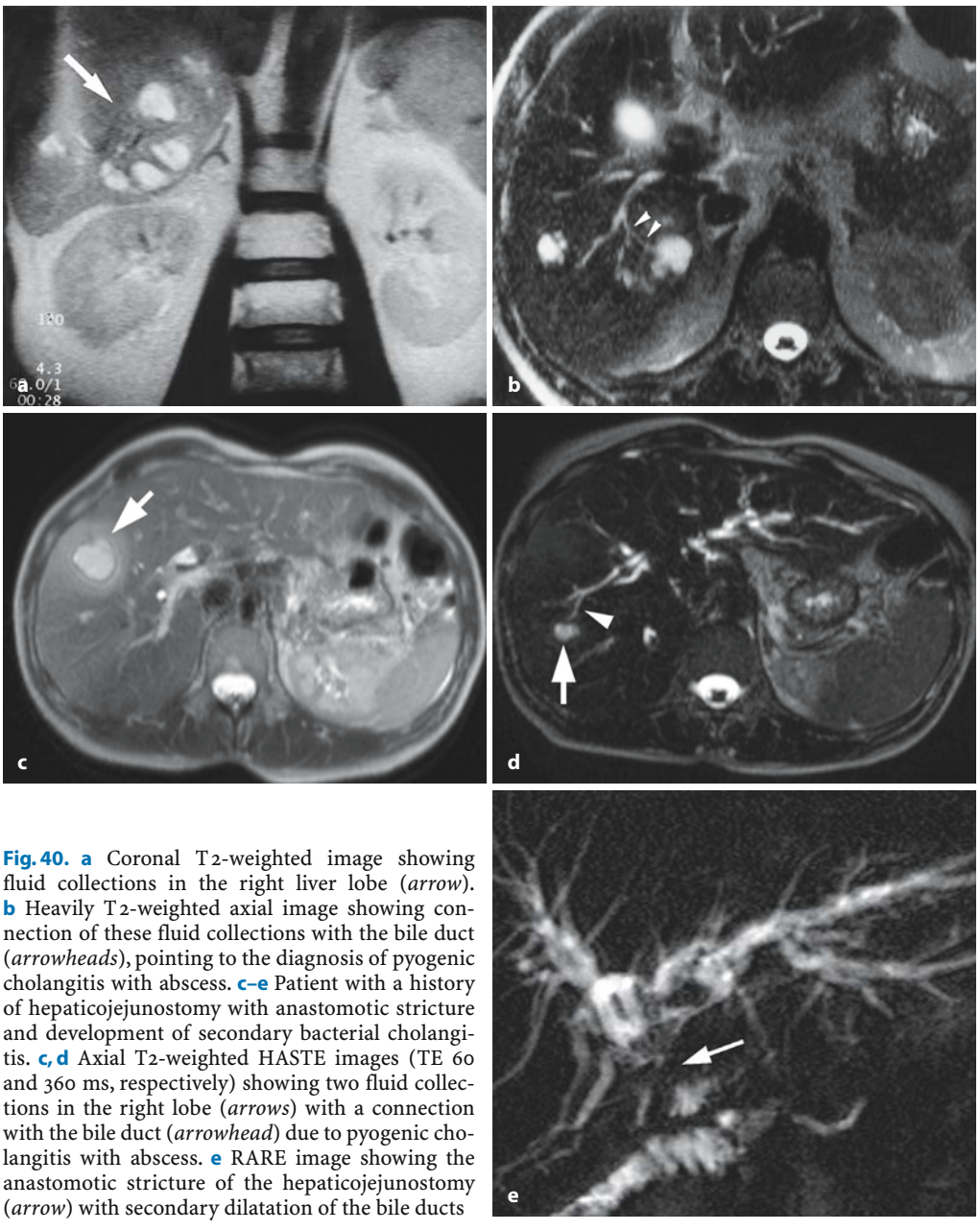

Fig. 40. a Coronal T2-weighted image showing fluid collections in the right liver lobe (*arrow*). **b** Heavily T2-weighted axial image showing connection of these fluid collections with the bile duct (*arrowheads*), pointing to the diagnosis of pyogenic cholangitis with abscess. **c–e** Patient with a history of hepaticojejunostomy with anastomotic stricture and development of secondary bacterial cholangitis. **c, d** Axial T2-weighted HASTE images (TE 60 and 360 ms, respectively) showing two fluid collections in the right lobe (*arrows*) with a connection with the bile duct (*arrowhead*) due to pyogenic cholangitis with abscess. **e** RARE image showing the anastomotic stricture of the hepaticojejunostomy (*arrow*) with secondary dilatation of the bile ducts

#41 Primary Sclerosing Cholangitis, General

Related topic: #76 (extrahepatic duct, primary sclerosing cholangitis)

KEY FACTS: DISEASE (CHAPMAN 1991)

- Chronic obliterative fibrotic inflammation of bile ducts
- Histology: destructive cholangitis with fibrous thickening of duct walls and with relatively few inflammatory cells
- 70 % of patients younger than 45 years of age at the time of diagnosis
- Ratio of women to men: 1 : 2
- Etiology: autoimmune
- Localization:
  - Both intra- and extrahepatic ducts: 72 % – 96 %
  - Intrahepatic ducts only: 1 % – 25 %
  - Extrahepatic ducts only: 3 %
- Cholangiographic classification: see #42, 43
- Associations:
  - Inflammatory bowel disease (up to 70 % of patients have ulcerative colitis)
  - Retroperitoneal fibrosis, Peyronie disease, Riedel thyroiditis, retro-orbital pseudotumor
  - Chronic pancreatitis (14 %; see also #169)
- Symptoms: usually chronic intermittent obstructive jaundice, fatigue, cholangitis, pruritus
- Diagnosis: primarily based on cholangiographic imaging findings
- Complications: see #44
- Prognosis: variable (some patients remain asymptomatic)
- *Note:* The term "primary" is used even when there is associated disease

References

Brandt DJ, MacCarty RL, Charboneau JW, LaRusso NF, Wiesner RH, Ludwig J (1988) Gallbladder disease in patients with primary sclerosing cholangitis. AJR Am J Roentgenol 150 : 571 – 574

Fulcher AS, Turner MA, Franklin KJ et al. (2000) Primary sclerosing cholangitis: evaluation with MR cholangiography – a case-control study. Radiology 215 : 71 – 80

Chapman RW (1991) Aetiology and natural history of primary sclerosing cholangitis – a decade of progress? Gut 32 : 1433 – 1435

MacCarty RL, LaRusso NF, Wiesner RH, Ludwig J (1983) Primary sclerosing cholangitis: findings on cholangiography and pancreatography. Radiology 149 : 39 – 44

#42 Primary Sclerosing Cholangitis, Early Disease (Type I)

Related topic: #76 (extrahepatic duct, primary sclerosing cholangitis)

KEY FACTS: MRI

- Cholangiographic description (Fig. 42, see also Fig. 43a; Majoie et al. 1991):
  - Segmental irregularity and narrowing, especially at duct bifurcations
  - No or only minor dilation
  - Pruning
- Cross-sectional images:
  - Lack of confluence of dilated intrahepatic ducts toward the hilum (presence of stenoses)
  - Direct demonstration of beaded appearance and/or pruning
  - T2-weighted images: sometimes presence of peribiliary "cuff" with low signal intensity (see, e.g., #8)
- Differential diagnosis: mainly primary biliary cirrhosis and other types of cirrhosis, diffuse sclerosing cholangiocarcinoma, lymphoma, polycystic liver disease, amyloidosis, liver necrosis (indicative finding: extrahepatic abnormalities)
- *Note:* Li-Yeng and Goldberg (1984) originally proposed four types of intrahepatic involvement. According to Majoie et al. (1991), a classification into three types is sufficient, since the original types I and II have the same clinical implications

References

Fulcher AS, Turner MA, Franklin KJ et al. (2000) Primary sclerosing cholangitis: evaluation with MR cholangiography – a case-control study. Radiology 215 : 71 – 80

Majoie CBLM, Reeders JWAJ, Sanders JB, Huibregtse K, Jansen PLM (1991) Primary sclerosing cholangitis: a modified classification of cholangiographic findings. AJR Am J Roentgenol 157 : 495 – 497

Li-Yeng C, Goldberg HI (1984) Sclerosing cholangitis: broad spectrum of radiographic findings. Gastrointest Radiol 9 : 39 – 47

Terada T, Nakanuma Y (1995) Intrahepatic cholangiographic appearance simulating primary sclerosing cholangitis in several hepatobiliary diseases: a postmortem cholangiographic and histopathological study in 154 livers at autopsy. Hepatology 22 : 75 – 81

Vitellas KM, Keogan MT, Freed KS et al. (2000) Radiologic manifestations of sclerosing cholangitis with emphasis on MR cholangiopancreatography. Radiographics 20 : 959 – 975

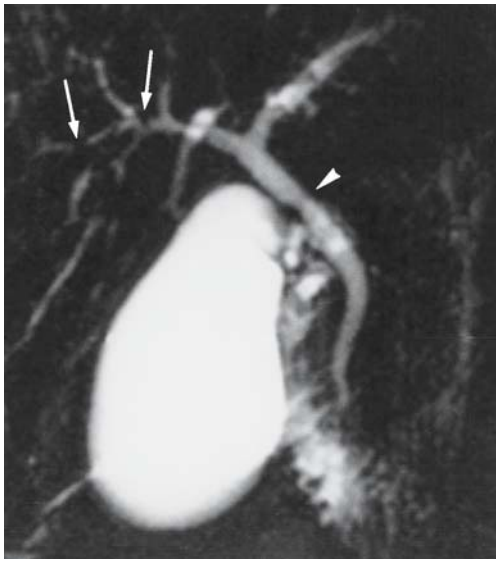

Fig. 42. Projective MR image showing stenoses of intrahepatic ducts (*arrows*) associated with low-grade stenosis of the common hepatic duct (*arrowhead*)

#43 Primary Sclerosing Cholangitis, Advanced Disease (Types II and III)

Related topic: #76 (extrahepatic duct: primary sclerosing cholangitis)

KEY FACTS: MRI

- Cholangiographic classification (Fig. 43a; Li-Yeng and Goldberg 1984; Majoie et al. 1991):
  - Type II (marked segmental narrowing and dilation, pruning, beading; sacculations resembling diverticula) (Fig. 43b)
  - Type III (peripheral duct obliteration; only narrowed central ducts remain)
- Type II abnormalities: more or less diagnostic
- Differential diagnosis for type III: Klatskin tumor, metastases, diffuse infiltrating hepatic tumors
- Most patients with PSC have associated imaging findings of cirrhosis
- *Note:* The key cholangiographic finding is a relative lack of dilation proximal to a stricture (related to diffuse periductal inflammation)

References

Bader TR, Beavers KL, Semelka RC (2003) MR imaging features of primary sclerosing cholangitis: patterns of cirrhosis in relationship to clinical severity of disease. Radiology 226 : 675 – 685

Fulcher AS, Turner MA, Yelon JA et al. (2000) Magnetic resonance cholangiopancreatography (MRCP) in the assessment of pancreatic duct trauma and its sequelae: preliminary findings. J Trauma 48 : 1001 – 1007

Li-Yeng C, Goldberg HI (1984) Sclerosing cholangitis: broad spectrum of radiographic findings. Gastrointest Radiol 9 : 39 – 47

Majoie CBLM, Reeders JWAJ, Sanders JB, Huibregtse K, Jansen PLM (1991) Primary sclerosing cholangitis: a modified classification of cholangiographic findings. AJR Am J Roentgenol 157 : 495 – 497

Vitellas KM, Keogan MT, Spritzer CE et al. (2000) MR cholangiopancreatography of bile and pancreatic duct abnormalities with emphasis on the single-shot fast spin-echo technique. Radiographics 20 : 939 – 957

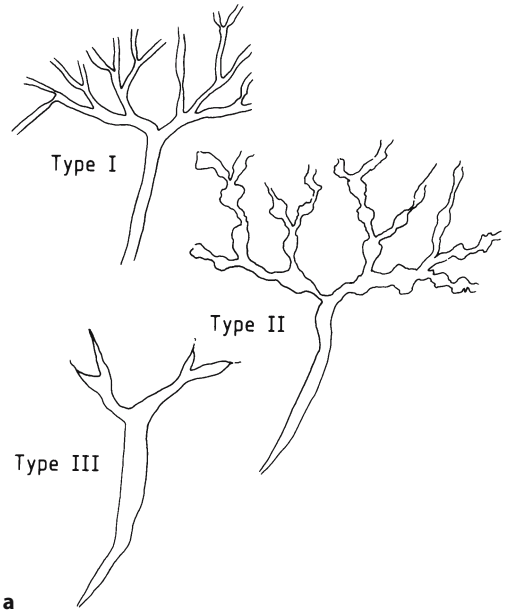

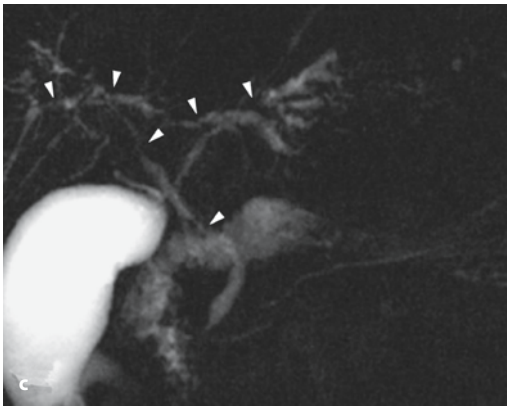

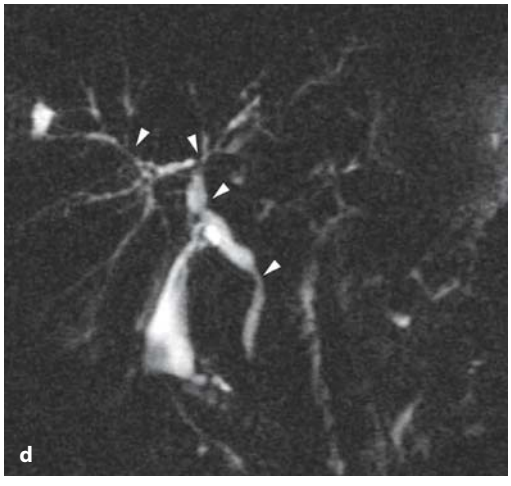

Fig. 43. **a** Type I–III cholangiographic abnormalities. **b** Projective MR image showing saccular additions (*arrowheads*) and several stenoses (*arrows*). **c** Different patient. Projective image showing multiple intra- and extrahepatic bile duct stenoses (*arrowheads*) with segmental irregularity and narrowing in this patient with type II PSC. **d** Projective image (different patient) showing multiple intra- and extrahepatic bile duct stenoses (*arrowheads*) in PSC type II

#44 Atypical and Complicated Primary Sclerosing Cholangitis

Related topic: #76 (extrahepatic duct, primary sclerosing cholangitis)

KEY FACTS: DISEASE

- Complications:
  - Biliary cirrhosis
  - Stone disease (8%; Fig. 44c)
  - Bacterial cholangitis
  - Cholangiocarcinoma (10%)

KEY FACTS: MRI

- Atypical presentation:
  - Bile lakes (differential diagnosis with biloma, abscess)
  - Segmental disease (differential diagnosis with cholangiocarcinoma may be difficult)
- Cirrhosis: see #36, 37
- Intrahepatic lithiasis: see #33
- Features that should arouse suspicion of cholangiocarcinoma:
  - Visualization of a polypoid mass larger than 1 cm
  - Rapid progression of stricture disease
  - Marked upstream dilation
- *Note:* In advanced primary sclerosing cholangitis with severe anatomical distortion, detection of stones requires particular attention (differential diagnosis stone versus stricture may be difficult)

References

Dodd GD, Niedzwiecki GA, Campbell WL, Baron RL (1997) Bile duct calculi in patients with primary sclerosing cholangitis. Radiology 203 : 443 – 447

MacCarty RL, la Russo NF, May GR et al. (1985) Cholangiocarcinoma complicating primary sclerosing cholangitis: cholangiographic appearances. Radiology 156 : 43 – 46

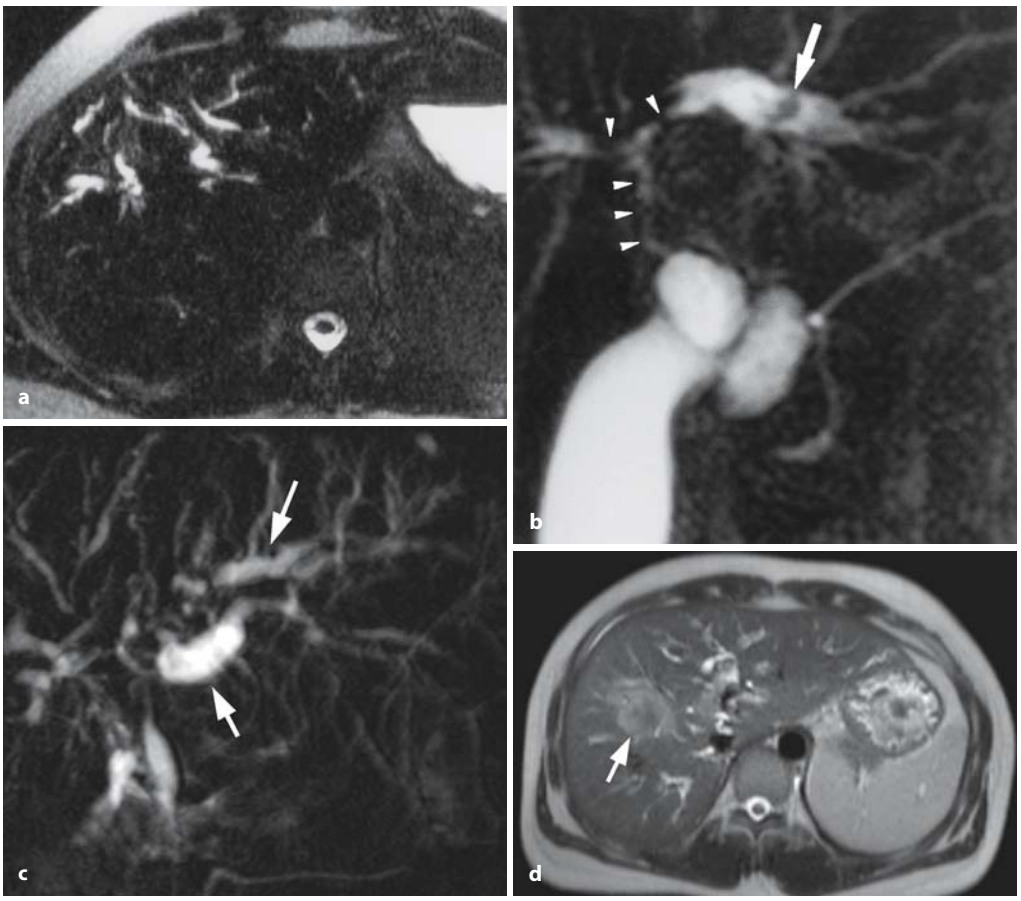

Fig. 44 a–d. **a** Segmental dilation of intrahepatic bile ducts in primary sclerosing cholangitis. **b** Projective MR image showing narrowing of the extrahepatic duct and bifurcation (*arrowheads*) and saccular dilation of the left hepatic duct, with presence of an intraductal stone (*arrow*). **c, d** Projective image (different patient) showing multiple bile duct stenoses due to known PSC. Note the marked dilatation of several intrahepatic ducts (*arrows*). This atypical finding should suggests the possibility of cholangiocarcinoma. **d** T2-weighted HASTE image (TE 60) confirmed the presence of a mass lesion. Final diagnosis was cholangiocarcinoma

#45 Secondary Sclerosing Cholangitis

Related topic: #40 (bacterial cholangitis)

KEY FACTS: DISEASE

- Chronic biliary inflammation and fibrosis attributable to local predisposing conditions
- Can be considered as the chronic form of pyogenic (obstructive) cholangitis (see #40)
- Causes: similar to acute cholangitis (e.g., stone disease, postoperative or posttraumatic stricture, papillary stenosis, chronic pancreatitis with bile duct narrowing; Fig. 45)
- Complications:
  - Severe duct stricture
  - Biliary cirrhosis

KEY FACTS: MRI

- Features of acute cholangitis (see #40)
- Specific findings:
  - Duct narrowing, diminished arborization, pruning (fibrosis)
  - Intraluminal concretions common

References

Amor A, Chapoutot C, Michel J, Pageaux GP, Larrey D, Michel H (1995) Les cholangites sclerosantes secondaires. Presse Med 24 : 948 – 952

Park MS, Yu JS, Kim KW, et al. (2001) Recurrent pyogenic cholangitis: comparison between MR cholangiography and direct cholangiography. Radiology 220 : 677 – 682

Wilson C, Auld CD, Schlinkert R et al. (1989) Hepatobiliary complications in chronic pancreatitis. Gut 30 : 520 – 527

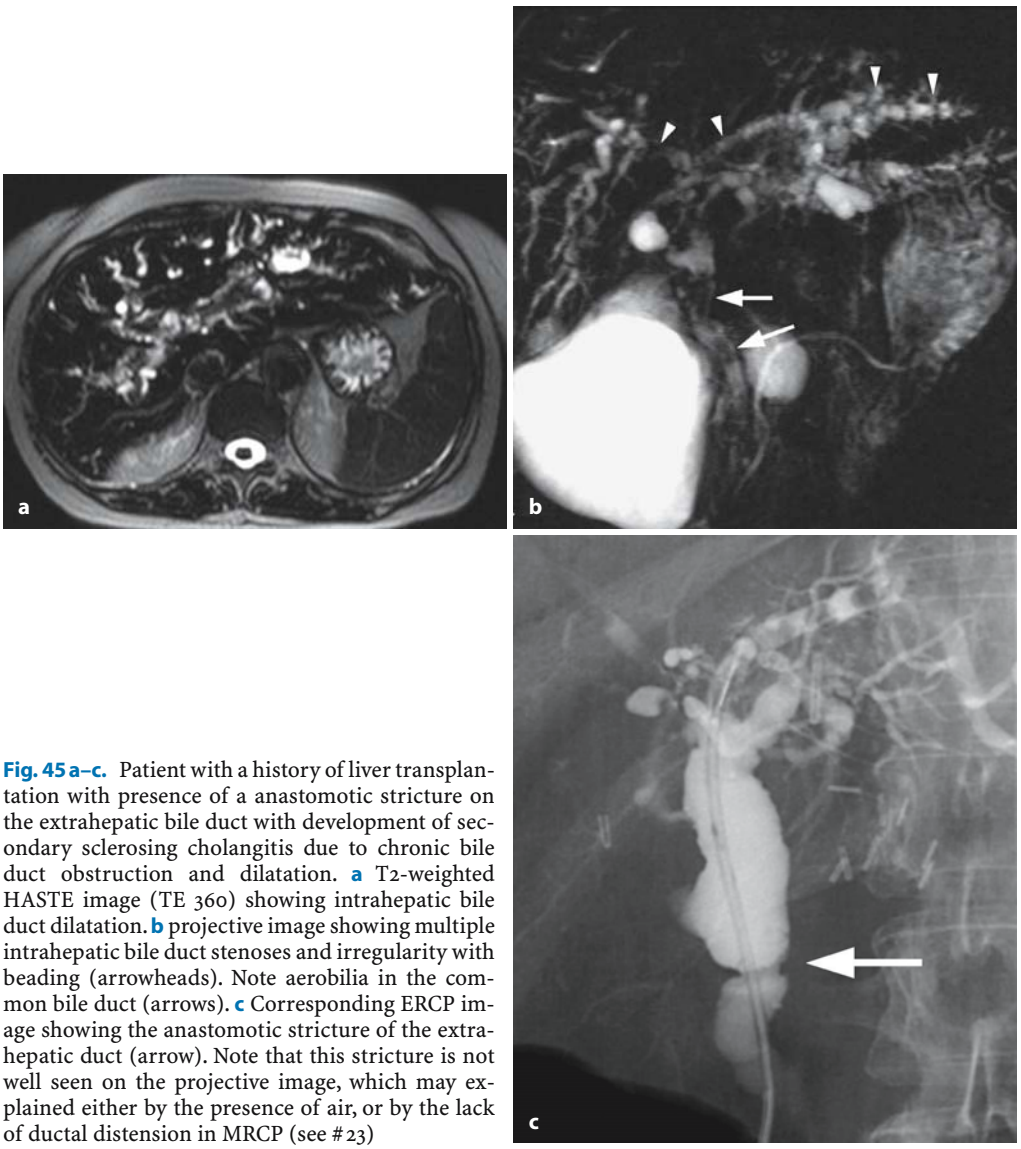

Fig. 45 a–c. Patient with a history of liver transplantation with presence of a anastomotic stricture on the extrahepatic bile duct with development of secondary sclerosing cholangitis due to chronic bile duct obstruction and dilatation. **a** T2-weighted HASTE image (TE 360) showing intrahepatic bile duct dilatation. **b** projective image showing multiple intrahepatic bile duct stenoses and irregularity with beading (arrowheads). Note aerobilia in the common bile duct (arrows). **c** Corresponding ERCP image showing the anastomotic stricture of the extrahepatic duct (arrow). Note that this stricture is not well seen on the projective image, which may explained either by the presence of air, or by the lack of ductal distension in MRCP (see #23)

#46 Oriental Cholangitis

KEY FACTS: DISEASE

- Chronic/recurrent infection of bile ducts
- Synonyms: recurrent pyogenic cholangitis, Hong Kong disease, intrahepatic pigment stone disease
- Pathology:
  - Inflammation of the biliary tree and surrounding parenchyma
  - Duct wall destruction, obliteration of peripheral ducts
  - Fibrosis, especially around portal tracts
  - Typically inflammation and fibrosis of the vaterian sphincter complex
  - Typically formation of pigment stones (bacterial deconjugation of bilirubin)
- Incidence:
  - Rare in the West, but common in South-East Asia
  - Third most common cause of acute abdomen in Hong Kong after appendicitis and perforated peptic ulcer
- Location: lateral segment of left lobe and posterior segment of right lobe most commonly involved
- Etiology (hypotheses):
  - Parasitic infection (*Clonorchis sinensis*, *Ascaris*) as initiating factor
  - Bacterial infection (*E. coli*) related to malnutrition
- Symptoms: recurrent attacks of fever, chills, abdominal pain, jaundice
- Complications: abscess (18%), segmental/lobar atrophy or even destruction

KEY FACTS: MRI

- Typical features (Fig. 46):
  - Marked dilation of large intrahepatic ducts
  - Strictures of intrahepatic ducts, mainly of left duct
  - Decreased arborization of smaller intrahepatic radicles (pruning)
  - Intrahepatic bile ducts filled with pigment stones and sludge
  - Marked dilation of common bile duct (68%), choledocholithiasis (30%)
  - Segmental hepatic atrophy
  - Abscesses
- *Note:* ERCP may underestimate the abnormalities if contrast medium does not pass a severe stenosis (Fig. 46)
- *Note:* Pigment stones characteristically have a high density on CT

References

Afagh A, Pancu D (2004) Radiologic findings in recurrent pyogenic cholangitis. J Emerg Med 26:343–346

Chau EM, Leong LL, Chan FL (1987) Recurrent pyogenic cholangitis: ultrasound evaluation compared with endoscopic retrograde cholangiopancreatography. Clin Radiol 38:79–85

Federle MP, Cello JP, Laing FC, Jeffrey RB Jr (1982) Recurrent pyogenic cholangitis in Asian immigrants: use of ultrasonography, computed tomography, and cholangiography. Radiology 143:151–156

Lim LH (1991) OCH: pathologic, clinical and radiologic features. AJR Am J Roentgenol 157:1–8

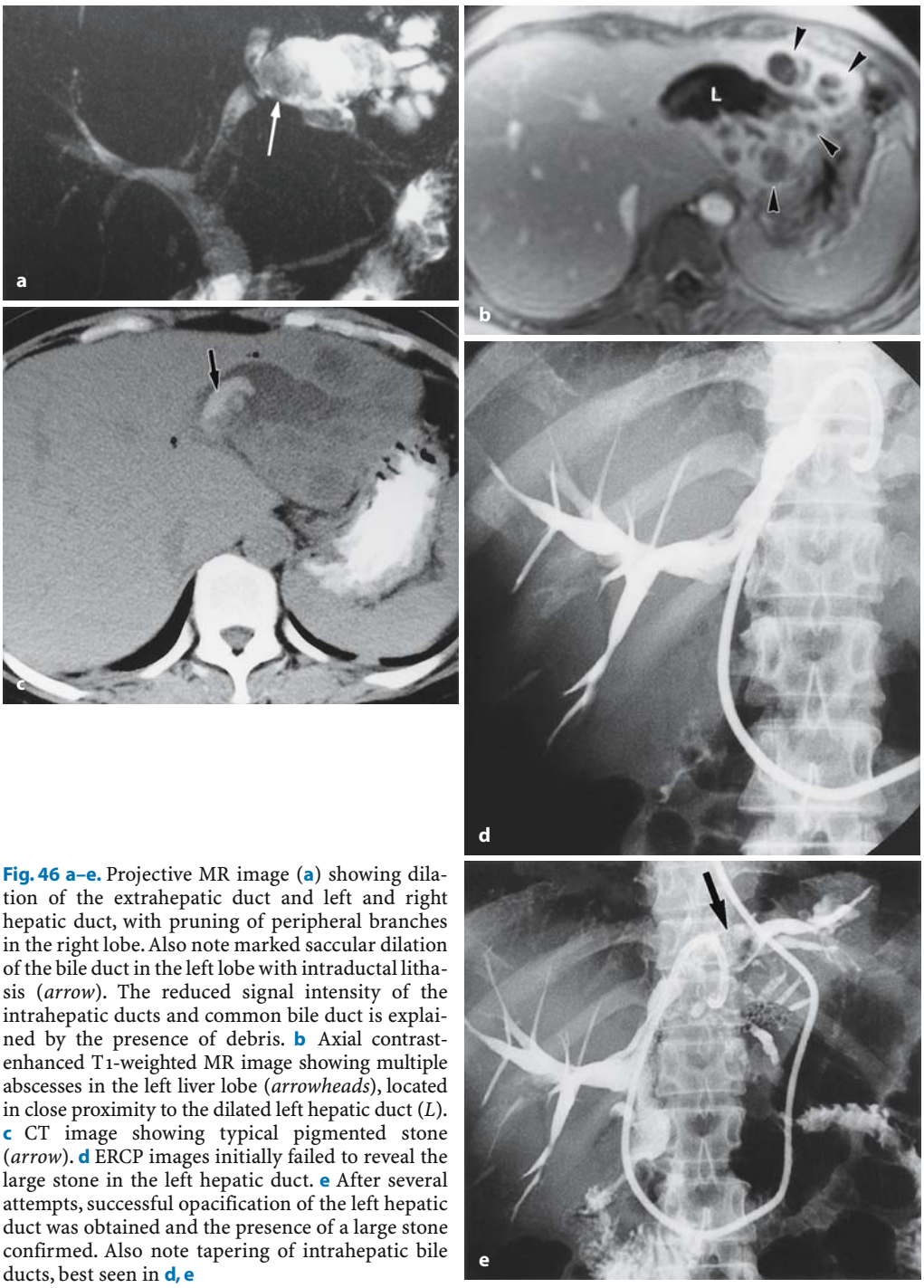

Fig. 46 a–e. Projective MR image (**a**) showing dilation of the extrahepatic duct and left and right hepatic duct, with pruning of peripheral branches in the right lobe. Also note marked saccular dilation of the bile duct in the left lobe with intraductal lithasis (*arrow*). The reduced signal intensity of the intrahepatic ducts and common bile duct is explained by the presence of debris. **b** Axial contrast-enhanced T1-weighted MR image showing multiple abscesses in the left liver lobe (*arrowheads*), located in close proximity to the dilated left hepatic duct (*L*). **c** CT image showing typical pigmented stone (*arrow*). **d** ERCP images initially failed to reveal the large stone in the left hepatic duct. **e** After several attempts, successful opacification of the left hepatic duct was obtained and the presence of a large stone confirmed. Also note tapering of intrahepatic bile ducts, best seen in **d, e**

#47 Echinococcosis

KEY FACTS: DISEASE

- Infection with *Echinococcus granulosus:* most common (hydatid disease)
  - Histology:
    Endocyst (= parasitic component of capsule): (a) inner germinative layer (= brood capsule), (b) cyst membrane (chitin)
    Pericyst (= granulation tissue)
  - Endemic to many parts of Australia, Africa, and the Middle East
  - Organs mainly affected: liver (73 %), lung (14 %), peritoneum (12 %)
  - Symptoms: pain, recurrent jaundice (biliary obstruction by membrane fragments)
  - Eosinophilia in 20 % – 50 %
  - Complications: intrabiliary rupture (66 %), intraperitoneal rupture (13 %), suppuration (13 %), intrathoracic rupture (6 %)
- Echinococcus multilocularis: rare

KEY FACTS: MRI

- Typical features of hydatid disease (Fig. 47 a, b):
  - Floating membranes within a fluid-containing and encapsulated lesion
  - The floating membranes usually have low signal intensity; this is not an absolute criterion, however
  - Signal intensity of fluid: usually high, may be low (hydatid sand)
- Calcifications (seen in 10 % – 30 %) usually not visible on MRI
- If rupture has occurred:
  - Interruption of cyst wall
  - Filling defects (hydatid sand and/or daughter cyst) in a dilated bile duct
- Echinococcus multilocularis has a more atypical presentation; lesions may mimic either metastases or pyogenic abscesses (Fig. 47 c – f)

References

Kumar R, Reddy SN, Thulkar S (2002) Intrabiliary rupture of hydatid cyst: diagnosis with MRI and hepatobiliary isotope study. Br J Radiol 75 : 271 – 274

Mortelé KJ, Wiesner W, Zou KH et al. (2004) Asymptomatic nonspecific serum hyperamylasemia and hyperlipasemia: spectrum of MRCP findings and clinical implications. Abdom Imaging 29 : 109 – 114

von Sinner W (1991) New diagnostic signs in hydatid disease: radiography, ultrasound, CT, and MRI correlated to pathology. Eur J Radiol 12 : 150 – 159

Zargar SA, Khuroo MS, Khan BA, Dar MY, Alai MS, Koul P (1992) Intrabiliary rupture of hepatic hydatid cyst: sonographic and cholangiographic appearances. Gastrointest Radiol 17 : 41 – 45

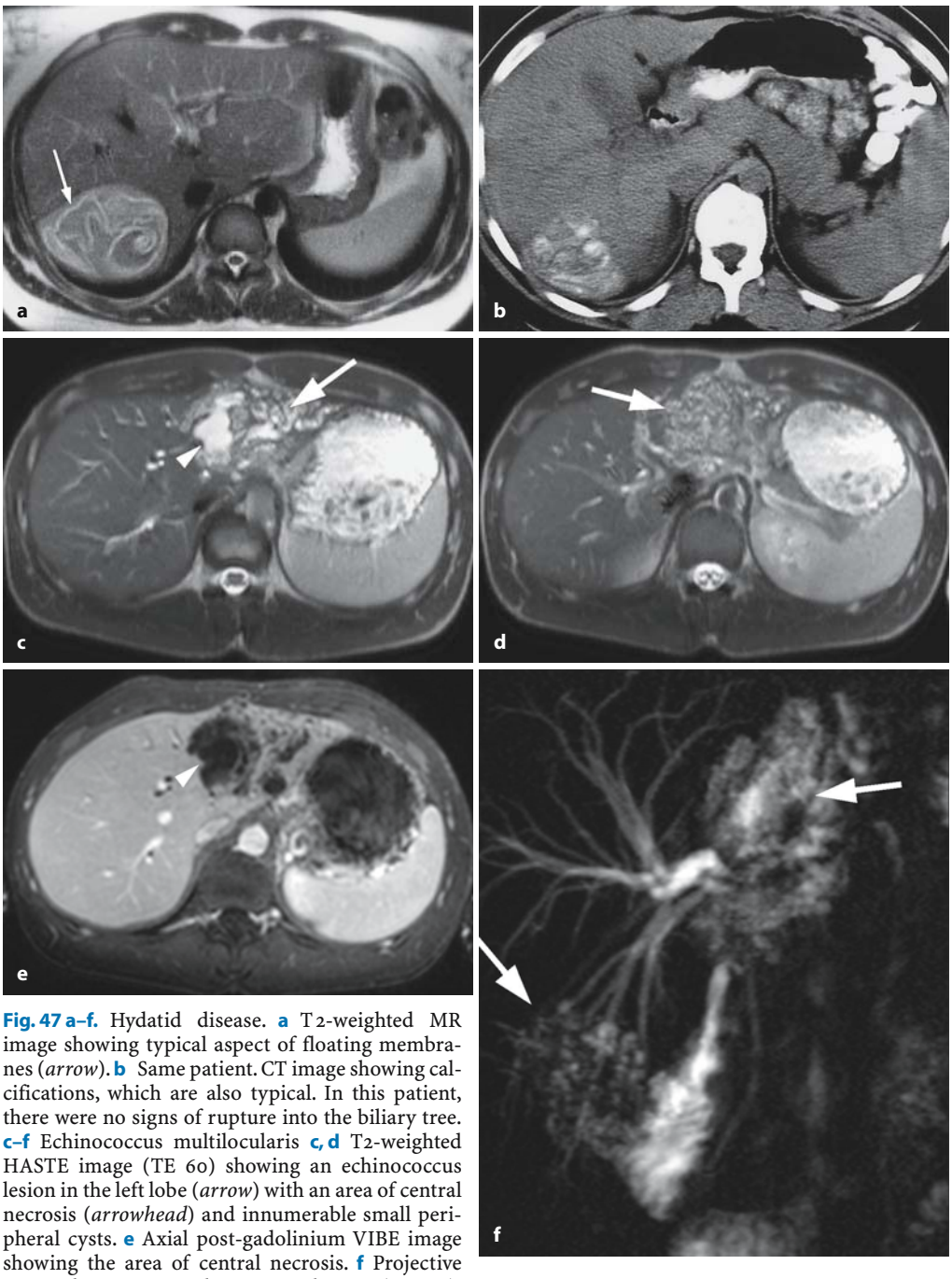

Fig. 47 a–f. Hydatid disease. **a** T2-weighted MR image showing typical aspect of floating membranes (*arrow*). **b** Same patient. CT image showing calcifications, which are also typical. In this patient, there were no signs of rupture into the biliary tree. **c–f** Echinococcus multilocularis **c, d** T2-weighted HASTE image (TE 60) showing an echinococcus lesion in the left lobe (*arrow*) with an area of central necrosis (*arrowhead*) and innumerable small peripheral cysts. **e** Axial post-gadolinium VIBE image showing the area of central necrosis. **f** Projective image showing two echinococcus lesions (*arrows*), one in the left lobe and a second in the right lobe (not shown on the axial images)

2.3 Traumatic, Postoperative, and Iatrogenic Abnormalities

#48 Sequelae of Direct Liver Trauma

Related topics: #113 (blunt gallbladder trauma), #181 (pancreatic duct injury)

KEY FACTS: DISEASE

- Incidence: severe bile duct injury after upper abdominal trauma is rare (< 0.1%; Dawson et al. 1991)
- Mechanism: hepatic laceration extending into a bile duct
- Complications:
  - Obstruction with or without stone formation
  - Bile leakage
  - Biloma formation
  - Partial liver atrophy

KEY FACTS: MRI

- MRI may show ductal narrowing or obstruction, bile leakage, etc. (Fig. 48 a, b)
- *Note:* "Periportal cuffing" (Fig. 48 c): (= fluid around venous tributaries)
  - Synonyms: "periportal halo," "periportal tracking"
  - Commonly seen after blunt hepatic trauma
  - May also be seen as a normal finding after hepatic transplantation and in patients with acute hepatitis, cirrhosis, AIDS, veno-occlusive disease, congestive heart failure, etc. (Lawson et al. 1993)
- Some types of injury may present with hilar stenoses, possibly mimicking neoplastic disease (Fig. 48 d–f)

References

Dawson DL, Johansen KH, Jurkovich GJ (1991) Injuries to the portal triad. Am J Surg 161 : 545 – 551

Fulcher AS, Turner MA (2002) MR cholangiopancreatography. Radiol Clin North Am 40 : 1363 – 1376

Lawson TL, Thorsen MK, Erickson SJ, Perret RS, Quiroz FA, Foley WD (1993) Periportal halo: a CT sign of liver disease. Abdom Imaging 18 : 42 – 46

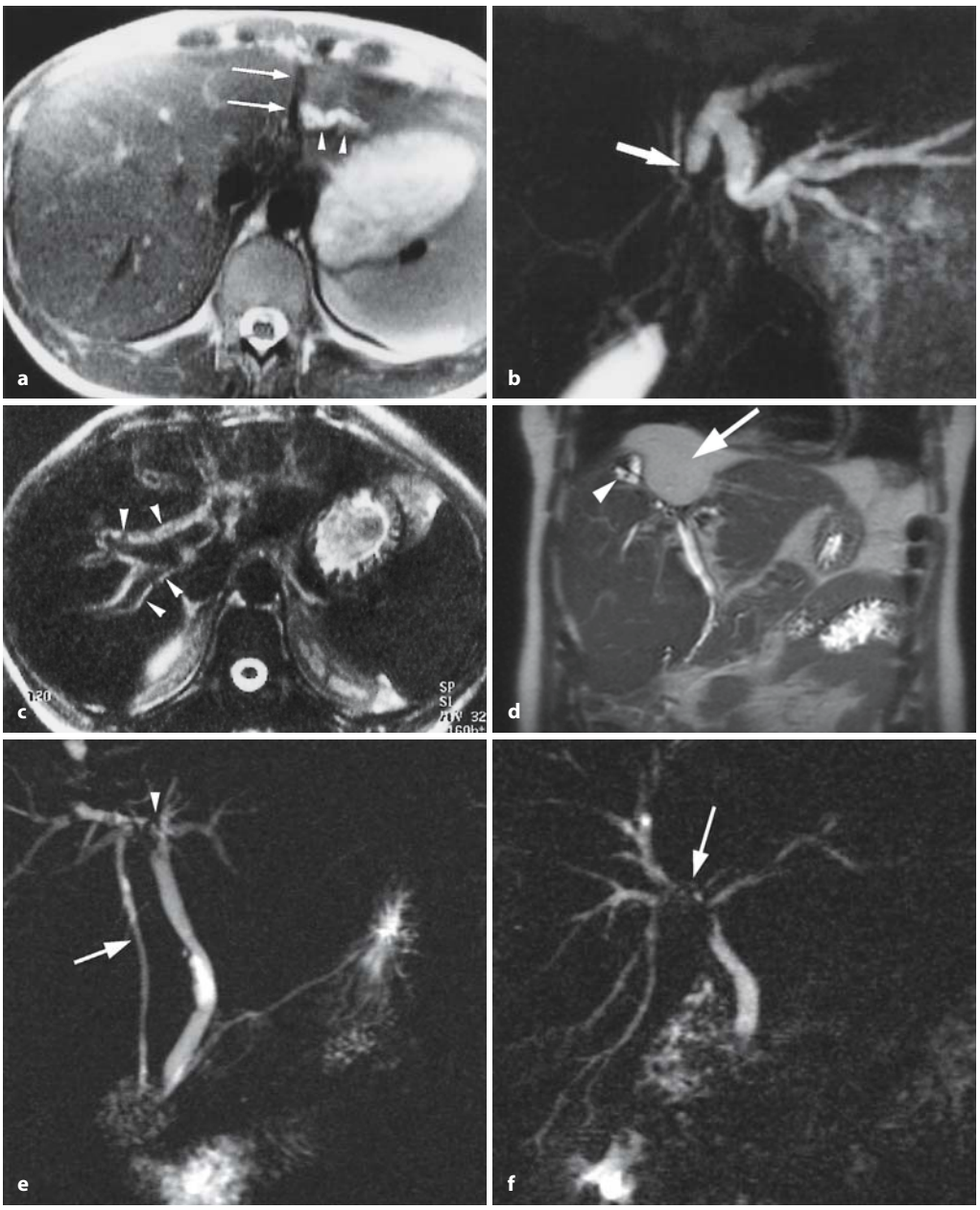

Fig. 48 a–f. Axial T2-weighted MR image (**a**) showing a hypointense laceration in the left liver lobe (*arrows*) and a dilated left hepatic duct (*arrowheads*). **b** Projective MR image showing occlusion of the bile duct secondary to the laceration (*arrow*). **c** Different patient. Heavily T2-weighted MR image showing "periportal cuffing" (*arrowheads*). **d, e** Patient with history of segmentectomy of the liver. **d** Coronal T2-weighted HASTE image (TE 60) showing the segmentectomy with fat interposition (*arrow*), together with right intrahepatic bile duct dilatation (*arrow-head*). **e** Projective image reveals a focal stenosis of the right hepatic duct (*arrowhead*), corresponding to a postoperative cicatricial stenosis. Note the unusually large right segmental posterior bile duct (*arrow*) related to hypertrophy of the right lobe. **f** Patient with a history of surgical treatment of a (suicidal) gunshot causing extensive liver damage. Postoperatively, progressive jaundice was observed. Projective image showing a focal hilar cicatricial bile duct stenosis (*arrow*) with secondary dilatation of the intrahepatic bile ducts

#49 After Hepaticojejunostomy: Anastomotic Stricture

Related topics: #29 (postoperative anatomy: after hepat(ic)ojejunostomy), #56 (recurrent tumor after hepaticojejunostomy)

KEY FACTS: DISEASE

- Incidence: up to 23 % (Bismuth et al. 1978; Lane et al. 1973)
- Mechanisms:
  - Fibrosis
  - Recurrent neoplasm (see #56)
- Complications:
  - Stone formation
  - Cholangitis

KEY FACTS: MRI

- Dilation of intrahepatic bile ducts nearly invariably present
- Typical features of fibrotic strictures (Fig. 49):
  - Usually short
  - Limited to anastomosis
  - Smooth delineation
  - No mass lesion on cross-sectional images
- *Note:* In comparison with PTC, MRCP may overestimate strictures; ERCP is usually impossible

References

Bismuth H, Franco D, Corlette MB, Hepp J (1978) Long-term results of Roux-en-y hepaticojejunostomy. Surg Gynecol Obstet 146 : 161 – 167

Lane CE, Sawyers JL, Riddel DH, Scott HW Jr (1973) Long-term results of Roux-en-y hepatocholangiojejunostomy. Ann Surg 177 : 714 – 722

Pavone P, Laghi A, Catalano C et al. (1997) MR cholangiography in the examination of patients with biliary-enteric anastomoses. AJR Am J Roentgenol 169 : 807 – 811

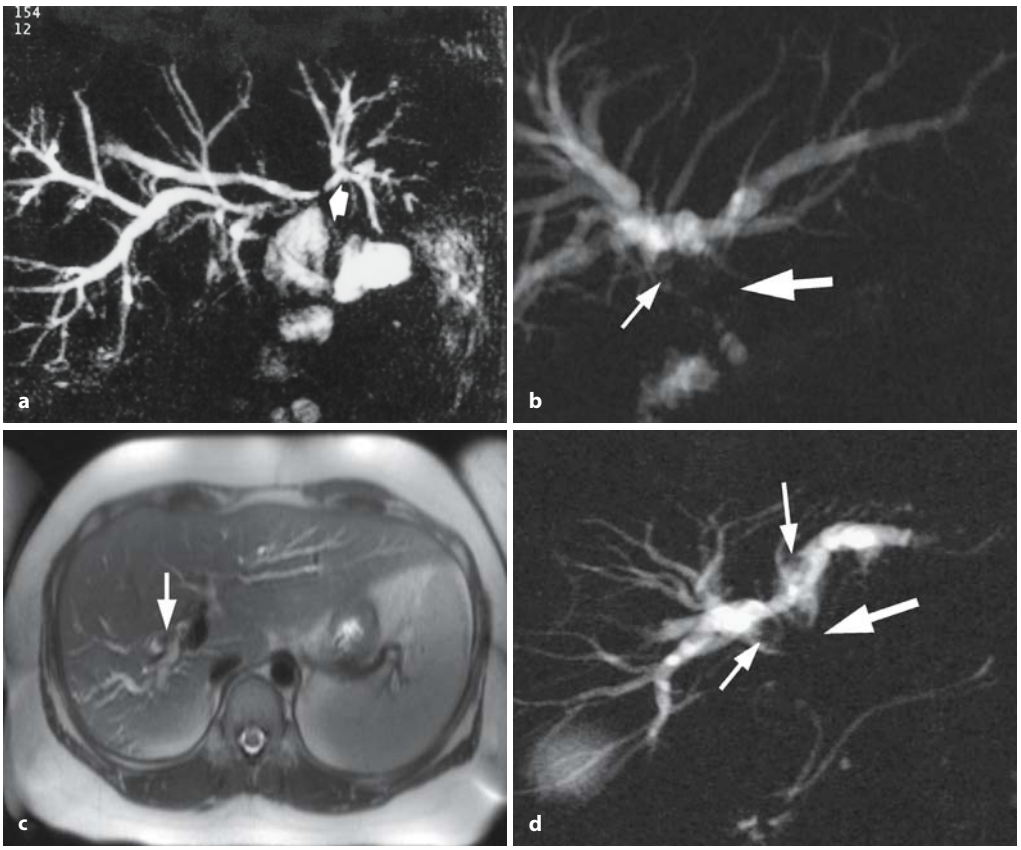

Fig. 49. **a** Projective MR image showing a short stricture of a hepaticojejunal anastomosis (*arrow*). **b,c** Patient with history of hepaticojejunostomy. **b** Projective image showing an anastomotic stricture (*large arrow*) with a stone (*small arrow*) and secondary dilatation of the intrahepatic bile ducts. **c** T2-weighted HASTE image showing the intrahepatic bile duct dilatation and the stone (*arrow*) **d** Different patient. Projective image showing a stricture of the hepaticojejunostomy (*large arrow*) with secondary intrahepatic bile duct dilatation and stones (*small arrows*)

#50 After Hepatic Transplantation (1): Ischemia

Related topics: #80, 81 (extrahepatic bile duct, complications after hepatic transplantation)

KEY FACTS: DISEASE

- Biliary complications after liver transplantation are common (up to 37%; Lerut et al. 1987; Ward et al. 1990)
- Ischemia is an important cause of biliary injury
- Mechanism: bile ducts receive their blood supply from the hepatic artery (not portal vein); any abnormality leading to decreased arterial inflow may cause ischemia
- Common causes:
  - Hepatic artery thrombosis (7% of transplants)
  - Severe arterial stenosis (1%)
  - Prolonged cold ischemic graft perfusion time
- Complications (occurring in up to 50%):
  - Stricture formation (multifocal)
  - Leakage of bile with or without biloma
  - Diffuse dilation
  - Intraductal debris, sloughed mucosa, clot

KEY FACTS: MRI (FIG. 50)

- Typical findings:
  - Multiple irregularities/strictures typically involving both the intrahepatic ducts and the proximal common hepatic duct
  - Bile duct dilation
  - Nonanastomotic leakage, biloma formation
  - Presence of multiple intraluminal filling defects
- Differential diagnosis: e.g., primary sclerosing cholangitis, chronic rejection, cholangitis
- See also #81

References

Lerut T, Gordon RD, Iwatsuki S et al. (1987) Biliary tract complications in human orthotopic liver transplantation. Transplantation 43 : 47 – 51

Ward EM, Kiely MJ, Maus TP, Wiesner RH, Krom RA (1990) Hilar biliary strictures after liver transplantation: cholangiographic and percutaneous treatment. Radiology 177 : 259 – 263

Zajko AB, Campbell WL, Logsdon GA et al. (1987) Cholangiographic findings in hepatic artery occlusion after liver transplantation. AJR Am J Roentgenol 149 : 485 – 489

Zoepf T, Maldonado-Lopez EJ, Hilgard P, et al. (2005) Diagnosis of biliary strictures after liver transplantation: which is the best tool? World J Gastroenterol 11 : 2945 – 2948

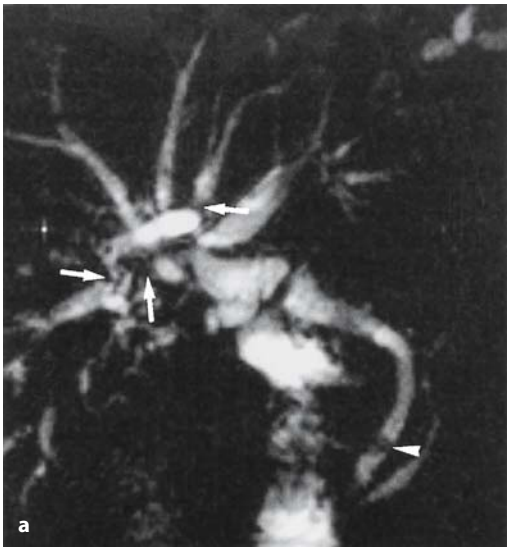

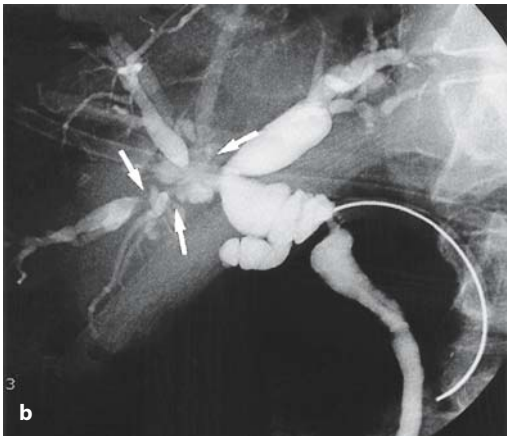

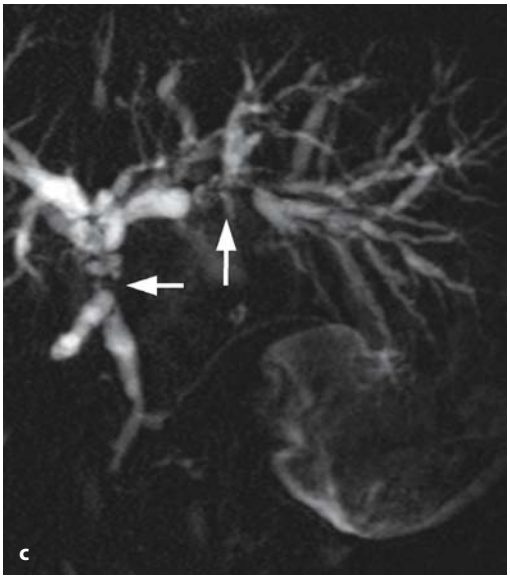

Fig. 50 a, b. Projective MR image (**a**) and ERCP image (**b**) showing several strictures of bifurcation and the right intrahepatic duct (*arrows*). There is also an anastomotic stricture. Also shown in **a** is a small stone in the distal common bile duct (*arrowhead*). **c** Different patient. Projective image showing irregular strictures of the common hepatic duct and the left hepatic duct (*arrows*)

#51 After Hepatic Transplantation (2): Other Complications

Related topics: #80, 81 (extrahepatic bile duct, complications after hepatic transplantation)

KEY FACTS: DISEASE

- Other complications of orthotopic liver transplantation apart from ischemia include:
  - Stone formation
  - Biloma (may occur secondary to ischemia)
  - Hematoma (common in the immediate postoperative period)
  - Abscess
  - Portal/hepatic vein thrombosis
  - Acute rejection
  - Chronic rejection
  - Viral hepatitis
  - Anastomotic stricture/leakage

KEY FACTS: MRI

- Hematomas (Fig. 51) have a variable signal intensity, depending on their age (see Table 51 for a simplified classification). Moreover, the central and peripheral parts of a hematoma may display a different signal intensity
- Bilomas have signal intensity features typical of fluid
- Acute rejection: may give the intrahepatic biliary tree a primary sclerosing cholangitis type of appearance (narrowing, stretching, and separation, reflecting edema and cellular infiltration)
- Chronic rejection: disappearance of small bile ducts ("vanishing bile ducts," see #39), nonanastomotic strictures, ductal irregularity, intraductal casts, etc.
- *Note:* A common finding after liver transplantation is the presence of periportal lymphedema related to surgical disruption of lymphatic channels. It should not be erroneously interpreted as biliary dilation (see #37, 48)

References

Bauman J, Campbell WL, Demetris AJ, Zajko AB (1988) Intrahepatic cholangiographic abnormalities in liver transplants: correlation with biopsy evidence of rejection and other disorders. AJR Am J Roentgenol 152 : 275 – 279

Dominguez R, Cuervas-Mons V, Van Thiel DH, Lecky JW, Starzl TE (1986) Radiographic features of liver allograft rejection. Gastrointest Radiol 11 : 326 – 329

Moncorge C, Baudin F, Vigouroux C et al. (1989) Transplantation hepatique chez l'adulte: prise en charge postoperatoire et evolution au cours des premiers mois. Ann Fr Anesth Reanim 8 : 497 – 517

Zoepf T, Maldonado-Lopez EJ, Hilgard P, et al. (2005) Diagnosis of biliary strictures after liver transplantation: which is the best tool? World J Gastroenterol 11 : 2945 – 2948

Table 51.1 Simplified classification of hematomas

Age of hematoma	Composition	Signal intensity on T1	Signal intensity on T2
Hyperacute (<1 h)	OxyHb	Low/intermediate	High
Acute (<3–4 days)	Intracellular deoxyHb Extracellular deoxyHb (lysis)	Intermediate Intermediate	Low High
Subacute (months/years)	MetHb	High	High
Chronic	MetHb + hemosiderin (periphery)	Low at periphery	Low at periphery

OxyHb, oxyhemoglobin; deoxyHb, deoxyhemoglobin; MetHb, methemoglobin.

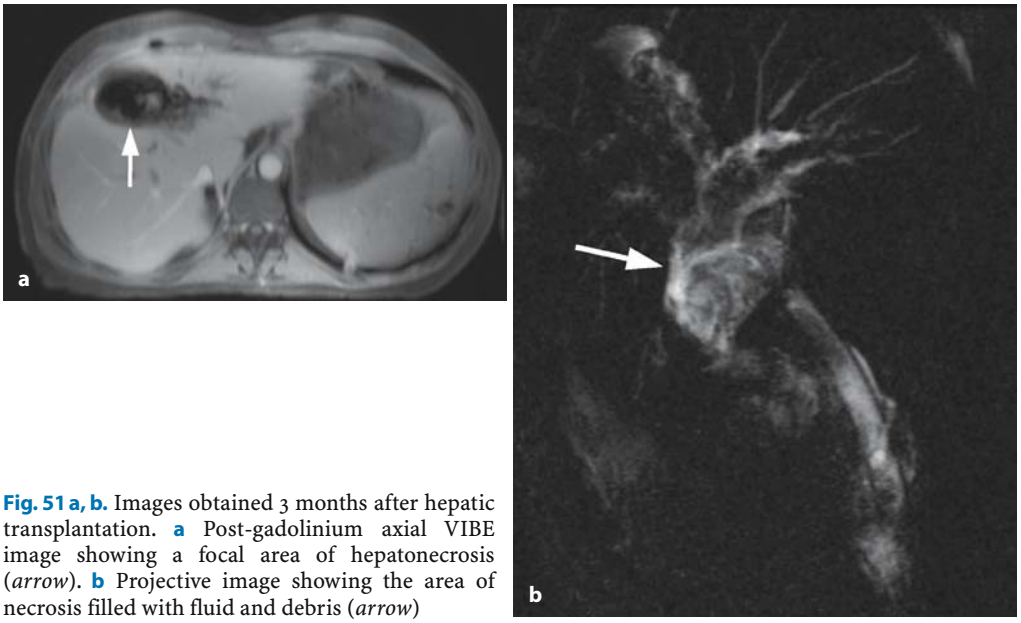

Fig. 51 a, b. Images obtained 3 months after hepatic transplantation. **a** Post-gadolinium axial VIBE image showing a focal area of hepatonecrosis (*arrow*). **b** Projective image showing the area of necrosis filled with fluid and debris (*arrow*)

#52 After Cholecystectomy: Stricture/Transection of an Aberrant Bile Duct

Related topics: #27 (variable junction of the posterior right hepatic duct), #82 (after cholecystectomy: stricture of the common bile duct)

KEY FACTS: DISEASE

- Inadvertent transection of an aberrant bile duct (see #27)
- Complications:
  - Stenosis
  - Occlusion
  - Bile leakage
  - Infection (cholangitis)
  - Partial liver atrophy
- *Note:* Other anatomical variations that increase the risk of bile duct injury during laparoscopic cholecystectomy include the following (Fig. 52a):
  - Low bifurcation of the common bile duct (see #63)
  - Very low or very high insertion of the cystic duct (see #93)
  - Short cystic duct
  - Parallel course of cystic and hepatic ducts
  - Cystic duct entering the common hepatic duct along its medial surface

KEY FACTS: MRI (FIG. 52)

- Depending on the severity of the injury, MR images may show:
  - Mild to severe segmental intrahepatic bile duct dilation
  - Focal narrowing of an accessory bile duct
  - Subhepatic/hilar bile collection
- *Note:* In comparison with ERCP, MRCP may under- or overestimate the severity of the stenosis (see also Fig. 27c, d)

References

Davidoff AM, Pappas TN, Murray EA et al. (1992) Mechnisms of major bile duct injury during laparoscopic cholecystectomy. Ann Surg 215: 196–202

Deziel DJ, Millikan KW, Economou SG, Doolas A, Ko ST, Airan MC (1993) Complications of laparoscopic cholecystectomy: a national survey of 4.292 hospitals and 77.604 cases. Am J Surg 165: 9–14

Vitellas KM, Keogan MT, Spritzer CE et al. (2000) MR cholangiopancreatography of bile and pancreatic duct abnormalities with emphasis on the single-shot fast spin-echo technique. Radiographics 20: 939–957

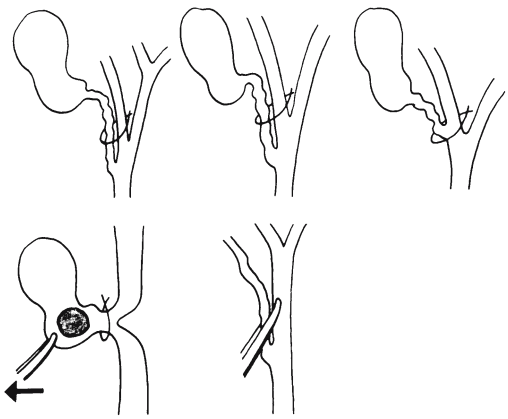

a

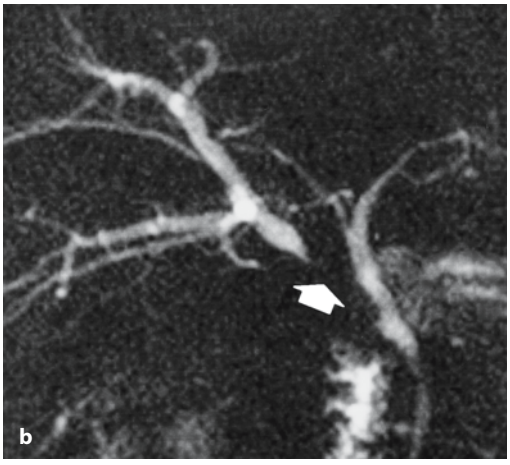

Fig. 52. **a** Some anatomical variations predisposing to bile duct injury. *1*, low insertion of the right posterior duct close to the cystic duct; *2*, low bifurcation; *3*, cystic duct draining into the right hepatic duct; *4*, very short cystic duct; *5*, long parallel course of the cystic duct and common hepatic duct. (Reprinted with permission from Kune and Sali 1980). **b** Patient who had had a laparoscopic cholecystectomy now presenting with fever. Projective MR image showing dilated right posterior biliary branches with an aberrant insertion. Note severe narrowing of the distalmost portion of this aberrant duct (*arrow*), probably related to direct trauma during surgery

#53 Biliary Complications of Percutaneous Procedures

KEY FACTS: DISEASE (GAZZANIGA ET AL. 1991; VAN THIEL ET AL. 1993)

- Complications of PTC and other percutaneous interventions:
  - Bacteremia
  - Sepsis
  - Subcapsular hematoma
  - Bile leak
  - Biloma
  - Peritonitis
  - Arteriovenous fistula
  - Vasculobiliary fistula
- Complication rate:
  - PTC using the Chiba needle: 1.8 %
  - PTC combined with external drainage: 10 % – 15 %
  - Liver biopsy: < 1 %

KEY FACTS: MRI

- Biloma, hematoma, etc.: see # 51
- MR detection of small arteriovenous fistulae and vasculobiliary fistulae requires a special technique (preferably three-dimensional breathhold contrast-enhanced MRI; Gaa et al. 1997; Rofsky et al. 1999; Fig. 53)

References

Gazzaniga GM, Gaffioni A, Bondanza G, Bararolo C, Filauro M (1991) Percutaneous transhepatic biliary drainage: 12 year experience. Hepatogastroenterology 38 : 154 – 59

Rofsky, NM, Lee VS, Laub G, et al. (1999) Abdominal MR imaging with a volumetric interpolated breath-hold examination. Radiology 212 : 876 – 884

Van Thiel DH, Gavaler JS, Wright H, Tzakis A (1993) Liver biopsy: its safety and complications as seen at a liver transplant center. Transplantation 55 : 1087 – 1090

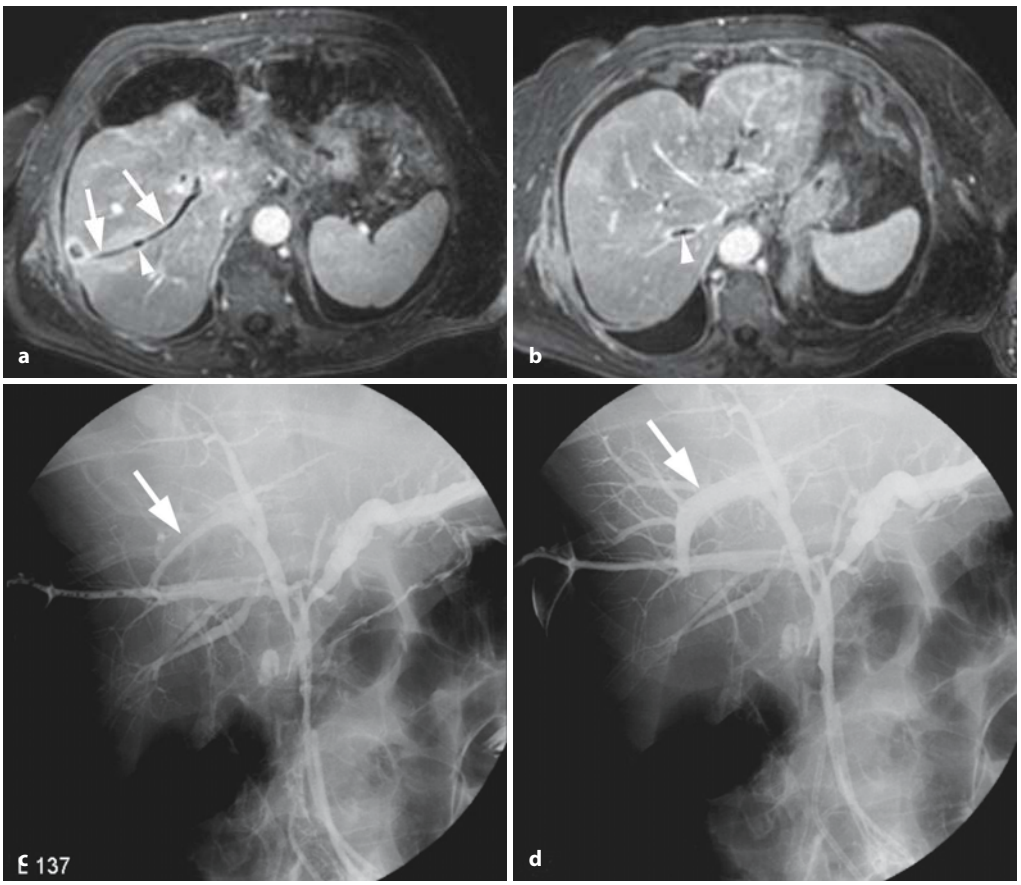

Fig. 53 a–d. Patient who underwent a PTC procedure complicated by a biliary venous fistula. **a, b** Post-gadolinium axial VIBE images obtained in the venous phase showing the percutaneous drain (*arrows*) complicated by a thrombus in the right hepatic vein (*arrowheads*) due to a biliary venous fistula. **c, d** Corresponding ERCP images showing the opacification of the right hepatic vein when contrast is injected through the percutaneous drain (*arrows*)

2.4 Malignant Tumors

#54 Intrahepatic (Peripheral) Cholangiocarcinoma (1): Ductal Changes

Related topics: #87, 88 (extrahepatic cholangiocarcinoma)

KEY FACTS: DISEASE

- Malignant tumor originating from the epithelium of small and peripheral intrahepatic bile ducts
- Histology: adenocarcinoma, characteristically with large central core of fibrotic tissue relatively devoid of malignant cells; may also contain mucoid material
- Classification: mass forming, peri-ductal-infiltrating, and intraductal-growing types (Lim 2003)
- To be distinguished from other types of cholangiocarcinoma:
  - Klatskin tumor (70 %; see #87)
  - Distal duct type (10 %; see #88)
- Incidence:
  - Second most common primary malignant liver tumor after hepatocellular carcinoma
  - ± 20 % of cholangiocarcinomas
- Predisposing factors: ulcerative colitis, choledochal cyst (see #68), Caroli's disease (see #30), infection by *Clonorchis sinensis*
- Symptoms: pain, jaundice
- Spread: predominantly local
- Complications:
  - Biliary obstruction/cholangitis
  - Intrahepatic satellite nodules (65 %)
- Prognosis: poor (5-year survival rate, 1 %)

KEY FACTS: MRI

- Cholangiographic features (Fig. 54):
  - Focal stricture most common
  - Other presentations: diffuse narrowing, polypoid intraluminal mass
- Nonspecific unless cross-sectional images show characteristic features (see #55)
- Focal or segmental intrahepatic bile duct dilation may be an early sign on cross-sectional images

!

References

Choi BI, Han JK, Shin YM, Baek SY, Han MC (1995) Peripheral cholangiocarcinoma: comparison of MRI with CT. Abdom Imaging 20 : 357 – 60

Kawarada Y, Mizumoto R (1984) Cholangiocellular carcinoma of the liver. Am J Surg 147 : 354 – 359

Lim JH (2003) Cholangiocarcinoma: morphologic classification according to growth pattern and imaging findings. AJR Am J Roentgenol 181 : 819 – 827

Nichols DA, MacCarty RL, Gaffey TA (1983) Cholangiographic evaluation of bile duct carcinoma. AJR Am J Roentgenol 141 : 1291 – 1294

Soyer P, Bluemke DA, Reichle R et al. (1995) Imaging of intrahepatic cholangiocarcinoma. 1. Peripheral cholangiocarcinoma. AJR Am J Roentgenol 165 : 1427 – 1431

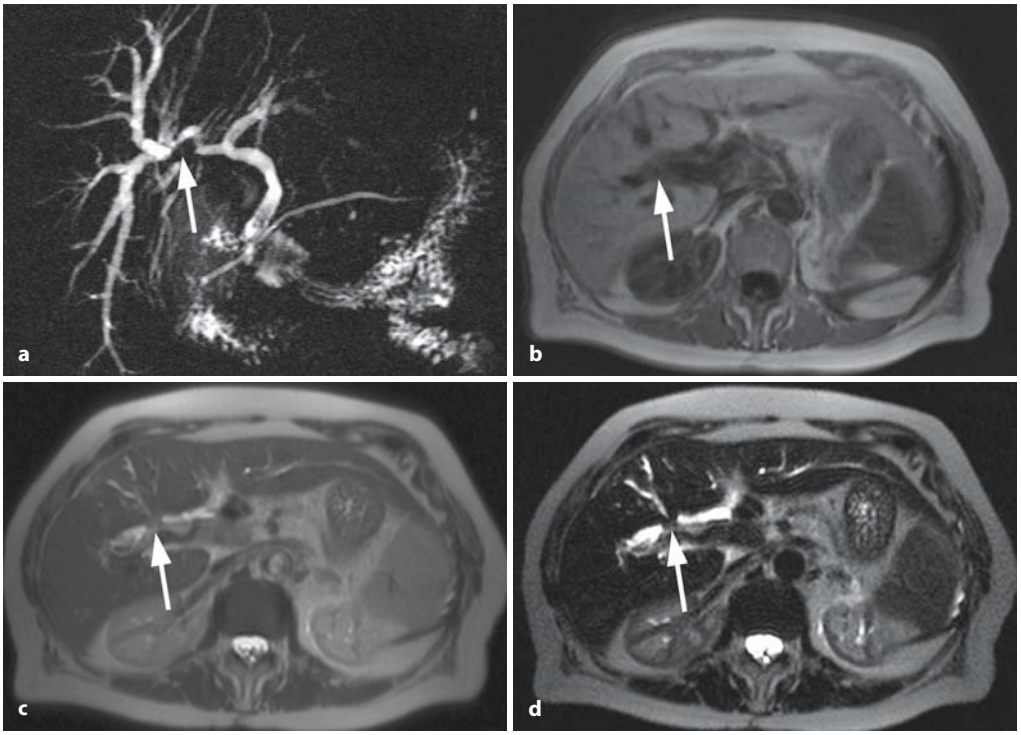

Fig. 54 a–d. Projective image (**a**) showing a focal stenosis (*arrow*) on the right hepatic duct with secondary bile duct dilatation. Axial T1-weighted image (**b**) and T2-weighted HASTE images (**c, d**; TE 60 and 360) showing a small mass centered on the right hepatic duct: small cholangiocarcinoma

#55 Intrahepatic (Peripheral) Cholangiocarcinoma (2): Enhancement Pattern

Related topics: #87, 88 (extrahepatic cholangiocarcinoma)

KEY FACTS: MRI

- Most intrahepatic cholangiocarcinomas can be visualized on cross-sectional images
- Signal intensity:
  - T1: low
  - T2: variable (isointense to markedly hyperintense; Vilgrain et al. 1997)
- Contrast-enhanced images:
  - May show early moderate peripheral enhancement (also seen in some metastases and hepatocellular carcinomas)
  - Characteristic feature: hyperintense central core on delayed contrast-enhanced images (Tani et al. 1991; Honda et al. 1993; Fig. 55)
- Mechanism of delayed enhancement:
  - Central part of tumor usually contains a large extravascular, extracellular contrast distribution volume
  - Contrast slowly accumulates in this part of the tumor by diffusion
- *Note:* Other features distinguishing intrahepatic cholangiocarcinoma from hepatocellular carcinoma:
  - Tumor extension into the portal vein less common
  - Segmental atrophy more common
  - Usually less hypervascular (arterial phase)

References

Han JK, Choi B, Kim A, et al. (2002) Cholangiocarcinoma: pictorial essay of CT and cholangiographic findings. RadioGraphics 22 : 173

Lacomis JM, Baron RL, Oliver JH, Nalesnik MA, Federle MP (1997) Cholangiocarcinoma: delayed CT contrast enhancement patterns. Radiology 203 : 98 – 104

Lim JH (2003) Cholangiocarcinoma: morphologic classification according to growth pattern and imaging findings. AJR Am J Roentgenol 181 : 819 – 827

Tani K, Kubota Y, Yamaguchi T et al. (1991) MR imaging of peripheral cholangiocarcinoma. J Comp Assist Tomogr 15 : 975 – 978

Vilgrain V, Van Beers BE, Flejou JF et al. (1997) Intrahepatic cholangiocarcinoma: MRI and pathologic correlation in 14 patients. J Comput Assist Tomogr 21 : 59 – 65

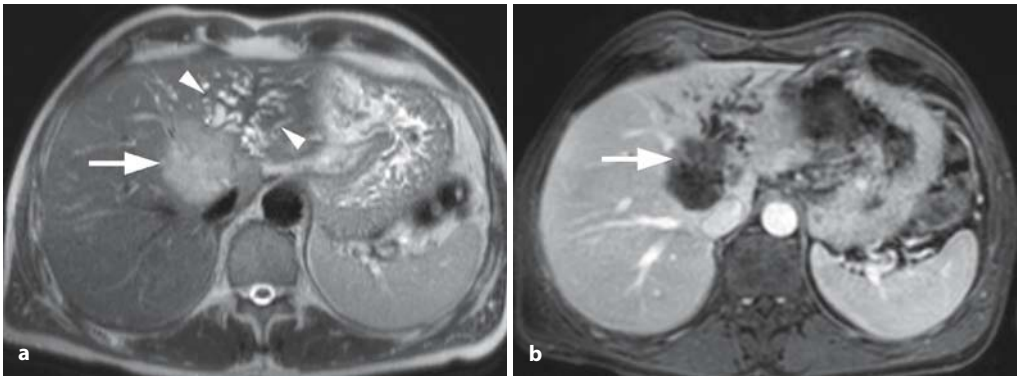

Fig. 55 a–d. **a** Axial T2-weighted HASTE image showing a T2 moderately hyperintense mass (*arrow*) with obstruction of the left intrahepatic duct (*arrowheads*). **b** Axial contrast-enhanced T1-weighted VIBE image obtained in the arterial phase showing this mass to be hypointense, with only slight peripheral enhancement (*arrow*).

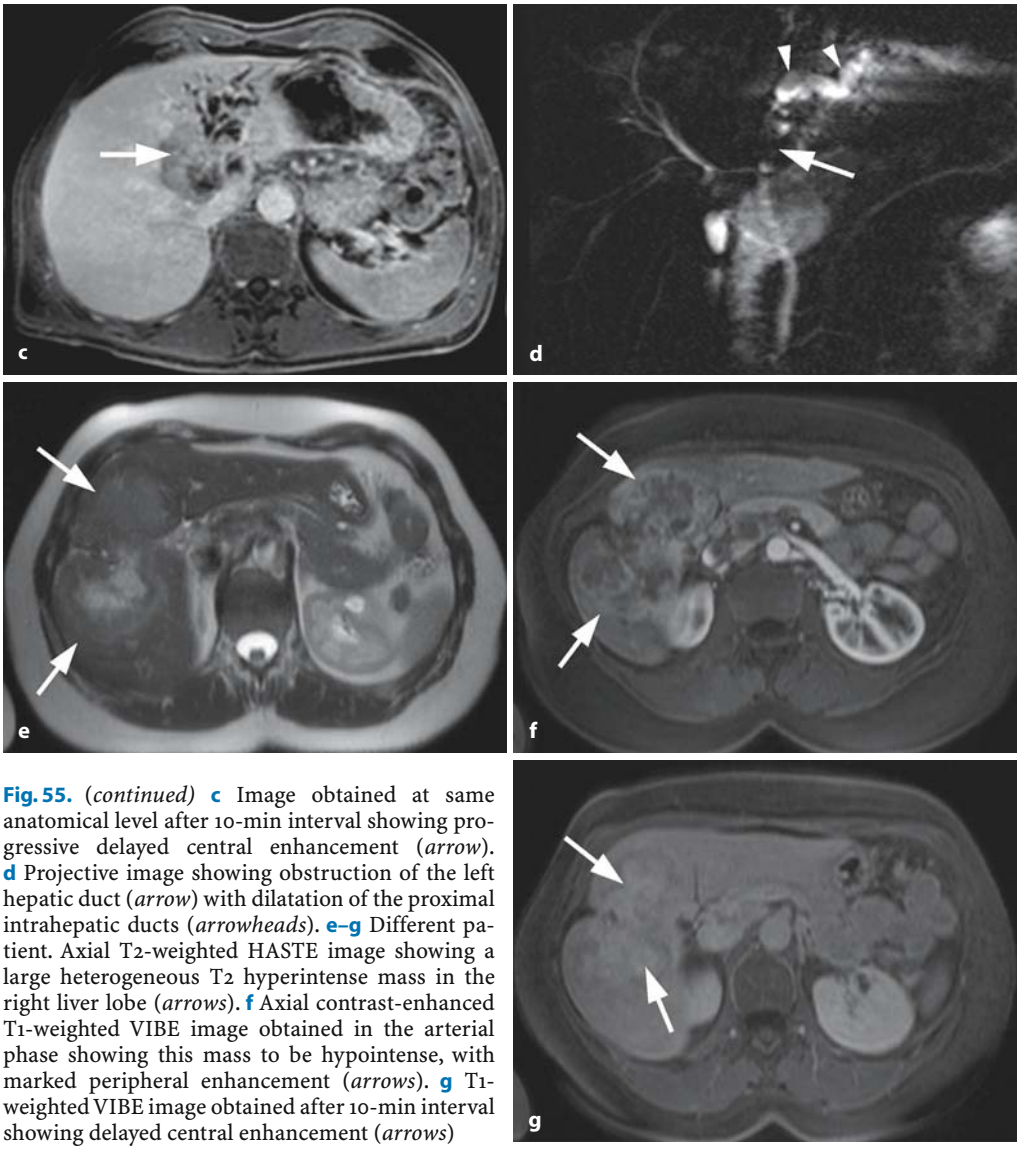

Fig. 55. (*continued*) **c** Image obtained at same anatomical level after 10-min interval showing progressive delayed central enhancement (*arrow*). **d** Projective image showing obstruction of the left hepatic duct (*arrow*) with dilatation of the proximal intrahepatic ducts (*arrowheads*). **e–g** Different patient. Axial T2-weighted HASTE image showing a large heterogeneous T2 hyperintense mass in the right liver lobe (*arrows*). **f** Axial contrast-enhanced T1-weighted VIBE image obtained in the arterial phase showing this mass to be hypointense, with marked peripheral enhancement (*arrows*). **g** T1-weighted VIBE image obtained after 10-min interval showing delayed central enhancement (*arrows*)

#56 Recurrent Tumor After Hepat(ic)ojejunostomy

Related topics: #29 (postoperative anatomy: after hepat(ic)ojejunostomy), #49 (after hepaticojejunostomy: anastomotic stricture)

KEY FACTS: DISEASE

- Although most hepaticojejunostomies are performed in patients with benign conditions, the technique may be part of a curative or palliative treatment of malignant neoplasms
- Sometimes combined with partial liver resection
- Biliary obstruction caused by tumor recurrence is not uncommon

KEY FACTS: MRI (FIG. 56)

- Cholangiographic images: usually not specific
  - Stricture(s) (suspect if long, irregular, nonanastomotic)
  - Dilation of proximal bile ducts
- Cross-sectional images (diagnostic if the tumor is sufficiently large):
  - Mass lesion

References

Nordback IH, Hruban RH, Cameron JL (1992) Second primary lesion in the biliary tree after successful resection of ampullary carcinoma. Surgery 112 : 111 – 115

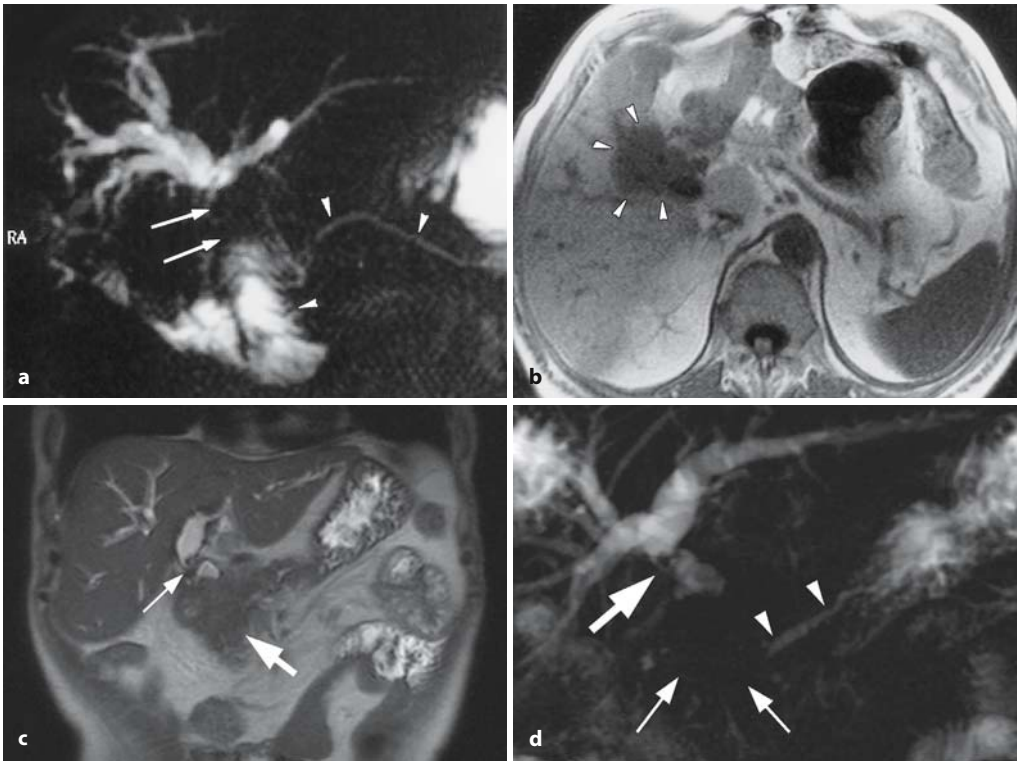

Fig. 56. a, b Patient had previously undergone a Whipple operation for ampullary carcinoma. **a** Projective MR image showing jejunal loop and normal pancreatic duct (*arrowheads*). The biliary ducts, however, are dilated secondary to a stenosis of the hepatojejunal anastomosis (*arrows*). **b** Axial T1-weighted image showing the tumor as a hypointense mass (*arrowheads*). **c, d** Patient who underwent a palliative hepaticojejunostomy for pancreatic carcinoma, with recurrent progressive jaundice. **c** Coronal T2-weighted HASTE image showing progression of the tumor in the pancreatic head (large arrow), with obliteration and obstruction of the hepaticojejunostomy (*small arrow*). **d** projective image showing the obstructed hepaticojejunostomy (*arrow*) with dilated intrahepatic bile ducts. Note the slightly enlarged pancreatic duct (arrowheads) and the "black hole" corresponding to the tumor (*small arrows*).

#57 Recurrent Tumor: Diagnostic Problems Related to the Presence of Endoprostheses

KEY FACTS: ENDOPROSTHESES

- Placement of an endoprosthesis is the treatment of choice in patients with unresectable bile duct carcinoma
- Types:
  - Plastic endoprostheses
  - Metallic endoprostheses (e.g., wall stent)
- Metallic endoprostheses provide longer stent patency but are much more expensive

KEY FACTS: MRI

- Plastic endoprostheses (Fig. 57a):
  - Cause no artifacts and are usually seen as a thin, hypointense, tubular structure surrounded by fluid
  - May be invisible if not surrounded by fluid
- Metallic endoprostheses (Fig. 57b):
  - Typically cause a *signal void* in and around the stent (local dephasing)
  - This metallic artifact may preclude the detection of recurrent tumor (Fig. 57c, d) and the evaluation of stent patency

References

Adam A, Chetty N, Roddie M, Yeung E, Benjamin IS (1991) Self-expandable stainless steel endoprostheses for treatment of malignant bile duct obstruction. AJR Am J Roentgenol 156 : 321 – 325

Irie H, Honda H, Kuroiwa T et al. (2001) Pitfalls in MR cholangiopancreatographic interpretation. Radiographics 21 : 23 – 37

Merkle EM, Boll DT, Weidenbach H et al. (2001) Ability of MR cholangiography to reveal stent position and luminal diameter in patients with biliary endoprostheses: in vitro measurements and in vivo results in 30 patients. AJR Am J Roentgenol 176 : 913 – 918

O'Brien S, Hatfield AR, Craig PI, Williams SP (1995) A three year follow-up of self expanding metal stents in the endoscopic palliation of longterm survivors with malignant biliary obstruction. Gut 36 : 618 – 621

Watanabe Y, Dohke M, Ishimori T et al. (1999) Diagnostic pitfalls of MR cholangiopancreatography in the evaluation of the biliary tract and gallbladder. Radiographics 19 : 415 – 429

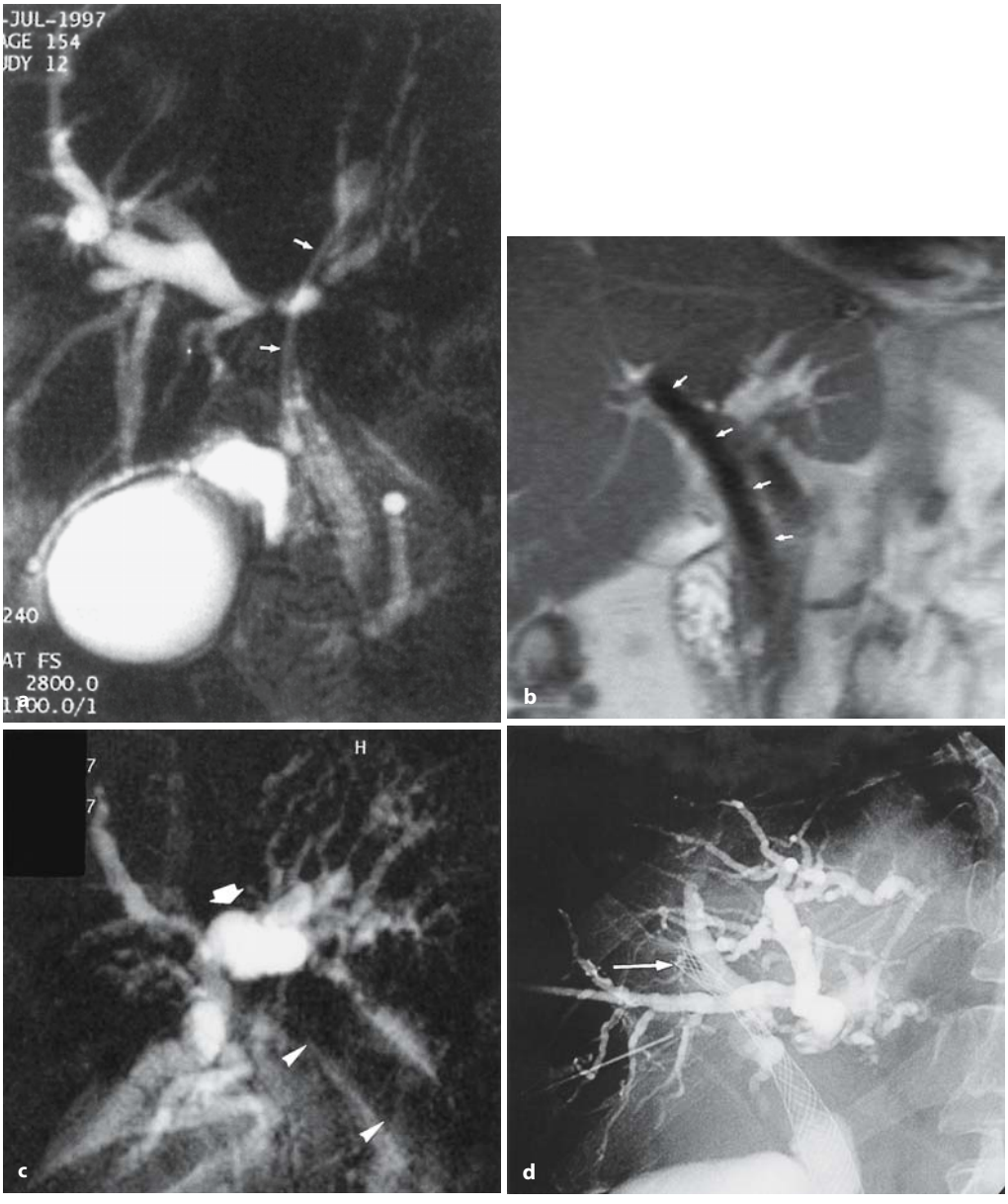

Fig. 57. **a** Plastic endoprothesis in patient with Klatskin tumor. This type of endoprothesis does not cause artifact and is seen as a thin, fluid-filled structure (*arrows*). **b** Example of appearance of wall stent on cross-sectional images (*arrows*) in a different patient. **c, d** Patient with cholangiocarcinoma who had previously undergone palliative placement of a wall stent. **c** Projective MR image showing dilation of intrahepatic bile ducts (*arrow*) and signal void caused by the stent (*arrowheads*). **d** Image obtained with PTC showing more clearly the dislodgement of the stent with the tip outside the biliary system (*arrow*) as well as narrowing of the stent caused by compression by tumor. The presence of tumor within a stent is not usually detected by MRCP because of the metallic artifact

#58 Hepatocellular Carcinoma, General

KEY FACTS: DISEASE

- Malignant tumor originating from hepatocytes
- Pathology (multistep progression): regenerative nodule, dysplastic nodule, dysplastic nodule with subfocus of hepatocellular carcinoma, small hepatocellular carcinoma (< 2 cm), hepatocellular carcinoma (Earls et al. 1996)
- 80 % – 90 % of all primary liver tumors
- Incidence:
  - United States/Europe: 0.2 % – 0.8 %
  - Asia: 5.5 % – 20 %
- Peak age: sixth to seventh decade (fibrolamellar hepatocellular carcinoma: < 40 years)
- Etiology:
  - Cirrhosis (particularly macronodular type)
  - Chronic hepatitis B, C (12 % of patients develop hepatocellular carcinoma)
  - Metabolic diseases: hemochromatosis, α_1-antitrypsin deficiency, porphyria cutanea tarda
  - Aflatoxin
- Growth pattern:
  - Solitary massive (27 % – 59 %)
  - Multicentric small nodular (15 % – 26 %)
  - Diffuse microscopic (15 % – 51 %)
- α-Fetoprotein elevated in the majority of patients (not in cholangiocarcinoma)
- *Note:* Portal vein invasion occurs in 25 % – 40 %

KEY FACTS: MRI

- Relationship between signal intensity and histology (signal intensity relative to normal liver): Table 58 a (Earls et al. 1996)
- Practical hints concerning focal lesions in cirrhotic livers: !
  - Lesions slightly hyperintense on T 2-weighted images are always suspect for hepatocellular carcinoma
  - Small lesions hypointense on T 1- and T 2-weighted images are most likely to be benign (siderotic nodules)
  - Most other combinations of signal intensity characteristics can be seen in both benign and malignant lesions
- Arterial blood supply with respect to histology: see Table 58 b
- Obtaining arterial-phase contrast-enhanced MR images is critical for: !
  - Accurate detection of small hepatocellular carcinoma foci
  - Differentiation of hepatocellular carcinoma from typical regenerative and dysplastic nodules and other types of focal lesions
- Other features of hepatocellular carcinoma (Freeny et al. 1992):
  - Large tumors: usually heterogeneous (e. g., hemorrhage, necrosis)
  - Fibrous pseudocapsula (12 % in the United States)
  - Vascular invasion (typically direct extension in portal vein characterized by caliber expansion and enhancement of tumor thrombus)
  - Signs of underlying cirrhosis

References

Earls JP, Theise ND, Weinreb JC et al. (1996) Dysplastic nodules and hepatcellular carcinoma: thin-section MR imaging of explanted cirrhotic livers with pathologic correlation. Radiology 201 : 207 – 214

Freeny PC, Baron RL, Teefey SA (1992) Hepatocellular carcinoma: reduced frequency of typical findings with dynamic contrast-enhanced CT in a non-Asian population. Radiology 182 : 143 – 148

Matsui O, Kadoya M, Kameyama T et al. (1991) Benign and malignant nodules in cirrhotic livers: distinction based on blood supply. Radiology 178 : 493 – 497

Table 58.1a. Stepwise development of hepatocellular carcinoma from a regenerative nodule: signal intensity characteristics

Histology	Signal intensity	
	T1	T2
Regenerative nodule (RN)	Isointense/hyperintense	Isointense
Siderotic regenerative nodule	Hypointense	Hypointense
Dysplastic nodule (DN)	Hyperintense	Hypointense
Siderotic dysplastic nodule	Hypointense	Hypointense
Dysplastic nodule with subfocus of HCC	Hyperintense	Hypointense
Small HCC	Hyperintense	Variable
HCC	Variable	Variable

HCC, hepatocellular carcinoma.

Table 58.1b. Stepwise development of hepatocellular carcinoma from a regenerative nodule: arterial blood supply

Histology	Arterial blood supply
Regenerative and dysplastic nodules	Hypovascular (96%)
Dysplastic nodule with subfocus of HCC	Usually hypovascular
Small HCC	Usually hypervascular
HCC	Hypervascular (up to 95%)

HCC, hepatocellular carcinoma.

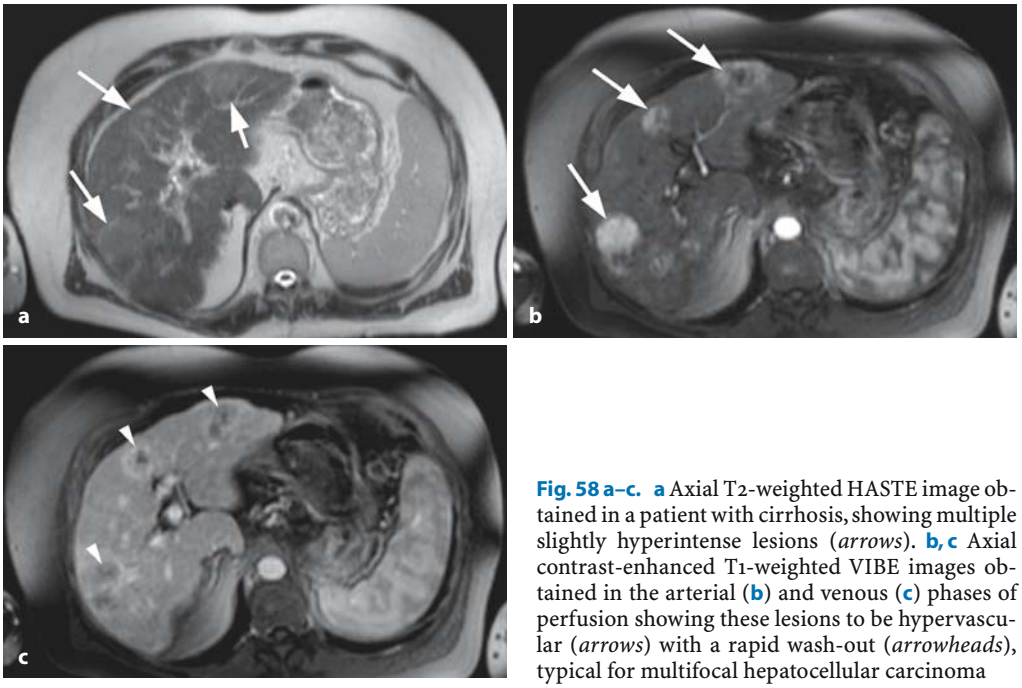

Fig. 58 a–c. **a** Axial T2-weighted HASTE image obtained in a patient with cirrhosis, showing multiple slightly hyperintense lesions (*arrows*). **b, c** Axial contrast-enhanced T1-weighted VIBE images obtained in the arterial (**b**) and venous (**c**) phases of perfusion showing these lesions to be hypervascular (*arrows*) with a rapid wash-out (*arrowheads*), typical for multifocal hepatocellular carcinoma

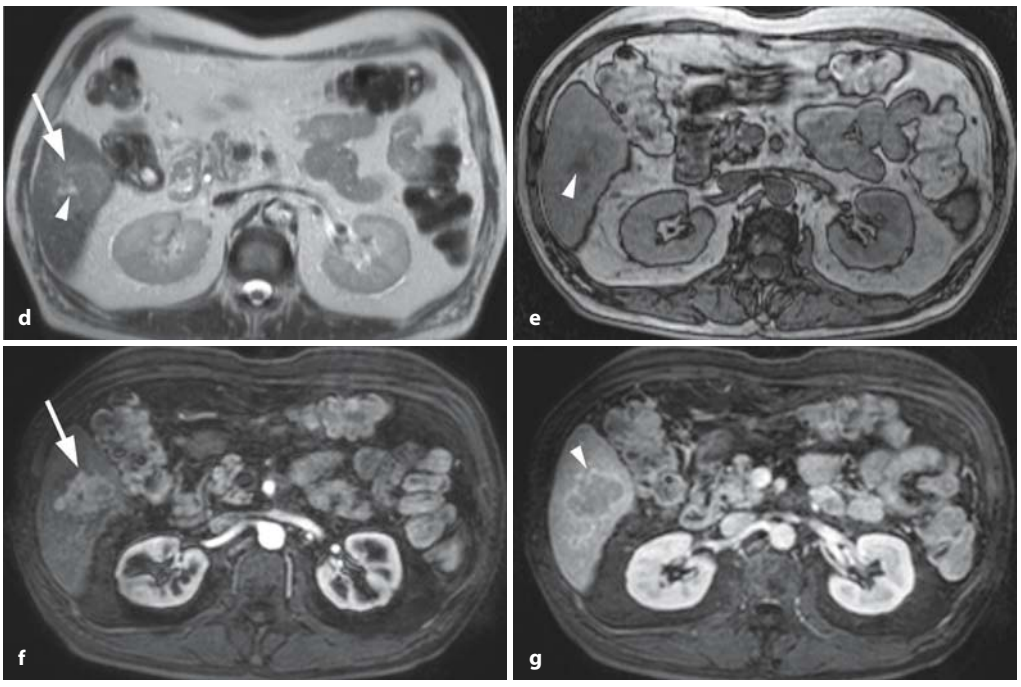

Fig. 58 d–g. (*continued*) **d** Axial T2-weighted HASTE image showing a slightly hyperintense lesion (*arrow*) with a central high signal intensity focus (*arrowhead*), possibly due to central fat or necrosis. **e** Axial T1-weighted image "out of phase" shows that this central high signal intensity focus drops (*arrowhead*) in signal, thus suggesting the presence of fat. **f, g** Axial contrast-enhanced T1-weighted VIBE images obtained in the arterial (**f**) and venous (**g**) phases showing the lesion to be hypervascular (*arrow*) with a rapid wash-out and presence of a (pseudo-) capsule (*arrowhead*). Histologic diagnosis: hepatocellular carcinoma

#59 Hepatocellular Carcinoma, Biliary Invasion

KEY FACTS: DISEASE

- While portal vein invasion by hepatocellular carcinoma is common, biliary invasion is relatively rare

KEY FACTS: MRI

- Imaging findings may include the following:
  - Focal stenosis
  - Scattered irregular strictures (infiltrating type)
  - Polypoid intraluminal mass (rare)

References

Kojiro M, Kawabata K, Kawano Y, Shirai F, Takemoto N, Nakashima T (1982) Hepatocellular carcinoma presenting as intrabile duct tumor growth: a clinicopathologic study of 24 cases. Cancer 49 : 2144 – 2147

Lee NW, Wong KP, Siu KF, Wong J (1984) Cholangiography in hepatocellular carcinoma with obstructive jaundice. Clin Radiol 35 : 119 – 123

Soyer P, Laissy JP, Bluemke DA, Sievert A, Menu Y (1995) Bile duct involvement in hepatocellular carcinoma: MR demonstration. Abdom Imaging 20 : 118 – 121

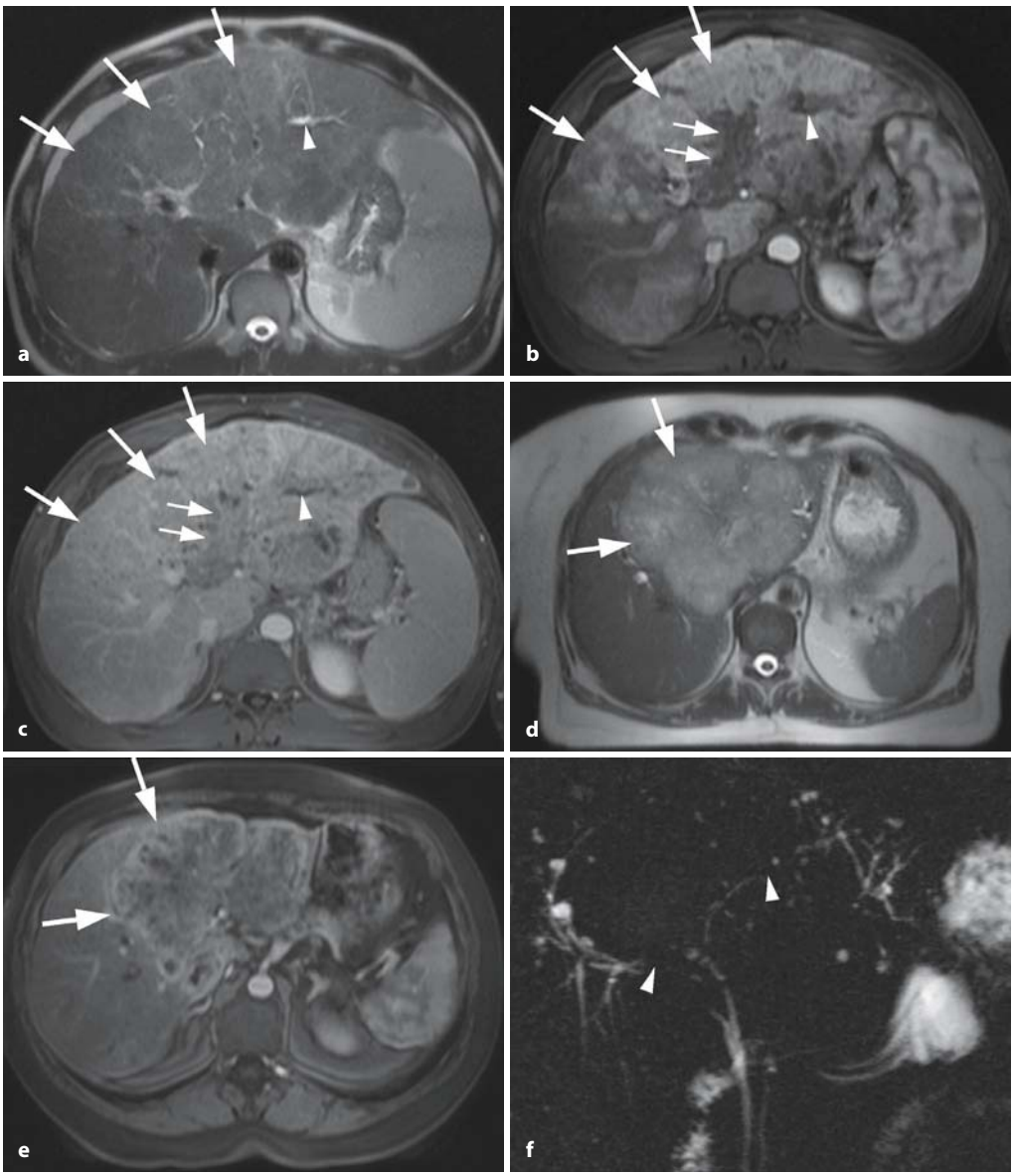

Fig. 59 a–c. **a** Axial T2-weighted HASTE image showing a large slightly hyperintense infiltrating mass (*arrows*) with secondary left hepatic bile duct dilatation due to invasion (*arrowhead*). **b, c** Axial contrast-enhanced T1-weighted VIBE images obtained in the arterial (**b**) and venous (**c**) phase showing this infiltrating mass to be hypervascular (*arrows*). Note the invasion and secondary thrombosis of the left portal vein (*small arrows*) and the dilated left hepatic bile ducts (*arrowhead*). **d–f** Different patient. **d** Axial T2-weighted HASTE image showing a large slightly hyperintense mass (*arrows*). **e** Axial contrast-enhanced T1-weighted VIBE images obtained in the arterial phase showing this to be a hypervascular mass (*arrows*). **f** Projective image showing the intrahepatic bile ducts to be severely displaced with multiple obliterations due to invasion (*arrowheads*)

#60 Metastases

Related topics: #91 (bile duct involvement by other extrabiliary neoplasms), #196 (secondary pancreatic tumors)

KEY FACTS: DISEASE

- Liver is the most common metastatic site after regional lymph nodes
- Organ of origin: colon (42%), stomach (23%), pancreas (21%), breast (14%), lung (13%)

KEY FACTS: MRI

- Displacement, stenosis, encasement, obstruction, separation, and diminished arborization may all be seen
- Care should be taken not to confuse cystic/necrotic metastases with simple cysts, particularly on heavily T2-weighted images (solid component invisible; see #193):
  - Metastases commonly containing a large necrotic or cystic component include metastases of mucinous carcinoma, colon carcinoma, sarcoma, melanoma, lung carcinoma, and endocrine tumors
  - Diagnostic clues: solid peripheral component; rim enhancement (Fig. 193)
- Contrast-enhanced scans:
  - Arterial phase (± 25 s): *hypovascular* primary tumors: peripheral rim enhancement or no enhancement; *hypervascular* primary tumors (e.g., renal cell carcinoma, malignant melanoma, endocrine tumors, adrenal carcinoma): rim enhancement or global enhancement
  - Hepatic phase (± 70 s): usually hypointense
  - Delayed phase (5–10 min): peripheral low-intensity halo is typical ("washout" of contrast medium; Mahfouz et al. 1994)

References

Mahfouz AE, Hamm B, Wolf KJ (1994) Peripheral washout: a sign of malignancy on dynamic gadolinium-enhanced MR images of focal liver lesions. Radiology 190 : 49–52

Van Hoe L, Bosmans H, Aerts P, Baert AL, Fevery J, Kiefer B, Marchal G (1996) Focal liver lesions fast T2-weighted MR imaging with half-Fourier rapid acquisition with relaxation enhancement. Radiology 201 : 817–823

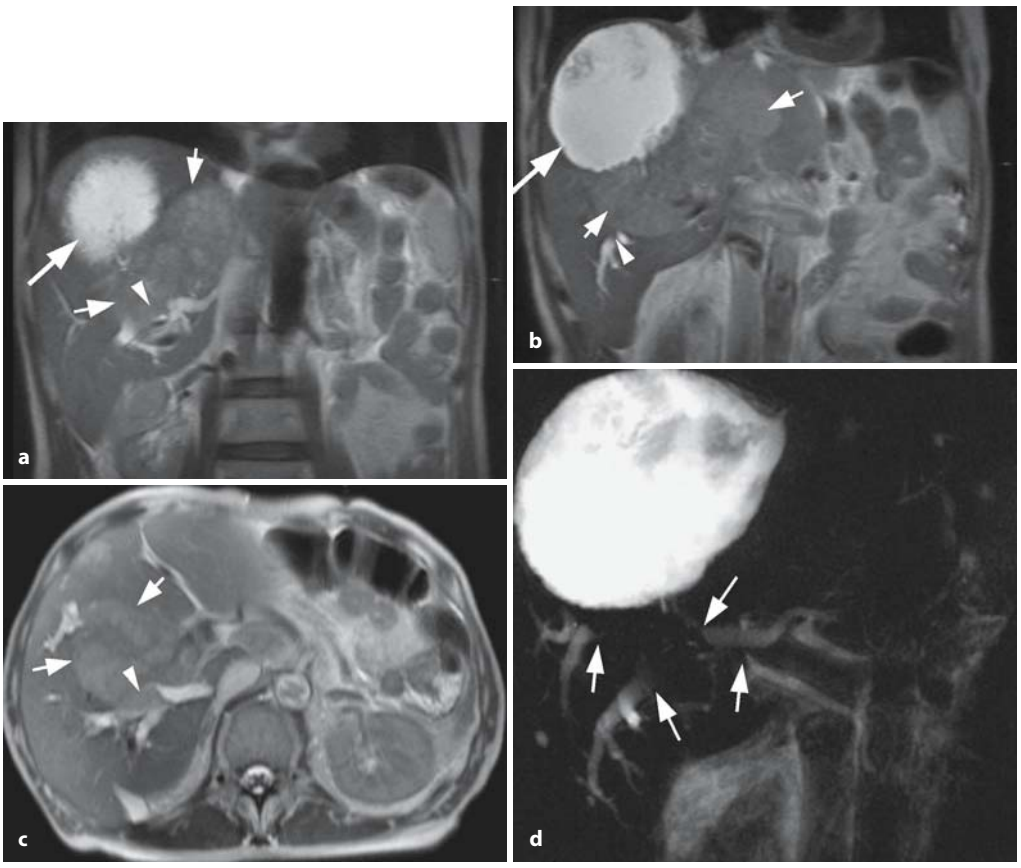

Fig. 60 a–d. Patient with a history of radiofrequency ablation of liver metastases. **a, b** Coronal and **c** axial T2-weighted HASTE images showing a large necrotic lesion (*arrow*) secondary to the known RF ablation, together with multiple recurrent liver metastases (*small arrows*), with secondary bile duct invasion and biliary dilatation (*arrowheads*). **d** Projective image showing dilated bile ducts due to invasion by metastatic disease (*arrows*). Note the large necrotic mass secondary to the RF ablation

Extrahepatic Bile Duct

3 Extrahepatic Bile Duct

3.1 Normal Anatomy and Variants

#61 Normal Anatomy, Terminology, and Size

KEY FACTS

- *Common hepatic duct:* portion of bile duct above the cystic duct and below the bifurcation
- *Common bile duct:* portion above the papilla and below the cystic duct
- Normal maximal diameter:
  - Simplifying rule: 5 mm for patients up to age 50, plus 1 mm per decade over age 50 (duct walls are composed of elastic fibers; loss of elasticity may occur with age)
  - In fact, a wide range of diameters are encountered in "normal" asymptomatic patients; diameters up to 10 mm may be observed in individuals under 50 years, even in the absence of disease (Fig. 61)
  - A normal bile duct diameter does not rule out (obstructive) disease
  - After cholecystectomy, dilatation of the common bile duct occurs; the increase in diameter is usually small (<1 mm), however (Feng and Song 1995)

References

Feng B, Song Q (1995) Does the common bile duct dilate after cholecystectomy? Sonographic evaluation in 234 patients. AJR Am J Roentgenol 165 : 859 – 861

Lasser RB, Silvis SE, Vennes JA (1978) The normal cholangiogram. Am J Dig Dis 23 : 586 – 590

Rohrman CA, Baron RL (1989) Biliary complications of pancreatitis. Radiol Clin North Am 27 : 93 – 104

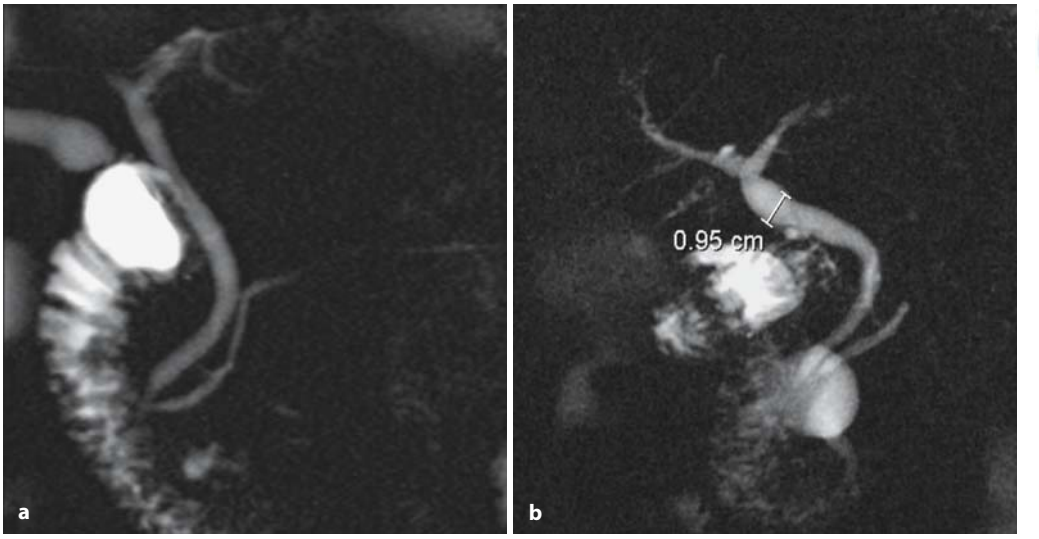

Fig. 61. **a** Projective image obtained in an asymptomatic patient showing a normal common hepatic and common bile duct. **b** Projective image obtained in an asymptomatic 80-year-old patient. Diameters up to 10 mm may be observed in this age group

#62 Variant Anatomy (1): Narrow Aspect of the Pancreatic Segment

KEY FACTS: ANATOMY

- Course of the normal bile duct (Fig. 62 a):
  - Through the pancreatic parenchyma (± 65 %)
  - In a groove in the posterior aspect of the pancreatic head (± 25 %)
  - Posterior to the pancreatic head and totally extrapancreatic (± 10 %)
- If the distal common bile duct courses through the pancreatic parenchyma, it may be smaller in diameter than the suprapancreatic portion

KEY FACTS: MRI

- Diagnostic clues (Fig. 62):
  - Gradual tapering
  - Absence of mass lesion
  - Intrapancreatic site of the common bile duct on axial images
- Widening of the distalmost part of the common bile duct is sometimes observed (corresponding to the presphincteric segment that is located outside the pancreas)
- Differential diagnosis: e.g., acute or chronic pancreatitis, pancreatic neoplasms

References

Van Hoe L, Mermuys K, Vanhoenacker P (2004) MRCP pitfalls. Abdom Imaging 29 : 360 – 387

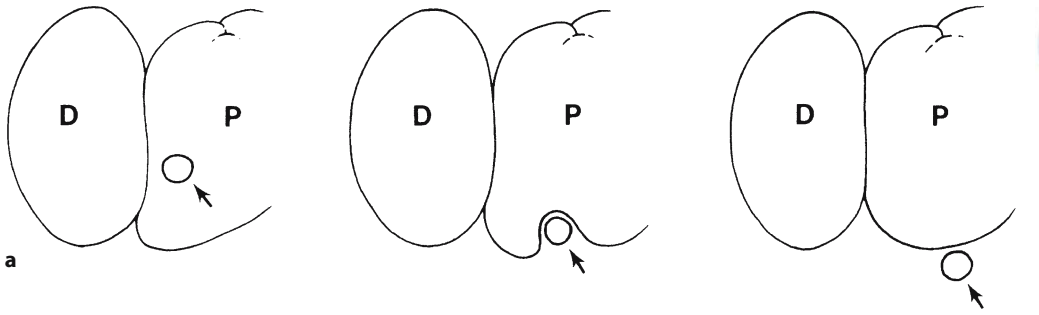

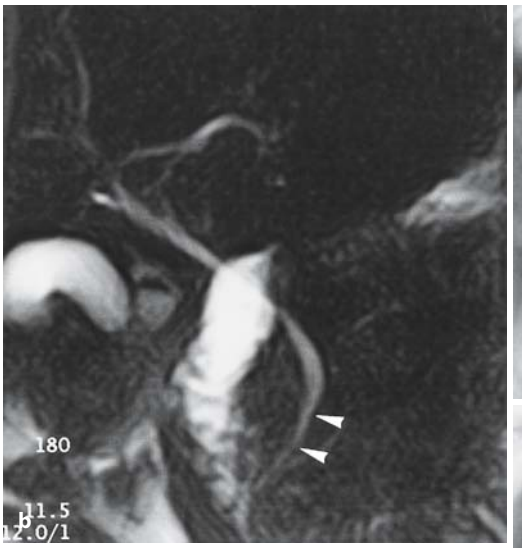

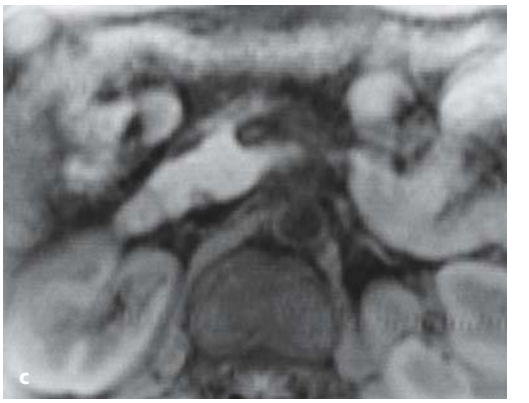

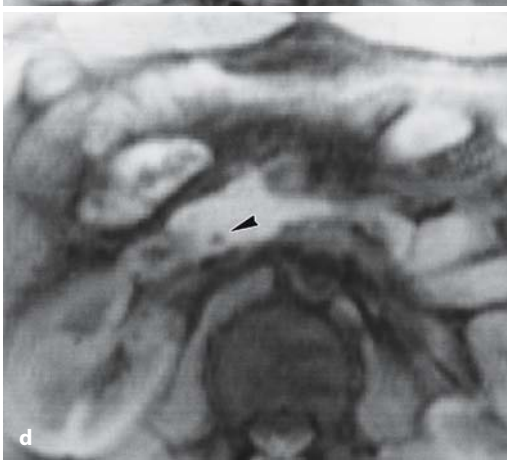

Fig. 62. **a** Variations in the anatomic relationship of the common bile duct and the head of the pancreas. *Left*, intrapancreatic course; *center*, in dorsal groove; *right*, extrapancreatic. (From Rohrman and Baron 1989, with permission). **b–d** Projective image showing apparent narrowing of the distal part of the common bile duct (*arrowheads*). **c**, **d** Axial T1-weighted images showing the intrapancreatic location of the distalmost portion of the common bile duct (*arrowhead* in **d**)

#63 Variant Anatomy (2): Location of the Bifurcation

Related topic: #82 (after cholecystectomy: stricture of the common bile duct)

KEY FACTS

- Right and left main hepatic ducts usually join up just outside the porta hepatis (± 1 cm under the edge of the liver)
- However, the site of union may be much lower:
  - In extreme cases, the right and left ducts drain separately into the duodenum
  - In individuals with low union or nonunion, the cystic duct drains into the right hepatic duct
- *Note:* Low bifurcation is clinically significant in that it carries an increased risk for injury during (laparoscopic) cholecystectomy (see Fig. 52 a)

References

Taylor AJ, Bohorfoush AG (1997) Normal anatomy of the biliary tree. In: Taylor AJ, Bohorfoush AG (eds) Interpretation of ERCP. Lippincott-Raven, Philadelphia, pp 59–76

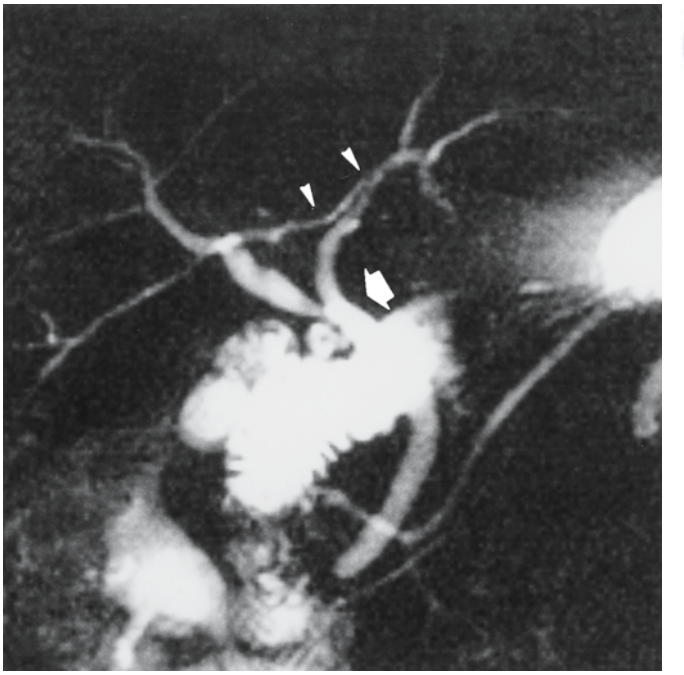

Fig. 63. Projective MR image showing low bifurcation; the cystic duct drains into the bile duct just below the bifurcation (*arrow*). Also note the right posterior hepatic duct draining into left hepatic duct (*arrowheads*) and pancreas divisum (see #140)

#64 Variant Anatomy (3): Impression by Blood Vessels

KEY FACTS: ANATOMY

- The common hepatic duct is accompanied by:
  - The portal vein (posteriorly)
  - The hepatic artery (medially)
  - The right hepatic artery and cystic artery (posteriorly)
- An aberrant cystic artery may also cross anterior to hepatic duct
- Blood vessels (usually the right hepatic artery) may cause an impression on the posterior aspect of the common hepatic duct

KEY FACTS: MRI

- MRCP may overestimate vascular impressions or falsely "create" impressions by the following mechanism:
  - Bile duct and vessel contained in one section (volume averaging)
  - Flow-related intravascular signal void reduces "overall" signal per voxel
  - Focally decreased signal intensity of a ductal segment suggests narrowing or external compression (Fig. 64b)
- Diagnostic clues:
  - Typical location and shape
  - Coronal cross-sectional images show crossing vessel (Fig. 64a)

References

Reuther G, Kiefer B, Tuchman A (1996) Cholangiography before biliary surgery: single-shot MR cholangiography versus intravenous cholangiography. Radiology 198 : 561 – 566

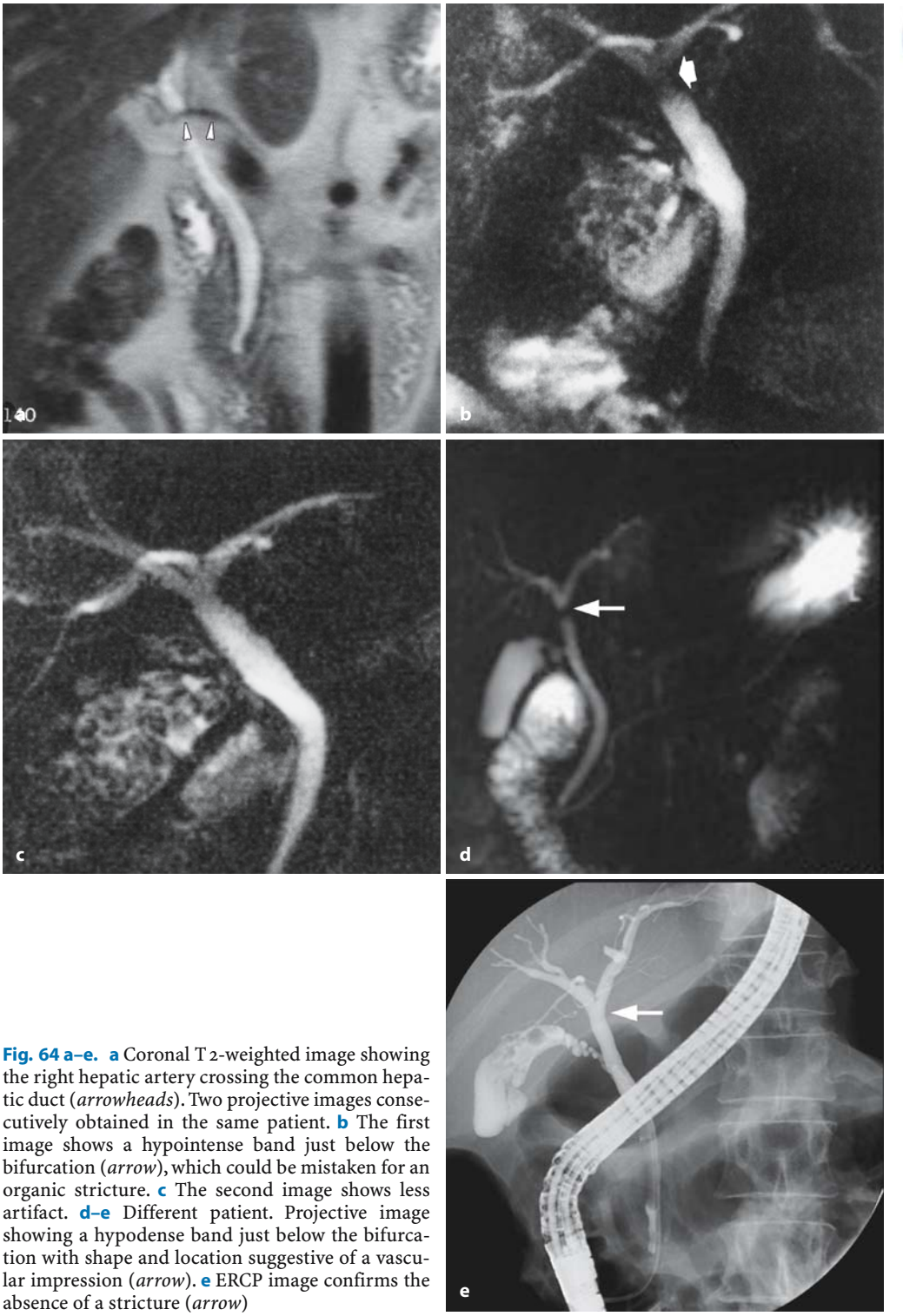

Fig. 64 a–e. **a** Coronal T 2-weighted image showing the right hepatic artery crossing the common hepatic duct (*arrowheads*). Two projective images consecutively obtained in the same patient. **b** The first image shows a hypointense band just below the bifurcation (*arrow*), which could be mistaken for an organic stricture. **c** The second image shows less artifact. **d–e** Different patient. Projective image showing a hypodense band just below the bifurcation with shape and location suggestive of a vascular impression (*arrow*). **e** ERCP image confirms the absence of a stricture (*arrow*)

#65 Postoperative Anatomy: After Hepatic Transplantation

Related topics: #80, 81 (complications after hepatic transplantation)

KEY FACTS: TECHNIQUE

- Three types of biliary anastomoses exist:
  - Choledocho-choledochostomy (Fig. 65) (most common type)
  - Choledochojejunal anastomosis
  - Choledocho-cholecysto-choledochal anastomosis (least common type)
- The gallbladders are usually removed
- Both cystic duct stumps are usually preserved
- Nonobstructive dilation is common:
  - Usually occurs in the initial postoperative period
  - Generally does not resolve with time
  - Mean donor dilation: 0.8 mm (in 15% of patients more than 3 mm)
  - Possible mechanisms: low-grade ischemia; postcholecystic reservoir effect; dysfunction of the vaterian sphincter complex (damage to neural reflex arcs)
- Size mismatch between the donor and the native common bile duct is also common

KEY FACTS: MRI

- Normal variants that may mimic disease (Fig. 65b):
  - Size mismatch
  - Mild, nonobstructive dilation of donor and/or native extrahepatic duct
- Differential diagnosis with pathologic narrowing:
  - Lack of dilation of intrahepatic bile ducts
  - Liver function tests

References

Campbell WL, Foster RG, Miller WJ, Lecky JW, Zajko AB, Lee KY (1992) Changes in intrahepatic bile duct caliber in liver transplant patients without evidence of biliary obstruction. AJR Am J Roentgenol 158 : 997 – 1000

Silvis S, Rohrmann C, Ansel H (eds) (1995) Endoscopic retrograde cholangiopancreatography. Igaku-Shoin, New York, p 289

Zoepf T, Maldonado-Lopez EJ, Hilgard P, et al. (2005) Diagnosis of biliary strictures after liver transplantation: which is the best tool? World J Gastroenterol 11 : 2945 – 2948

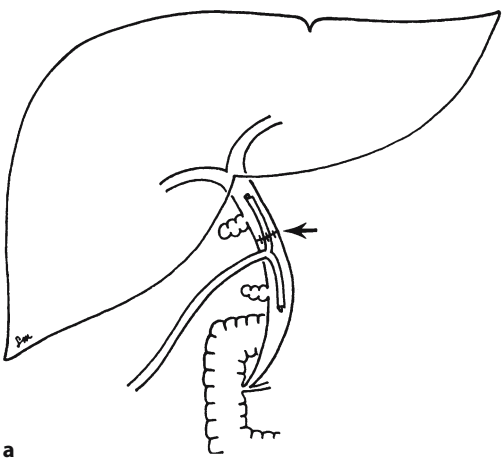

a

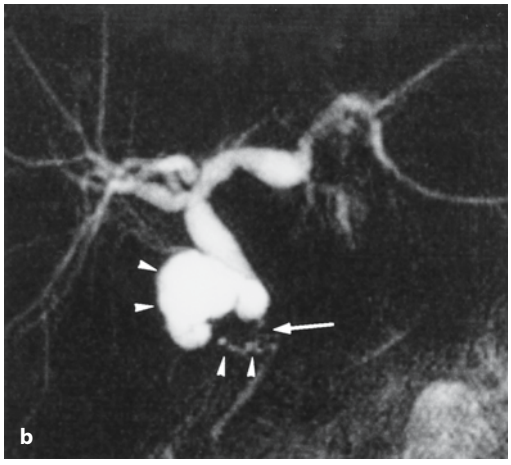

b

Fig. 65. **a** Choledocho-choledochal anastomosis in hepatic transplantation. The anastomosis is located in between the two cystic duct stumps. *Note:* The use of a T tube is not universal. (Reprinted with permission from Silvis et al. 1995). **b** Projective MR image obtained a few days after hepatic transplantation showing marked size mismatch between donor and native common bile duct, as well as between the two cystic duct remnants (*arrowheads*). Also note apparent narrowing of anastomosis (*arrow*), most likely related to edema. Clinically and biochemically, there were no signs of biliary obstruction

#66 Postoperative Anatomy: After the Whipple Procedure

Related topic: #29 (postoperative anatomy: after hepat(ic)ojejunostomy)

KEY FACTS: TECHNIQUE

- Types:
  - *Classical Whipple* operation: radical pancreaticoduodenectomy with removal of the pancreatic head, associated biliary tree, duodenum, and gastric antrum
  - *Modified Whipple* procedure: the pylorus and first portion of the duodenum are left intact. The advantages of the modified procedure include maintenance of intact gastric reservoir capacity and decreased incidence of jejunal ulceration and bile reflux
- The following anastomoses are made (Fig. 66 a):
  - Hepaticojejunostomy
  - Pancreatojejunostomy
  - Duodenojejunostomy
- Indications:
  - Resection of tumor located in right hemipancreas
  - Diversion of bile system or main pancreatic duct

KEY FACTS: MRI

- The hepatojejunal and pancreatojejunal anastomoses are usually clearly visible (Fig. 66 b)
- Criteria for a normal anastomosis: see #29
- Critical elements of technique: administration of oral contrast agent (e.g., tap water) and spasmolytic drug
- Good distention of the jejunal loop enables recognition of the following:
  - Normal valvulae conniventes (important to differentiate jejunum from a mass, pseudocyst, etc.)
  - Exact location of the anastomosis

References

Schopohl J, Zöckler CE, Draese K (1986) Modified Whipple surgical procedure. Chirurg 57 : 517 – 521

Taylor AJ, Bohorfoush AG (1997) Interpretation of ERCP. Lippincott-Raven, Philadelphia, p 298

Trerotola SO, Jones B, Crist DW, Cameron JL (1989) Pylorus-preserving Whipple pancreaticoduodenectomy: postoperative evaluation. Radiology 171 : 735 – 738

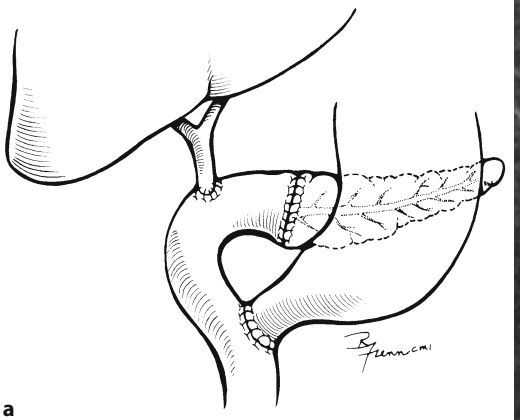

a

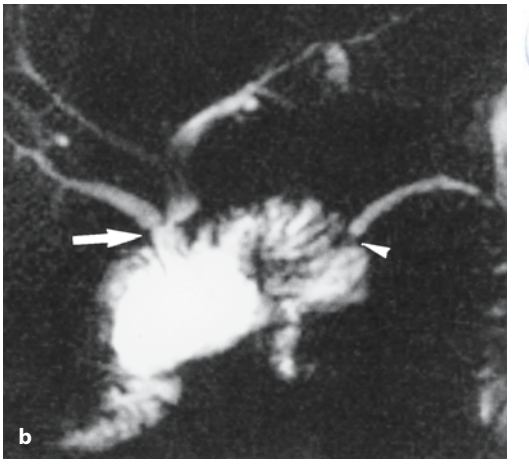

b

Fig. 66. **a** Modified Whipple procedure. (Reprinted with permission from Taylor and Bohorfoush 1997). **b** Projective image showing normal aspect of hepaticojejunal (*arrow*) and pancreatojejunal (*arrowhead*) anastomoses

#67 Aerobilia

Related topic: # 73 (stones in the common bile duct: pitfalls in diagnosis)

KEY FACTS: GENERAL

- Causes:
  - ERCP/PTC (most common)
  - Biliary surgery
  - Bilioenteric fistulas (see # 103)
  - Patent papilla (see Fig. 124)

KEY FACTS: MRI

- Signal void (absence of protons)
- Differentiation from stones:
  - Appearance: often more elongated, margins less clear
  - Presence of an air–fluid level on axial images (most reliable sign) (Fig. 67)
  - Change in shape/location after patient repositioning (ventral versus dorsal decubitus)
- *Note:* MRI underestimates aerobilia compared to CT; in some patients with large amounts of air, however, susceptibility may mimic bile duct stenoses at projective MRCP (Fig. 67 c, d)

References

Irie H, Honda H, Kuroiwa T et al. (2001) Pitfalls in MR cholangiopancreatographic interpretation. Radiographics 21 : 23 – 37

Reinhold C, Bret P (1996) MR cholangiopancreatography. Abdom Imaging 21 : 105 – 116

Van Hoe L, Mermuys K, Vanhoenacker P (2004) MRCP pitfalls. Abdom Imaging 29 : 360 – 387

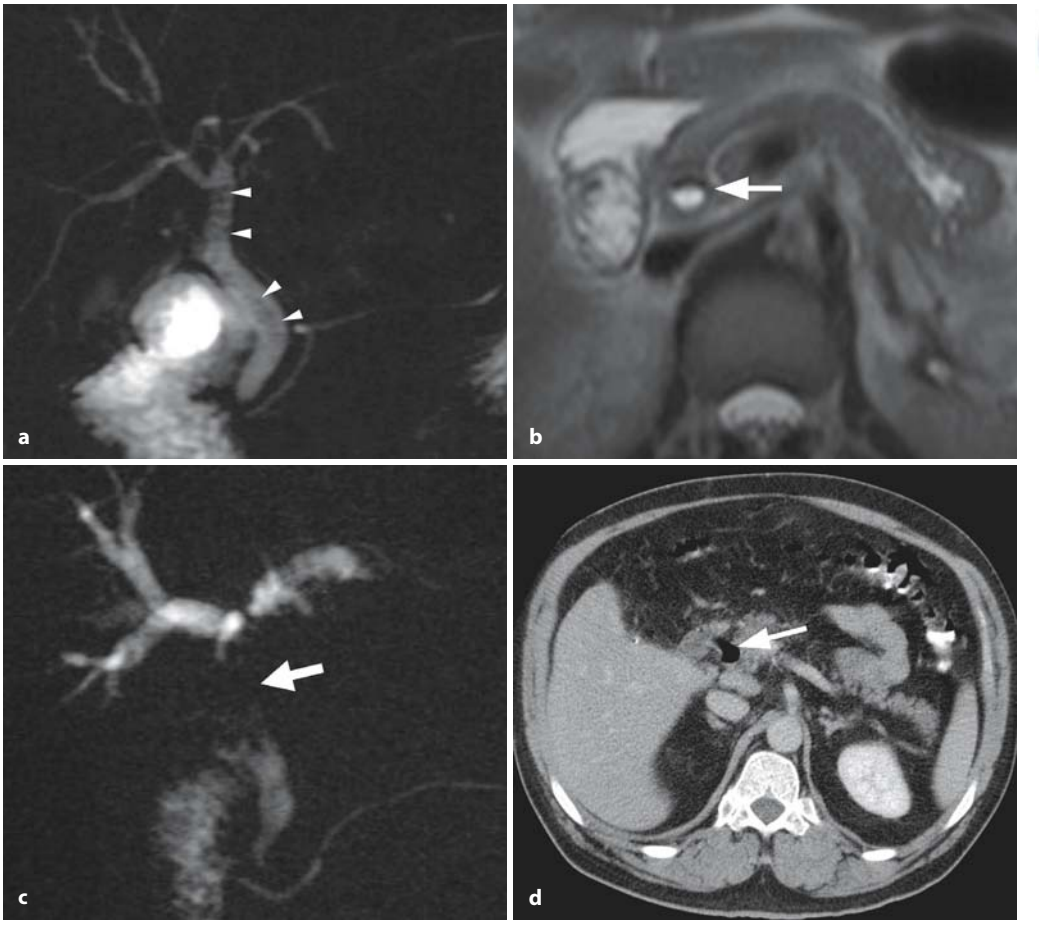

Fig. 67 a–d. **a** Projective image showing multiple uniform rounded areas of signal void in the common bile duct and the common hepatic duct (*arrowheads*). **b** Axial T2-weighted HASTE image (TE 60) showing an air–fluid level in the common bile duct (*arrow*), diagnostic of intraluminal air. **c, d** Different patient. Projective image showing a large area of signal loss in the common hepatic duct (*arrow*). **d** Axial CT image showing air in the common bile duct (*arrow*). Extensive aerobilia was the cause of the signal loss at MRI

3.2 Benign Nontraumatic Abnormalities

#68 Developmental Abnormalities (1): Choledochal Cyst

Related topics: #30 (Caroli's disease), #126 (choledochocele)

KEY FACTS: DISEASE

- Cystic dilation of the extrahepatic bile duct (type I bile duct cyst; see #30)
- 50 % – 80 % of bile duct cysts
- Patients present during childhood or adolescence
- Ratio of women to men: 3 : 1
- Etiology: anomalous junction of the pancreatic duct and common bile duct (long common channel; see also #123)
- Mechanism: free reflux of pancreatic enzymes in the biliary tree with weakening of the wall of the common bile duct
- Associations:
  - Dilation/stenosis or atresia of other portions of biliary tract
  - Gallbladder anomalies
  - Polycystic liver disease
  - Gallbladder carcinoma
- Complications:
  - Stones in the common bile duct (8 % – 70 %)
  - Recurrent pancreatitis (1 % – 34 %)
  - Cholangitis (20 %)
  - Malignant transformation (3 % – 28 %; age, > 20 years)
  - Biliary cirrhosis (1 % – 13 %)
  - Rupture with bile duct peritonitis (1.8 %)
  - Bleeding
- *Note:* The choledochal cysts seen in neonates with biliary atresia (#69) are considered to represent a separate entity

KEY FACTS: MRI

- Typical features:
  - Markedly dilated extrahepatic bile duct
  - The hallmark is a long common channel (Fig. 68 a – f)
  - No or only mild intrahepatic bile duct dilation; abrupt changes of caliber
  - Usually saccular in configuration
- Irregular ductal contours may herald malignant degeneration

!

References

De Wilde V, Elewaut A, De Vos MP, Hendrix R, Barbier F (1991) Choledochal cysts in the adult. Endoscopy 23 : 4 – 7

Fulcher AS, Turner MA (1999) MR pancreatography: a useful tool for evaluating pancreatic disorders. Radiographics 19 : 5 – 24

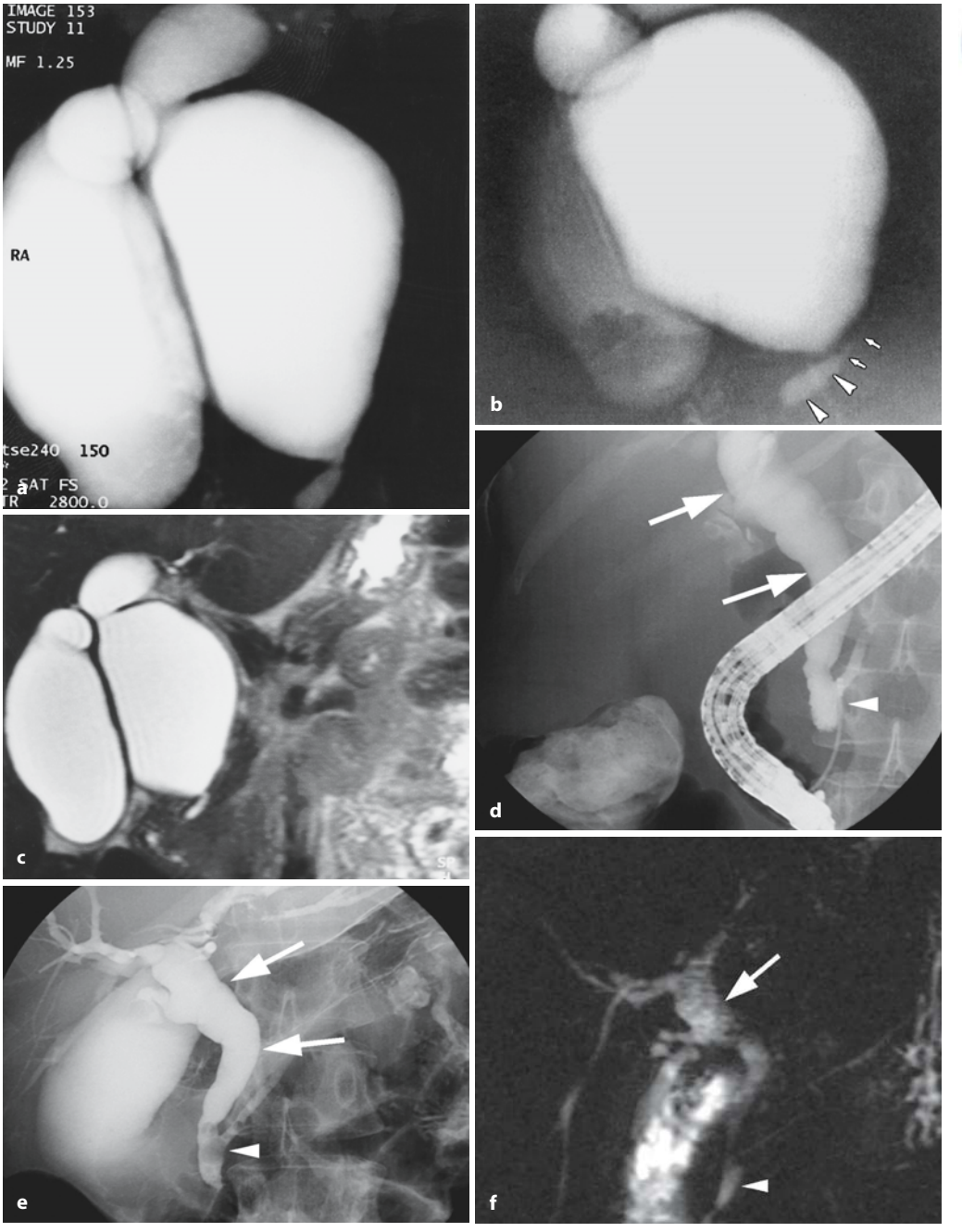

Fig. 68 a–f. **a, b** Projective MR images showing marked saccular dilation of the common bile duct. The pancreatic duct joins the common bile duct just below the dilated segment (*arrows* in **b**). Note the long common channel (*arrowheads*). Also note the dilated gallbladder containing a stone. **c** Same patient. Coronal cross-sectional image showing the position of a choledochal cyst in relation to the liver. **d–f** Different Patient. ERCP images showing a fusiform dilatation of the common bile duct and the common hepatic duct (*arrows*) compatible with a type I bile duct cyst. Note long common channel (*arrowhead*) and aerobilia (*arrowhead* in e). **f** Projective image showing dilated common hepatic duct (*arrow*) and long common channel (*arrowhead*). Image quality is suboptimal due to aerobilia and respiratory artifact

#69 Developmental Abnormalities (2): Atresia

KEY FACTS: DISEASE

- Progressive inflammation, fibrosis, and obliteration of bile ducts
- Most common cause of chronic cholestasis in infants and children
- Classification:
  - Type I: atresia of the distal part of the common bile duct
  - Type II: atresia of the extrahepatic duct; normal bifurcation and intrahepatic ducts
  - Type III (most common): disease extending proximally into the porta hepatis
- Associated disease: developmental choledochal cyst of the neonate
- Symptoms: jaundice, pale stools
- Diagnosis: hepatobiliary scintigraphy (sensitivity up to 97%, lower specificity)
- Treatment:
  - Correctable type (type I and II): hepaticojejunostomy
  - Uncorrectable type (type III): usually Kasai operation: hepatic *porto*jejunostomy (anastomosis between jejunal limb and cut surface of the fibrous mass replacing the hepatic duct radicles at the porta hepatis)
  - Liver transplantation
- Complications (occurring even in patients with "successful" bilioenteric anastomoses):
  - Chronic cholangitis
  - Extensive hepatic fibrosis
  - Portal hypertension
- Differential diagnosis (clinical): neonatal cholangitis
- *Note:* True *agenesis* of extrahepatic bile ducts is rare

KEY FACTS: MRI

- Typical features:
  - No visualization of extrahepatic bile duct
  - "Periportal thickening" (corresponding to periportal fibrosis)
- Remarks:
  - Knee or surface coils should be used as much as possible (high-resolution imaging)
  - Atresia can only be ruled out if the *entire* extrahepatic bile duct is identified
  - Evaluation on the integrity of the intrahepatic ducts in infants is difficult because normal ducts are barely visible at MRI
  - MRI may beuseful for postoperative follow up (Fig. 69 a, b)

References

Engelskirchen R, Holschneider AM, Gharib M, Vente C (1991) Biliary atresia – a 25 year survey. Eur J Pediatr Surg 1:154–160

Guibaud L, Lachaud A, Touraine R et al. (1998) MR cholangiography in neonates and children: feasibility and preliminary applications. AJR Am J Roentgenol 170:27–31

Kasai M, Suzuki H, Ohashi E, Ohi R, Chiba T, Okamoto A (1978) Technique and results of operative management of biliary atresia. World J Surg 2:571–580

Krause D, Cercueil JP, Dranssart M et al. (2002) MRI for evaluating congenital bile duct abnormalities. J Comput Assist Tomogr 26:541–552

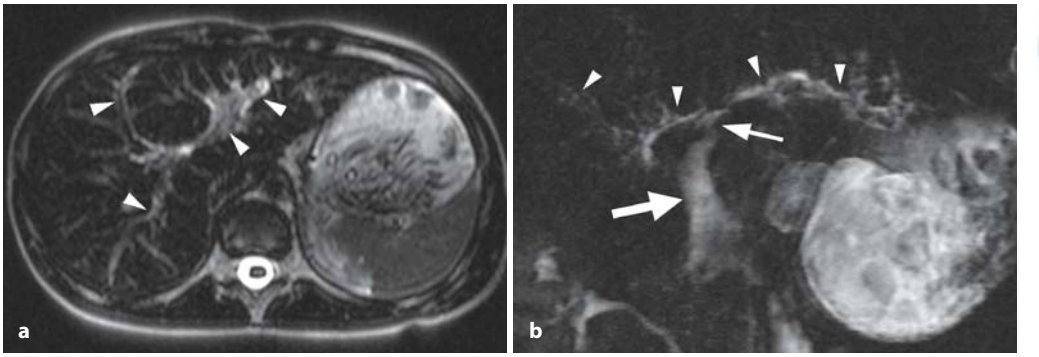

Fig. 69 a, b. Patient with biliary atresia treated by Kasai operation. **a** Axial T2-weighted HASTE image (TE 360) showing discrete dilatation of the left intrahepatic bile ducts (*arrowheads*). **b** Projective image showing the jejunal limb (*large arrow*) and the anastomosis (*small arrow*) due to the Kasai operation. The intrahepatic bile ducts are markedly irregular (*arrowheads*) with discrete dilatation of the left intrahepatic bile duct. These findings are due to chronic cholangitis and hepatic fibrosis secondary to the atresia, and are commonly observed, even after successful bilioenteric anastomosis

#70 Web

Related topic: #73 (stones in the common bile duct: pitfalls in diagnosis)

KEY FACTS

- Valvulae in the common bile duct
- Histology: folds or plates containing fibrous and muscular tissue with a redundant epithelial surface
- Rare

KEY FACTS: MRI

- Typical features:
  - Less than 1 mm thick
  - Elongated aspect
  - Sharply marginated
  - Not completely surrounded by bile
- Remarks:
  - The MRCP appearance of a web may differ from its ERCP appearance (absence of distention in MRCP) (Fig. 70)
  - Occasionally, differentiation between a web and a stone may be difficult (see Fig. 73)

References

Belsito AA, Cramer GG, Dickinson PB (1977) Normal biliary tree. In: Stewart E, Vennes J, Geenen J (eds) Atlas of endoscopic retrograde cholangiopancreatography. Mosby, Saint Louis, pp 88–123

Dolar ME, Ates KB, Dalay AR, Caner ME, Sasmaz N, Sahin B (1993) Congenital stricture of the common hepatic duct due to a web: an unusual case without jaundice. Hepatogastroenterology 40:194–195

Papaziogas B, Lazaridis C, Pavlidis T et al. (2002) Congenital web of the common bile duct in association with cholelithiasis. J Hepatobiliary Pancreat Surg 9:271–273

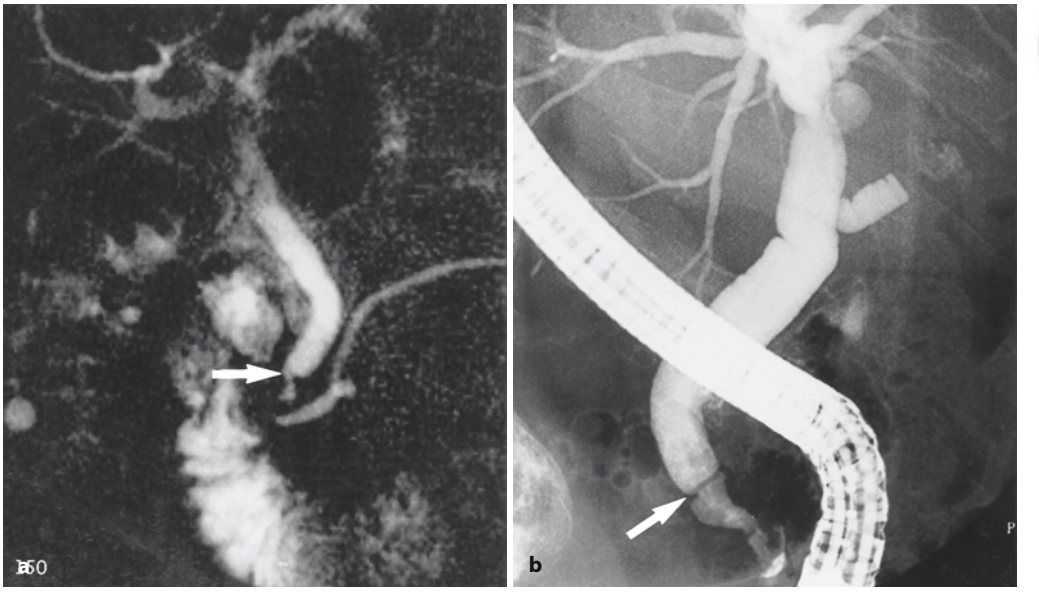

Fig. 70 a, b. **a** Projective MR image and **b** ERCP image showing web in the distal common bile duct (*arrows*). Note collapse of the distal segment of the common bile duct in **a**, resulting in a different morphologic appearance of the web

#71 Mirizzi Syndrome

KEY FACTS: DISEASE

- Extrinsic right-sided compression of the common bile duct by a large gallstone impacted in the cystic duct, gallbladder neck, or cystic duct remnant, accompanied by chronic inflammatory reaction
- Types:
  - Type 1: simple type
  - Type 2: fistula between the gallbladder and common hepatic duct
- More common in patients with anomalous low insertion of the cystic duct into the common hepatic duct with a parallel course of the ducts
- Associated disease: gallbladder carcinoma (see #22; Miller and Sica 1996)

KEY FACTS: MRI

- Typical features:
  - Type 1: smooth, focal, laterally scalloped narrowing of the common bile duct caused by a stone in the gallbladder neck/cystic duct (Fig. 71a, b)
  - Type 2: stone located at the junction of the cystic duct and common hepatic duct, partially located within the bile duct; no smooth lateral compression (Fig. 71c–f)
  - In both types, infiltration of fat surrounding the junction may be seen (inflammation)
- The presence of a soft tissue mass around the cystic duct and/or in the hepatic portal should arouse suspicion of associated neoplastic disease (usually gallbladder carcinoma; see #22)
- Differential diagnosis of smooth extrinsic bile duct narrowing: extrinsic inflammatory process, acute cholecystitis with gallbladder enlargement, pancreatic pseudocysts, choledochal varices

References

Binmoeller KF, Thonke F, Soehendra N (1993) Endoscopic treatment of Mirizzi's syndrome. Gastrointest Endoscop 39:532–536

Koehler RE, Melson GL, Lee JK, Long J (1979) Common hepatic duct obstruction by cystic duct stone: Mirizzi syndrome. AJR Am J Roentgenol 132:1007–1009

Miller FH, Sica GT (1996) Mirizzi syndrome associated with gallbladder cancer and biliary-enteric fistulas. Case report. AJR Am J Roentgenol 167:95–97

Redaelli CA, Buchler MW, Schilling MK et al. (1997) High coincidence of Mirizzi syndrome and gallbladder carcinoma. Surgery 121:58–63

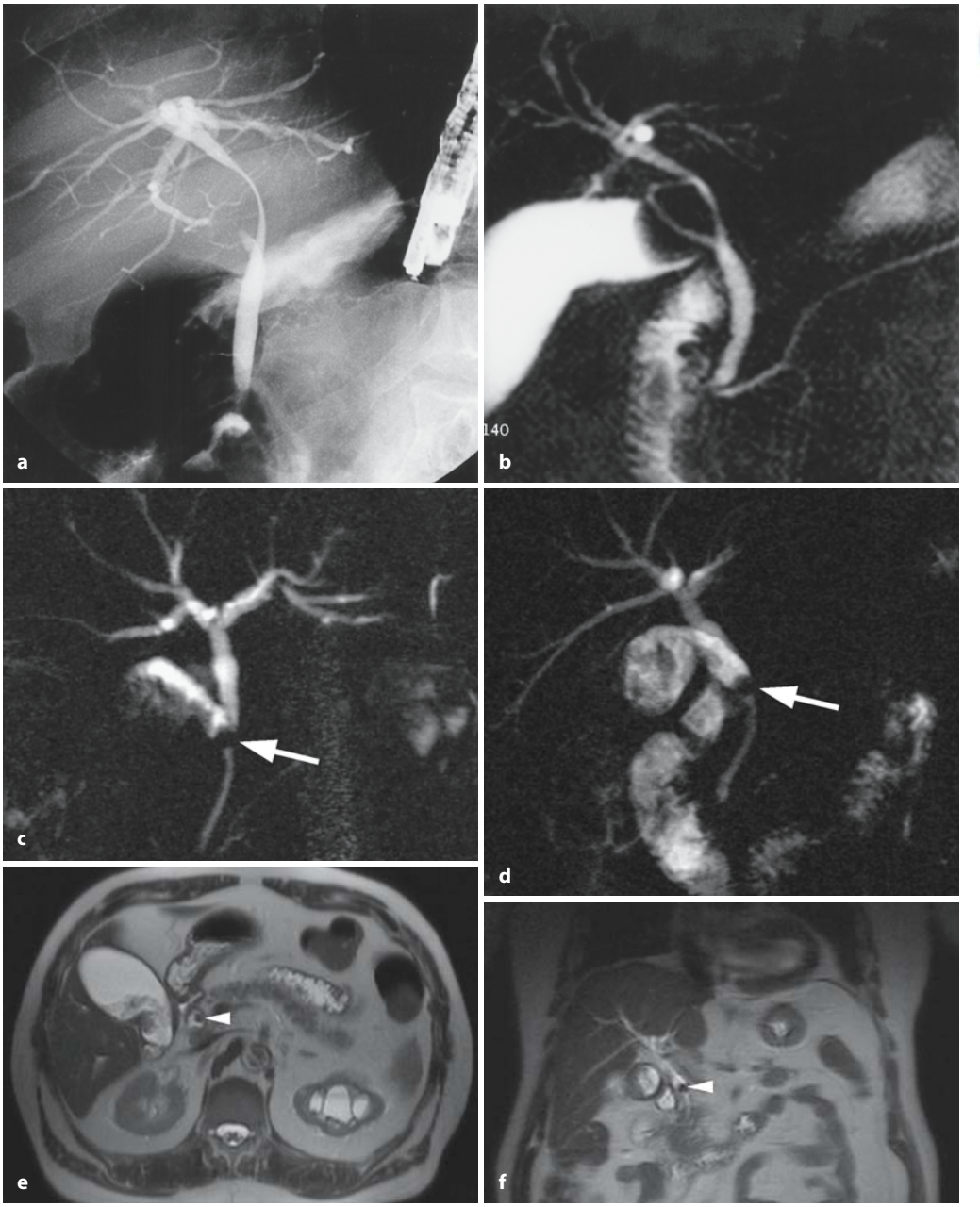

Fig. 71 a–f. Type I Mirizzi syndrome. **a** ERCP image showing smooth lateral impression on the extrahepatic bile duct. **b** Projective MR image showing an impacted stone in the gallbladder neck **c–f**. Type II Mirizzi syndrome. **c, d** Projective image showing an impacted stone at the junction of the cystic duct and common hepatic duct (*arrow*) with secondary obstruction and intrahepatic bile duct dilatation. **e, f** Axial (**e**) and coronal (**f**) T2-weighted HASTE image (TE 60) showing the impacted stone at the junction (*arrowhead*)

#72 Stones in the Common Bile Duct

Related topics: #33 (intrahepatic bile duct lithiasis), #125 (vaterian sphincter complex, impacted stone)

KEY FACTS: DISEASE

- Most common cause of bile duct obstruction
- Found in 12 % – 15 % of patients undergoing cholecystectomy
- Types:
  - In Western countries, most (95 % of) patients with choledocholithiasis have *secondary* choledocholithiasis, i. e., the stones have migrated from the gallbladder into the common bile duct
  - *Primary* choledocholithiasis is found in individuals of Asian or Eastern cultures and is associated with parasitic infection
- Predisposing factors:
  - Cholecystolithiasis
  - Bile duct stenosis
  - Dysfunction of the vaterian sphincter complex (see # 127)
- Associated disease: cholangitis
- Symptoms (75 %): jaundice, chills, fever
- Complications:
  - Acute pancreatitis (see # 151)
  - Duct stricture
  - Fistula (e. g., bilioenteric; see # 74)
  - Bacterial cholangitis (see # 75)
  - Liver abscess (see # 40)
  - Secondary sclerosing cholangitis (see # 45)

KEY FACTS: MRI

- MR is highly accurate in the diagnosis of bile duct lithiasis (Topal et al. 2003; Tayler et al. 2002; Kim et al. 2002)
- The large majority of stones are seen as T 1- and T 2-hypointense structures surrounded by bile
- Differential diagnosis: aerobilia (see # 67)
- Pitfalls: see # 73
- *Note:* 20 % – 35 % of stones occur in nondilated ducts (Reinhold and Bret 1996)

References

Kim TK, Kim BS, Kim JH et al. (2002) Diagnosis of intrahepatic stones: superiority of MR cholangiopancreatography over endoscopic retrograde cholangiopancreatography. AJR Am J Roentgenol. 179 : 429 – 434Reinhold C, Bret PM (1996) Current status of MR cholangiopancreatography. AJR Am J Roentgenol 1285 – 1295

Taylor AC, Little AF, Hennessy OF et al. (2002) Prospective assessment of magnetic resonance cholangiopancreatography for noninvasive imaging of the biliary tree. Gastrointest Endosc 55 : 17 – 22

Topal B, Van de Moortel M, Fieuws S et al. (2003) The value of magnetic resonance cholangiopancreatography in predicting common bile duct stones in patients with gallstone disease. Br J Surg 90 : 42 – 47

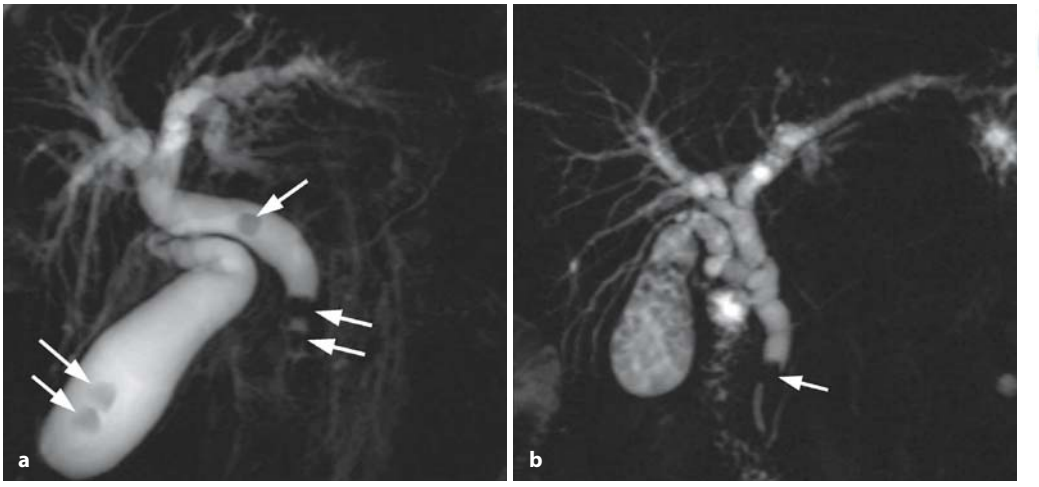

Fig. 72. **a** Projective image showing several stones in the gallbladder and in the common bile duct (*arrows*) **b** Different patient. Projective image showing multiple small stones in the gallbladder and an impacted stone in the distal common bile duct (*arrow*), with secondary bile duct dilatation

#73 Stones in the Common Bile Duct (2): Pitfalls in Diagnosis with MRCP/ERCP

Related topics: #67 (aerobilia), #70 (web), #125 (impacted stone), #122 (vaterian sphincter complex, pseudocalculus sign)

KEY FACTS

- False-negative diagnoses on MRCP are usually caused by a lack of fluid surrounding the stone:
  - Lack of ductal distention (e.g., primary sclerosing cholangitis, intermittent obstruction)
  - Stone impacted in sphincteric segment (see #125)
  - Very large stone; multiple stones with or without sludge
- Causes of a false-positive diagnosis on MRCP:
  - Bile duct web (rare) (see #70 and Fig. 73a, b)
  - Inverted sphincteric segment ("pseudocalculus sign"; see #122)
  - Aerobilia (see #67)
  - Flow artifact (Sugita et al. 2003; Van Hoe et al. 2004)
- Causes of a false-negative diagnosis on ERCP:
  - Small stone invisible due to overfilling/superimposition of contrast medium (intrinsic limitation of projective technique)
  - Proximal displacement of stones during filling with contrast medium (Fig. 73c–d)

References

Irie H, Honda H, Kuroiwa T et al. (2001) Pitfalls in MR cholangiopancreatographic interpretation. Radiographics 21 : 23 – 37

Sugita R, Sugimura E, Itoh M et al. (2003) Pseudolesion of the bile duct caused by flow effect: a diagnostic pitfall of MR cholangiopancreatography. AJR Am J Roentgenol. 180 : 467 – 471

Van Hoe L, Mermuys K, Vanhoenacker P (2004) MRCP pitfalls. Abdom Imaging 29 : 360 – 387

Watanabe Y, Dohke M, Ishimori T et al. (1999) Diagnostic pitfalls of MR cholangiopancreatography in the evaluation of the biliary tract and gallbladder. Radiographics 19 : 415 – 429

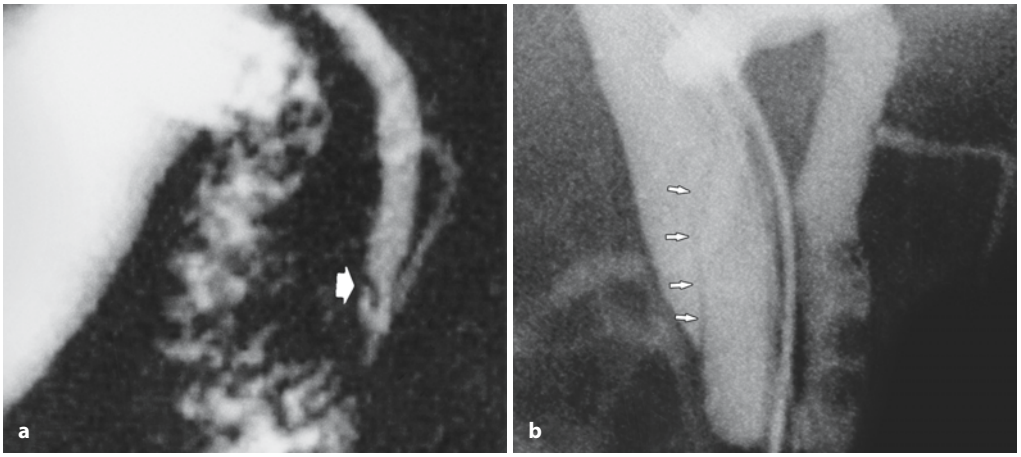

Fig. 73a–f. **a** Projective MR image showing hypointense elongated structure in the distal common bile duct (*arrow*), which was initially interpreted as lithiasis. **b** ERCP showing that this lesion represented a web (*arrows*).

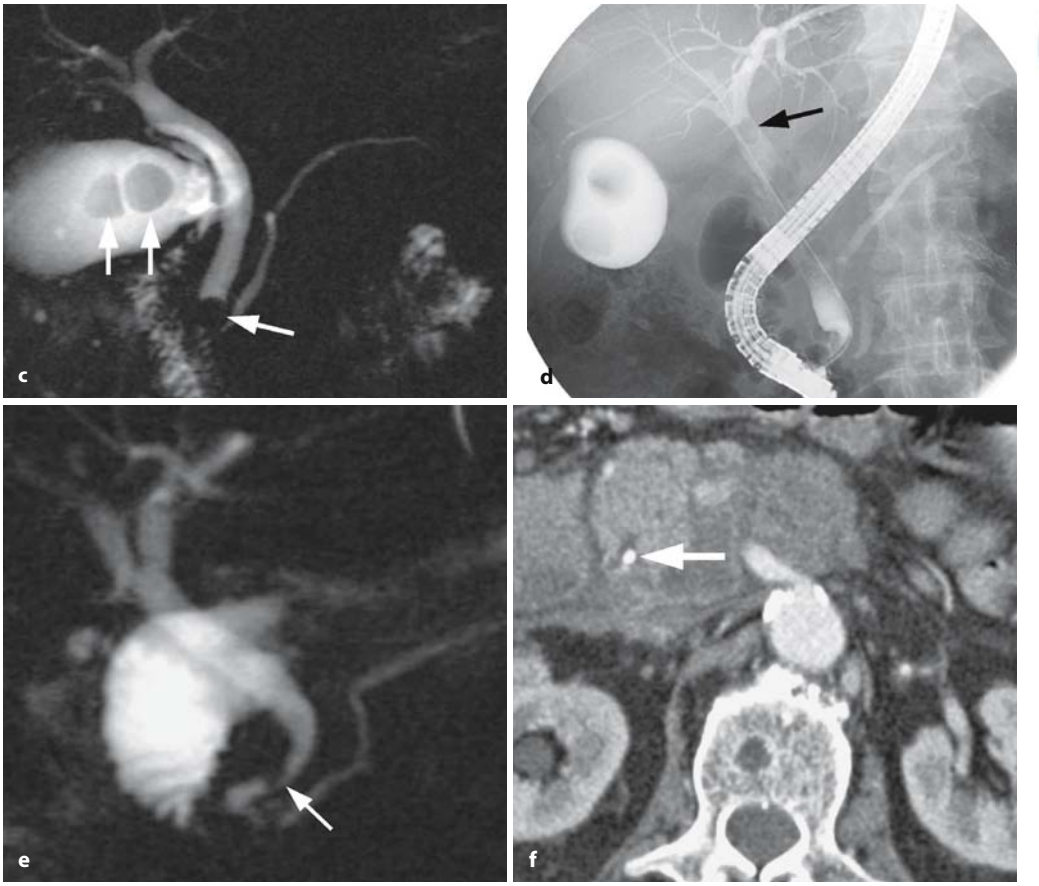

Fig. 73. (*continued*) **c, d** Different patient. Projective image showing two large stones in the gallbladder and an impacted stone in the distal common bile duct (*arrows*). **d** ERCP image shows no stone in the distal common bile duct; the stone now has a more proximal position (*arrow*). **e, f** Different patient. Projective image showing a hypointense structure along the medial wall of the distal common bile duct (*arrow*), not quite typical for a stone. **f** CT image shows heavily calcified bile duct stone (*arrow*)

#74 Stones Complicated by Fistula

Related topic: #166 (complications of chronic pancreatitis)

KEY FACTS: DISEASE

- Fistulas occur in up to 7% of patients with common bile duct stones
- Most common types (decreasing order of frequency):
  - Choledochoduodenal fistula
  - Choledochogastric fistula
  - Choledochojejunal fistula
  - Choledochocolonic fistula
  - Choledochopleural fistula
- Other causes of fistula with the common bile duct:
  - Peptic ulcer disease
  - Hepatic hydatid disease (Ponchon et al. 1989)
  - Trauma (usually surgical)
  - Gallbladder disease (see #103)

KEY FACTS: MRI

- In typical cases, fistulas are seen as bandlike T2-hyperintense structures communicating with the common bile duct (Fig. 74)
- Small fistulas containing air rather than fluid are probably more difficult to visualize
- *Note:* If significant periductal inflammation is present, fistulas may be difficult to assess with projective MRCP; in such cases, heavily T2-weighted cross-sectional images are quite useful to avoid superimposition of fluid/edema (Fig. 74)

References

Ikeda S, Okada Y (1975) Classification of choledochoduodenal fistula and its etiological significance. Gastroenterology 69 : 130 – 137

Ponchon T, Gallez JF, Valette PJ, Chavaillon A, Bory R (1989) Endoscopic treatment of biliary tract fistulas. Gastrointest Endoscop 35 : 490 – 498

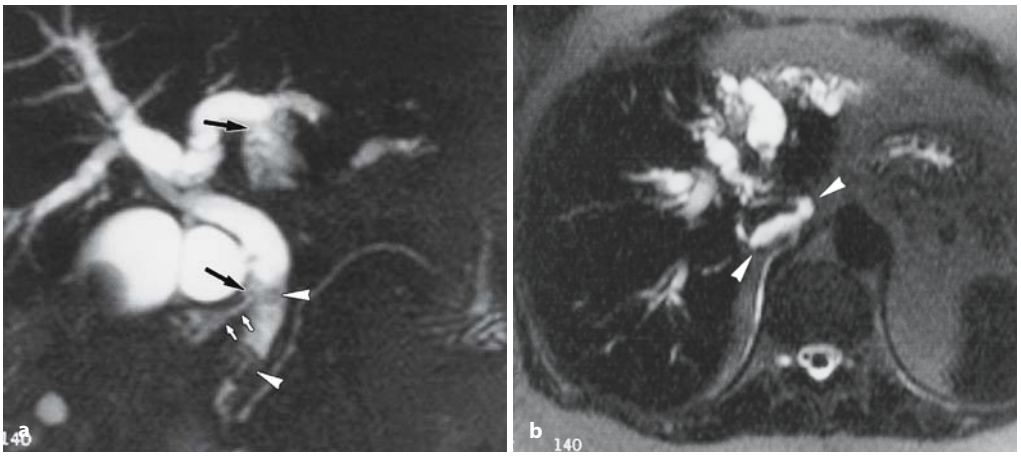

Fig. 74 a, b. **a** Projective MR image showing stones in the distal common bile duct (*arrowheads*) and rupture of both the left intrahepatic bile duct and the common bile duct (*arrows*). **b** Heavily T2-weighted axial image showing presence of fluid around the vena cava and in the proximity of the right diaphragmatic crus (*arrowheads*)

#75 Bacterial Cholangitis

Related topic: #40 (intrahepatic bile ducts: bacterial cholangitis)

KEY FACTS: DISEASE

- See #40

KEY FACTS: MRI

- Typical feature: mucosal irregularities (Fig. 75)
- *Note:* MRCP is less sensitive than ERCP in the detection of subtle abnormalities (lack of distention)
- Differential diagnosis:
  - Primary sclerosing cholangitis (see #76)
  - Bile duct varices (may cause narrowing with an undulated aspect; see #79)

References

Bader TR, Braga L, Beavers KL, Semelka RC (2001) MR imaging findings of infectious cholangitis. Magn Reson Imaging 19:781–788

Sinanan MN (1992) Acute cholangitis. Infect Dis Clin North Am 6:571–599

Taylor AJ, Bohorfoush AG (1997) Inflammation of the biliary tract. In: Taylor AJ, Bohorfoush AG (eds) Interpretation of ERCP. Lippincott-Raven, Philadelphia, pp 77–125

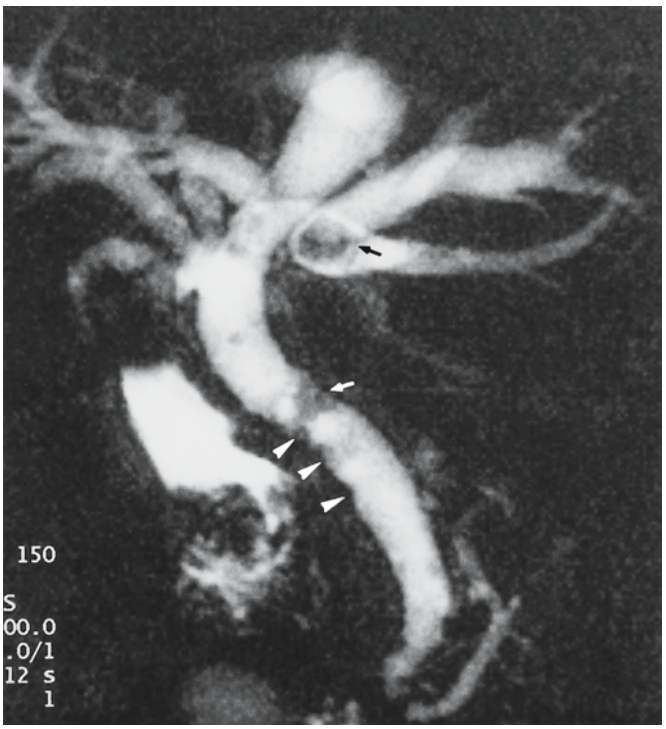

Fig. 75. Projective image showing irregular contours of the common bile duct (*arrowheads*). Also note the presence of two stones (*arrows*)

#76 Primary Sclerosing Cholangitis

Related topics: #41–44 (intrahepatic bile ducts, primary sclerosing cholangitis)

KEY FACTS: DISEASE

- See #41–44

KEY FACTS: MRI

- Typical findings in different stages of disease (Fig. 76a; Majoie et al. 1991):
  - Type I: marginal irregularities (differential diagnosis with cholangitis)
  - Type II: focal stenosis (if solitary, differential diagnosis with cholangiocarcinoma, metastasis, traumatic stricture)
  - Type III: diffuse, irregular narrowing (differential diagnosis with sclerosing carcinoma, metastases)
  - Type IV: diverticular outpouchings, sacculations (typical)
- Key features:
  - Usually multiple strictures
  - Relative lack of dilation proximal to a stricture
  - Involvement of intra- and extrahepatic ducts

References

Chapman RW (1991) Aetiology and natural history of primary sclerosing cholangitis – a decade of progress? Gut 32 : 1433–1435

Fulcher AS, Turner MA, Franklin KJ et al. (2000) Primary sclerosing cholangitis: evaluation with MR cholangiography – a case-control study. Radiology 215 : 71–80

MacCarty RL, LaRusso NF, Wiesner RH, Ludwig J (1983) Primary sclerosing cholangitis: findings on cholangiography and pancreatography. Radiology 149 : 39–44

Majoie CB, Reeders JWAJ, Sanders JB, Huibregtse K, Jansen PLM (1991) Primary sclerosing cholangitis: a modified classification of cholangiographic findings. AJR Am J Roentgenol 157 : 495–497

Vitellas KM, Keogan MT, Freed KS et al. (2000) Radiologic manifestations of sclerosing cholangitis with emphasis on MR cholangiopancreatography. Radiographics 20 : 959–975

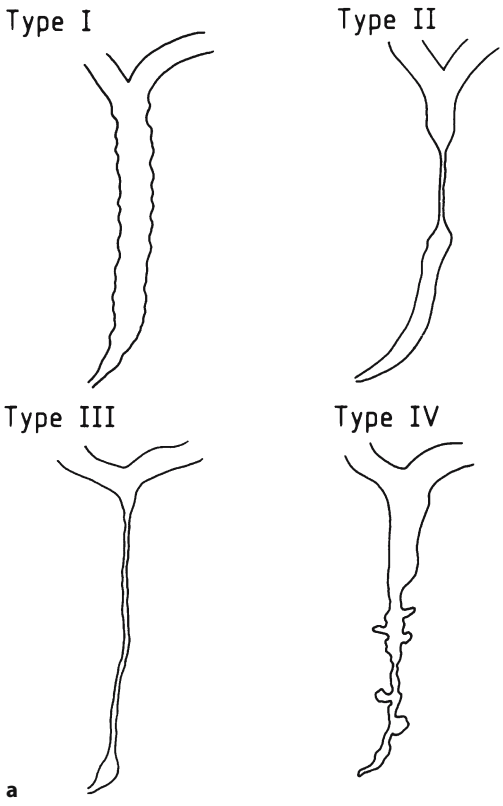

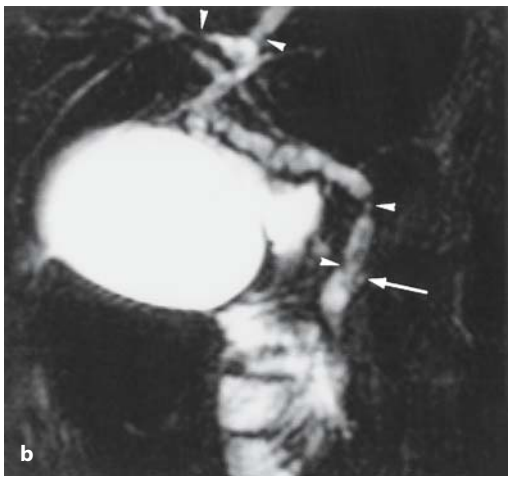

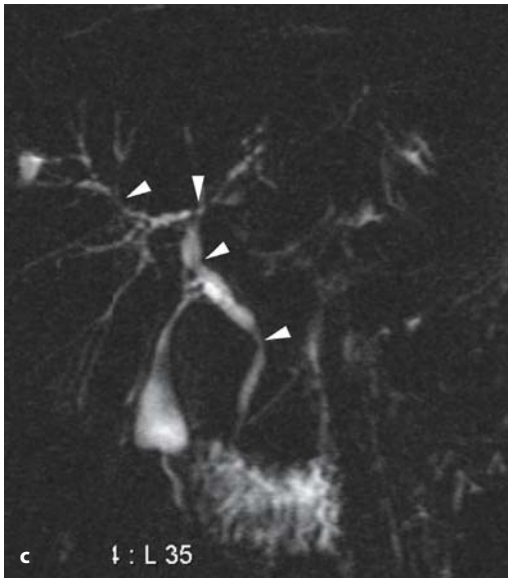

Fig. 76. **a** Type I–IV cholangiographic abnormalities. **b** Projective MR image showing multiple focal stenoses of intra- and extrahepatic bile ducts (*arrowheads*). Saccular outpouchings may also be present (*arrow*). **c** Different patient. Projective image showing multiple focal stenoses of the intra- and extrahepatic bile ducts (*arrowheads*)

#77 Common Bile Duct Stenosis in Acute Pancreatitis

Related topics: # 151 – 157 (acute pancreatitis)

KEY FACTS: DISEASE

- A variety of diseases may cause hyperbilirubinemia in patients with acute pancreatitis
- In a minority of these patients, a stenosis of the common bile duct can be demonstrated
- Causes of common bile duct stenosis:
  - Pancreatic edema (usually transient)
  - Complications of pancreatitis (e. g., pseudocysts)
  - Coexistent or underlying disease (e. g., common bile duct stones)

KEY FACTS: MRI (FIG. 77)

- MR appearance of the common bile duct in edematous pancreatitis:
  - Commonly normal
  - Smooth, gradual tapering may be observed
- Differential diagnosis: chronic pancreatitis, pancreatic cancer (see clinical data/cross-sectional images/aspect of the pancreatic duct)

References

Frieden JH (1965) The significance of jaundice in acute pancreatitis. Arch Surg 90 : 435 – 441

Rohrmann CA, Baron RL (1989) Biliary complications of pancreatitis. Radiol Clin North Am 27 : 93 – 104

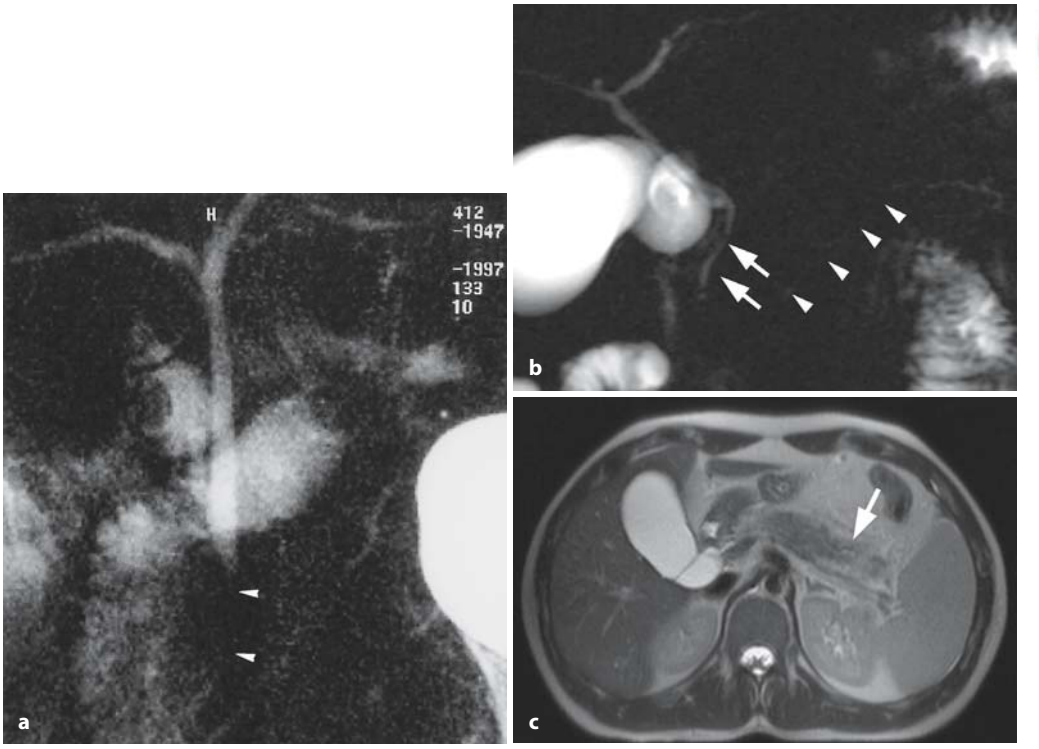

Fig. 77. **a** Patient with acute pancreatitis. Projective MR image showing severe narrowing of the distal (intrapancreatic) part of the common bile duct (*arrowheads*). Also note increased background signal intensity due to peripancreatic fluid/edema. **b, c** Different patient. Projective image showing discrete narrowing of the distal common bile duct (*arrows*) and apparent absence of the main pancreatic duct due to pancreatic oedema (*arrowheads*). **c** Axial T2-weighted HASTE image (TE 60) showing increased signal intensity of the pancreatic tissue, particularly in the tail (*arrow*)

#78 Common Bile Duct Stenosis in Chronic Pancreatitis

Related topics: #159–167 (chronic pancreatitis)

KEY FACTS: DISEASE

- Incidence:
  - Prevalence of clinically relevant common bile duct stenosis in chronic alcoholic pancreatitis: ± 9 %
- Causes:
  - Fibrosis
  - Pseudocyst(s)
  - Inflammatory mass
- Symptoms/signs:
  - Abdominal pain (not specific)
  - Jaundice (may also be related to hepatocellular damage)
- Complication: secondary sclerosing cholangitis with or without cirrhosis (see #45)

KEY FACTS: MRI

- Typical MR features (Fig. 78):
  - Long, smooth, gentle, progressive narrowing of entire pancreatic portion of the common bile duct (differential diagnosis with carcinoma: usually abrupt narrowing)
  - Signs of attraction/distortion not uncommon (Fig. 78b)
  - Displacement if direct compression by pseudocyst is present
- The distalmost segment of the intrapancreatic common bile duct may widen slightly again before it narrows to enter the sphincter ("hourglass" appearance), thus reflecting the extrapancreatic location of the distalmost part of the common bile duct (see Fig. 163b)
- *Note:* Atypical patterns of common bile duct narrowing are not uncommon (see #164, "double duct sign" in chronic pancreatitis)

References

Rohrmann CA, Baron RL (1989) Biliary complications of pancreatitis. Radiol Clin North Am 27: 93–104

Stahl TJ, Allen MO, Ansel HJ, Vennes JA (1988) Partial biliary obstruction caused by chronic pancreatitis. An appraisal of indications for surgical biliary drainage. Ann Surg 207: 26–32

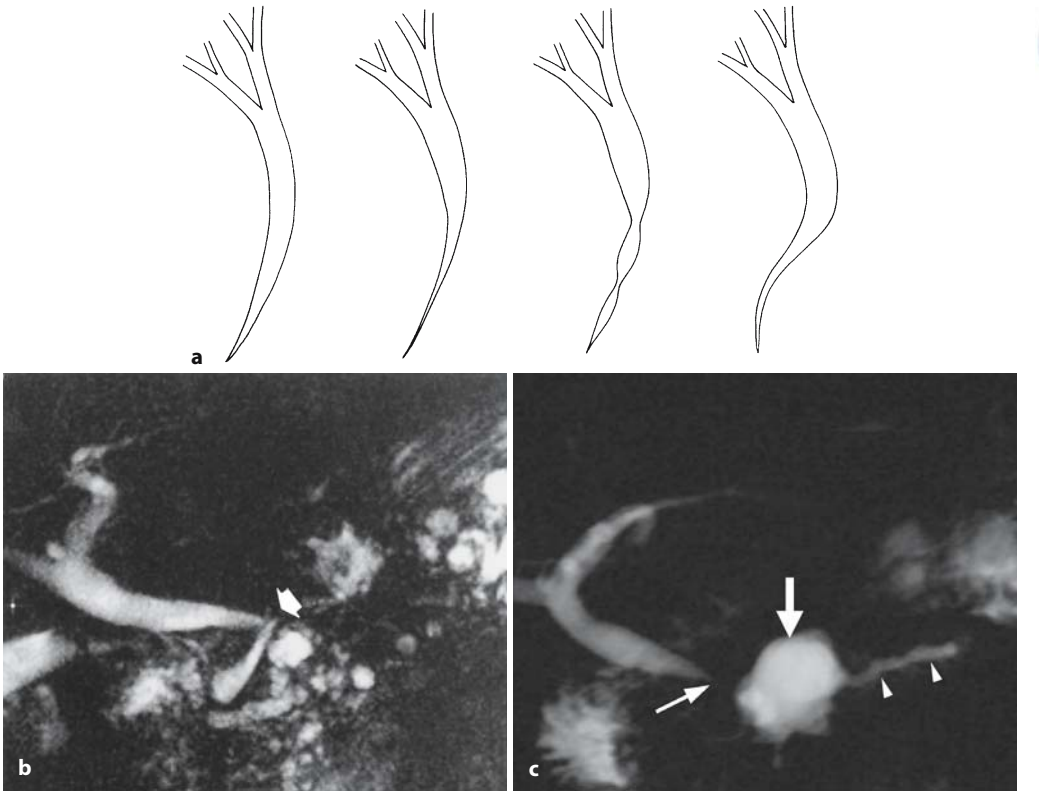

Fig. 78. **a** Typical configurations of the common bile duct in chronic pancreatitis. From *left* to *right*: normal; gradual tapering; alternating stenosis and dilation; focal medial or lateral deflection, usually due to pseudocyst and/or fibrosis. (From Rohrman and Baron 1989, with permission). **b** Projective MR image showing displacement and marked angulation of the common bile duct (*arrow*), caused by extensive parenchymal fibrosis in a patient with severe chronic pancreatitis. **c** Different patient. Attraction and smooth progressive stenosis of the distal common bile duct (*small arrow*) caused by fibrosis. Note pancreatic pseudocyst (*large arrow*) and dilatation of pancreatic duct (*arrowheads*) in this patient with severe chronic pancreatitis

#79 Other Benign Causes of Bile Duct Narrowing

KEY FACTS: DISEASE

- Other benign causes of bile duct narrowing include:
  - Retroperitoneal fibrosis
  - Reactive lymph node enlargement
  - Ectopic pancreas (see also # 145)
  - Benign tumors (adenoma, hamartoma; Allaire et al. 1988)
  - Bile duct varices resulting from portal vein occlusion (Fig. 79; see also # 112; Kim and Chew 1988)
  - Duplication cyst of the duodenum
  - Other cysts (post-traumatic, postinfection, idiopathic)

KEY FACTS: MRI

- Findings depend on type of underlying disease
- Patients with cavernous transformation of portal vein typically show "pseudocholangiocarcinoma sign" (irregular, undulating narrowing and nodular extrinsic defects; Fig. 79)

References

Allaire GS, Rabin L, Ishak KG, Sesterhenn IA (1988) Bile duct adenoma: a study of 152 cases. Am J Surg Pathol 12 : 708 – 715

Bayraktar Y, Balkanci F, Ozenc A et al. (1995) The "pseudo-cholangiocarcinoma sign" in patients with cavernous transformation of the portal vein and its effect on the serum alkaline phosphatase and bilirubin levels. Am J Gastroenterol 90 : 2015 – 2019

Kim S, Chew FS (1988) Choledochal varices. AJR Am J Roentgenol 150 : 578 – 580

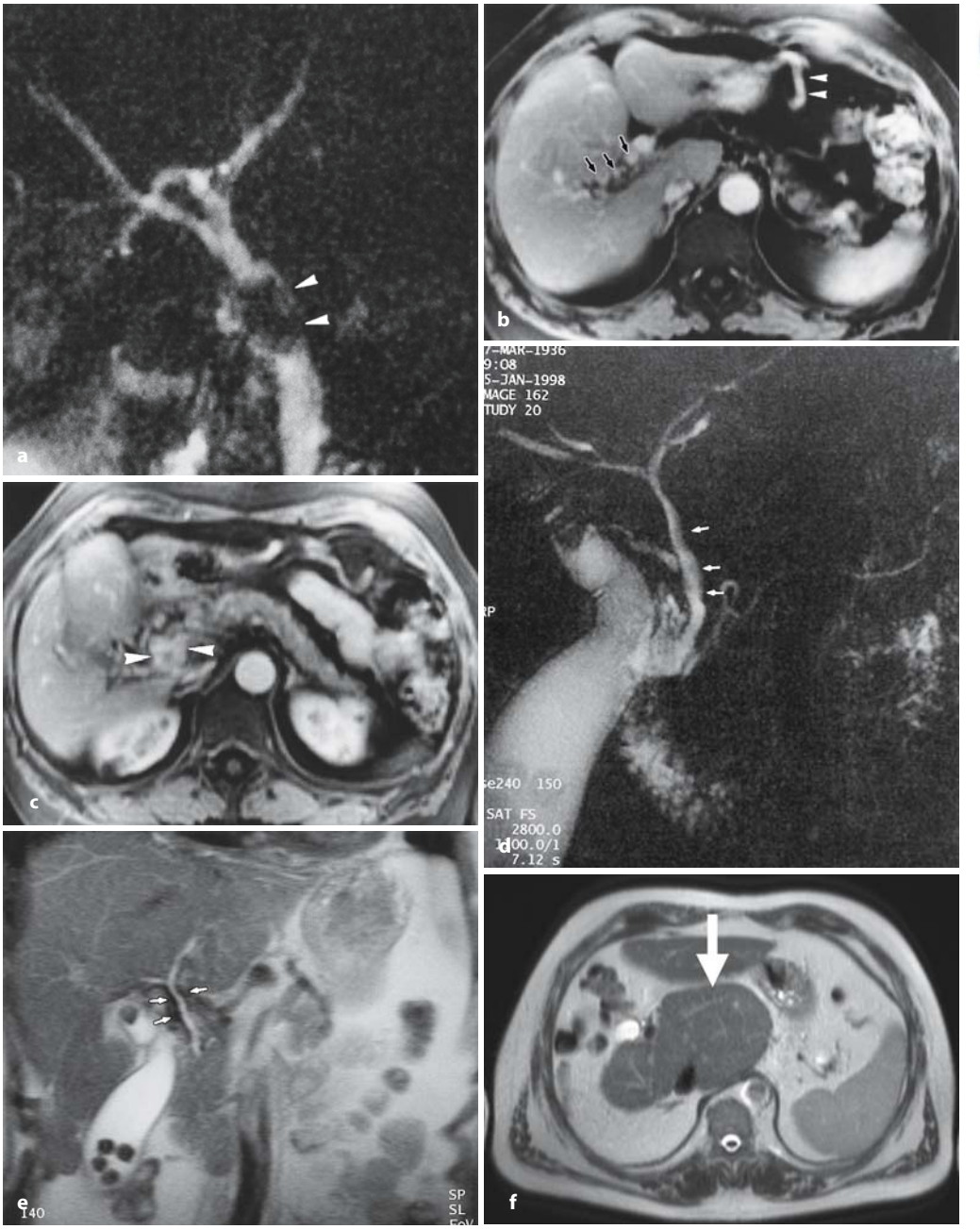

Fig. 79 a–c. **a** Projective MR image showing severe narrowing of the proximal extrahepatic duct (*arrowheads*), possibly an impacted stone or a polypoid tumor. Axial contrast-enhanced T1-weighted images showing the absence of a normal portal vein with the formation of multiple collaterals (cavernous transformation) (*arrows* in **b**) and extrahepatic venous collaterals (*arrowheads* in **b**). The focal narrowing of the bile duct is explained by the presence of large peribiliary venous collaterals (*arrowheads* in **c**). **d–e** Another patient with long-standing thrombosis of the portal vein. **d** Projective MR image showing undulated aspect of the extrahepatic bile duct (*arrows*). **e** Cross-sectional image obtained in the coronal plane showing flow void in peribiliary varices (*arrows*). **f–h** Patient with cirrhosis

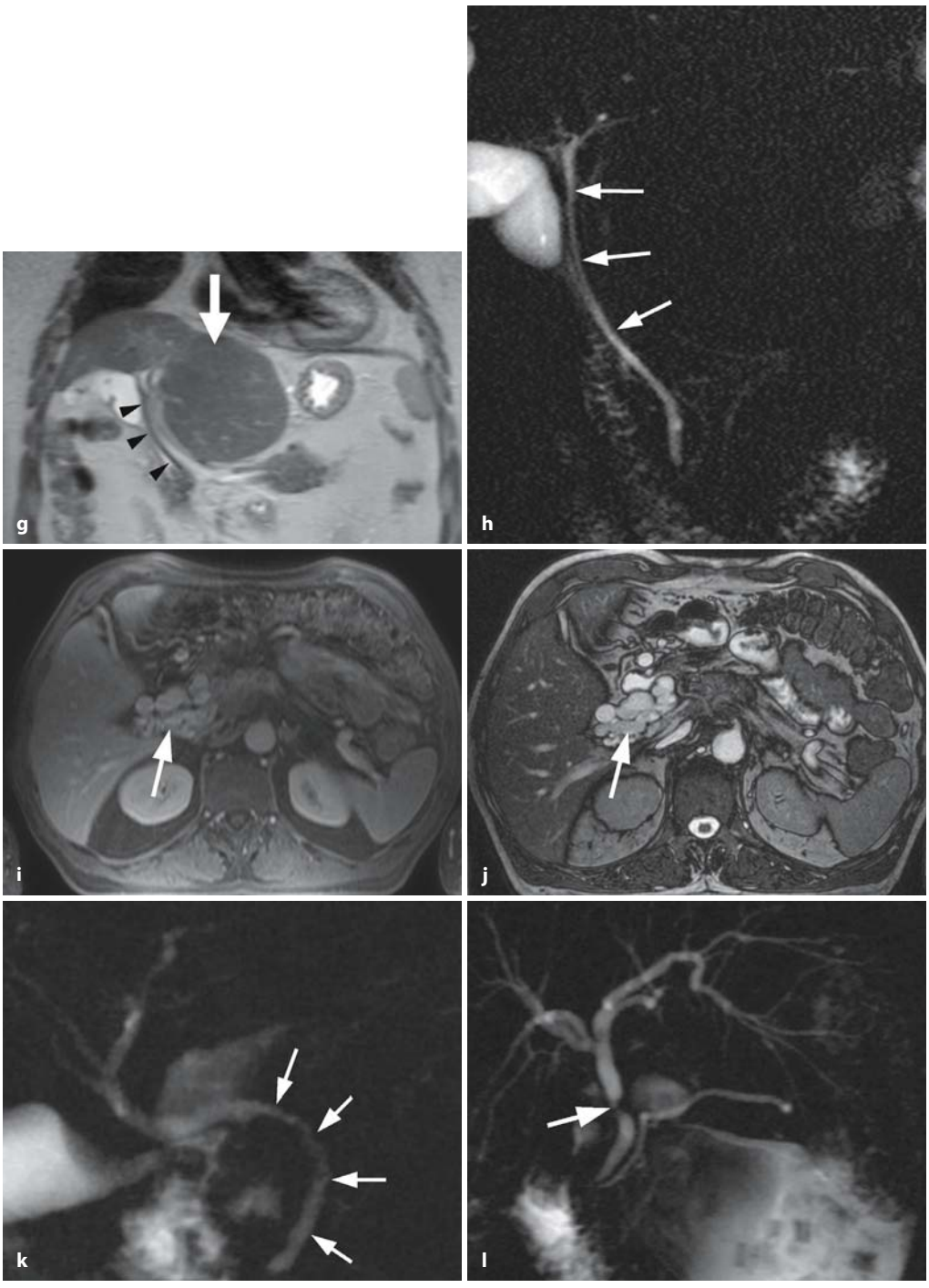

Fig. 79 a – n. (*continued*)

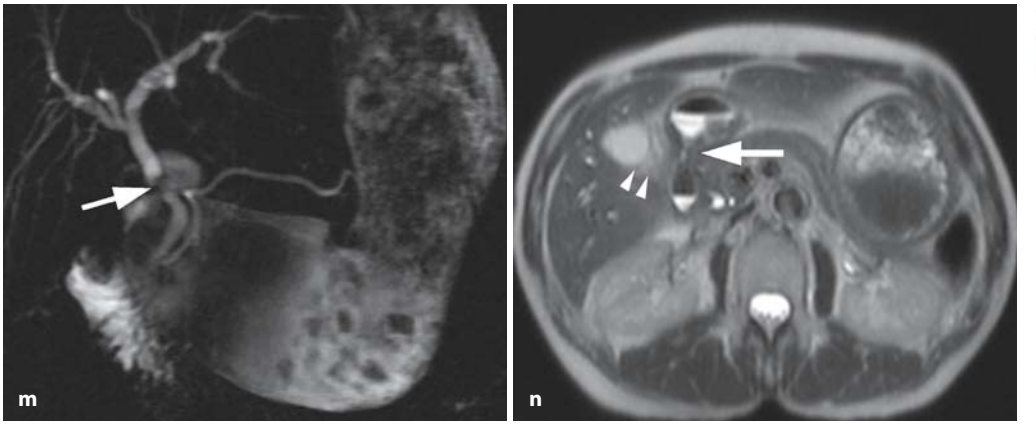

Fig. 79 f–h. (*continued)* Axial (**f**) and coronal (**g**) T2-weighted HASTE images showing marked hypertrophy of the caudate lobe (*arrows*) with secondary displacement of common hepatic duct and common bile duct (*arrowheads*). **h** Projective image showing lateral deviation and narrowing of the common hepatic and common bile duct (*arrows*). **i–k** Different patient with long-standing portal vein thrombosis. Axial contrast-enhanced T1-weighted VIBE image (**i**) obtained in the venous phase, and axial True-FISP image (**j**) showing the absence of a normal portal vein with cavernous transformation and large venous collaterals (*arrows*). **k** Projective image showing nodging and focal narrowing of the common bile duct due to the presence of venous collaterals (*arrows*). **l–n** Patient with a large bulbar ulcer with secondary inflammatory changes in the liver hilum and proximal common bile duct. **l, m** Projective images showing focal narrowing of the proximal common bile duct (*arrow*). Note the large stomach due to gastric outlet obstruction. **n** Axial T2-weighted HASTE image showing wall thickening of the pylorus and bulbar area (*arrow*) due to the ulcer. Note the secondary infiltration in the liver hilum and around the gallbladder (*arrowhead*)

3.3 Traumatic, Postoperative, and Iatrogenic Abnormalities

#80 After Hepatic Transplantation (1): Anastomotic Stricture

Related topics: #50, 51 (intrahepatic bile ducts, complications after hepatic transplantation), #65 (anatomy after hepatic transplantation)

KEY FACTS: DISEASE

- Incidence:
  - Choledocho-choledochal anastomoses: at least 5%
  - Choledochojejunal anastomoses: up to 27%
- Causes:
  - Excessively tight anastomotic suturing
  - Scar formation (fibrosis)
- Differential diagnosis with other causes of obstruction:
  - Ischemic stricture (see #81)
  - Strictures at the level of T tube insertion
  - Stones, blood clot, sloughed mucosa
  - Extrinsic compression (e.g., biloma, hematoma)
- Other complications of extrahepatic bile ducts after hepatic transplantation:
  - Anastomotic leakage
  - Nonanastomotic leakage (usually secondary to ischemia or from T tube insertion site)

KEY FACTS: MRI (FIG. 80)

- Typical features:
  - Usually short
  - Only involves the point of anastomosis
  - Smoothly marginated

References

Holbert BL, Campbell WL, Skolnick ML (1995) Evaluation of the transplanted liver and postoperative complications. Radiol Clin North Am 33: 521–540

Sheng R, Zaiko AB, Campbell WL, Abu-Elmagd K (1993) Biliary strictures in hepatic transplant patients: prevalence and types in patients with primary sclerosing cholangitis vs those with other liver diseases. AJR Am J Roentgenol 161: 297–300

Ward J, Sheridan MB, Guthrie JA et al. (2004) Bile duct strictures after hepatobiliary surgery: assessment with MR cholangiography. Radiology 231: 101–108

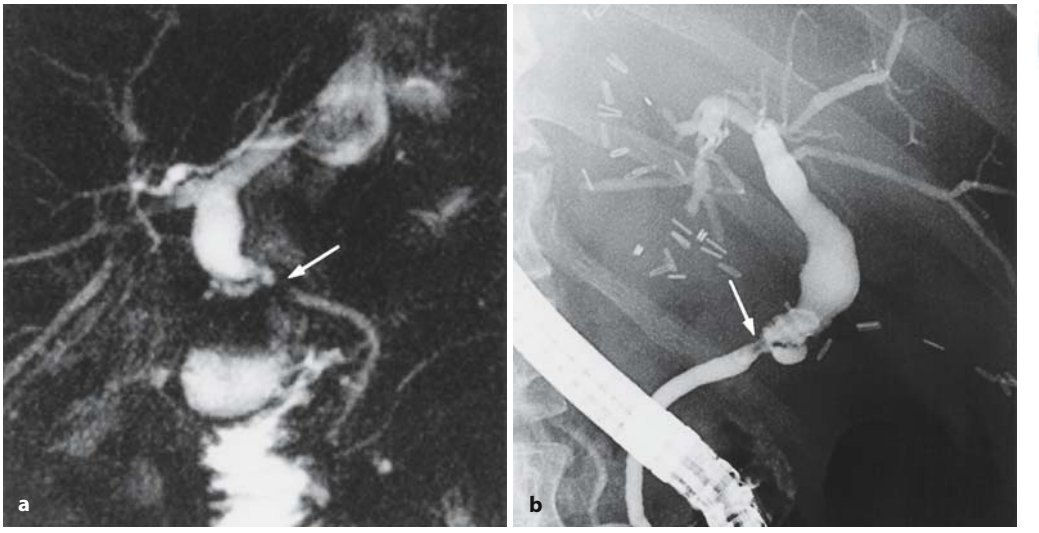

Fig. 80 a, b. **a** Projective MR image suggesting the presence of an anastomotic stricture (*arrow*). **b** ERCP confirms the presence of a stricture (*arrow*). Balloon dilation was performed. Note that the severity of the stricture is overestimated in **a**

#81 After Hepatic Transplantation (2): Ischemic Stricture

Related topics: #50, 51 (intrahepatic bile ducts, complications after hepatic transplantation), #65 (extrahepatic bile duct: anatomy after hepatic transplantation)

KEY FACTS: DISEASE

- Pathophysiology: in addition to the hepatic artery, the gastroduodenal artery and branches from the celiac trunk and superior mesenteric artery help supply the native biliary tree. Following liver transplantation, all but the hepatic artery blood supply is lost
- Complications of ischemia:
  - Stricture
  - Nonanastomotic leakage of bile with or without biloma
  - Diffuse dilation/stasis/cholangitis
  - Intraductal debris, sloughed mucosa, clot, stone formation (found in 6%–29% of patients that have undergone transplantations)

KEY FACTS: MRI

- Typical findings (Fig. 81):
  - Multiple irregularities/strictures typically involving both intrahepatic ducts and proximal common hepatic duct
  - Minimal irregularity usually first develops in the donor common hepatic duct
  - An irregular cast of sloughed mucosa may develop and cause proximal duct dilation
  - Strictures are usually relatively short and multifocal
- Differential diagnosis: e.g., primary sclerosing cholangitis, bacterial cholangitis
- See also #50

References

Holbert BL, Campbell WL, Skolnick ML (1995) Evaluation of the transplanted liver and postoperative complications. Radiol Clin North Am 33: 521–540

Lerut T, Gordon RD, Iwatsuki S et al. (1987) Biliary tract complications in human orthotopic liver transplantation. Transplantation 43: 47–51

Ward EM, Kiely MJ, Maus TP, Wiesner RH, Krom RA (1990) Hilar biliary strictures after liver transplantation: cholangiographic and percutaneous treatment. Radiology 177: 259–263

Zoepf T, Maldonado-Lopez EJ, Hilgard P, et al. (2005) Diagnosis of biliary strictures after liver transplantation: which is the best tool? World J Gastroenterol 11: 2945–2948

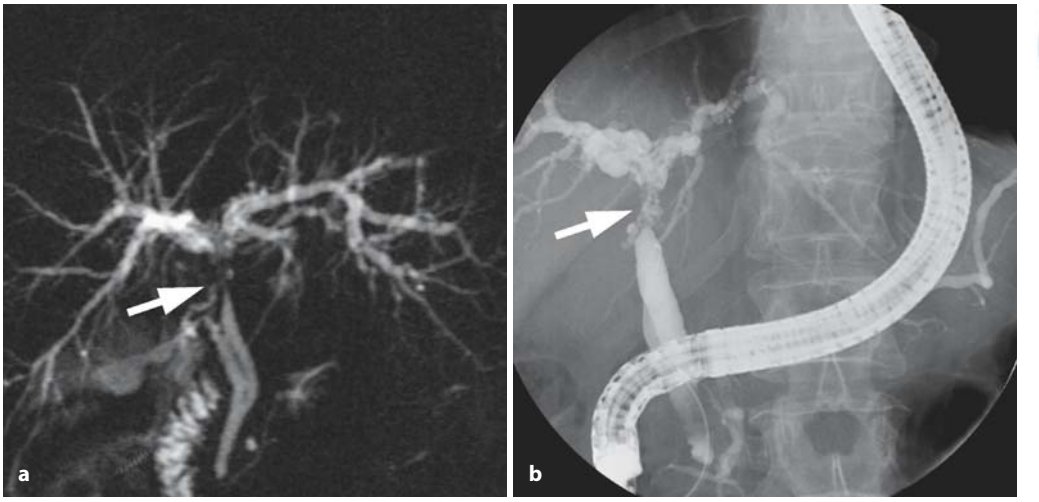

Fig. 81 a, b. Patient after liver transplantation. **a** Projective image showing a stricture of the proximal extrahepatic bile duct (*arrow*). **b** Corresponding ERCP image confirming the stricture with irregular aspect (*arrow*)

#82 After Cholecystectomy (1): Stricture of the Common Bile Duct

Related topics: #27 (variable junction of the posterior right hepatic duct), #52 (after cholecystectomy: stricture/transection of an aberrant bile duct), #63 (variant anatomy: location of bifurcation), #83 (after cholecystectomy: bile leak), #84 (post-cholecystectomy syndrome), #93 (normal and variant anatomy of cystic duct), #114 (complications with cystic duct remnant)

KEY FACTS: DISEASE

- Incidence:
  - After conventional cholecystectomy: 0.1% (Andren-Sandberg et al. 1985)
  - After laparoscopic cholecystectomy: at least 0.6% (Deziel et al. 1993)
- Tends to occur when the cystic duct is clamped and ligated close to its junction with the common hepatic duct (Fig. 82 a)
- Anatomic variations that increase the risk of bile duct injury during laparoscopic cholecystectomy: see #52 (Davidoff et al. 1992)
- Mechanism: failure to recognize these variants may lead to mistaking the common hepatic duct for the cystic duct and to inadvertent ligation or resection of a portion of the common hepatic duct
- Classification: see Fig. 82 b

KEY FACTS: MRI

- Stenoses are usually seen near the insertion of the cystic duct or at the bifurcation (Fig. 82 c – e)
- Morphologic features: usually short and regular
- *Note:* In some patients with severe stenoses, ERCP only shows a cutoff. MRCP may give more relevant preoperative information by revealing the distance between the proximal end of the lesion and the bifurcation

References

Andren-Sandberg A, Alinder G, Bengmark S (1985) Accidental lesions of the bile ducts at cholecystectomy: pre- and perioperative factors of importance. Ann Surg 201 : 328 – 332

Davidoff AM, Pappas TN, Murray EA et al. (1992) Mechanisms of major biliary injury during laparoscopic cholecystectomy. Ann Surg 215 : 196 – 202

Deziel DJ, Millikan KW, Economou SG, Dodas A, Ko ST, Airan MC (1993) Complications of laparoscopic cholecystectomy: a national survey of 4.292 hospitals and analysis of 77.604 cases. Am J Surg 165 : 9 – 14

Khalid TR, Casillas VJ, Montalvo BM et al. (2001) Using MR cholangiopancreatography to evaluate iatrogenic bile duct injury. AJR Am J Roentgenol 177 : 1347 – 1352

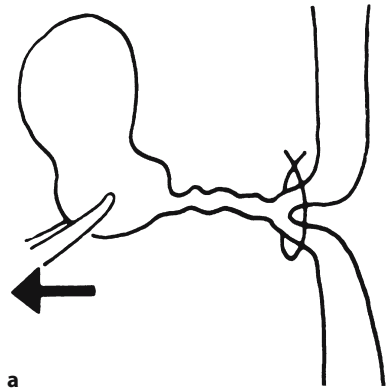

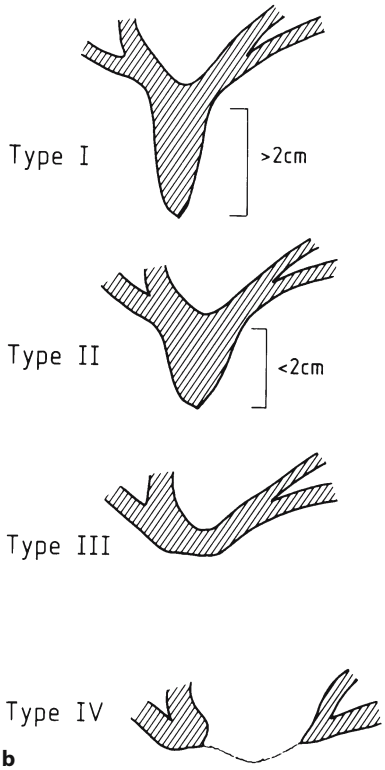

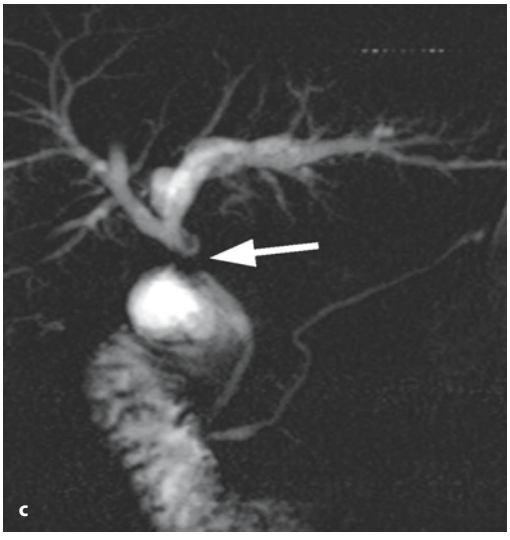

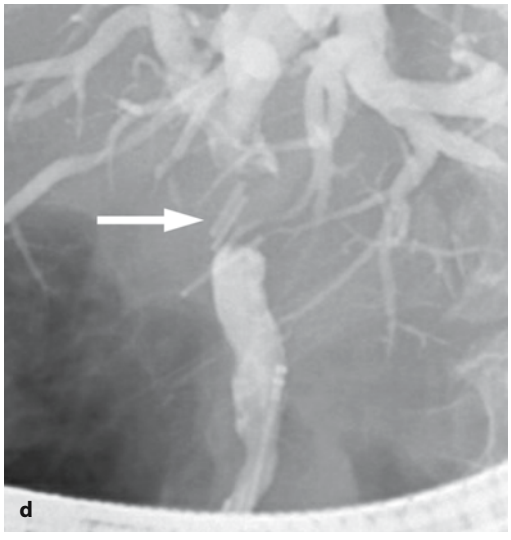

Fig. 82. **a** Possible mechanism of common bile duct injury. Traction on the common bile duct during cholecystectomy can cause disruption or inclusion in a clamp or ligature (see also Fig. 52a). (Reprinted with permission from Kune and Sali 1980). **b** Classification of benign bile duct injuries (Bismuth). *Type I:* remaining common hepatic duct greater than 2 cm; *type II:* common hepatic duct less than 2 cm; *type III:* injuries extending to the bifurcation; *type IV:* injuries extending to the distal portion of the right and left hepatic duct, with lack of communication between the two ductal systems. **c** Patient with signs of biliary obstruction after laparoscopic cholecystectomy. Projective images showing a focal narrowing/absence of the proximal extrahepatic bile duct with secondary intrahepatic bile duct dilatation (*arrows*). **d** Corresponding ERCP image showing severe narrowing of proximal extrahepatic bile duct and presence of clips (*arrow*)

#83 After Cholecystectomy (2): Bile Leak

Related topics: #27 (variable junction of the posterior right hepatic duct), #52 (after cholecystectomy: stricture/transection of an aberrant bile duct), #63 (variant anatomy: location of the bifurcation), #82 (after cholecystectomy: stricture of the common bile duct), #84 (post-cholecystectomy syndrome), #93 (normal and variant anatomy of the cystic duct), #114 (complications with cystic duct remnant)

KEY FACTS: DISEASE

- Causes:
  - Leakage at the end of the remaining cystic duct (see #114)
  - Leakage from damaged common bile duct or right hepatic duct
- Predisposing factors: anatomic variants (see #82)

– Complications:
  - Bile peritonitis
  - Biloma
  - Abscess

KEY FACTS: MRI (FIG. 83)

- Bile collection in close proximity of the common bile duct
- The actual connection with the common bile duct can usually be demonstrated or at least suspected
- Differential diagnosis:
  - Hemorrhage (e.g., after inadequate ligation of cystic artery; typical signal intensity)
  - "Normal" postoperative collection (seen in up to 20 % of patients): a mixture of blood and bile is often seen in the first week after surgery and resolves gradually

References

Davidoff AM, Pappas TN, Murray EA et al. (1992) Mechanisms of major biliary injury during laparoscopic cholecystectomy. Ann Surg 215 : 196 – 202

Deziel DJ, Millikan KW, Economou SG, Dodas A, Ko ST, Airan MC (1993) Complications of laparoscopic cholecystectomy: a national survey of 4.292 hospitals and analysis of 77.604 cases. Am J Surg 165 : 9 – 14

Neff CC, Simeone JF, Ferruci JT Jr, Mueller PR, Wittenberg J (1983) The occurrence of fluid collections following routine abdominal surgical procedures: sonographic survey in asymptomatic postoperative patients. Radiology 146 : 463 – 466

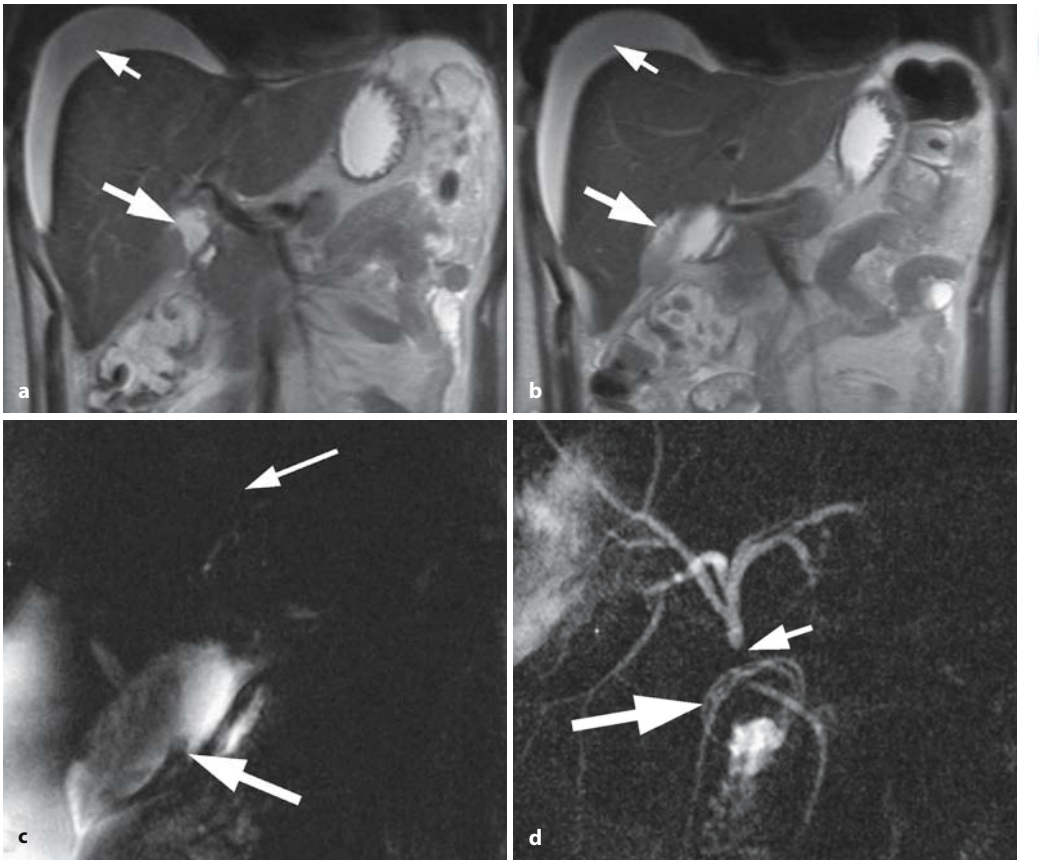

Fig. 83 a–d. Patient complaining of pain after laparoscopic cholecystectomy. **a, b** Coronal T2-weighted HASTE image (TE 60) showing ascites (*small arrow*) and a fluid collection located in the liver hilum (*large arrow*). **c** Projective image showing the fluid collection (biloma) (*large arrow*); the absence of intrahepatic bile duct dilatation (*small arrow*) is related to the presence of a persisting biliary leak. The patient was treated with percutaneous drainage of the biloma. **d** Follow-up projective image 1 month later showing the drain, no residual collection visible (*large arrow*). The intrahepatic bile ducts are visible again. Note the development of a secondary fibrotic stricture on the proximal extrahepatic bile duct (*small arrow*)

#84 Post-cholecystectomy Syndrome

Related topics: #52 (after cholecystectomy: stricture/transection of an aberrant bile duct), #82 (after cholecystectomy: stricture of the common bile duct), #83 (after cholecystectomy: bile leak), #93 (normal and variant anatomy of the cystic duct), #114 (complications with cystic duct remnant)

KEY FACTS

- Definition: symptoms recurring/persisting after cholecystectomy
- Incidence of severe symptoms: 2.6%–32%
- Causes:
  - *Biliary:* incomplete surgery (retained stone in cystic duct remnant; overlooked common bile duct stone); operative trauma (bile duct stricture; leakage of bile with or without peritonitis); bile duct pathology (fibrosis of vaterian sphincter complex; biliary dyskinesia; biliary fistula)
  - *Extrabiliary:* disease overlooked during preoperative evaluation (e.g., pancreatitis, hepatitis); new disease
- In symptomatic patients, stones in the cystic or common bile duct may be found in up to 34% (Fig. 84; Marotta et al. 1989)
- *Note:* Delayed remote abscess formation is another (probably rare) complication that may occur after peritoneal spillage of gallstones during (laparoscopic) cholecystectomy

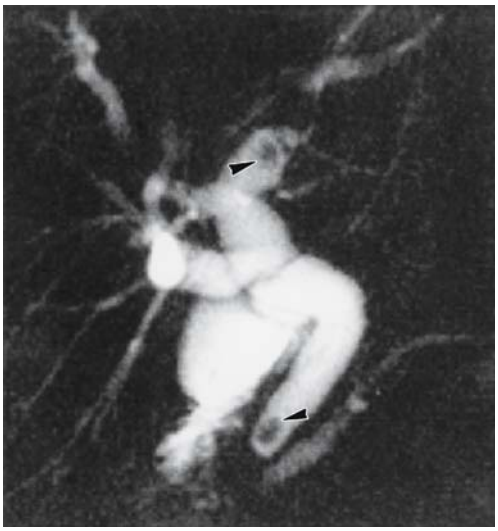

Fig. 84. Projective MR image obtained in patient with persistent complaints after cholecystectomy showing stones in the distal common bile duct and left hepatic duct (*arrowheads*)

References

Marotta F, Hada R, Morello P et al. (1989) ERCP in the assessment of patients with postcholecystectomy syndrome: benefits and limitations. Nether J Med 35:232–240

McGahan JP, Stein M (1995) Complications of laparoscopic cholecystectomy: imaging and intervention. AJR Am J Roentgenol 165:1089–1097

Moossa AR, Easter DW, vanSonnenberg E, Casola G, D'Agostino H (1993) Laparoscopic injuries to the bile duct. A cause of concern. Ann Surg 218:215–216

Rubini G, Dimonte M (1999) Postcholecystectomy syndrome: evaluation by biliary cholescintigraphy and MR cholangiopancreatography. Clin Nucl Med 24:784–788

#85 Bile Duct Trauma Related to Nonbiliary Surgery

KEY FACTS: DISEASE

- Bile duct injury may occur during gastrectomy, pancreatectomy, partial hepatectomy, portocaval shunting, etc.
- Mechanisms:
  - Direct injury
  - Vascular injury (the blood supply of the middle part of the common bile duct depends entirely on two paracholedochal arteries; injury to these arteries can lead to ischemia and stricture formation)

KEY FACTS: MRI

- Most common finding: stricture and/or bile leak (Fig. 85)

References

Khalid TR, Casillas VJ, Montalvo BM et al. (2001) Using MR cholangiopancreatography to evaluate iatrogenic bile duct injury. AJR Am J Roentgenol 177 : 1347 – 1352

Lillemoe KD, Pitt HA, Cameron JL (1990) Postoperative bile duct strictures. Surg Clin North Am 70 : 1355 – 1380

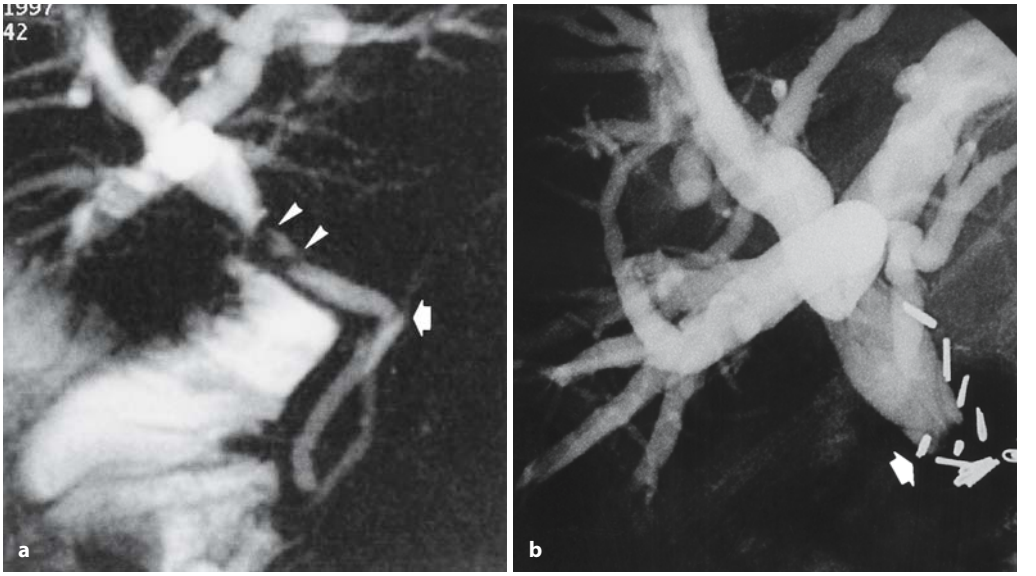

Fig. 85 a, b. Patient who underwent gastrectomy 5 years earlier. **a** Projective MR image showing a relatively short stricture of the common hepatic duct (*arrowheads*). Also note the attraction of the more distal extrahepatic duct due to fibrosis (*arrow*). **b** PTC image showing occlusion of the common hepatic duct (*arrow*). Despite the short length of the stricture, percutaneous dilation was not possible and the patient was referred for surgery

#86 Choledochoduodenostomy with Sump Syndrome

KEY FACTS: DISEASE

- "Sump": reservoir located at the lowest point of a drainage system, collecting fluid and debris
- "Sump syndrome": cholangitis and biliary obstruction caused by the accumulation of debris and ingested material in the bile ducts
- Incidence of sump syndrome: 0.14 % – 1.3 % of choledochoduodenostomies (Hawes et al. 1992)
- Mechanism: reflux of gas, intestinal contents, and contrast medium into the intrahepatic bile ducts (Fig. 86 a)
- Note on choledochoduodenostomy:
  - Indications: multiple or unremovable common bile duct stones, chronic pancreatitis, postoperative stricture, ampullary stenosis
  - Considered by some as a valuable alternative to endoscopic papillotomy and biliary lithotripsy (Berlatzky and Freund 1990)

KEY FACTS: MRI (FIG. 86 b)

- The common bile duct has a large diameter
- Debris and stones are usually clearly seen as hypointense structures within the lumen
- If the bile duct contains a large amount of air (which is not unusual), the interpretation may become difficult

References

Berlatzky Y, Freund HR (1990) Primary choledochoduodenostomy for benign obstructive biliary tract disease. J Clin Gastroenterol 12 : 420 – 422

Escudero-Fabre A, Escallon A, Sack J, Halpern NB, Aldrete JS (1991) Choledochoduodenostomy. Analysis of 71 cases followed for 5 to 15 years. Ann Surg 213 : 643 – 644

Hawes DR, Pelsang RE, Janda RC, Lu CC (1992) Imaging of the biliary sump syndrome. AJR Am J Roentgenol 158 : 315 – 319

Silvis S, Rohrmann C, Ansel H (eds) (1995) Endoscopic retrograde cholangiopancreatography. Igaku-Shoin, New York, p 287

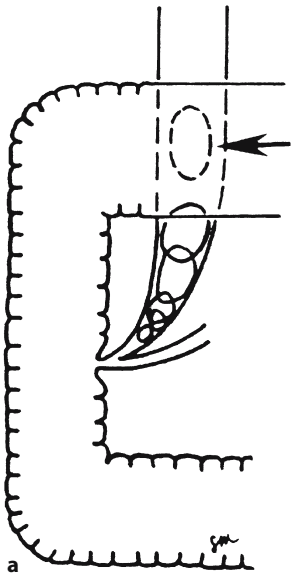

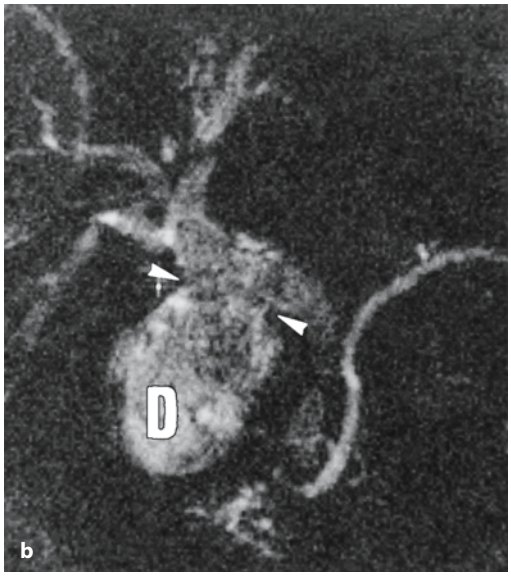

Fig. 86. **a** Choledochoduodenostomy (*arrow*). Stones, debris, and sludge may collect in the excluded segment of the distal common bile duct. (Reprinted with permission from Silvis et al. 1995). **b** Patient who underwent choledochoduodenostomy and presented with fever. Projective MR image showing connection (*arrowheads*) between the extrahepatic bile duct and the first part of the duodenum (*D*). Note low overall signal intensity of the bile ducts, related to presence of air and debris

3.4 Malignant Tumors

#87 Extrahepatic Cholangiocarcinoma (1): Klatskin Tumor

Related topics: #54, 55 (intrahepatic cholangiocarcinoma), #88 (extrahepatic cholangiocarcinoma: distal duct type)

KEY FACTS: DISEASE

- Cholangiocarcinoma involving the proximal common hepatic duct and sometimes the bifurcation (= hilar cholangiocarcinoma)
- Histology: varies from well-differentiated adenocarcinoma to anaplastic carcinoma
- Incidence: 70 % of cholangiocarcinomas
- Age peak: sixth to seventh decade
- Growth pattern:
  - Focal stenotic
  - Diffuse sclerosing
  - Polypoid (least common)
- Classification: see Fig. 87 a (Deviere et al. 1988)
- Predisposing factors:
  - Inflammatory bowel disease
  - Primary sclerosing cholangitis (see #41–44)
  - Caroli's disease (see #30)
  - Choledochal cysts (see #68)
  - *Clonorchis sinensis* infection
- Symptoms: painless jaundice, cholangitis, weight loss
- Spread:
  - Most are locally infiltrative
  - Invasion of portal vein unusual
  - Lymphatic spread: most often in common bile duct nodes
  - Infiltration of the liver (23 %)
  - Peritoneal seeding (9 %)
  - Hematogenous: extremely rare

KEY FACTS: MRI (FIG. 87 b–f)

- Projective images:
  - Usually stenotic lesion (usually 1–3 cm in length, may be longer; contour may be smooth or irregular)
  - Nodular intraluminal components not uncommon
  - Differential diagnosis: trauma, bile duct surgery, compression by metastatic lymph nodes, lymphoma, hepatocellular carcinoma, or gallbladder carcinoma
- Cross-sectional images:
  - Mass located at the liver hilum causing intrahepatic bile duct dilation
  - Signal intensity on T2-weighted images: well-differentiated and mucin-containing types are hyperintense; the scirrhous type is moderately hyperintense (or more or less isointense)

- Enhancement pattern: heterogeneous progressive enhancement
- Other features: lobar atrophy, segmental portal vein occlusion without caliber expansion of the vein, hilar lymph node enlargement
- Small (<1–2 cm) and infiltrating tumors are usually not clearly visible

- *Note:* In the absence of surgical antecedents, strictures involving the region of the porta hepatis or the midportion of the extrahepatic duct are almost invariably malignant, regardless of their appearance

References

Deviere J, Baize M, De Toeuf J, Cremer M (1988) Long-term follow-up of patients with hilar malignant stricture treated by endoscopic biliary drainage. Gastrointest Endosc 34 : 95 – 101

Guthrie JA, Ward J, Robinson PJ (1996) Hilar cholangiocarcinomas: T 2-weighted spin echo and gadolinium-enhanced FLASH MR imaging. Radiology 201 : 347 – 351

Nichols DA, MacCarty RL, Gaffey TA (1983) Cholangiographic evaluation of bile duct carcinoma. AJR Am J Roentgenol 141 : 1291 – 1294

Park MS, Kim TK, Kim KW et al. (2004) Differentiation of extrahepatic bile duct cholangiocarcinoma from benign stricture: findings at MRCP versus ERCP. Radiology 233 : 234 – 240

Soyer P, Bluemke DA, Reichle R et al. (1995) Imaging of intrahepatic cholangiocarcinoma. 2. Hilar cholangiocarcinoma. AJR Am J Roentgenol 165 : 1433 – 1436

Yeh TS, Jan YY, Tseng JH et al. (2000) Malignant perihilar biliary obstruction: magnetic resonance cholangiopancreatographic findings. Am J Gastroenterol 95 : 432 – 440

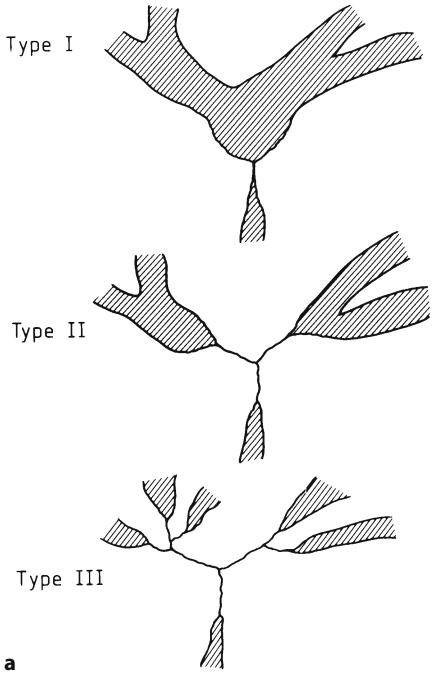

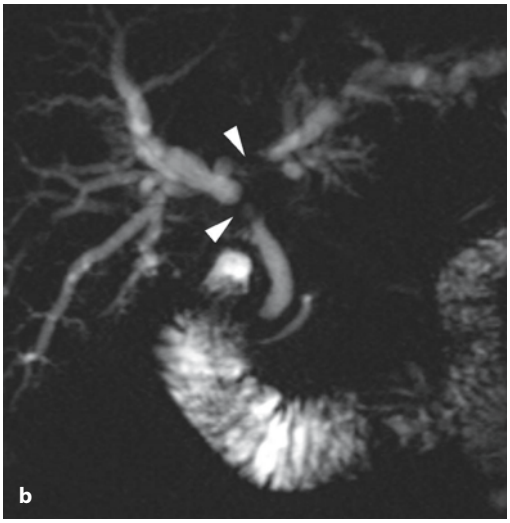

Fig. 87. **a** Classification of malignant hilar stenoses (Bismuth). *Type I:* tumors involving the proximal common hepatic duct, sparing the bifurcation; *type II:* tumors of the bifurcation involving the more distal hepatic ducts; *type III:* tumors of the bifurcation extending up to and involving secondary hepatic ducts. **b–f** Projective image (**b**) and corresponding ERCP image (**c**) showing a long stricture of the proximal common hepatic duct and bifurcation (*arrowheads*) with secondary intrahepatic bile duct dilatation: Klatskin tumor type II. **d** T1-weighted FLASH image showing a hypointense soft tissue mass in the liver hilum (*arrow*). **e** Axial contrast-enhanced T1-weighted VIBE image obtained in the arterial phase showing only slight peripheral enhancement (*arrow*). **f** Same image obtained after 10-min interval showing the typical delayed central enhancement, characteristic for a cholangiocarcinoma (*arrow*)

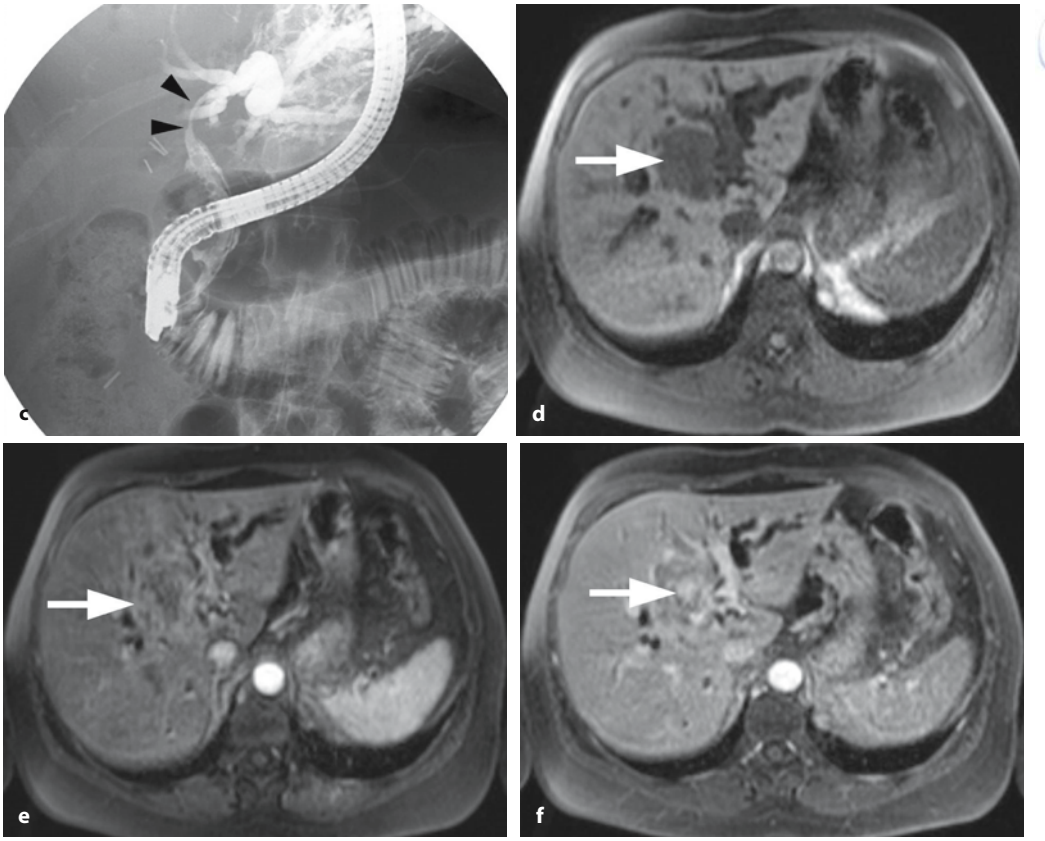

Fig. 87. (*continued*)

#88 Extrahepatic Cholangiocarcinoma (2): Distal Duct Type

Related topics: #54, 55 (intrahepatic cholangiocarcinoma), #87 (Klatskin tumor)

KEY FACTS: DISEASE

- Definition: cholangiocarcinoma located below the proximal part of the common hepatic duct (usually within the mid-extrahepatic biliary tree)
- Macroscopic appearance: mass encasing the bile duct or rounded intraluminal mass
- Usually small
- Incidence: 10 % of cholangiocarcinomas
- Predisposing disease: see # 87
- Better prognosis than Klatskin tumor (higher probability of surgical cure; Nichols et al. 1983)

KEY FACTS: MRI (FIG. 88)

- Projective images:
  - Usually focal stenosis
  - Rarely polypoid mass
- Cross-sectional images:
  - Mass lesion (if sufficiently large)
  - T 1: hypointense; T 2: variable, usually moderately hyperintense
  - With or without enlarged lymph nodes

References

Kim JH, Kim MJ, Chung JJ et al. (2002) Differential diagnosis of periampullary carcinomas at MR imaging. Radiographics 22 : 1335 – 1352

Nichols DA, MacCarty RL, Gaffey TA (1983) Cholangiographic evaluation of bile duct carcinoma. AJR Am J Roentgenol 141 : 1291 – 1294

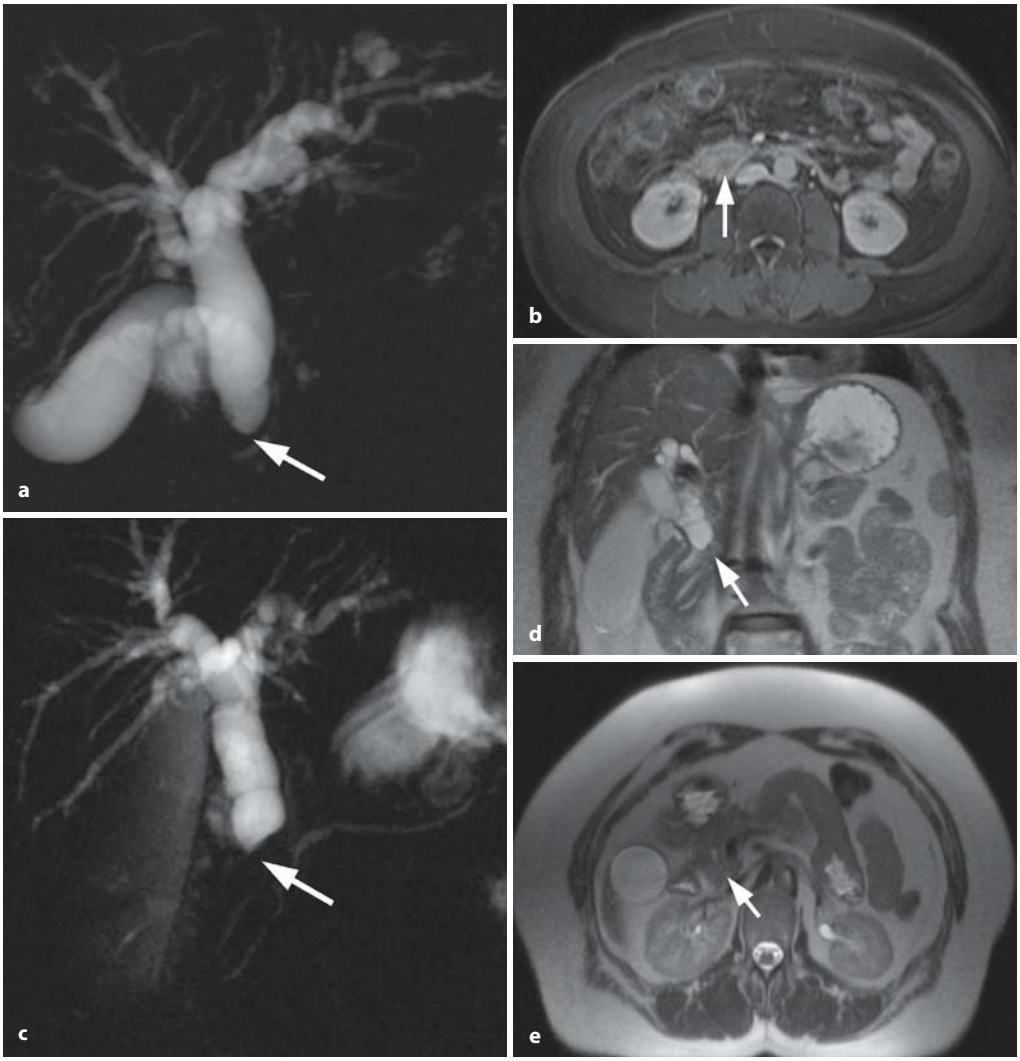

Fig. 88. a, b Projective image (**a**) showing marked bile duct dilatation with an abrupt stenosis in the distal common bile duct (*arrow*). **b** Axial contrast-enhanced T1-weighted VIBE image obtained in the venous phase showing a small hypo-intense lesion in the distal common bile duct, corresponding to a small cholangiocarcinoma (*arrow*) **c–e** Different patient. Projective image (**c**) showing marked bile duct dilatation with an abrupt stenosis in the distal common bile duct (*arrow*). **d, e** Coronal and axial T2-weighted HASTE images (TE 60) showing a slightly hyperintense infiltrating mass in the pancreatic head (*arrow*). Final diagnosis: cholangiocarcinoma

#89 Bile Duct Involvement by Gallbladder Carcinoma

Related topics: # 115 – 118 (gallbladder carcinoma)

KEY FACTS: DISEASE (SEE ALSO # 115 – 118)

- Incidence of biliary tree stenosis/obstruction in gallbladder carcinoma: 50 %
- Mechanisms of involvement of bile duct:
  - Gallbladder carcinomas have a propensity for direct centripetal extrahepatic spread
  - Bile duct compression/invasion by metastatic lymph nodes

KEY FACTS: MRI (FIG. 89)

- Cholangiographic appearance: indistinguishable from Klatskin tumors
- Characteristic features (see # 115 – 118):
  - Focal or diffuse thickening of the gallbladder wall
  - Abnormal gallbladder bed
  - Sometimes large mass directly invading the liver

References

Lane J, Buck JL, Zeman RK (1989) Primary carcinoma of the gallbladder: a pictorial essay. Radiographics 9 : 209 – 228

Schwartz LH, Black J, Fong Y et al. (2002) Gallbladder carcinoma: findings at MR imaging with MR cholangiopancreatography. J Comput Assist Tomogr 26 : 405 – 410

Silvis S, Rohrmann C, Ansel H (eds) (1995) Endoscopic retrograde cholangiopancreatography. Igaku-Shoin, New York, p 287

Thorsen MK, Quiroz F, Lawson TL, Smith DF, Foley WD, Stewart ET (1984) Primary biliary carcinoma: CT evaluation. Radiology 152 : 479 – 483

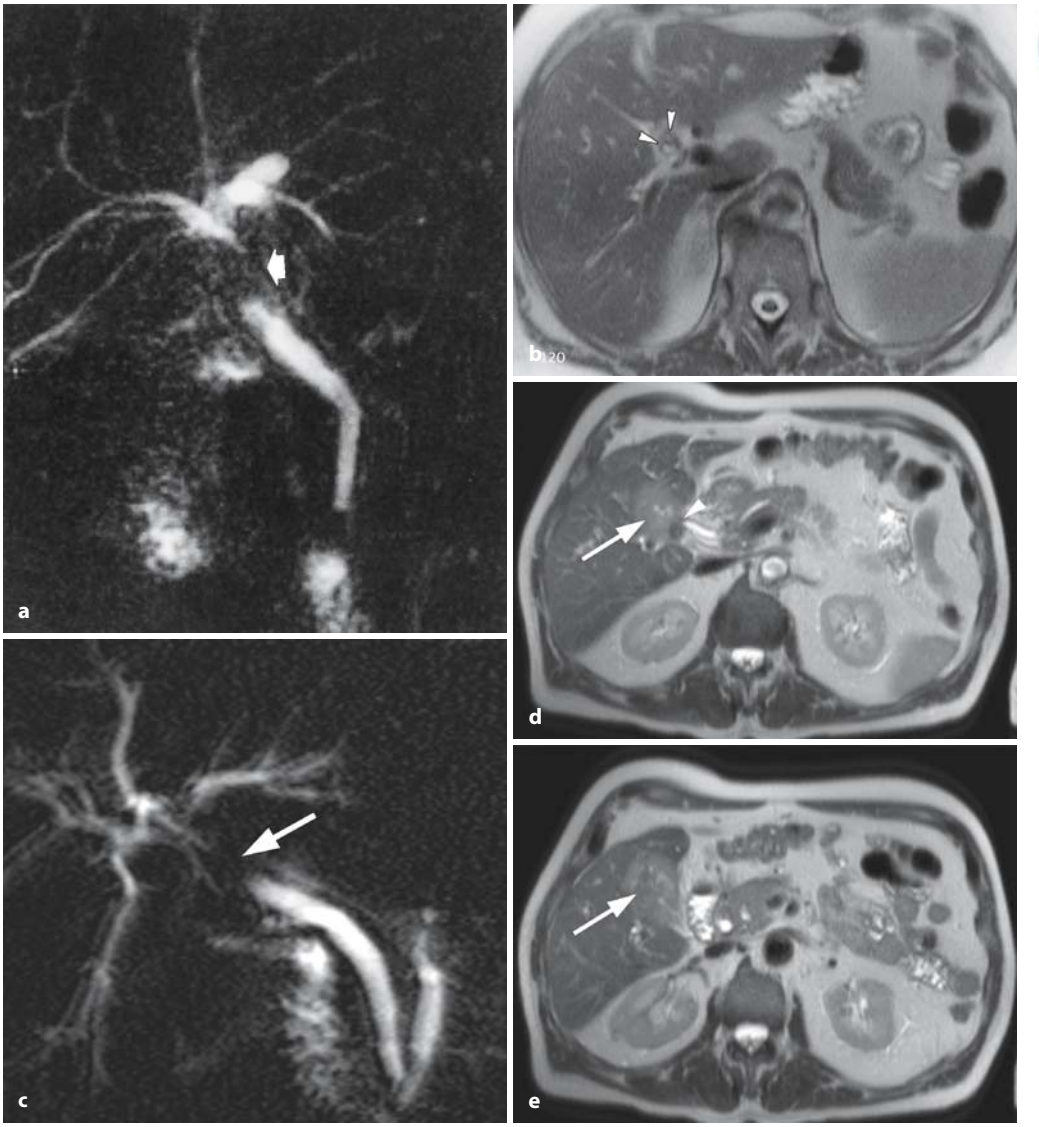

Fig. 89. **a, b** Patient who had previously undergone "routine" cholecystectomy. Histology revealed gallbladder carcinoma with positive section margins. **a** Projective MR image obtained 3 weeks after surgery showing narrowing of the proximal common hepatic duct (*arrow*). **b** Axial T2-weighted image obtained at the level of the stenosis showing a small hypointense soft tissue mass around the narrowed bile duct (*arrowheads*), representing infiltrating tumor. **c–e** Different patient. Projective image (**c**) showing severe narrowing of the proximal common hepatic bile duct (*arrow*) with secondary intrahepatic bile duct dilatation. **d, e** Axial T2-weighted HASTE image (TE 60) showing an infiltrating hyperintense mass originating from the gallbladder (*arrow*) and invading the adjacent bile duct (*arrowhead*)

#90 Bile Duct Involvement by Pancreatic Carcinoma

Related topics: #133 (vaterian sphincter complex, invasion by pancreatic carcinoma), #185–195 (pancreatic carcinoma)

KEY FACTS: DISEASE

- Pancreatic carcinoma commonly occurs in the pancreatic head (60 %–70 %)
- Secondary involvement of the biliary tree is common

KEY FACTS: MRI (FIG. 90)

- Stenosis:
  - Abrupt transition with or without "shouldering"
  - Median length: several centimeters
  - Usually irregular contours
- May also become manifest as obstruction
- Location:
  - Usually intrapancreatic segment of the common bile duct
  - Midsegment of the common bile duct: in pancreatic tumors extending cranially
- *Note:* The diagnosis of pancreatic carcinoma can be made with confidence if:
  - Cross-sectional images show a mass lesion located in the pancreatic head
  - Both the common bile duct and the pancreatic duct show typical irregular narrowing with abrupt transition (typical "double duct" sign)

References

Baert AL, Rigauts H, Marchal G (1994) Ductal adenocarcinoma. In: Baert AL (ed) Radiology of the pancreas. Springer, Berlin Heidelberg New York, pp 129–172

Freeny PC (1989) Radiological diagnosis and staging of pancreatic ductal adenocarcinoma. Radiol Clin North Am 27 : 121–128

Kim JH, Kim MJ, Chung JJ et al. (2002) Differential diagnosis of periampullary carcinomas at MR imaging. Radiographics 22 : 1335–1352

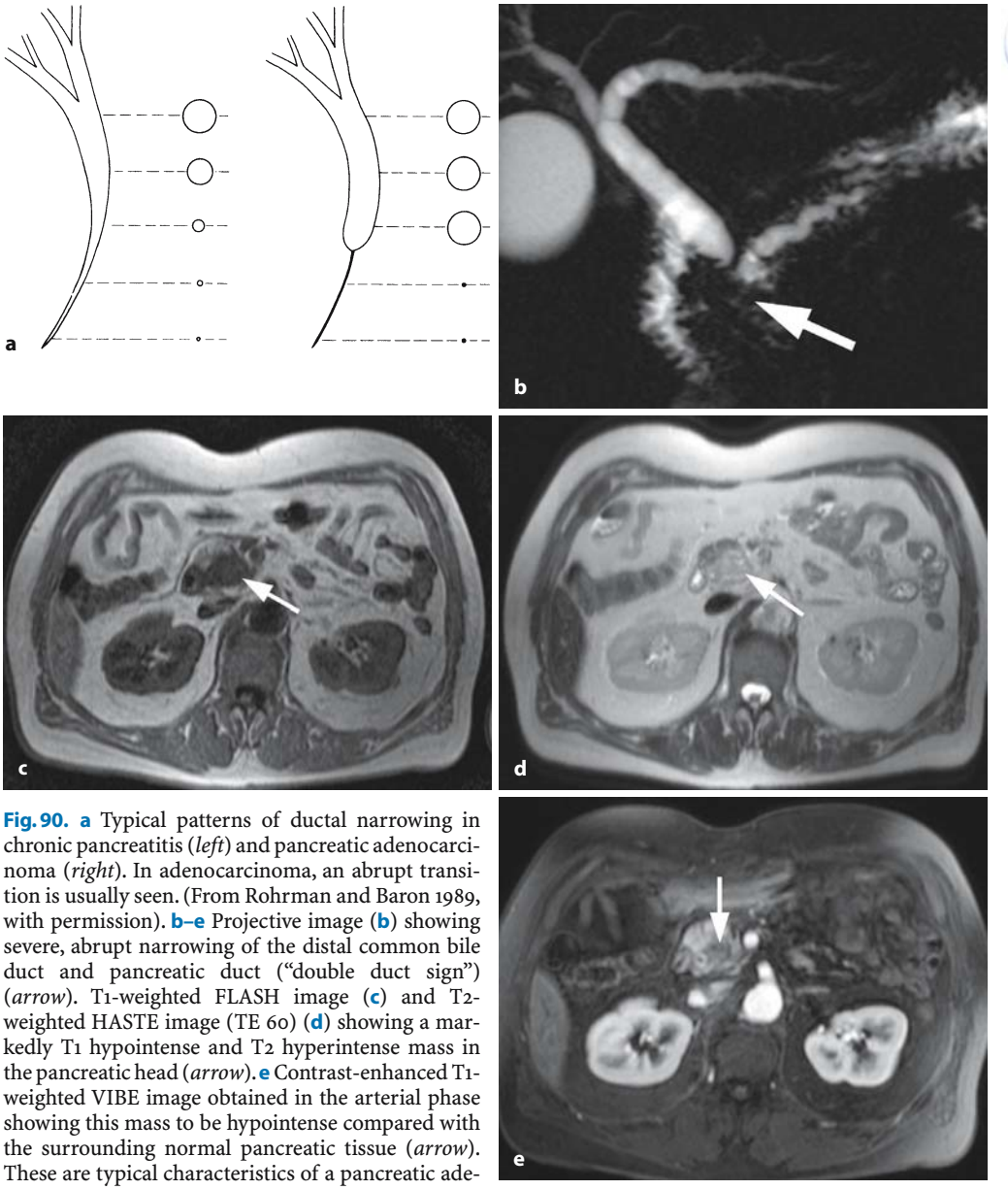

Fig. 90. a Typical patterns of ductal narrowing in chronic pancreatitis (*left*) and pancreatic adenocarcinoma (*right*). In adenocarcinoma, an abrupt transition is usually seen. (From Rohrman and Baron 1989, with permission). **b–e** Projective image (**b**) showing severe, abrupt narrowing of the distal common bile duct and pancreatic duct ("double duct sign") (*arrow*). T1-weighted FLASH image (**c**) and T2-weighted HASTE image (TE 60) (**d**) showing a markedly T1 hypointense and T2 hyperintense mass in the pancreatic head (*arrow*). **e** Contrast-enhanced T1-weighted VIBE image obtained in the arterial phase showing this mass to be hypointense compared with the surrounding normal pancreatic tissue (*arrow*). These are typical characteristics of a pancreatic adenocarcinoma

#91 Bile Duct Involvement by Other Extrabiliary Neoplasms

Related topics: #60 (intrahepatic bile ducts, metastases), #196 (secondary pancreatic tumors)

KEY FACTS: DISEASE

- Incidence: at least 10 % of tumors involving the bile ducts
- Causes:
  - Metastatic disease (usually lymph node metastases in pericholedochal lymphatics)
  - Lymphoma

KEY FACTS: MRI (FIG. 91)

- Projective images show a varying appearance:
  - Smooth eccentric compression
  - Smooth or irregular concentric narrowing
  - Polypoid intraluminal mass (metastases represent ± 10 % of polypoid bile duct tumors; Ponette et al. 1994)
- Cross-sectional images usually enable identification of enlarged lymph nodes

References

Ponette E, Biebau G, Gelin J et al. (1994) Imaging of polypoid endoluminal growing bile duct tumors. J Belge Radiol 77 : 157 – 161

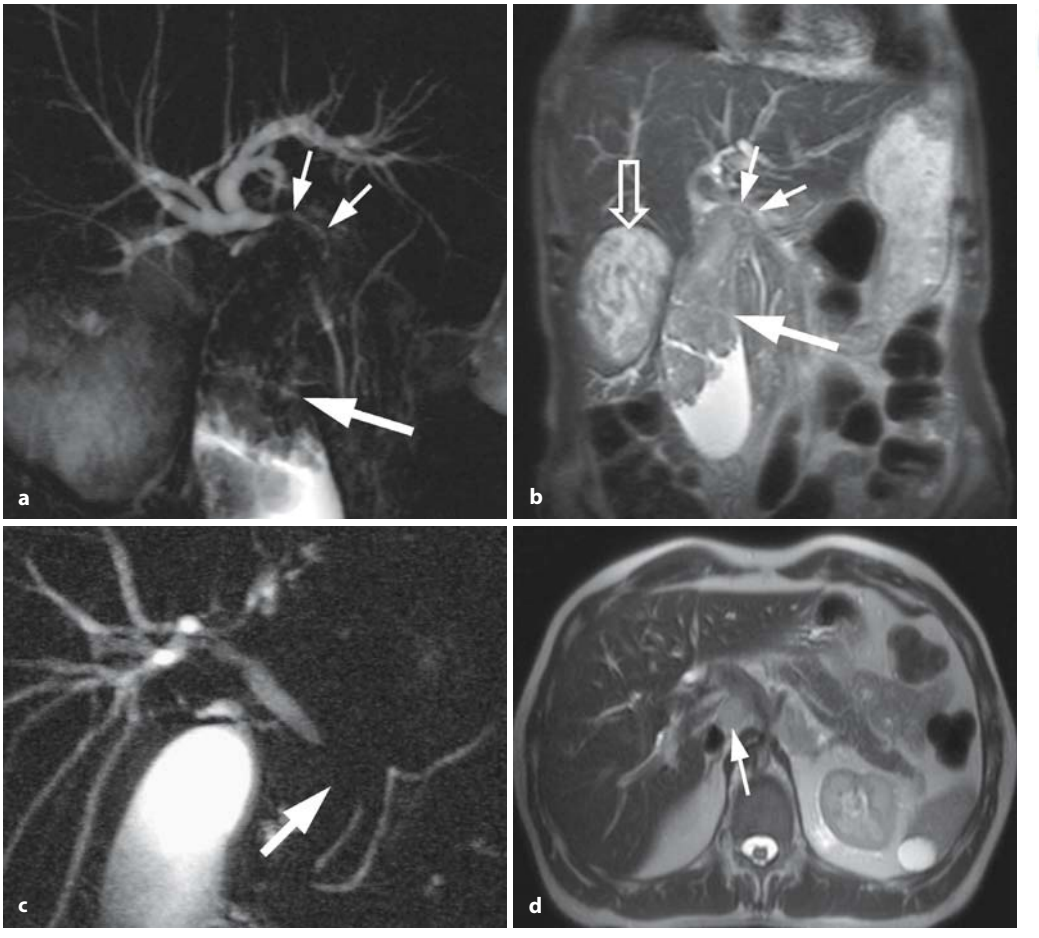

Fig. 91. a, b Patient with a known malignant melanoma. Projective image (**a**) and coronal T2-weighted HASTE image (**b**) showing a distended gallbladder filled with solid tissue (*large arrow*): gallbladder metastasis. Secondary invasion of the proximal common hepatic duct is also observed (*small arrows*). Note the partially necrotic liver metastasis adjacent to the gallbladder (*open arrow*). **c, d** Patient with known lymphoma. **c** Projective image showing a medial deviation and severe narrowing of the distal common bile duct (*arrow*). **d** T2-weighted HASTE image showing a large retroperitoneal adenopathy adjacent to the common bile duct, causing extrinsic compression and stenosis (*arrow*)

Gallbladder and Cystic Duct

4 Gallbladder and Cystic Duct

4.1 Normal Anatomy and Variants

#92 Gallbladder

KEY FACTS: ANATOMY (GORE ET AL. 1994)

- The gallbladder is located in a fossa on the lower surface of the liver between the right and left lobes
- Normal wall thickness: < 2–3 mm
- Divided into four parts: fundus, body, infundibulum, and neck

KEY FACTS: VARIANTS

- Location (e.g., may be intrahepatic, suprahepatic, retroperitoneal)
- Content: sludge (calcium bilirubinate granules and cholesterol crystals), commonly found during prolonged fasting and hyperalimentation (Fig. 92a, b)
- Classification of septa:
  - *Longitudinal septum* (= duplication; 1 in 3000 to 1 in 12000);
  - *Isolated transverse septum*
  - *Phrygian cap:* 2%–6% of population, kinking/folding of fundus and sometimes septum; Fig. 92c, d)
- Size ("cholecystomegaly" vs. "microgallbladder")

KEY FACTS: MRI (BRET AND REINHOLD 1997)

- Signal intensity of gallbladder content:
  - T2: hyperintense
  - T1: variable, depending on the composition and concentration of bile (higher signal intensity in patients fasting for several hours; Demas et al. 1985)
- The normal gallbladder wall is thin and hypointense relative to retroperitoneal fat on non-fat-suppressed snapshot T2-weighted MR images
- Signal intensity of sludge (Fig. 92a, b):
  - T1: hyperintense
  - T2: slightly hypointense (differential diagnosis with stones: shape)

References

Bret P, Reinhold C (1997) MRI of the gallbladder. In: Rossi P (ed) Biliary tract radiology. Springer, Berlin Heidelberg New York, pp 59–69

Demas BE, Hricak H, Moseley M et al. (1985) Gallbladder bile: an experimental study in dogs using MR imaging and proton MR spectroscopy. Radiology 157: 453–455

Freeny PC, Stevenson GW (1994) Margulis and Burhenne's alimentary tract Radiology, 5th edn. Mosby, St Louis

Gore RM, Ghahremani GG, Fernbach SK (1994) Gallbladder: anomalies and anatomic variants. In: Gore RM, Levine MS, Laufer I (eds) Textbook of gastrointestinal radiology. Saunders, Philadelphia, pp 1621–1635

Hakansson K, Christoffersson JO, Leander P et al. (2002) On the appearance of bile in clinical MR cholangiopancreatography. Acta Radiol 43: 401–410

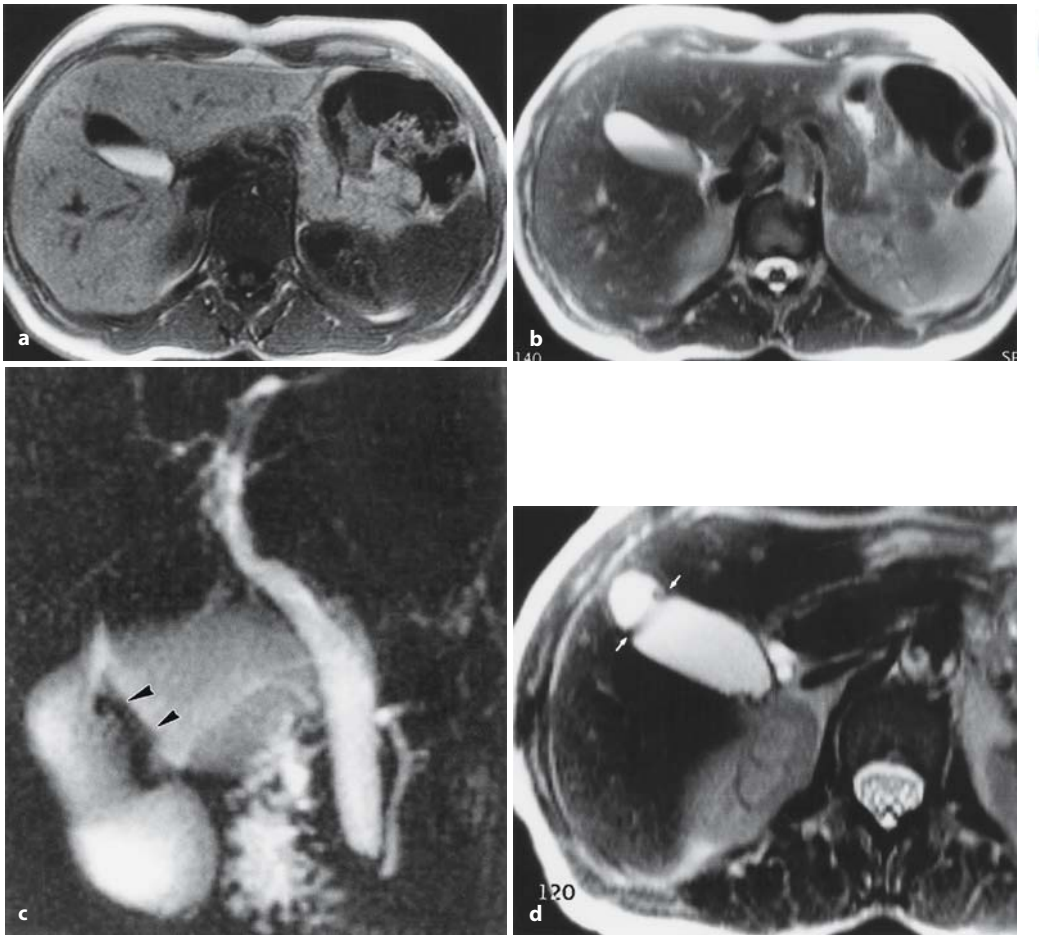

Fig. 92 a, b. Sludge. **a** T1- and **b** T2-weighted images showing sludge in dependent portion of the gallbladder. **c, d** Phrygian cap. **c** Projective image showing folding of fundus with larger diameter of the distal part and presence of a septum (*arrowheads*). **d** Axial T2-weighted image showing septum (*arrows*). Note higher signal intensity of bile within the fundus

#93 Cystic Duct

Related topics: #27, 28 (intrahepatic bile ducts, variant anatomy), #82, 83 (extrahepatic duct, complications after cholecystectomy)

KEY FACTS: ANATOMY

- Average diameter: 1.8 mm
- Average length: 2–4 cm
- Course: classically serpiginous with tight S-shaped bends
- Location:
  - Distal part usually posterior to the common bile duct (95%)
  - May run parallel to the common hepatic duct for a short distance
  - In 10%, the two ducts have a long parallel course
- Insertion: the point at which the cystic duct joins the bile duct is quite variable (Shaw et al. 1993) (Fig. 93a):
  - Upper part of bile duct (including left or right hepatic duct): ± 30%
  - Middle part: ± 60%
  - Lower part: ± 10%

KEY FACTS: MRI

- Small, tubular fluid-containing structure between the gallbladder and bile duct
- Usually easily recognized due to its characteristic location and "folded" appearance
- Identification of anatomic variants (high and low insertion, long parallel course) is important if (laparoscopic) cholecystectomy is planned (see #52, 82, 83) (Fig. 93b, c)

References

Schulte SJ (1994) Embryology, normal variation, and congenital anomalies of the gallbladder and biliary tract. In: Freeny PC, Stevenson GW (eds) Marqulis and Burhenne's alimentary tract radiology. Mosby, St. Louis, pp 1251–1274

Shaw MJ, Dorscher PJ, Vennes JA (1993) Cystic duct anatomy: an endoscopic perspective. Am J Gastroenterol 88: 2102–2106

Silvis SE (1995) The normal bile duct. In: Silvis S, Rohrmann C, Ansel H (eds) Endoscopic retrograde cholangiopancreatography. Igaku-Shoin, New York, pp 168–192

Turner MA, Fulcher AS (2001) The cystic duct: normal anatomy and disease processes. Radiographics 21: 3–22

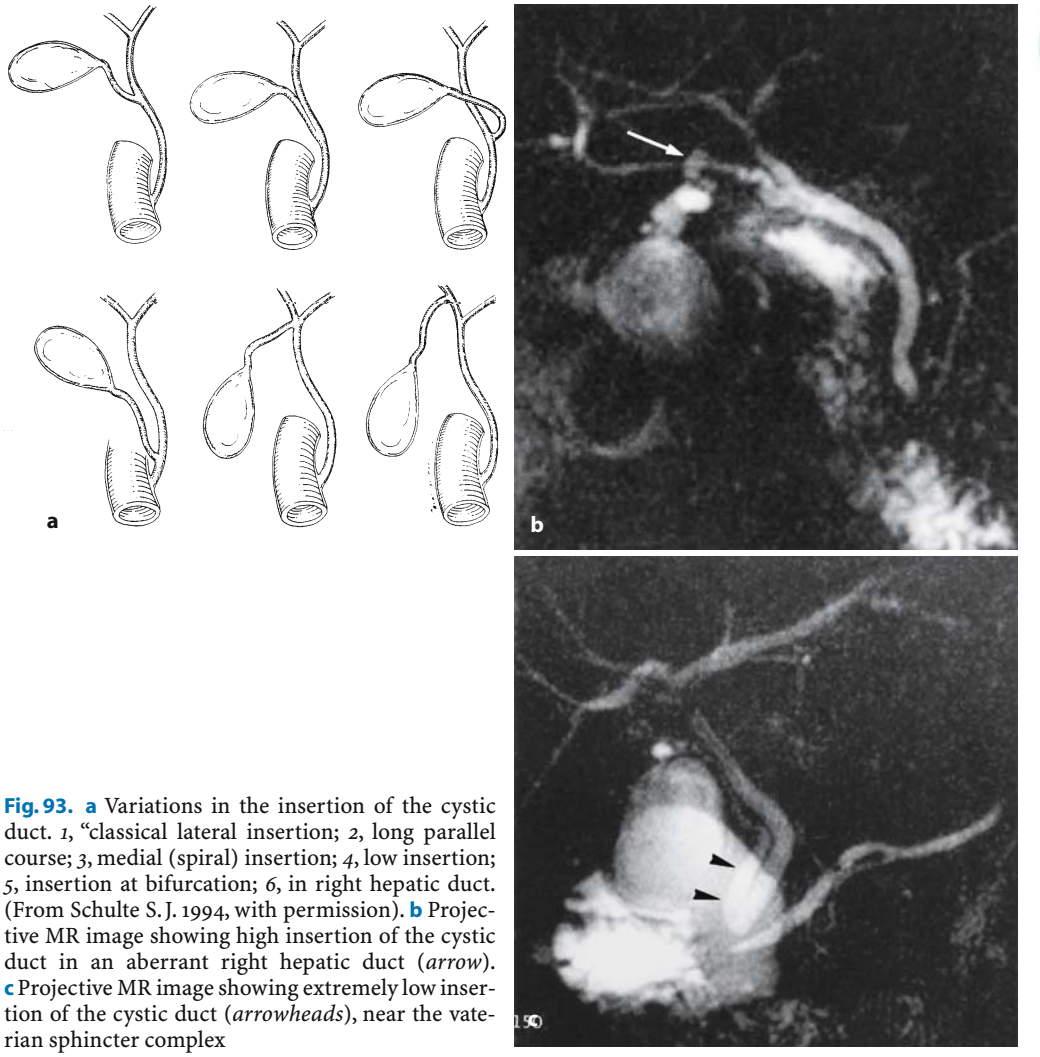

Fig. 93. **a** Variations in the insertion of the cystic duct. *1*, "classical lateral insertion; *2*, long parallel course; *3*, medial (spiral) insertion; *4*, low insertion; *5*, insertion at bifurcation; *6*, in right hepatic duct. (From Schulte S. J. 1994, with permission). **b** Projective MR image showing high insertion of the cystic duct in an aberrant right hepatic duct (*arrow*). **c** Projective MR image showing extremely low insertion of the cystic duct (*arrowheads*), near the vaterian sphincter complex

4.2 Benign Nontraumatic Abnormalities

#94 Cholecystolithiasis, Classical Appearance

Related topic: #72 (stones in the common bile duct)

KEY FACTS: DISEASE

- Incidence: depends on age and sex (25% in women over 50 years)
- Ratio of women to men: 3:1
- Types:
  - Cholesterol stones (± 80% in Western countries): pure cholesterol (10%); cholesterol plus calcium (70%)
  - Pigment stones (calcium bilirubinate)
- Predisposing factors for cholesterol stones:
  - Estrogens (female sex, pregnancy)
  - Obesity
  - High age
  - Hypertriglyceridemia
  - Clofibrate therapy
- Predisposing factors for pigment stones:
  - Hemolytic disease (e.g., spherocytosis, prosthetic cardiac valves)
  - Cirrhosis
  - High age
  - Biliary disease (e.g., stricture)
- Symptoms and complications:
  - Biliary colic
  - Pancreatitis
  - Acute and chronic cholecystitis
  - Fistula
  - Cancer of gallbladder (incidence doubled)

KEY FACTS: MRI

- Signal intensity:
  - Most commonly hypointense on T1- and T2-weighted images
  - May be partially or (more rarely) entirely hyperintense on T1 (Fig. 94a, b)
- Comments:
  - Cross-sectional T2-weighted images are more sensitive than projective and T1-weighted images
  - Ultrasonography is the primary modality for detection of stones in the gallbladder

References

Baron RL, Shuman WP, Lee SP et al. (1989) MRI appearance of gallstones in vitro at 1.5 T: correlation with chemical composition. AJR Am J Roentgenol 153:497–502

Bret P, Reinhold C (1997) MRI of the gallbladder. In: Rossi P (ed) Biliary tract radiology. Springer, Berlin Heidelberg New York, pp 59–69

Calvo MM, Bujanda L, Heras I, et al. (2002) Magnetic resonance cholangiography versus ultrasound in the evaluation of the gallbladder. J Clin Gastroenterol 34:233–236

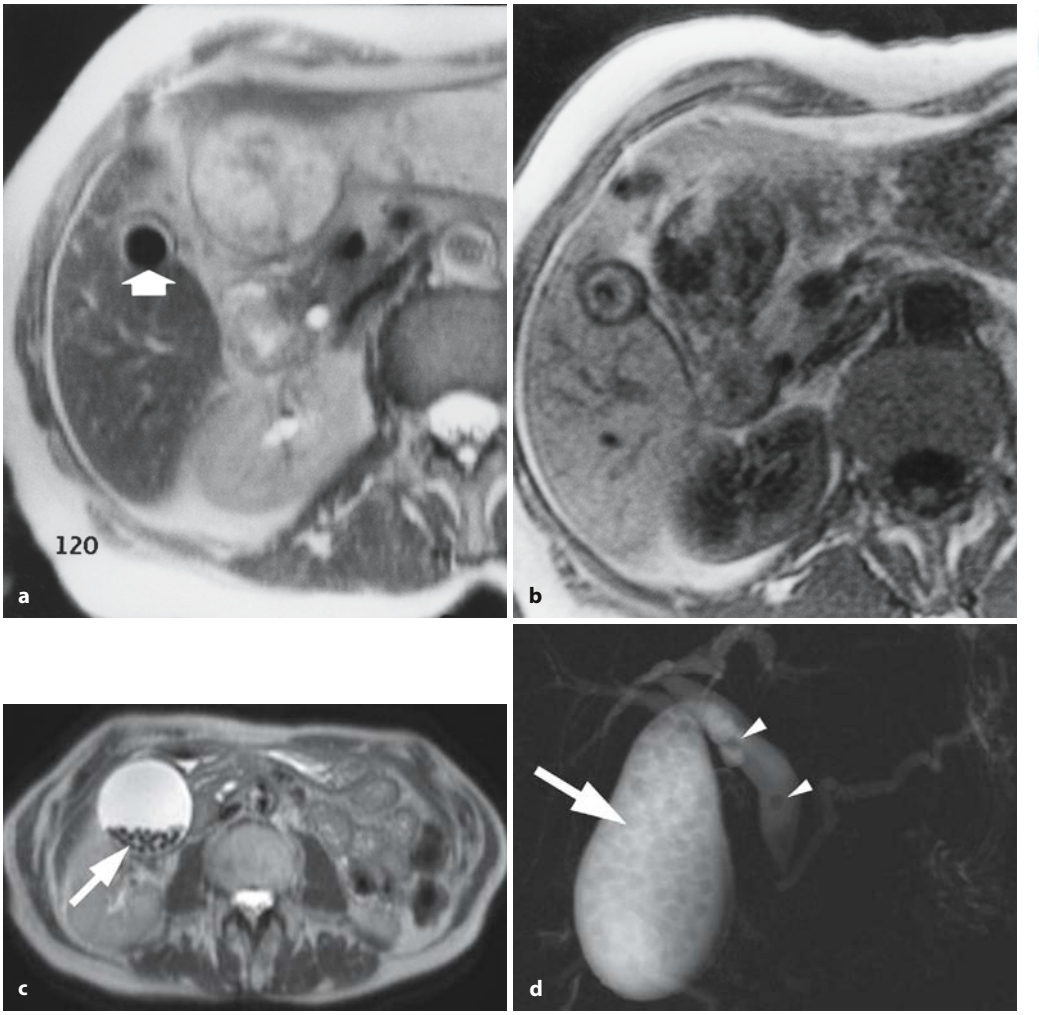

Fig. 94. a, b T2-weighted image (**a**) showing a gallstone as a rounded hypointense structure in the gallbladder lumen (*arrow*). Note the thick, hyperintense gallbladder wall. **b** T1-weighted image showing a gallstone containing two layers: a hyperintense outer layer and a hypointense (calcified) core. The outer hypointense layer corresponds to the thickened wall of the gallbladder. **c, d** Different patient. T2-weighted HASTE image (**c**) and projective image (**d**) showing multiple small gallstones (*arrow*). Note several common bile duct stones (*arrowheads*)

#95 Cholecystolithiasis, Variant Appearance

KEY FACTS: MRI

- Floating stones (Fig. 95a): causes and mechanisms:
  - Relatively pure cholesterol stones
  - Gas-containing stones
  - Rise in specific gravity of bile
- Gas-containing stones:
  - Dehydration of older stones → internal shrinkage → nitrogen gas filling ("crow-foot" or "Mercedes-Benz" sign) → hypointense central core
- The central core may also contain water and appear as a hyperintense "star" (Fig. 95b)
- Gallstones may be missed if they are not surrounded by fluid:
  - Microgallbladder
  - Chronic cholecystitis
  - Small stones impacted in the infundibulum/cystic duct

References

Baron RL, Shuman WP, Lee SP et al. (1989) MRI appearance of gallstones in vitro at 1.5 T: correlation with chemical composition. AJR Am J Roentgenol 153 : 497 – 502

Bret P, Reinhold C (1997) MRI of the gallbladder. In: Rossi P (ed) Biliary tract radiology. Springer, Berlin Heidelberg New York, pp 59 – 69

Moeser PM, Julian S, Karstaedt N, Sterchi M (1988) Unusual presentation of cholelithiasis on T1-weighted MR imaging. J Comput Assist Tomogr 12 : 150 – 152

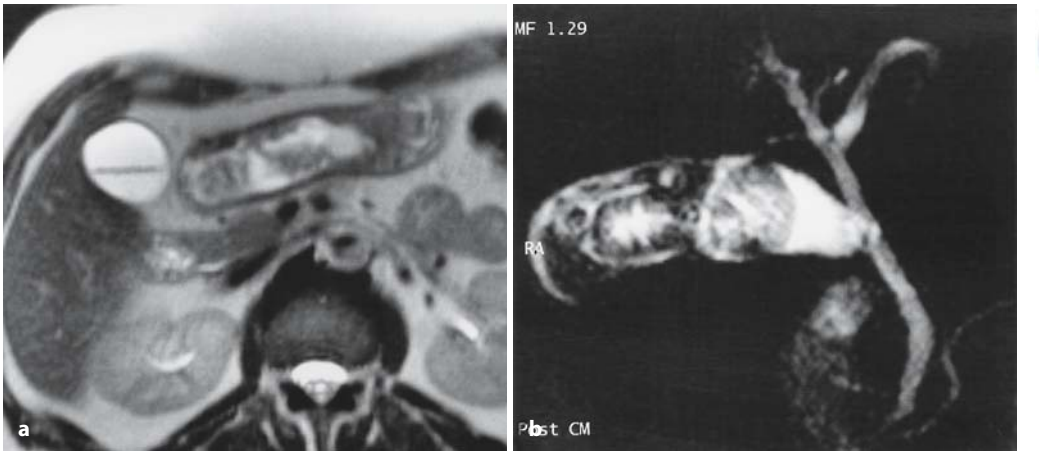

Fig. 95. **a** Axial T2-weighted image showing floating stones. **b** Projective MR image showing gallstones with hyperintense central core

#96 Acute Cholecystitis

KEY FACTS: DISEASE

- Acute inflammation of the gallbladder
- Age peak: fifth to sixth decade
- Types/mechanism:
  - Calculous cholecystitis (90 %): related to cystic duct obstruction by impacted stone
  - Acalculous cholecystitis (10 %): gallbladder wall ischemia secondary to distention (e. g., associated with severe trauma, prolonged fasting)
- Predisposing factor: cholecystolithiasis
- Diagnosis: usually clinical
- Complications:
  - Intramural abscess (see # 98)
  - Gangrene (see # 99)
  - Perforation (see # 100)
  - Empyema

KEY FACTS: MRI (FIG. 96)

- T 2-weighted images:
  - Wall thickening (intramural edema)
  - Increased signal intensity of wall (intramural edema)
  - Hydrops
- T1-weighted images:
  - Usually (not always) low signal intensity of bile, related to high fluid content (sign with differentiating value only in patients fasting for 8 – 12 h; Pu et al. 1994)
- Contrast-enhanced images:
  - Marked enhancement of the gallbladder wall (not specific)
  - Transient enhancement of adjacent liver parenchyma
- Differential diagnosis with chronic cholecystitis: high signal intensity of the gallbladder wall on heavily T 2-weighted images (Fig. 96)

References

Kim KW, Park M, Yu J, et al. (2003) Acute cholecystitis at T2-weighted and manganese-enhanced T1-weighted MR cholangiography: preliminary study. Radiology 227 : 580 – 584

Loud PA, Semelka RC, Kettritz U, Brown JJ, Reinhold C (1996) MRI of acute cholecystitis: comparison with the normal gallbladder and other entities. Magn Reson Imaging 14 : 349 – 355

Pu Y, Yamamoto F, Igimi H et al. (1994) A comparative study of the usefulness of magnetic resonance imaging in the diagnosis of acute cholecystitis. J Gastroenterol 29 : 192 – 198

Weissleder R, Stark DD, Compton CC, Simeone JF, Ferruci JT (1988) Cholecystitis: diagnosis by MR imaging. Magn Reson Imaging 6 : 345 – 348

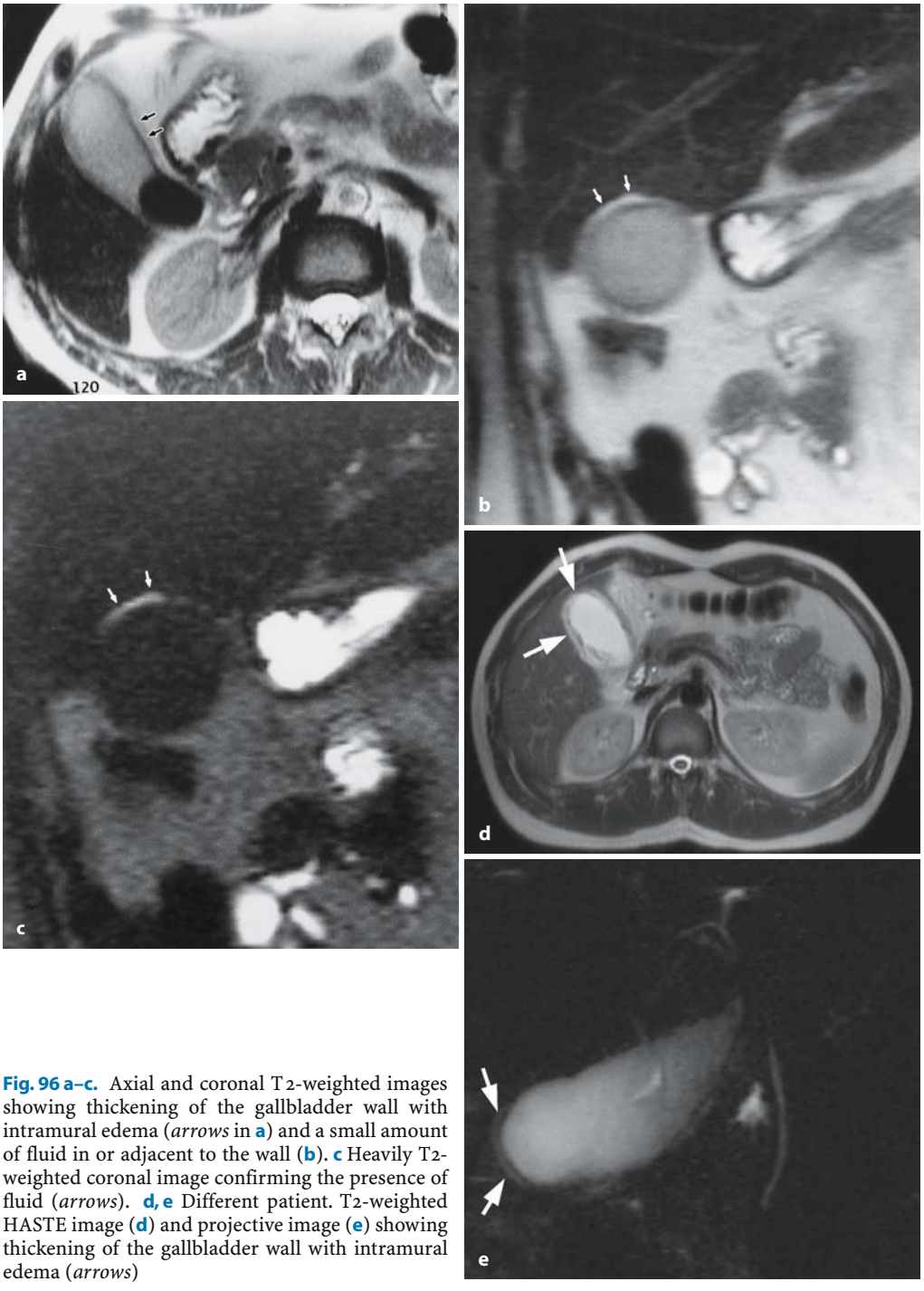

Fig. 96 a–c. Axial and coronal T2-weighted images showing thickening of the gallbladder wall with intramural edema (*arrows* in **a**) and a small amount of fluid in or adjacent to the wall (**b**). **c** Heavily T2-weighted coronal image confirming the presence of fluid (*arrows*). **d, e** Different patient. T2-weighted HASTE image (**d**) and projective image (**e**) showing thickening of the gallbladder wall with intramural edema (*arrows*)

#97 Acute Cholecystitis with Pericholecystitis

KEY FACTS: DISEASE

- Acute cholecystitis with transmural extension of inflammation

KEY FACTS: MRI (FIG. 97)

- In patients with acute cholecystitis, the following features are commonly seen:
  - Moderate hyperintensity of the adjacent fat (edema, inflammation)
  - Fluid around the gallbladder
- The inflammation may extend to the common bile duct, duodenum, and/or hepatic flexure of colon
- *Note:* Detection of small amounts of fluid requires the use of heavily T2-weighted images (see double echo technique, #2)

References

Weissleder R, Stark DD, Compton CC, Simeone JF, Ferruci JT (1988) Cholecystitis: diagnosis by MR imaging. Magn Reson Imaging 6:345–348

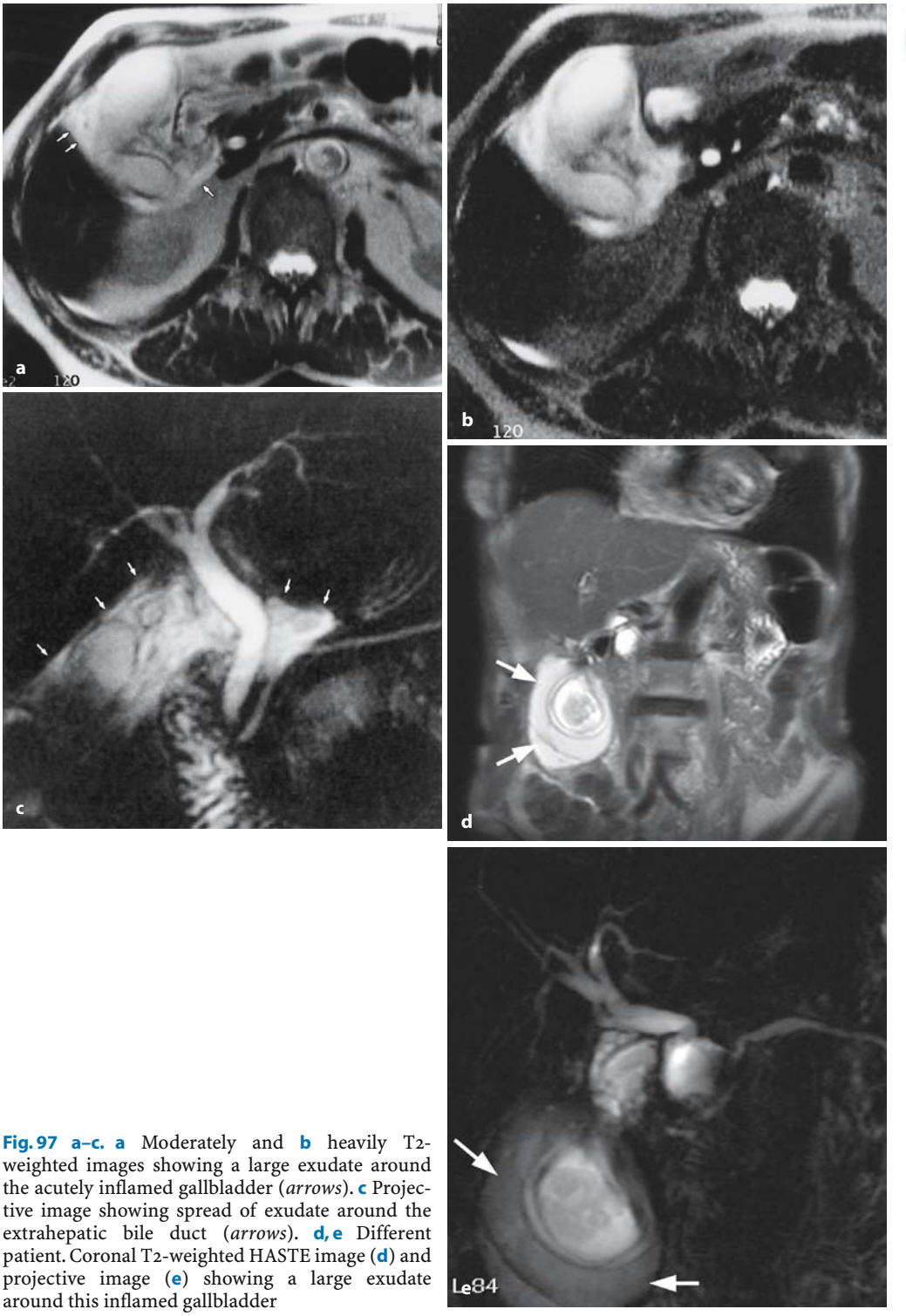

Fig. 97 a–c. **a** Moderately and **b** heavily T2-weighted images showing a large exudate around the acutely inflamed gallbladder (*arrows*). **c** Projective image showing spread of exudate around the extrahepatic bile duct (*arrows*). **d, e** Different patient. Coronal T2-weighted HASTE image (**d**) and projective image (**e**) showing a large exudate around this inflamed gallbladder

#98 Complications of Acute Cholecystitis (1): Intramural Abscess

KEY FACTS: DISEASE

- Acute cholecystitis with the presence of pus in the gallbladder wall
- Incidence: 2 % – 20 %
- Mechanism: focal necrosis
- Other common locations of abscesses include:
  - Gallbladder bed
  - Peritoneal cavity

KEY FACTS: MRI

- Signs of acute cholecystitis plus a well-delineated fluid-containing area in the gallbladder wall (Fig. 98)
- Sometimes, circumferential intramural collections are observed with associated mucosal desquamation (Fig. 98 e – h)

References

Weissleder R, Stark DD, Compton CC, Simeone JF, Ferruci JT (1988) Cholecystitis: diagnosis by MR imaging. Magn Reson Imaging 6 : 345–348

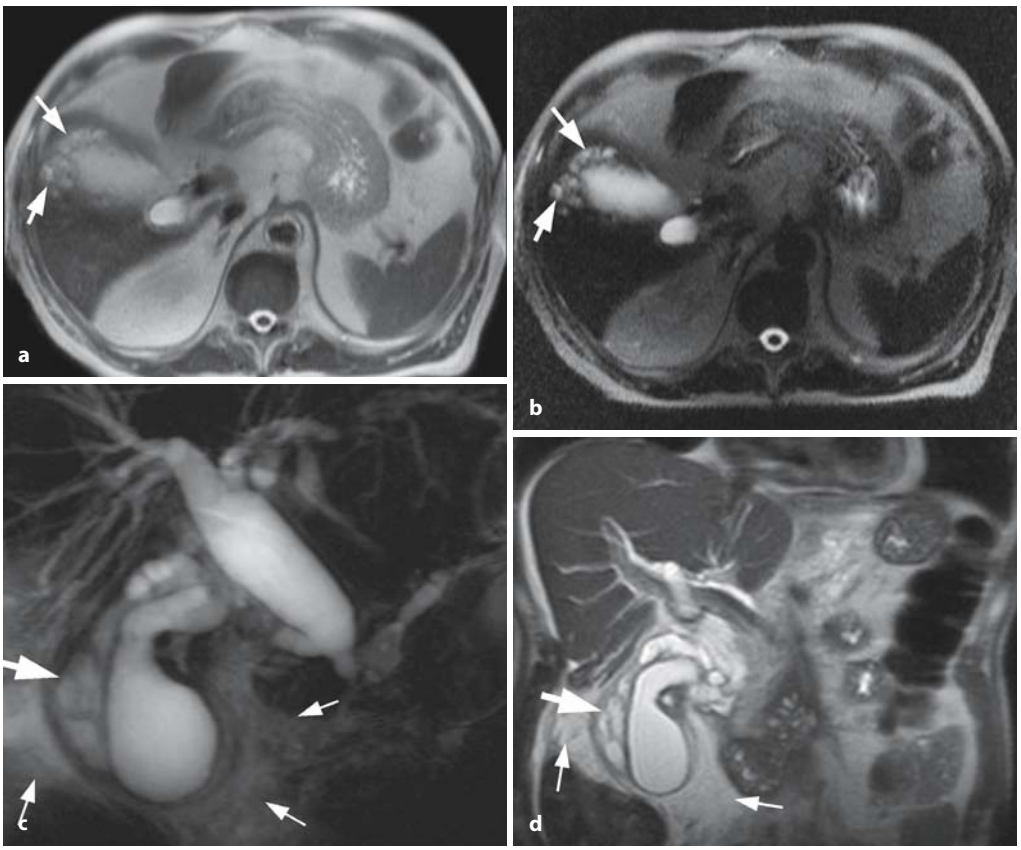

Fig. 98 a, b. Moderately (**a**) and heavily (**b**) T2-weighted HASTE images showing multiple intramural fluid collections: small intramural abscesses (*arrows*). Note that, in this case, the imaging features could be confused with those of focal adenomyomatosis (see Fig. 109). **c–e** Different patient. Projective image (**c**), coronal (**d**) and axial (**e**) T2-weighted HASTE images showing a large intramural fluid collection (*large arrow*) and an extensive exudate around the gallbladder (*small arrows*) due to a severe acute cholecystitis with intramural abscess.

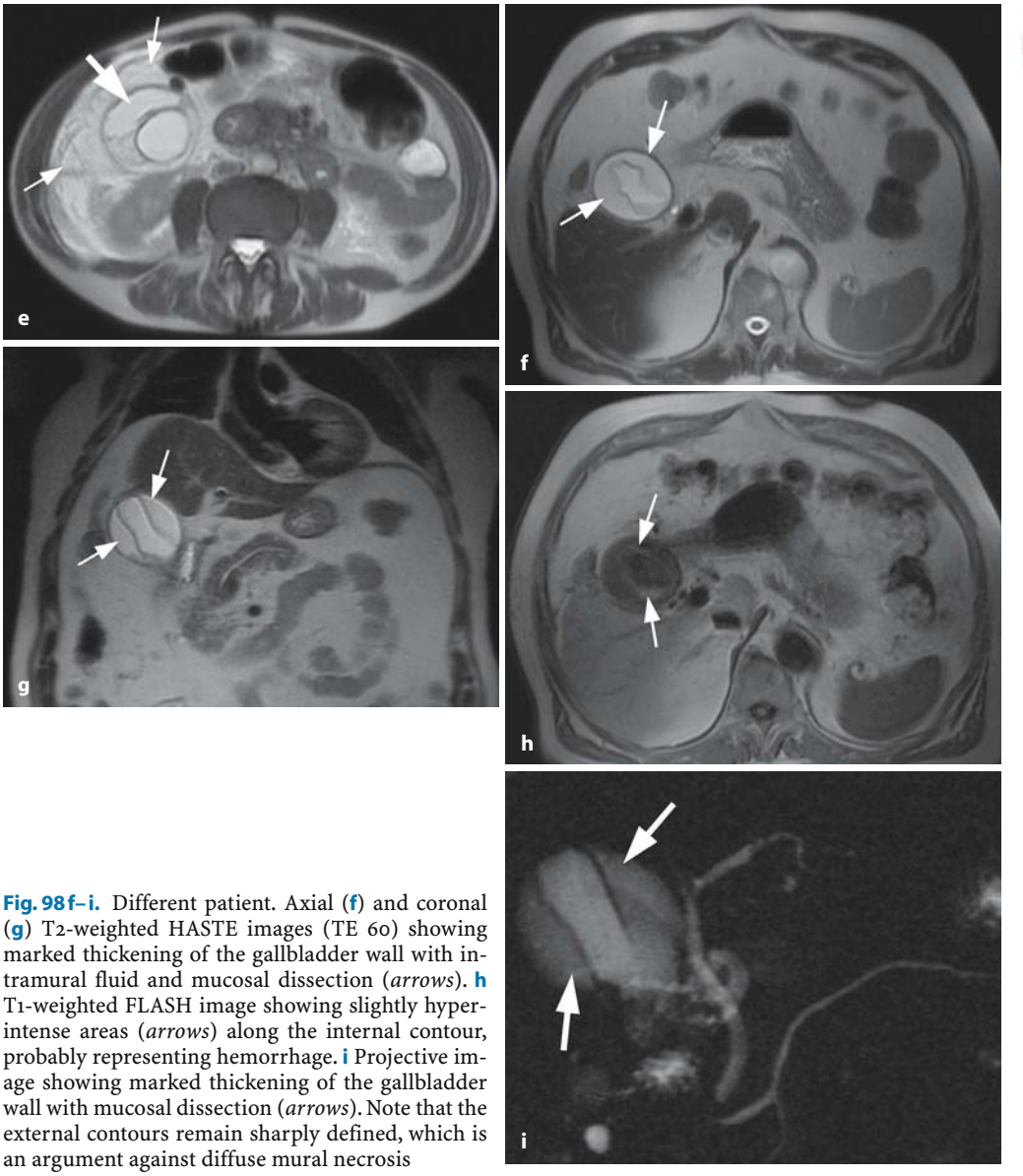

Fig. 98 f–i. Different patient. Axial (**f**) and coronal (**g**) T2-weighted HASTE images (TE 60) showing marked thickening of the gallbladder wall with intramural fluid and mucosal dissection (*arrows*). **h** T1-weighted FLASH image showing slightly hyperintense areas (*arrows*) along the internal contour, probably representing hemorrhage. **i** Projective image showing marked thickening of the gallbladder wall with mucosal dissection (*arrows*). Note that the external contours remain sharply defined, which is an argument against diffuse mural necrosis

#99 Complications of Acute Cholecystitis (2): Gangrene

KEY FACTS: DISEASE

- Severe inflammation of the gallbladder with mural necrosis
- Underlying conditions: marked distention, vasculitis, diabetes, torsion
- Complication: perforation

KEY FACTS: MRI (FIG. 99)

- Appearance of the wall:
  - Loss of definition (important feature)
  - Thickening
  - Heterogeneous aspect (mucosal ulcers, hemorrhage, necrosis, etc.)
  - Discontinuous mucosal enhancement (Singh and Sagar 2005)
- Other features that may be observed:
  - Microabscess
  - Intraluminal debris or membranes (desquamated mucosa)

References

Jeffrey RB, Laing FC, Wong W, Callen PW (1983) Gangrenous cholecystitis: diagnosis by ultrasound. Radiology 148 : 219 – 221

Singh AK, Sagar P (2005) Gangrenous cholecystitis: prediction with CT imaging. Abdom Imaging 30 : 218 – 221

Teefey SA, Baron RL, Radke HM, Bigler SA (1991) Gangrenous cholecystitis: new observations on sonography. J Ultrasound Med 10 : 603 – 606

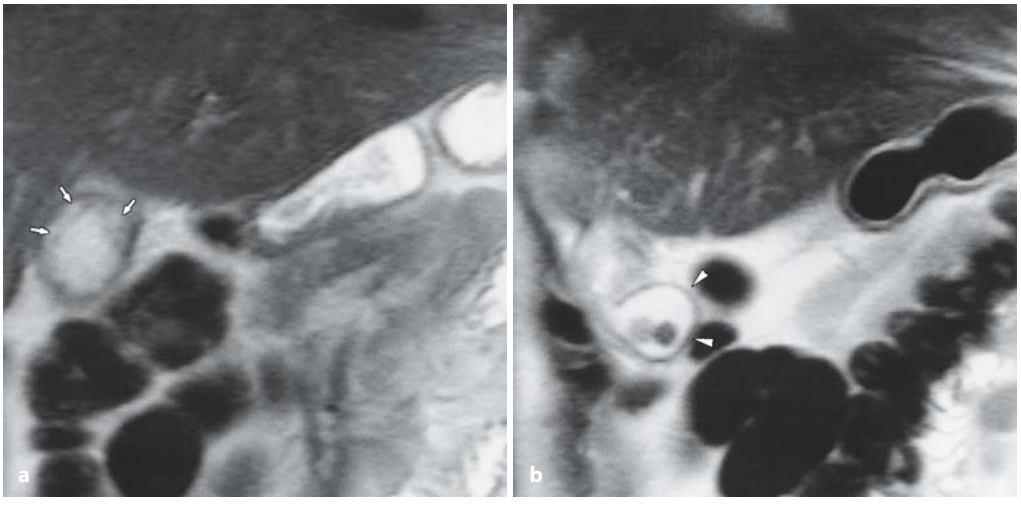

Fig. 99 a, b. Coronal T2-weighted MR images showing a markedly thickened gallbladder wall containing slightly hyperintense areas (*arrows* in **a**; possibly necrosis). Also note loss of definition of internal contours. The wall of the fundus of the gallbladder still has a normal appearance (*arrowheads* in **b**)

#100 Complications of Acute Cholecystitis (3): Perforation

KEY FACTS: DISEASE

- Focal rupture of the gallbladder wall
- Incidence: 3%–15% of patients with acute cholecystitis
- Types:
  - Contained (localized) perforation (contained by omentum or adhesions produced by recurrent inflammation)
  - Free perforation (less common)
- Location of wall defect: usually in the fundus
- Relative surgical emergency; percutaneous drainage can be useful
- Free perforation is associated with a high mortality rate (up to 30%)

KEY FACTS: MRI (FIG. 100)

- Signs of acute cholecystitis plus focal defect of wall
- Appearance of abscess:
  - Well-demarcated fluid-containing lesion
  - Usually (not always) relative thick wall
  - Communication with the gallbladder lumen may be visible

References

Siskind BN, Hawkins HB, Cinti DC, Zeman RK, Burrell MI (1987) Gallbladder perforation. An imaging analysis. J Clin Gastroenterol 9 : 670 – 678

Sood B, Jain M, Khandelwal N, Singh P, Suri S (2002) MRI of perforated gall bladder. Australas Radiol 46 : 438 – 440

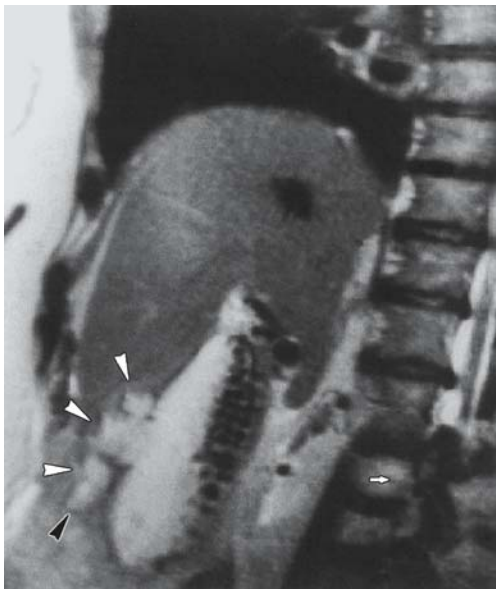

Fig. 100. Sagittal T2-weighted MR image showing fluid collection located between the gallbladder and liver (*arrowheads*) and communicating with the gallbladder lumen: perforated acute cholecystitis with abscess

#101 Acute Emphysematous Cholecystitis

KEY FACTS: DISEASE

- Acute inflammation with ischemia of the gallbladder wall and complicated by infection with gas-producing organisms
- Organism: *Clostridium perfringens*
- Mechanism: occlusion of the cystic artery secondary to cystic duct obstruction with edema
- Predisposing factors: diabetes (20 %–30 % of cases of acute emphysematous cholecystitis)
- Complications:
  - Gangrene (75 %)
  - Perforation (20 %)
  - Mortality (15 %)

KEY FACTS: MRI (FIG. 101)

- Presence of gas:
  - In the gallbladder wall
  - In the gallbladder lumen
  - In the pericholecystic tissue (if perforation has occurred)
  - In bile ducts (not obligate)
- Differential diagnosis of intraluminal gas:
  - Cholecystoenteric fistula (see # 103)
  - Incompetent sphincter of Oddi
  - After biliary surgery/ERCP
- Differential diagnosis of intramural gas: air-containing abscess with or without fistula

References

Koenig T, Tamm EP, Kawashima A (2004) Magnetic resonance imaging findings in emphysematous cholecystitis. Clin Radiol 59(5): 455 – 458

McMillin K (1985) Computed tomography of emphysematous cholecystitis. J Comp Assist Tomogr 9 : 330 – 332

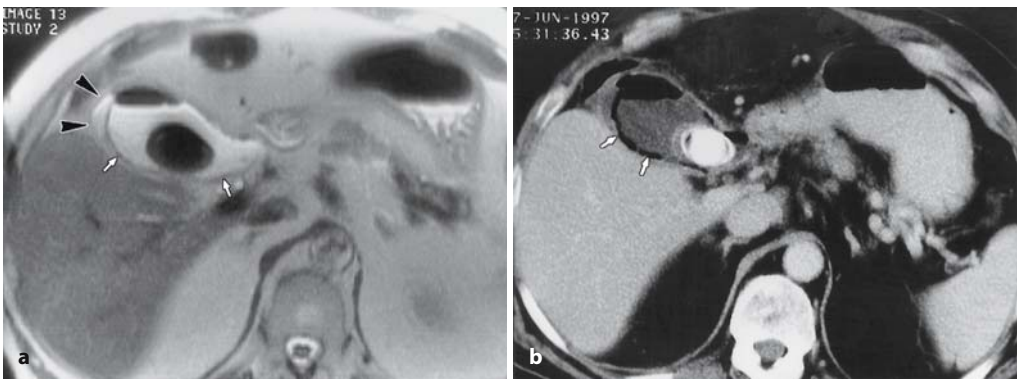

Fig. 101 a, b. **a** Axial T2-weighted MR image showing a gallbladder with a large stone and an air–fluid level. Also note pericholecystic fluid (*arrowheads*) and low signal intensity of gallbladder wall (*arrows*). **b** CT image showing the intramural air more clearly (*arrows*). In this patient, acute emphysematous cholecystitis was complicated by perforation

#102 Peridiverticulitis of the Gallbladder

KEY FACTS: DISEASE

- Definition: inflammation of true gallbladder diverticula (i. e., diverticula containing all mural layers, including muscle)
- Incidence: very rare

KEY FACTS: MRI

- Typical features (Fig. 102):
  - Signs of acute inflammation (fluid, edema, wall thickening)
  - Visualization of one or more diverticula
- Differential diagnosis: adenomyomatosis associated with acute cholecystitis

References

Chan-Wilde C, Chew R, Foong WC, Wee A (1990) Adenomyomatosis of the gallbladder: the NUH experience. Ann Acad Med Singapore 19:389–392

Gore RM, Ghahremani GG, Fernbach SK (1994) Gallbladder: anomalies and anatomic variants. In: Gore RM, Levine MS, Laufer I (eds) Textbook of gastrointestinal radiology. Saunders, Philadelphia, pp 1621–1635

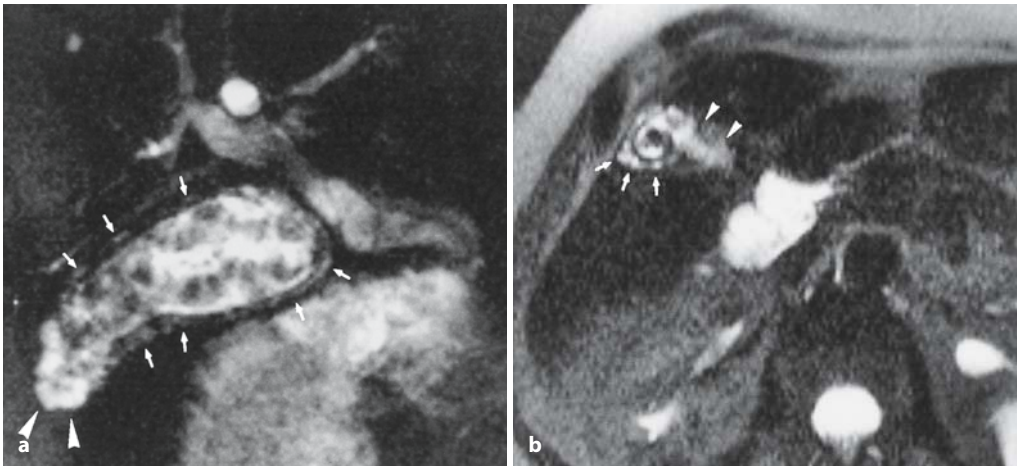

Fig. 102 a, b. **a** Projective image showing a gallbladder filled with stones. Note the presence of multiple small fluid "collections" within the wall (*arrows*) and large diverticula in the fundus (*arrowheads*). **b** Same patient. Heavily T2-weighted axial image showing diverticular outpouchings in the fundus (*arrows*) and pericholecystic fluid (*arrowheads*). Pathology revealed gallbladder diverticulosis with diverticulitis and mural necrosis. The largest outpouchings located in the fundus probably represent diverticula. The smaller hyperintense areas seen elsewhere in the gallbladder wall may represent either diverticula or areas of necrosis

#103 Cholecystoenteric Fistula

KEY FACTS: DISEASE

- Abnormal communication between the gallbladder and digestive tract
- Usually older patients (> 65 years)
- Most common causes:
  - Cholecystolithiasis with or without acute cholecystitis (90 %)
  - Peptic ulcer disease (6 %)
  - Carcinoma
  - Colonic diverticulitis
- Communication with duodenum in 70 %, with colon in 26 %
- Gallstone ileus is a possible complication:
  - Erosion of stone in the gastrointestinal tract
  - Stones may be "hung up" at narrow portions of the gastrointestinal tract, e. g., ligament of Treitz, ileocecal valve, sigmoid colon

KEY FACTS: MRI (FIG. 103)

- Typical features:
  - Air in the gallbladder lumen
  - Air in the biliary tract if the cystic duct is patent
  - Focal or diffuse thickening of the gallbladder wall (depending on underlying disease)
  - Inflammatory changes around the gallbladder
  - Direct visualization of the fistula

References

Beltran MA, Csendes A (2005) Mirizzi syndrome and gallstone ileus: an unusual presentation of gallstone disease. J Gastrointest Surg 9 : 686 – 689

Haff RC, Wise L, Ballinger WF (1971) Biliary-enteric fistulas. Surg Gynecol Obstet 133 : 84 – 88

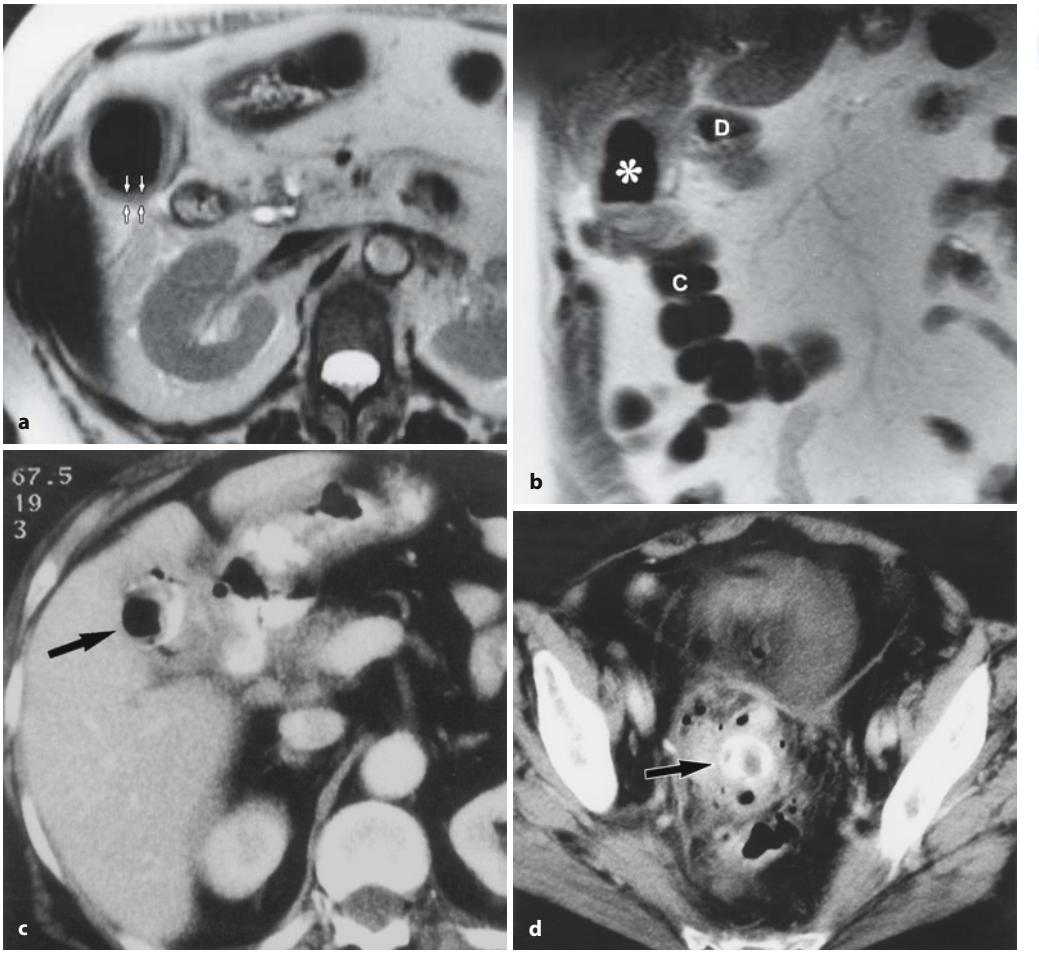

Fig. 103 a–d. Patient with antecedent sigmoid diverticulitis now presenting with signs of obstruction. **a** Axial and **b** coronal T2-weighted images showing the gallbladder with a thickened wall (*arrows* in **a**) and a markedly hypointense lumen. Note that neither the colon (*C*) nor the duodenum (*D*) can be separated from the gallbladder wall in **b**. *Asterisk*, air in the gallbladder lumen. **c** Same patient. CT image showing the gallbladder (*arrow*) containing air and orally administered contrast medium, thus suggesting the presence of a cholecystoduodenal fistula. **d** Same patient. CT image of pelvis showing gallstone impacted in the sigmoid colon (*arrow*). Note the presence of diverticula and inflammatory changes. The final diagnosis was cholecystitis with cholecystoduodenal fistula and spontaneous migration of a gallstone into the colon

#104 Chronic Cholecystitis

KEY FACTS: DISEASE

- Chronic inflammation of the gallbladder wall
- Histology: chronic inflammatory cell infiltrate throughout all the layers of the wall which becomes thickened with fibrosis
- Most common form of gallbladder inflammation
- Causes/associated disease:
  - Cholecystolithiasis
  - (Intermittent) cystic duct obstruction
- Symptoms:
  - Patients may be asymptomatic
  - Recurrent right upper quadrant pain

KEY FACTS: MRI (FIG. 104)

- Morphologic features:
  - Smooth or irregular thickening of the gallbladder wall
  - Gallbladder shrinkage may be a prominent feature (Fig. 104 c, d)
- Signal intensity: hypointense aspect of the gallbladder wall and adjacent fat on heavily T 2-weighted images (no edema/fluid; Fig. 104 a, b)
- Dynamic contrast-enhanced MRI: smoothly delineated early enhancement of mucosa and muscle and more delayed enhancement of subserosa (fibrosis) (Demachi et al. 1997)
- Decreased contraction after cholecystokinin administration (see # 19)
- Differential diagnosis:
  - Acute cholecystitis: presence of fluid/edema (best seen on heavily T 2-weighted images)
  - Carcinoma: more heterogeneous aspect; irregularly delineated enhancement; secondary signs of malignancy

References

Brugge WR, Brand DL, Atkins HL, Lane BP, Abel WG (1986) Gallbladder dyskinesia in chronic acalculous cholecystitis. Dig Dis Sci 31 : 461 – 467

Demachi H, Matsui O, Hoshiba K et al. (1997) Dynamic MRI using a surface coil in chronic cholecystitis and gallbladder carcinoma: radiologic and histopathologic correlation. J Comp Assist Tomogr 21 : 643 – 51

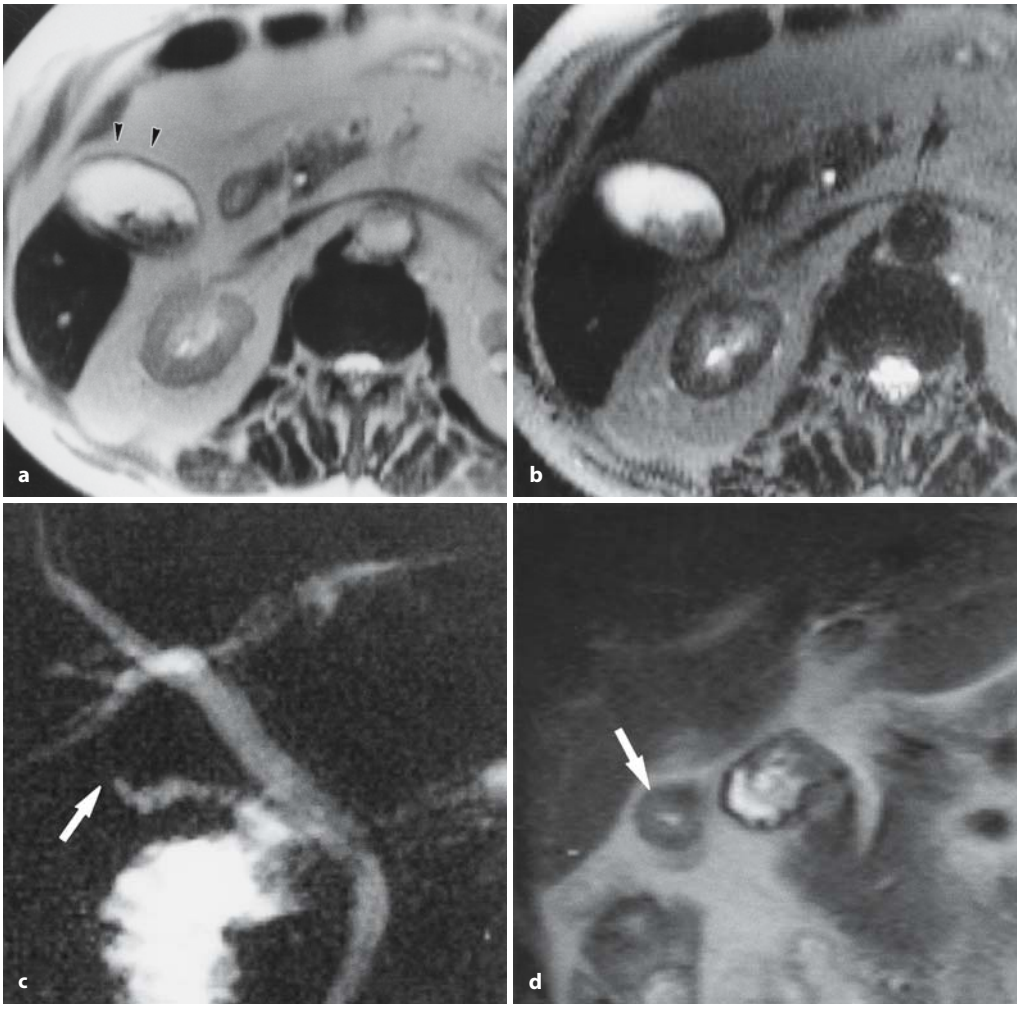

Fig. 104. a, b Moderately T2-weighted MR image showing a thickened gallbladder wall. Note the presence of a thin, hyperintense halo around the gallbladder (*arrowheads*), possibly fluid or fat. **b** Heavily T2-weighted image showing that this "halo" and the surrounding fat are isointense, which excludes fluid and suggests chronic (rather than acute) inflammation. **c, d** Other patient. **c** Projective MR image showing a normal cystic duct. The gallbladder is invisible, however (*arrow*). **d** Cross-sectional T2-weighted image obtained in the coronal plane showing a shrunken gallbladder with a thickened wall and nearly no intraluminal fluid (*arrow*), thus explaining the findings in Fig. 104c

#105 Xanthogranulomatous Cholecystitis

KEY FACTS: DISEASE

- Chronic inflammatory disorder of the gallbladder
- Histology:
  - Multiple yellow–brown intramural formations, severe proliferative fibrosis, foamy histiocytes
  - Newer lesions often contain necrotic areas
- Incidence: 0.7 % – 10.6 %
- Etiology (hypotheses):
  - Intramural extravasation of bile with xanthogranulomatous reaction
  - Chronic infection
- Clinical presentation: similar to chronic cholecystitis
- Significance: may simulate gallbladder carcinoma, both clinically and radiologically (Cossi et al. 1987)

KEY FACTS: MRI (FIG. 105)

- Marked wall thickening, usually diffuse
- Signal intensity:
  - Dependent on histologic composition
  - T1: relatively high signal intensity (fat) (Joerg et al. 1989)
  - Areas of iso- to slightly high signal on T2-weighted images correspond with areas of abundant xanthogranulomas at pathologic examination
  - Areas with very high signal itensity on T2-weighted images correspond with necrosis and/or abscesses
- Contrast-enhanced images: heterogeneous enhancement of the wall
- Differential diagnosis:
  - Abscess (more focal)
  - Tumor (features pointing to xanthogranulomatous cholecystitis are the presence of necrotic areas, diffuse involvement of the gallbladder wall, and preservation of the mucosal line)
  - Adenomymatosis (presence of pseudodiverticula)
  - Cholesterolosis

References

Chun KA, Ha HK, Yu ES et al. (1997) Xanthogranulomatous cholecystitis: CT features with emphasis on differentiation from gallbladder carcinoma. Radiology 203 : 93 – 97

Cossi AF, Scholz FJ, Aretz HT, Larsen CR (1987) Computed tomography of xanthogranulomatous cholecystitis. Gastrointest Radiol 12 : 154 – 155

Joerg A, Cussenot O, Houlle D, Despoisse JM, Le Duc A (1989) La pyelonephrite xanthogranulomateuse. Interêt de l'imagerie par resonance magnetique. Ann Urol Paris 23 : 232 – 235

Shuto R, Kiyosue H, Komatsu E, Matsumoto S, Kawano K, Kondo Y, Yokoyama S, Mori H (2004) CT and MR imaging findings of xanthogranulomatous cholecystitis: correlation with pathologic findings. Eur Radiol 14 : 440 – 446, Epub 2003 Aug 6

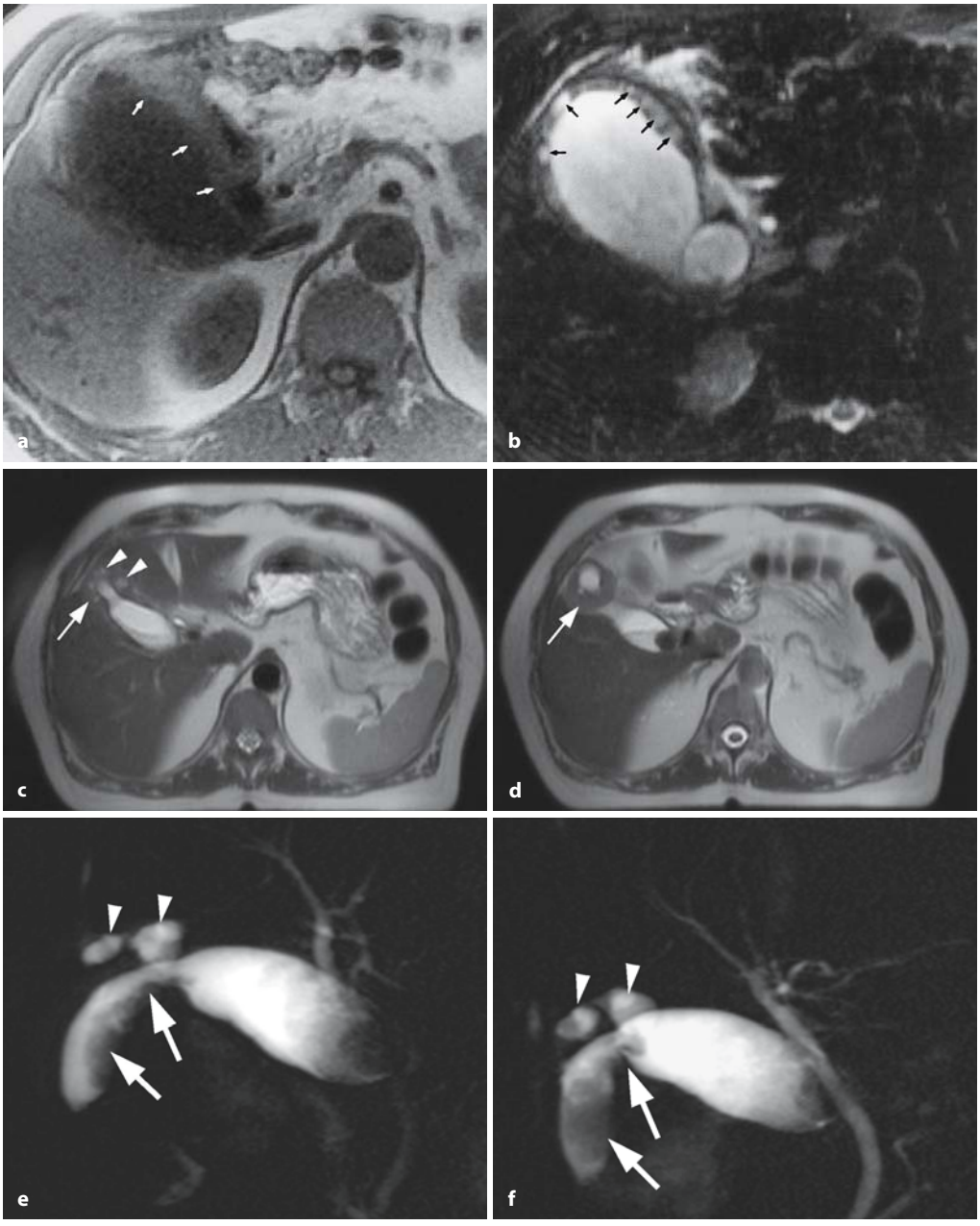

Fig. 105 a–f. **a** T1-weighted image showing a thickened gallbladder wall with relatively high signal intensity (*arrows*). **b** Heavily T2-weighted image showing several hyperintense foci in the wall (*arrows*). Also note fluid in the gallbladder fossa, caused by superimposed acute inflammation. **c, d** Different patient. Axial T2-weighted HASTE images (TE 60) (**c, d**) showing marked focal wall thickening of the fundus of the gallbladder (*arrows*), with intramural fluid collections (*arrowheads*). **e, f** Projective images showing focal narrowing of the gallbladder lumen (*arrows*) near the fundus with intramural fluid collections (*arrowheads*)

#106 Cholesterolosis

KEY FACTS: DISEASE

- Benign non-neoplastic, noninflammatory gallbladder abnormality
- Histology:
  - Accumulation of foamy, cholesterol-laden histiocytes in the subepithelial lamina propria, producing villus-like mucosal protrusions
  - The mucosal protrusions may become sufficiently distended to produce tiny macroscopic excrescences or small polyps
- Incidence: common (found in up to 30 % of patients undergoing routine cholecystectomy)
- Age/sex distribution unknown
- Types:
  - Strawberry gallbladder = diffuse cholesterolosis = lipid cholecystitis = planar form (no luminal protrusions)
  - Cholesterol polyp = polypoid form (see # 107)
- No relationship with blood cholesterol or atherosclerosis
- May be a cause of chronic biliary pain (Kmiot et al. 1994)

KEY FACTS: MRI

- No specific MRI features have been described

References

Berk RN, Van der Vegt JH, Lichtenstein JE (1983) The hyperplastic cholecystoses: cholesterolosis and adenomyomatosis. Radiology 146 : 593 – 601

Kmiot WA, Perry EP, Donovan IA et al. (1994) Cholesterolosis in patients with chronic alcalculous biliary pain. Br J Surg 81 : 112 – 115

Lubera RJ, Climie ARW, Kling GE (1967) Cholecystitis and the hyperplastic cholesteroloses: a clinical, radiological and pathology study. Am J Dig Dis 12 : 696 – 704

Salmenkivi K (1964) Cholesterolosis of the gallbladder: a clinical study based on 269 cholecystectomies. Acta Chir Scand 324 [Suppl]: 1 – 93

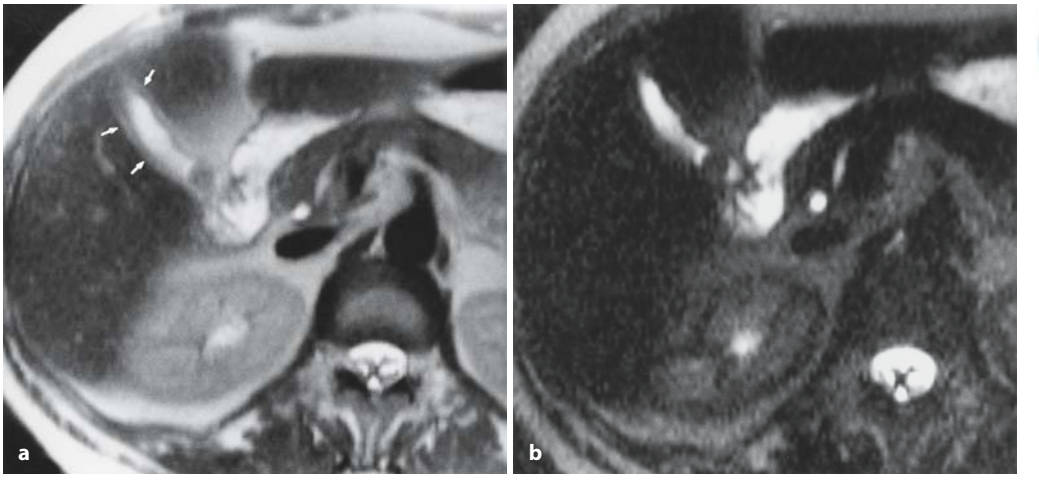

Fig. 106. **a** Moderately T2-weighted image showing a small gallbladder with a thickened wall with the same intensity as fat (*arrows*). **b** Same patient. Heavily T2-weighted image reveals that the wall has a low signal intensity, thus ruling out acute inflammation. Histology revealed diffuse cholesterolosis. It is unclear whether the high signal intensity of the gallbladder wall in **a** is related to the increased fat content

#107 Cholesterol Polyp

KEY FACTS: DISEASE

- Polypoid form of cholesterolosis (see #106)
- 90% of all gallbladder polyps
- No malignant potential

KEY FACTS: MRI (FIG. 107)

- Polypoid-like intraluminal lesion, single or (more frequently) multiple
- The diagnosis is especially likely if the lesion is small (< 1 cm) and if multiple polyps are present
- Signal intensity: not known
- Differential diagnosis of solitary cholesterol polyp:
  - Adenoma (most common benign neoplasm)
  - Carcinoma (15% – 25% patients present with a polypoid mass, usually greater than 2 cm)
  - Adherent stone
  - Metastasis
  - Neurinoma, granuloma, hemangioma, etc.

References

Berk RN, Van der Vegt JH, Lichtenstein JE (1983) The hyperplastic cholecystoses: cholesterolosis and adenomyomatosis. Radiology 146 : 593 – 601

Price RP, Stewart ET, Foley WD, Dodds WJ (1982) Sonography of polypoid cholesterolosis. AJR Am J Roentgenol 139 : 1197 – 1198

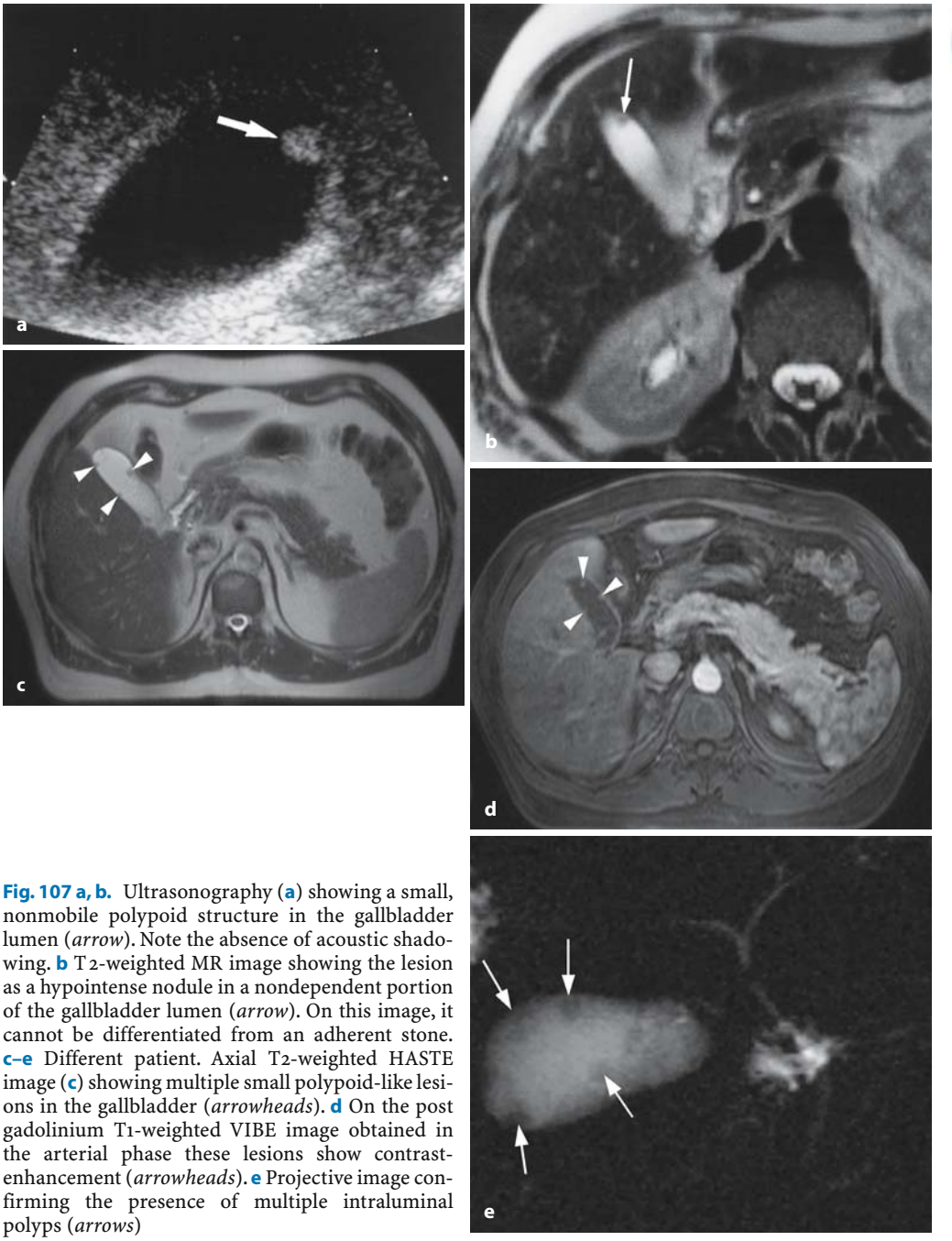

Fig. 107 a, b. Ultrasonography (**a**) showing a small, nonmobile polypoid structure in the gallbladder lumen (*arrow*). Note the absence of acoustic shadowing. **b** T2-weighted MR image showing the lesion as a hypointense nodule in a nondependent portion of the gallbladder lumen (*arrow*). On this image, it cannot be differentiated from an adherent stone. **c–e** Different patient. Axial T2-weighted HASTE image (**c**) showing multiple small polypoid-like lesions in the gallbladder (*arrowheads*). **d** On the post gadolinium T1-weighted VIBE image obtained in the arterial phase these lesions show contrast-enhancement (*arrowheads*). **e** Projective image confirming the presence of multiple intraluminal polyps (*arrows*)

#108 Diffuse Adenomyomatosis

KEY FACTS: DISEASE

- Benign non-neoplastic, noninflammatory gallbladder abnormality
- Histology:
  - Exaggeration of the normal infoldings of the luminal epithelium (Rokitanski-Asshoff sinuses) associated with proliferation of the smooth muscle
  - These infoldings correspond to intramural 'pseudo'-diverticula (i.e., outpouchings not containing all mural layers)
  - Occasionally, the diverticula may pass all the way through the wall
- Incidence: 5 % of cholecystectomies
- Develops with increasing age
- Ratio of women to men: 3 : 1
- Associations:
  - Gallstones
  - Cholesterolosis in 33 %

KEY FACTS: MRI

- The diagnosis depends on the simultaneous demonstration of:
  - Mural thickening
  - Pseudodiverticula ("pearl necklace sign")
- Visualization of small pseudodiverticula is only possible when heavily T 2-weighted images are obtained (effective TE as large as possible; Fig. 108)
- *Note:* If the intramural diverticula are too small to be visualized by MRI, the appearance is nonspecific

References

Haradome H, Ichikawa T, Sou H et al. (2003) The pearl necklace sign: an imaging sign of adenomyomatosis of the gallbladder at MR cholangiopancreatography. Radiology 227 : 80 – 88

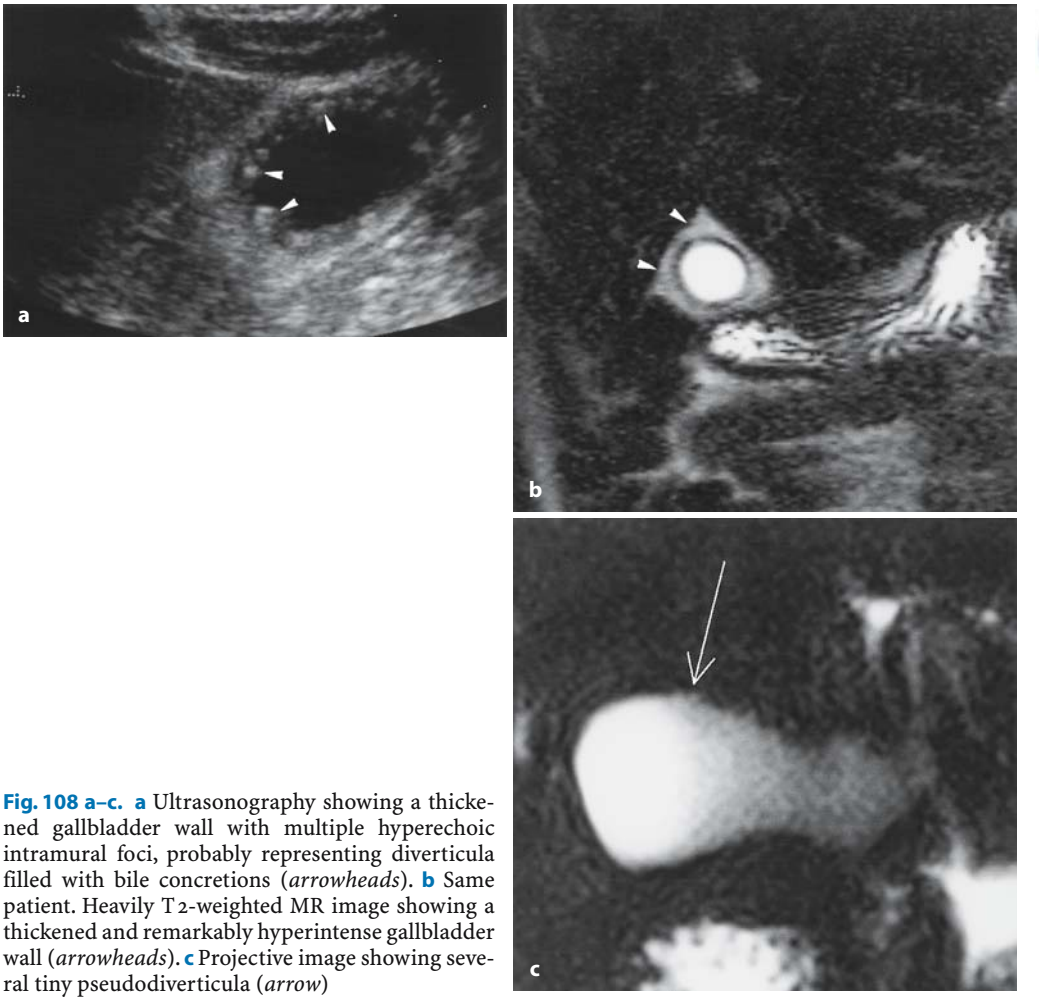

Fig. 108 a–c. **a** Ultrasonography showing a thickened gallbladder wall with multiple hyperechoic intramural foci, probably representing diverticula filled with bile concretions (*arrowheads*). **b** Same patient. Heavily T2-weighted MR image showing a thickened and remarkably hyperintense gallbladder wall (*arrowheads*). **c** Projective image showing several tiny pseudodiverticula (*arrow*)

#109 Focal Adenomyomatosis

KEY FACTS: DISEASE

- More common than diffuse adenomyomatosis
- Usually located in the fundus
- Cystic spaces are arranged in a circle and may communicate with the lumen through a central umbilicated depression
- Associated disease: gallbladder cancer (found in 6.4% of patients in one series; Ohtani et al. 1992)

KEY FACTS: MRI

- Characteristic signs:
  - Multiple diverticular outpouchings at the fundus (Fig. 109)
  - Small central sessile "mass" may be seen
  - Focal wall thickening

References

Boukadoum M, Siddiky MA, Zerhouni EA, Stitik FP (1984) CT demonstration of adenomyomatosis of the gallbladder. J Comput Assist Tomogr 8 : 177

Gerard PS, Berman D, Zafaranloo S (1990) CT and ultrasound of gallbladder adenomyomatosis mimicking carcinoma. J Comput Assist Tomogr 14 : 490 – 491

Ohtani T, Shirai Y, Tsukada K, Muto T (1992) Relationship between gallbladder carcinoma and the segmental type of adenomyomatosis of the gallbladder. Cancer 69 : 2647 – 2652

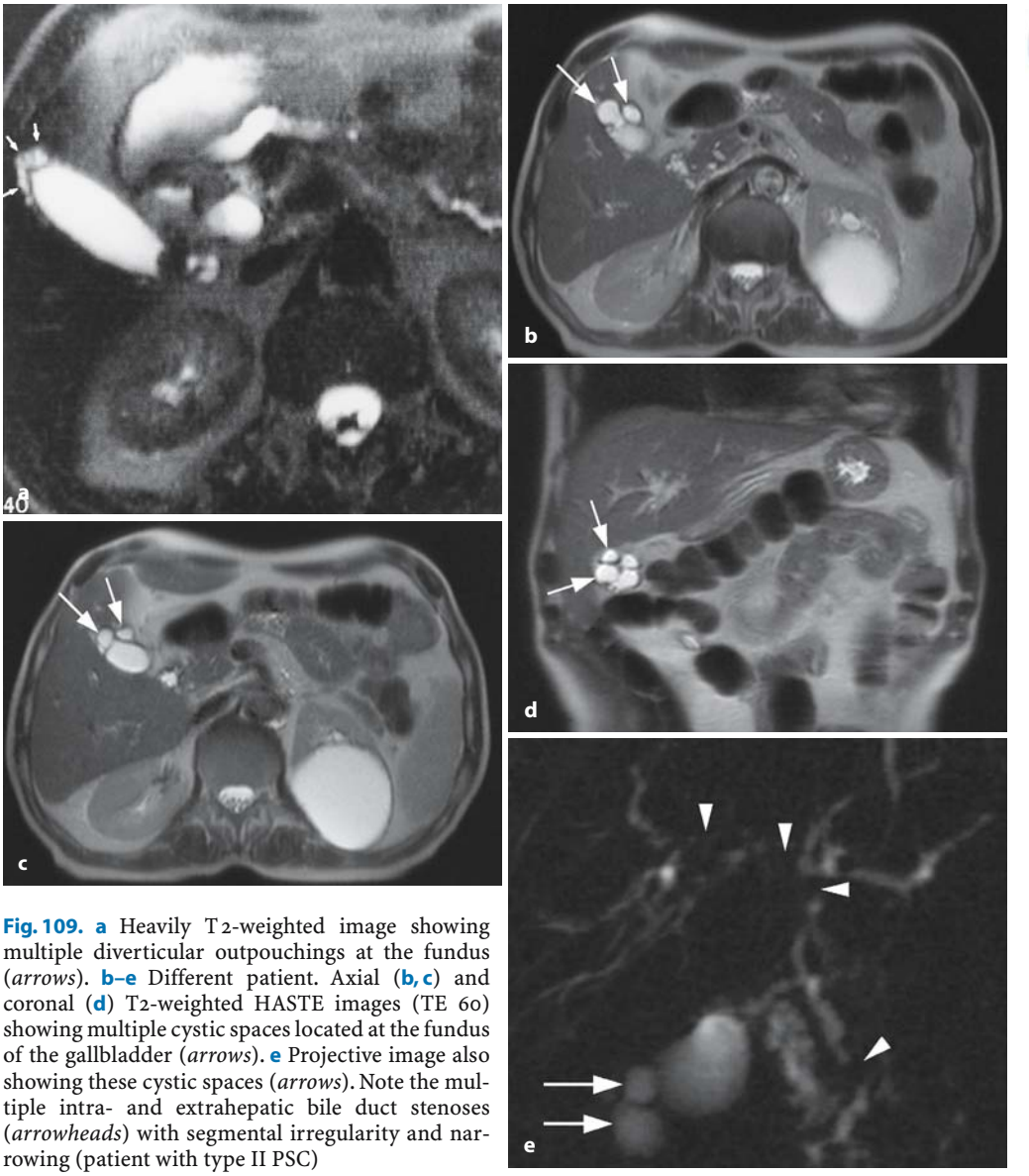

Fig. 109. a Heavily T2-weighted image showing multiple diverticular outpouchings at the fundus (*arrows*). **b–e** Different patient. Axial (**b, c**) and coronal (**d**) T2-weighted HASTE images (TE 60) showing multiple cystic spaces located at the fundus of the gallbladder (*arrows*). **e** Projective image also showing these cystic spaces (*arrows*). Note the multiple intra- and extrahepatic bile duct stenoses (*arrowheads*) with segmental irregularity and narrowing (patient with type II PSC)

#110 Porcelain Gallbladder

KEY FACTS: DISEASE

- Chronic calcifying cholecystitis
- Histology: calcium incrustation of the gallbladder wall, either continuous or punctate
- Incidence: 0.6 % – 0.8 % of cholecystectomy patients
- Ratio of women to men: 5 : 1
- Association: gallstones nearly always present
- Symptoms: minimal
- Complication: gallbladder carcinoma (up to 22 %; see # 115)

KEY FACTS: MRI

- If there is marked mural calcification, the gallbladder wall appears hypointense on T1- and T2-weighted images (Fig. 110)
- *Note:* MRI is less sensitive than CT for detecting calcifications (Fig. 110). Moreover, MRI is less specific: a thickened wall with low signal intensity may correspond to fibrosis, intramural air (see # 101), and calcifications

References

Berk RN, Armbuster TG, Salzstein SL (193) Carcinoma in the porcelain gallbladder. Radiology 106 : 29 – 31

Kane RA, Jacobs R, Katz J, Costello P (1984) Porcelain gallbladder: ultrasound and CT appearance. Radiology 152 : 137 – 141

Rickes S, Ocran K (2002) Images in clinical medicine. Porcelain gallbladder. N Engl J Med 346 : e4

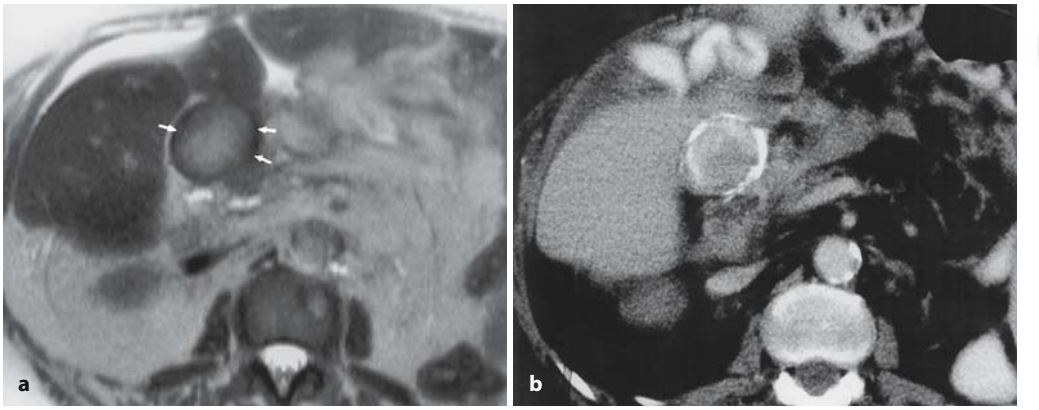

Fig. 110. **a** T 2-weighted MR image showing a thikkened gallbladder wall with very low signal intensity (*arrows*). **b** Corresponding CT image showing extensive calcification of the gallbladder wall. Note ascites as an incidental finding

#111 Reactive Thickening of the Gallbladder Wall

Related topics: #34 (acute hepatitis), #36 (cirrhosis), #151–157 (acute pancreatitis)

KEY FACTS: DISEASE

- Extrinsic causes of wall thickening include:
  - Acute hepatitis (see #34)
  - Hypoalbuminemia
  - Ascites
  - Cirrhosis (see #36)
  - Veno-occlusive disease
  - Heart failure
  - Acute pancreatitis
- Differential diagnosis: contracted gallbladder after eating, cholecystitis, tumor, AIDS, primary sclerosing cholangitis, …

KEY FACTS: MRI (FIG. 111)

- Typical features (reflecting diffuse mural edema):
  - Homogeneously thickened wall
  - High signal intensity on T2-weighted images
  - Preservation of mucosal line
- Differential diagnosis: distinguishing features:
  - With tumor and xanthogranulomatous cholecystitis: homogeneous aspect of thickened wall
  - With acute cholecystitis: concentric "symmetric" aspect of thickened wall; more homogeneous aspect; absence of pericholecystitic fluid; small size of the gallbladder lumen
- *Note:* diffuse mural edema may be caused by a shift of fluid from the intravascular to the extravascular space (venous congestion, hypoproteinemia) or to passive diffusion of extracellular fluid

References

Shlaer W, Leopold GR, Scheible FW (1981) Sonography of thickened gallbladder wall: a non-specific finding. AJR Am J Roentgenol 136 : 337–339

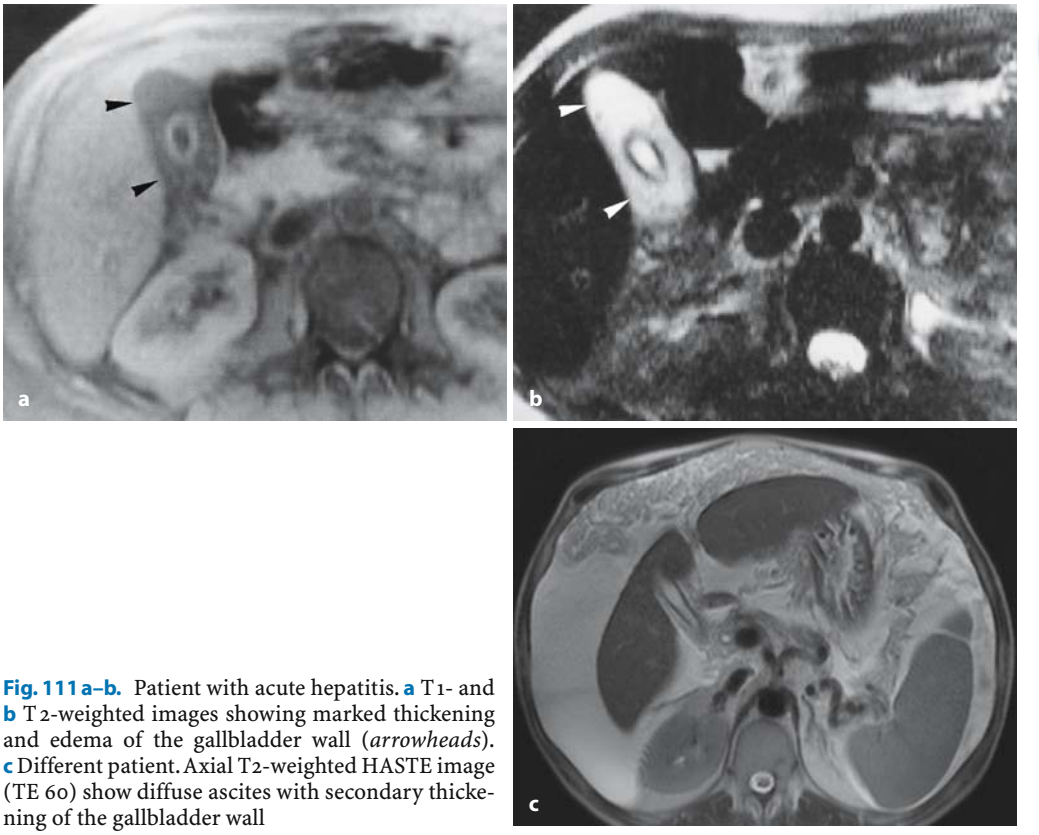

Fig. 111 a–b. Patient with acute hepatitis. **a** T1- and **b** T2-weighted images showing marked thickening and edema of the gallbladder wall (*arrowheads*). **c** Different patient. Axial T2-weighted HASTE image (TE 60) show diffuse ascites with secondary thickening of the gallbladder wall

#112 Varices in the Gallbladder Wall

Related topic: #79 (extrahepatic bile duct, other benign causes of bile duct narrowing)

KEY FACTS: DISEASE

- Causes:
  - Portal vein thrombosis
  - Chronic portal hypertension
- Mechanisms:
  - Increased "backward" pressure in the cystic vein
  - Veins in the gallbladder wall may act as a bypass around a focally thrombosed extrahepatic segment of the portal vein (blood flows from the cystic vein to gallbladder varices to hepatic parenchyma)

KEY FACTS: MRI (FIG. 112)

- Features on contrast-enhanced images:
  - Thickening of the gallbladder wall
  - Presence of multiple serpiginous vessels

References

Marchal G, Van Holsbeeck M, Tshibwabwa-Ntumba E et al. (1985) Dilation of the cystic veins in portal hypertension: sonographic demonstration. Radiology 154:187–189

West MS (1991) Gallbladder varices: imaging findings in patients with portal hypertension. Radiology 179:179–182

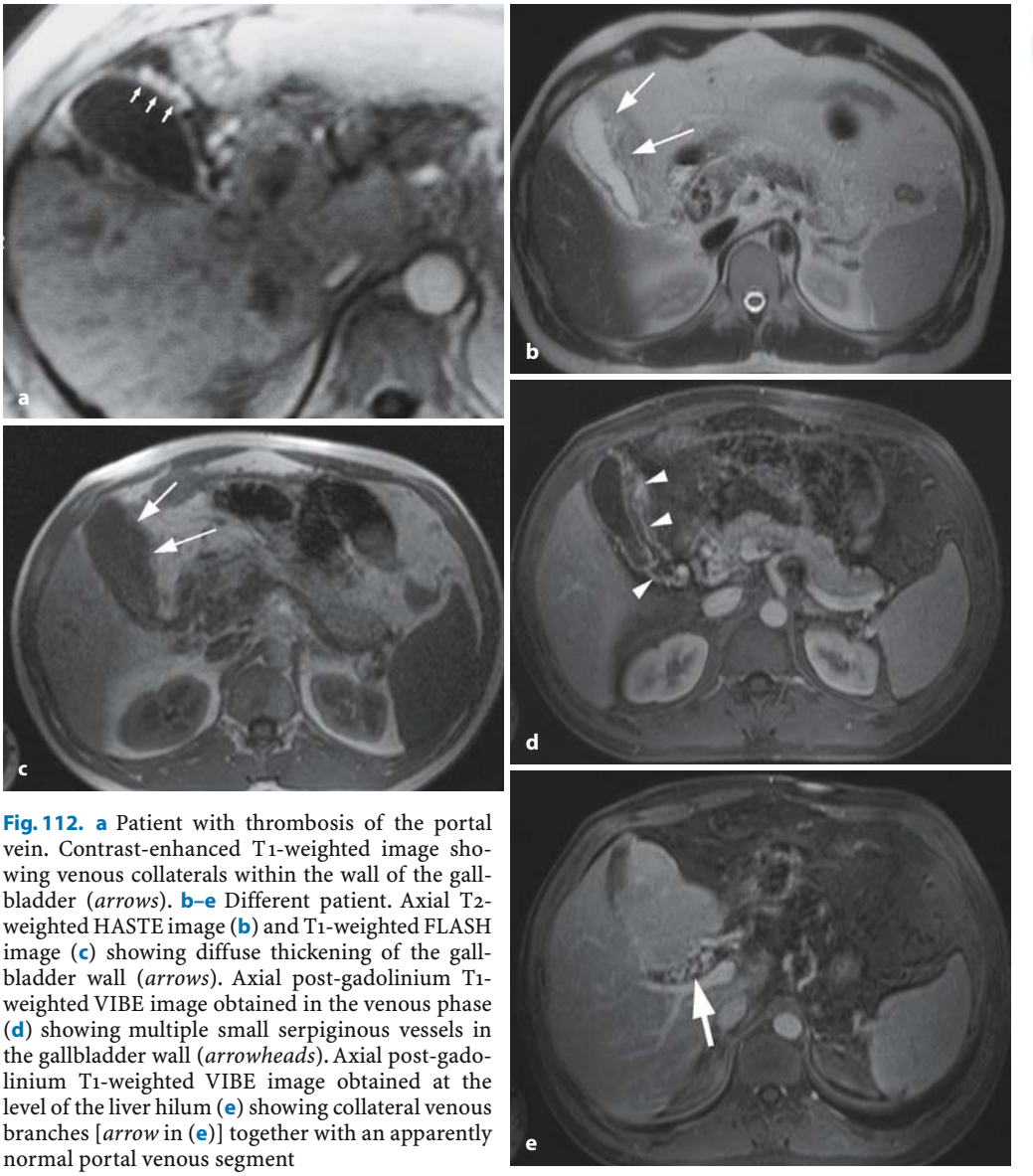

Fig. 112. a Patient with thrombosis of the portal vein. Contrast-enhanced T1-weighted image showing venous collaterals within the wall of the gallbladder (*arrows*). **b–e** Different patient. Axial T2-weighted HASTE image (**b**) and T1-weighted FLASH image (**c**) showing diffuse thickening of the gallbladder wall (*arrows*). Axial post-gadolinium T1-weighted VIBE image obtained in the venous phase (**d**) showing multiple small serpiginous vessels in the gallbladder wall (*arrowheads*). Axial post-gadolinium T1-weighted VIBE image obtained at the level of the liver hilum (**e**) showing collateral venous branches [*arrow* in (**e**)] together with an apparently normal portal venous segment

4.3 Traumatic, Postoperative, and Iatrogenic Abnormalities

#113 Blunt Gallbladder Trauma

Related topics: #48 (sequelae of direct liver trauma), #181 (pancreatic duct injury)

KEY FACTS: DISEASE

- Gallbladder injury occurs in 2%–3% of patients with severe blunt abdominal trauma
- Types of injury:
  - Contusion (i.e., intramural/intraluminal bleeding without rupture)
  - Laceration (i.e., perforation of the wall)
  - Avulsion (i.e., disconnection of the vascular pedicle)
- Associations:
  - Liver laceration
  - Duodenal rupture

KEY FACTS: MRI

- Common findings:
  - Blood in the gallbladder lumen (signal intensity: see #51; Fig. 113)
  - Ill-defined contour of the gallbladder wall with or without focal defect
  - Fluid/blood around the gallbladder
- Other possible findings:
  - Absence of enhancement of the gallbladder wall (avulsion)
  - Pseudoaneurysm (rare) (Fig. 113)
  - Collapsed gallbladder (rupture)

References

Jeffrey RB Jr, Federle MP, Laing FC, Wing VW (1986) Computed tomography of blunt trauma to the gallbladder. J Comput Assist Tomogr 10 : 756 – 758

Kim PN, Lee KS, Kim IV, Bae WK, Lee BH (1994) Gallbladder perforation: comparison of US findings with CT. Abdom Imaging 19 : 239 – 242

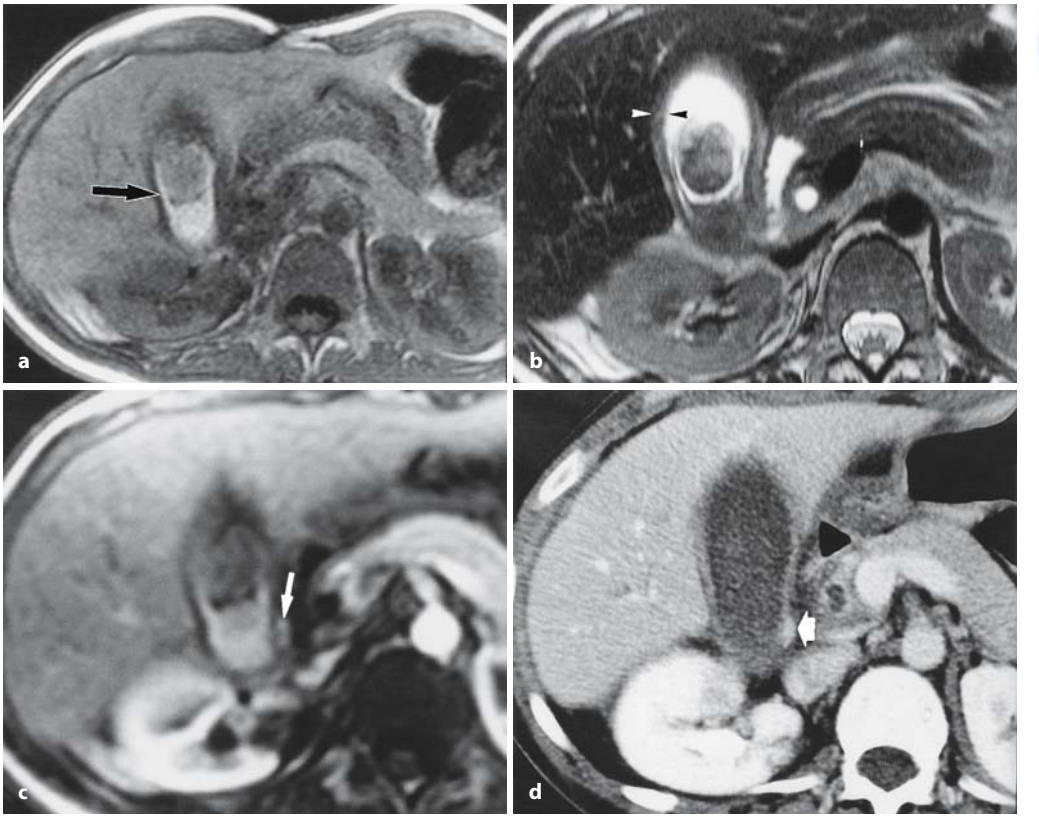

Fig. 113 a–d. Patient who was victim of a blunt abdominal trauma. **a** T 1- and **b** T 2-weighted images showing mixed signal intensity of the gallbladder content: hematoma with clot formation (*arrow*). Note marked thickening of the gallbladder wall in **b** (*arrowheads*). **c** Contrast-enhanced MR image obtained in the late arterial phase showing an enhancing structure in the gallbladder wall (*arrow*): small post-traumatic pseudoaneurysm. **d** CT confirming the presence of a small pseudoaneurysm (*arrow*). (Figure courtesy of D. Perdieus)

#114 After Cholecystectomy: Complications with Cystic Duct Remnant

Related topics: #52 (after cholecystectomy: stricture/transection of an aberrant bile duct), #82, 83 (extrahepatic duct: complications after cholecystectomy), #84 (postcholecystectomy syndrome)

KEY FACTS: DISEASE

- After cholecystectomy, almost 50% of patients have a cystic duct remnant measuring between 1 and 6 cm in length
- Complications with the cystic duct remnant account for 10% of reoperations after cholecystectomy
- Most common problems in the early postoperative phase:
  - Retained lithiasis
  - Fistula
  - Bile leakage
- Most common problems in the late postoperative phase:
  - Retained/recurrent lithiasis
  - Neurinoma, suture granuloma
  - "Recurrent gallbladder": large cystic duct stumps can function like a residual gallbladder with inflammatory changes. This typically causes late-onset pain several months or years after cholecystectomy

KEY FACTS: MRI

- Most common imaging findings:
  - Early phase: fluid collection around the cystic duct remnant (leakage)
  - Early and late phase: stone in the cystic duct remnant (Fig. 114)

References

Bodvall B, Overgaard B (1966) Cystic duct remnant after cholecystectomy: incidence studied by cholangiography in 500 cases and significance in 103 reoperations. Ann Surg 163:382–390

Rubini G, Dimonte M (1999) Postcholecystectomy syndrome: evaluation by biliary cholescintigraphy and MR cholangiopancreatography. Clin Nucl Med 24:784–788

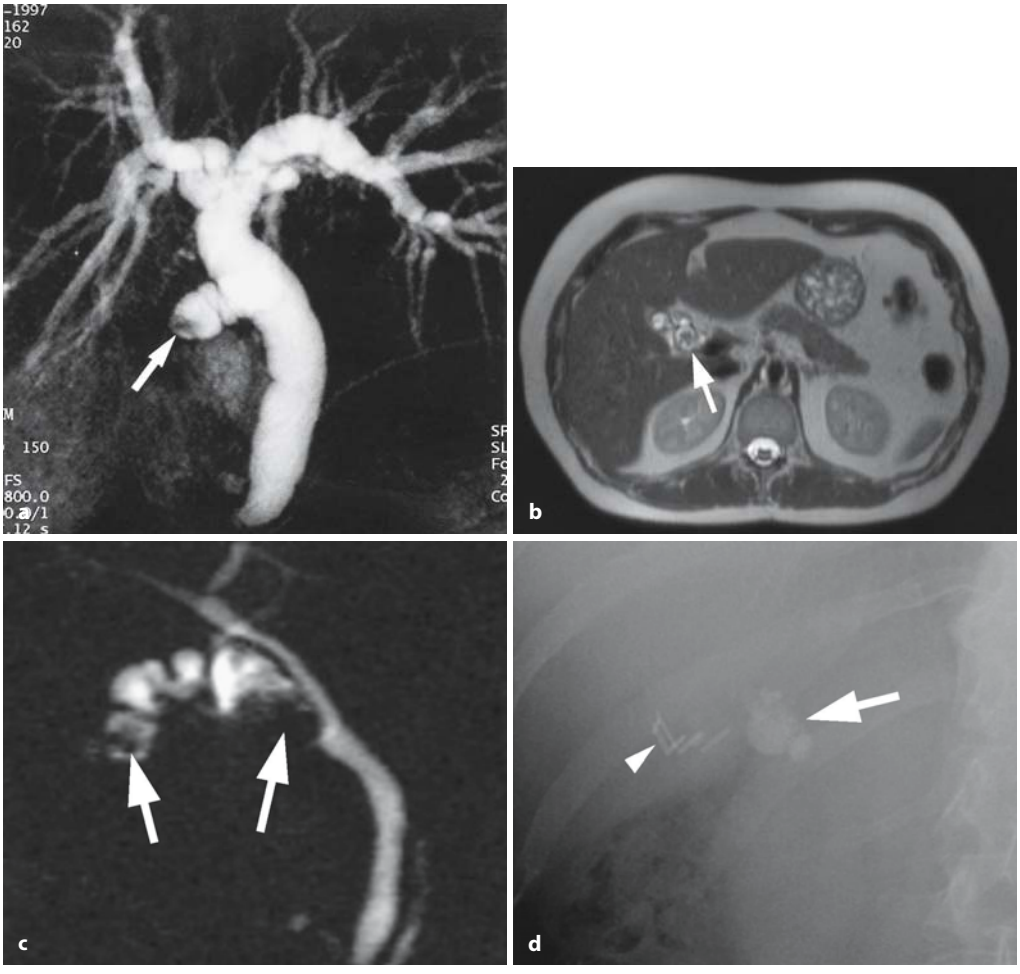

Fig. 114. **a** Projective MR image showing a small stone in the cystic duct remnant (*arrow*). **b–d** Different patient. Axial T2-weighted HASTE image (**b**), projective image (**c**), and conventional X-ray image (**d**), showing multiple stones in the cystic duct remnant after cholecystectomy (*arrows*). Note the operation clips in (**d**) (*arrowhead*)

4.4 Malignant Tumors

#115 Gallbladder Carcinoma, General

KEY FACTS: DISEASE

- Histology: variable (from well-differentiated to anaplastic)
- Incidence:
  - Most common biliary cancer
  - Found in 0.4 % – 0.6 % of biliary tract operations
- Peak age: sixth to seventh decade
- Ratio of women to men: 3 : 1
- Location: usually body, fundus
- Predisposing factors/associated disease:
  - Porcelain gallbladder (incidence of carcinoma up to 22 %; see # 110)
  - Gallstones (in 65 % – 98 %; carcinoma occurs in only 1 % of patients with stones, however)
  - Chronic cholecystitis
  - Anomalous pancreaticobiliary duct union (see # 123)
  - Focal adenomyomatosis (see # 109)
- Symptoms: either signs of malignancy or signs of cholecystitis
- 75 % unresectable at the time of diagnosis
- 88 % mortality rate within 1 year

KEY FACTS: MRI

- Morphologic appearance:
  - Mass replacing the gallbladder (40 % – 70 %)
  - Focal/diffuse asymmetric irregular wall thickening (15 % – 30 %; Fig. 115)
  - Polypoid intraluminal mass (15 % – 25 %)
- Signal intensity:
  - Like most other neoplasms: T 1, hypointense; T 2, moderately hyperintense
  - Usually heterogeneous
- Contrast-enhanced images: typically ill-defined enhancement in the early phase
- Gallstones commonly present
- Differential diagnosis:
  - Xanthogranulomatous cholecystitis (see # 105; Chun et al. 1997)
  - Adenomyomatosis (see # 108; Gerard et al. 1990)
  - Acute/chronic cholecystitis (see # 96, 104)
  - Metastases (50 % malignant melanoma)
  - Leukemia, lymphoma
  - Benign polyps
  - Direct invasion of gallbladder by other tumors (e. g., hepatic, duodenal)
- Signs of extramural spread: see # 116 – 118

References

Chun KA, Ha HK, Yu ES et al. (1997) Xanthogranulomatous cholecystitis: CT features with emphasis on differentiation from gallbladder carcinoma. Radiology 203 : 93 – 97

Demachi H, Matsui O, Hoshiba K et al. (1997) Dynamic MRI using a surface coil in chronic cholecystitis and gallbladder carcinoma: radiologic and histopathologic correlation. J Comp Assist Tomogr 21 : 643 – 651

Franquet T, Montes M, Ruiz de Azua Y, Jimenez FJ, Cozcolluella R (1991) Primary gallbladder carcinoma: imaging findings in 50 patients with pathologic correlation. Gastrointest Radiol 16 : 143 – 148

Gerard PS, Berman D, Zafaranloo S (1990) CT and ultrasound of gallbladder adenomyomatosis mimicking carcinoma. J Comp Assist Tomogr 14 : 490 – 491

Schwartz LH, Black J, Fong Y et al. (2002) Gallbladder carcinoma: findings at MR imaging with MR cholangiopancreatography. J Comput Assist Tomogr 26 : 405 – 410

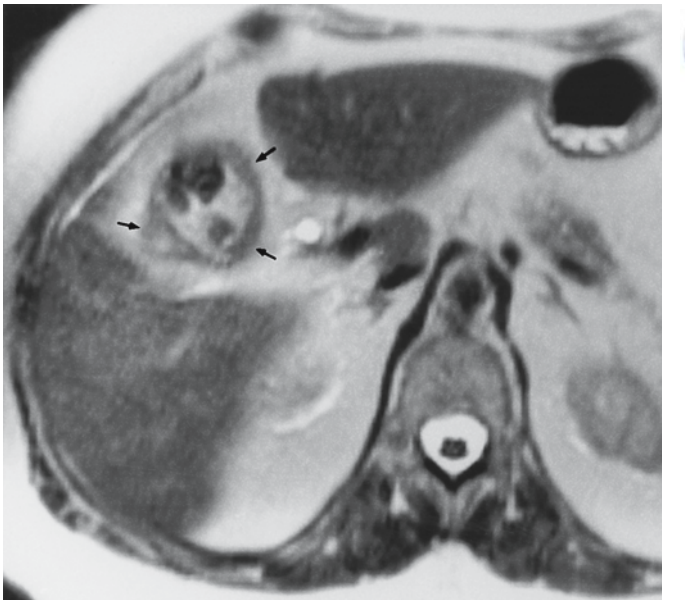

Fig. 115. T 2-weighted MR image showing asymmetric wall thickening (*arrows*) associated with multiple stones: carcinoma

#116 Spread of Gallbladder Carcinoma (1): Direct Invasion of Liver Parenchyma and/or Biliary Tree

Related topic: #89 (extrahepatic bile duct, involvement by gallbladder carcinoma)

KEY FACTS: DISEASE

- Local spread to the liver and/or biliary tree occurs in up to 80% of cases (Kumar and Aggarwal 1994)
- Mechanism: venous drainage of the gallbladder ends in adjacent liver substance
- Other routes of spread:
  - Duodenum (12%) or colon (9%)
  - Lymphatic (see #117)
  - Peritoneal (see #118)
  - Hematogenous (see #118)

KEY FACTS: MRI (FIG. 116)

- MR features of liver invasion:
  - Abnormal aspect of the gallbladder bed with absence of clear separation between the gallbladder and liver
  - Soft tissue mass in hepatic parenchyma cranial to the gallbladder and/or in the liver hilum
  - Narrowing of the common hepatic duct (see #89) or intrahepatic ducts
- Differential diagnosis: e.g., cholangiocarcinoma, metastases, lymphoma, hepatocellular carcinoma
- *Note:* Coronal images should be obtained to evaluate intrahepatic spread

References

Kumar A, Aggarwal S (1994) Carcinoma of the gallbladder: CT findings in 50 cases. Abdom Imaging 19:304–308

Schwartz LH, Black J, Fong Y et al. (2002) Gallbladder carcinoma: findings at MR imaging with MR cholangiopancreatography. J Comput Assist Tomogr 26:405–410

Yamaguchi K, Enjoji M (1988) Carcinoma of the gallbladder. A clinicopathology of 103 patients and a newly proposed staging. Cancer 62:1425–1432

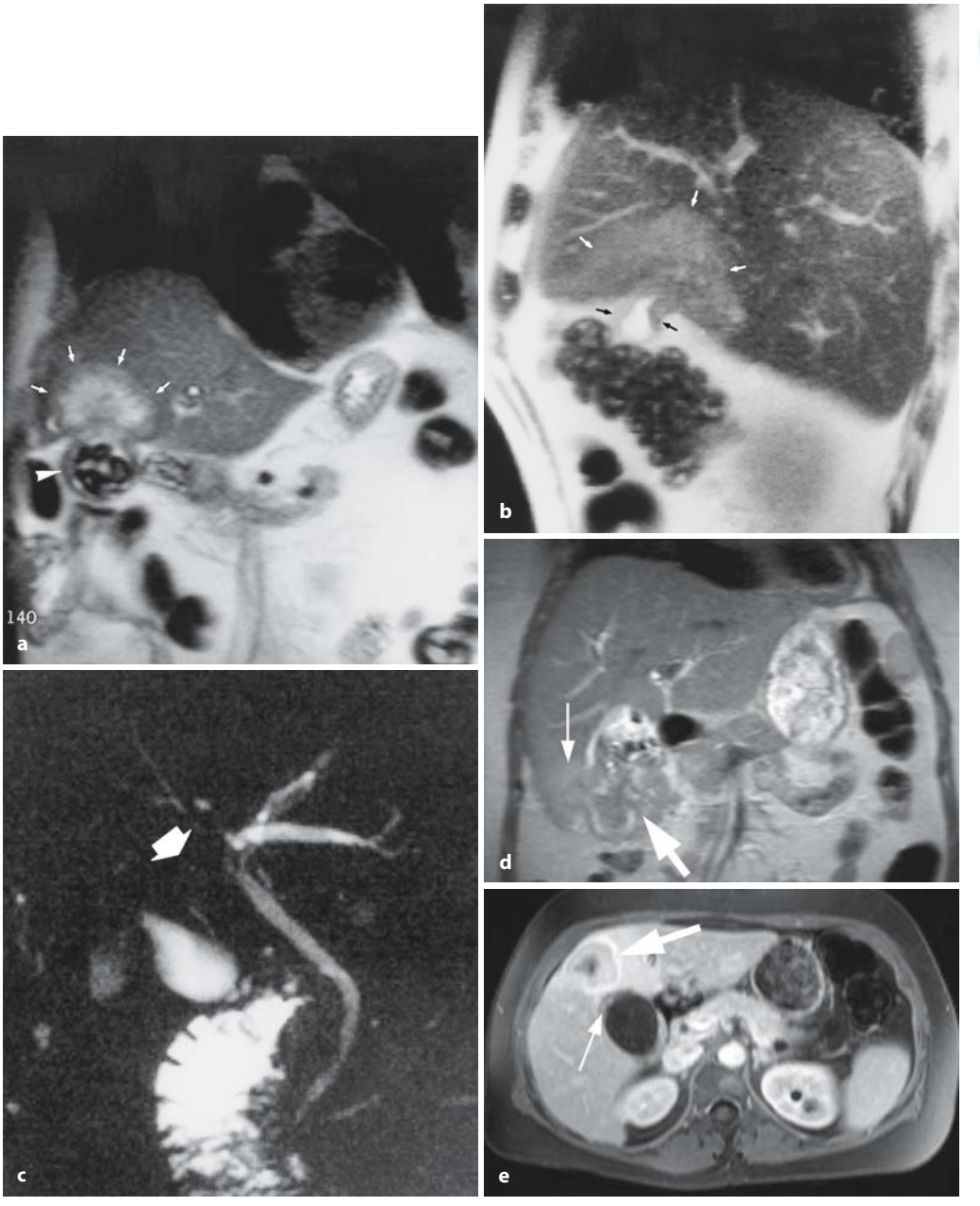

Fig. 116 a–c. **a** Coronal T2-weighted image showing a large mass in the right liver lobe (*arrows*), discrete thickening of the gallbladder wall (*arrowhead*), and absence of a fatty interface between the gallbladder and liver: gallbladder carcinoma with direct hepatic invasion. **b** Sagittal cross-sectional image obtained in a different patient showing similar abnormalities as in **a** (*arrows*). c Same patient as in **b**. Projective image showing amputation of bile ducts in the right liver lobe (*arrow*). **d–e** Different patient. Coronal T2-weighted HASTE image (TE 60) (**d**) showing a slightly hyperintense mass in the gallbladder fossa (*large arrow*), with extension into the adjacent liver parenchyma (*small arrow*). **e** Axial post-gadolinium T1-weighted VIBE images obtained in the venous phase showing ring enhancement of the intrahepatic mass (*large arrow*) together with focal thickening of the gallbladder wall (*small arrow*)

#117 Spread of Gallbladder Carcinoma (2): Lymph Node Metastases

KEY FACTS: DISEASE

- Second most common route of spread, after direct invasion of the liver/biliary tree
- Incidence: average 17 %; 63 % in stage III carcinoma (i. e., carcinoma invading adjacent organs such as the duodenum, liver, and colon)
- Anatomy: lymphatics of the gallbladder descend around the bile duct, merge with lymph nodes posterior to the pancreas, portal vein, and common hepatic artery, and finally drain into the interaortocaval nodes (Shirai et al. 1992)
- The prevalence of metastases to the different types of regional lymph nodes corresponds to this pathway (Ohtani et al. 1993)
- Hepatic hilar nodes usually *not* involved
- According to Tsukada et al. (1997), gallbladder cancer with lymph node metastases limited to the cystic and pericholedochal lymph nodes can be cured in more than 50 % of cases

KEY FACTS: MRI

- Specific location of lymph node: see above
- Criteria for malignancy (Ohtani et al. 1993; Fig. 117):
  - Size greater than 10 mm (positive predictive value, 93 %)
  - Lobulated appearance (positive predictive value, 93 %)
  - Heterogeneous enhancement (positive predictive value, 86 %)
- Projective images may show narrowing of the common bile duct (compression by paracholedochal nodes)
- *Note:* Accurate preoperative assessment of the extent of metastases may be useful for planning radical surgery (Shirai et al. 1992; Tsukada et al. 1997)
- Differential diagnosis: other tumors (e. g., pancreatic carcinoma) with lymph node metastases

References

Kumar A, Aggarwal S (1994) Carcinoma of the gallbladder: CT findings in 50 cases. Abdom Imaging 19 : 304 – 308

Ohtani T, Shirai Y, Tsukada K, Hatakeyama K, Muto T (1993) Carcinoma of the gallbladder: CT evaluation of lymphatic spread. Radiology 189 : 875 – 880

Schwartz LH, Black J, Fong Y et al. (2002) Gallbladder carcinoma: findings at MR imaging with MR cholangiopancreatography. J Comput Assist Tomogr 26 : 405 – 410

Shirai Y, Yoshida K, Tsukada K, Ohtani T, Muto T (1992) Identification of the regional lymphatic system of the gallbladder by vital staining. Br J Surg 79 : 659 – 662

Tsukada K, Kurosaki I, Uchida K et al. (1997) Lymph node spread from carcinoma of the gallbladder. Cancer 80 : 661 – 667

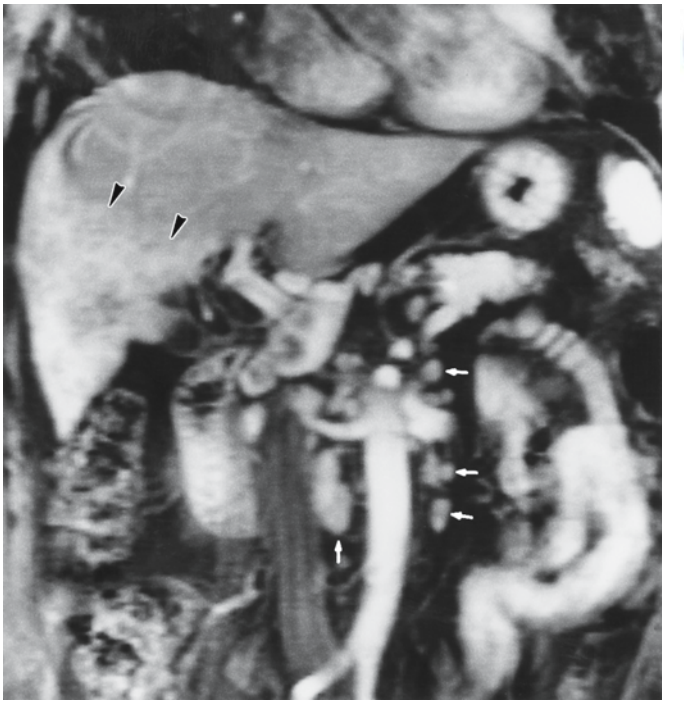

Fig.117. Contrast-enhanced image obtained in the coronal plane showing multiple enlarged retroperitoneal lymph nodes (*arrows*). Also note the abnormal enhancement of the caudal part of the right liver lobe secondary to invasion by the gallbladder tumor (*arrowheads*; same patient as in Fig. 116 b, c)

#118 Spread of Gallbladder Carcinoma (3): Other Metastases

KEY FACTS: DISEASE

- Local spread to adjacent organs such as the stomach, duodenum, and hepatic colonic flexure is relatively common
- Hematogenous spread:
  - Intrahepatic dissemination may occur secondary to spread into branches of the portal vein
  - Distant metastases are rare
- Peritoneal metastases: found in ± 6% (Buhr et al. 1996)
- Ovarian metastases (rare)
- *Note:* A problem that has arisen recently is the risk of implantation metastases following laparoscopic cholecystectomy (seeding may occur along the trocar pathways)

KEY FACTS: MRI

- Liver metastases: see # 60 (Fig. 118)
- Findings in peritoneal metastatic disease:
  - Ascites
  - Thickening of parietal peritoneum
  - Marked enhancement of peritoneum (Low et al. 1997)

References

Buhr J, Hürten M, Heinrichs CM, Graf M, Padberg WM (1996) Implantation metastases following laparoscopic cholecystectomy in gallbladder carcinoma. Dtsch Med Wochenschr 121 : 57 – 61

Kriplani AK, Jayant S, Kapur BML (1992) Laparoscopy in primary carcinoma of the gallbladder. Gastrointest Endosc 38 : 326 – 329

Low RN, Barone RM, Lacey C, Sigeti JS, Alzate GD, Sebrechts CP (1997) Peritoneal tumor: MR imaging with dilute oral barium and intravenous gadolinium-containing contrast agents compared with unenhanced MR imaging and CT. Radiology 204 : 513 – 520

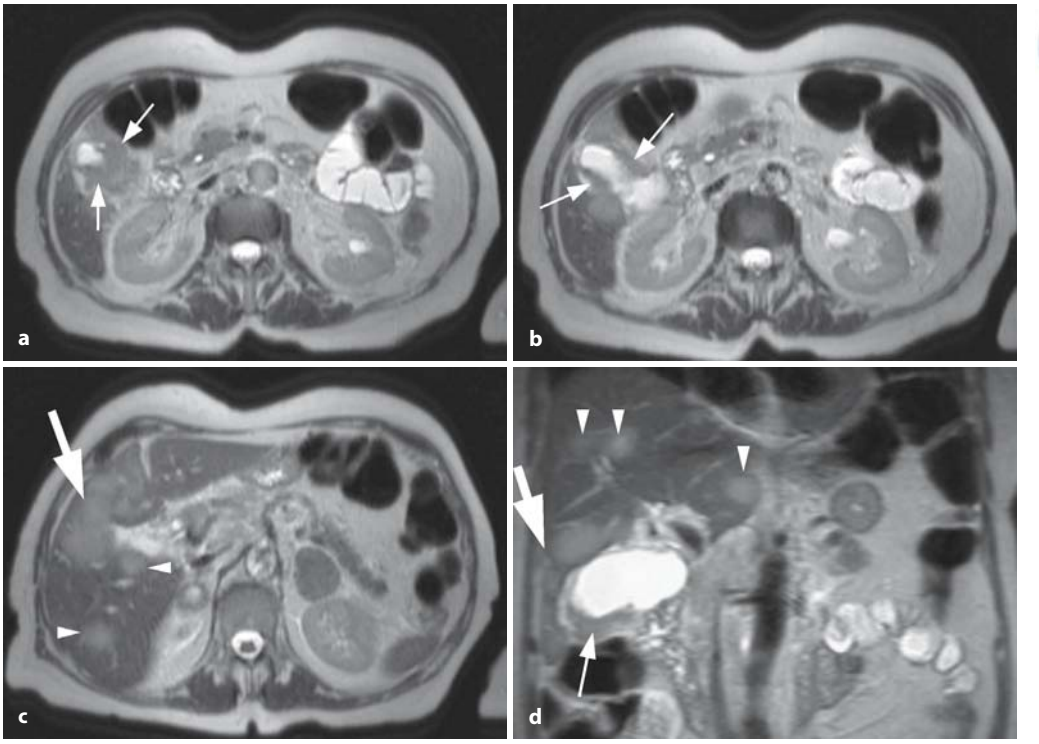

Fig. 118 a–d. Axial (**a–c**) and coronal (**d**) T2-weighted HASTE image (TE 60) showing diffuse thickening of the gallbladder wall (*small arrows*) with extension into the adjacent liver parenchyma (*large arrow*). Several hepatic metastases are seen (*arrowheads*)

Vaterian Sphincter Complex

5 Vaterian Sphincter Complex

5.1 Normal Anatomy and Variants

119 Normal Anatomy

KEY FACTS: ANATOMY

- The vaterian sphincter complex includes the distal (intramural) part of the common bile duct and pancreatic duct, the papilla, and the surrounding smooth muscle (sphincter of Oddi) (Fig. 119 a)
- Length of vaterian sphincter complex: 10 – 15 mm
- Course: oblique in a laterocaudal direction
- Diameter of intramural duct: a few millimeters
- In 60 % – 80 % of individuals, the pancreatic and bile ducts unite to form a *common channel* (length, 2 – 15 mm; average, 5 mm; Misra and Dwivedi 1990; see # 123)
- The slightly dilated distal segment of the common channel is also called the *ampulla*
- The *papilla* forms an endoluminal protrusion at the medial wall of the duodenum and contains the *orifice*
- Size of papilla: usually less than 10 – 15 mm
- Shape of papilla: variable (may be polypoid)
- Location of papilla:
  - Usually (92 %) located at the posteromedial wall of the mid-descending duodenum
  - Can be anywhere between the pylorus and the ligament of Treitz
- Location of minor papilla: 1 – 2 cm proximal to the major papilla

KEY FACTS: MRI

- If MRI is performed during relaxation of the sphincter, images show the distal portion of the pancreatic duct and common bile duct as thin, fluid-containing structures connected with the duodenum (Fig. 119 b)
- Nonvisualization is a normal variant if only single images are obtained (see # 120; Van Hoe et al. 1998)
- The papilla may be seen as an endoluminal protrusion at the medial wall of the duodenum

References

Misra SP, Dwivedi M (1990) Pancreaticobiliary ductal union. Gut 31 : 1144 – 1149

Stewart E, Vennes J, Geenen J (1977) Atlas of endoscopic retrograde cholangiopancreatography. Mosby, St Louis, p 41

Van Hoe L, Gryspeerdt S, Vanbeckevoort D et al. (1998) Normal Vaterian sphincter complex: evaluation of morphology and contractility with dynamic single-shot MR cholangiography. AJR 170 : 1497 – 1500

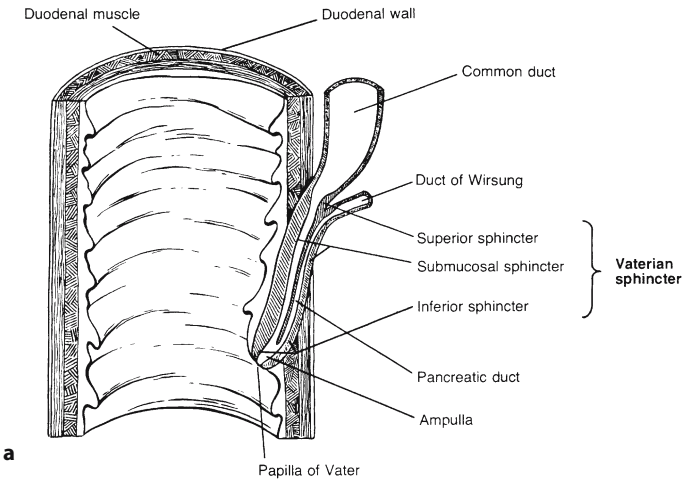

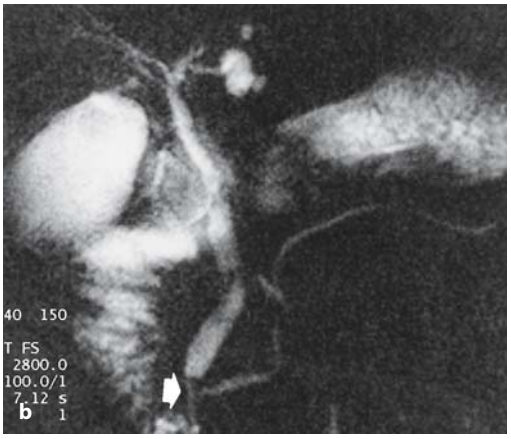

Fig. 119. **a** Anatomy of the vaterian sphincter complex. The common bile duct and pancreatic duct become invested by smooth muscle fibers as they approach the duodenal wall. This is reflected by a marked decrease in internal diameter. (Reprinted with permission from Stewart et al. 1977). **b** Projective MR image showing the distal common bile duct and pancreatic duct joining to form a common channel. Note the (normal) abrupt change in diameter of the distalmost part of the common bile duct (*arrow*)

#120 Normal Contractile Activity

Related topics: #13 (dynamic evaluation of vaterian sphincter complex), #128 (sphincter dysfunction, features on dynamic MRCP)

KEY FACTS: PHYSIOLOGY

- The vaterian sphincter complex functions as an independent motor unit that regulates the flow of bile and pancreatic secretions
- Following a meal, the gallbladder contracts and the sphincter relaxes, allowing free flow of bile into the duodenum. This response is mediated by cholecystokinin
- On manometric studies, the sphincter exhibits a basal pressure of 15 ± 5 mm Hg. Superimposed on the basal tone are high-amplitude phasic wave contractions occurring at a mean frequency of 4 ± 0.5 per min. These contractions measure 150 ± 16 mmHg in amplitude and have a duration of 4.3 ± 0.5 s

KEY FACTS: DYNAMIC MRI

- Serial breathhold MRI using a single-shot technique (kinematic MRCP) allows visualization of the vaterian sphincter complex in 95 % of normal patients (Van Hoe et al. 1998; Kim et al. 2002)
- Normal features:
  - On serial images, the aspect of the vaterian sphincter complex shows temporal variability: it is either not shown or is shown as a narrow ductal segment
  - The distal aspect of the presphincteric segment of the common bile duct also shows temporal variability in shape, which is related to the contractile activity of the sphincter (Fig. 120 a)
- *Note:* Forceful contraction of the sphincter is not uncommonly asociated with disappearance of fluid in the adjacent portion of the duodenum. This may be a helpful feature in the interpretation of dynamic studies of the sphincter (see Figs. 122 b, c, 125)

References

Staritz M (1988) Pharmacology of the sphincter of Oddi. Endoscopy 20 : 171 – 174

Van Hoe L, Gryspeerdt S, Vanbeckevoort D et al. (1998) Normal Vaterian sphincter complex: evaluation of morphology and contractility with dynamic single-shot MR cholangiography. AJR 170 : 1497 – 1500

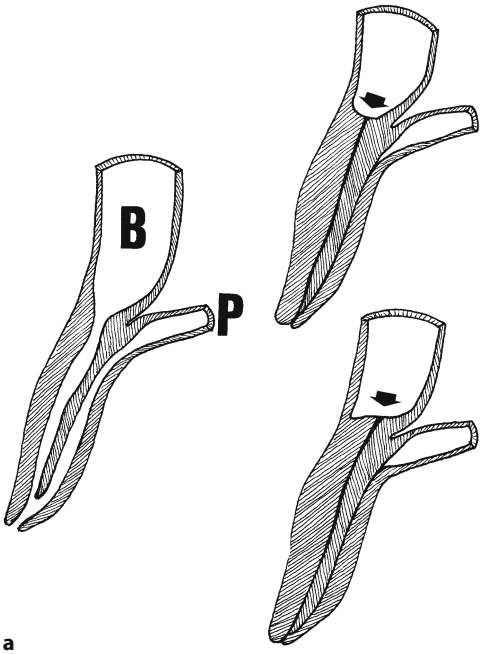

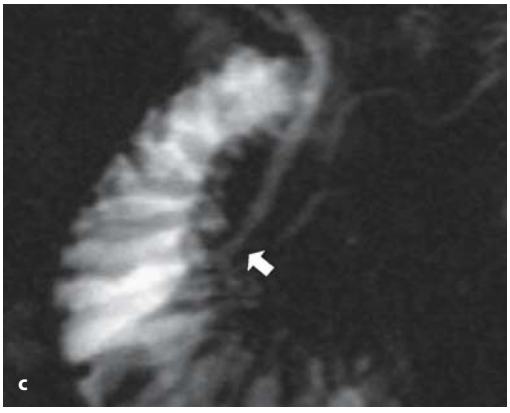

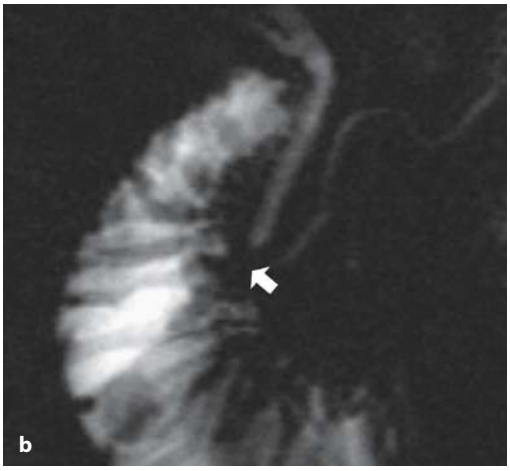

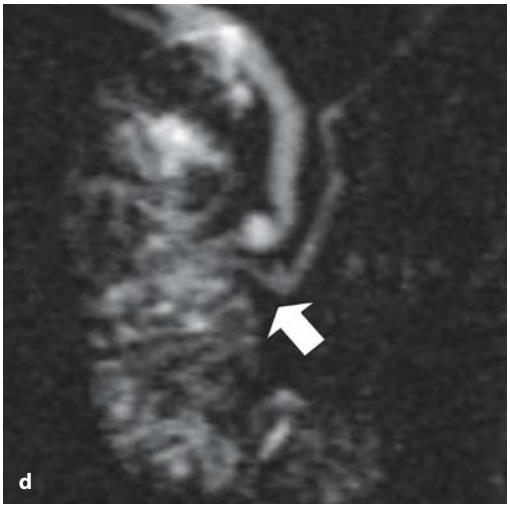

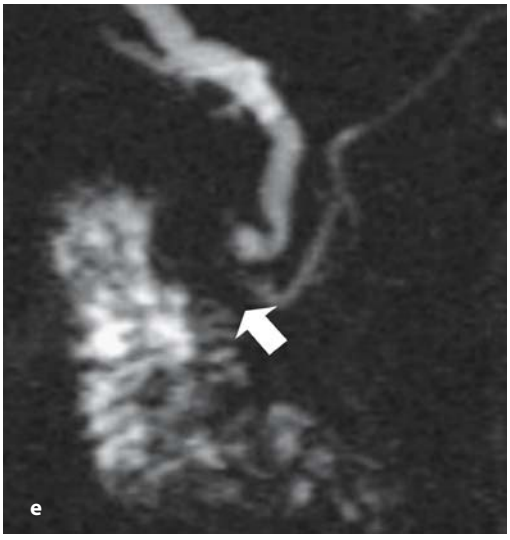

Fig. 120. **a** Functional activity of the sphincter and its influence on the appearance of the distalmost portions of the bile duct (*B*) and pancreatic duct (*P*). *Left*, the sphincter is relaxed. *Right*, contraction of the sphincter causes obliteration of the lumina of both ducts. The distal aspect of the presphincteric segment of the bile duct may be flat, slightly concave (*bottom right, arrow*), or slightly convex (*top right, arrow*). **b, c** Projective images obtained at 30-s intervals. The images show the variable appearance of the intramural portion of the common bile duct, which is invisible in (**b**) and can clearly been seen in (**c**) (*arrow*). **d, e** Different patient. Projective images with an interval of 130-s. These images also show the variable appearance of the intramural portions of the pancreatic duct and bile duct: they are clearly visible in (**d**) (relaxation) and invisible in (**e**) (contraction) (*arrow*)

#121 Variant Anatomy (1): Type of Junction

KEY FACTS: ANATOMY

- The junction between the distal common bile duct and the pancreatic duct can be classified as follows:
  - Y-type junction (± 70 %)
  - V-type junction (± 20 %)
  - U-type junction (± 10 %)
  - Other types (rare)
- In less than 0.2 % of patients, the common bile duct and pancreatic ducts have separate orifices

References

Bocker V, Stolte M (1979) Functionelle Morphologie. In: Ottenjann R, Classen M (eds) Gastroenterologische Endoskopie. Enke, Stuttgart, pp 142 – 149

Wiedmeyer DA, Sewart ET, Taylor AJ (1993) Radiologic evaluation of structure and function of the sphincter of Oddi. Gastrointest Endoscop Clin North Am 3 : 13 – 40

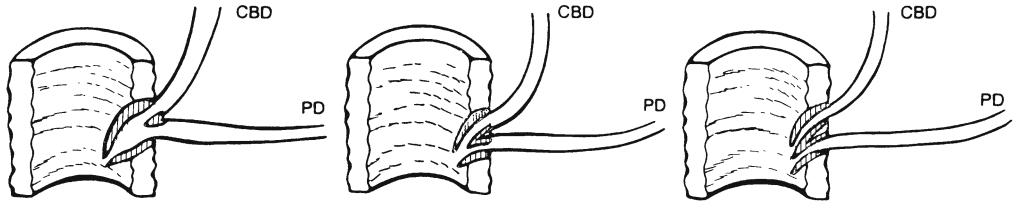

a

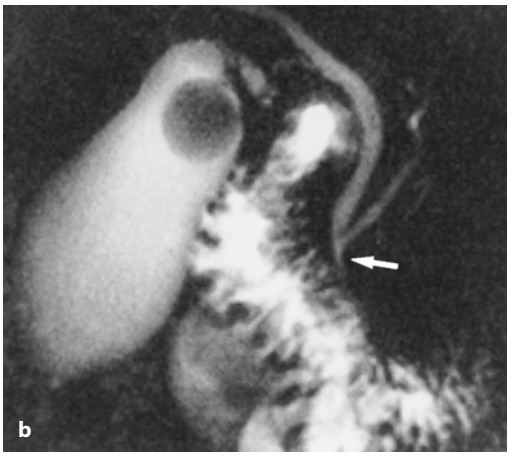

b

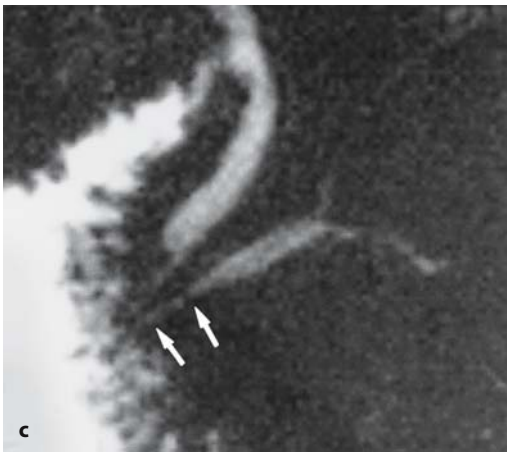

c

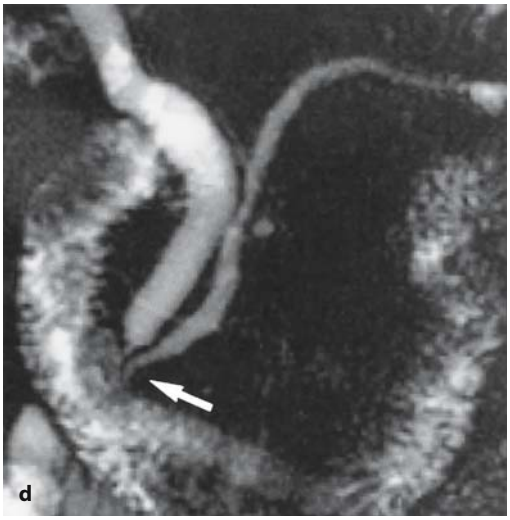

d

Fig. 121. **a** Y-type (*left*), V-type (*center*), and U-type junction (*right*). *CBD*, common bile duct; *PD*, pancreatic duct. (Reprinted with permission from Wiedmeyer et al. 1993). **b–d** Projective images showing junction with **b** Y-type, **c** V-type, and **d** U-type morphology (*arrows*)

#122 Variant Anatomy (2): "Pseudocalculus" Sign

Related topics: #73 (stones in common bile duct: pitfalls in diagnosis), #125 (impacted stone)

KEY FACTS

- Pseudocalculus sign: concave aspect of distal border of suprasphincteric part of the common bile duct, mimicking a stone (Fig. 122)
- Cause: forceful contraction of the sphincter with retrograde "invagination"
- Normal variant
- Potential cause of false-positive MR diagnosis of common bile duct lithiasis (if dynamic imaging is not performed)

References

Ferruci J, Wittenberg J, Stone L, Dreyfuss J (1976) Hypotonic cholangiography with glucagon. Radiology 118 : 466 – 467

Van Hoe L, Gryspeerdt S, Vanbeckevoort D et al. (1998) Normal Vaterian sphincter complex: evaluation of morphology and contractility with dynamic single-shot MR cholangiography. AJR 170 : 1497 – 1500

Van Hoe L, Mermuys K, Vanhoenacker P (2004) MRCP pitfalls. Abdom Imaging 29 : 360 – 387

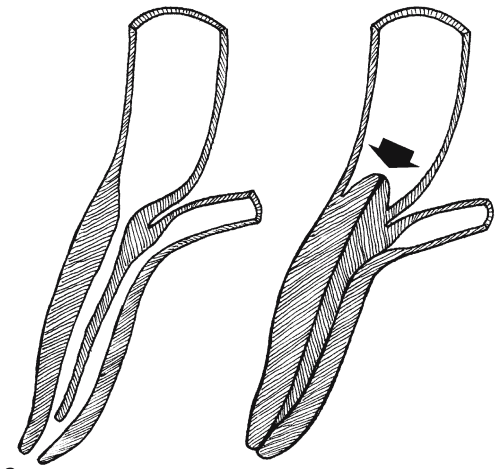

a

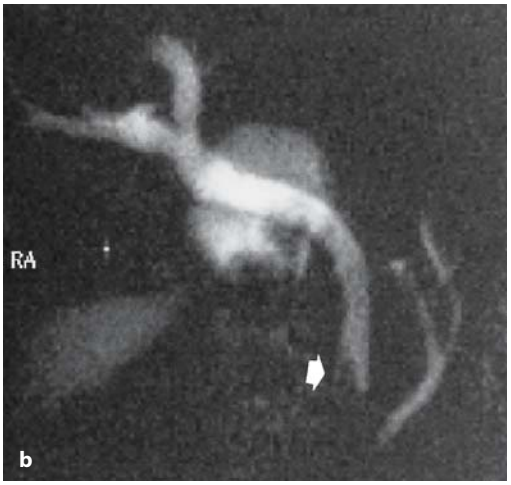

b

Fig. 122 a – g. **a** Pseudocalculus sign. *Left*, the sphincter is relaxed. *Right*, forceful contraction of the sphincter leads to retrograde invagination (*arrow*). **b, c** Projective image obtained during contraction showing pseudocalculus sign (*arrow*). **c** Projective image obtained 10 s later showing normal sphincter area (*arrows*). Note the absence of fluid in the second portion of the duodenum in **b**

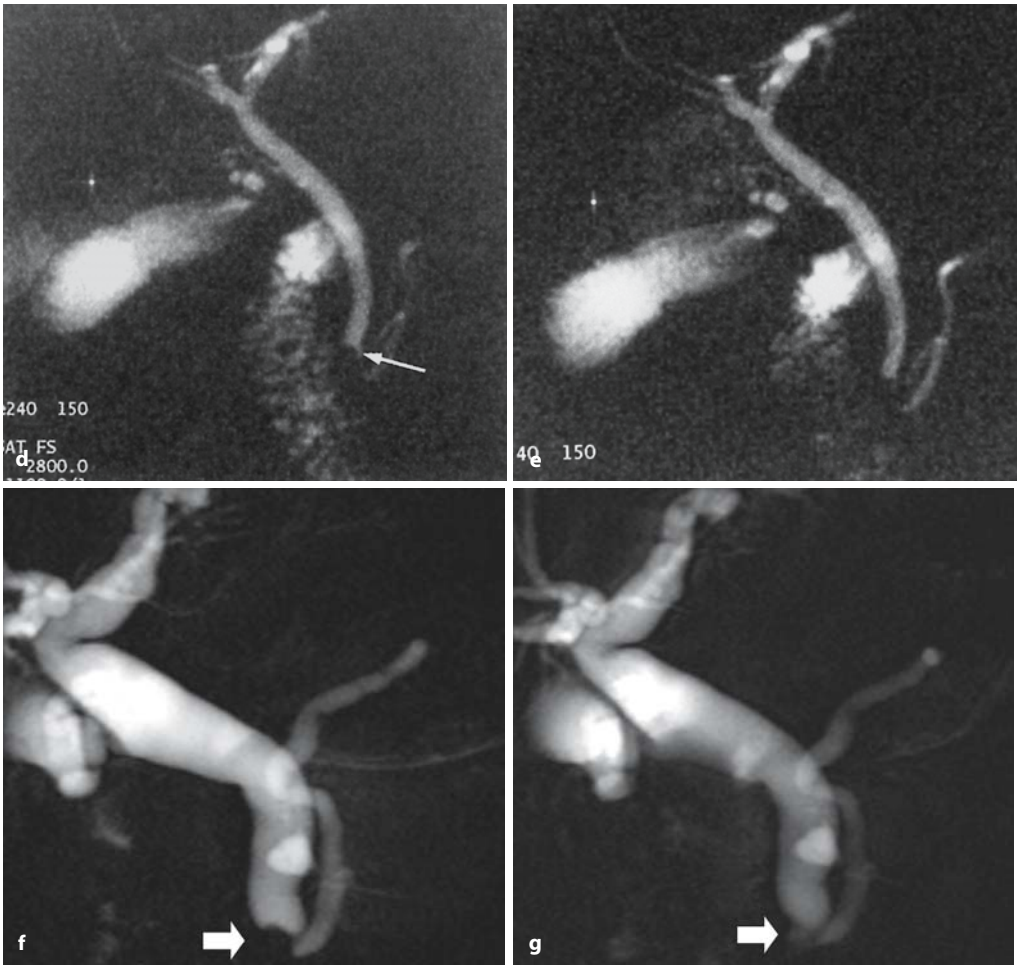

Fig. 122 a–g. (*continued*) **d, e** Other patient. Projective images obtained within a 15-s interval. Again, the aspect of the distal common bile duct in **d** could erroneously be interpreted as a small stone (*arrow*). **f, g.** Different patient. Projective image during forceful sphincter contraction (**f**) showing retrograde invagination resulting in the pseudocalculus sign (*arrow*). Projective image obtained 20-s later (**g**) showing a normal sphincter area (*arrow*)

#123 Variant Anatomy (3): Length of Common Channel

KEY FACTS

- In 60%–80%, the pancreatic and bile ducts unite to form a common channel (length, 2–15 mm; average, 5 mm; Kochhar et al. 1989)
- Presence of an *anomalous pancreaticobiliary duct union* (common channel greater than 15 mm in length) may predispose to intrabiliary reflux of pancreatic juice and formation of a choledochal cyst (see #68)
- *Note:* A key factor in the evaluation of the length of the common channel is adequate visualization of the exact location of the papilla. In MRI, sufficient filling of the duodenum with fluid is an essential prerequisite
- *Note:* Techniques to ensure that the duodenum is filled with fluid during an MRCP study:
  - Dynamic (repetitive) scanning (mechanism: intermittent passage of fluid)
  - Injection of a spasmolytic agent (possible mechanism: increased outflow of bile and/or gastric content; see #21)
  - Oral administration of water

References

Hand BH (1962) An anatomical study of the choledochoduodenal area. Br J Surg 50 : 486

Hosoki T, Hasuike Y, Takeda Y et al. (2004) Visualization of pancreaticobiliary reflux in anomalous pancreaticobiliary junction by secretin-stimulated dynamic magnetic resonance cholangiopancreatography. Acta Radiol 45 : 375–382

Kochhar R, Nagi B, Chawla S et al (198) The clinical spectrum of anomalous pancreaticobiliary junction. Surg Endoscop 3 : 83–86

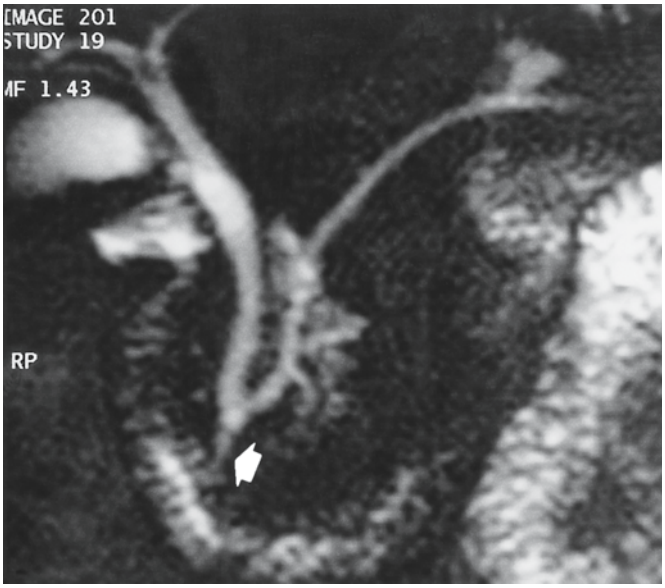

Fig. 123. Projective image showing a relatively long common channel (± 16 mm; *arrow*)

#124 Variant Anatomy (4): Papilla in or Adjacent to a Duodenal Diverticulum

KEY FACTS: ANATOMY

- Incidence of duodenal diverticula: 5 % – 10 % (Shemesh et al. 1987)
- Anatomic relationship to papilla:
  - Papilla on the rim of the diverticulum (most common)
  - Papilla in the diverticulum (may be a cause of failed ERCP)
- Associations:
  - Increased incidence of common bile duct stones
  - Possibly also increased incidence of pancreatitis (Osnes et al. 1981)

KEY FACTS: MRI (FIG. 124)

- Appearance of diverticula: paraduodenal structures containing:
  - Fluid
  - Air
  - Air and fluid (with air–fluid level)
- The terminal ducts may be narrowed as they pass around the diverticulum
- If the papilla is within the diverticulum, intermittent reflux of air may be seen (may be interpreted as a stone if dynamic imaging is not performed)
- Duodenal diverticula may mimic cystic neoplasms of the pancreas when filled only with fluid (Macari et al. 2003)

References

Balci NC, Noone T, Akun E et al. (2003) Juxtapapillary diverticulum: findings on MRI. J Magn Reson Imaging 17 : 487 – 492

Macari M, Lazarus D, Israel G, Megibow A (2003) Duodenal diverticula mimicking cystic neoplasms of the pancreas: CT and MR imaging findings in seven patients. AJR Am J Roentgenol 180 : 195 – 199

Osnes M, Lootveit T, Larsen S, Aune S (1981) Diverticula and their relationship to age, sex, and biliary calculi. Scand J Gastroenterol 16 : 103 – 107

Shemesh E, Friedman E, Czesniak A, Bat L (1987) The association of biliary and pancreatic anomalies with periampullary duodenal diverticula. Correlation with clinical presentations. Arch Surg 122 : 1055 – 1057

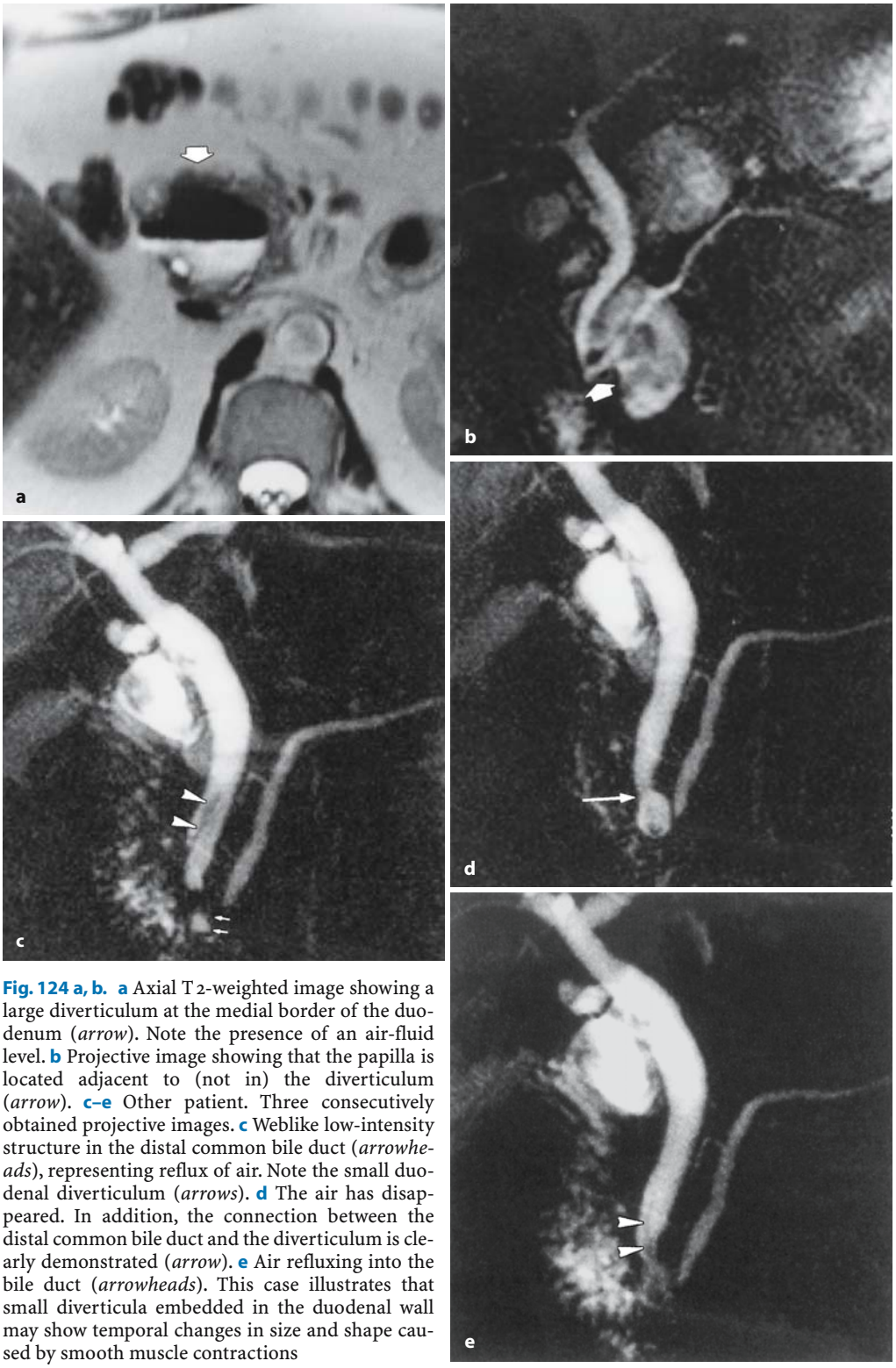

Fig. 124 a, b. **a** Axial T 2-weighted image showing a large diverticulum at the medial border of the duodenum (*arrow*). Note the presence of an air-fluid level. **b** Projective image showing that the papilla is located adjacent to (not in) the diverticulum (*arrow*). **c–e** Other patient. Three consecutively obtained projective images. **c** Weblike low-intensity structure in the distal common bile duct (*arrowheads*), representing reflux of air. Note the small duodenal diverticulum (*arrows*). **d** The air has disappeared. In addition, the connection between the distal common bile duct and the diverticulum is clearly demonstrated (*arrow*). **e** Air refluxing into the bile duct (*arrowheads*). This case illustrates that small diverticula embedded in the duodenal wall may show temporal changes in size and shape caused by smooth muscle contractions

5.2 Benign Nontraumatic Abnormalities

#125 Impacted Stone

Related topics: #73 (stones in common bile duct: pitfalls in diagnosis), #122 (pseudocalculus sign)

KEY FACTS: DISEASE

- Stone located in the intramural portion of the common bile duct, leading to either transient or persistent blockage and edema of the ampulla of Vater
- Clinical signs/complications:
  - Acute painful jaundice
  - Acute pancreatitis
  - Fistula formation
- *Note:* In the majority of cases, gallstones pass into the duodenum after a few days (Kelly 1980)

KEY FACTS: MRI

- Stones that are not surrounded by fluid are invisible on MRCP
- Dynamic (repetitive) scanning is mandatory to diagnose small stones impacted in the distalmost portion of the common bile duct and to differentiate true lithiasis from the "pseudocalculus" effect (true lithiasis has an unchanged shape throughout the study) (Fig. 125 a – c; see also #122)
- Dynamic scanning also helps to avoid false-negative diagnoses: stones are best seen on images obtained during sphincter relaxation (Fig. 125 d, e)

References

Chan Y-L, Chan ACW, Lam WWM et al. (1996) Choledocholithiasis: comparison of MR cholangiography and endoscopic retrograde cholangiography. Radiology 200 : 85 – 89

Guibaud L, Bret PM, Reinhold C, Atri M, Barkun AN (1995) Bile duct obstruction and choledocholithiasis: diagnosis with MR cholangiography. Radiology 197 : 109 – 115

Kelly TR (1980) Gallstone pancreatitis: the timing of surgery. Surgery 88 : 345 – 350

Van Hoe L, Mermuys K, Vanhoenacker P (2004) MRCP pitfalls. Abdom Imaging 29 : 360 – 387

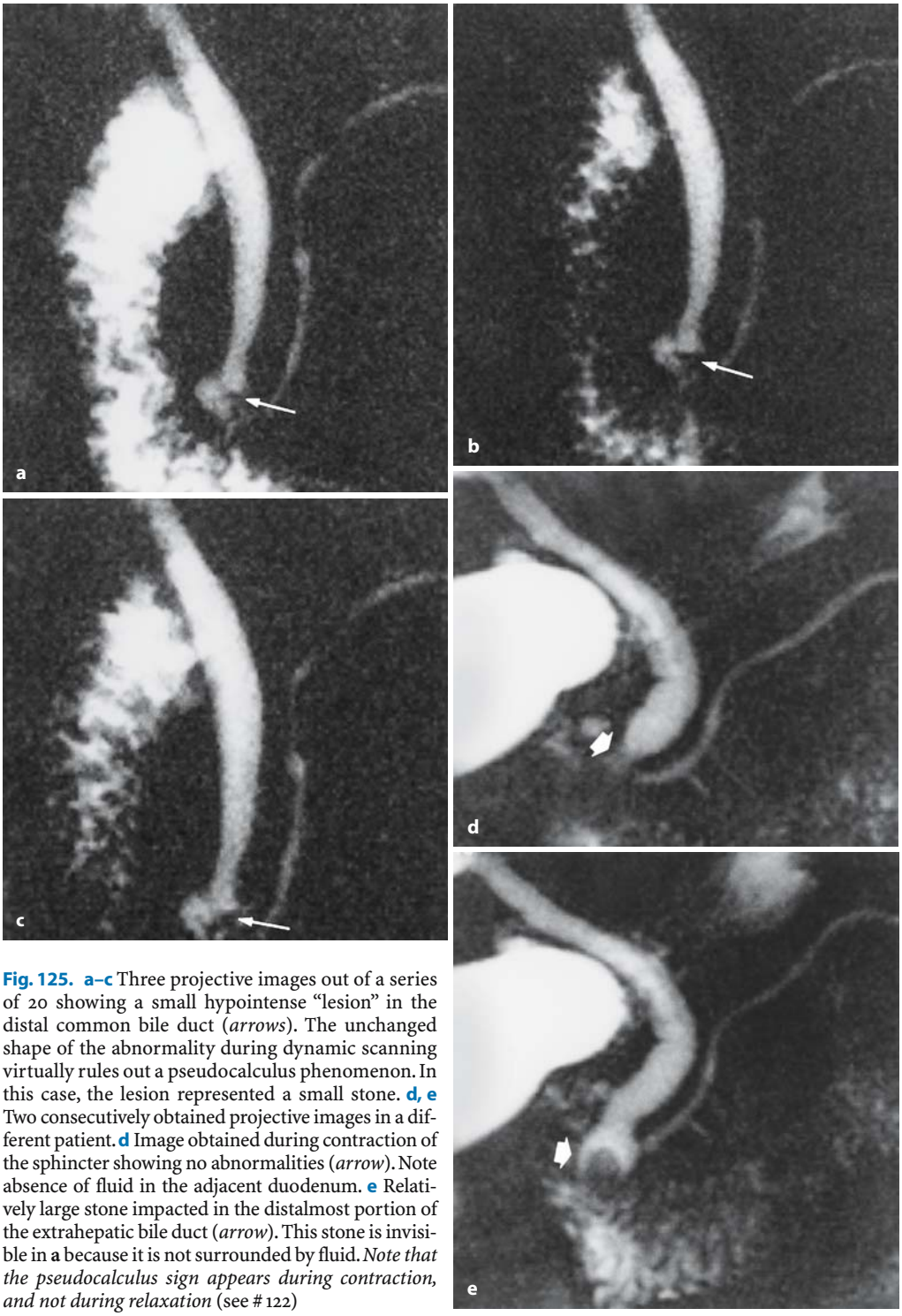

Fig. 125. a–c Three projective images out of a series of 20 showing a small hypointense "lesion" in the distal common bile duct (*arrows*). The unchanged shape of the abnormality during dynamic scanning virtually rules out a pseudocalculus phenomenon. In this case, the lesion represented a small stone. **d, e** Two consecutively obtained projective images in a different patient. **d** Image obtained during contraction of the sphincter showing no abnormalities (*arrow*). Note absence of fluid in the adjacent duodenum. **e** Relatively large stone impacted in the distalmost portion of the extrahepatic bile duct (*arrow*). This stone is invisible in **a** because it is not surrounded by fluid. *Note that the pseudocalculus sign appears during contraction, and not during relaxation* (see # 122)

#126 Choledochocele

Related topics: #30 (Caroli's disease), #68 (choledochal cysts)

KEY FACTS: DISEASE

- Cystic dilation of the distal/intramural portion of the common bile duct with herniation of the common bile duct into the duodenum (similar to ureterocele)
- Represents type III bile duct cyst (see #30)
- Often manifests in adulthood
- Etiology:
  - Congenital: diverticulum of the distal common bile duct; stenosis of the ductal orifice
  - Acquired: stone passage → inflammation → stenosis of the orifice
- Symptoms: nausea, vomiting, episodic abdominal pain
- Stones/sludge often present

KEY FACTS: MRI (FIG. 126)

- Typical appearance:
  - Rather than being narrowed, the intramural portion of the common bile duct is broadened and clubbed
  - The papilla bulges into the duodenum

References

De Backer AI, Van den Abbeele K, De Schepper AM et al. (2000) Choledochocele: diagnosis by magnetic resonance imaging. Abdom Imaging 25 : 508 – 510

Venu RP, Geenen JE, Hogan WJ (1984) Role of ERCP in the diagnosis and treatment of choledochocele. Gastroenterology 87 : 1144 – 1149

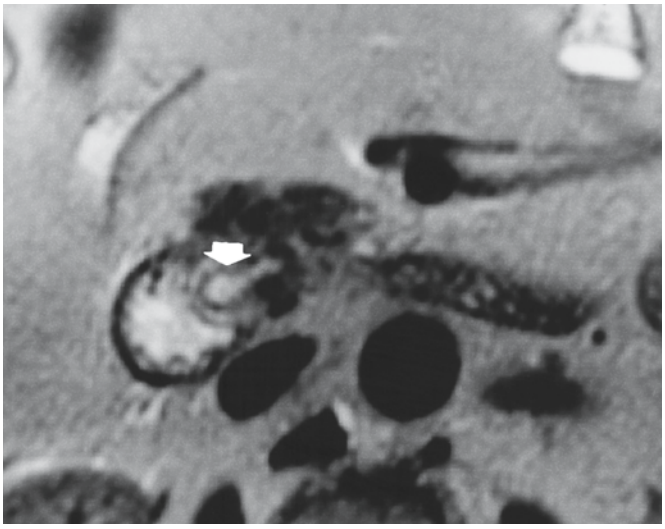

Fig. 126. Axial T 2-weighted image showing broadened aspect of the distal (intramural) part of the common bile duct (*arrow*)

#127 Sphincter Dysfunction, General

KEY FACTS: DISEASE

- Clinical entity resulting from the impedance of biliary and/or pancreatic flow
- Most common in middle-aged women
- Underlying disorder:
  - Structural narrowing (fibrosis): *papillary stenosis*
  - Motor abnormality: *dyskinesia*
- Predisposing factors: prior cholecystectomy; stone passage
- Symptoms: biliary colic
- Objective diagnostic criteria (Hogan et al. 1987):
  - Elevation of transaminases and alkaline phosphatase (twice the normal value), documented on two different occasions
  - Dilation of extrahepatic bile duct (> 12 mm)
  - Delayed emptying on ERCP (> 45 min)
- Classification:
  - Type I: all three criteria fulfilled
  - Type II: one or two criteria fulfilled
  - Type III: no criteria fulfilled
- Gold standard for diagnosis: manometry. If dyskinesia is present, abnormalities include (Toonly et al. 1997):
  - Most common: elevation of basal pressure (> 40 mmHg)
  - Increased frequency of phasic wave contractions (more than eight per min)
- Other diagnostic techniques that have been proposed:
  - ^{99m}Tc-hepato-iminodiacetic acid (HIDA) scan (delayed transit from the common bile duct to the bowel)
  - Secretin test with measurement of pancreatic duct diameter (see also # 19)
  - Fatty meal test with measurement of bile duct diameter (see also # 19)
- Treatment:
  - Type I: sphincterotomy
  - Type II: sphincterotomy if manometry is positive
  - Type III: medication
- Complications:
  - Chronic obstructive pancreatitis (see # 168)
  - Secondary sclerosing cholangitis (see # 45; Tarnasky et al. 1997)

References

Hogan WJ, Geenen JE, Dodds WJ (1987) Dysmotility disturbances of the biliary tract: classification, diagnosis, and treatment. Semin Liver Dis 7: 302 – 311

Tarnasky PR, Hoffman B, Aabakken L et al. (1997) Sphincter of Oddi dysfunction is associated with chronic pancreatitis. Am J Gastroenterol 92: 1125 – 1129

Toonly J, Roberts-Thomson IC, Dent J, Lee J (1985) Manometric studies in patients with suspected sphincter of Oddi dysfunction. Gastroenterology 88: 1243 – 1250

#128 Sphincter Dysfunction, Features on Dynamic MRCP

Related topic: #120 (vaterian sphincter complex: normal contractile activity)

KEY FACTS

- The following morphologic patterns may be seen on dynamic MRCP:
  - "Type A": nonvisualization of sphincter segment (Fig. 128 a, c–e)
  - "Type B": absence of variability in shape on serial breathhold images (Fig. 128 b, f–j)
- These morphologic abnormalities of the vaterian sphincter complex may be associated with dilation of the common bile duct and pancreatic duct (not always present)
- *Note:* Detection of these abnormalities requires use of a dedicated MR technique and specific attention to the morphology of the vaterian sphincter complex on consecutive images

References

Van Hoe L, Vanbeckevoort D, Gryspeerdt S et al. (1997) MR cholangiography of periampullary lesions: potential pitfalls in diagnosis. Radiology 205 (P) : 709

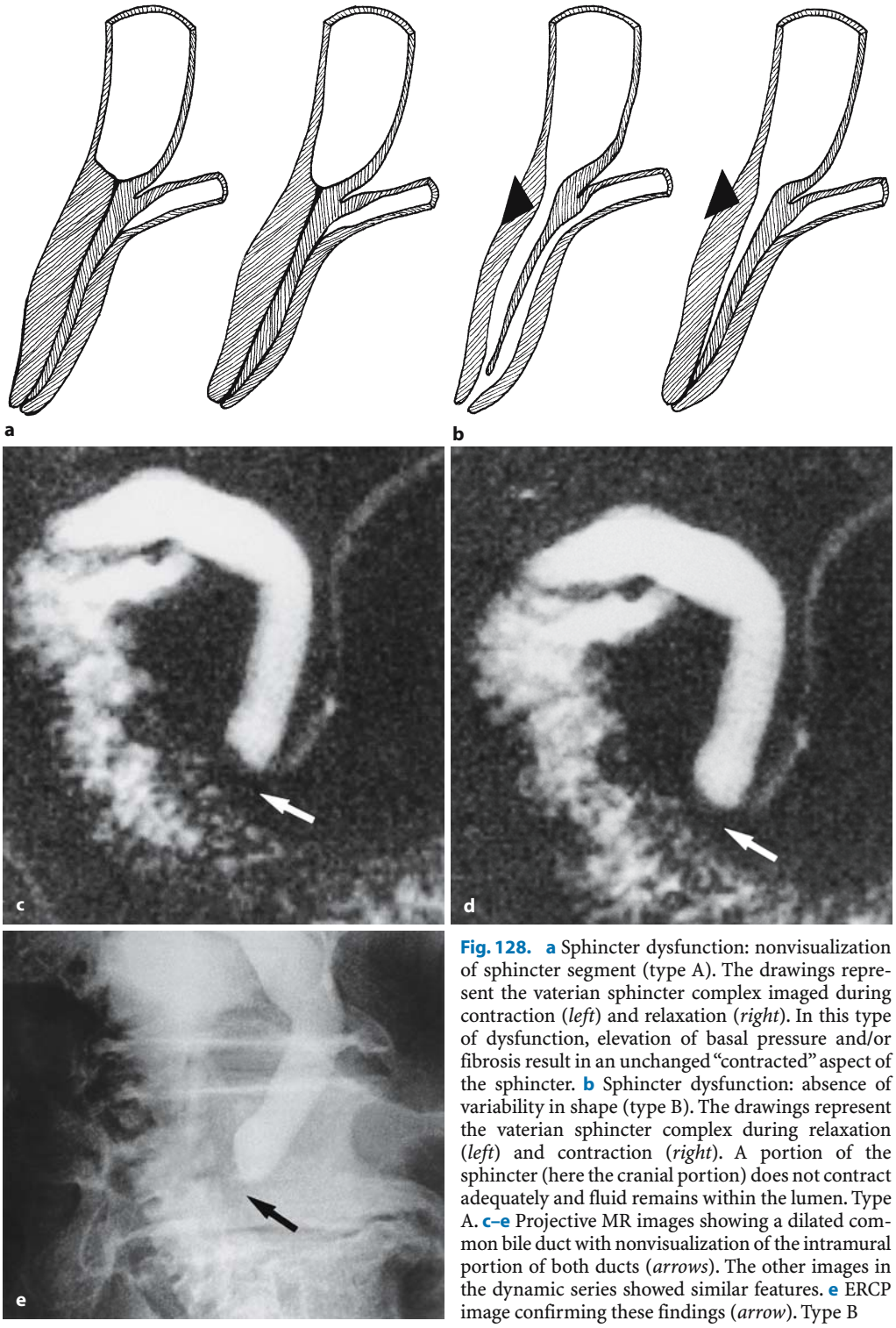

Fig. 128. **a** Sphincter dysfunction: nonvisualization of sphincter segment (type A). The drawings represent the vaterian sphincter complex imaged during contraction (*left*) and relaxation (*right*). In this type of dysfunction, elevation of basal pressure and/or fibrosis result in an unchanged "contracted" aspect of the sphincter. **b** Sphincter dysfunction: absence of variability in shape (type B). The drawings represent the vaterian sphincter complex during relaxation (*left*) and contraction (*right*). A portion of the sphincter (here the cranial portion) does not contract adequately and fluid remains within the lumen. Type A. **c–e** Projective MR images showing a dilated common bile duct with nonvisualization of the intramural portion of both ducts (*arrows*). The other images in the dynamic series showed similar features. **e** ERCP image confirming these findings (*arrow*). Type B

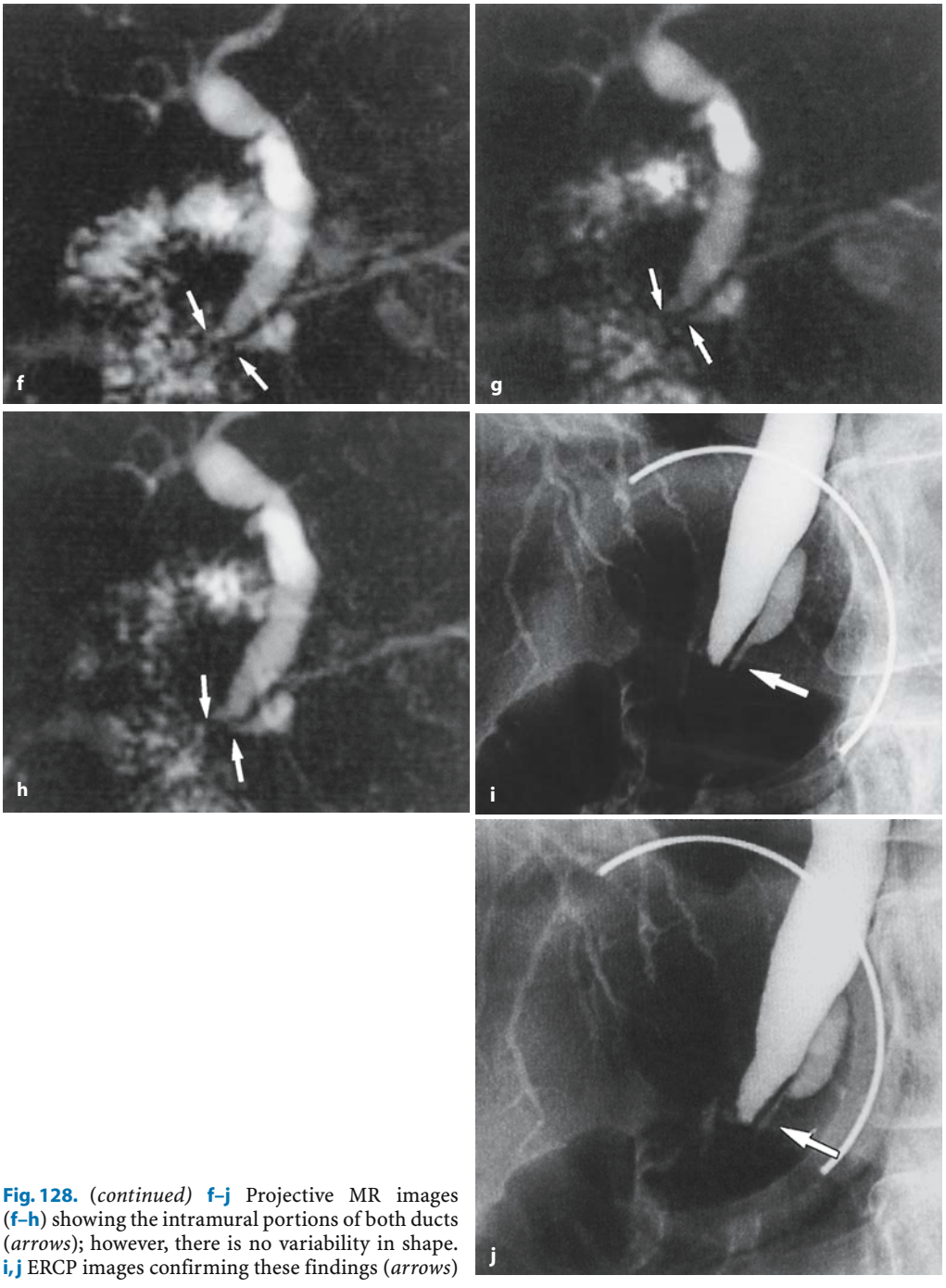

Fig. 128. (*continued*) **f–j** Projective MR images (**f–h**) showing the intramural portions of both ducts (*arrows*); however, there is no variability in shape. **i, j** ERCP images confirming these findings (*arrows*)

#129 Sphincter Dysfunction, False-Negative Diagnosis on Dynamic MRCP

KEY FACTS: MRI

- While dynamic MRCP provides information on the presence of contractile activity, it does not actually show the *passage* of bile into the duodenum
- In some patients with papillary dyskinesia, ERCP shows delayed emptying of the common bile duct despite the presence of contractile activity; this feature is not shown on MRCP (Fig. 129)
- *Note:* In order to overcome this limitation, the use of provocative tests has been proposed (Mariani et al. 2003). Further studies are required to determine the role of MRCP in comparison with ERCP/manometry.

References

Mariani A, Curioni S, Zanello A, et al. (2003) Secretin MRCP and endoscopic pancreatic manometry in the evaluation of sphincter of Oddi function: a comparative pilot study in patients with idiopathic recurrent pancreatitis. Gastrointest Endosc 58 : 847 – 852

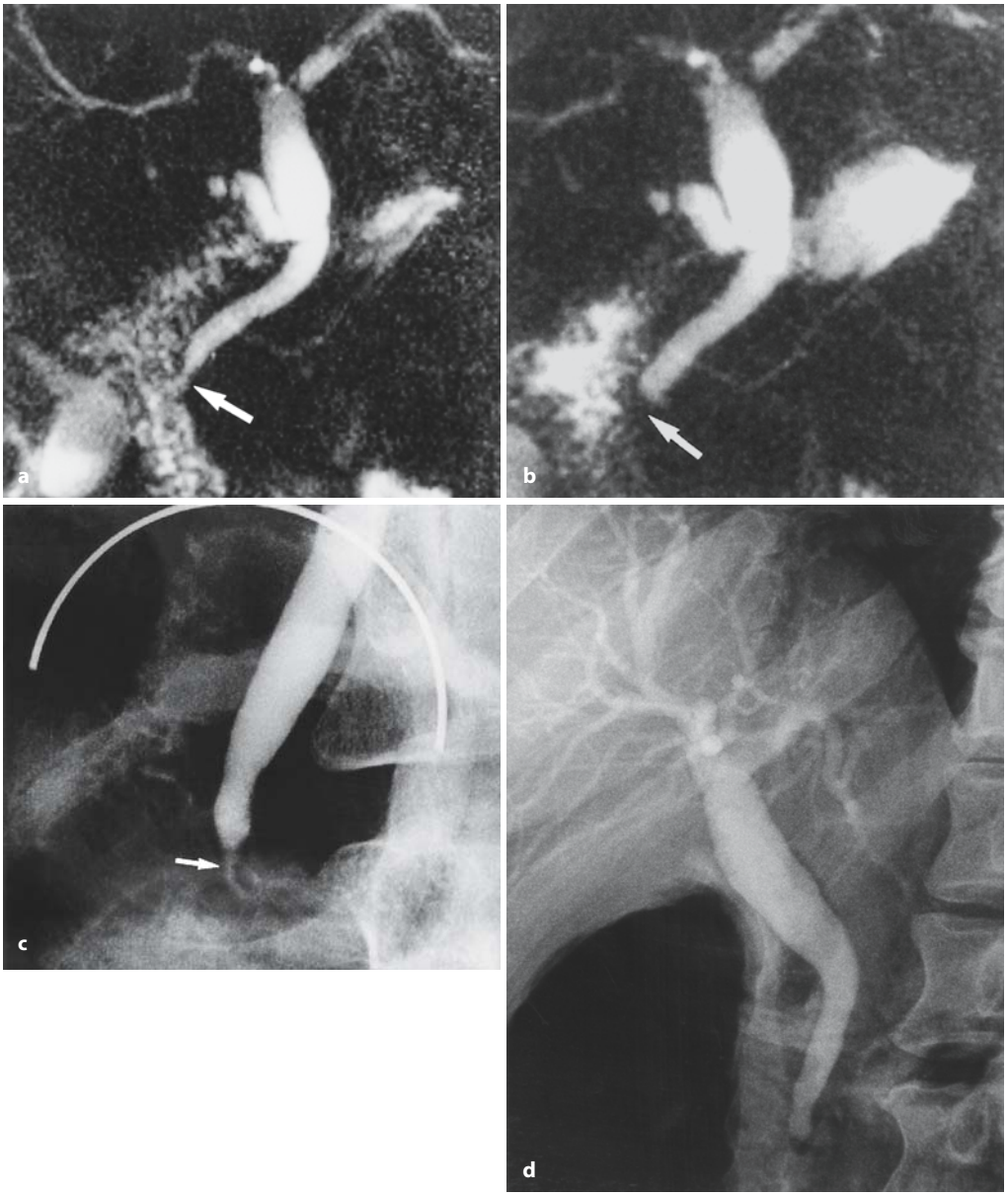

Fig. 129 a–d. Projective MR images showing apparently normal contractility of the sphincter: **a** sphincter relaxation with visualization of the intramural segment; **b** contraction (*arrows*). **c** ERCP image showing apparently normal distal (intramural) portion of bile duct (*arrow*). **d** However, 1-h delayed ERCP image shows bile ducts still filled with contrast medium, thus suggesting sphincter dysfunction (see # 127, diagnostic criteria). Surprisingly, manometry showed normal contractility and normal baseline pressure. The final diagnosis was sphincter dysfunction, however, mainly because the symptoms disappeared after sphincterotomy

#130 Benign Tumors

KEY FACTS: DISEASE

- Histology of ampullary tumors:
  - Adenoma most common
  - Other types: leiomyoma, neurofibroma, hemangioma, hamartoma
- Incidence: 0.04 % – 0.62 %
- Age peak: 50 – 70 years
- Associations (adenoma):
  - Familial polyposis coli
  - Gardner syndrome
- Adenoma is considered a precancerous lesion (Yamaguchi and Enjoji 1991)

KEY FACTS: MRI

- Typical features (Fig. 130 a):
  - Dilation of pancreatic duct and bile ducts
  - Bulging papilla (= generously sized papilla protruding into the lumen) with or without soft tissue mass
- Differential diagnosis (usually impossible by MRI):
  - Non-neoplastic causes of bulging papilla: impacted gallstone; choledochocele; papillitis (Fig. 130 b)
  - Malignant tumors (see # 132, 133)

References

Seifert E, Schulte F, Stolte M (1992) Adenoma and carcinoma of the duodenum and papilla of Vater: a clinicopathologic study. Am J Gastroenterol 87 : 37 – 42

Yamaguchi K, Enjoji M (1991) Adenoma of the ampulla of Vater: putative precancerous lesion. Gut 32 : 1558 – 1561

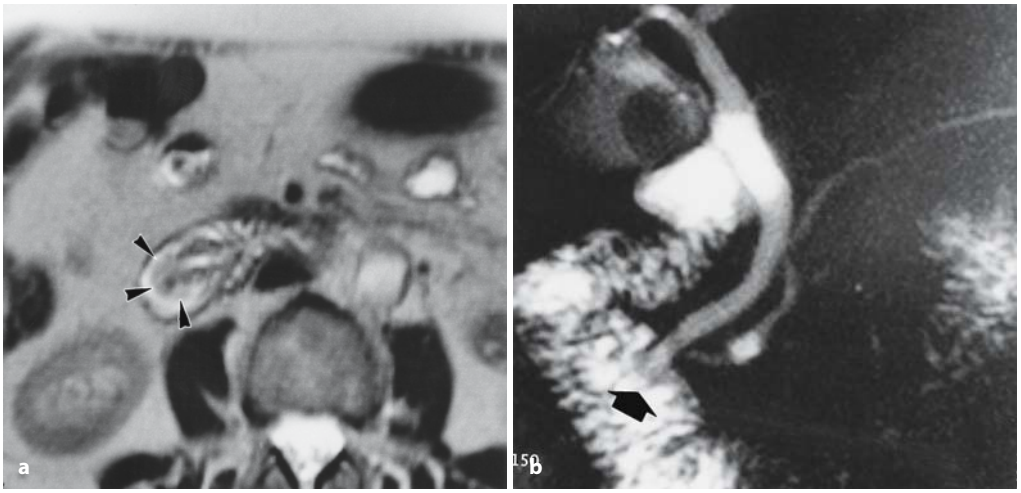

Fig. 130. a Axial T2-weighted image showing enlarged papilla bulging into the duodenal lumen (*arrowheads*). The final diagnosis was tubulovillous adenoma. **b** Different patient. Projective image showing prominent papilla ("bulging papilla"; *arrow*). In this patient, the final diagnosis was papillary edema, most likely secondary to stone passage

5.3 Traumatic, Postoperative, and Iatrogenic Abnormalities

#131 Sequelae/Complications of ERCP

KEY FACTS: DISEASE

- Complication rate: between 4.6% and 12%, depending on the type of procedure (diagnostic, manometry, sphincterotomy) (Cotton and Chong 1995)
- Complications of diagnostic ERCP:
  - Pancreatitis (most common)
  - Infection
  - Sepsis (0.8%)
  - Aspiration pneumonia (0.1%)
- Complications of sphincterotomy (Catalano et al. 1997):
  - Overall complication rate: 10%
  - Most common: hemorrhage, perforation (0.4% – 2.1%), pancreatitis
  - Mortality rate: 0.3%

KEY FACTS: MRI

- Pancreatitis (see #151)
- Perforation:
  - Paraduodenal collection containing fluid and/or air
  - May spread in retroperitoneum
  - A defect may be demonstrated in the wall of the distal common bile duct
- Bleeding:
  - Collection with typical signal intensity of blood (see #51)
- *Note:* After sphincterotomy, the distalmost portions of the bile duct and pancreatic duct may have an unusual appearance (Fig. 131):
  - Abnormally "broad" aspect
  - Absence of normal contractions
  - Irregular contours
  - Intraluminal air

References

Catalano O, Lapiccirella G, Rotondo A (1997) Papillary injuries and duodenal perforation during endoscopic retrograde sphincterotomy: radiological findings. Clin Rad 52 : 688 – 691

Cotton P, Chong W (1995) Complications of ERCP and therapy. In: Silvis S, Rohrmann C, Ansel H (eds) Endoscopic retrograde cholangiopancreatography. Igaku-Shoin, New York, pp 446 – 469

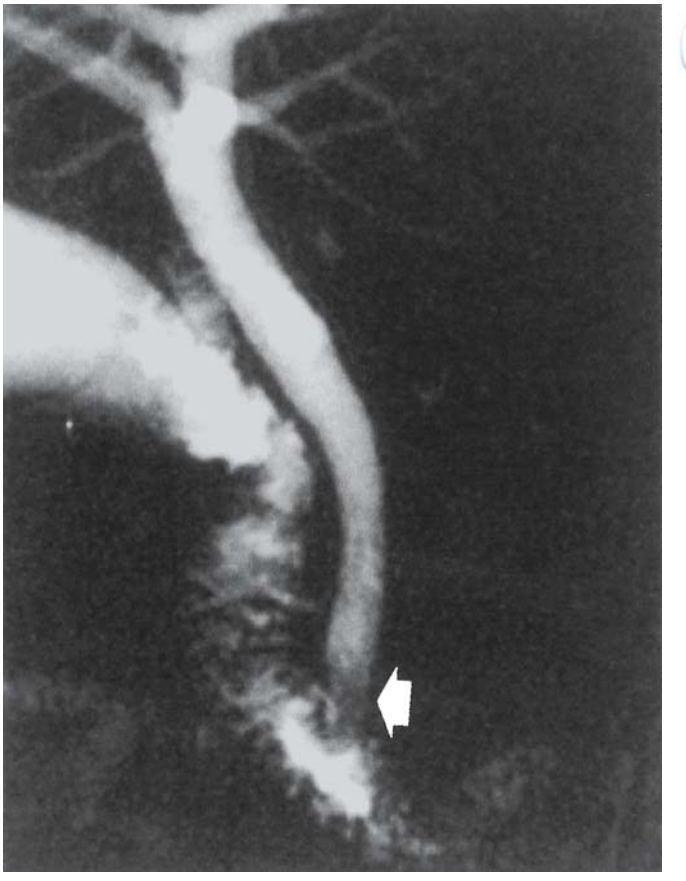

Fig. 131. Projective image obtained in a patient who underwent papillotomy showing abnormally broad aspect of the distal common bile duct (*arrow*). Note decreased signal intensity of the distalmost portion of the common bile duct, most likely caused by presence of air

5.4 Malignant Tumors

#132 (Peri-)Ampullary Carcinoma

KEY FACTS: DISEASE

- Carcinomas of the papilla, ampulla, and adjacent structures are collectively referred to as periampullary carcinomas
- Usually adenocarcinomata; tend to be smaller than more proximal biliary neoplasms
- In many cases, it is impossible to determine the exact origin (e.g., duodenum, papilla proper, ampulla)
- Age peak: 60 years
- Symptoms: icterus, duodenal obstruction, weight loss
- Resectable in 80 % – 95 %
- Relatively good prognosis (5-year survival rate, 35 % – 60 %)

KEY FACTS: MRI (FIG. 132)

- Typical features on projective images:
  - Dilation of the common bile duct and pancreatic duct
  - Abrupt irregular narrowing or occlusion of the distalmost portions of both ducts ("double duct" sign)
  - Signs of fixation (no contractile activity)
  - Enlarged "bulging" papilla with or without soft tissue mass (Fig. 132)
- Cross-sectional images:
  - Sometimes small mass lesion in the lateral part of the pancreatic head
  - Signal intensity and contrast uptake pattern: similar to pancreatic carcinoma
- Differential diagnosis:
  - Adenocarcinoma of pancreatic head invading the vaterian sphincter complex (see # 133)
  - Distal cholangiocarcinoma (diagnosis more likely if the pancreatic duct diameter is normal)
  - Other tumors (e.g., gastrinoma, carcinoid, adenoma, metastasis)
  - Non-neoplastic causes of papillary obstruction (e.g., impacted stone with edema)

References

Geier A, Nguyen HN, Gartung C et al. (2000) MRCP and ERCP to detect small ampullary carcinoma. Lancet 356 : 1607 – 1608

Irie H, Honda H, Shinozaki K et al. (2002) MR imaging of ampullary carcinomas. J Comput Assist Tomogr 26 : 711 – 717

Kim JH, Kim MJ, Chung JJ et al. (2002) Differential diagnosis of periampullary carcinomas at MR imaging. Radiographics 22 : 1335 – 1352

Semelka RC, Kelekis N, John G et al. (1997) Ampullary carcinoma: demonstration by current MR techniques. J Magn Reson Imaging 7 : 153 – 156

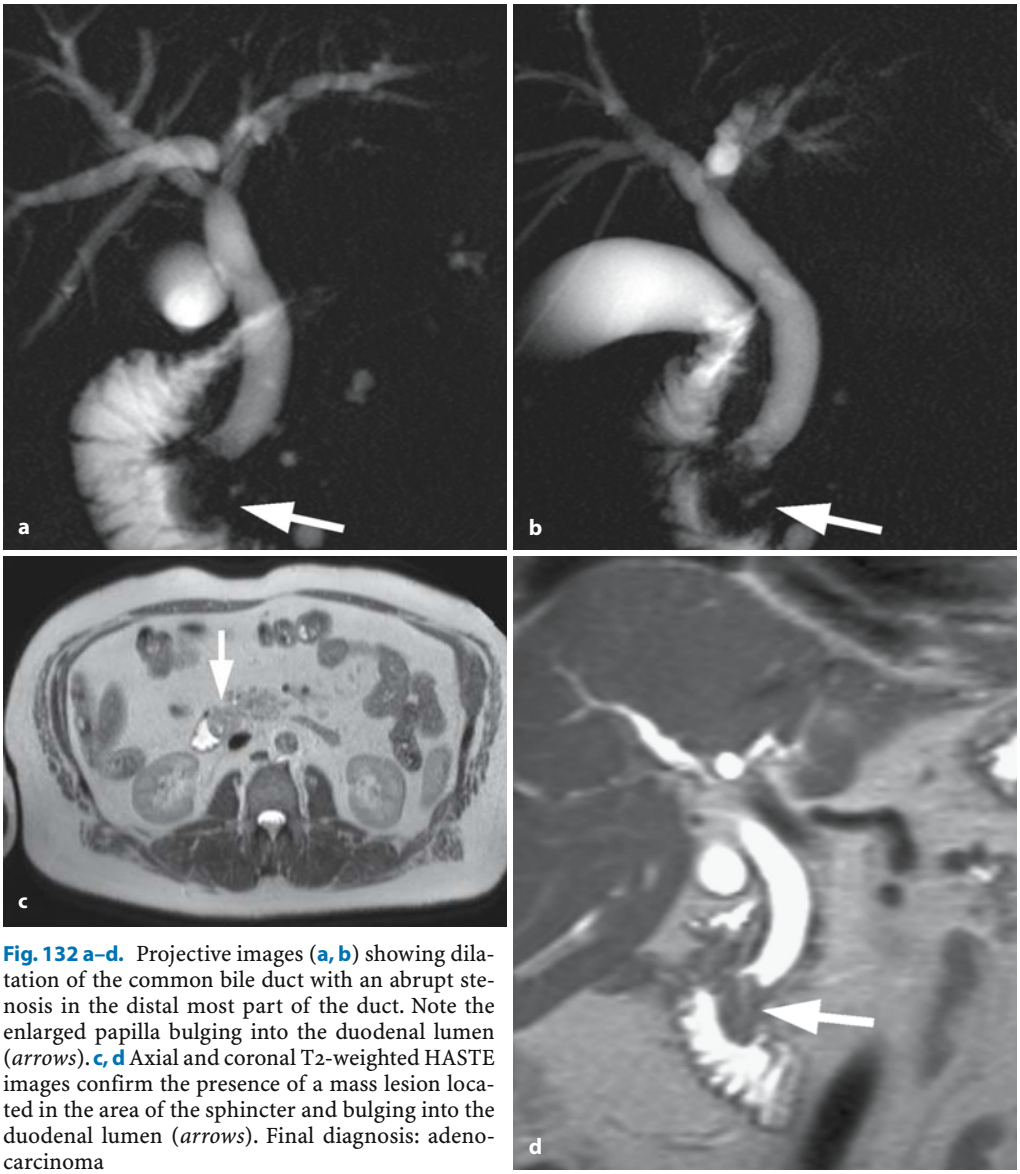

Fig. 132 a–d. Projective images (**a, b**) showing dilatation of the common bile duct with an abrupt stenosis in the distal most part of the duct. Note the enlarged papilla bulging into the duodenal lumen (*arrows*). **c, d** Axial and coronal T2-weighted HASTE images confirm the presence of a mass lesion located in the area of the sphincter and bulging into the duodenal lumen (*arrows*). Final diagnosis: adenocarcinoma

#133 Carcinoma of the Pancreatic Head Invading the Vaterian Sphincter Complex

Related topics: #90 (extrahepatic duct: involvement by pancreatic carcinoma), #185–195 (pancreatic adenocarcinoma)

KEY FACTS: DISEASE

- See #185

KEY FACTS: MRI

- See also #90
- Typical features:
  - Stenosis of the distal common bile duct and pancreatic duct, commonly manifested as "invisible ducts"
  - Unchanged aspect during dynamic evaluation
  - Mass lesion in the pancreatic head
- Differential diagnosis with primary ampullary carcinoma (see #132): usually difficult or even impossible
- Pancreatic carcinomas with a more proximal location may present with the "four-segment sign" or involve the pancreatic duct only, thus making ampullary carcinoma unlikely (Kim et al. 2002)

References

Kelekis NL, Semelka RC (1995) Carcinoma of the pancreatic head area. Diagnostic imaging: magnetic resonance imaging. Rays 20 : 289–303

Kim JH, Kim MJ, Chung JJ et al. (2002) Differential diagnosis of periampullary carcinomas at MR imaging. Radiographics 22 : 1335–1352

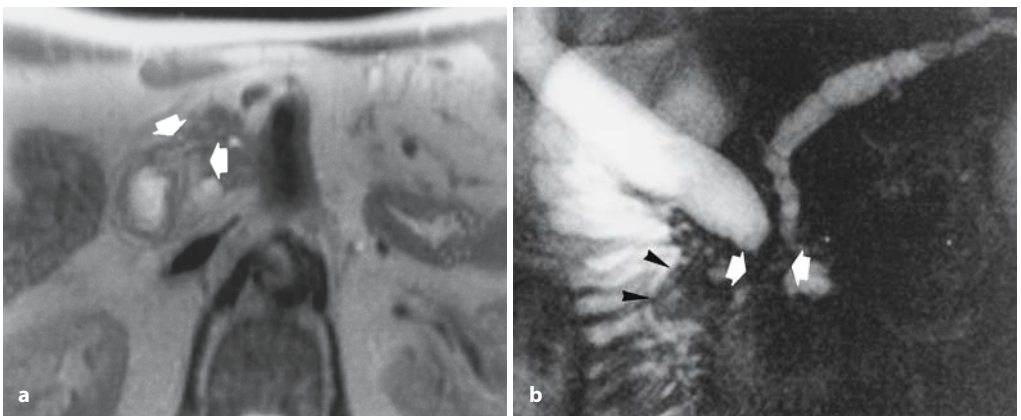

Fig. 133 a, b. Axial T2-weighted image (**a**) showing slightly hyperintense area in the lateral part of the pancreatic head, corresponding to pancreatic adenocarcinoma. **b** Projective image obtained in the same patient showing a dilated common bile duct and pancreatic duct with abrupt narrowing in the pancreatic head (double duct sign; *arrows*). Also note prominent papilla (*arrowheads*)

Pancreatic Ducts

1 Pancreatic Ducts

6.1 Normal Anatomy and Variants

#134 Normal Pancreas: Location and Signal Intensity

KEY FACTS

- The pancreas is a retroperitoneal organ crossing the lumbar spine at level L 2
- The head of the pancreas lies within the duodenal sweep, while the tail is usually directed towards the splenic hilum
- After splenectomy, the pancreatic tail migrates cranially and dorsally (Fig. 134)
- Length of duct: ranging from 9.5 to over 25 cm (average, 16 cm)
- Normal maximal anteroposterior diameters of the head and body: 3.5 and 2.2 cm, respectively
- Signal intensity of normal pancreatic parenchyma:
  - T 1: high intensity (equal to or higher than signal intensity of liver, due to aqueous protein in the acini; see also Fig. 10)
  - T 2: relatively hypointense (lower than signal intensity of spleen)
- T 1-weighted images with fat suppression provide the best delineation of the pancreatic borders

References

Mitchell DG, Winston CB, Outwater EK, Ehrlich SM (1995) Delineation of the pancreas with MR imaging: multiobserver comparison of five pulse sequences. J Magn Reson Imaging 5 : 193 – 199

Semelka RC, Ascher SM (1993) MR imaging of the pancreas. Radiology 188 : 593 – 602

Winston CB, Mitchell DG, Outwater EK, Ehrlich SM (1995) Pancreatic signal intensity on T 1-weighted fat saturation MR images: clinical correlation. J Magn Reson Imaging 5 : 267 – 271

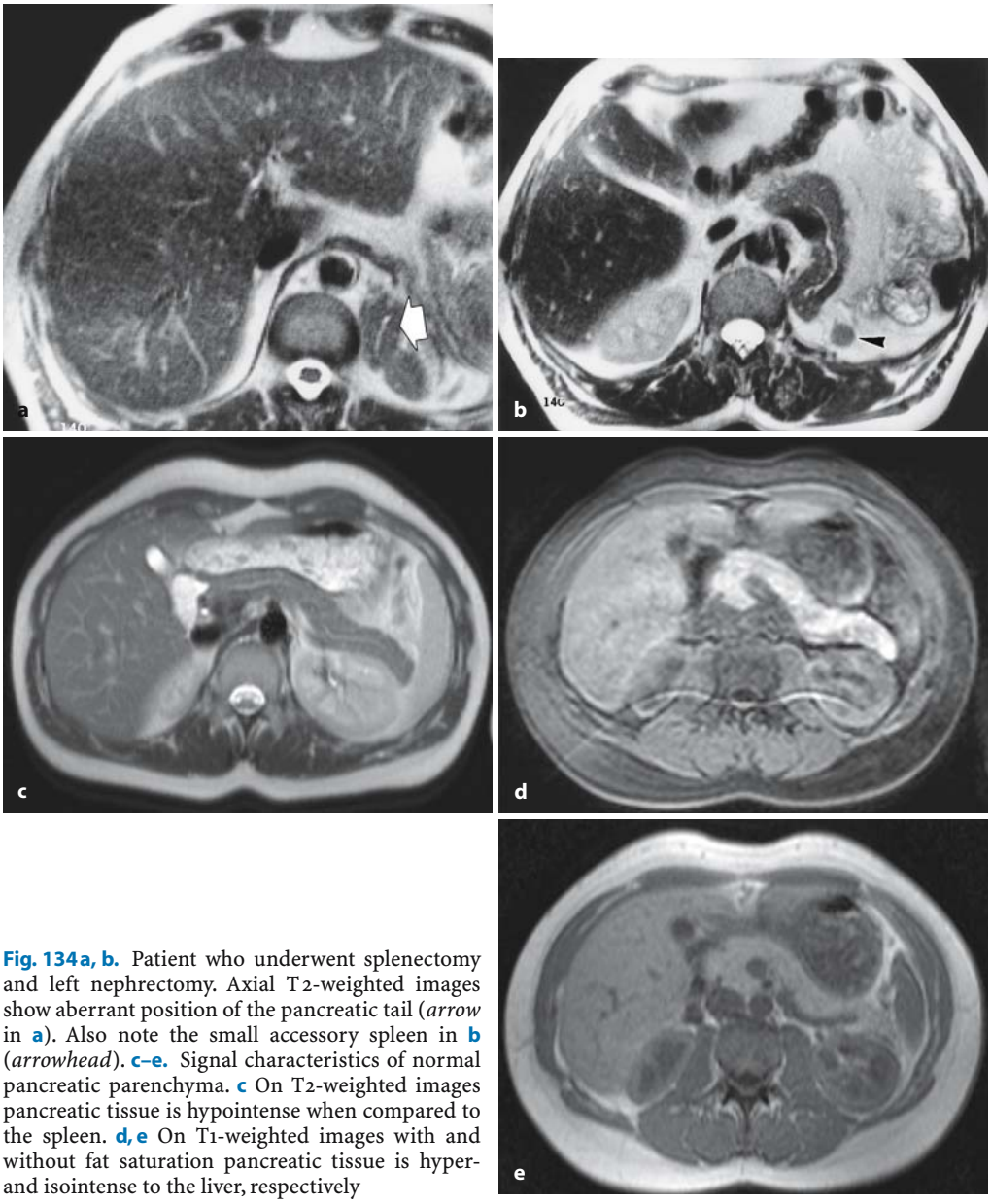

Fig. 134a, b. Patient who underwent splenectomy and left nephrectomy. Axial T2-weighted images show aberrant position of the pancreatic tail (*arrow* in **a**). Also note the small accessory spleen in **b** (*arrowhead*). **c–e.** Signal characteristics of normal pancreatic parenchyma. **c** On T2-weighted images pancreatic tissue is hypointense when compared to the spleen. **d, e** On T1-weighted images with and without fat saturation pancreatic tissue is hyper- and isointense to the liver, respectively

#135 Classical Ductal Anatomy

KEY FACTS: ANATOMY

Features of the normal main pancreatic duct include:

- Size
  - Reported maximum diameter: < 5 mm (increases with age)
  - The caliber is greatest in the head and tapers smoothly to the tail
- Common types of course:
  - "Sigmoid" configuration (ascending-horizontal-ascending; 34.5 %)
  - "Pistol" configuration (ascending-horizontal-horizontal; 27.6 %)

Features of normal side branches include:

- Number: 15 – 30
- Taper gently as they course into the parenchyma
- In the body and tail, branch points appear at regular intervals
- All the body and tail side branches should be uniform (the presence of one or two mildly ectatic branches is still considered normal)
- The side branches in the pancreatic head that course inferiorly to serve the uncinate process are variable in number, length, and caliber

KEY FACTS: MRI

- The normal pancreatic duct is usually visible on MRCP, both on cross-sectional and projective images; the latter type of image is best suited to visualize the entire pancreatic duct
- Normal side branches are usually *not* seen on MRCP
- Occasionally, large normal side branches may be seen in the pancreatic head

References

Laubenberger J, Büchert M, Schneider B, Blum B, Hennig J, Langer M (1995) Breath-hold projection magnetic resonance cholangio-pancreaticography (MRCP): a new method for the examination of the bile and pancreatic ducts. Magn Reson Med 33 : 18 – 23

Reinhold C, Bret P (1996) MR cholangiopancreatography. Abdom Imaging 21 : 105 – 116

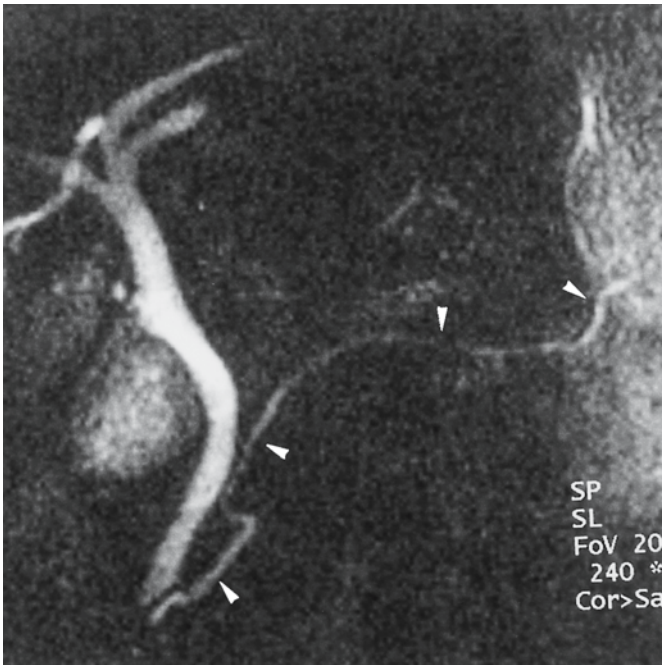

Fig. 135. Projective image shows sigmoid configuration of the pancreatic duct (*arrowheads*)

#136 Classical Ductal Anatomy in Pancreatic Head

KEY FACTS: ANATOMY

- Normal development of the dorsal anlage (see Fig. 140 a):
  - Develops into the tail, body, and cranial portion of the head
  - Drains into the minor papilla through the accessory duct of Santorini
- Normal development of the ventral anlage:
  - Forms the caudal portion of the pancreatic head
  - Drains into the major papilla through the distal portion of the duct of Wirsung
- Normal ductal fusion and variants (see also # 137):
  - In 60 % of patients, the duct of the ventral pancreas (Wirsung) fuses with the dorsal duct to become the primary continuation of the main pancreatic duct; the duct of Santorini remains patent but has a small diameter (usually 1 mm less than the diameter of the duct of Wirsung)
  - In 30 %, the duct of Santorini regresses further and loses its direct connection with the duodenum at the minor papilla
  - In 3 % – 7 %, there is pancreas divisum: no fusion (see # 140)
- Comment on anatomy:
  - The *ventral pancreas* corresponds to the *posterior* part of the pancreatic head
  - The *dorsal pancreas* corresponds to the *anterior* part of pancreatic head and the body and tail

KEY FACTS: MRI

- The duct of Wirsung is clearly visualized in the large majority of patients
- Visualization of the duct of Santorini is variable; in most patients, it is barely visible or not seen at all

References

Millbourn E (1960) Calibre and appearance of the pancreatic ducts and relevant clinical problems: a roentgenographic and anatomic study. Acta Chir Scand 118 : 286 – 303

Reinhold C, Bret P (1996) MR cholangiopancreatography. Abdom Imaging 21 : 105 – 116

Taylor AJ, Bohorfoush AG (1997) Interpretation of ERCP. Lippincott-Raven, Philadelphia, p 210

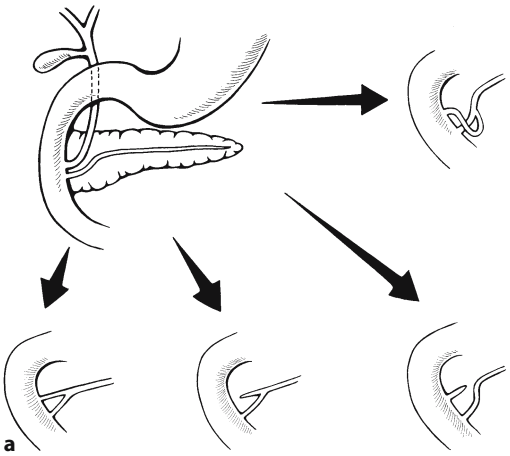

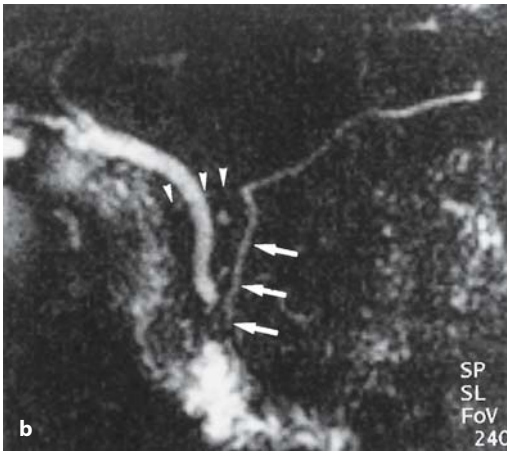

Fig. 136. **a** Variation of accessory duct appearance: *1*, bifid configuration (see #137); *2*, *3*, incomplete duct of Santorini; *4*, ansa pancreatica (see #138). (From Taylor and Bohorfoush 1997, with permission). **b** Projective image showing normal aspect of the main pancreatic duct draining into the papilla major (*arrows*). The duct of Santorini is hardly visible (*arrowheads*)

#137 Variant Anatomy (1): "Bifid" Configuration with a Prominent Duct of Santorini

Related topic: # 140 (pancreas divisum)

KEY FACTS: MRI

- In some patients, the duct of Santorini is clearly seen
- Types:
  - "Bifid" ductal configuration (common): both ducts have approximately the same size and are connected (Fig. 137)
  - "Dominant duct of Santorini" (± 3 %): variant of the bifid configuration in which the duct of Santorini has the largest diameter
- Differential diagnosis with pancreas divisum (# 140):
  - The ventral and dorsal systems are connected
  - The ventral duct (Wirsung) is always clearly visible and does not arborize

References

Leyendecker JR, Elsayes KM, Gratz BI et al. (2002) MR cholangiopancreatography: spectrum of pancreatic duct abnormalities. AJR Am J Roentgenol 179 : 1465 – 1471

Sigfusson BF, Wehlin L, Lindström CG (1983) Variants of pancreatic duct system of importance in endoscopic retrograde cholangiopancreatography. Acta Radiol Diagn 24 : 113 – 128

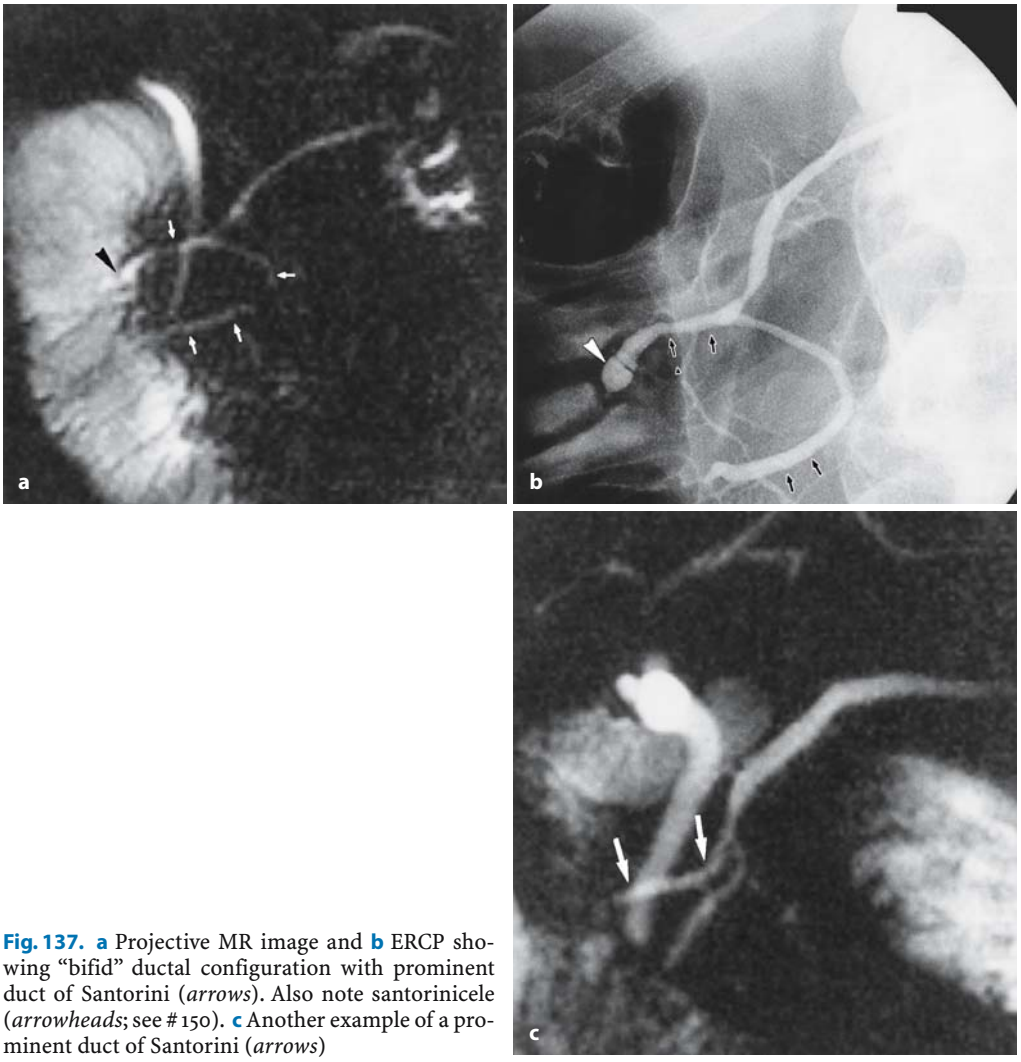

Fig. 137. **a** Projective MR image and **b** ERCP showing "bifid" ductal configuration with prominent duct of Santorini (*arrows*). Also note santorinicele (*arrowheads*; see # 150). **c** Another example of a prominent duct of Santorini (*arrows*)

#138 Variant Anatomy (2): Ansa Pancreatica and Ductal Loops

KEY FACTS

- The accessory duct of Santorini usually has a fairly direct course from the pancreatic neck to the duodenum
- Occasionally, this duct has a reversed S-shaped appearance and is connected with an uncinate process side branch: ansa pancreatica (see Fig. 136 a)
- Loops may be seen in the head, neck, and body (Fig. 138)
- Ansa pancreatica may be associated with chronic pancreatitis (Tanaka et al. 1992)

References

Dawson W, Langman J (1961) An anatomical-radiological study on the pancreatic duct pattern in man. Anat Rec 139 : 51 – 56

Tanaka T, Ichiba Y, Miura Y, Itoh H, Dohi K (1992) Variations of the pancreatic ducts as a cause of chronic alcoholic pancreatitis; ansa pancreatica. Am J Gastroenterol 87 : 806

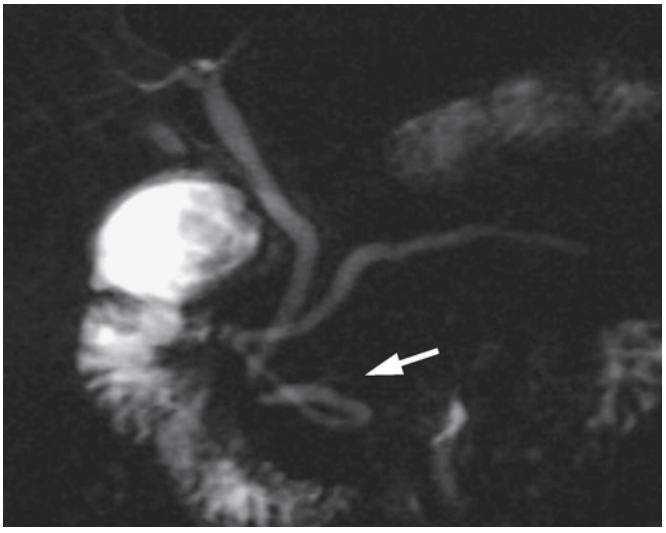

Fig. 138. Projective image obtained in a asymptomatic volunteer showing a prominent ductal loop (*arrow*)

#139 Variant Anatomy (3): Focal Narrowing at the Junction

KEY FACTS

- Narrowing at the site of fusion of the dorsal and ventral ducts ("fusion narrowing")
- 3% in autopsy series
- Typical features (Fig. 139):
  - Length: usually a few millimeters
  - Characteristic location: takeoff of the accessory duct, the original drainage conduit for the dorsal pancreas
- Differential diagnosis with pathologic stenosis:
  - Typical location
  - Subtle narrowing, short length
  - Lack of proximal dilation, abnormal side branches, or other ductal changes

References

Belber JP, Bill K (1977) Fusion anomalies of the pancreatic ductal system: differentiation from pathologic states. Radiology 122 : 637 – 642

Sivak MV, Sullivan BH (1976) Endoscopic retrograde pancreatography: analysis of the normal pancreatogram. Am J Dig Dis 21 : 263 – 269

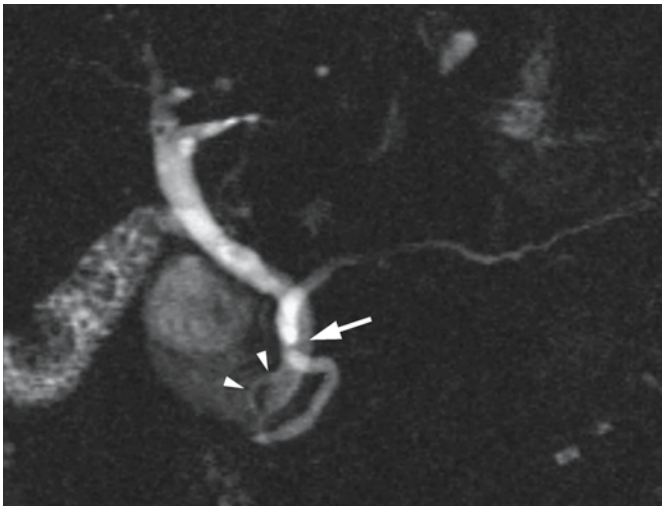

Fig. 139. Projective image showing typical fusion narrowing (*arrow*) located at the takeoff of the accessory duct (*arrowheads*)

#140 Variant Anatomy (4): Pancreas Divisum

Related topics: #137 (bifid configuration with a prominent duct of Santorini), #141 (uneven lipomatosis), #150 (santorinicele)

KEY FACTS: GENERAL

- The dorsal and ventral pancreatic anlage fail to fuse in the eighth week of fetal life (Fig. 140a)
- Incidence:
  - 3%–7% of the normal population
  - 12%–26% of patients with idiopathic recurrent pancreatitis
- Ductal anatomy:
  - Duct of Wirsung (ventral duct) originates from the major papilla and terminates within 1–7 cm
  - The duct of Wirsung typically has a small diameter and an arborizing pattern
  - The dorsal duct originates from the papilla minor and drains the entire dorsal pancreas
- Types:
  - Complete pancreas divisum (most common)
  - Incomplete pancreas divisum (much less common): the ventral and dorsal systems remain connected through small-caliber branch ducts
- Clinical significance: increased incidence of acute and chronic pancreatitis (the orifice of the minor papilla is too small to adequately drain the volume of secretions produced by the pancreatic body and tail; Delhaye et al. 1988)

KEY FACTS: MRI (FIG. 140)

- Pancreas divisum can accurately be demonstrated by MRI
- Key cholangiographic findings:
  - Visualization of the dorsal duct draining into the duodenum via the papilla minor, separated from the distal common bile duct (see also Figs. 63, 67)
  - No connection between the dorsal and ventral ductal system
  - The ventral duct may be small (29%) or invisible (71%)
- Signs on axial cross-sectional images:
  - Visualization of the duct of Santorini ventrally in the pancreatic head clearly separated from the common bile duct. The duct of Santorini is usually clearly seen because of its more or less horizontal course
  - Enlargement of the pancreatic head (not always present)
  - Flat cleft separating the dorsal and ventral pancreatic moieties (not always present; see also #141)
- *Note:* MRCP is probably less accurate than ERCP in the differentiation of complete and incomplete pancreas divisum

References

Bret P, Reinhold C, Taourel P, Guibaud L, Atri M, Barkun AN (1996) Pancreas divisum: evaluation with MRCP. Radiology 199 : 99 – 103

Delhaye M, Engelholm L, Cremer M (1988) Pancreas divisum: controversial clinical significance. Dig Dis 6 : 30 – 39

Gregg JA (1977) Pancreas divisum: its association with pancreatitis. Am J Surg 134 : 539 – 543

Mortelé KJ, Segatto E, Ros PR (2004) The infected liver: radiologic-pathologic correlation. RadioGraphics 24 : 937 – 955

Taylor AJ, Bohorfoush AG (1997) Interpretation of ERCP. Lippincott-Raven, Philadelphia, p 210

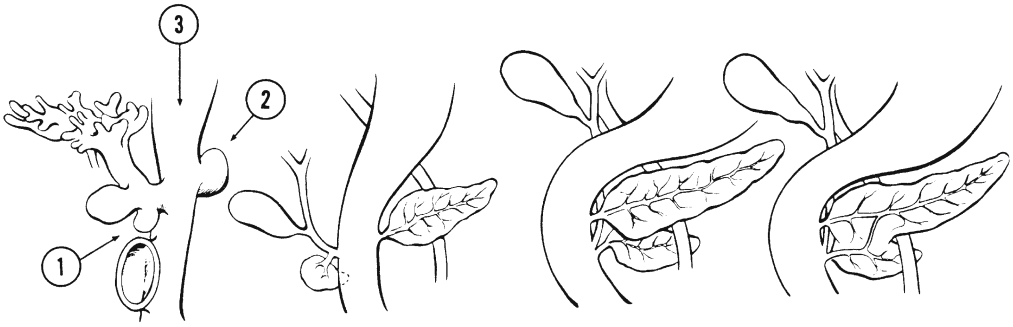

Fig. 140. a Embryologic development of the pancreas (from *left* to *right*). Both the ventral pancreas (*1*) and dorsal pancreas (*2*) are buds off the foregut (*3*). The ventral pancreas develops as a separate anlage and rotates posteriorly as maturation occurs. In pancreas divisum, the ventral and dorsal pancreas are adjacent to each other; however, the two ductal systems remain separated. (From Stewart et al. 1997, with permission).

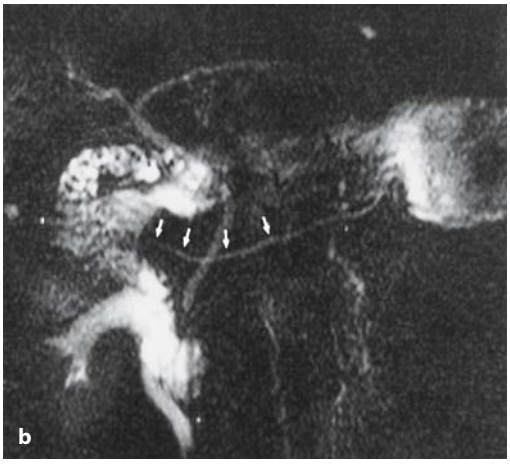

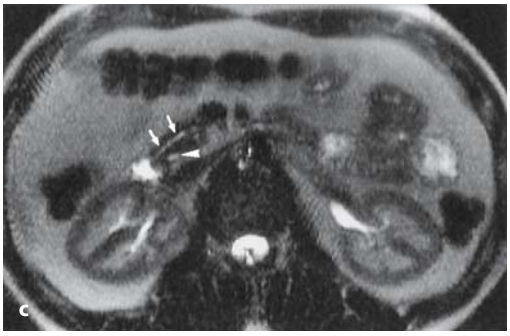

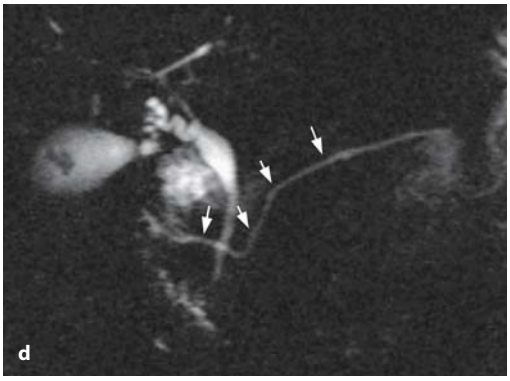

Fig. 140 b–c. **b** Projective MR image showing classical ductal anatomy in pancreas divisum. The duct of Wirsung is not visible. **c** Heavily T2-weighted axial image showing duct of Santorini located ventrally in the pancreatic head (*arrows*) and clearly separated from the common bile duct (*arrowhead*). **d** Projective image showing the classical ductal anatomy in pancreas divisum, with a clearly visible dorsal ductal system (duct of Santorini) and an invisible ventral ductal system (duct of Wirsung).

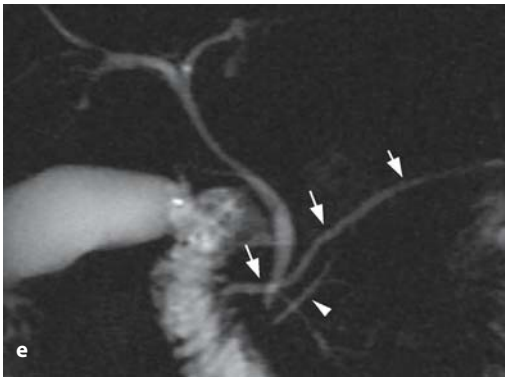

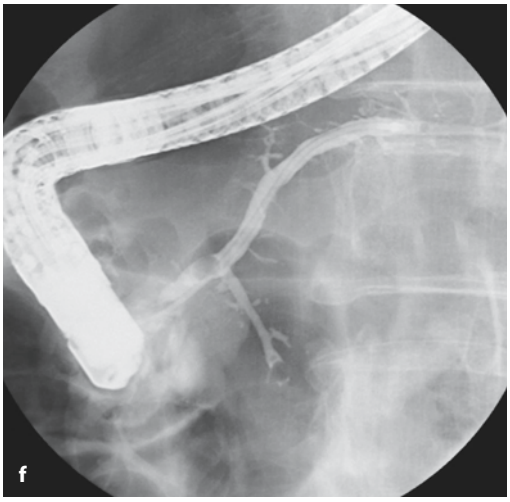

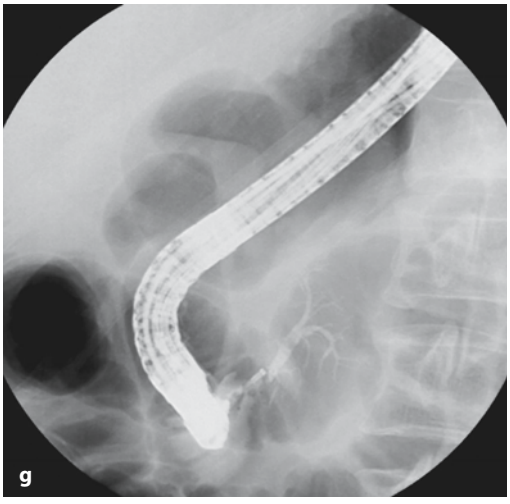

Fig. 140. (*continued*) **e–g** Projective image (**e**) showing a separate dorsal (*arrows*) and ventral (*arrowhead*) pancreatic ductal system. Note that the ventral ductal system is small but still visible. ERCP images with contrast injection in the papilla minor (**f**) and major (**g**) showing the separate dorsal and ventral ductal system.

#141 Variant Anatomy (5): Uneven Lipomatosis

KEY FACTS: GENERAL

- Marked difference in fat content between the dorsal and ventral pancreas (the dorsal moiety contains more fat)
- Incidence: ± 3 %
- May be associated with pancreas divisum
- Etiology:
  - Related to separate embryologic development of both moieties
  - Precise mechanism not known
- Importance: may mimic focal pancreatic mass on ultrasonography, CT, and MRI (Marchal et al. 1989; Matsumoto et al. 1995)

KEY FACTS: MRI (FIG. 141)

- Signal intensity (reflecting the degree of lipomatosis):
  - T1-weighted images: anterior part of the pancreatic head more hyperintense than the posterior part
  - T1-weighted images with fat suppression: anterior part less hyperintense
  - T2-weighted images: aspect depends on the technique used
- Key finding: straight demarcation between the ventral and dorsal parts of the pancreatic head. This line of transition corresponds to the level of fusion between the two embryonal portions of the organ

References

Marchal G, Verbeken E, Van Steenbergen W, Baert AL, Lauweryns J (1989) Uneven lipomatosis: a pitfall in pancreatic sonography. Gastrointest Radiol 14 : 233 – 237

Matsumoto S, Mori H, Miyake H et al. (1995) Uneven fatty replacement of the pancreas: evaluation with CT. Radiology 194 : 453 – 458

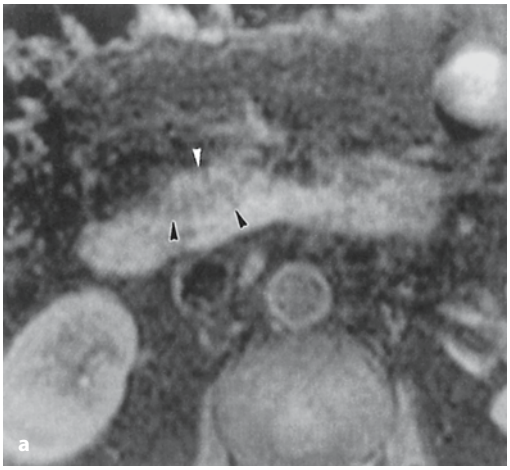

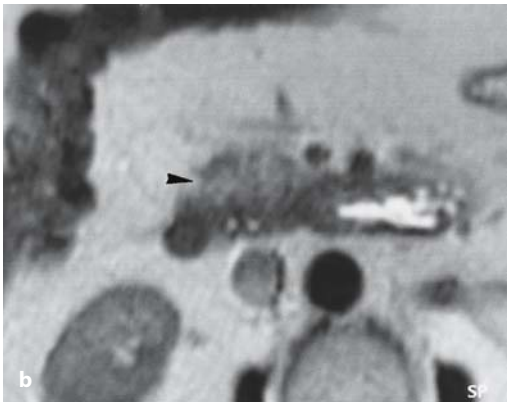

Fig. 141 a–f. **a** T1-weighted image with fat suppression showing ventral part of the pancreatic head as hypointense compared to dorsal part (*arrowheads*). **b** T2-weighed image showing the opposite relationship.

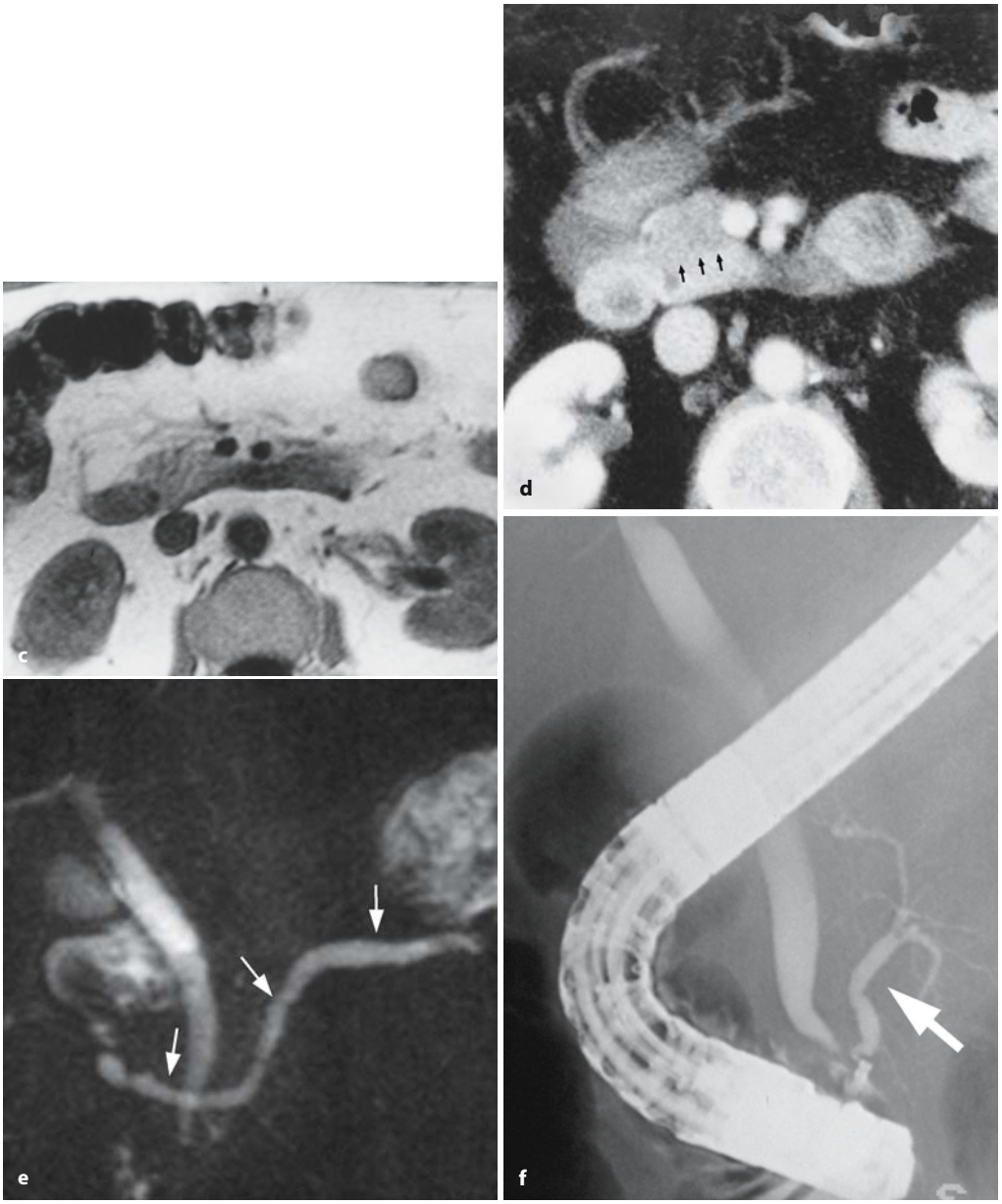

Fig. 141. (*continued*) **c** Non-fat-suppressed T1-weighted image showing no difference in signal intensity. **d** CT image showing ventral part as hypodense. Note the straight demarcation line (*arrows*). Same patient. All these "abnormalities" are consistent with increased fat content in the anterior part of the pancreatic head. **e** Same patient. Projective image showing a clearly visible dorsal ductal system (duct of Santorini) (*arrows*), with Santorinicele, and an invisible ventral ductal system (duct of Wirsung). **f** ERCP image with contrast injection in the papilla major show opacification of the small ventral ductal system (*arrow*). In this patient, the uneven lipomatosis was associated with pancreas divisum

#142 Variant Anatomy (6): Lobulations of the Pancreatic Head

KEY FACTS: GENERAL

- Variants in the lateral contour of the pancreatic head (and neck)
- Incidence: up to 35 %
- Classification (taking into account the orientation of the lobule):
  - Anterior (29 %)
  - Posterior (56 %)
  - Horizontal (15 %) (Ross et al. 1996)
- Mechanism: probably a spectrum of fusion patterns of the dorsal and ventral embryonal parts of the pancreas
- Importance: marked focal convexity can be mistaken for tumor

KEY FACTS: MRI

- Cross-sectional images show marked focal convexity of the lateral contour of the pancreatic head (Fig. 142 a)
- Projective images may show a duct branch in an unusual lateral position (Fig. 142 b)
- Key finding: isointensity with the rest of the pancreas on all pulse sequences

References

Ross B, Brooke Jeffrey R, Mindelzun R (1996) Normal variations in the lateral contour of the head and neck of the pancreas mimicking neoplasm: evaluation with dual-phase helical CT. AJR Am J Roentgenol 166 : 799 – 801

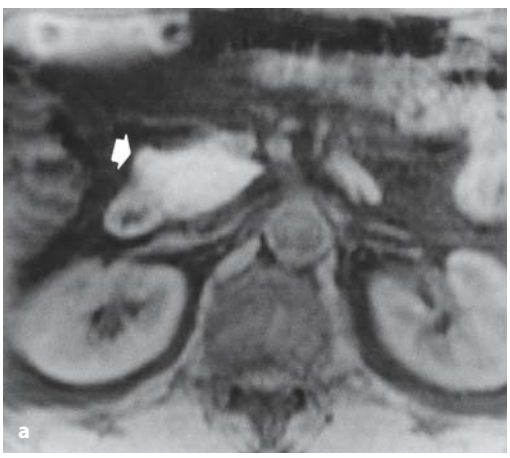

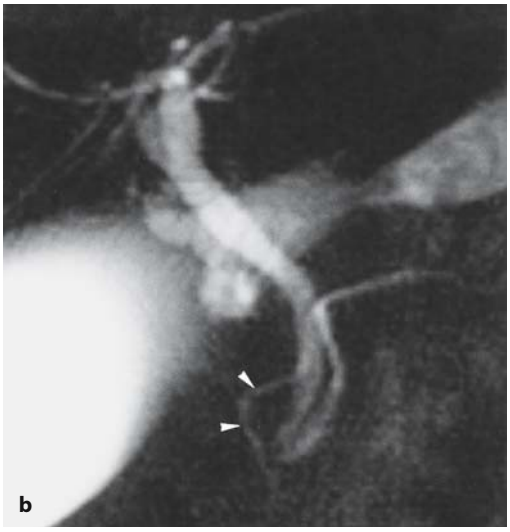

Fig. 142. **a** T1-weighted image showing lobulated lateral contour of the pancreatic head (*arrow*). **b** Different patient. Projective image showing duct of Santorini projecting to the right of the common bile duct (*arrowheads*), which is an indirect sign of a far lateral position of (part of) the pancreatic head

#143 Developmental Abnormalities (1): Agenesis of the Dorsal Pancreas

KEY FACTS: DISEASE

- Types of agenesis:
  - Agenesis of the ventral pancreas (extremely rare)
  - Complete agenesis of the dorsal pancreas (rare)
  - Incomplete development or hypoplasia of the dorsal pancreas: short pancreas and duct system (rare)
  - Complete pancreatic agenesis: (extremely rare; early neonatal death)
- Complications:
  - Endocrine insufficiency (diabetes)
  - Exocrine insufficiency (steatorrhea)

KEY FACTS: MRI (FIG. 143)

- Cross-sectional images show absence or hypoplasia of the dorsal pancreas
- Projective images show a short pancreatic duct
- *Note:* On ERCP, agenesis may be misinterpreted as a pathologic obstruction

References

Macari M, Giovanniello G, Blair L, Krinsky G (1998) Diagnosis of agenesis of the dorsal pancreas with MR pancreatography. AJR Am J Roentgenol 170 : 144 – 146

Wang JT, Lin JT, Chuang CN et al. (1990) Complete agenesis of the dorsal pancreas: a case report and review of the literature. Pancreas 5 : 493 – 497

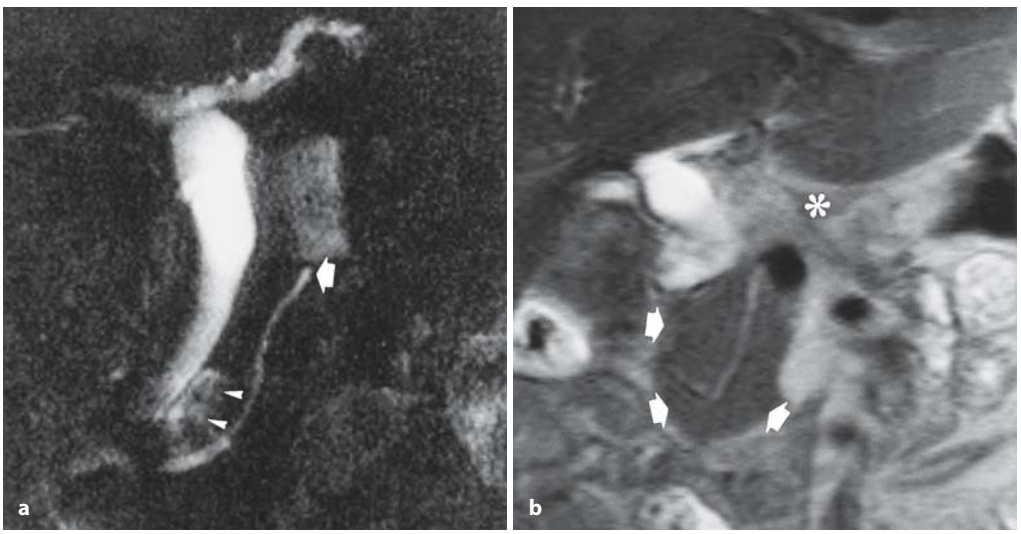

Fig. 143. a Projective image showing short pancreatic duct with abrupt termination (*arrow*). Note the incidental finding of a small duodenal diverticulum (*arrowheads* in **a**). **b** Cross-sectional image obtained in coronal plane showing normal pancreatic head (*arrows*) and absence of pancreatic body/tail (*asterisk*). (Figure courtesy of L. Storms and J. Agneessens)

#144 Developmental Abnormalities (2): Annular Pancreas

KEY FACTS: DISEASE

- Ring of normal pancreatic tissue encircles the duodenum
- Incidence: 0.05 %
- Age at presentation (bimodal peak):
  - Childhood (usually neonatal period): 50 %
  - Adulthood: 50 %
- Pathogenesis: abnormal migration of the ventral pancreas
- Location:
  - Second portion of the duodenum: 85 %
  - First portion: 15 %
- Associated with other congenital anomalies in 75 %
  - Duodenal atresia, stenosis or diaphragm
  - Down syndrome
  - Situs inversus (Fig. 144 d, e)
  - Pancreas divisum (36 %) (the annular duct drains into the ventral duct system)
- Symptoms:
  - Persistent vomiting (neonate)
  - Frequently no symptoms
- Complications (40 % – 50 %)
  - Ulcer disease
  - Pancreatitis

KEY FACTS: MRI (FIG. 144)

- Key features:
  - The pancreatic duct surrounds the duodenum
  - Apparent wall thickening of the duodenum

References

Choi JY, Kim MJ, Kim JH et al. (2004) Annular pancreas: emphasis on magnetic resonance cholangiopancreatography findings. J Comput Assist Tomogr 28 : 528 – 532

Glazer GM, Margulis AR (1979) Annular pancreas: etiology and diagnosis using ERCP. Radiology 133 : 303 – 306

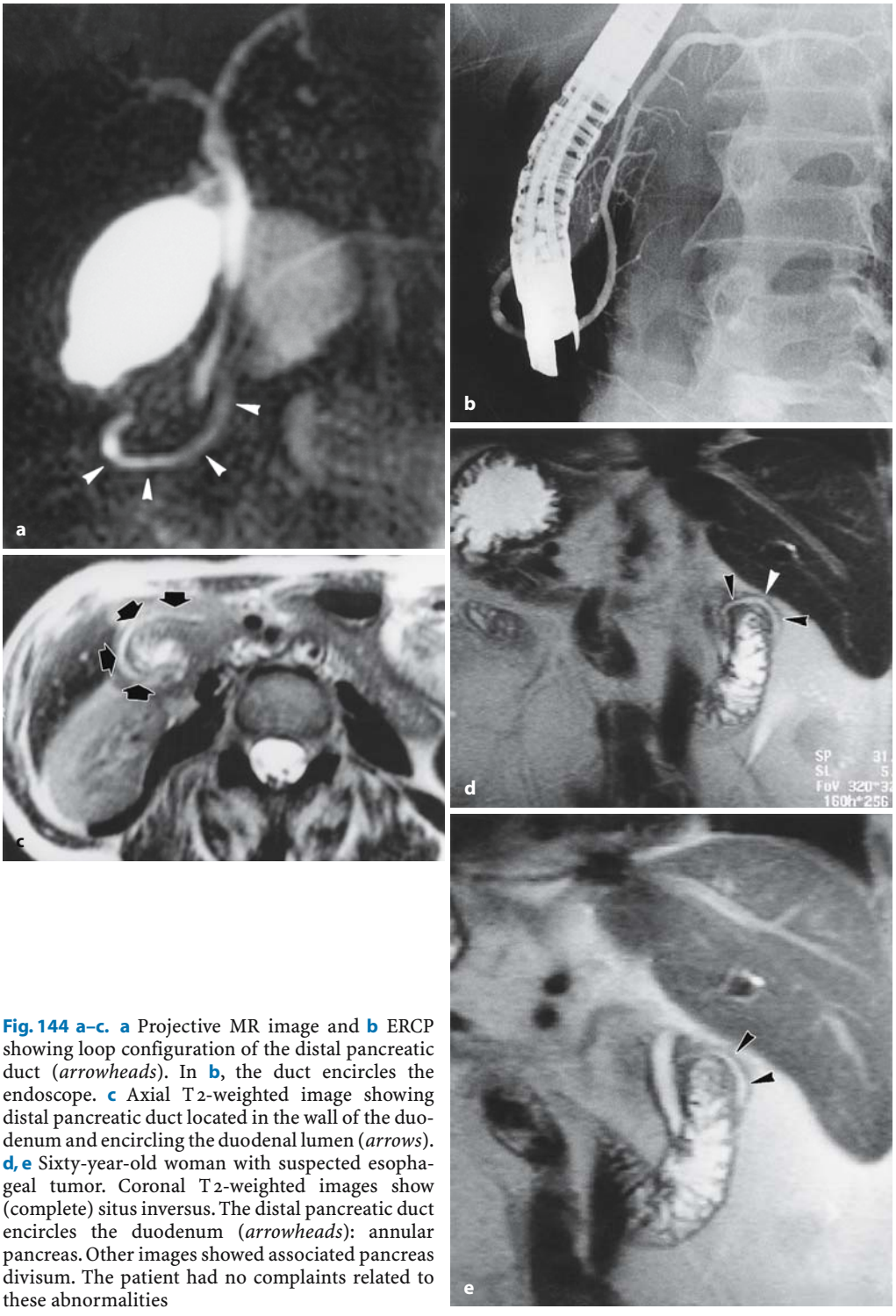

Fig. 144 a–c. **a** Projective MR image and **b** ERCP showing loop configuration of the distal pancreatic duct (*arrowheads*). In **b**, the duct encircles the endoscope. **c** Axial T2-weighted image showing distal pancreatic duct located in the wall of the duodenum and encircling the duodenal lumen (*arrows*). **d, e** Sixty-year-old woman with suspected esophageal tumor. Coronal T2-weighted images show (complete) situs inversus. The distal pancreatic duct encircles the duodenum (*arrowheads*): annular pancreas. Other images showed associated pancreas divisum. The patient had no complaints related to these abnormalities

#145 Developmental Abnormalities (3): Ectopic Pancreas

KEY FACTS: DISEASE

- Pancreatic tissue that is present outside the normal confines of the pancreas
- Incidence: 1 % – 2 % of autopsies
- Location:
  - Wall of stomach (26 % – 38 %)
  - Duodenum (28 % – 36 %)
  - Jejunum (16 %)
  - Many other sites
- Size: usually less than 2 cm
- Usually asymptomatic
- Complications:
  - Acute or chronic pancreatitis
  - Ulceration with bleeding
  - Neoplastic transformation
  - Cystic dystrophy (secondary to obstruction)

KEY FACTS: MRI

- Abnormal mass in the gastric or duodenal wall, with characteristically high signal intensity on T1-weighted images and relatively low signal intensity on T2-weighted images (Fig. 145)
- Cystic dystrophy is characterized by the presence of cystic formations surrounded by inflammation (Fékété et al. 1996)
- *Note:* In view of its small size, it is likely that ectopic pancreatic tissue is commonly overlooked on MRI

References

Fékété F, Noun R, Sauvanet A, Réjou JF, Bernades P, Belghiti J (1996) Pseudotumor developing in heterotopic pancreas. World J Surg 20 : 295 – 298

Lai EC, Tompkins RK. Heterotopic pancreas: review of a 26-year experience. Am J Surg 151 : 697 – 700

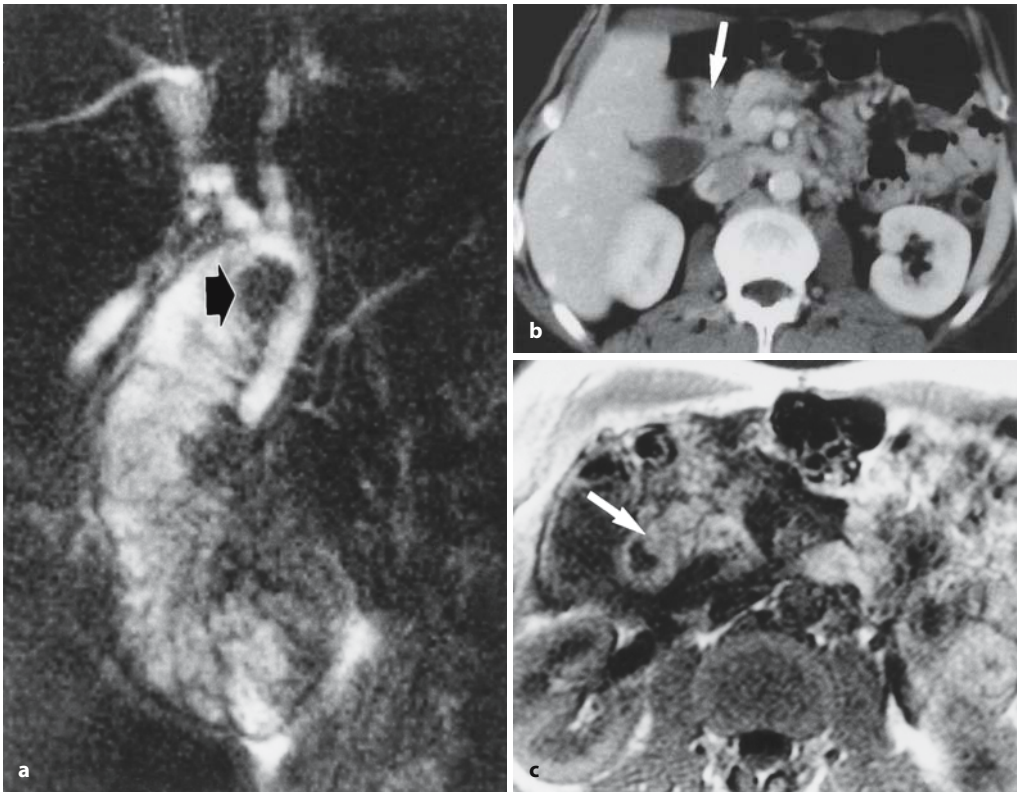

Fig. 145 a–c. **a** Projective MR image showing filling defect at medial border of the duodenum (*arrow*). Note increased signal intensity of background tissue, related to pancreatitis. **b** CT image showing a soft tissue mass at this location (*arrow*), initially interpreted as a duodenal tumor. **c** T1-weighted MR image showing this "mass" to have high signal intensity (*arrow*), similar to normal pancreatic tissue

#146 Developmental Abnormalities (4): Partial Duplication

KEY FACTS: DISEASE

- Incidence depends on type:
  - Duplication of the main duct in the body and tail: 10 %
  - Duplication of both duct and parenchyma: very rare
- Association: duplication of stomach or intestine communicating with the main pancreatic duct through an anomalous duct and pancreatic lobe (Hoffman et al. 1987)

KEY FACTS: MRI

- Ductal duplication: projective images show two parallel ducts in the pancreatic body/tail (see Fig. 168)
- Parenchymal duplication:
  - Projective images: visualization of a second duct with variable course
  - Cross-sectional images: visualization of an accessory pancreatic lobe, most commonly in close connection with the stomach
  - The aberrant duct may terminate in a cystic structure representing a gastric duplication cyst (Hoffman et al. 1987)

References

Agha FP (1987) Duplex ventral pancreas. Gastrointest Radiol 12 : 23 – 25

Hoffman M, Sugerman HJ, Heuman D, Turner MA, Kisloff B (1987) Gastric duplication cyst communicating with aberrant pancreatic duct: a rare cause of recurrent acute pancreatitis. Surgery 101 : 369 – 372

Kikuchi K, Nomiyama T, Miwa M, Harasawa S, Miwa T (1983) Bifid tail of the pancreas: a case presenting as a gastric submucosal tumor. Am J Gastroenterol 78 : 23 – 27

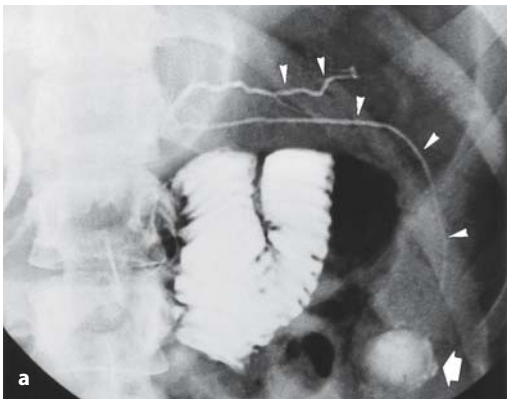

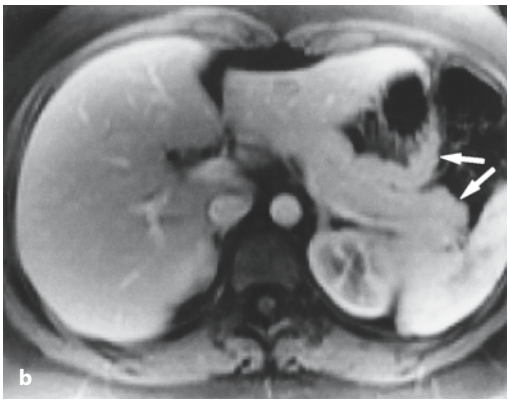

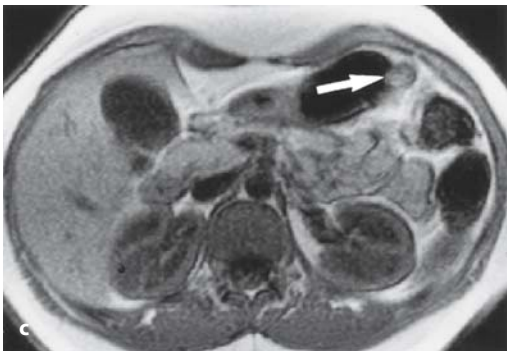

Fig. 146 a–c. **a** ERCP showing "normal" upper pancreatic duct (*arrowheads*) and second lower pancreatic duct coursing in a caudal direction (*arrowheads*) and connected with a cystic lesion (either pseudocyst or gastric duplication cyst; *arrow*). **b** Axial T1-weighted contrast-enhanced MR image showing bifurcation of the pancreatic tail (*arrows*). The ventral part of the pancreatic tail is situated in close proximity to the wall of the stomach. **c** Non-contrast-enhanced T1-weighted image obtained at a more caudal level showing the caudal end of the aberrant pancreatic tail, still in close proximity to the wall of the stomach (*arrow*)

#147 The Elderly Pancreas

KEY FACTS: GENERAL

- Common changes in elderly patients: fatty infiltration, periductal and lobular fibrosis, hyperplasia of the ductular epithelium

KEY FACTS: MRI

- The following changes may be seen:
  - Atrophy of pancreatic parenchyma
  - Decreased signal intensity on T1-weighted images (fibrosis)
  - Changes in the main pancreatic duct: discrete caliber irregularities, diffuse ectasia, strikingly straight appearance (Fig. 147)
  - Dilation of side branches
- Significance: differentiation with chronic pancreatitis may be difficult

References

Jones SN, McNeil NI, Lees WR (1989) The interpretation of retrograde pancreatography in the elderly. Clin Radiol 40 : 393 – 396

Schmitz-Moormann P, Himmelmann GW, Brandes JW et al. (1985) Comparative radiological and morphological study of the human pancreas. Pancreatitis-like changes in postmortem ductograms. Possible implications for ERCP. Gut 26 : 406 – 414

Winston CB, Mitchell DG, Outwater EK, Ehrlich SM (1995) Pancreatic signal intensity on T1-weighted fat saturation MR images: clinical correlation. J Magn Reson Imaging 5 : 267 – 271

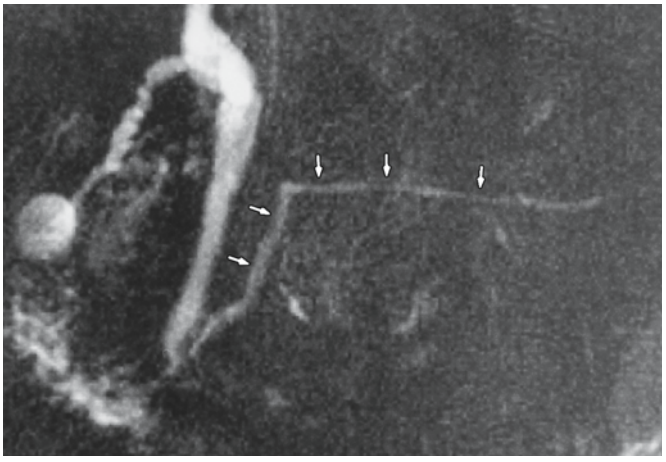

Fig. 147. Seventy-six-year old patient. Projective image showing markedly straight appearance of the pancreatic duct (*arrows*). This patient had no clinical signs that suggested the presence of pancreatic disease

#148 Postoperative Anatomy (1): After Partial Resection

Related topics: #66 (extrahepatic bile duct: anatomy after the Whipple procedure), #184 (complications of partial pancreatic resection)

KEY FACTS: TECHNIQUE

- Indications: usually tumor or conditions requiring ductal decompression (e.g., chronic pancreatitis with stricture formation and proximal ductal dilation)
- Surgical techniques:
  - Whipple procedure (see #66)
  - "Simple" resection of the pancreatic tail
  - Duval procedure: resection of the pancreatic tail with end-to-end pancreatojejunostomy
  - Puestow procedure: side-to-side pancreaticojejunostomy

KEY FACTS: MRI

- The exact appearance depends on the type of surgery performed; close correlation with the surgical report is imperative when defining the normal postoperative anatomy
- Technical requirements for a successful MRCP study: adequate distention of the anastomosed jejunal loop (recognition of valvulae conniventes)
- Differential diagnosis: collapsed bowel loops may mimic abscesses and fluid collections

References

Freed KS, Paulson EK, Frederick MG, Keogan MT, Pappas TN (1997) Abdomen after a Puestow procedure: postoperative CT appearance, complications, and potential pitfalls. Radiology 203:790–794

Rossi RL, Heiss FW, Braasch JW (1985) Surgical management of chronic pancreatitis. Surg Clin North Am 65:79–101

Taylor AJ, Bohorfoush AG (1997) Pancreatic duct – miscellaneous. In: Taylor AJ, Bohorfoush AG (eds) Interpretation of ERCP. Lippincott-Raven, Philadelphia, pp 291–303

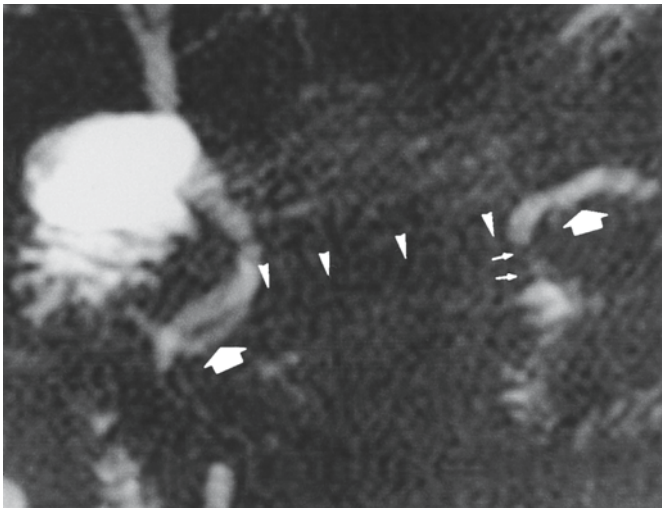

Fig. 148. Projective image obtained in a patient who underwent a partial pancreatectomy showing absence of the pancreatic duct in the body of the pancreas (*arrowheads*). Note the presence of the pancreatic duct in the pancreatic head and tail (*arrows*). The pancreatojejunal anastomosis is also visualized (*small arrows*), although the jejunal loop is suboptimally filled with fluid. Note the slightly dilated aspect of the pancreatic duct in the tail of the pancreas

#149 Postoperative Anatomy (2): After Pancreatic Transplantation

Related topics: #182, 183 (complications after pancreatic transplantation)

KEY FACTS: TECHNIQUE

- Indication: restoration of endogenous secretion of insulin in patients with severe diabetes
- Commonly performed together with renal transplantation (diabetic nephropathy)
- Procedure:
  - The graft is placed within the peritoneal cavity in the pelvis
  - Exocrine pancreatic secretions are managed by bladder drainage via an interposed duodenal segment
  - The celiac trunk and superior mesenteric artery of the donor are usually implanted with a common aortic patch on the common iliac artery

KEY FACTS: MRI

- The graft is usually seen in the right iliac fossa extending cephalad, parallel to the ascending colon
- The diameter of the graft depends on surgical factors (grafts that are stretched within the flank appear thinner) and may be temporarily increased in the immediate postoperative period (edema)
- Signal intensity is similar to pancreatic tissue in situ:
  - T 1: approximately as intense as the renal cortex
  - T 2: intermediate
- The pancreatic duct should show regular contours and gradual tapering towards the tail

References

Gore RM, Levine MS, Laufer I (eds) (1994) Textbook of gastrointestinal radiology. Saunders, Philadelphia, p 2204

Kelcz F, Sollinger HW, Pirsch JD (1991) MRI of the pancreas transplant: lack of correlation between imaging and clinical status. Magn Reson Med 21 : 30 – 38

Pozniak MA, Propeck PA, Kelcz F, Sollinger H (1995) Imaging of pancreas transplants. Rad Clin North Am 33 : 581 – 594

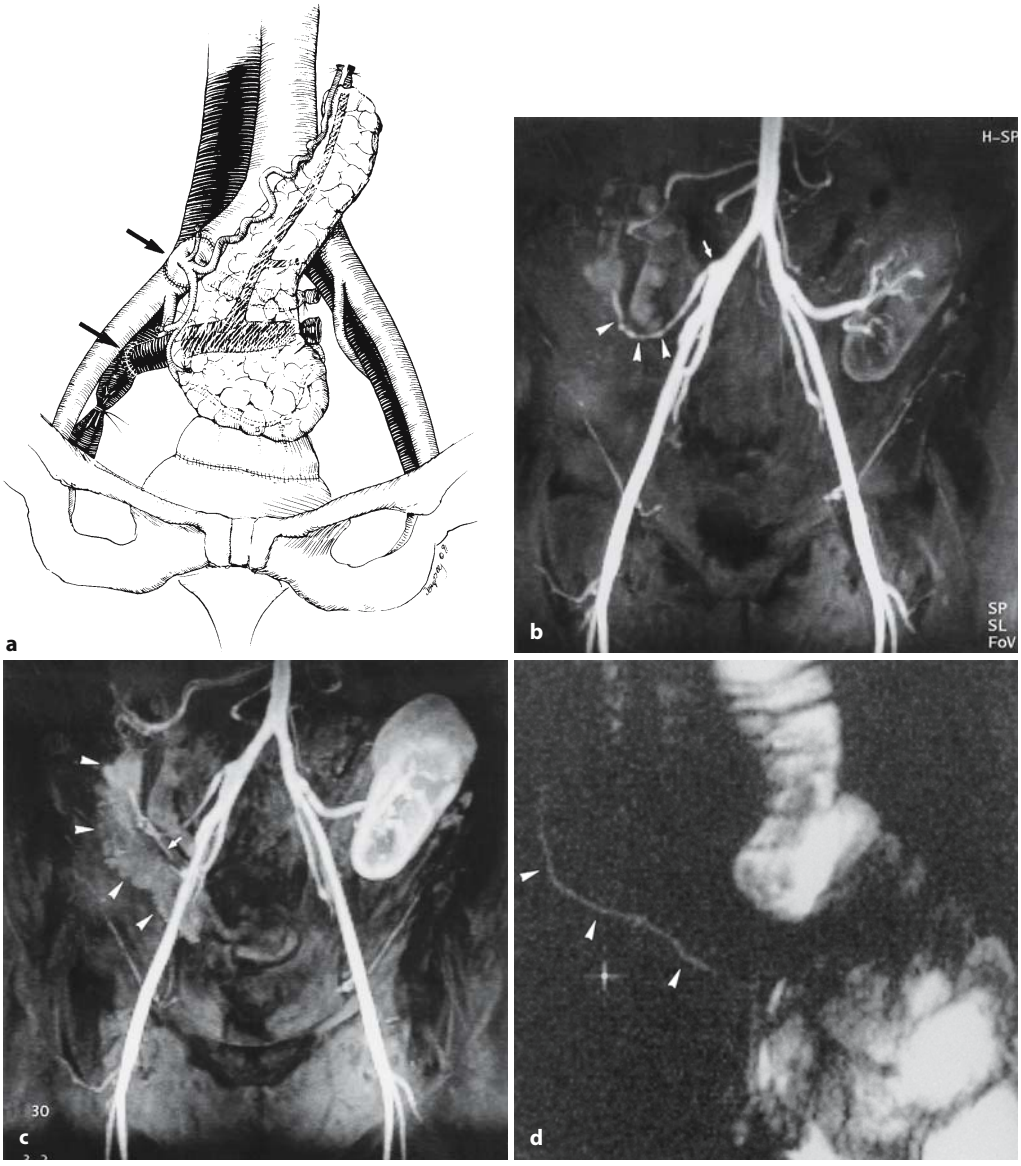

Fig. 149. **a** Pancreatic transplant anatomy. A duodenocystostomy is used for exocrine drainage. An aortic patch and the portal vein are used for anastomoses with the iliac vessels (*arrows*). (Reprinted with permission from Gore et al. 1994). **b–d** Normal vascular and ductal anatomy. In this patient, the transplant pancreas is situated in the right iliac fossa. **b** Contrast-enhanced MR angiogram obtained in the "early" arterial phase showing aorta, iliac arteries, aortic patch (*arrow*), and splenic artery (*arrowheads*). Note initial cortical enhancement of the renal transplant in the left fossa. The pancreas is invisible. **c** Contrast-enhanced MR angiogram obtained in the "late" arterial phase showing homogeneous enhancement of the pancreatic parenchyma (*arrowheads*) and discrete opacification of the splenic vein (*arrow*). **d** Projective image showing pancreatic duct of normal size (*arrowheads*)

6.2 Benign Nontraumatic Abnormalities

#150 Santorinicele and Wirsungocele

Related topic: #140 (pancreas divisum)

KEY FACTS: DISEASE

- Focal dilation at the termination of the dorsal or ventral duct
- Similar to choledochocele (see #126) and ureterocele
- Most common in elderly patients
- Etiology: probably a combination of outflow obstruction (small accessory orifice) and weakness of the distal duct wall, either congenital or acquired
- Commonly, but not necessarily, associated with pancreas divisum (see also #140 and Fig. 137)
- May be the underlying disorder in patients with recurrent attacks of acute pancreatitis
- Symptoms may improve after accessory sphincterotomy

KEY FACTS: MRI

- Santorinicele (Fig. 150 a, b):
  - Pancreas divisum (see #140)
  - Focal dilation at the termination of the accessory duct
- Wirsungocele (Fig. 150 c, d):
  - Focal dilation of the termination of the duct of Wirsung

References

Manfredi R, Costamagna G, Brizi MG et al. (2000) Pancreas divisum and "santorinicele": diagnosis with dynamic MR cholangiopancreatography with secretin stimulation. Radiology 217 : 403–408

Eisen G, Schutz S, Metzler D, Baillie J, Cotton B (1994) Santorinicele: new evidence for obstruction in pancreas divisum. Gastrointest Endoscop 40 : 73–76

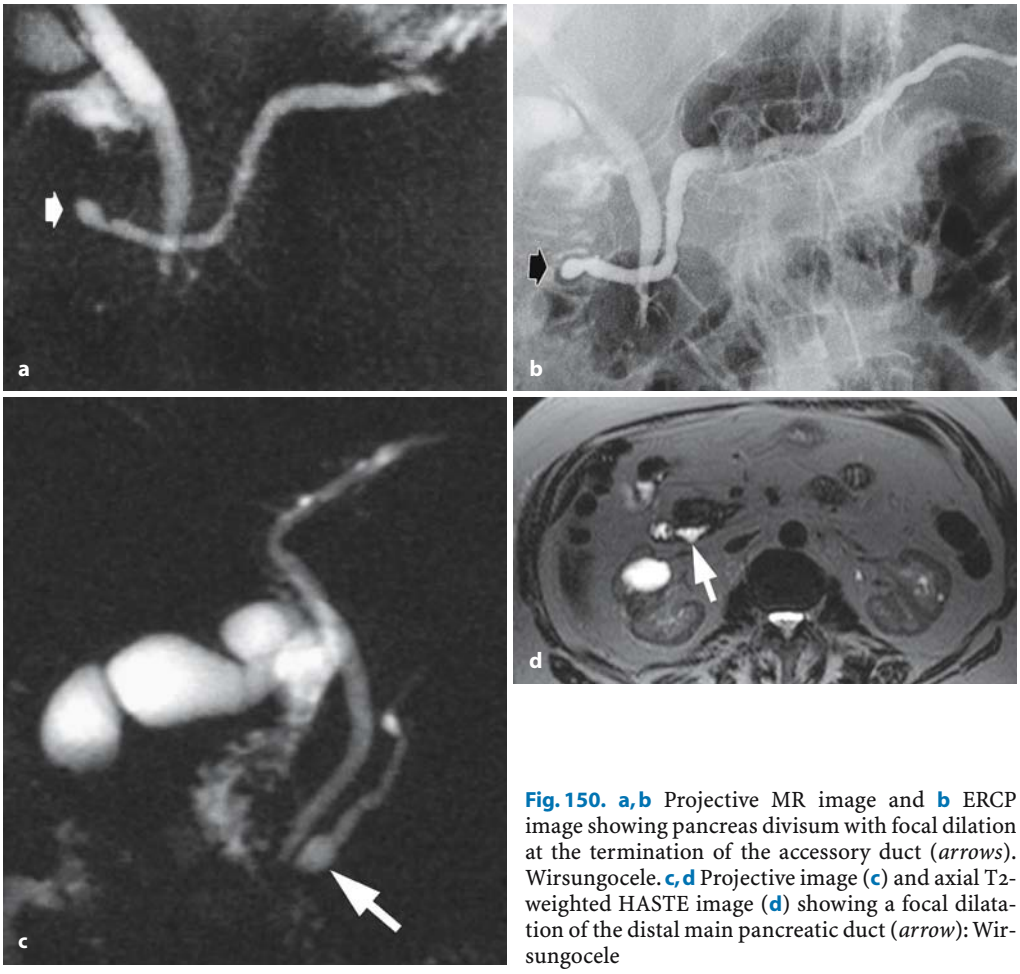

Fig. 150. a, b Projective MR image and **b** ERCP image showing pancreas divisum with focal dilation at the termination of the accessory duct (*arrows*). Wirsungocele. **c, d** Projective image (**c**) and axial T2-weighted HASTE image (**d**) showing a focal dilatation of the distal main pancreatic duct (*arrow*): Wirsungocele

#151 Acute Pancreatitis, General

KEY FACTS: DISEASE

- Acute inflammatory disease of the pancreas producing temporary changes with restoration of normal anatomy and function
- Causes:
  - Biliary disease (± 60 %)
  - Alcoholism (± 30 %)
  - Other causes (e.g., hypercalcemia, hypertriglyceridemia, drugs)
- Clinical prognostic scores: Ranson score, Imrie score, Acute Physiology and Chronic Health Evaluation (APACHE) score
- Imaging classification (Balthazar 1994; Balthazar et al. 1985):
  - Grades A, B: edematous pancreatitis (see # 152)
  - Grade C: acute pancreatitis with associated peripancreatic inflammation (see # 153)
  - Grades D, E: acute pancreatitis with ill-defined fluid collection/phlegmon (see # 154)
- This grading system was developed for CT (Balthazar 1994) and constitutes the basis for calculation of the severity index (see # 155)
- Associations/predisposing factors:
  - Small gallstones (common)
  - Wide cystic duct
  - Common channel between the common bile duct and pancreatic duct
  - Cholesterolosis of gallbladder
- Symptoms: upper abdominal pain, nausea, vomiting (often non-specific)
- Typically elevated amylase and lipase levels (sensitivity, 80 % – 90 %)
- Complications (mainly occur in patients with stage D or E disease):
  - Necrosis (see # 155)
  - Pseudocyst (10 %) (with or without infection; see # 156)
  - Hemorrhage (3 %)
  - Venous thrombosis (see # 157)
  - Pseudoaneurysm (see # 157)
  - Biliary obstruction (see # 77)
  - Abscess (2 % – 20 %)
  - Ascites
- *Note:* It has been stated that ERCP with sphincterotomy may be indicated in all patients with severe (biliary) pancreatitis; it is unclear whether MRCP might be useful in selecting candidates for sphincterotomy

References

Balthazar EJ (1994) Pancreatitis. In: Gore RM, Levine MS, Laufer I (eds) Textbook of gastrointestinal radiology. Saunders, Philadelphia, pp 2132 – 2160

Balthazar EJ, Ranson JHC, Naidich JP, Megibow AJ, Caccavale R, Cooper MM (1985) Acute pancreatitis: prognostic value of CT. Radiology 156 : 767 – 772

Chalmers AG (1997) The role of imaging in acute pancreatitis. Eur J Gastroenterol Hepatol 9 : 106 – 116

Curran FT, Neoptolemos JP (1995) Acute biliary pancreatitis. Ann Ital Chir 66 : 197 – 202

#152 Edematous Pancreatitis (Grades A and B)

KEY FACTS: DISEASE

- Classification:
  - Grade A: no macroscopic changes
  - Grade B: disease confined to the pancreas
- Prognosis: most patients have a mild and uncomplicated clinical course

KEY FACTS: MRI

- Cross-sectional images (Fig. 152):
  - Grade A: pancreas appears normal
  - Grade B: focal or diffuse enlargement; contour irregularities; increased signal intensity on T2-weighted images (focal or diffuse); normal aspect of peripancreatic fat; small intrapancreatic fluid collections may be seen together with hypoenhancing areas
- Projective images:
  - Usually normal
  - Pancreatic duct may be diffusely involved with stretching
  - Conversely, it may show mild ectasia
  - Occasionally, subtle intraluminal filling defects are seen

References

Amano Y, Oishi T, Takahashi M et al. (2001) Non-enhanced magnetic resonance imaging of mild acute pancreatitis. Abdom Imaging 26 : 59 – 63

Gryspeerdt S, Van Hoe L, Baert AL (1998) MRI of pancreatitis. In: Heuck A, Reiser M (eds) Magnetic resonance imaging of the abdomen and pelvis. Springer, Berlin Heidelberg New York, pp 91 – 108

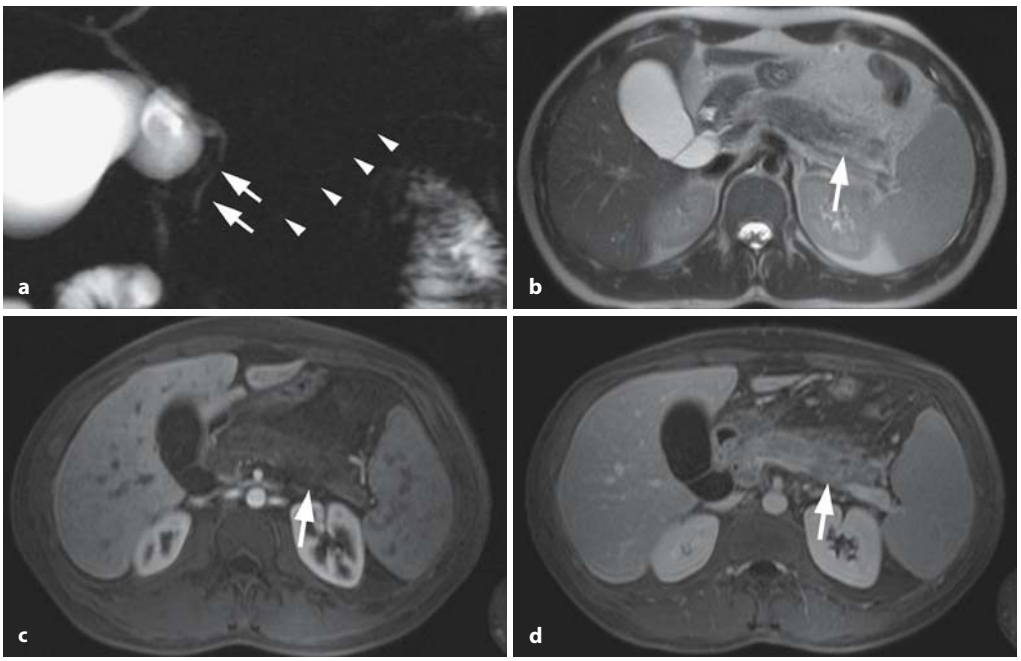

Fig. 152 a–d. Same patient as in Fig. 77 b,c with acute pancreatitis. **a** Projective image showing discrete narrowing of the distal common bile duct (*arrow*) and apparent partial absence of the main pancreatic duct due to pancreatic edema (*arrowheads*). **b** Axial T2-weighted HASTE image (TE 60) showing increased signal of the pancreatic tissue, particularly in the tail (*arrow*). **c, d** Axial contrast-enhanced T1-weighted VIBE images obtained in the arterial (**c**) and venous (**d**) phase showing marked absence of pancreatic enhancement in the arterial phase, with delayed enhancement in the venous phase (*arrows*). This is secondary to acute pancreatitis and pancreatic edema

#153 Acute Pancreatitis with Peripancreatic Inflammation (Grade C)

KEY FACTS: DISEASE

- Incidence: 40 % – 50 % of patients with acute pancreatitis
- Mechanism: because the pancreas does not have a well-developed capsula, secretions are commonly discharged into the retroperitoneum

KEY FACTS: MRI

- Cross-sectional images: identical to grade B, plus peripancreatic fluid/edema (best appreciated on heavily T2-weighted MR images; Fig. 153)
- Projective images:
  - Ductal changes: identical to grade B
  - Not uncommonly, the pancreatic duct is obscured by overlying fluid
- *Note:* The presence of peripancreatic fluid may be the first and/or only sign of acute pancreatitis on MRI

!

References

Gryspeerdt S, Van Hoe L, Baert AL (1998) MRI of pancreatitis. In: Heuck A, Reiser M (eds) Magnetic resonance imaging of the abdomen and pelvis. Springer, Berlin Heidelberg New York, pp 91 – 108

Saïfuddin A, Ward J, Ridgway J, Chalmers AG (1993) Comparison of MR and CT scanning in severe acute pancreatitis: initial experience. Clin Radiol 48 : 111 – 116

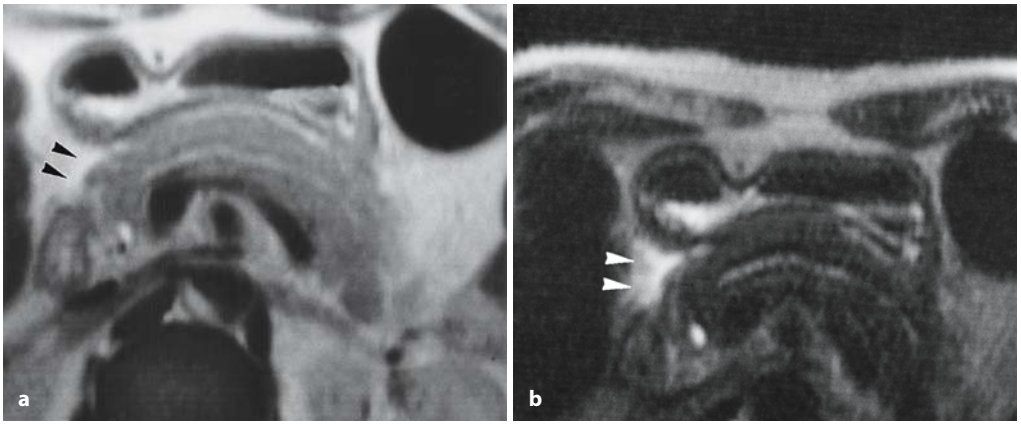

Fig. 153. **a** Moderately and **b** heavily T2-weighted MR images showing hyperintense aspect of fat adjacent to the pancreatic head (*arrowheads*): peripancreatic inflammation

#154 Acute Pancreatitis with Ill-Defined Fluid Collection/Phlegmon (Grades D and E)

KEY FACTS: DISEASE

- Definition of phlegmon: solid mass characterized by edema, infiltration of inflammatory cells, and necrosis
- Incidence: up to 50% of patients with acute pancreatitis
- Classification:
  - Grade D: small and usually single, ill-defined fluid collection or phlegmon
  - Grade E: two or more large phlegmonous collections with or without the presence of gas
- Spread: primarily in anterior pararenal and interfascial spaces
- Evolution: commonly associated with abscess formation and necrosis; mortality rate between 4% and 40%

KEY FACTS: MRI

- Typical appearance of fluid collections (Fig. 154 a–d):
  - Pure water (remains visible on T2-weighted images with very long TE)
  - Typically located around the pancreas and in the anterior pararenal space. Other locations include the lesser sac, posterior pararenal space, mesocolon, mesenterium, psoas compartment, mediastinum, pleura, pericardium
- Typical appearance of phlegmon (Fig. 154 b–d):
  - Ill-defined structure with heterogeneous content
  - Signal intensity on T2: mixed, usually with both hyperintense and hypointense portions (e.g., necrotic debris, blood)
- *Note:* MRI appears to be more accurate than CT for differentiating between pure fluid collections and phlegmons (these may exhibit fluid density on CT). Therefore, predrainage MRI should be performed in patients with subacute pancreatic collections to avoid attempts to drain "collections" actually representing necrotic debris (Morgan et al. 1997; Fig. 154)

References

Balthazar EJ (1994) Pancreatitis. In: Gore RM, Levine MS, Laufer I (eds) Textbook of gastrointestinal radiology. Saunders, Philadelphia, pp 2132–2160

Balthazar EJ, Ranson JHC, Naidich JP, Megibow AJ, Caccavale R, Cooper MM (1985) Acute pancreatitis: prognostic value of CT. Radiology 156: 767–772

Morgan DE, Baron TH, Smith JK, Robbin ML, Kenney PJ (1997) Pancreatic fluid collections prior to intervention: evaluation with MR imaging compared with CT and US. Radiology 203: 773–778

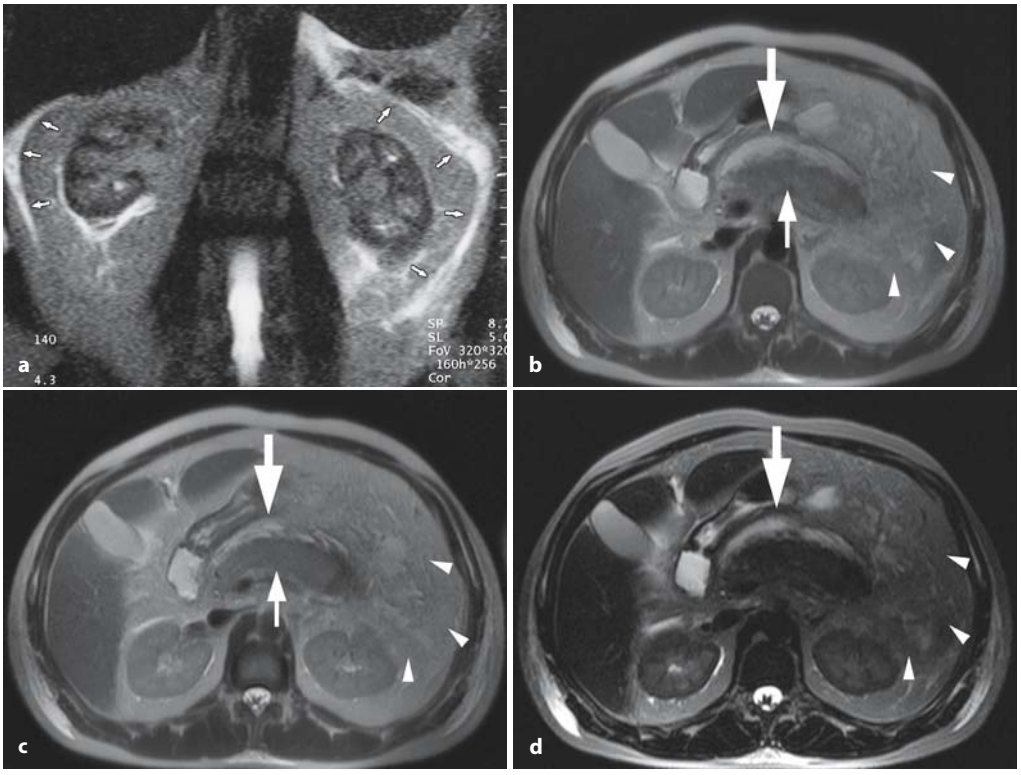

Fig. 154. a Heavily T2-weighted image showing classical spread of pancreatic fluid collections into the left and right interfascial space (*arrows*). **b–d** Axial T2-weighted HASTE images with short TE (TE 60) (**b, c**) and long TE (TE 360) (**d**) showing an enlarged slightly hyperintense heterogeneous pancreas (*small arrow*), with peripancreatic exudate/phlegmon (*arrowheads*), and a fluid collection anterior to the pancreas (*large arrow*)

#155 Complications of Acute Pancreatitis (1): Necrosis

KEY FACTS: DISEASE

- Classification:
  - A: less than 30 % of pancreatic parenchyma
  - B: 30 % – 50 %
  - C: more than 50 %
- Detection of necrosis has important prognostic implications (Ranson et al. 1985):
  - No necrosis: almost no mortality
  - Necrosis: up to 23 % mortality
- The extent of necrosis also appears to be important:
  - Less than 30 % of pancreatic parenchyma: no mortality
  - More than 50 %: 11 % – 25 % mortality
- The *severity index* is calculated by adding together a morphologic score reflecting the grade of disease (Sg) (see # 151) and a score reflecting the degree of necrosis (Sn) (Balthazar et al. 1990; Table 155)
- Mortality as a function of the severity index:
  - Severity index 0 – 3: 3 %
  - Severity index 4 – 6: 6 %
  - Severity index 7 – 10: 17 %
- If necrotic tissue becomes infected, the mortality rate rises to about 60%

KEY FACTS: MRI

- Typical features:
  - Signal intensity: necrosis has no specific features on non-contrast-enhanced scans
  - Contrast-enhanced scans: focal or diffuse absence of enhancement (Fig. 155)
  - Projective images: focal interruption of the pancreatic duct
- *Note:* Rapid injection of intravenous contrast media and adequate bolus timing are imperative for accurate detection of necrosis by MRI (Piironen et al. 1997)
- *Note:* Necrosis may develop a few days after the onset of acute pancreatitis and therefore may not be detected on the initial contrast-enhanced study

References

Balthazar EJ, Robinson DL, Megibow AJ, Ranson JH (1990) Acute pancreatitis: value of CT in establishing prognosis. Radiology 174 : 331 – 336

Miller FH, Keppke AL, Dalal K et al. (2004) MRI of pancreatitis and its complications: part 1, acute pancreatitis. AJR Am J Roentgenol 183 : 1637 – 1644

Piironen A, Kivisaari R, Pitkäranta P et al (1997) Contrast-enhanced MRI for the detection of acute hemorrhagic necrotizing pancreatitis. Eur Radiol 7 : 17 – 20

Ranson JHC, Balthazar E, Caccavale R, Cooper M (1985) Computed tomography and the prediction of abscess in acute pancreatitis. Ann Surg 201 : 656 – 665

Table 155.1a. Grade of disease (Sg)

Grade	Score (Sg)
A	0
B	1
C	2
D	3
E	4

Table 155.1b. Degree of necrosis (Sn)

Necrosis (%)	Score (Sn)
< 30	2
30 – 50	4
> 50	6

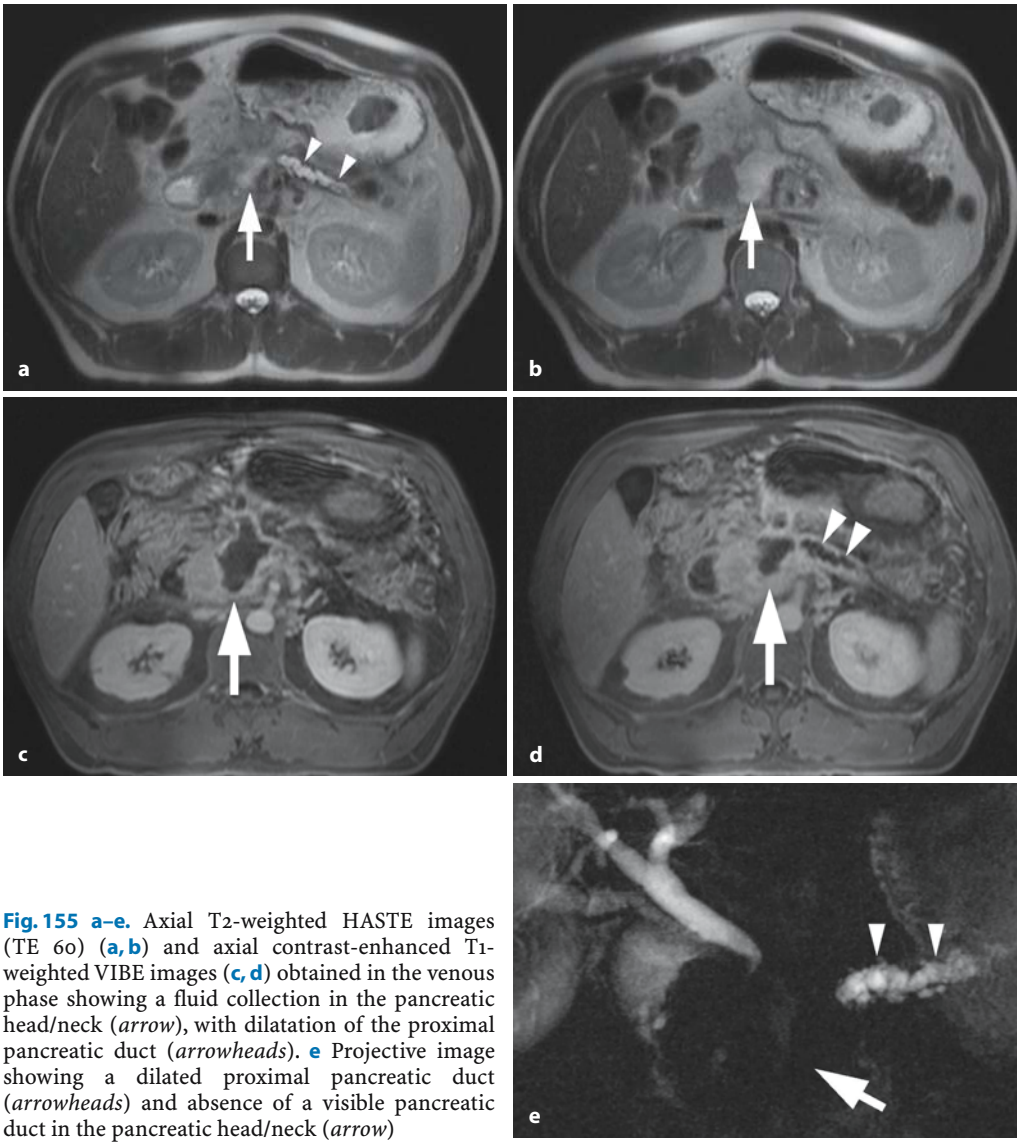

Fig. 155 a–e. Axial T2-weighted HASTE images (TE 60) (**a, b**) and axial contrast-enhanced T1-weighted VIBE images (**c, d**) obtained in the venous phase showing a fluid collection in the pancreatic head/neck (*arrow*), with dilatation of the proximal pancreatic duct (*arrowheads*). **e** Projective image showing a dilated proximal pancreatic duct (*arrowheads*) and absence of a visible pancreatic duct in the pancreatic head/neck (*arrow*)

#156 Complications of Acute Pancreatitis (2): Pseudocyst

Related topic: #165 (pseudocyst in chronic pancreatitis)

KEY FACTS: DISEASE

- Collection of pancreatic fluid encapsulated by fibrous tissue (no true epithelial lining)
- The transition from fluid collection (without fibrous "wall") to pseudocyst takes 4–6 weeks
- Incidence:
  - 90% of all cystic pancreatic masses
  - 2%–4% after initial attack of acute pancreatitis
  - 12% after several episodes of alcoholic pancreatitis
  - 10%–15% in chronic pancreatitis
- Other causes:
  - Obstructive tumor
  - Trauma
- Location:
  - Most commonly in the anterior pararenal space and omental bursa
  - Anywhere from the peripancreatic area to the pleura, groin, etc.
- Symptoms: persistent pain in a patient who is not seriously ill is typical
- Complications:
  - Rupture/fistula formation (e.g., into abdominal cavity, stomach)
  - Hemorrhage (with or without pseudoaneurysm)
  - Infection
- Treatment:
  - Surgery
  - Percutaneous drainage
  - Endoscopic drainage (cystogastrostomy or cystoduodenostomy)

KEY FACTS: MRI

- Typical features (Fig. 156):
  - Unilocular in 94%
  - Usually has the same intensity as water
  - May contain internal material (e.g., blood clot, cellular debris)
  - May have variable/mixed signal intensity if hemorrhagic
- Presence of air within a pseudocyst (hypointense on all sequences, sometimes with air–fluid level) suggests one of the following:
  - Infection (usually anaerobe bacteria)
  - Previous percutaneous, endoscopic, or surgical intervention
  - Fistula with gastrointestinal tract
- *Note:* MRI is less accurate than ERCP in demonstrating duct-pseudocyst communication

References

Ahearne PM, Baillie JM, Cotton PB, Baker ME, Meyers WC, Pappas TN (1992) An endoscopic retrograde cholangiopancreatography (ERCP)-based algorithm for the management of pancreatic pseudocysts. Am J Surg 163:111–115

Miller FH, Keppke AL, Dalal K et al. (2004) MRI of pancreatitis and its complications: part 1, acute pancreatitis. AJR Am J Roentgenol 183:1637–1644

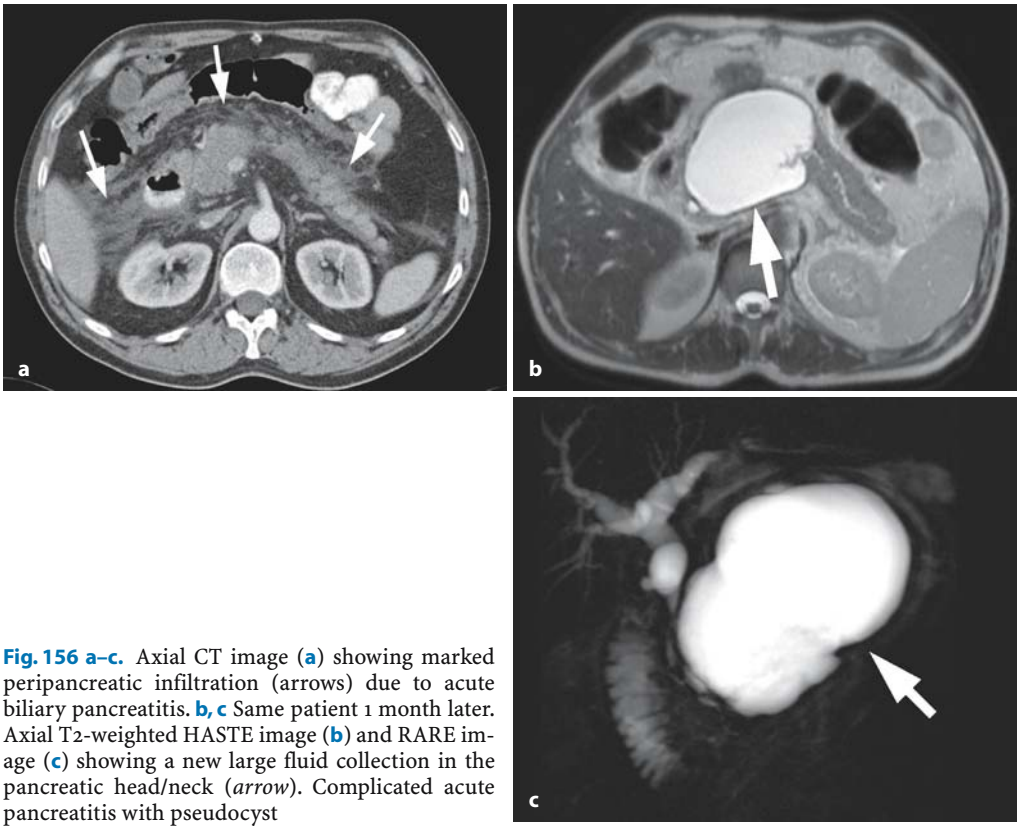

Fig. 156 a–c. Axial CT image (**a**) showing marked peripancreatic infiltration (arrows) due to acute biliary pancreatitis. **b, c** Same patient 1 month later. Axial T2-weighted HASTE image (**b**) and RARE image (**c**) showing a new large fluid collection in the pancreatic head/neck (*arrow*). Complicated acute pancreatitis with pseudocyst

#157 Complications of Acute Pancreatitis (3): Vascular Complications

Related topic: # 166 (vascular complications of chronic pancreatitis)

KEY FACTS: DISEASE

Arterial Complications: Pseudoaneurysm

- Up to 10 % of severe cases of acute pancreatitis
- Mechanism: pancreatic or peripancreatic blood vessel erosion (autodigestion of arterial walls by enzymes liberated in pancreatitis)
- May occur within 2 – 3 weeks to several years after an acute episode of pancreatitis
- Location:
  - Splenic and gastroduodenal arteries most commonly involved
  - May develop within a preexisting pseudocyst
- Complications: rupture with free hemorrhage in the duodenum, bile duct, lesser sac, peritoneal cavity, pancreatic duct, portal vein, etc.
- Treatment: usually therapeutic angiographic embolization (Mandel et al. 1987)

Venous Complications: Venous Thrombosis

- Incidence : up to 45 % of patients with acute pancreatitis
- Commonly involves the mesenteric–splenic confluence and may extend into the main portal vein
- Complication: varices of the gastric fundus
- Treatment for bleeding gastric varices: splenectomy

KEY FACTS: MRI

Pseudoaneurysm (Fig. 157)

- Typical features:
  - Signal intensity: variable, depends on type of sequence and flow velocity (the typical flow void may be absent in pseudoaneurysms with a small connection to the feeding artery)
  - Key finding on contrast-enhanced MRA: enhancement in the arterial phase
- *Note:* Fast injection of contrast media and accurate bolus timing are mandatory (Gaa et al. 1997)

Venous Thrombosis

- Typical features:
  - Absence of flow void
  - No enhancement
  - Presence of venous collaterals

References

Gaa J, Laub G, Georgi M (1997) Breath-hold three-dimensional gadolinium-enhanced dual-phase MR angiography in the abdomen: first clinical results. In: Oudkerk M, Edelman R (eds) High-power gradient MR-imaging. Blackwell Science, Berlin, pp 334 – 339

Mandel SR, Jaques PF, Sanofsky S, Mauro MA (1987) Non operative management of peripancreatic arterial aneurysms. A 10 years experience. Ann Surg 205 : 126 – 128

Vujic I (1989) Vascular complications of pancreatitis. Radiol Clin North Am 27 : 81 – 91

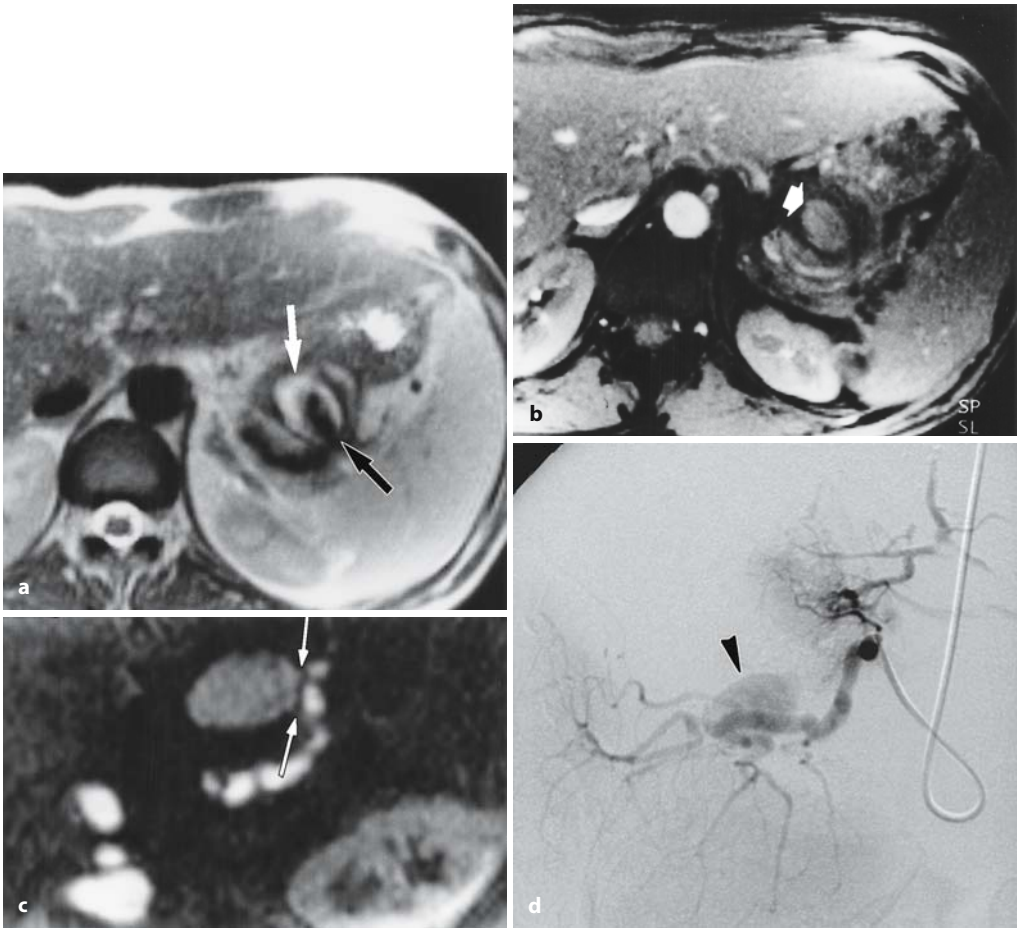

Fig. 157 a–d. Patient with chronic pancreatitis. **a** T2-weighted image showing pseudoaneurysm in close connection with the pancreatic tail (*arrows*). The hypointense signal in the center of the lesion is probably caused by flow-related signal void. **b** Time-of-flight (TOF) image confirming the presence of flow in the center of the lesion (*arrow*). **c** Contrast-enhanced image showing a connection with the splenic artery (*arrows*). **d** Catheter angiogram confirming the presence of a pseudoaneurysm (*arrowhead*)

#158 Recurrent (Relapsing) Pancreatitis

KEY FACTS: DISEASE

- Two or more episodes of acute pancreatitis
- Causes/associated disease (found in up to 80 % of patients):
  - Segmental stenosis of the pancreatic duct
  - Papillary obstruction/dysfunction (see # 127, 128)
  - Common bile duct calculi (see # 72), biliary sludge
  - Pancreas divisum (see # 140)
  - Anomalous union of pancreatobiliary duct system (see # 123)
  - Duodenal duplication cyst

KEY FACTS: MRI

- Signs of acute pancreatitis may be seen
- Signs of underlying disease (see respective entities)
- *Note:* The role of MRI is not to confirm the diagnosis of pancreatitis, but to detect (or rule out) underlying abnormalities

References

Asbun HJ, Rossi RL, Heiss FW, Shea JA (1993) Acute relapsing pancreatitis as a complication of papillary stenosis after sphincterotomy. Gastroenterology 104 : 1814 – 1817

Mori K, Nagakawa T, Ohta T et al. (1991) Acute pancreatitis associated with anomalous union of the pancreaticobiliary ductal system. J Clin Gastroenterol 13 : 673 – 677

Venu RP, Geenen JE, Hogan WJ, Stone J, Johnson GK, Soergel K (1989) Idiopathic recurrent pancreatitis. An approach to diagnosis and treatment. Dig Dis Sci 34 : 1943 – 1945

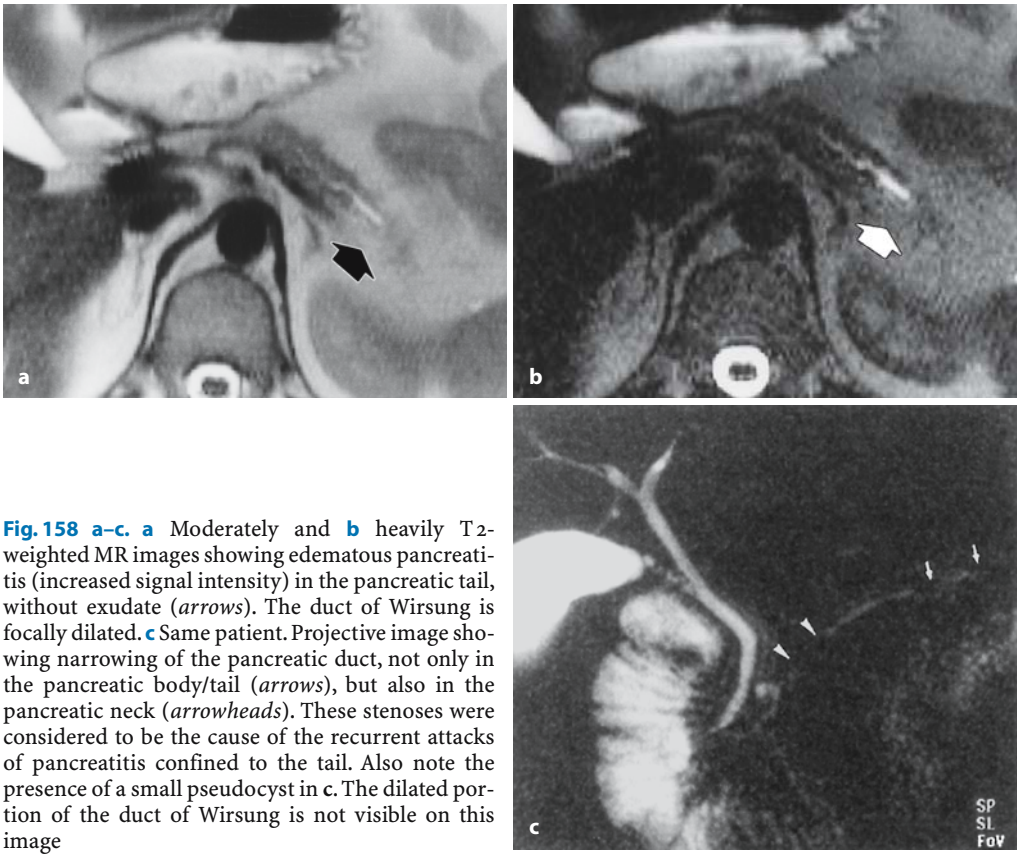

Fig. 158 a–c. **a** Moderately and **b** heavily T2-weighted MR images showing edematous pancreatitis (increased signal intensity) in the pancreatic tail, without exudate (*arrows*). The duct of Wirsung is focally dilated. **c** Same patient. Projective image showing narrowing of the pancreatic duct, not only in the pancreatic body/tail (*arrows*), but also in the pancreatic neck (*arrowheads*). These stenoses were considered to be the cause of the recurrent attacks of pancreatitis confined to the tail. Also note the presence of a small pseudocyst in **c**. The dilated portion of the duct of Wirsung is not visible on this image

#159 Chronic Pancreatitis, General

KEY FACTS: DISEASE

- Continuing inflammatory disease characterized by irreversible damage to pancreatic anatomy and function
- Types:
  - Chronic calcifying pancreatitis (most common)
  - Chronic obstructive pancreatitis (see # 168)
  - Nonalcoholic duct-destructive pancreatitis (see # 169)
  - Hereditary pancreatitis (see # 170)
  - Idiopathic
- Causes:
  - Alcoholism (75 %)
  - Others: e. g., hyperlipidemia, hyperparathyroidism, trauma
- Pathophysiology (main mechanism): intraductal precipitation of (calcified) concretions, with secondary obstruction, scar formation, etc.
- Pathophysiology (possible underlying mechanisms):
  - Alcohol-induced pancreatic secretion of protein
  - Formation of a mucosubstance
- Symptoms: epigastric pain, weight loss, steatorhea (80 %), diabetes (58 %)
- Differential diagnosis with malignant tumor of the pancreas:
  - Clinically, the differentiation between chronic pancreatitis and malignancy is often difficult
  - The two diseases may coexist
- Complications:
  - Pseudocyst (see # 165)
  - Vascular (see # 166)
  - Fistula (see # 166)
  - Biliary (see # 78)
- *Note:* In accordance with most textbooks and papers, the discussion on the pages that follow will refer to "chronic pancreatitis" as a single disease. However, the reader should be aware of the fact that chronic obstructive pancreatitis and nonalcoholic duct-destructive pancreatitis have quite characteristic imaging features that are clearly different from those seen in "classical" chronic pancreatitis. For a discussion of these entities, the reader is referred to # 168 and # 169

#160 Chronic Pancreatitis, Signal Intensity Changes and Enhancement Pattern

KEY FACTS: MRI

- Histology: normal pancreatic parenchyma is partially replaced by fibrotic tissue that contains no aqueous protein (no acini) and is less well vascularized
- Typical MR features (more commonly diffuse than focal; Fig. 160):
  - Loss of the normal high signal intensity on T1-weighted images
  - Decreased enhancement on dynamic contrast-enhanced sequences
- Differential diagnosis: the abnormalities described above are not specific and can be seen in:
  - Pancreatic cancer (with or without retro-obstructive pancreatitis; clues for differentiation: see # 167)
  - Acute pancreatitis
- *Note:* Punctate calcifications are the hallmark of chronic alcoholic pancreatitis. They are commonly invisible on MRI. Therefore, performing CT is always a good option when MRI findings suggest chronic pancreatitis, without being diagnostic

References

Semelka RC, Ascher SM (1993) MR imaging of the pancreas. Radiology 188 : 593 – 602

Sittek H, Heuck AF, Folsing C, Gieseke J, Reiser M (1995) Static and dynamic MR tomography of the pancreas: contrast media kinetics of the normal pancreatic parenchyma in pancreatic carcinoma and chronic pancreatitis. ROFO 162 : 396 – 403

Winston CB, Mitchell DG, Outwater EK, Ehrlich SM (1995) Pancreatic signal intensity on T1-weighted fat saturation MR images: clinical correlation. J Magn Reson Imaging 5 : 267 – 271

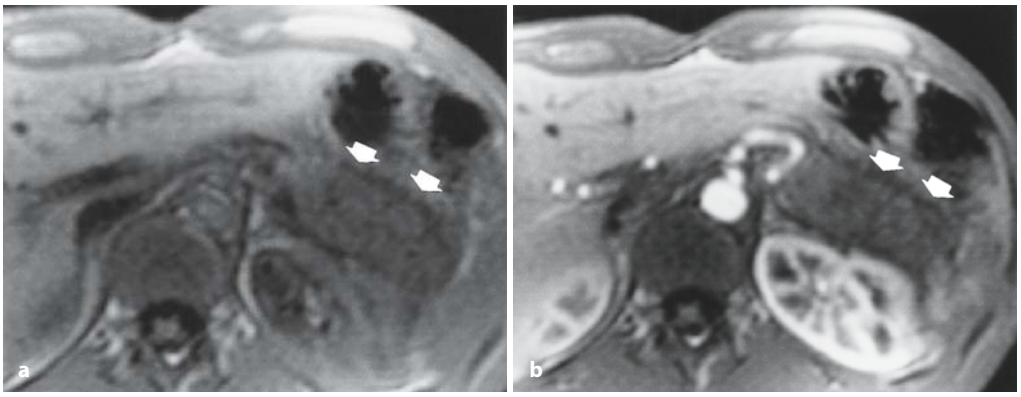

Fig. 160. **a** Non-contrast-enhanced T1-weighted MR image and **b** image obtained in the pancreatic phase of perfusion showing hypointense, hypoenhancing pancreas (*arrows*)

#161 Chronic Pancreatitis, Ductal Changes (1): ERCP Classification

KEY FACTS

- Basic elements of chronic pancreatitis: (a) changes in the main pancreatic duct, (b) changes in side branches, and (c) intraductal concretions
- ERCP classification (Cambridge classification; Axon 1989):
  - Mild CP: at least three abnormal side branches
  - Moderate CP: addition of main pancreatic duct changes
  - Marked CP: addition of one or more of the following: severe dilation (> 1 cm); marked mural irregularity; obstruction; opacification of large cavity (> 1 cm); intraductal filling defects
- Progressive changes in the main pancreatic duct: see Fig. 161 a
- Progressive changes in side branches: see Fig. 161 b

References

Axon AT (198) Endoscopic retrograde cholangiopancreatography in chronic pancreatitis. Cambridge classification. Radiol Clin North Am 27 : 39 – 50

Chari ST, Singer MV (1994) The problem of classification and staging of chronic pancreatitis. Proposals based on current knowledge of its natural history. Scand J Gastroenterol 29 : 949 – 960

Ponette E, Brys P, Van Steenbergen W (1994) Chronic pancreatitis: endoscopic retrograde cholangiopancreatography. In: Baert AL (ed) Radiology of the pancreas. Springer, Berlin Heidelberg New York, pp 106 – 115

Taylor AJ, Bohorfoush AG (1997) Pancreatic duct in inflammation of the pancreas. In: Taylor AJ, Bohorfoush AG (eds) Interpretation of ERCP. Lippincott-Raven, Philadelphia, pp 231 – 259

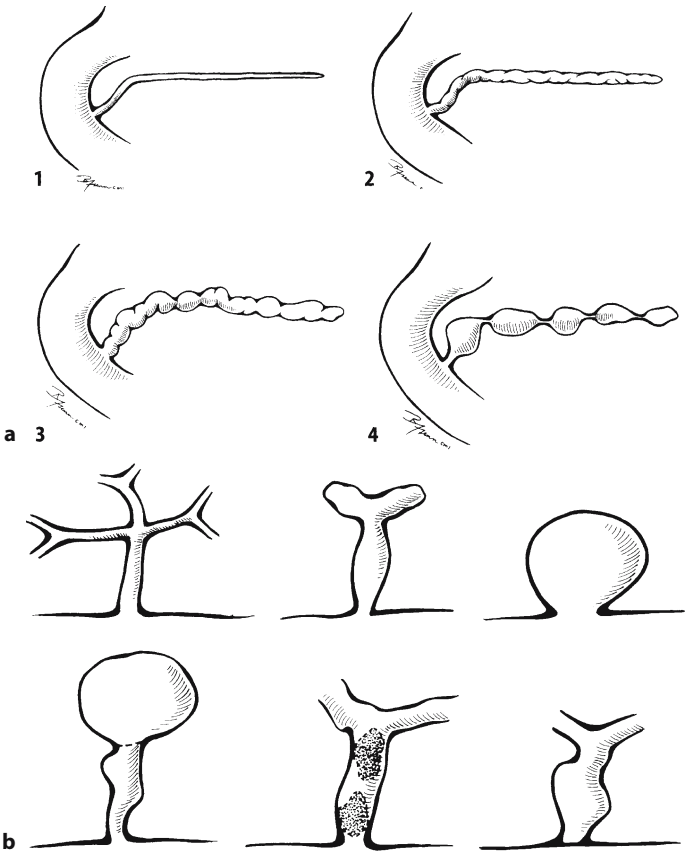

Fig. 161. **a** Changes in the main pancreatic duct. *1*, normal; *2*, mild irregularity; *3*, more pronounced irregularity; *4*, "chain of lakes". **b** Changes in the side branches. *1*, normal; *2*, early changes: mild narrowing at the base; *3*, marked cystic dilation of a side branch; *4*, cavitation and drainage from necrotic parenchyma; *5*, intraductal concretions; *6*, complete obstruction of side branch base. (From Taylor and Bohorfoush 1997, with permission)

#162 Chronic Pancreatitis, Ductal Changes (2): Early Disease

KEY FACTS: MRI

- With the exception of unpaired branches in the pancreatic head, normal side branches are not visible on MRCP
- Signs of early chronic pancreatitis:
  - Visualization of two or more side branches in the body and tail
  - Discrete irregularities of the main pancreatic duct (Fig. 162; differential diagnosis: senescent changes – see #147)
- *Note:* Although subtle caliber changes of the main pancreatic duct are usually clearly seen on projective MR cholangiography, MRCP is certainly not as sensitive as ERCP in the detection of the earliest stages of the disease for the following reasons:
  - Limitations in spatial resolution
  - Absence of ductal distention during imaging (no intraductal injection of contrast medium). Drugs stimulating the secretion of pancreatic juice can be helpful in this respect (see #19)

References

Fulcher AS, Capps GW, Turner MA (1999) Thoracopancreatic fistula: clinical and imaging findings. J Comput Assist Tomogr 23:181–187

Ponette E, Brys P, Van Steenbergen W (1994) Chronic pancreatitis: endoscopic retrograde cholangiopancreatography. In: Baert AL (ed) Radiology of the pancreas. Springer, Berlin Heidelberg New York, pp 106–115

Takehara Y, Ichijo K, Tooyama N et al. (1994) Breath-hold MR cholangiopancreatography with a long-echo-train fast spin-echo sequence and a surface coil in chronic pancreatitis. Radiology 192:73–78

Taylor AJ, Bohorfoush AG (1997) Pancreatic duct in inflammation of the pancreas. In: Taylor AJ, Bohorfoush AG (eds) Interpretation of ERCP. Lippincott-Raven, Philadelphia, pp 231–259

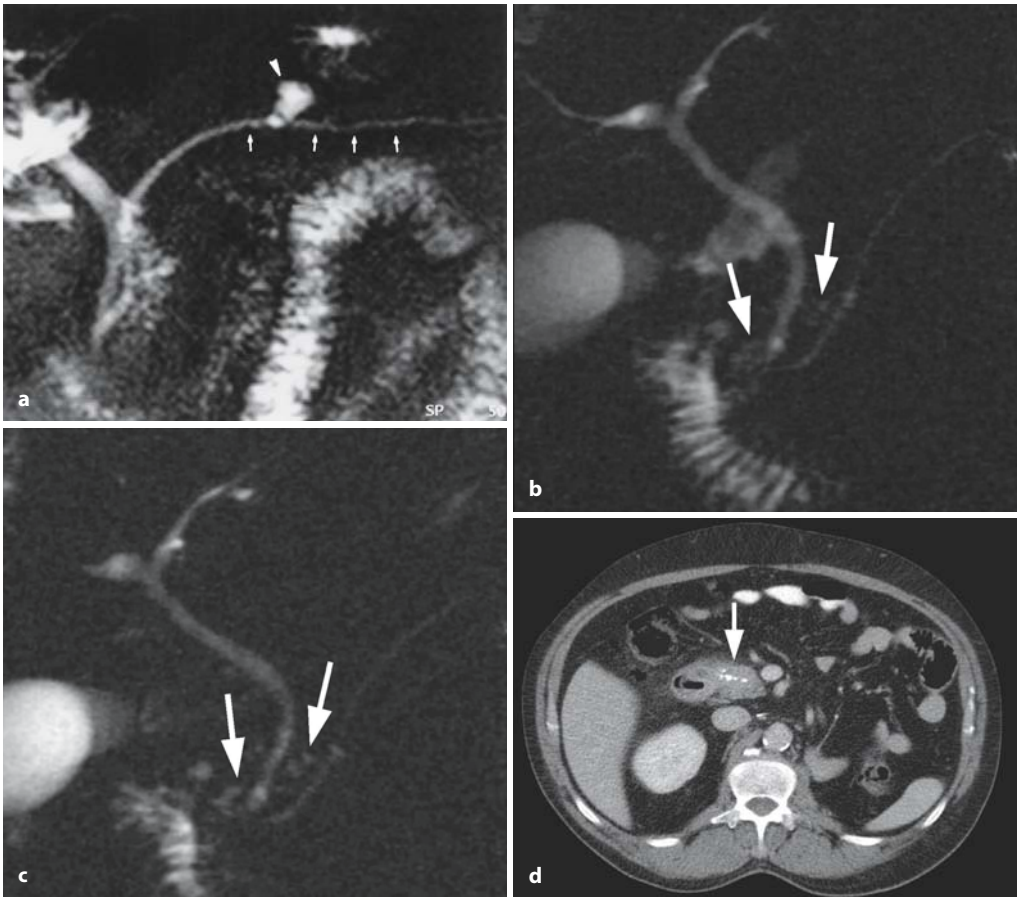

Fig. 162. **a** Projective MR image showing discrete ductal irregularities (*arrows*). Also note the presence of a small pseudocyst (*arrowhead*). **b–d** Projective images (**b, c**) showing multiple dilated side branches in the pancreatic head (*arrows*). **d** Axial CT image showing multiple calcifications in the pancreatic head (*arrow*) confirming the diagnosis of chronic pancreatitis

#163 Chronic Pancreatitis, Ductal Changes (3): Advanced Disease

Related topic: #78 (common bile duct stenosis in chronic pancreatitis)

KEY FACTS: MRI

- Typical features of the main pancreatic duct:
  - Dilation and tortuosity
  - Short areas of narrowing (strictures greater than 1 cm are less common but not rare)
  - Intraductal stones
- Typical features of side branches:
  - *Dilation and blunting* of side branches
  - *Nipping*, i.e., narrowing of the side branch base with respect to the more peripheral part (Fig. 163 c–e)
  - *Clubbing*, i.e., peripheral dilation instead of tapering (Fig. 163 c–e)
- Differential diagnosis:
  - Obstructive dilation: more uniform dilation of the main duct and side branches, without focal stenoses, nipping, or clubbing (see #168)
  - Pancreatic neoplasm (see #187)
- *Note:* MRCP is particularly useful in cases in which ERCP shows *obstruction* of the main pancreatic duct: the differential diagnosis between a tumor, tight stenosis, intraductal lithiasis, etc. is usually easy to make with MRCP

References

Fulcher AS, Capps GW, Turner MA (1999) Thoracopancreatic fistula: clinical and imaging findings. J Comput Assist Tomogr 23:181–187#

Ponette E, Brys P, Van Steenbergen W (1994) Chronic pancreatitis: endoscopic retrograde cholangiopancreatography. In: Baert AL (ed) Radiology of the pancreas. Springer, Berlin Heidelberg New York, pp 106–115

Takehara Y, Ichijo K, Tooyama N et al. (1994) Breath-hold MR cholangiopancreatography with a long-echo-train fast spin-echo sequence and a surface coil in chronic pancreatitis. Radiology 192:73–78

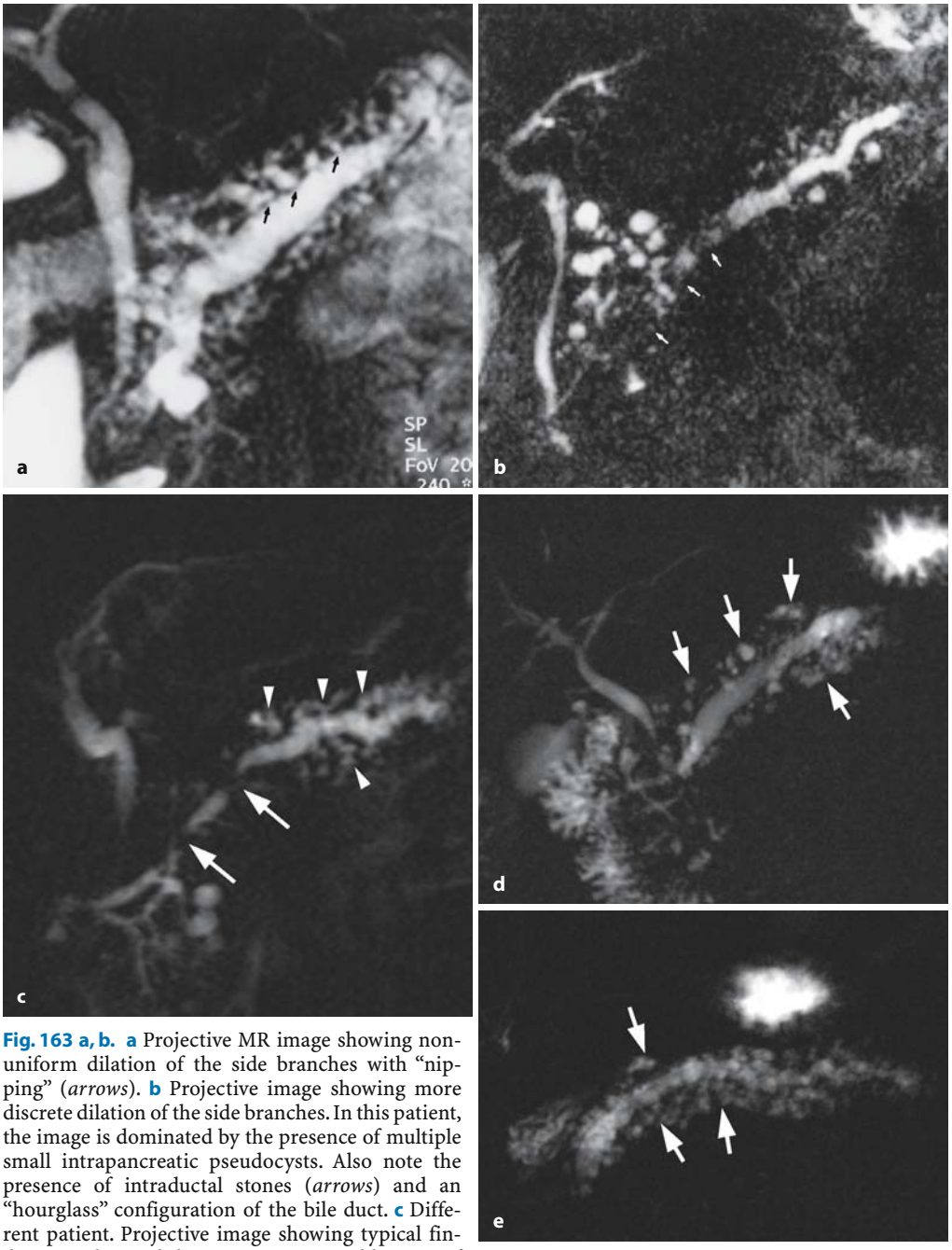

Fig. 163 a, b. **a** Projective MR image showing non-uniform dilation of the side branches with "nipping" (*arrows*). **b** Projective image showing more discrete dilation of the side branches. In this patient, the image is dominated by the presence of multiple small intrapancreatic pseudocysts. Also note the presence of intraductal stones (*arrows*) and an "hourglass" configuration of the bile duct. **c** Different patient. Projective image showing typical findings in advanced chronic pancreatitis: dilatation of the pancreatic duct with two stenoses (*arrows*), and dilatation of the side branches with "nipping" and "clubbing" (*arrowheads*). **d, e.** Projective images in different patient showing diffuse dilation of the main pancreatic duct and of several side branches, with "nipping" and "clubbing"

#164 Atypical Ductal Changes in Chronic Pancreatitis

KEY FACTS

Marked Diffuse Dilation of Ducts

- May be caused by distal intraductal stone, orificial stenosis, etc.
- Differential diagnosis:
  - Small papillary tumor (see # 130, 132)
  - Dysfunction of the vaterian sphincter complex (see # 127)
  - Intraductal mucinous neoplasm (see # 199)

Focal Narrowing

- Focal narrowing of the main pancreatic duct may be the only sign on MRCP in patients with chronic pancreatitis (Fig. 164 a)
- Differential diagnosis:
  - Acute pancreatitis
  - Duct-destructive chronic pancreatitis (see # 169)
  - Neoplasm (usually shows more irregular narrowing)
  - Rare causes: e. g., granulomatous disease
- Clues in the differential diagnosis with pancreatic cancer: see # 167

Double Duct Sign (Fig. 164 b – d)

- Narrowing of the pancreatic duct and the adjacent segment of the common bile duct
- Although this sign is more classically seen in malignancy, it may also be observed in patients with chronic pancreatitis (differential diagnosis: more gradual narrowing, kinking, etc.; see # 167)

References

Ponette E, Brys P, Van Steenbergen W (1994) Chronic pancreatitis: endoscopic retrograde cholangiopancreatography. In: Baert AL (ed) Radiology of the pancreas. Springer, Berlin Heidelberg New York, pp 106 – 115

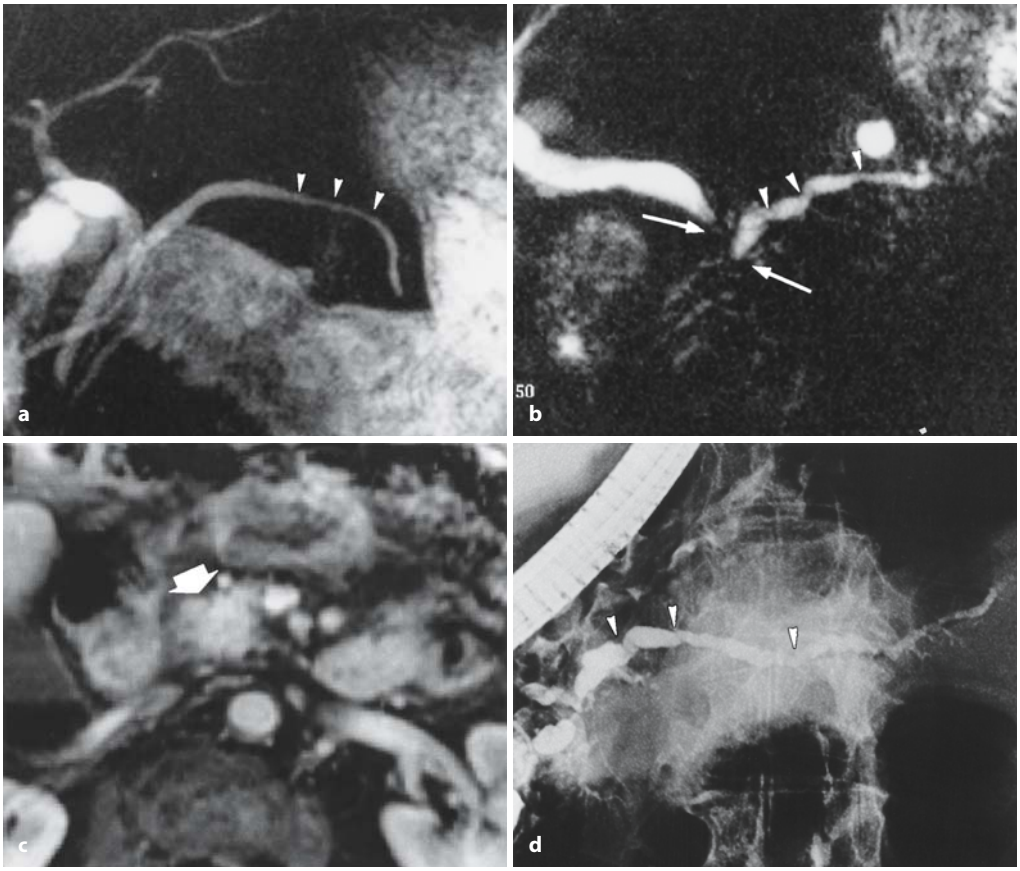

Fig. 164. **a** Projective MR image showing ductal narrowing in the pancreatic body (*arrowheads*), without associated abnormalities. **b–d** Double duct sign in chronic pancreatitis. **b** Projective MR image showing double duct sign (arrows), possibly indicating a pancreatic tumor. Also note the multiple short stenoses of the pancreatic duct (*arrowheads*) and pseudocysts. **c** Contrast-enhanced T1-weighted image showing normal enhancement of the pancreatic head (*arrow*): no signs of a tumor. **d** ERCP confirming the presence of multiple stenoses (*arrowheads*). Chronic pancreatitis was confirmed by biopsy and follow-up

#165 Complications of Chronic Pancreatitis (1): Pseudocyst

Related topic: #156 (pseudocyst in acute pancreatitis)

KEY FACTS: DISEASE

- Definition, classification, etc.: see #156
- Can occur in chronic pancreatitis with or without superimposed acute pancreatitis
- Treatment: surgical or endoscopic drainage

KEY FACTS: MRI

- Signal intensity: although most pseudocysts exhibit fluid intensity, the signal intensity may be variable if blood degradation products are present within the pseudocyst
- Uncomplicated pseudocyst: differential diagnosis:
  - Simple cyst
  - Mucinous neoplasm (see #198): may be indistinguishable from pseudocysts on MRCP; clinical history, puncture with aspiration, and/or ERCP may provide important clues
- Differential diagnosis of complicated (hemorrhagic) pseudocyst:
  - Phlegmon (may also contain hemorrhage)
  - Hemorrhagic tumor (diagnostic clues: associated signs of chronic pancreatitis, secondary signs of malignancy, presence and degree of upstream ductal dilation and atrophy, visualization of solid components)
- *Note:* Small intrapancreatic pseudocysts are very common in chronic pancreatitis; similar small fluid collections may be seen in:
  - Acute pancreatitis
  - Pancreatic carcinoma (more focal)

References

Ahearne PM, Baillie JM, Cotton PB, Baker ME, Meyers WC, Pappas TN (1992) An endoscopic retrograde cholangiopancreatography (ERCP)-based algorithm for the management of pancreatic pseudocysts. Am J Surg 163 : 111 – 115

Sand JA, Seppannen SK, Nordback IH (1997) Intracystic hemorrhage in pancreatic pseudocysts: initial experiences of a treatment protocol. Pancreas 14 : 187 – 191

van Sonnenberg E, Wittich GR, Casola G et al. (1989) Percutaneous drainage of infected and noninfected pancreatic pseudocysts: experience in 101 cases. Radiology 170 : 757 – 761

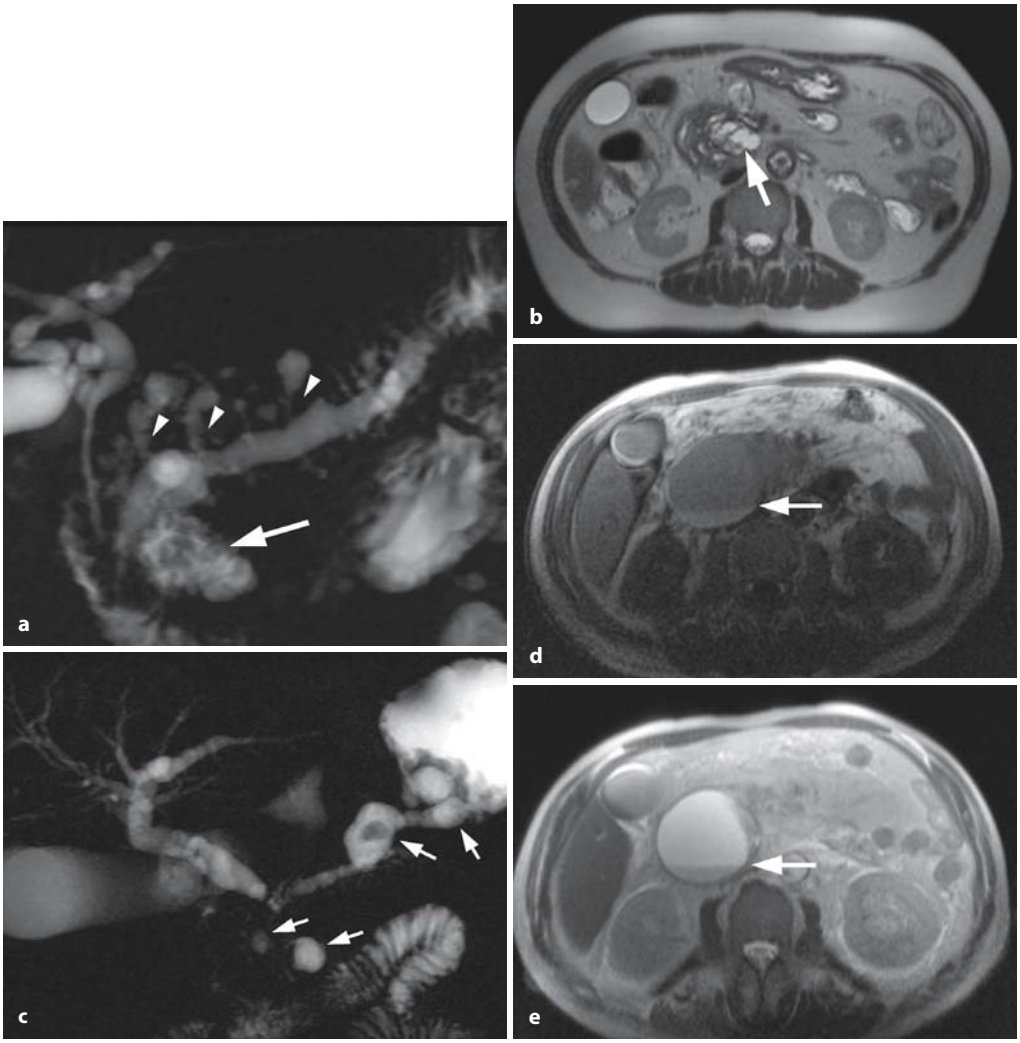

Fig. 165 a, b. Projective image (**a**) showing typical findings in advanced chronic pancreatitis: dilatation of the main pancreatic duct, prominent dilatation of the side branches with "nipping" (*arrowheads*) and a pseudocyst in the pancreatic head (*arrow*). Axial T2-weighted HASTE image (**b**) showing the fluid collection in the pancreatic head: pseudocyst (*arrow*). **c** Different patient. Projective image showing two small pseudocysts in the pancreatic head and several peripancreatic pseudocysts extending towards the stomach (*arrows*). **d, e** Different patient. Axial T1 weighted FLASH image (**d**) and T2-weighted HASTE image (**e**) showing a large hemorrhagic pancreatic pseudocyst with fluid–fluid level (*small arrow*)

#166 Complications of Chronic Pancreatitis (2): Other Complications

Related topics: #74 (common bile duct stones complicated by fistula), #157 (vascular complications in acute pancreatitis)

KEY FACTS: DISEASE

Vascular Complications

- See #157
- Types:
  - Pseudoaneurysm (encountered in 6%–10% of patients)
  - Venous thrombosis

Fistula

- Pancreatic fluid may penetrate several organs/cavities and create fistulas:
  - Pleura: pathway usually via the lesser sac to the aortic or esophageal hiatus
  - Peritoneum (pancreatic ascites): via the lesser sac and foramen of Winslow
  - Portal vein
- May develop de novo or secondary to rupture of a pseudocyst

KEY FACTS: MRI

- Vascular complications: see #157 (Fig. 166 d–f)
- Fistula: usually best seen on coronal heavily T2-weighted cross-sectional images; both the rupture of the pancreatic duct and the connection with the pleura may be demonstrated by MRCP (Fig. 166 a–c)

References

Fulcher AS, Capps GW, Turner MA (1999) Thoracopancreatic fistula: clinical and imaging findings. J Comput Assist Tomogr 23:181–187

Maule WF, Reber HA (1985) Diagnosis and management of pancreatic pseudocysts, pancreatic ascites, and pancreatic fistulas. In: Go VLM, Gardner JD, Brooks FP et al. (eds) The exocrine pancreas: biology, pathobiology and diseases. Raven, New York, pp 601–610

Miller FH, Keppke AL, Wadhwa A et al. (2004) MRI of pancreatitis and its complications: part 2, chronic pancreatitis. AJR Am J Roentgenol 183:1645–1652

Sankaran S, Sugawa C, Walt AJ (1979) Value of endoscopic retrograde pancreatography in pancreatic ascites. Surg Gynecol Obstet 148:185–192

Vujic I (1989) Vascular complications of pancreatitis. Radiol Clin North Am 27:81–91

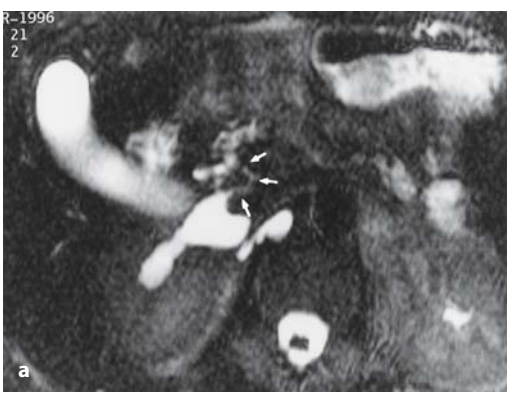

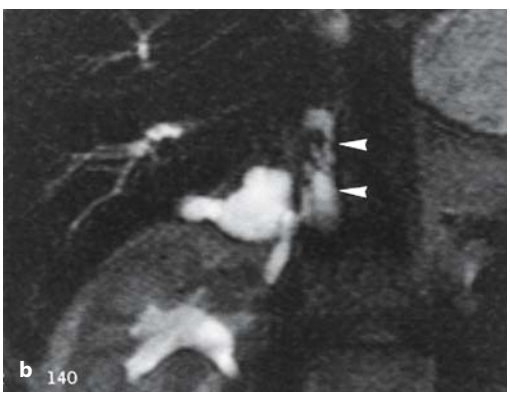

Fig. 166. a Heavily T2-weighted axial image (**a**) showing communication (*arrows*) between the distal pancreatic duct and a retroperitoneal collection. Coronal images (**b, c**) showing connection between the retroperitoneal collection and the right pleural space (*arrowheads*)

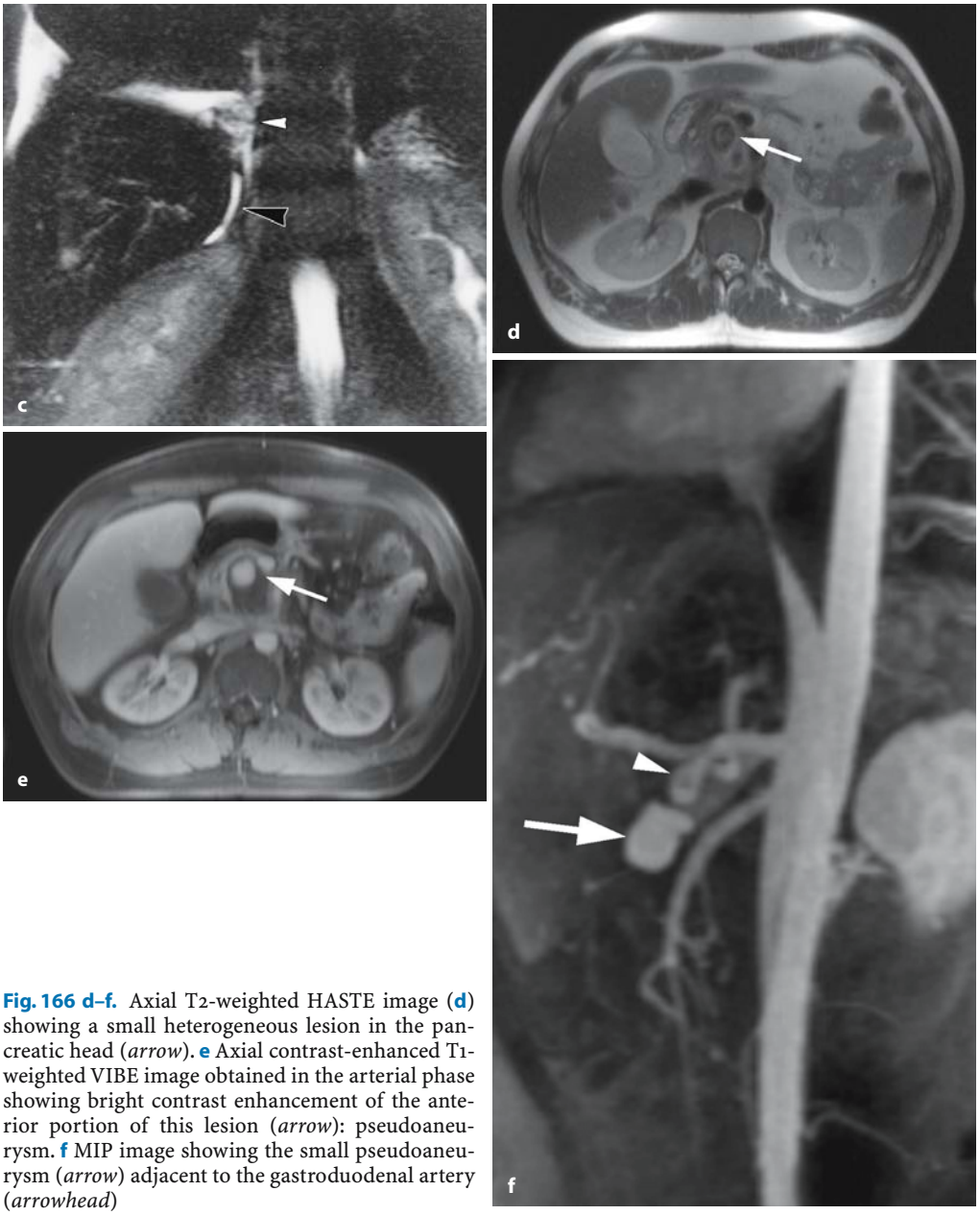

Fig. 166 d–f. Axial T2-weighted HASTE image (**d**) showing a small heterogeneous lesion in the pancreatic head (*arrow*). **e** Axial contrast-enhanced T1-weighted VIBE image obtained in the arterial phase showing bright contrast enhancement of the anterior portion of this lesion (*arrow*): pseudoaneurysm. **f** MIP image showing the small pseudoaneurysm (*arrow*) adjacent to the gastroduodenal artery (*arrowhead*)

#167 Chronic Pancreatitis with Focal Inflammatory Mass

KEY FACTS: DISEASE

- A focal inflammatory mass is seen in up to 30% of patients with chronic pancreatitis (up to 49% in some series; Luetmer et al. 1989), most commonly in the pancreatic head
- Etiology:
  - Superimposed acute pancreatitis
  - Possibly a specific chronic inflammatory process
- Symptoms: patients with chronic pancreatitis and pancreatic head enlargement commonly have severe pain

KEY FACTS: MRI

! Together with the segmental type of chronic pancreatitis (see #164), this entity commonly poses problems in the differential diagnosis with pancreatic carcinoma. The following features suggest chronic pancreatitis:

- On projective images:
  - Dilation of the main pancreatic duct *distal* to the site of stenosis (i.e., downstream)
  - Abnormal side branches *distal* to the site of stenosis
  - Intraductal stones
  - Multiple pseudocysts at different locations
  - Side branches: nipping, clubbing, distorted appearance
  - Signs of attraction of the common bile duct (suggesting fibrosis; see #78)
  - Smooth tapering of the common bile duct
  - Duct-penetrating sign (Ichikawa et al. 2001)
- On cross-sectional images:
  - CT: calcifications within the mass
  - Visualization of dilated side branches traversing the suspect area (Fig. 167a–d) (in malignant tumors, obstructed side branches are seen adjacent to, but not within the mass; see Fig. 187a)
  - No atrophy or uniform atrophy of the gland
  - Focal mass with relatively high signal intensity on non-fat-suppressed T1-weighted images (most reliable sign but not always present) (Fig. 167k–n)
  - Focal mass not presenting a a "black hole" on early-phase dynamic contrast-enhanced images (Fig. 167k–n, compare to Fig. 1 and Fig 186a–f)

References

Büchler M, Malfertheiner M, Friess H, Senn T, Beger HG (1990) Chronic pancreatitis with inflammatory mass in the head of the pancreas: a specific entity? In: Beger HG (ed) Chronic pancreatitis. Springer, Berlin Heidelberg New York, pp 41–46

Ichikawa T, Sou H, Araki T et al. (2001) Duct-penetrating sign at MRCP: usefulness for differentiating inflammatory pancreatic mass from pancreatic carcinomas. Radiology 221:107–116

Ishihara T, Yamaguchi T, Tsuyuguchi T, Hayasake A, Saisho H (1996) Characteristic findings of ERCP in the diagnosis of chronic pancreatitis with inflammatory mass. Nippon Shokakibyo Gakkai Zasshi 93:725–731

Luetmer PH, Stephens DH, Ward EM (1989) Chronic pancreatitis: reassessment with current CT. Radiology 171:353–357

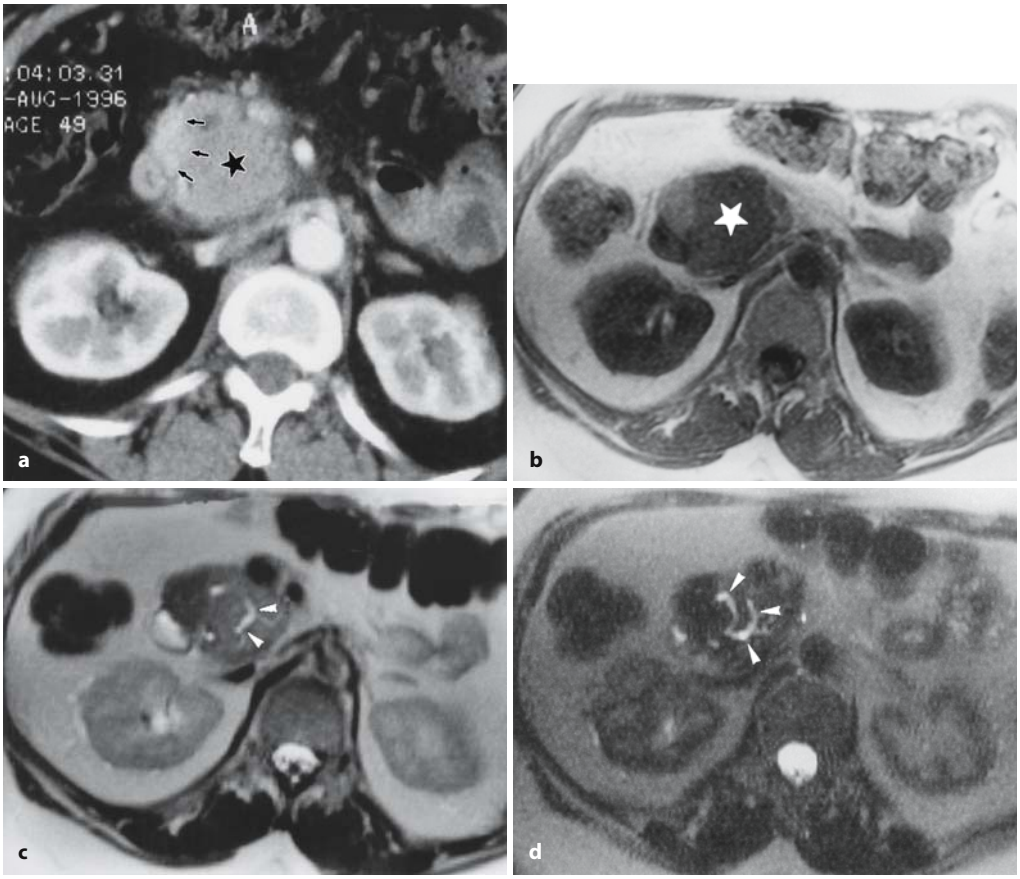

Fig. 167 a–d. Patient with chronic pancreatitis. **a** CT image showing enlargement and decreased iodine uptake of the pancreatic head (*asterisk*): Tumor? Note the normal enhancement more laterally (*arrows*). **b** T1-weighted MR image showing the enlarged part of the pancreatic head as markedly hypointense (*asterisk*), which is still consistent with a tumor. **c** Moderately and **d** heavily T2-weighted images showing dilated side branches (*arrowheads*): this rules out a tumor.

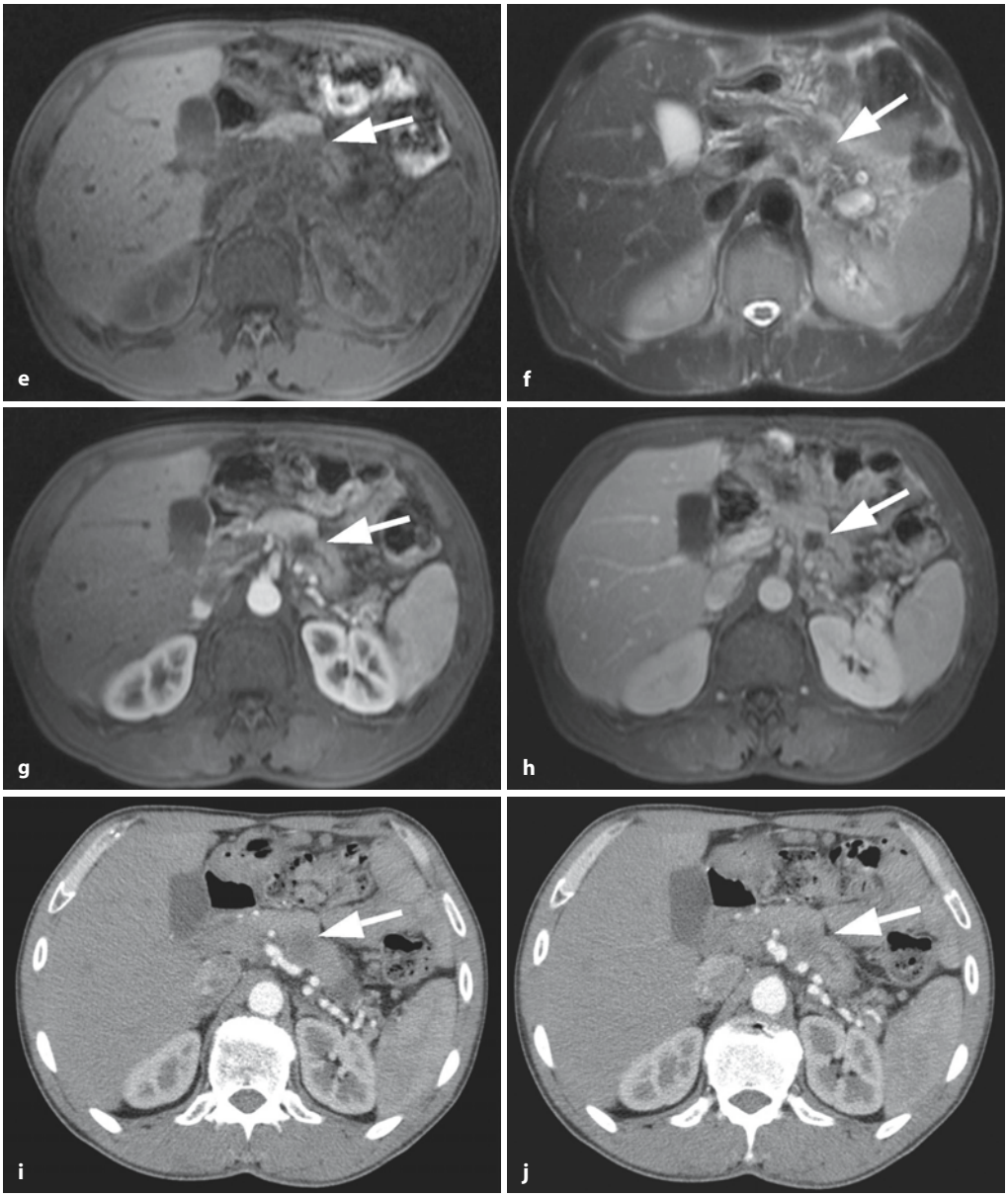

Fig. 167 e–j. T1-(**e**) and T2-(**f**)weighted images showing a focal lesion in the pancreatic tail that appears as a T1-hypointense and T2-hyperintense mass (*arrow*). Axial contrast-enhanced T1-weighted VIBE images obtained in the arterial (**g**) and venous (**h**) phase showing this mass to be hypovascular (*arrow*). Axial CT images (**i, j**) also confirm the presence of a small hypointense mass in the pancreatic tail (*arrow*). Needle biopsy and lack of evolution over a period of 9 months proved this mass to be a focal inflammatory mass.

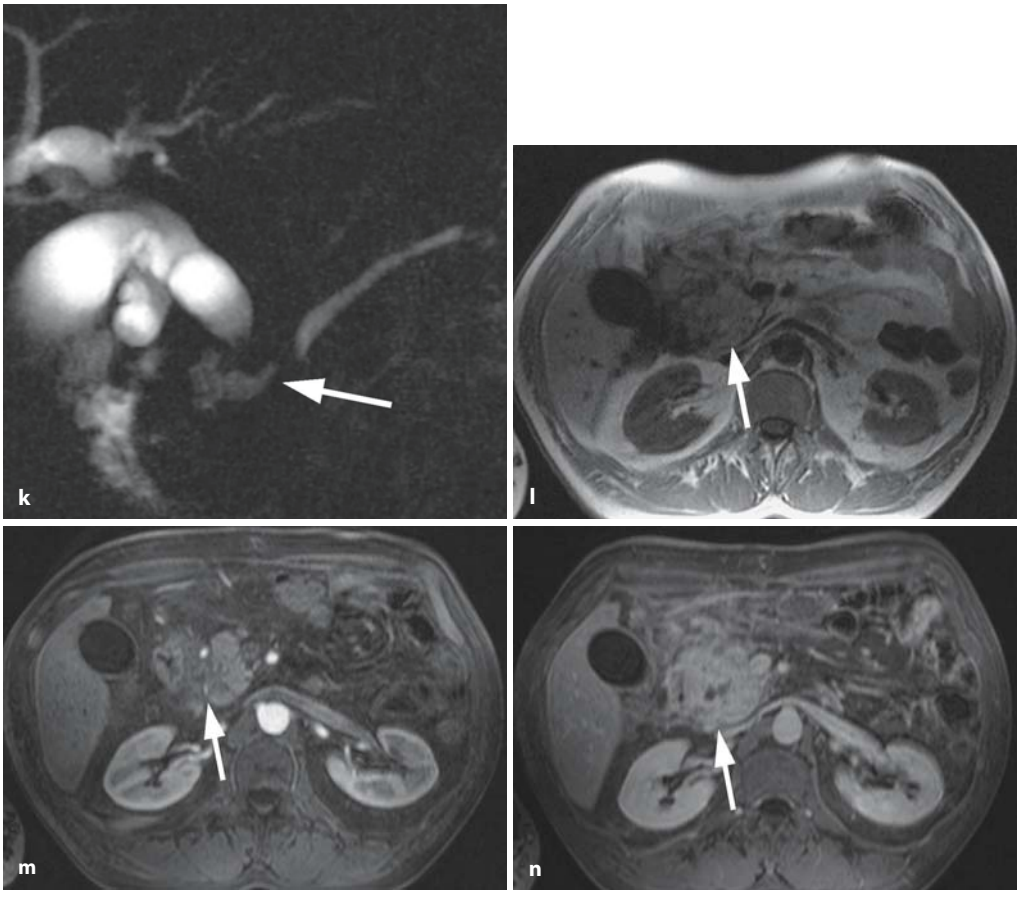

Fig. 167 k–n. **k** Projective image showing a double-duct sign (*arrow*). **l** Axial T1-weighted image showing an enlarged pancreatic head (*arrow*) with small hypointense areas at the duodenal groove. **m** Axial contrast-enhanced T1-weighted VIBE image obtained in the arterial phase showing decreased/delayed uptake of contrast medium (*arrow*). **n** Image obtained in the venous phase showing late enhancement of this mass (*arrow*). The enhancement features together with the relatively high signal intensity at T1-weighted images favour the diagnosis of a focal inflammatory mass. Because of increasing biochemical abnormalities, surgery was performed. Final diagnosis: groove pancreatitis, no tumor

#168 Chronic Obstructive Pancreatitis

Related topic: #194 (adenocarcinoma with retro-obstructive pancreatitis)

KEY FACTS: DISEASE

- Pancreatitis related to (caused by) obstruction of the main pancreatic duct
- Histology: evenly distributed chronic parenchymal inflammation with preservation of the ductal epithelium. Intraductal stones are uncommon (except as a causal factor)
- Cause: either benign (e.g., papillary stenosis) or malignant
- Complications: endocrine and/or exocrine insufficiency may develop if less than 40% of the parenchyma lies beyond the obstruction
- Therapy: removal of obstructive component

KEY FACTS: MRI (FIG. 168, SEE ALSO FIG. 182B)

- Typical features:
  - Uniform dilation of the main pancreatic duct
  - Commonly relative sparing or mild uniform dilation of side branches
  - No intraluminal filling defects (except as a causal factor)
  - Intraparenchymal pseudocysts may be seen
  - Diminished signal intensity of parenchyma on T1-weighted MRI (fibrosis)
- *Note:* Chronic obstructive pancreatitis is commonly seen in patients with ductal adenocarcinoma. This may cause problems in determining the exact proximal extent of the tumor (both tumor and pancreatitis are hypointense on T2-weighted images). In such cases, tumor delineation may be improved by obtaining contrast-enhanced scans (see #1a–d, 15, 194)

References

Freeny PC (1989) Classification of pancreatitis. Radiol Clin North Am 27:1–3

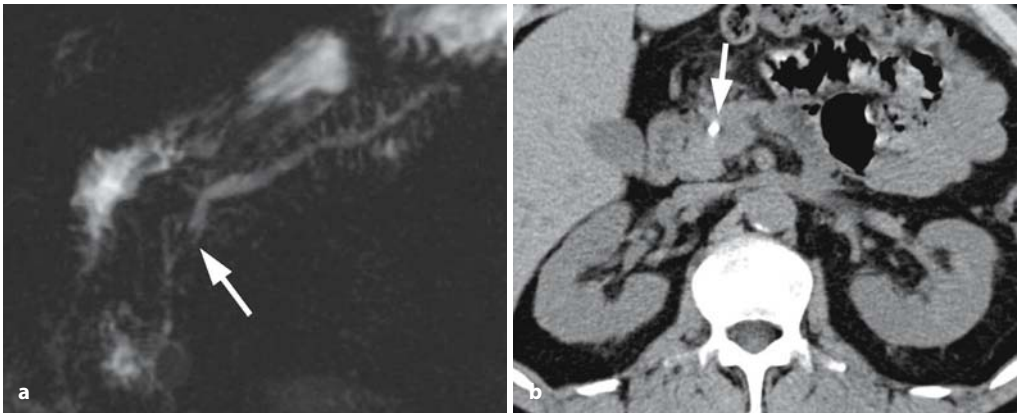

Fig. 168 a, b. **a** Projective image showing dilatation of the pancreatic duct in the body/tail secondary due to an intraductal stone (*arrow*). **b** Axial CT image confirming the presence of a stone in the pancreatic head (*arrow*)

#169 Nonalcoholic Duct-Destructive Chronic Pancreatitis (auto-immune pancreatitis)

KEY FACTS: DISEASE (ECTORS ET AL. 1997)

- Probably identical to chronic sclerosing pancreatitis
- Type of chronic pancreatitis with specific histologic features
- Histology: periductal inflammation causing duct obstruction and focal duct destruction. The infiltrate consists mainly of lymphocytes and is associated with periductal and interlobular fibrosis
- Incidence: not known, probably not rare
- No characteristic age or sex distribution
- Causes: probably auto-immune related
- Associated diseases: auto-immune or related diseases such as Sjögren's syndrome, primary sclerosing cholangitis, and chronic ulcerative colitis
- Symptoms (variable):
  - No symptoms
  - Obstructive jaundice
  - Signs of acute pancreatitis
- Remission has been observed after administration of steroids

KEY FACTS: MRI (FIG. 169)

- Focal or more diffuse mass-like enlargement of the pancreas
- Signal intensity:
  - T1: hypointense
  - T2: variable, depending on the histologic composition (fibrosis versus active inflammation)
- Other features:
  - Hypovascular
  - Causes narrowing of the main pancreatic duct (regular or irregular); narrowing of the CBD may be associated
  - Sometimes multiple biliary stenoses
  - Mimics tumor
- Features that distinguish nonalcoholic duct-destructive chronic pancreatitis from pancreatic cancer:
  - No extrapancreatic spread
  - Less pronounced ductal dilation/parenchymal atrophy proximal to the lesion
  - Sometimes smooth rim of contrast enhancement and/or signal intensity alteration at the anterior and posterior border of pancreatic parenchyma (pathognomonic finding)

References

Bogomoletz W (1997) Duct destructive chronic pancreatitis. A new insight into the pathology of idiopathic non-alcoholic chronic pancreatitis. Gut 41 : 272 – 273

Ectors N, Maillet B, Aerts R et al. (1997) Non-alcoholic duct destructive chronic pancreatitis. Gut 41 : 263 – 268

Irie H, Honda H, Baba S et al. (1998) Auto-immune pancreatitis: CT and MR characteristics. AIR; 170 : 1323 – 1327

Sahani DV, Kalva SP, Farrell J et al. (2004) Autoimmune pancreatitis: imaging features. Radiology 233 : 345 – 352

Van Hoe L, Gryspeerdt S, Ectors N et al. (1998) Non-alcoholic duct destructive chronic pancreatitis: imaging findings. AJR Am J Roentgenol 170 : 643 – 647

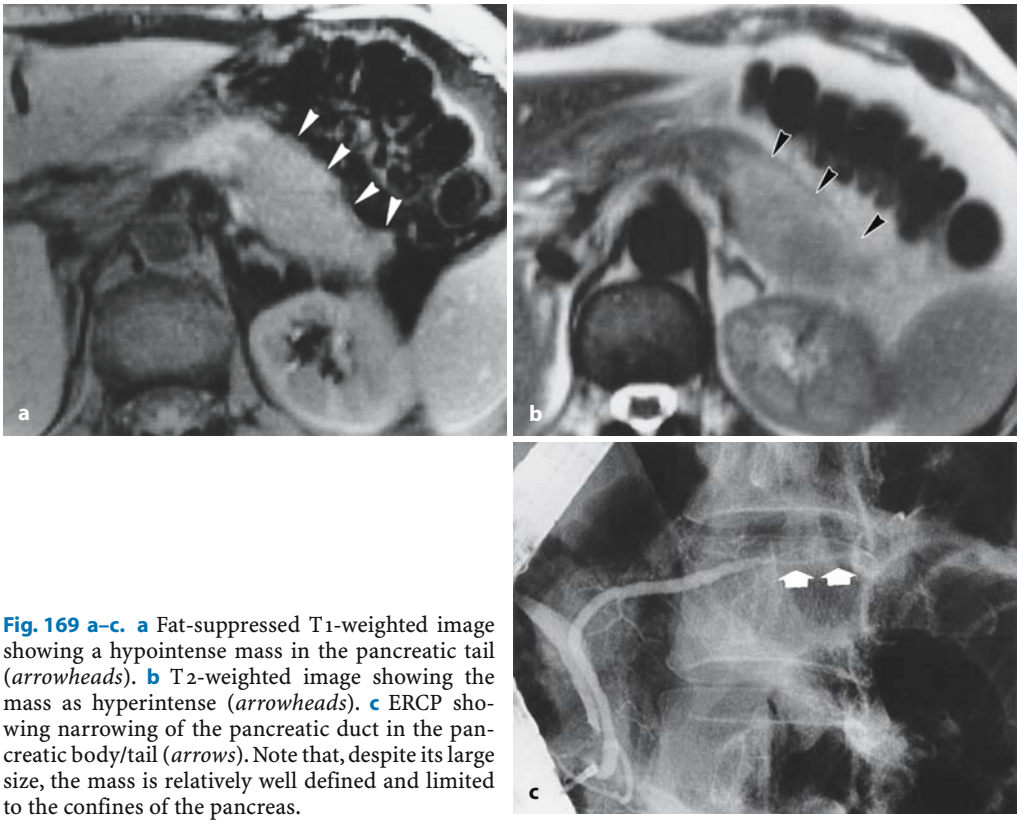

Fig. 169 a–c. **a** Fat-suppressed T1-weighted image showing a hypointense mass in the pancreatic tail (*arrowheads*). **b** T2-weighted image showing the mass as hyperintense (*arrowheads*). **c** ERCP showing narrowing of the pancreatic duct in the pancreatic body/tail (*arrows*). Note that, despite its large size, the mass is relatively well defined and limited to the confines of the pancreas.

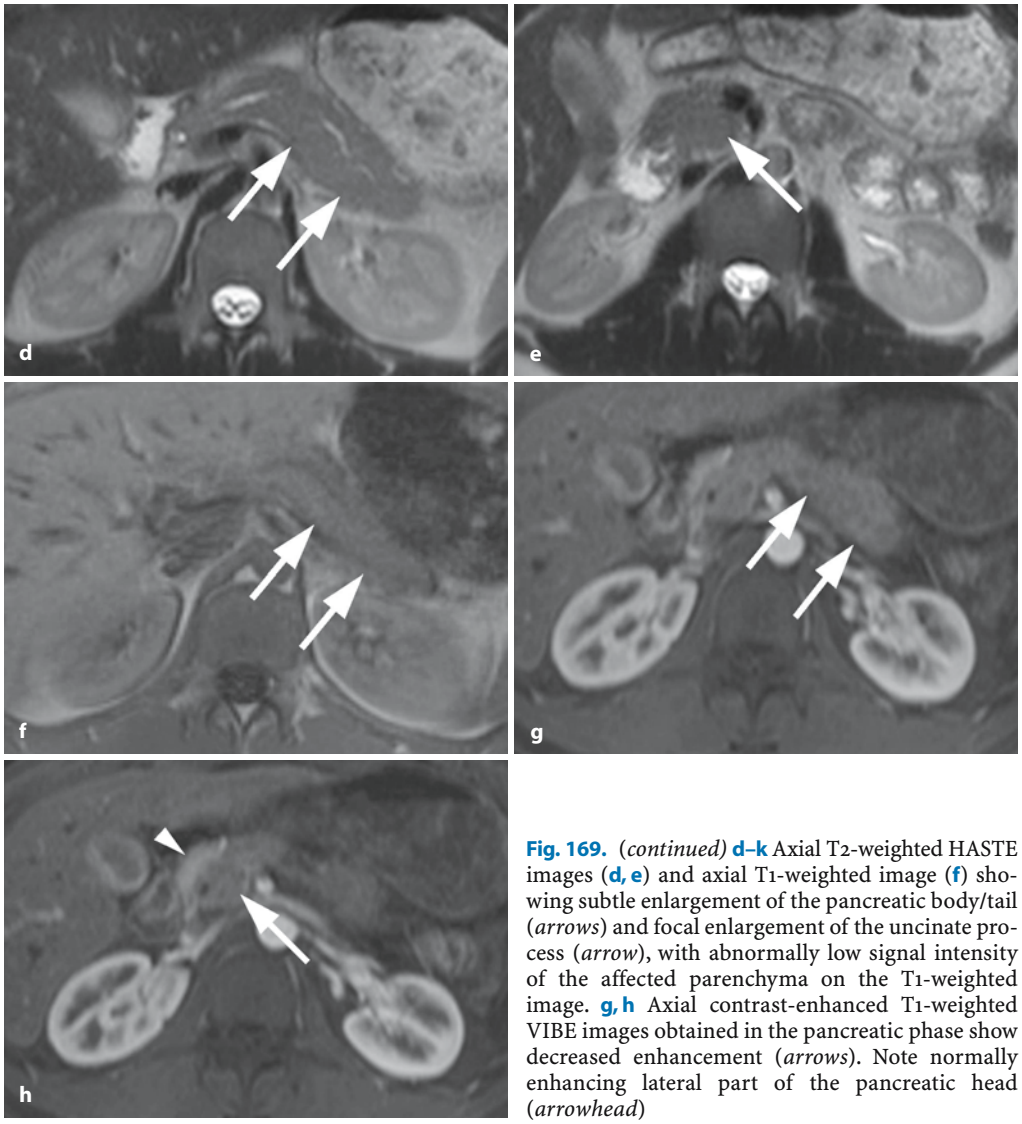

Fig. 169. (*continued*) **d–k** Axial T2-weighted HASTE images (**d, e**) and axial T1-weighted image (**f**) showing subtle enlargement of the pancreatic body/tail (*arrows*) and focal enlargement of the uncinate process (*arrow*), with abnormally low signal intensity of the affected parenchyma on the T1-weighted image. **g, h** Axial contrast-enhanced T1-weighted VIBE images obtained in the pancreatic phase show decreased enhancement (*arrows*). Note normally enhancing lateral part of the pancreatic head (*arrowhead*)

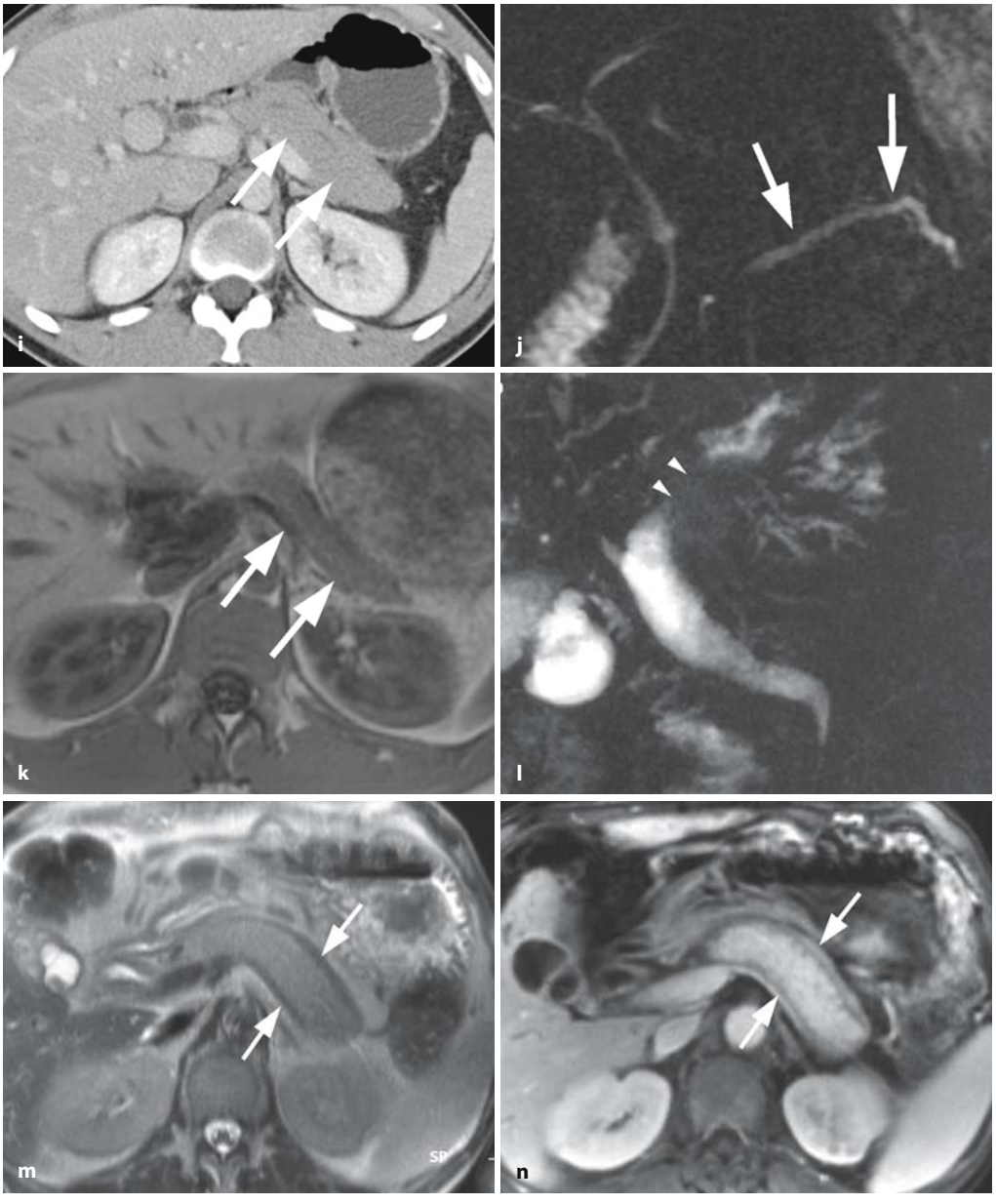

Fig. 169. (*continued*) **i** Axial CT image in the venous phase confirming the enlargement of the pancreatic body/tail with decreased iodine uptake (*arrows*). **j** Projective image showing subtle dilatation of the pancreatic duct in the body/tail (*arrows*), with narrowing in the head/neck. **k** Axial T1-weighted image after 1 month steroid therapy shows an important regression of the findings (*arrows*) confirming the diagnosis of autoimmune pancreatitis. **l–n** Single-slice MRCP image obtained in a different patient shows severe narrowing of the CBD and proximal biliary dilatation. **m** Axial T2-weighted image shows bizarre appearance of pancreatic parenchyma with presence of peripheral (ventral and dorsal) hypointense bands (*arrows*). **n** Axial contrast-enhanced T1-weighted image shows poor uptake of contrast material in this region (*arrows*). The patient was known with primary sclerosing cholangitis and also had a severe stenosis at the hepatic hilum [*arrowheads* in (**l**). At the time of admission, a rapid clinical deterioration was observed. However, spectacular improvement was noted after steroid administration

#170 Hereditary Pancreatitis

KEY FACTS: DISEASE

- Form of chronic pancreatitis with autosomal dominant inheritance
- Cause: mutation of the cationic trypsinogen gene
- Clinical onset: usually between 2 and 12 years (mean, 7 years)
- Symptoms: attacks of acute abdominal pain
- Complications:
  - Exocrine and/or endocrine insufficiency (10 % – 30 %)
  - Pseudocyst formation (17 %)
  - Thrombosis of splenic vein (5 %)

KEY FACTS: MRI (FIG. 170)

- Typical features:
  - Moderate to marked dilation of the main pancreatic duct (commonly more than 1 – 2 cm)
  - Typically large intraductal calculi
- Other features:
  - Signs of acute pancreatitis
  - Signs of complications (see also # 165, 166)
- Differential diagnosis: other types of chronic pancreatitis (age is often the most important clue)

References

Niederau C, Luthen R (1997) Hereditary pancreatitis is due to a mutation of the cationic trypsinogen gene. Z Gastroenterol 35 : 363 – 365

Perrault J (1994) Hereditary pancreatitis. Gastroenterology Clin North Am 23 : 743 – 752

Rohrmann CA, Surawicz CM, Hutchinson D, Silverstein FE, White TT, Marchioro TL (1981) The diagnosis of hereditary pancreatitis by pancreatography. Gastrointest Endosc 27 168 – 173

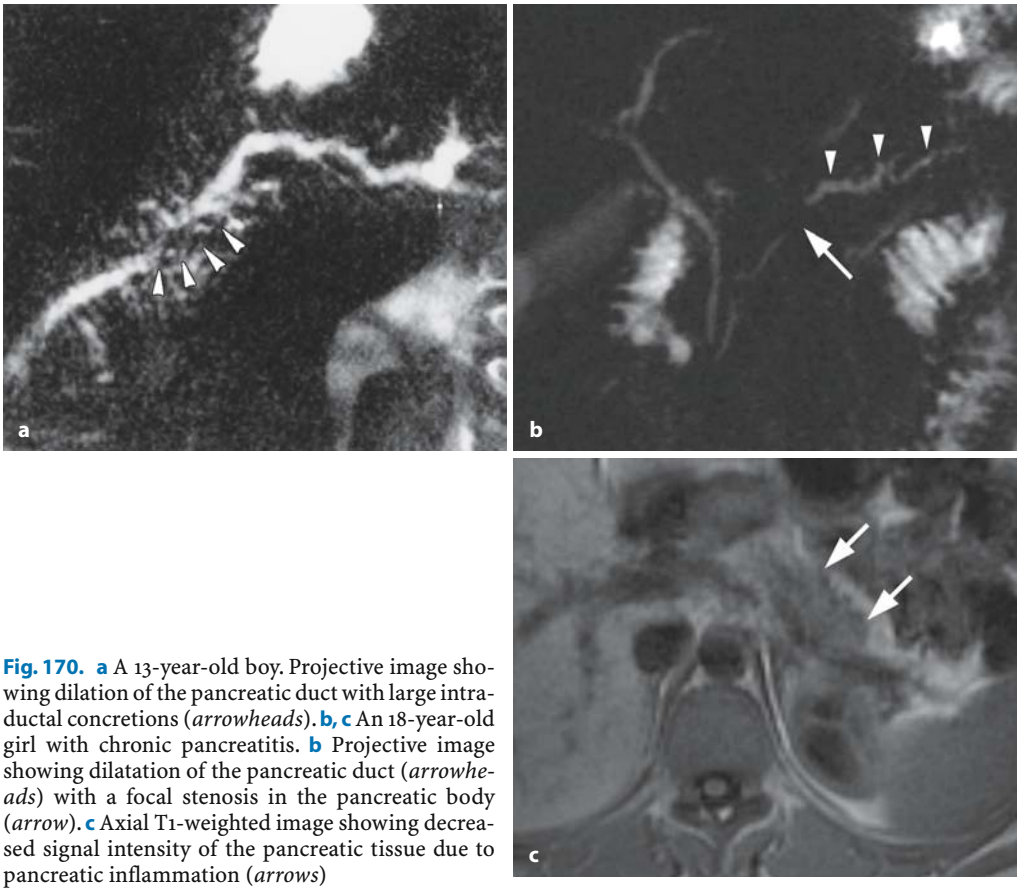

Fig. 170. **a** A 13-year-old boy. Projective image showing dilation of the pancreatic duct with large intraductal concretions (*arrowheads*). **b, c** An 18-year-old girl with chronic pancreatitis. **b** Projective image showing dilatation of the pancreatic duct (*arrowheads*) with a focal stenosis in the pancreatic body (*arrow*). **c** Axial T1-weighted image showing decreased signal intensity of the pancreatic tissue due to pancreatic inflammation (*arrows*)

#171 Simple True Cyst

Related topics: #31 (hepatic cysts), #172 (cysts in von Hippel-Lindau disease)

KEY FACTS: DISEASE

- Definition: cyst lined by an epithelial layer
- Histology: clear cystic fluid; inner surface lined with ductal cells
- Incidence: less common than pseudocysts
- Types:
  - Congenital cysts (associated with polycystic disease in other organs)
  - Acquired cysts: retention cysts (arising from obstruction of pancreatic duct); parasitic cysts
- Usually solitary; if multiple, underlying disease is common (see #172)
- Usually asymptomatic; jaundice is possible

KEY FACTS: MRI

- T1 hypointense, T2 hyperintense
- Homogeneous, no solid components, unilocular
- May compress the common bile duct or pancreatic duct (rare) (Fig. 171)
- Differential diagnosis (may be difficult):
  - Features suggesting *pseudocyst:* clinical history; connection with pancreatic duct; associated signs of chronic pancreatitis; multiple cystic lesions
  - Features suggesting *cystic tumor* (see #175, 198): peripheral rim of solid tissue; irregular contours; mural nodules
  - Lymphangioma (see #173)

References

Heindryckx E, Van Steenbergen W, Van Vaerenbergh W, Van Hoe L, Vanbeckevoort D, Ectors N, Baert AL. Solitary true cyst of the pancreas: case report. Eur Radiol (in press)

Kim YH, Saini S, Sahani D, Hahn PF, Mueller P, Auh Y (2005) Imaging diagnosis of cystic pancreatic lesions: pseudocyst versus nonpseudocyst. RadioGraphics 25 : 671 – 685

Mao C, Greenwood S, Wagner S, Howard JM (1992) Solitary true cyst of the pancreas in an adult. Int J Pancreatol 12 : 181 – 186

Sperti C, Pasquali C, Constantino V, Perasole A, Liessi G, Pedrazzoli S (1995) Solitary true cyst of the pancreas in adults. Int J Pancreatol 18 : 161 – 67

Zhang X, Mitchell DG, Dohke M, Holland GA, Parker L (2002) Pancreatic cysts: depiction on single-shot fast spin-echo MR images. Radiology 223 : 547 – 553

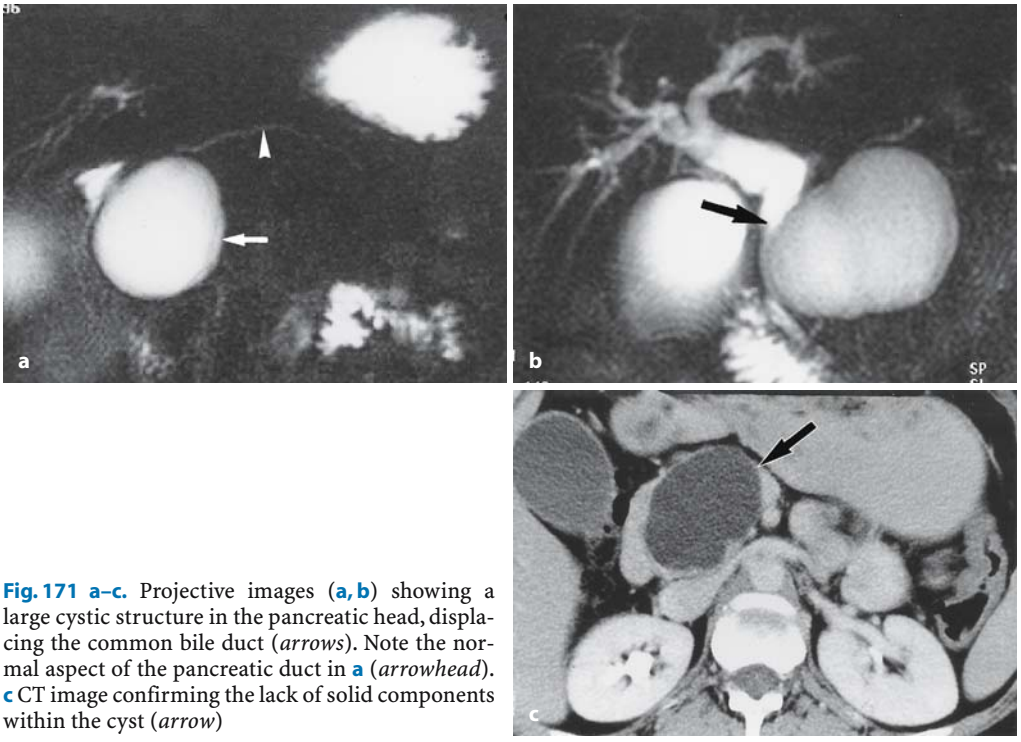

Fig. 171 a–c. Projective images (**a, b**) showing a large cystic structure in the pancreatic head, displacing the common bile duct (*arrows*). Note the normal aspect of the pancreatic duct in **a** (*arrowhead*). **c** CT image confirming the lack of solid components within the cyst (*arrow*)

#172 Cysts in Von Hippel-Lindau Disease

Related topic: # 171 (simple true cyst)

KEY FACTS: DISEASE

- Von Hippel-Lindau disease: autosomal disorder associated with abnormal tissue growth in different organs (e. g., retinal angiomatosis, hemangioblastoma of the central nervous system, renal cell carcinoma, adrenal pheochromocytoma)
- Incidence: pancreatic cysts are found in 72 % of patients with von Hippel-Lindau disease
- Number of cysts: varies from a few cysts to polycystic transformation of the entire organ
- Other pancreatic abnormalities seen with increased frequency in von Hippel-Lindau disease: serous cystadenoma, islet cell tumor, adenocarcinoma
- Other diseases associated with the presence of (multiple) pancreatic cysts:
  - Adult polycystic kidney disease
  - Cystic fibrosis (see # 174)

KEY FACTS: MRI

- Pancreatic cysts are easily recognized (Fig. 172)

References

Horton WA, Wong V, Eldridge R (1976) Von Hippel-Lindau disease: clinical and pathological manifestations in nine families with 50 affected members. Arch Intern Med 136 : 769 – 777

Hough DM, Stephens DH, Johnson CD, Binkovitz LA (1994) Pancreatic lesions in von Hippel-Lindau disease: prevalence, clinical significance, and CT-findings. AJR Am J Roentgenol 162 : 1091 – 1094

Neumann HP, Dinkel E, Brambs H et al. (1991) Pancreatic lesions in the von Hippel Lindau syndrome. Gastroenterology 101 : 465 – 471

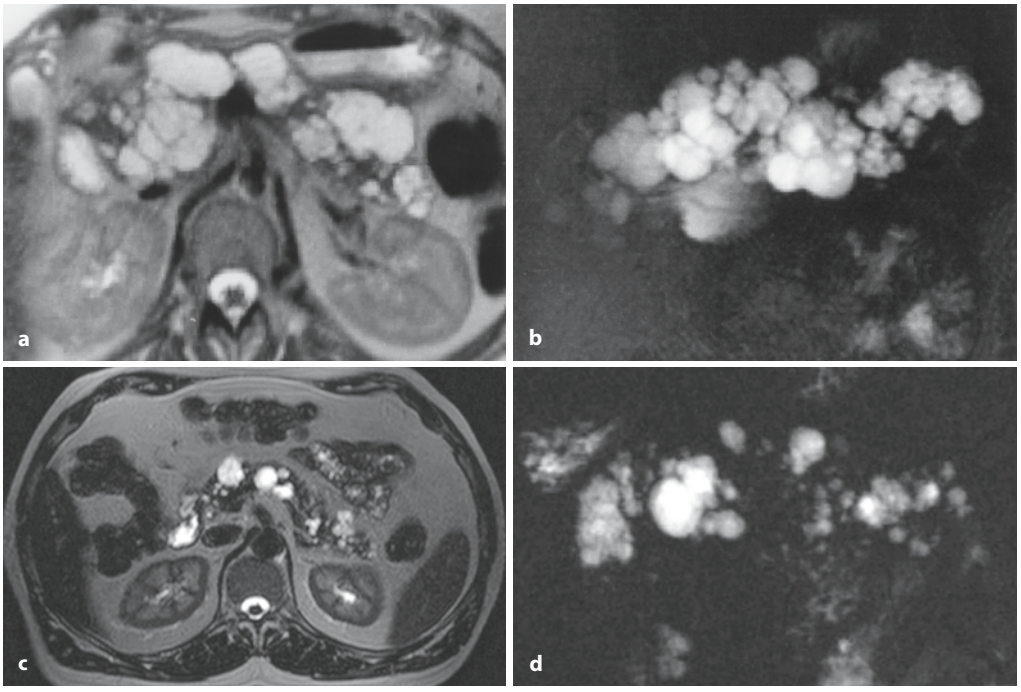

Fig. 172. **a, b** Axial T 2-weighted image and **b** projective image showing multiple cysts throughout the pancreas. **c, d** Other patient with Von Hippel-Lindau Disease. Axial T2-weighted image (TE 360) (**c**) and projective image (**d**) showing multiple cysts scattered throughout the pancreas

#173 Lymphangioma

KEY FACTS: DISEASE

- Rare benign "tumor," actually representing ectasia of lymphatic channels
- Most common in children
- Location:
  - Neck and axilla (95%)
  - Numerous other locations have been reported
- May contain serous fluid or chyle
- Abdominal lymphangiomas may also contain fat if lymphatic flow is received from the mesentery

KEY FACTS: MRI

- Fluid-containing lesion without characteristic features
  - Uni- or multilocular, round or elongated
  - May contain fat or calcifications
  - Located within or adjacent to the pancreas
- Differential diagnosis: simple cyst, pseudocyst, mucinous cystic neoplasm

References

Khandelwal M, Lichtenstein GR, Morris JB, Furth EE, Long WB (1995) Abdominal lymphangioma masquerading as a pancreatic cystic neoplasm. J Clin Gastroenterol 20:142–144

Pandolfo I, Scribano E, Gaeta M, Fiumara F, Longo M (1985) Cystic lymphangioma of the pancreas: CT demonstration. J Comp Assist Tomogr 9:209–210

Salimi Z, Fishbein M, Wolverson MK, Johnson FE (1991) Pancreatic lymphangioma: CT, MRI, and angiographic features. Gastrointest Radiol 16:248–250

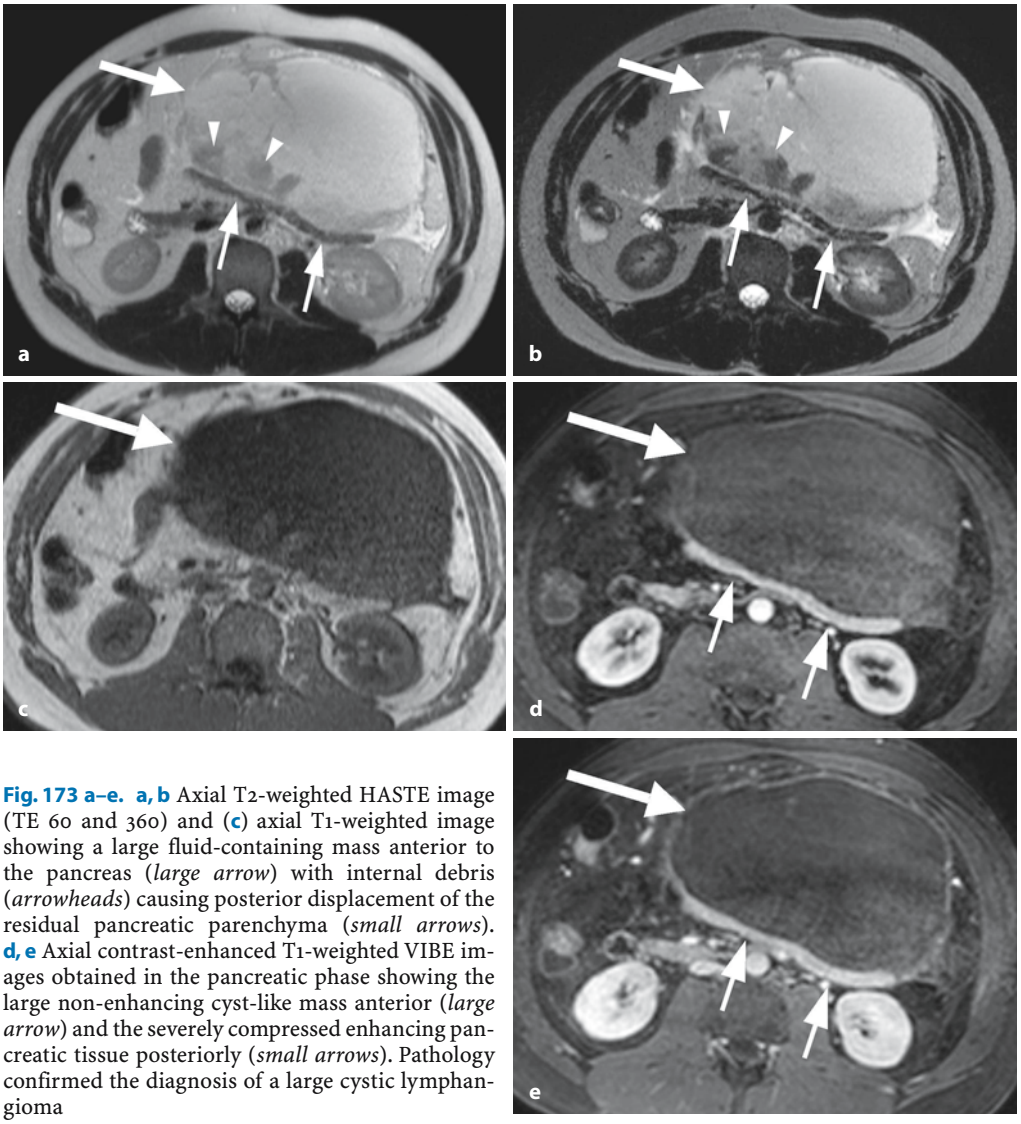

Fig. 173 a–e. **a, b** Axial T2-weighted HASTE image (TE 60 and 360) and (**c**) axial T1-weighted image showing a large fluid-containing mass anterior to the pancreas (*large arrow*) with internal debris (*arrowheads*) causing posterior displacement of the residual pancreatic parenchyma (*small arrows*). **d, e** Axial contrast-enhanced T1-weighted VIBE images obtained in the pancreatic phase showing the large non-enhancing cyst-like mass anterior (*large arrow*) and the severely compressed enhancing pancreatic tissue posteriorly (*small arrows*). Pathology confirmed the diagnosis of a large cystic lymphangioma

#174 Cystic Fibrosis

KEY FACTS: DISEASE

- Autosomal recessive multisystem disorder with widespread abnormalities of mucus-secreting exocrine glands
- Incidence: 1 in 1500
- Pancreatic disease (pathophysiology):
  - Decreased secretion of chloride, sodium, and water, followed by precipitation of relatively insoluble proteins and obstruction of small pancreatic ducts
  - Progressive dilation of the acini and ducts with secondary fibrosis, atrophy, lipomatous degeneration, and/or cyst formation
- Morphologic types:
  - Diffuse fatty pancreas
  - Combination of fat and fibrotic parenchyma residuals (liposclerosis)
  - Atrophy and fibrosis
  - Numerous cysts (pancreatic cystosis)
- Clinical features: acute pancreatitis, diabetes mellitus, cirrhosis, exocrine pancreatic insufficiency, obstructive lung disease, chronic pulmonary infection
- Prognosis: mainly determined by the progression of pulmonary obstruction and infection

KEY FACTS: MRI

- MRI findings may reflect the various stages of the disease. Appearance on T1-weighted images:
  - Mottled hyperintensity (partial fatty replacement)
  - Lobulated hyperintense pancreas (nearly complete fatty replacement)
  - Diffuse hyperintense pancreas (complete fatty replacement) (Fig. 174)
  - Atrophic or hypotrophic pancreas with normal signal intensity
  - Multiple hypointense areas corresponding to cysts (probably rare)
- Differential diagnosis depends on the stage: chronic pancreatitis (atrophy and fibrosis), von Hippel-Lindau disease (multiple pancreatic cysts)

References

Ferrozzi F, Bova D, Campodonico F et al. (1996) Cystic fibrosis: MR assessment of pancreatic damage. Radiology 198 : 875 – 879

Hernanz-Schulman M, Teele RL, Perez-Atayde et al. (1986) Pancreatic cystosis in cystic fibrosis. Radiology 158 : 629 – 631

King LJ, Scurr ED, Murugan N et al. (2000) Hepatobiliary and pancreatic manifestations of cystic fibrosis: MR imaging appearances. Radiographics 20 : 767 – 777

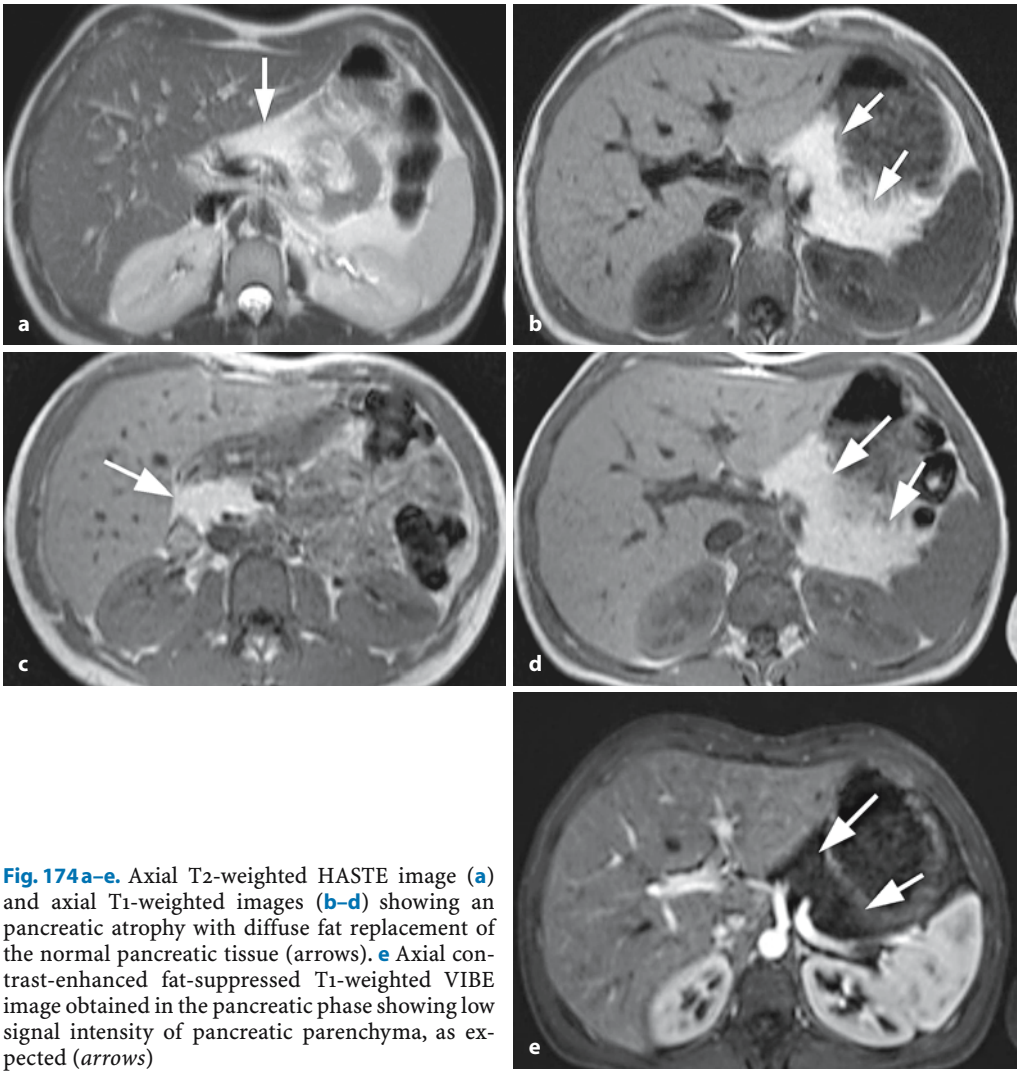

Fig. 174 a–e. Axial T2-weighted HASTE image (**a**) and axial T1-weighted images (**b–d**) showing an pancreatic atrophy with diffuse fat replacement of the normal pancreatic tissue (arrows). **e** Axial contrast-enhanced fat-suppressed T1-weighted VIBE image obtained in the pancreatic phase showing low signal intensity of pancreatic parenchyma, as expected (*arrows*)

#175 Microcystic Serous Cystadenoma

Related topics: #176 (macrocystic serous cystadenoma), #198 (mucinous cystic neoplasm)

KEY FACTS: DISEASE

- Glycogen-containing cystic tumor, virtually always benign
- Histology: small cysts containing proteinous fluid separated by thin connective tissue septa; the cysts are lined with a monolayer of epithelial cells
- ± 50 % of all cystic pancreatic neoplasms
- Ratio of women to men: 4 : 1
- Most commonly observed in middle-aged and elderly women
- Diagnosis: the cytoplasm of the cuboidal cells stains darkly (red) with periodic acid–Schiff (PAS). This positivity for PAS disappears after pretreatment with amylase, thus identifying glycogen
- Can occur anywhere in the pancreas
- Predisposing factor: von Hippel-Lindau disease

KEY FACTS: MRI

- Well-defined lesion containing multiple small (< 2 cm) cysts (Fig. 175)
- Contrast-enhanced scans usually show enhancement of septa and peripheral part of tumor (Fig. 175)
- Central calcifications (33 %): usually not observed on MRI scans
- The cysts never communicate with the pancreatic ducts (differential diagnosis with pseudocyst)
- Features distinguishing this entity from mucinous neoplasms (#198):
  - Large number of cysts
  - Small size of the cysts (< 2 cm)
  - Rich arterial blood supply

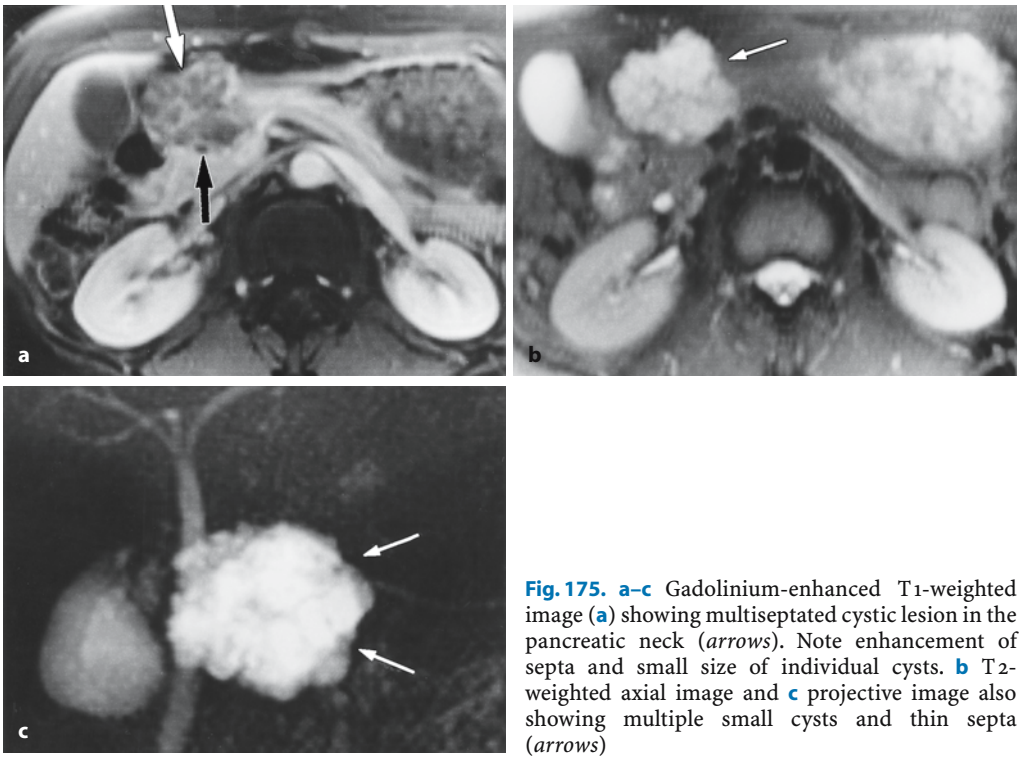

Fig. 175. a–c Gadolinium-enhanced T1-weighted image (**a**) showing multiseptated cystic lesion in the pancreatic neck (*arrows*). Note enhancement of septa and small size of individual cysts. **b** T2-weighted axial image and **c** projective image also showing multiple small cysts and thin septa (*arrows*)

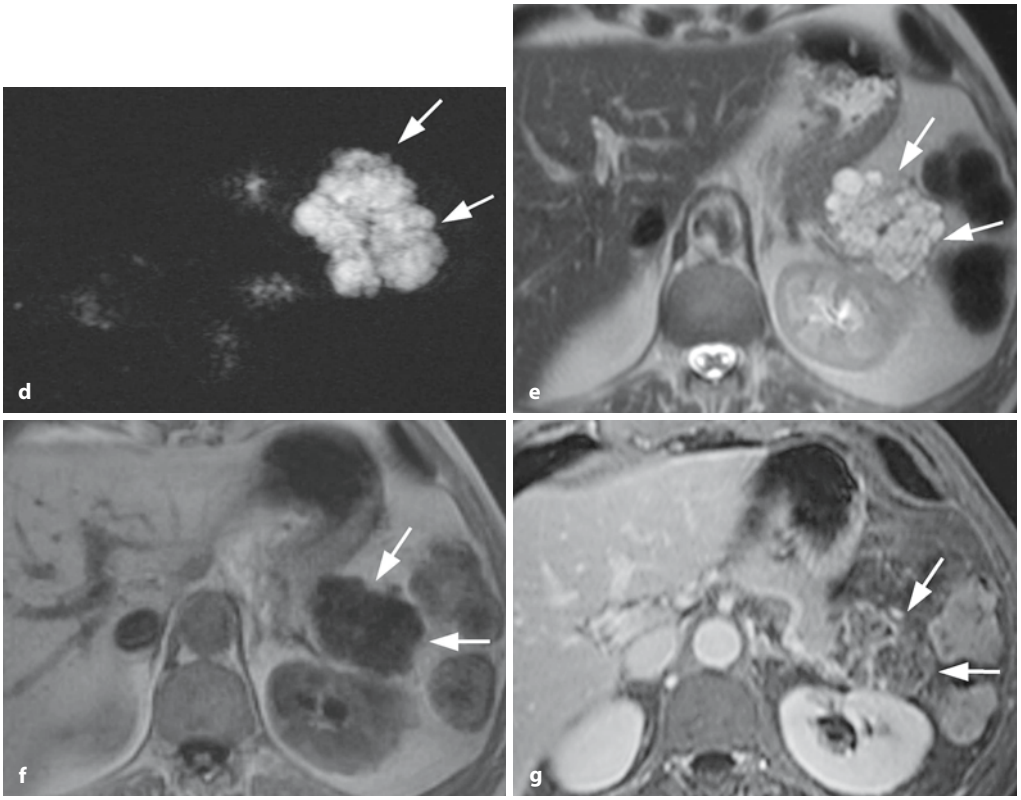

Fig. 175 d–g. (*continued)* Different patient. Projective image (**d**) and T2-weighted HASTE image (**e**) showing a multiseptated cystic lesion in the pancreatic tail containing multiple small cysts (*arrows*). **f** Axial T1-weighted image showing this lesion to be diffusely hypointense due to the multiple cysts (*arrows*). **g** Axial contrast-enhanced T1-weighted VIBE image obtained in the portal venous phase showing septal enhancement (*arrows*). Note the small size of the individual cysts

References

Compagno J, Oertel J (1978) Microcystic adenomas of the pancreas (glycogen-rich cystadenomas): a clinicopathologic study of 34 cases. Am J Clin Pathol 69 : 289 – 298

Kim YH, Saini S, Sahani D, Hahn PF, Mueller P, Auh Y (2005) Imaging diagnosis of cystic pancreatic lesions: pseudocyst versus nonpseudocyst. RadioGraphics 25 : 671 – 685

Procacci C, Graziani R, Bicego E et al. (1997) Serous cystadenoma of the pancreas: report of 30 cases with emphasis on the imaging findings. J Comp Assist Tomogr 21 : 373 – 382

#176 Macrocystic Serous Cystadenoma

Related topics: #175 (microcystic serous cystadenoma), #198 (mucinous cystic neoplasm)

KEY FACTS: DISEASE

- Macrocystic variant of serous cystadenoma (cysts may measure up to 8 cm, often with one large dominant cyst and several smaller daughter cysts)
- Histology: similar to the microcystic variant
- Extremely rare
- Only benign cases reported

KEY FACTS: MRI (FIG. 176)

- Identical to MR features of mucinous cystic tumor (see #198)

References

Lewandrowski K, Warshaw A, Comptom C (1992) Macrocystic cystadenoma of the pancreas: a morphologic variant differing from microcystic adenoma. Hum Pathol 23 : 871 – 875

Mori K, Takeyama S, Hirosawa H et al. (1995) A case of macroscopic serous cystadenoma of the pancreas. Int J Pancreatol 17 : 91 – 93

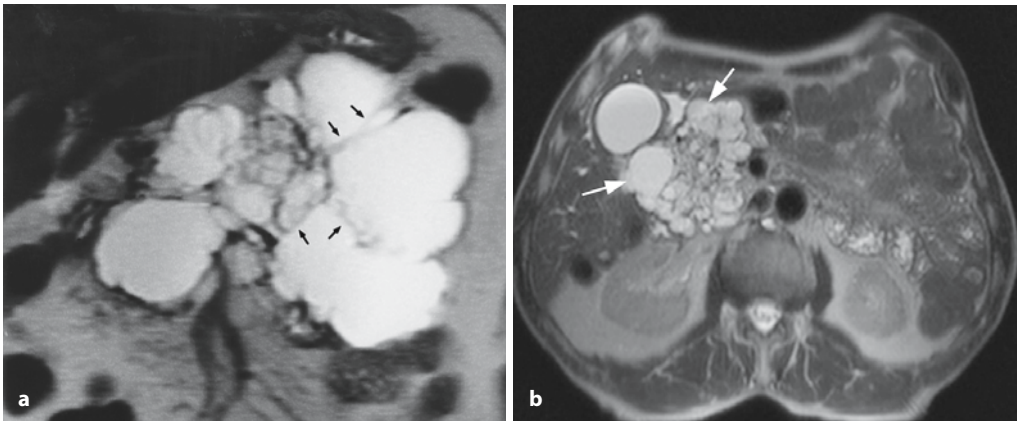

Fig. 176. a Coronal T2-weighted image showing cystic lesion with multiple septa (*arrows*) and several large cystic components. **b** Different patient. T2-weighted HASTE image (TE 60) showing a large multiseptated cystic lesion in the pancreatic head containing innumerable cysts. Note the presence of several larger cystic components (*arrows*)

#177 Benign Neuroendocrine Tumors

Related topic: #197 (malignant neuroendocrine tumors)

KEY FACTS: DISEASE

- Synonym: islet cell tumors
- Histology: tumors composed of neuroendocrine cells characterized by the expression of neuroendocrine markers
- Incidence: 0.4 % – 1.5 % of autopsies
- Nearly 85 % of endocrine pancreatic tumors are functioning tumors
- The incidence of malignancy is correlated with:
  - Histologic subtype (see #197): insulinomas are usually benign (> 90 %); all other subtypes are more likely to be malignant
  - Size: the smaller the tumor, the less likely malignant behavior is (Buetow et al. 1995)
- Predisposing factor: type-1 multiple endocrine neoplasia (MEN)

KEY FACTS: MRI

- Signal intensity:
  - T1: nearly invariably hypointense
  - T2: variable, most commonly hyperintense, sometimes (partially) cystic (Fig. 177 a – f and g – j)
- On dynamic contrast-enhanced scans, most endocrine tumors enhance more than the surrounding pancreatic parenchyma (rich arterial blood supply)
- The conspicuity on contrast-enhanced scans is variable and depends on:
  - The "baseline" intensity of the tumor and surrounding parenchyma
  - The degree of vascularization of both tissues
  - The imaging parameters (e.g., delay between the injection and the scan) (Fig. 177 n – q)
- Aspect on contrast-enhanced scans
  - Hyperintense (common)
  - Hypointense with hyperintense enhancing rim (common)
  - Isointense (hypointense tumors not uncommonly become invisible after intravenous administration of contrast agent) (Fig. 177 n – q)
  - Hypointense
- *Note:* Benign functioning tumors (particularly insulinomas and gastrinomas) are usually small (< 2 cm in the large majority of cases); detection requires an optimized technique and special attention
- *Note:* Gastrinomas associated with type-1 multiple endocrine neoplasia syndrome are even smaller (< 1 cm), commonly multicentric, and predominantly located in the wall of the duodenum
- Differential diagnosis of hypervascular pancreatic tumors:
  - Primary: endocrine tumors; serous cystic tumor (enhancement of periphery and septa); solid and papillary cystic neoplasm (rare)
  - Secondary: metastases from angiosarcoma, melanoma, carcinoid, renal adenocarcinoma, adrenal carcinoma, thyroid carcinoma, etc.

References

Buetow PC, Parrino TV, Buck JL et al. (1995) Islet cell tumors of the pancreas: pathologic-imaging correlation among size, necrosis and cysts, calcification, malignant behaviour, and functional status. AJR Am J Roentgenol 165 : 1175 – 1179

Kraus BB, Ros PR (1994) Insulinoma: diagnosis with fat-suppressed MR imaging. AJR Am J Roentgenol 162 : 69 – 70

Pavone P, Mitchell DG, Leonetti F et al. (1993) Pancreatic beta-cell tumors: MRI. J Comput Assist Tomogr 17 : 403 – 407

Sheth S, Hruban RK, Fishman EK (2002) Helical CT of islet cell tumors of the pancreas: typical and atypical manifestations. AJR Am J Roentgenol 179 : 725 – 730

Van Hoe L, Vanbeckevoort D, Baert AL (1997) Endocrine tumors of the pancreas: computed tomography and magnetic resonance imaging. Chir Gastroenterol 13 : 301 – 306

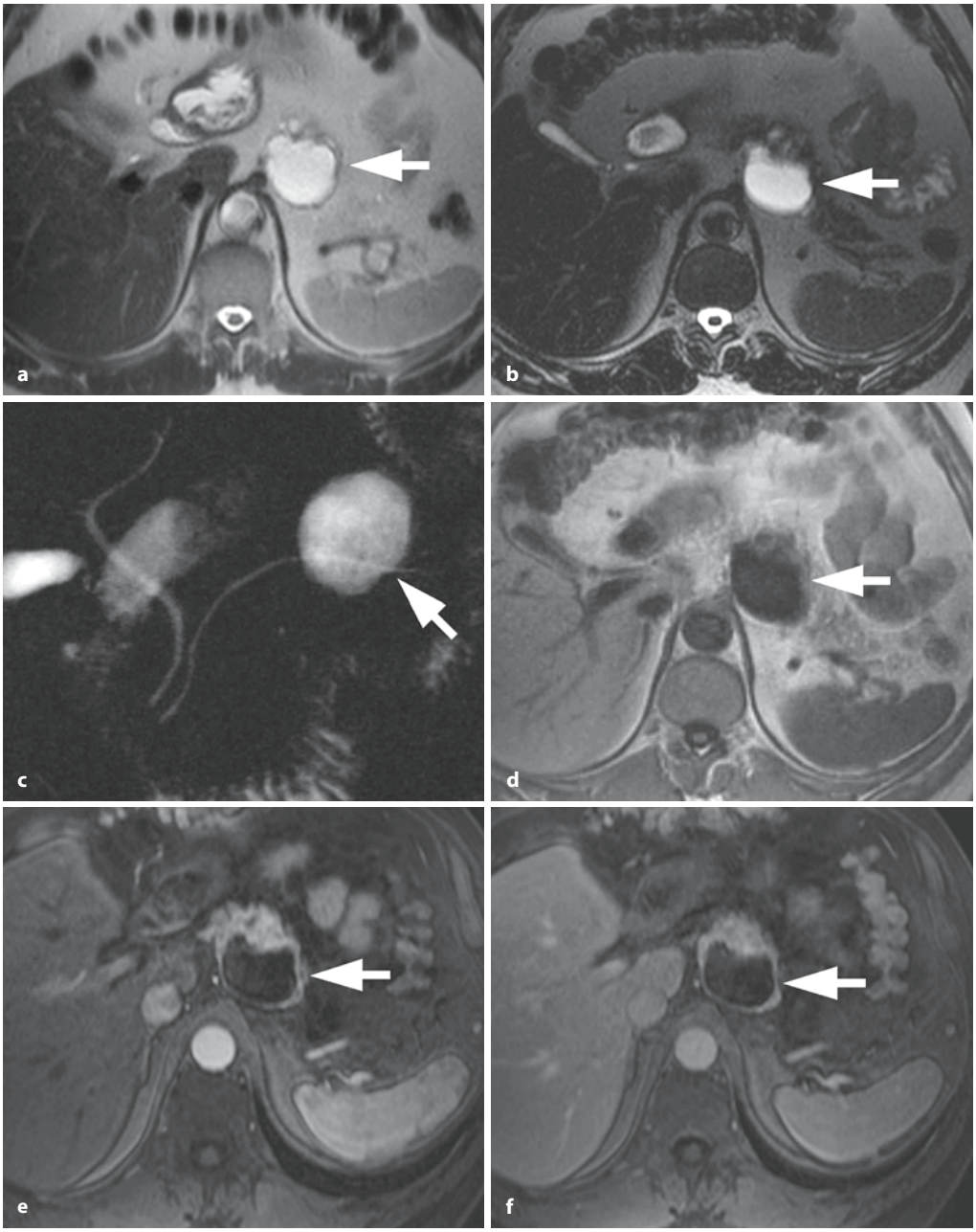

Fig. 177 a–f.

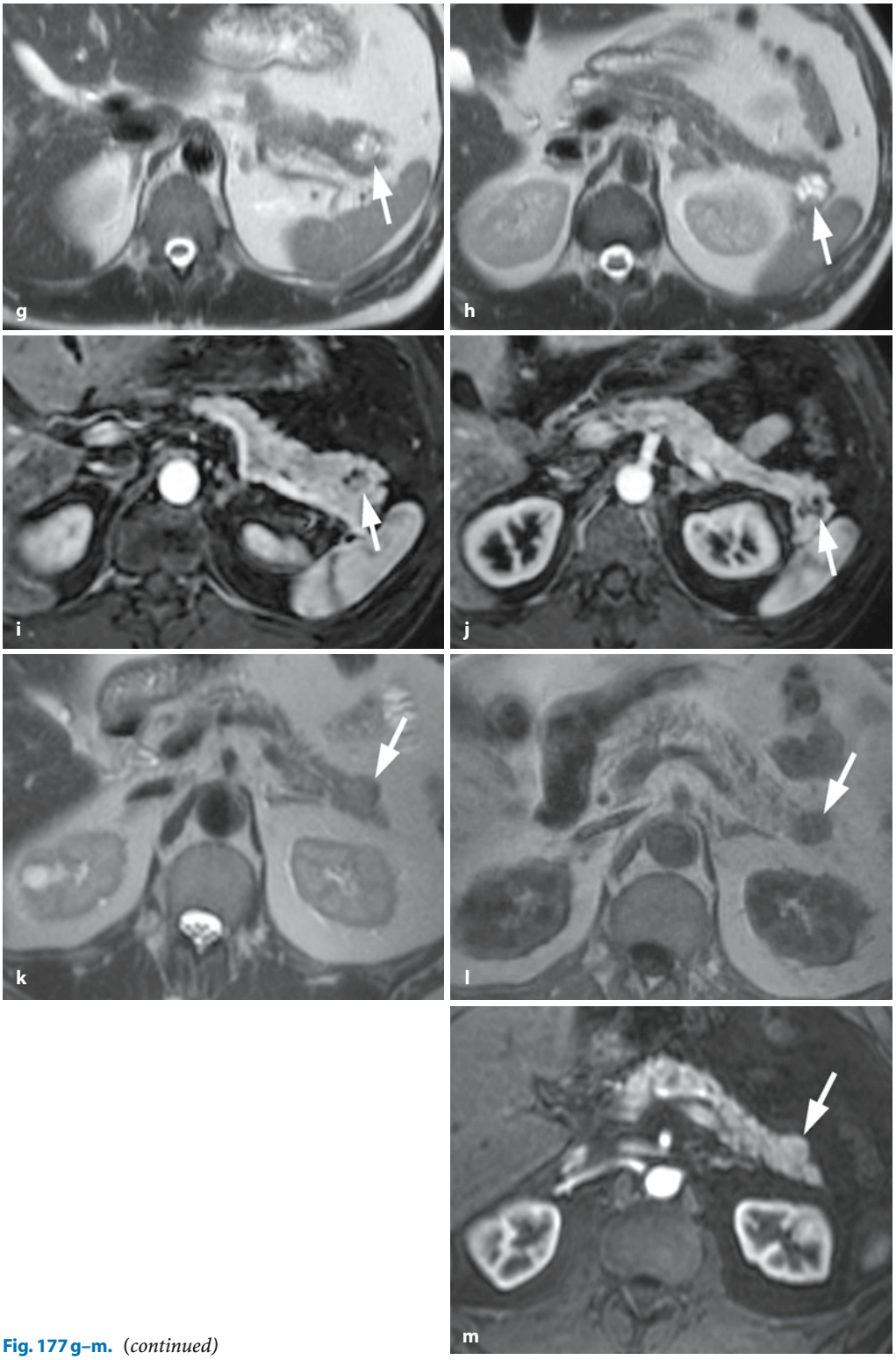

Fig. 177 g–m. (*continued*)

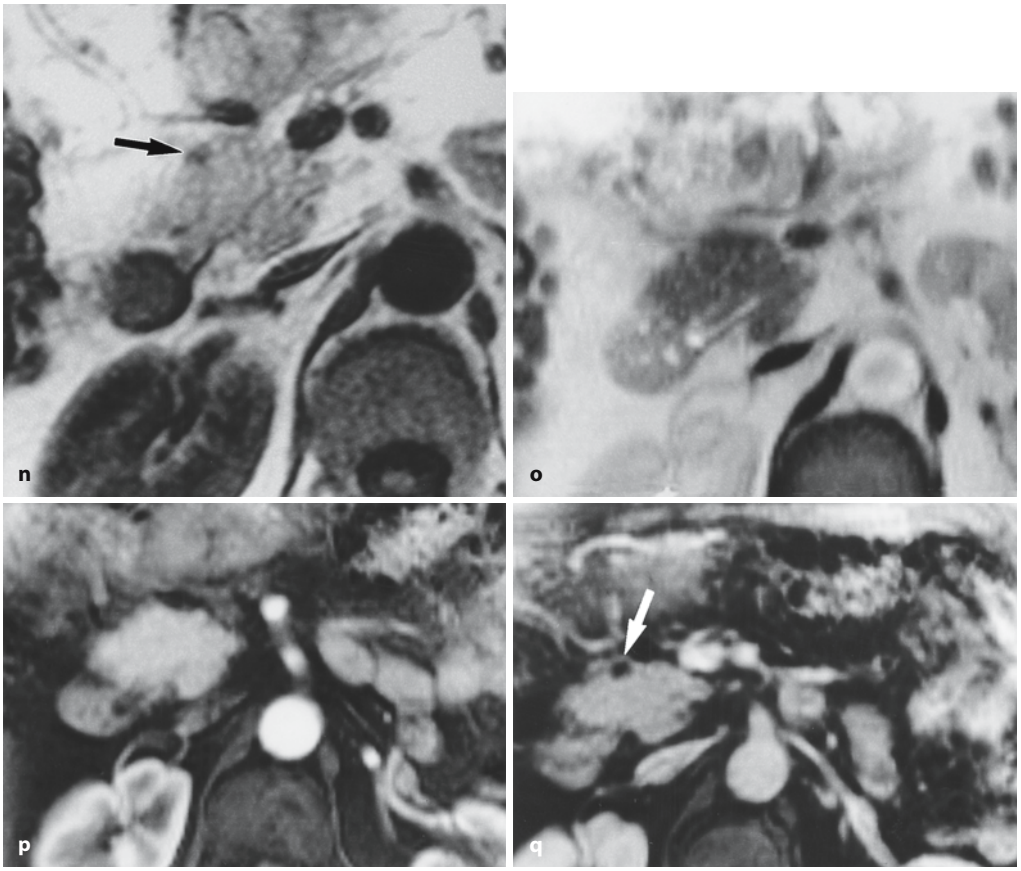

Fig. 177 a–f. Axial T2-weighted HASTE images (**a, b**) (TE 60 and 360) and projective image (**c**) showing a tick-walled cystic lesion in the pancreatic body (*arrow*). Axial pre- (**d**) and post-contrast (**e, f**) T1-weighted images show a strong enhancement of the anterior wall of this cystic lesion (*arrow*). Final diagnosis: cystic neuroendocrine tumor without obvious signs of malignancy. **g–j** Patient with MEN-I syndrome and multiple neuroendocrine pancreatic tumors. **g, h** Axial T2-weighted HASTE images and (**i, j**) axial contrast-enhanced T1-weighted VIBE images obtained in the pancreatic phase show two partially cystic lesions in the pancreatic tail. **k–m** Different patient. Axial T2-weighted HASTE image (**k**) showing an anterior bulge in the pancreatic tail. Axial T1-weighted image (**l**) reveals a hypointense nodule at this location (*arrow*). **m** Axial contrast-enhanced T1-weighted VIBE image obtained in the pancreatic phase showing this mass to be isointense to the surrounding normal pancreatic tissue (*arrow*), this feature points to the strong enhancement of the lesion. **n–q** Patient with insulinoma. **n** T1-weighted image showing small hypointense lesion in the pancreatic neck (*arrow*). **o** The lesion is isointense on the T2-weighted image. **p** Contrast-enhanced T1-weighted image obtained in the pancreatic phase fails to reveal the lesion. **q** The lesion becomes hypointense again on images obtained in the portal venous phase (*arrow*). These features point to strong enhancement in the early phase and early washout of contrast medium

#178 Schwannoma

KEY FACTS: DISEASE

- Tumor derived from the lining cells of the nerve sheath (Schwann cells)
- Synonyms: neurinoma, neurilemmoma
- Pathology:
  - Typically well encapsulated, rounded
  - Cystic degeneration, necrosis, and hemorrhage common
  - Consists of Antoni A areas (high cellularity) and Antoni B areas (myxoid substance)
- To be distinguished from neurofibroma (proliferation of Schwann cells and fibroblasts; associated with Recklinghausen's disease, i. e., neurofibromatosis I)
- Incidence: 5 % – 10 % of tumors of the central nervous system; rare in the abdomen
- Age peak: 30 – 60 years
- Usually no symptoms

KEY FACTS: MRI (FIG. 178)

- Signal intensity: typically high signal intensity on T 2-weighted images (cystic/necrotic component, myxoid material)
- Usually strong enhancement
- Clues for differential diagnosis with other retroperitoneal tumors:
  - High signal intensity (T 2)
  - Rounded form, sharp delineation

References

Cerofolini E, Landi A (1991) MR of benign peripheral nerve sheath tumors. J Comput Assist Tomogr 15 : 593 – 597

Kim SH, Choi BI, Han MC, Kim YI (1992) Retroperitoneal neurilemoma: CT and MR findings. AJR Am J Roentgenol 159 : 1923 – 1026

Urban BA, Fishman EK, Hruban RH, Cameron JL (1992) CT findings in cystic schwannoma of the pancreas. J Comp Assist Tomogr 16 : 492 – 493

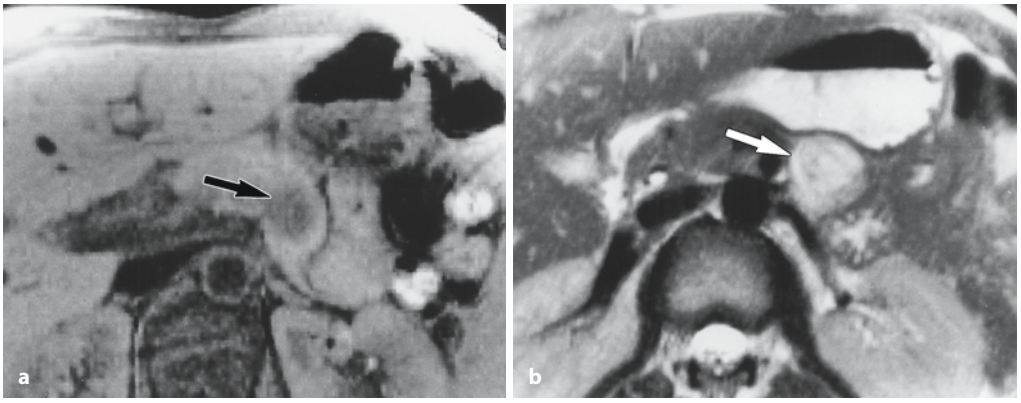

Fig. 178 a, b. **a** T1-weighted image showing a hypointense lesion apparently surrounded by pancreatic parenchyma (*arrow*). **b** T2-weighted image showing the tumor as a markedly hyperintense mass (*arrow*). The tumor originated from the mesenteric root adjacent to the pancreas

#179 Granulomatous Disease of the Pancreas

KEY FACTS: DISEASE

- Granulomatous involvement of the pancreas may (rarely) be seen in sarcoidosis, tuberculosis, fungal diseases, cat scratch disease, and lymphoma
- Sarcoidosis:
  - Granulomatous disease of unknown etiology
  - Lung and lymph nodes most commonly affected
  - Other organs sometimes involved: eyes, liver, skin, salivary glands, spleen, pericardium, peritoneum
  - Diagnosis: bronchoalveolar lavage (BAL)

KEY FACTS: MRI

- Common findings in abdominal sarcoidosis:
  - Enlarged lymph nodes
  - Hepatosplenomegaly
  - Focal lesions in liver and spleen
- Uncommon findings:
  - Focal lesion(s) in the pancreas with or without displacement of the pancreatic duct (Fig. 179)
  - Narrowing of the distal common bile duct (Toda et al. 1994)
  - Ascites (peritoneal involvement/congestive heart failure)
- Differential diagnosis: although rare, sarcoidosis should be considered in the differential diagnosis of focal pancreatic masses not typical of adenocarcinoma

References

Bonhomme A, Dhadamus A, De Bie P, Van Hoe L, Baert AL (1997) Pancreatic involvement in systemic sarcoidosis: CT findings. J Belge Radiol 80 : 116 – 117

Caldwell JH, Evans WE (1978) Granuloma (sarcoid?) of the pancreas. Am J Gastroenterol 69 : 320 – 322

Purdy DJ, Levine EJ, Forsthoefel KJ, Fromkes JJ (1994) Periampullary pseudotumor secondary to granulomatous disease. Am J Gastroenterol 89 : 2087 – 2088

Toda K, Souda S, Yoshikawa Y, Momiyama T, Ohshima M (1994) Narrowing of the distral common bile duct and the portal vein secondary to pancreatic sarcoidosis. Am J Gastroenterol 89 : 1259 – 1261

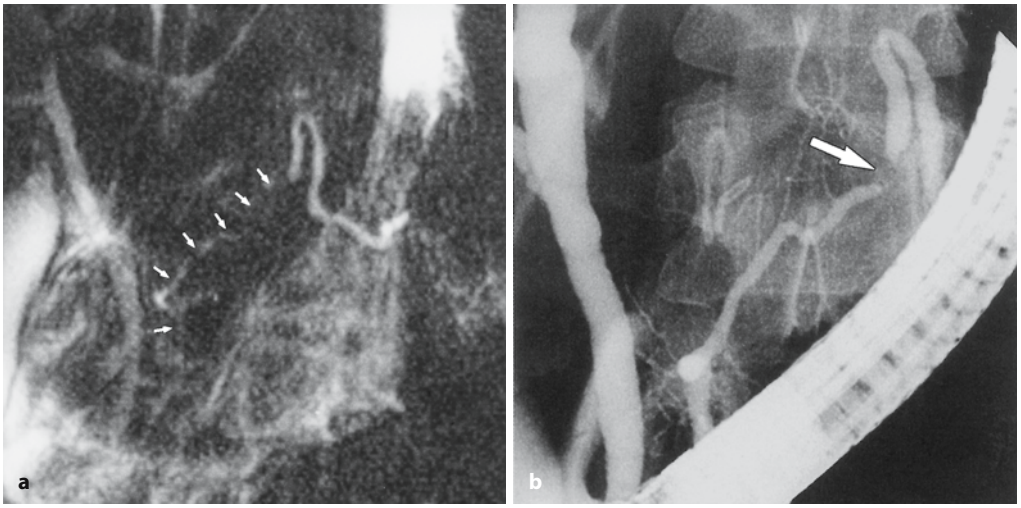

Fig. 179 a, b. Patient with sarcoidosis. **a** Projective MR image showing apparent narrowing of the pancreatic duct in the pancreatic body and neck (*arrows*). **b** ERCP image showing focal narrowing (*arrow*). Overestimation of the length of the stenosis by MRCP is related to the lack of distention (no retrograde injection of contrast material; see #23). Also note increased background signal intensity in **a**, caused by pancreatitis after ERCP

#180 Hemochromatosis

KEY FACTS: DISEASE

- Excess iron deposition in various parenchymal organs leading to organ damage
- Autosomal recessive inheritance
- Organs especially affected: liver, pancreas, heart
- Basic disorder: mucosal defect in the intestinal wall resulting in increased absorption of intestinal iron
- Symptoms: hyperpigmentation (90 %), hepatomegaly (90 %), arthralgia (50 %), diabetes (30 %), hypogonadism
- Complications:
  - Periportal fibrosis and cirrhosis
  - Hepatocellular carcinoma (14 % – 30 %)
- Differential diagnosis: secondary hemochromatosis (hemosiderosis) (Fig. 180 c):
  - Iron overload due to blood transfusions
  - Storage of iron mainly in the reticuloendothelial system (liver, spleen)
  - Little clinical significance

KEY FACTS: MRI

- Pancreatic parenchyma exhibits very low signal intensity on T 1- and T 2-weighted images
- Always associated with low signal intensity of liver tissue

References

Runge VM, Clanton JA, Smith FW et al. (1983) NMR of iron and copper disease states. AJR Am J Roentgenol 141 : 943 – 948

Yoon DY, Choi BI, Han JK, Park MO, Suh SJ (1994) MR findings in secondary hemochromatosis: transfusional versus erythropoietic. J Comput Asist Tomogr 18 : 416 – 419

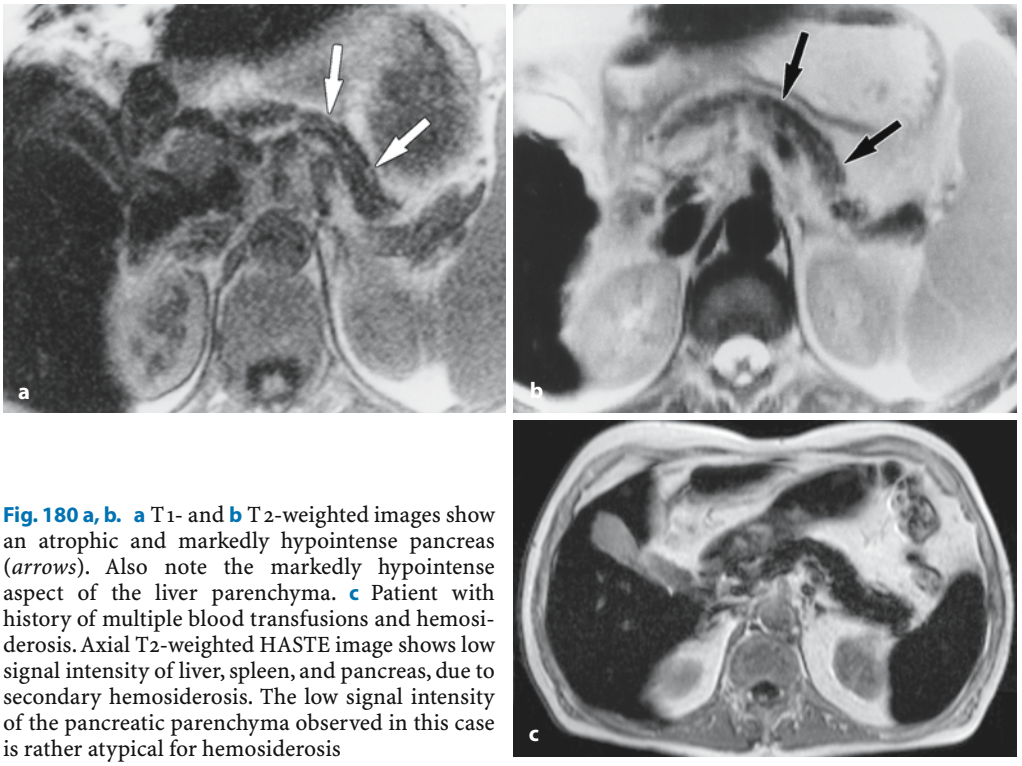

Fig. 180 a, b. **a** T1- and **b** T2-weighted images show an atrophic and markedly hypointense pancreas (*arrows*). Also note the markedly hypointense aspect of the liver parenchyma. **c** Patient with history of multiple blood transfusions and hemosiderosis. Axial T2-weighted HASTE image shows low signal intensity of liver, spleen, and pancreas, due to secondary hemosiderosis. The low signal intensity of the pancreatic parenchyma observed in this case is rather atypical for hemosiderosis

6.3 Traumatic, Postoperative, and Iatrogenic Abnormalities

#181 Pancreatic Duct Injury

Related topics: #48 (sequelae of direct liver trauma), #113 (blunt gallbladder trauma)

KEY FACTS: DISEASE

- Relatively uncommon: 1%–12% of all abdominal injuries
- Cause: blunt or penetrating injury
- Classification of pancreatic trauma:
  - Grade 1: contusion
  - Grade 2: small laceration
  - Grade 3: laceration with rupture of the main pancreatic duct
  - Grade 4: crush injury
- Most common location of laceration: pancreatic neck (compression against the first lumbar vertebra)
- Associated disease: other abdominal injuries in 90%
- Complications of grade 3 injuries:
  - Fistula
  - Pseudocyst
  - Stricture with or without recurrent pancreatitis
  - Focal necrosis
  - Abscess formation

KEY FACTS: MRI (FULCHER ET AL. 2000)

- MRI usually plays no role in the acute setting, but may be used for follow-up purposes
- (Continued) leakage, strictures, pseudocysts, atrophy, and/or ductal dilation may be shown

References

Carr ND, Cairns SJ, Lees WR, Russell RC (1989) Late complications of pancreatic trauma. Br J Surg 76:1244–1246

Fulcher AS, Turner MA, Yelon JA et al. (2000) Magnetic resonance cholangiopancreatography (MRCP) in the assessment of pancreatic duct trauma and its sequelae: preliminary findings. J Trauma 48:1001–1007

Van Hoe L, Gryspeerdt S, Oyen R, Baert AL (1996) Retroperitoneal trauma. In: Heller M (ed) Radiology of trauma. Springer, Berlin Heidelberg New York, pp 163–192

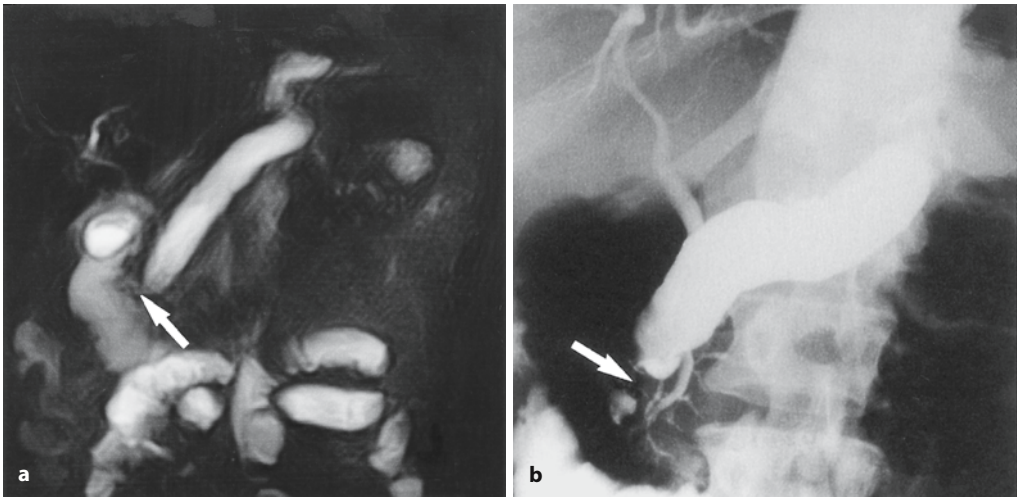

Fig. 181 a, b. **a** Projective MR image and **b** ERCP image showing marked dilation of the pancreatic duct secondary to ductal stenosis in the pancreatic head (*arrow*). The patient suffered a severe blunt trauma to the pancreas as a child

#182 Complications of Pancreatic Transplantation (1): Pancreatitis

Related topic: # 149 (postoperative anatomy: after pancreatic transplantation)

KEY FACTS: DISEASE

- Postoperative pancreatitis commonly occurs immediately after surgery and usually subsides within 4 weeks
- Incidence: 1.8 %
- Causes of *persistent* pancreatitis (acute/relapsing/chronic):
  - Urinary reflux
  - Stenosis/obstruction of the pancreatic duct or anastomosis
- Complications:
  - Fistula
  - Ascites
  - Pseudocyst

KEY FACTS: MRI

- Classical MR features of acute pancreatitis (see # 151 – 157)
  - Diffuse parenchymal edema
  - Peripancreatic fluid
- Features of chronic pancreatitis: see # 160 – 168 (Fig. 182 a, b)
- Pancreatic duct dilation may be observed if obstruction or reflux is present
- Signs of complications: pseudocysts, fistula, etc.
- *Note:* The differentiation between pancreatitis and rejection (see # 183) may be difficult. Features more or less specific for pancreatitis are:
  - Ductal dilation
  - Large fluid collections/ascites
  - Focal areas of necrosis

References

Moudry-Munns K, Gruessner A, Sutherland DE (1994) Analysis of United States pancreas transplant registration data. J Transplant Coordination 4 : 18 – 22

Yuh WT, Hunsicker LG, Nghiem DD et al. (1989) Pancreatic transplants: evaluation with MR imaging. Radiology 170 : 171 – 177

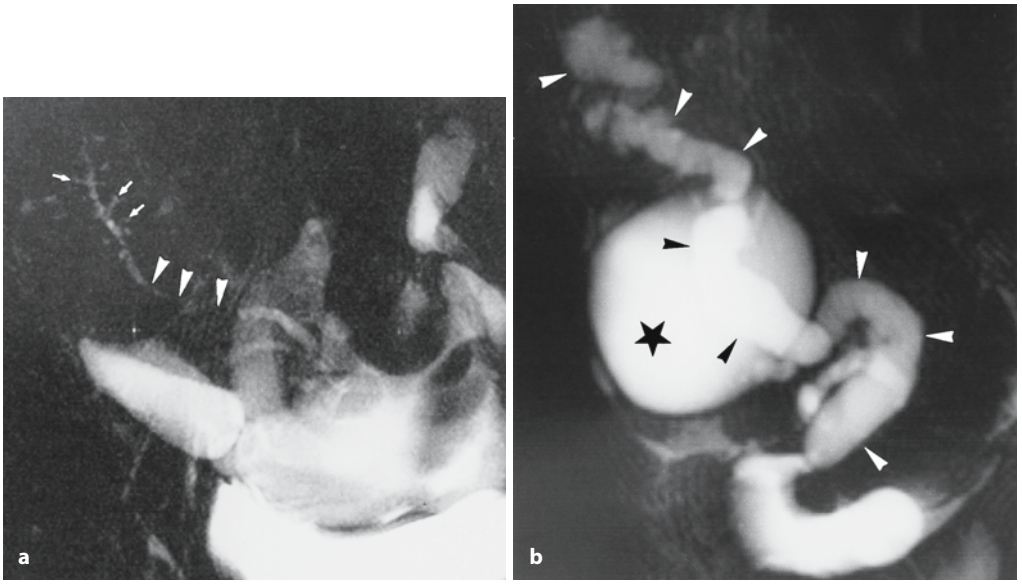

Fig. 182. a Projective image showing long segmental stenosis of the pancreatic duct (*arrowheads*). Also note the slight dilation of the pancreatic duct in the tail, with several dilated side branches (*arrows*). It remained unclear in this patient whether the stenosis was the primary lesion or a secondary lesion in preexisting chronic pancreatitis. **b** Projective MR image showing a dilated pancreatic duct (*arrowheads*), a small fluid exudate, and a large pseudocyst (*asterisk*): chronic obstructive pancreatitis secondary to an anastomotic stricture (see also # 168)

#183 Complications of Pancreatic Transplantation (2): Other Complications

Related topic: #149 (postoperative anatomy: after pancreatic transplantation)

KEY FACTS: DISEASE

- Major causes of graft loss include:
  - Rejection (35%)
  - Vascular thrombosis (12%–20%)
  - Sepsis (8%–22%)
- Other complications:
  - Hemorrhage
  - Infarction
  - Pseudoaneurysm (may be related to biopsy)
  - Anastomotic leak

KEY FACTS: MRI

- Acute rejection:
  - Usually large edematous graft (as in pancreatitis)
  - Dynamic contrast-enhanced MRI shows delayed parenchymal enhancement (probably not specific)
- Chronic rejection:
  - Small graft
  - Low signal intensity on T1- and T2-weighted images (fibrosis)
- Hematoma: signal intensity usually characteristic of blood (see #51)
- Abscess (Fig. 183):
  - Typical fluid collection with thick, irregular wall
  - Air–fluid level or multiple air bubbles may be seen
  - Differential diagnosis with pseudocyst, loculated ascites, and urinoma may be difficult
- Secretin-augmented MRCP and MR perfusion measurements have been proposed to differentiate between functional and dysfunctional grafts (Heverhagen et al. 2004)

References

Fernandez MP, Bernardino ME, Neylan JF, Olson RA (1991) Diagnosis of pancreatic transplant dysfunction: value of gadopentetate dimeglumine-enhanced MR imaging. AJR Am J Roentgenol 156:1171–1176

Snider JF, Hunter DW, Kuni CC, Castenada-Zuniga WR, Letourneau JG (1991) Pancreatic transplantation: radiologic evaluation of vascular complications. Radiology 178:749–753

Heverhagen JT, Wagner HJ, Ebel H et al. (2004) Pancreatic transplants: noninvasive evaluation with secretin-augmented MR pancreatography and MR perfusion measurements – preliminary results. Radiology 233:273–280

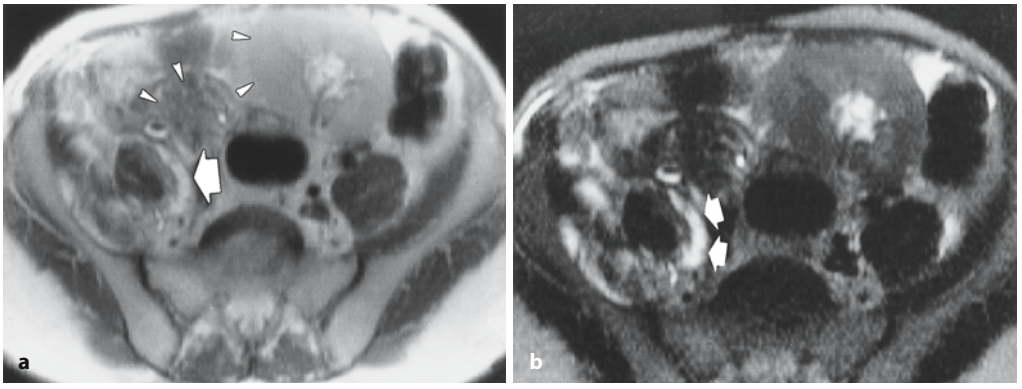

Fig. 183 a, b. **a** Moderately T2-weighted image showing transplanted pancreas and kidney (*arrowheads*). Also note the small hyperintense area more dorsally (*arrows*). **b** Heavily T2-weighted image confirming the presence of fluid in the psoas compartment (*arrows*). The final diagnosis was psoas abscess

#184 Complications of Partial Pancreatic Resection

Related topic: #148 (postoperative anatomy: after partial resection)

KEY FACTS: DISEASE

- Surgical procedures: see #148
- Main complications:
  - Anastomotic leak
  - Anastomotic stenosis
  - Tumor recurrence
  - Intraductal lithiasis

KEY FACTS: MRI

- Specific features depend on the type of disease (e.g., stricture, fluid collection)
- *Note:* Adequate visualization of the normal and pathologic anastomosis requires sufficient filling of the draining jejunal loop
- *Note:* Once early postoperative edema has disappeared, anastomotic leaks and stenoses as well as recurrent tumor are usually easily recognized

References

Lepanto L, Gianfelice D, Déry R, Dagenais M, Lapointe R, Roy A (1994) Postoperative changes, complications, and recurrent disease after Whipple's operation: CT features. AJR Am J Roentgenol 163 : 841 – 846

Trerotola SO, Jones B, Crist DW, Cameron JL (1989) Pylorus-preserving Whipple pancreaticoduodenectomy: postoperative evaluation. Radiology 171 : 735 – 738

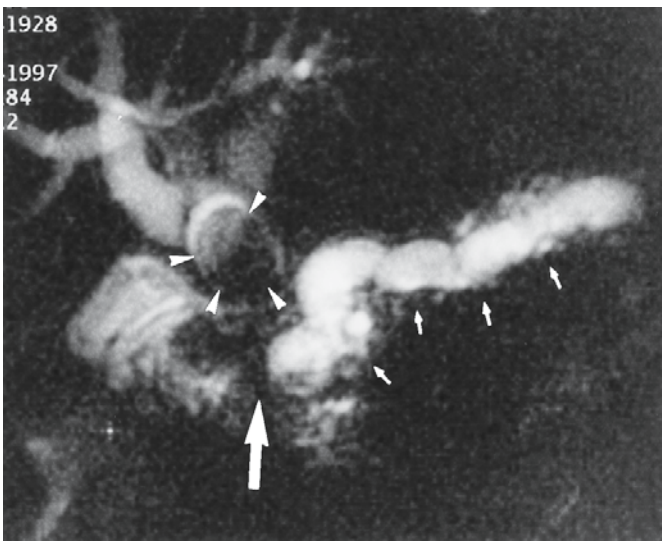

Fig. 184. Patient who had undergone a Whipple operation and subsequently presented with jaundice. Projective MR image showing marked obstructive dilation of the pancreatic duct, secondary to an anastomotic stricture (*arrows*). The intraheptratic ducts are also dilated and contain a large stone (*arrowheads*)

6.4 Malignant Tumors and Tumors with Malignant Potential

#185 Adenocarcinoma, General

KEY FACTS: DISEASE

- Fourth to fifth leading cause of cancer death in the United States
- Incidence in autopsy series: 2%
- Age peak: seventh decade
- Resectable at presentation: 8%–15%
- CA 19-9 increased in 80%–90%
- Origin:
  - Exocrine ductal epithelium: 99%
  - Acinar portion of the pancreatic gland: 1%
- Extent (Cubilla et al. 1979)
  - 65% of patients have advanced local disease or distant metastases
  - 21% have local disease with spread to regional lymph nodes
  - 14% have tumor confined to the pancreas
- Metastases
  - Liver: 30%–60%
  - Regional lymph nodes: 15%–28%
  - Peritoneum: 7%–10%
  - Other sites: e.g., lung, pleura, bone
- Symptoms:
  - Epigastric pain radiating to the back
  - Obstructive jaundice
  - New-onset diabetes, steatorrhea
- Five-year survival rate: 1%–5%

References

Cubilla AL, Fitzgerald PJ (1979) Cancer of the pancreas (nonendocrine): a suggested morphological classification. Semin Oncol 6 : 285–297

Warshaw AL, Fernandez-del Castillo C (1992) Pancreatic carcinoma. New Engl J Med 326 : 455–465

#186 Adenocarcinoma, Signal Intensity

KEY FACTS: MRI

- Signal intensity:
  - Nearly invariably hypointense on T1-weighted magnetization-prepared snapshot gradient echo images (see #9)
  - May be isointense, however, if the surrounding pancreatic tissue is abnormal (pancreatitis)
  - Iso- or hyperintense on T2-weighted images
  - Usually hypointense on contrast-enhanced scans
- Technical remarks about contrast-enhanced scans:
  - Rapid bolus injection is mandatory
  - Timing is important: imaging should be done in the pancreatic phase (± 40 s after injection)
- *Note:* Value of sequences:
  - T1 much better than T2 for tumor detection
  - Magnetization-prepared snapshot gradient echo particularly reliable
  - Contrast-enhanced scans often required for preoperative evaluation (assessment of vascular anatomy, detection of lymph node metastases)

References

Gabata T, Matsui O, Kadoya M et al. (1994) Small pancreatic adenocarcinomas: efficacy of MR imaging with fat suppression and gadolinium enhancement. Radiology 193 : 683 – 688

Ichikawa T, Haradome H, Hachiya J et al. (1997) Pancreatic ductal adenocarcinoma: preoperative assessment with helical CT versus dynamic MR imaging. Radiology 202 : 655 – 662

Kelekis NL, Semelka RC (1997) MRI of pancreatic tumors. Eur Radiol 7 : 875 – 886

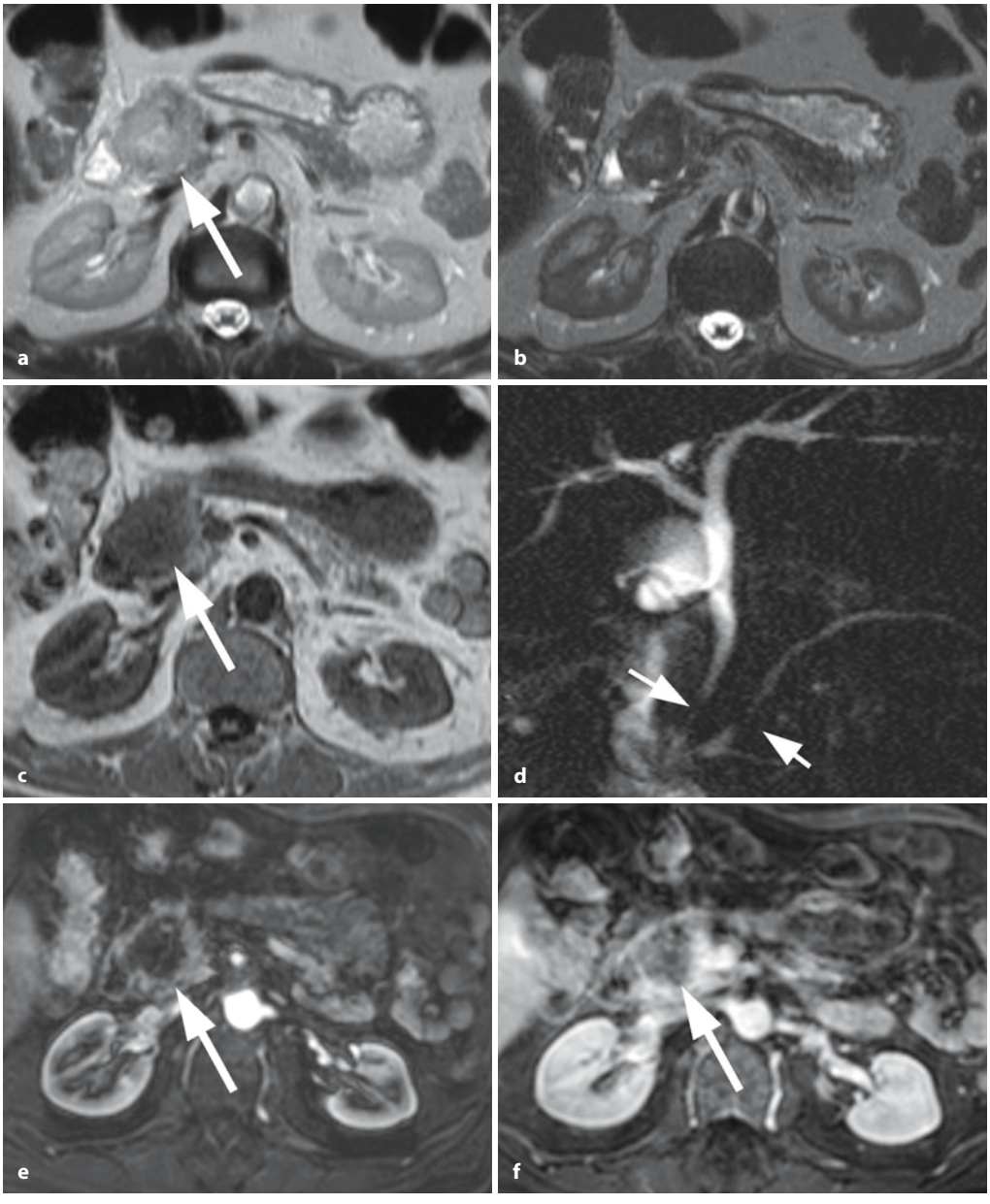

Fig. 186 a–f. Axial T2-weighted HASTE images (TE 60 and 360) (**a, b**) and (**c**) axial T1-weighted image showing a focal lesion in pancreatic head (*arrows*): adenocarcinoma. The lesion is markedly hypointense to normal pancreatic tissue on the T1-weighted image. **d** Projective image showing focal narrowing of the distal common bile duct and pancreatic duct, approximately at the same level (double duct sign) (*arrows*). Note nearly normal size of proximal pancreatic duct, which is an unusual finding. **e, f** Axial contrast-enhanced T1-weighted VIBE images obtained in the pancreatic and late venous phase showing no enhancement of the tumor in the pancreatic phase and only minimal enhancement of the tumor in the late venous phase (*arrow*)

#187 Adenocarcinoma, Ductal Changes

KEY FACTS: MRI

- Classical patterns of involvement of the main duct (Fig. 187a):
  - (Apparent) occlusion (> 50% on MRCP)
  - Stenosis, usually irregular with abrupt termination
  - Dilation of the proximal main duct
  - Double duct sign (Freeny et al. 1978; e.g., see #90, Fig. 187b–e, 188a, b); sometimes "four-segment sign" (Kim et al. 2002)

- Side branches may be:
  - Invisible (normal or obliterated)
  - Dilated (obstruction; may appear like bizarre cystic pockets located adjacent to the tumor)
  - Distorted/displaced
- Comments:
  - Long strictures of the pancreatic duct, especially in the body or tail, are most commonly malignant (see, however, #164, #167 and #169); short strictures are more common in chronic alcoholic pancreatitis
  - Projective images should be obtained routinely: subtle ductal changes may herald the presence of small tumors

References

Freeny PC, Bilbao MK, Katon RM (1976) "Blind" evaluation of endoscopic retrograde cholangiopancreatography (ERCP) in the diagnosis of pancreatic carcinoma: the "double duct" and other signs. Radiology 119 : 271 – 274

Kim JH, Kim MJ, Chung JJ et al. (2002) Differential diagnosis of periampullary carcinomas at MR imaging. Radiographics 22 : 1335 – 1352

Stewart E, Vennes J, Geenen J (1977) Atlas of endoscopic retrograde cholangiopancreatography. Mosby, St Louis, p 182

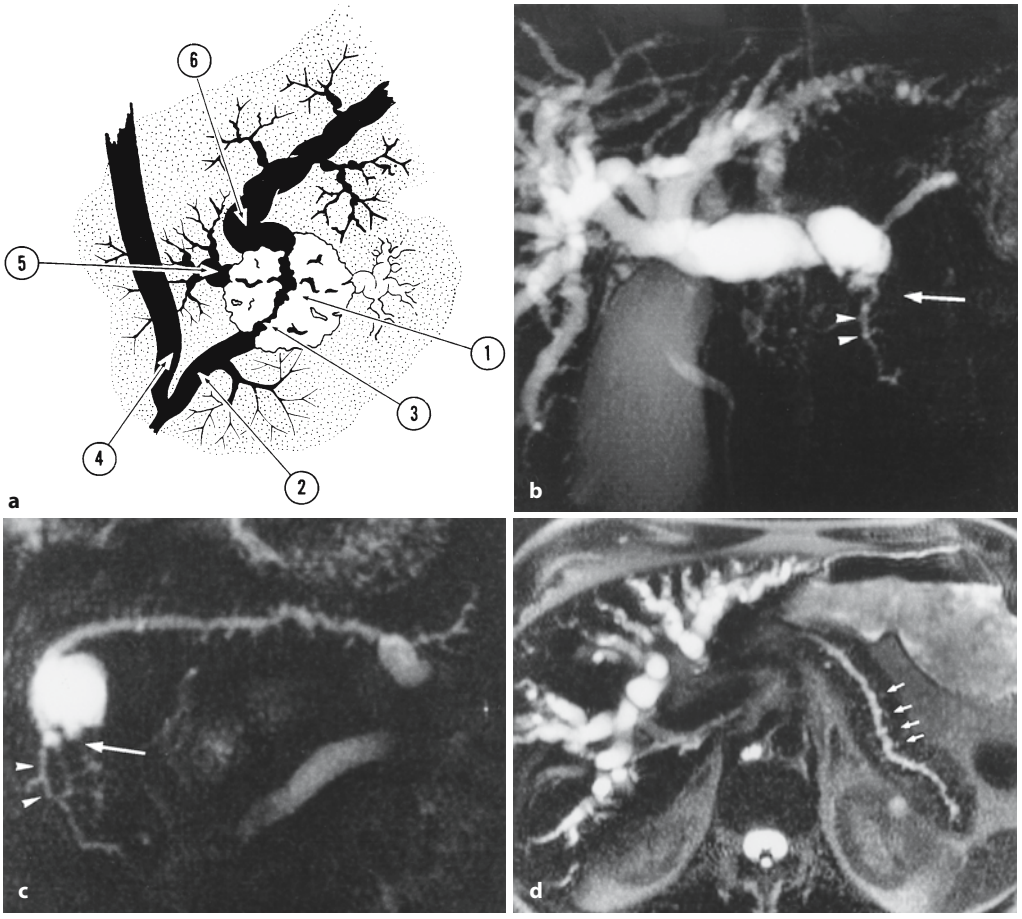

Fig. 187. **a** Ductal changes in pancreatic cancer. The tumor (*1*) causes abrupt narrowing of the pancreatic duct (*2*). Note the irregular contours of the stricture (*3*). The common bile duct (*4*) may be normal or stenotic at the same level. Dilated side branches are seen adjacent to the tumor mass (*5*). The proximal pancreatic duct shows dilation (*6*). Note that necrotic areas within the tumor may appear as small "cysts." In chronic pancreatitis, dilated side branches may be seen *within* an inflammatory mass, rather than adjacent to the mass (see # 167). (Reprinted with permission from Stewart et al. 1997). **b–d** Patient with cancer of pancreatic head. Projective images showing marked dilation of intrahepatic bile ducts with abrupt termination (*arrow* in **b**) and slightly dilated pancreatic duct that exhibits narrowing at the same level (*arrow* in **c**). Note the rather homogeneous dilation of side branches in **c** and the presence of a dilated side branch in the pancreatic head that is displaced by the tumor (*arrowheads* in **b,c**). The cystic lesion in the pancreatic neck proved to be a benign mucinous neoplasm (incidental finding). **d** Same patient. Heavily T 2-weighted axial image also showing rather uniform dilation of the side branches (*arrows*). The final diagnosis was infiltrating adenocarcinoma of the pancreatic neck

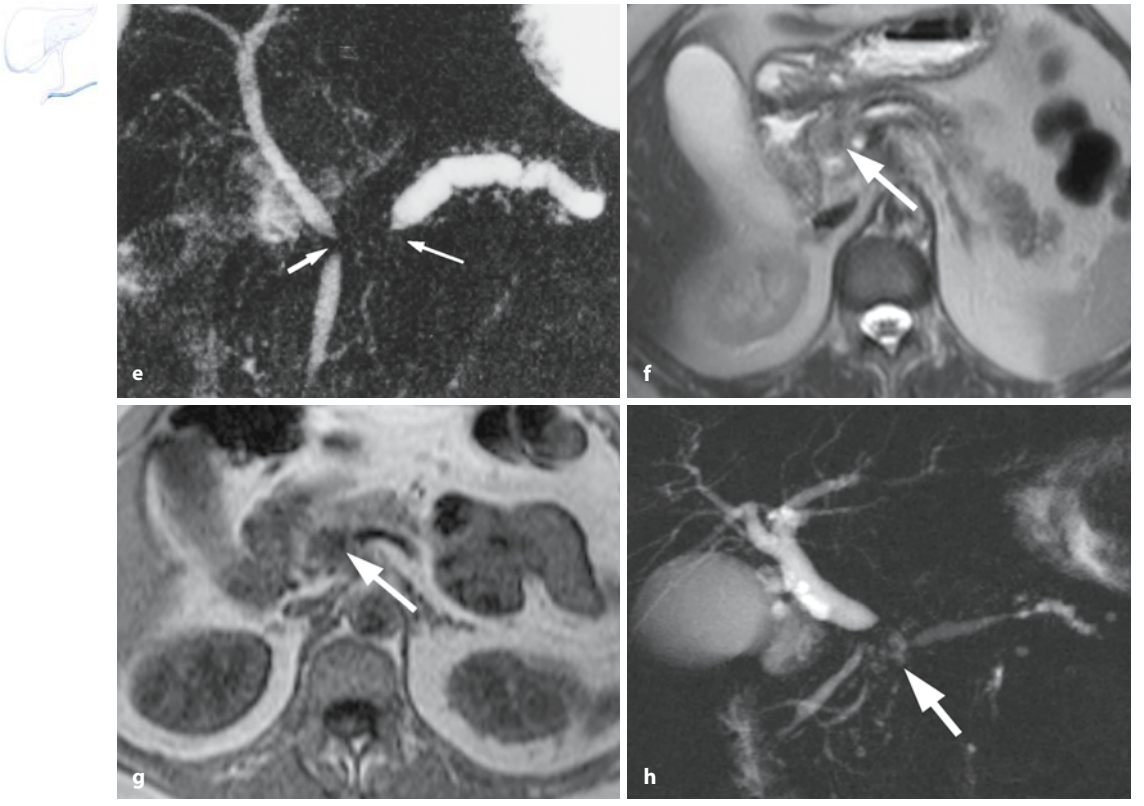

Fig. 187 a–j. (*continued*) **e** Projective image showing obliteration of the pancreatic duct associated with a short stricture of the common bile duct (double duct sign, *arrows*). **f–h** Axial T2-weighted HASTE image (**f**) and axial T1-weighted image (**g**) showing a small adenocarcinoma in the pancreatic head (*arrow*). As in most cases, the lesion is nearly isointense to normal pancreatic parenchyma on the T2-weighted images and clearly T1-hypointense. **h** Projective image showing dilatation of the proximal main pancreatic and common bile duct with an abrupt obliteration of the ducts (*arrow*). The distal main pancreatic and common bile duct have a normal appearance (four segment sign)

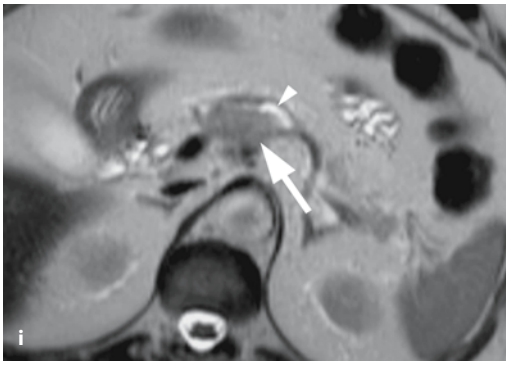

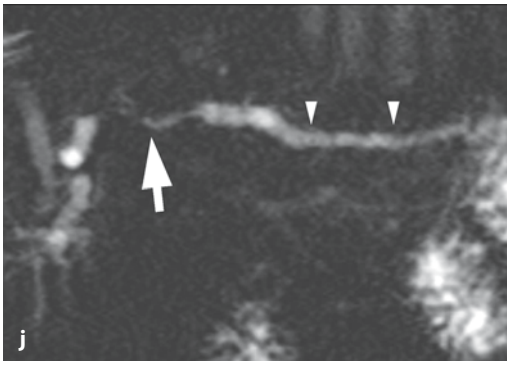

Fig. 187 a–j. (*continued*) **i, j** Axial T2-weighted HASTE image (**i**) showing a small adenocarcinoma in the pancreatic body (*arrow*) with narrowing of the main pancreatic duct and proximal dilatation (arrow–head). **j** Projective image showing dilatation of the proximal main pancreatic duct (*arrowheads*) with irregular narrowing in the pancreatic body (*arrow*)

#188 Variant Morphology of Adenocarcinoma (1): Degree of Obstruction

KEY FACTS: MRI

- Since most pancreatic adenocarcinomas originate in the main pancreatic duct, ductal obstruction occurs early in the course of disease. MRI correlates:
  - Dilation of the proximal main pancreatic duct
  - More or less uniform dilation of the proximal side branches
  - Variable degree of parenchymal atrophy
  - Small intrapancreatic pseudocysts in 10 %

- However, the absence of proximal dilation does not rule out pancreatic carcinoma (Fig. 188 c):
  - Tumor may develop in a side branch and invade the main pancreatic duct only in a more advanced stage
  - In patients with "dual" drainage ("bifid" ductal configuration, see also # 136), obstruction of the ventral duct does not necessarily implicate dilation of the dorsal ducts
  - Pancreas divisum (see # 190)

References

Fukumoto K, Nakajima M, Murakami K, Kawai K (1974) Diagnosis of pancreatic cancer by endoscopic cholangiopancreatography (ERCP). Am J Gastroenterol 60 : 210 – 213

Kim JH, Kim MJ, Chung JJ et al. (2002) Differential diagnosis of periampullary carcinomas at MR imaging. Radiographics 22 : 1335 – 1352

Muranaka T (1990) Morphologic changes in the body of the pancreas secondary to a mass in the pancreatic head. Analysis by CT. Acta Radiol 31 : 483 – 488

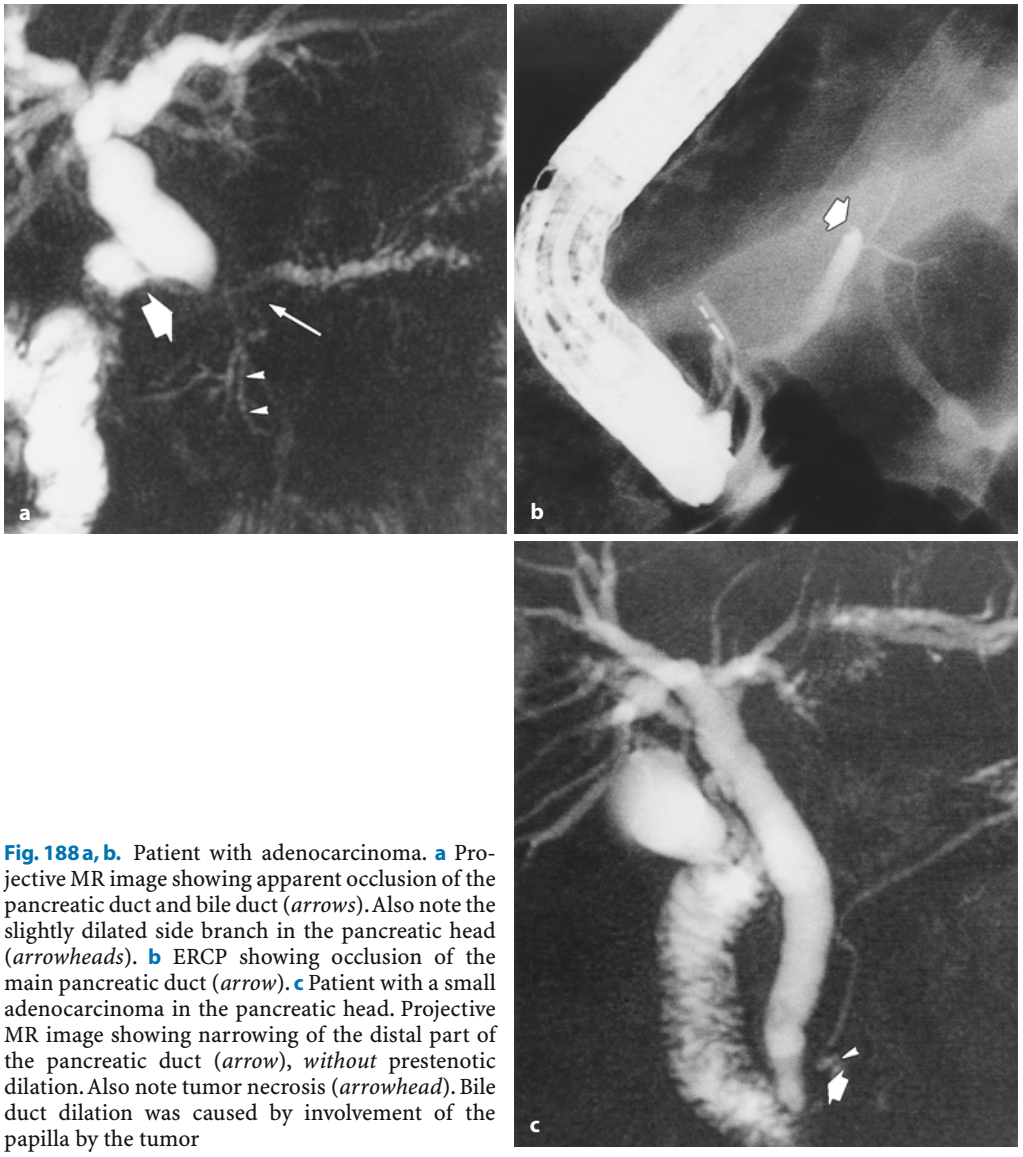

Fig. 188 a, b. Patient with adenocarcinoma. **a** Projective MR image showing apparent occlusion of the pancreatic duct and bile duct (*arrows*). Also note the slightly dilated side branch in the pancreatic head (*arrowheads*). **b** ERCP showing occlusion of the main pancreatic duct (*arrow*). **c** Patient with a small adenocarcinoma in the pancreatic head. Projective MR image showing narrowing of the distal part of the pancreatic duct (*arrow*), *without* prestenotic dilation. Also note tumor necrosis (*arrowhead*). Bile duct dilation was caused by involvement of the papilla by the tumor

#189 Variant Morphology of Adenocarcinoma (2): Necrosis/Cystic Degeneration

KEY FACTS: MRI

- Adenocarcinomas commonly contain T2-hyperintense areas
- These may correspond to:
  - Necrosis
  - Cystic components
- Occasionally, cystic/necrotic areas may be quite large (cystic adenocarcinoma; Fig. 189)
- Differential diagnosis:
  - Pseudocysts in chronic pancreatitis
  - Other cystic tumors (e.g., mucinous neoplasms)
  - Dilated side branches (see # 187)
- ERCP correlate of necrosis: extraductal extravasation of contrast material (38 %) (Bilabao and Katon 1977)

References

Bilabao MK, Katon RM (1977) Neoplasms of the pancreas. In: Stewart E, Vennes J, Geenen J (eds) Atlas of endoscopic retrograde cholangiopancreatography. Mosby, St Louis, pp 181 – 192

Sahani D, Prasad S, Saini S, Mueller P (2002) Cystic pancreatic neoplasms: evaluation by CT and magnetic resonance cholangiopancreatography. Gastrointest Endoscopy Clin N Am 12 : 657 – 672

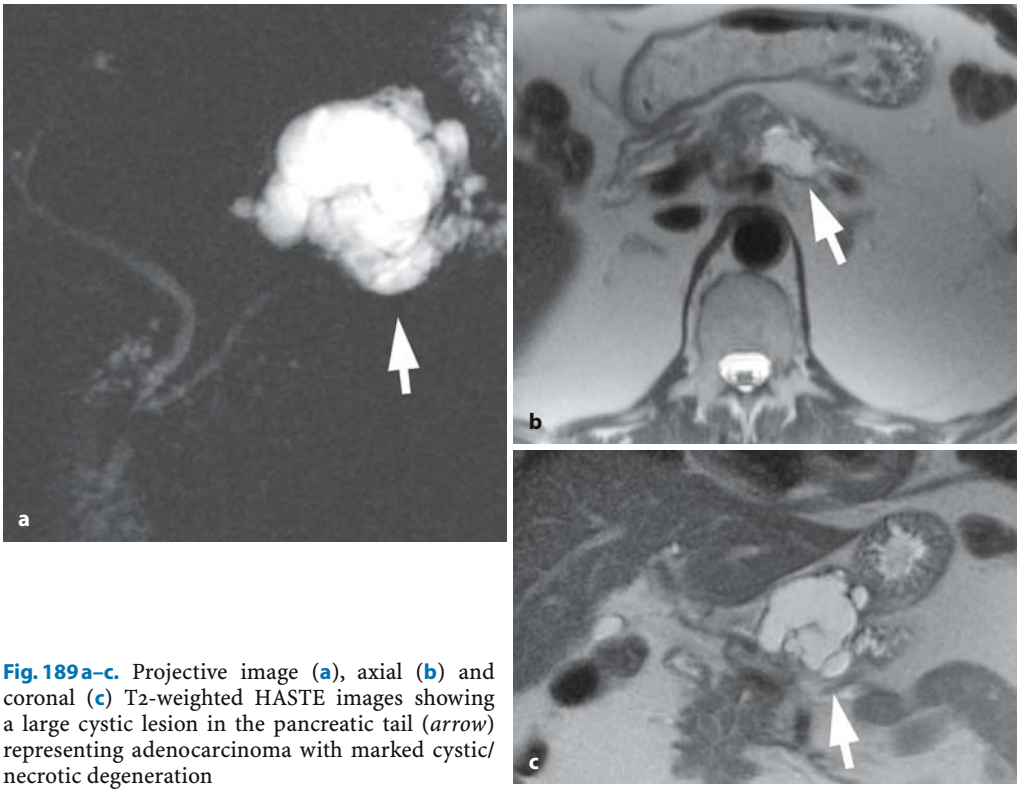

Fig. 189 a–c. Projective image (**a**), axial (**b**) and coronal (**c**) T2-weighted HASTE images showing a large cystic lesion in the pancreatic tail (*arrow*) representing adenocarcinoma with marked cystic/necrotic degeneration

#190 Adenocarcinoma in Pancreas Divisum

Related topic: # 140 (pancreas divisum)

KEY FACTS: MRI

- The "double duct sign" usually refers to concomitant stenosis or occlusion of the "main" pancreatic duct and common bile duct. It may, however, also refer to:
  - Stenosis of the common bile duct and a *side branch* of the main pancreatic duct
  - Stenosis of the common bile duct and the *ventral duct* (in pancreas divisum)
- *Note:* In complete pancreas divisum, obstruction of the ventral pancreatic duct is typically *not* associated with ductal dilation in the body and tail, except in cases where the tumor extends to the minor papilla or accessory duct (Fig. 190)

References

Kelekis NL, Semelka RC (1995) Carcinoma of the pancreatic head area. Diagnostic imaging: magnetic resonance imaging. Rays 20 : 289 – 303

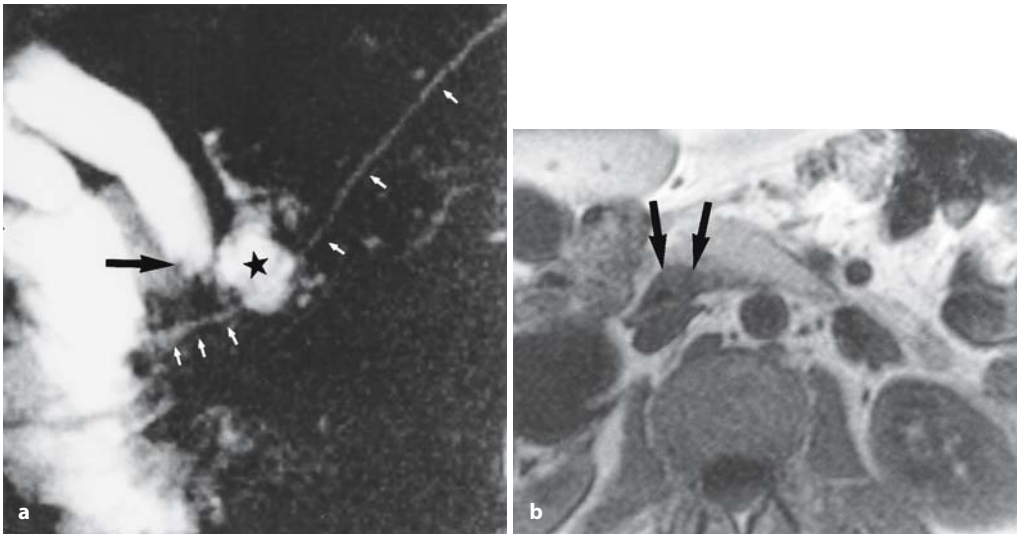

Fig. 190 a, b. Projective image (**a**) showing a normal pancreatic duct in the body/tail with a patent duct of Santorini (*small arrows*). Note the dilation of the common bile duct with abrupt narrowing (*arrow*). Also note the marked obstructive dilation of a side branch in the pancreatic head/neck (*asterisk*). **b** Axial T1-weighted image showing a small tumor in the posterior part of the pancreatic head (*arrows*). (Figure courtesy of C. Feys)

#191 Spread of Adenocarcinoma (1): Vascular Invasion

KEY FACTS: DISEASE

- Invasion of peripancreatic vessels usually indicates unresectability
- Incidence: ± 33 %
- Arterial encasement involves the superior mesenteric, splenic, celiac, hepatic, gastroduodenal, and left renal arteries, in descending order of frequency
- The veins most commonly affected are the splenic vein and portosplenic confluence

KEY FACTS: MRI

- Criteria for vascular invasion:
  - Narrowing/occlusion
  - Vessel partially or completely encircled by tumor (Loyer et al. 1996; Mitchell et al. 1987)
- In patients with pancreatic head cancer invading or compressing the superior mesenteric vein, visualization of dilated peripancreatic veins (that act as collaterals) may be another useful sign of unresectability (Fig. 191; Hommeyer et al. 1995):
  - Gastrocolic trunk
  - Anterior superior pancreaticoduodenal vein
  - Posterior superior pancreaticoduodenal vein
- Comments:
  - In many cases, diagnosis of vascular invasion is evident on non-contrast-enhanced scans (Fig. 191)
  - Dual-phase MRA can be used in conjunction with cross-sectional MRI and MRCP to provide a "complete" preoperative assessment of pancreatic neoplasms (Gaa et al. 1997)

References

Gaa J, Wendl K, Trede M, Georgi M (1997) New concepts in MR imaging of pancreatic carcinoma: the all-in-one approach. In: Oudkerk M, Edelman R (eds) High-power gradient MR-imaging. Blackwell Science, Berlin, pp 425 – 430

Hommeyer S, Freeny PC, Crabo LG (1995) Carcinoma of the head of the pancreas: evaluation of the pancreaticoduodenal veins with dynamic CT – potential for improved accuracy in staging. Radiology 196 : 233 – 238

Loyer EM, David CL, Dubrow RA, Evans DB, Charnsangavej C (1996) Vascular involvement in pancreatic adenocarcinoma: reassessment by thin-section CT. Abdom Imaging 21 : 202 – 206

Mitchell DG, Hill MC, Cooper R et al. (1987) The superior mesenteric artery fat plane: is obliteration pathognomonic of pancreatic carcinoma? J Comp Assist Tomogr 11 : 247 – 253

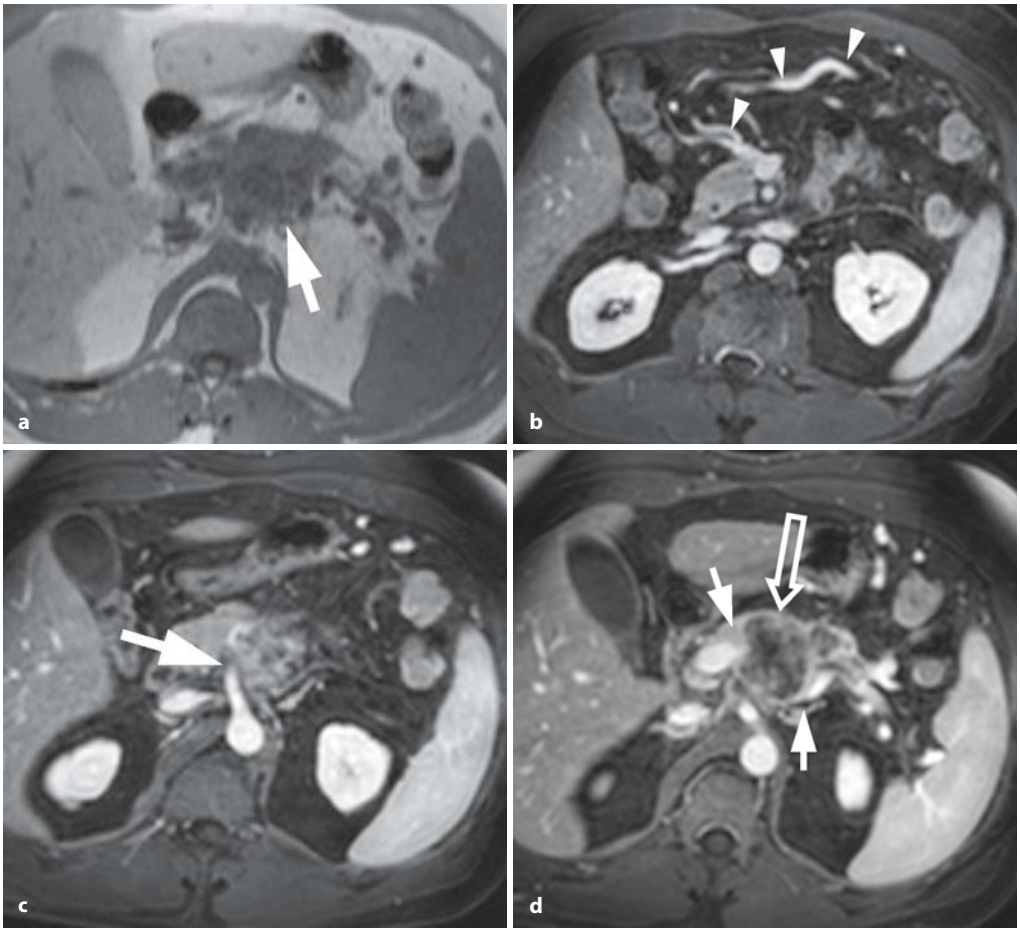

Fig. 191 a–d. Axial T1-weighted image (**a**) showing a large hypointense adenocarcinoma with clear extrapancreatic extension (*arrow*). **b–d** Axial contrast-enhanced T1-weighted VIBE images obtained in the venous phase show dilatation of the gastrocolic venous trunc with mesenteric venous collaterals [*arrowheads* in (**b**)]. Also seen is displacement of the celiac trunc [*large arrow* in (**c**)], and invasion of the venous confluence and splenic vein [*small arrows* in (**d**)]. Note the hypovascular adenocarcinoma [*open arrow* in (**d**)]

#192 Spread of Adenocarcinoma (2): Lymph Nodes

KEY FACTS: DISEASE

- Lymph node metastases are found in ± 50 % of patients (Megibow et al. 1995)
- Lymph nodes most commonly involved:
  - Cancer of the pancreatic head: retroperitoneal and superior pancreatic head groups
  - Cancer of the pancreatic body and tail: superior body and head groups

KEY FACTS: MRI

- Signal intensity of (enlarged) lymph nodes relative to surrounding fat:
  - T2 without fat suppression: variable, often more or less isointense
  - T2 with fat suppression: variable, commonly hyperintense
  - T1 without fat suppression: hypointense
  - T1 with fat suppression: commonly isointense
  - Contrast-enhanced images with fat suppression: hyperintense
- Limitations:
  - Detection of slightly enlarged peripancreatic nodes may be difficult because of limitations of spatial resolution (particularly in the third dimension; volume averaging), multiplicity of small structures present in the peripancreatic space (e.g., arteries, veins), and subtle differences in signal intensity from surrounding tissues
  - Detection of micrometastases in normal-sized nodes is impossible
- Importance: detection of enlarged lymph nodes by imaging studies has little clinical relevance because, in the absence of other signs of non-resectability, it does not represent a contra-indication for surgery

References

Kelekis NL, Semelka RC (1997) MRI of pancreatic tumors. Eur Radiol 7 : 875 – 886

Megibow AJ, Zhou XH, Rotterdam H et al. (1995) Pancreatic adenocarcinoma: CT versus MR imaging in the evaluation of resectability – report of the Radiology Diagnostic Oncology Group. Radiology 195 : 327 – 332

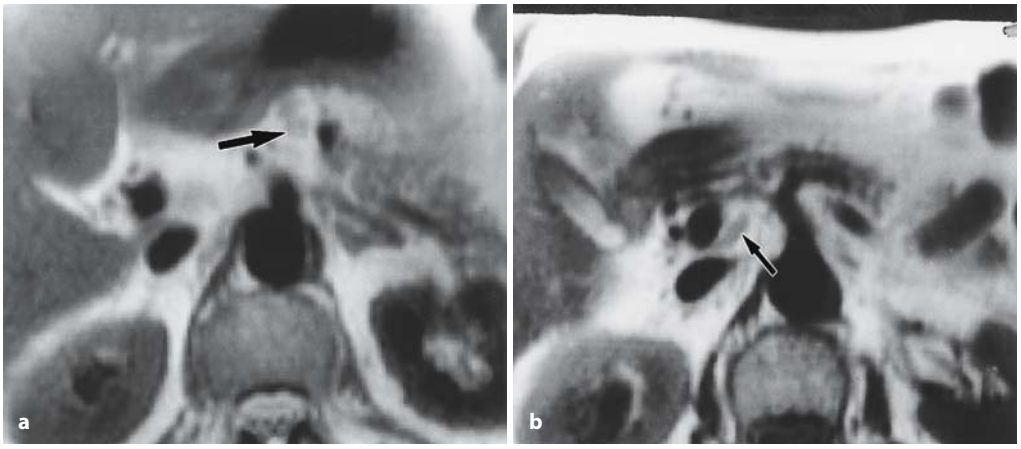

Fig. 192 a, b. Patient with pancreatic carcinoma. Images obtained using the "black blood" technique showing several enlarged **a** superior body and **b** portocaval nodes (*arrows*). Note that these nodes were invisible on the classical HASTE sequence

#193 Spread of Adenocarcinoma (3): Distant Metastases

KEY FACTS: DISEASE

- Incidence of hematogenous metastases in autopsy series: 85 % – 95 %
- Location (in descending order of frequency): liver, lungs, adrenals, kidneys, bones

KEY FACTS: MRI

- Hepatic metastases of pancreatic adenocarcinoma have a nonspecific appearance (see also #60):
  - T1: hypointense
  - T2: (minimally) hyperintense with or without central necrosis
  - Hypointense on contrast-enhanced scans, sometimes with peripheral rim enhancement
- Peritoneal metastases are usually not directly visualized; presence of ascites in patients with a pancreatic neoplasm and without signs of cirrhosis or portal vein thrombosis may be an indirect sign (Fig. 1)

References

Baert AL, Rigauts H, Marchal G (1994) Ductal adenocarcinoma. In: Baert AL (ed) Radiology of the pancreas. Springer, Berlin Heidelberg New York, pp 129 – 172

Kelekis NL, Semelka RC (1997) MRI of pancreatic tumors. Eur Radiol 7 : 875 – 886

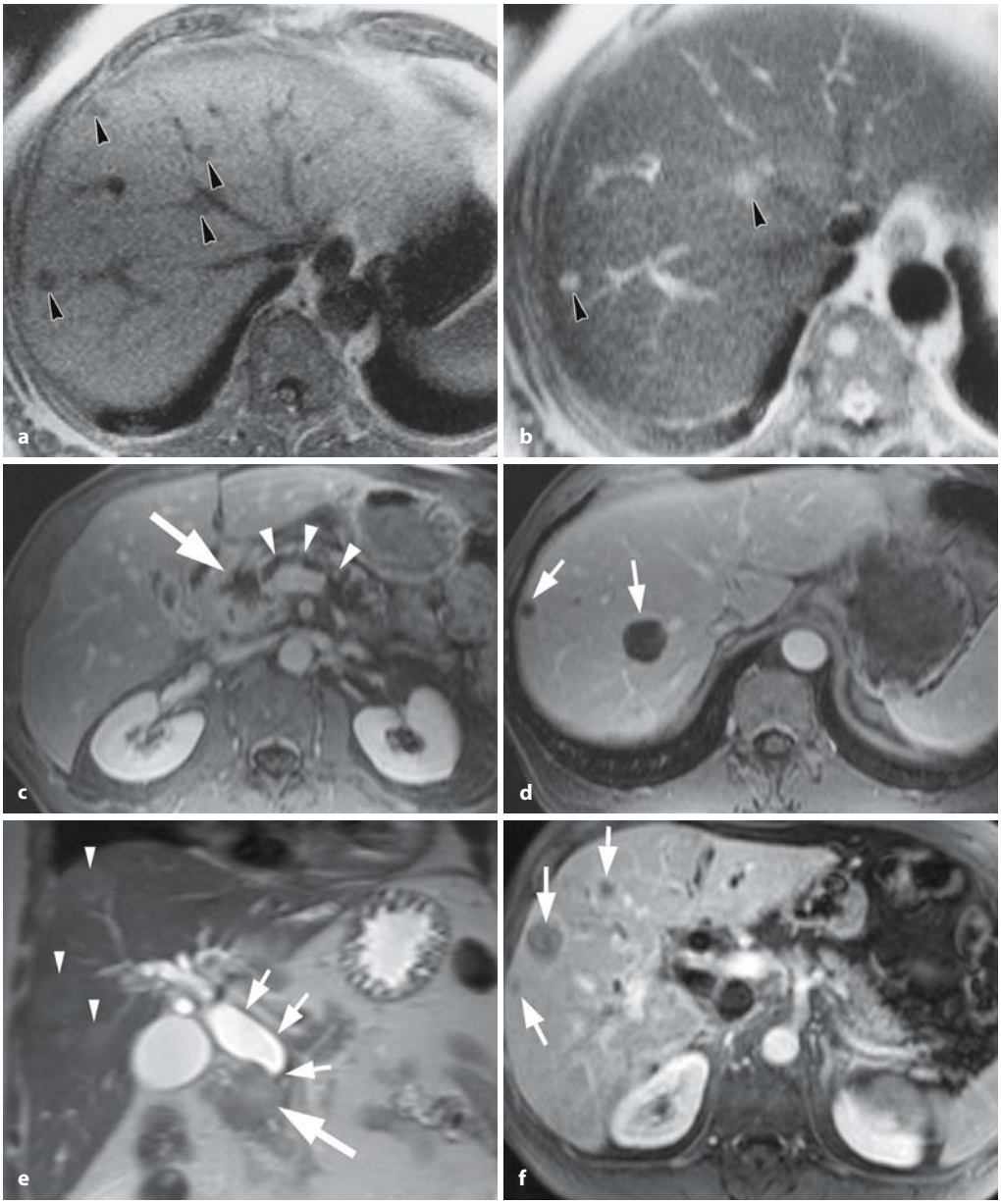

Fig. 193 a, b. **a** T1- and **b** T2-weighted images showing hepatic metastases as hypo- and slightly hyperintense, respectively (*arrowheads*). Note that the T1-weighted image shows more lesions. **c, d** Axial contrast-enhanced T1-weighted VIBE images obtained in the portovenous phase showing a hypoenhancing adenocarcinoma in the pancreatic head [*large arrow* in (**c**)], with retro-obstructive dilatation of the main pancreatic duct [*arrowheads* in (**c**)], and two rim-enhancing liver metastases in the right lobe [*small arrows* in (**d**)]. Because of the subtle enhancement, these lesions could be mistaken for cysts. **e, f** Coronal T2-weighted HASTE image (**e**) showing a hyperintense adenocarcinoma in the pancreatic head (*large arrow*) with obliteration and proximal dilatation of the common bile duct (*small arrows*), and multiple slightly hyperintense hepatic metastases (*arrowheads*). **f** Axial contrast-enhanced T1-weighted VIBE image obtained in the venous phase confirming the presence of multiple metastatic lesions in the liver (*arrows*)

#194 Adenocarcinoma with Retro-obstructive Pancreatitis

Related topic: #168 (chronic obstructive pancreatitis)

KEY FACTS: DISEASE

- Ductal obstruction by adenocarcinoma may cause:
  - Chronic obstructive pancreatitis (see #168)
  - Acute pancreatitis
- *Note:* Pancreatic cancer may also develop in patients with *preexisting* chronic pancreatitis (occurring in 2–4% of patients)

KEY FACTS: MRI

- Pancreatitis associated with adenocarcinoma may cause diagnostic problems for several reasons:
  - Ductal changes in chronic pancreatitis may be so dominant that the associated carcinoma is overlooked
  - Peripancreatic inflammatory changes in acute pancreatitis may jeopardize the diagnostic quality of projective MR images
  - Tumor detection may be difficult due to loss of the normal hyperintensity of surrounding pancreatic tissue on T1-weighted images
- Signs of pancreatitis indicate the need for obtaining immediate postcontrast gadolinium-enhanced scans for tumor detection (Fig. 194)
- Signs suggestive of carcinoma (see also #167):
  - Focal irregular ductal stenosis in a duct with an otherwise normal appearance (not absolute, see # 1)
  - Length of stenosis: > 1–2 cm (idem)
  - Abrupt termination of stenosis (idem)
  - Double duct sign (not absolute, see #164)
  - Focal markedly T1-hypointense mass, with parenchyma with an otherwise normal appearance
  - Markedly hypovascular solid focal mass causing ductal obstruction

References

Delmaschio A, Vanzulli A, Sironi S et al. (1991) Pancreatic cancer versus chronic pancreatitis: diagnosis with CA 19-9 assessment, US, CT, and CT-guided fine-needle biopsy. Radiology 178 : 95–99

Kelekis NL, Semelka RC (1997) MRI of pancreatic tumors. Eur Radiol 7 : 875–886

Shemesh E, Czerniak A, Nass S, Klein E (1990) Role of endoscopic retrograde cholangiopancreatography in differentiating pancreatic cancer coexisting with chronic pancreatitis. Cancer 65 : 893–896

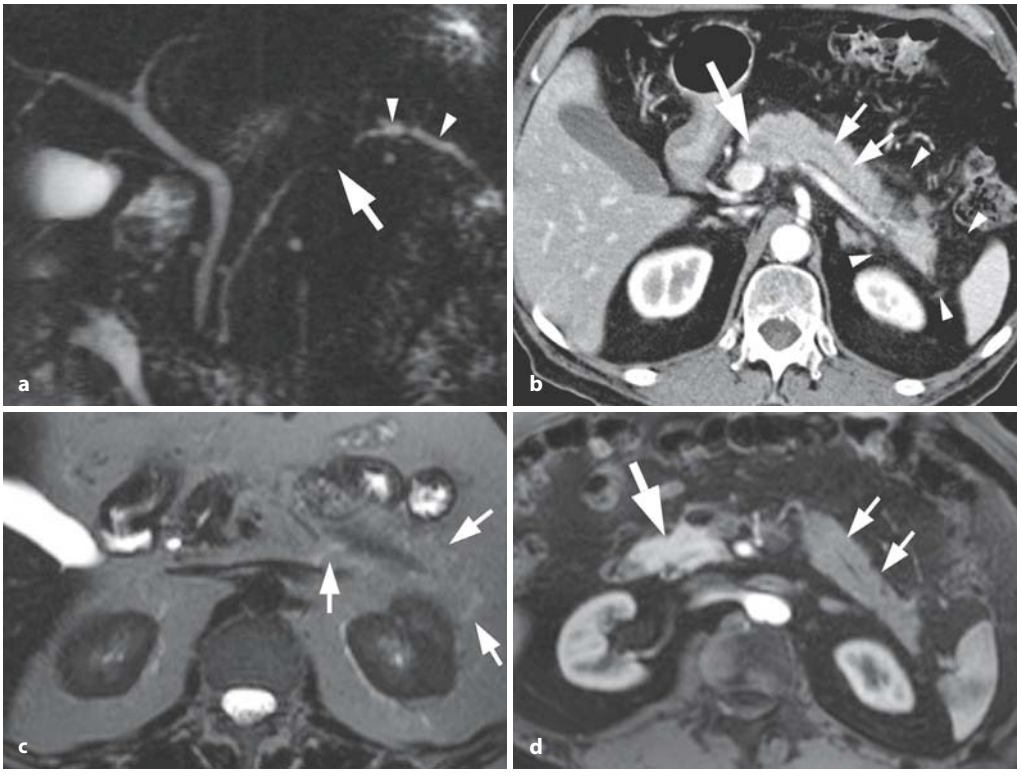

Fig. 194 a–d. Patient with adenocarcinoma and retro-obstructive pancreatitis. **a** Projective image showing a stenosis of the pancreatic duct (*arrow*) with proximal dilatation (*arrowheads*). **b** CT image showing a small pancreatic tumor (*large arrow*), prestenotic duct dilatation (*small arrows*), and subtle peripancreatic infiltration (*arrowheads*). **c** Axial T2-weighted HASTE image (TE 360) showing slightly increased signal intensity of the fat around pancreatic tail. **d** Axial contrast-enhanced T1-weighted VIBE image obtained in the pancreatic phase showing decreased enhancement of the pancreatic tail (*small arrows*) when compared to the head (*large arrow*). The findings in (**c**) and (**d**) point to the presence of retro-obstructive pancreatitis. Final diagnosis: adenocarcinoma

#195 Recurrent Adenocarcinoma

KEY FACTS: GENERAL

- Incidence: not rare:
  - Only 14% of patients with adenocarcinoma have tumor confined to the pancreas
  - Approximately 35% of metastatic lymph nodes cannot be removed during surgery; similarly, tumors encasing retroperitoneal vessels can only partially be removed
- Location: most commonly in close proximity to the superior mesenteric artery or celiac trunk

KEY FACTS: MRI

- Typical feature: infiltrating mass surrounding and encasing the superior mesenteric artery and/or celiac trunk

References

Coombs RJ, Zeiss J, Howard JM, Thomford NR, Merrick HW (1990) CT of the abdomen after the Whipple procedure: value of depicting postoperative anatomy, surgical complications and tumor recurrence. AJR Am J Roentgenol 154 : 1011 – 1014

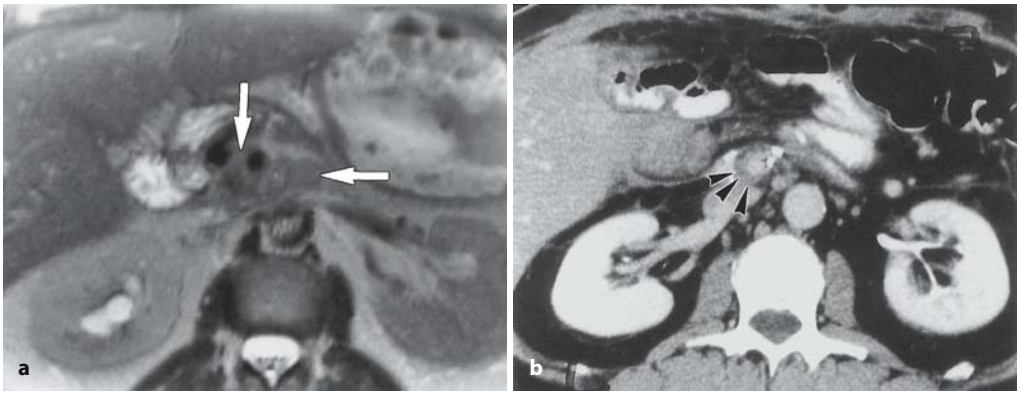

Fig. 195 a, b. Patient who underwent a Whipple operation for carcinoma in the pancreatic head. **a** T2-weighted image showing soft tissue mass (*arrows*) between the superior mesenteric artery and the aorta. **b** CT image obtained at a more caudal level also showing soft tissue cuff around the superior mesenteric artery (*arrowheads*)

#196 Secondary Pancreatic Tumors

Related topics: #60 (intrahepatic bile ducts: metastases), #91 (extrahepatic bile duct: involvement by other extrabiliary neoplasms)

KEY FACTS: DISEASE

- Most common secondary pancreatic tumors:
  - Lymphoma
  - Metastases from breast cancer, lung cancer (24% of patients with small cell lung cancer), cancer of the colon, renal cell carcinoma, and malignant melanoma
- Usually end-stage disease

KEY FACTS: MRI

- Pancreatic duct:
  - Typically no involvement or displacement only
  - Narrowing may occur but is less frequent
- Parenchyma: usually multiple locations
- Specific features:
  - Melanoma metastases may be T1-hyperintense
  - Renal cell carcinoma metastases are typically hypervascular (differential diagnosis with endocrine tumors)
- Key elements: clinical history/locations in other organs

References

Ehrlich A, Stalder G, Geller W, Sherlock P (1968) Gastrointestinal manifestations of malignant lymphoma. Gastroenterology 54 : 1115 – 1121

Roland CF, Van Heerden JA (1989) Nonpancreatic primary tumors with metastases to the pancreas. Surg Gynecol Obstet 168 : 345 – 347

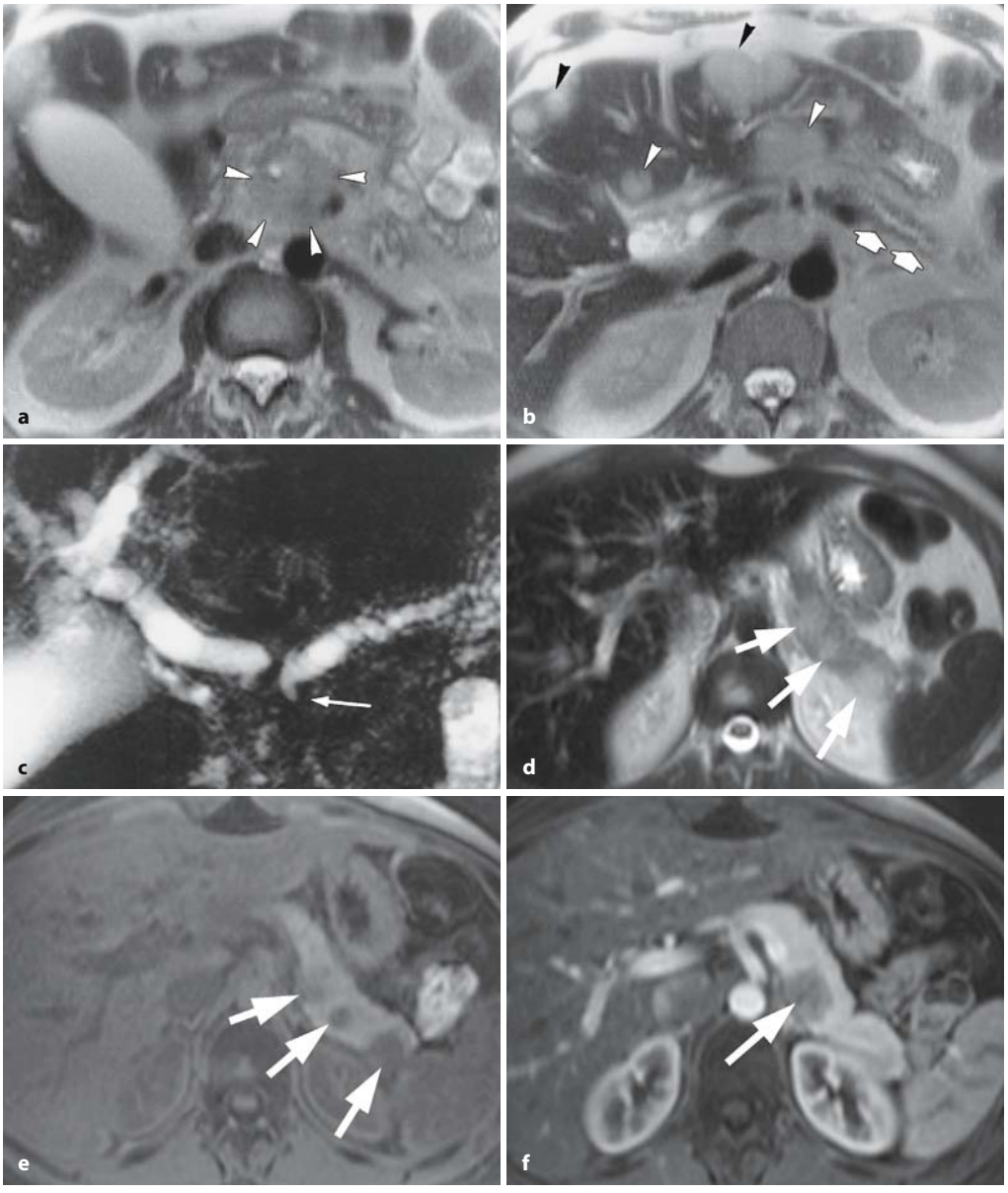

Fig. 196 a – c. Patient with lung cancer. **a, b** T2-weighted images showing a large mass in the pancreatic head (*arrowheads*), atrophy of the pancreatic tail (*arrows*), and multiple hepatic metastases (*arrowheads*). **c** Projective MR image showing double duct sign (*arrow*), which is an unusual finding in patients with pancreatic metastases. **d–f** Patient with esophageal myosarcoma and pancreatic metastases. Axial T2-weighted HASTE image (**d**) and axial T1 weighted image (**e**) showing multiple focal lesions in the pancreatic tail (arrows). Note the peripheral location of these masses and the absence of dilatation of the pancreatic duct. **f** Axial contrast-enhanced T1-weighted VIBE image (different position) obtained in the pancreatic phase showing poor vascularization of the metastatic lesion (*arrow*)

#197 Malignant Neuroendocrine Tumors

Related topic: #177 (benign neuroendocrine tumors)

KEY FACTS: DISEASE

- Incidence of malignancy with respect to subtype: see Table 197
- Other features:
  - Gastrinomas found in patients with type-1 multiple endocrine neoplasia syndrome are less likely to be malignant than isolated gastrinomas
  - Larger tumors (> 2 cm) are more commonly malignant

KEY FACTS: MRI

- Secreting tumors: see #177 (no morphologic features to distinguish between benign and malignant tumors)
- Nonsecreting tumors are usually large and centrally necrotic
- *Note:* Hepatic metastases of gastrinoma typically have a very high signal intensity on T2-weighted images and, therefore, may mimic hemangiomas. Solution: delayed contrast-enhanced MRI (Berger et al. 1996):
  - Gastrinoma metastases: hypo- or isointense
  - Hemangiomas: hyperintense

References

Berger JF, Laissy JP, Limot O et al. (1996) Differentiation between multiple liver hemangiomas and liver metastases of gastrinomas: value of enhanced MRI. J Comp Assist Tomogr 20 : 349 – 355

Marcos HB, Libutti SK, Alexander HR, et al. (2002) Neuroendocrine tumors of the pancreas in von Hippel-Lindau disease: spectrum of appearances at CT and MR imaging with histopathologic comparison. Radiology 225 : 751 – 758

Van Hoe L, Vanbeckevoort D, Baert AL (1997) Endocrine tumors of the pancreas: computed tomography and magnetic resonance imaging. Chir Gastroenterol 13 : 301 – 306

Table 197. Incidence of malignancy in neuroendocrine tumors

Tumor	Relative frequency (%)	Malignant (%)
Insulinoma	56	5–10
Gastrinoma	21	60
Glucagonoma	2.3	80
Vipoma	1.8	60
Nonfunctioning tumors	15	80–100

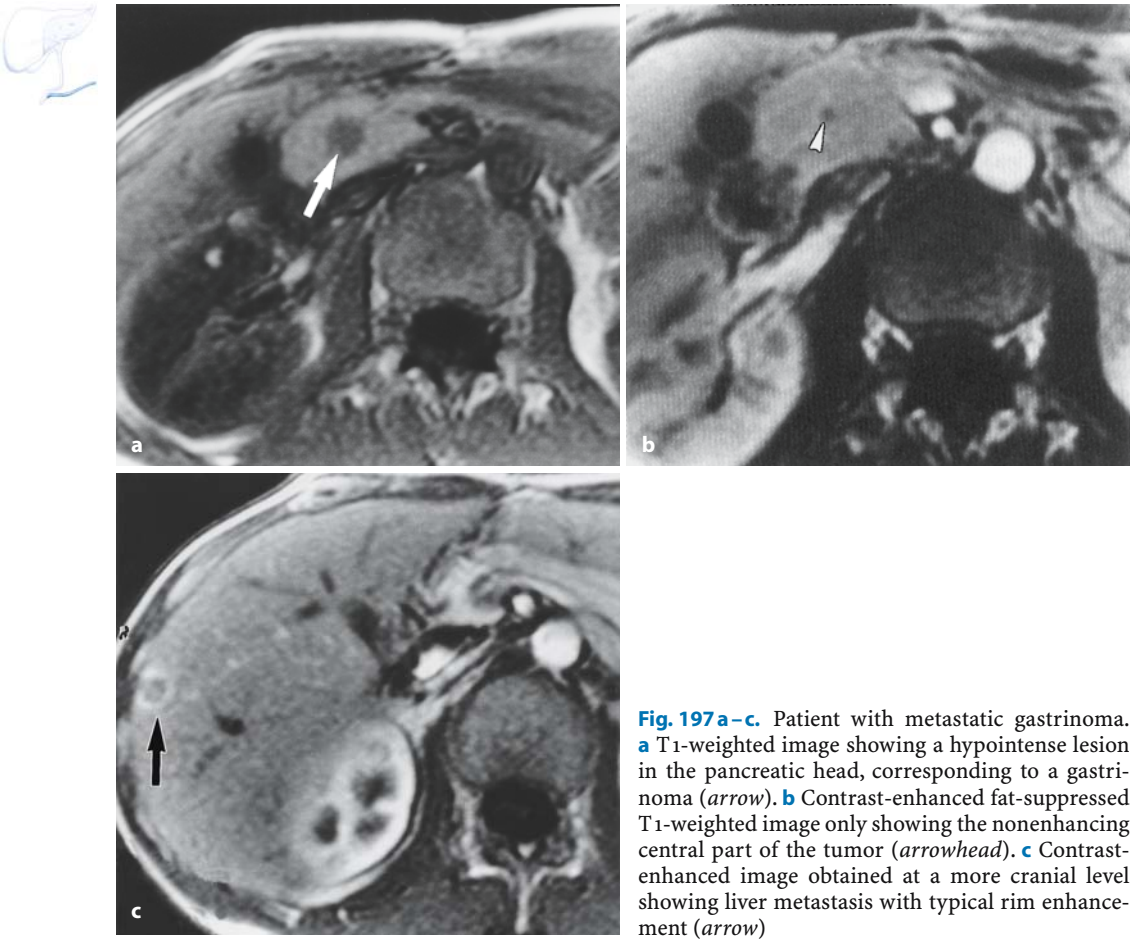

Fig. 197 a–c. Patient with metastatic gastrinoma. **a** T1-weighted image showing a hypointense lesion in the pancreatic head, corresponding to a gastrinoma (*arrow*). **b** Contrast-enhanced fat-suppressed T1-weighted image only showing the nonenhancing central part of the tumor (*arrowhead*). **c** Contrast-enhanced image obtained at a more cranial level showing liver metastasis with typical rim enhancement (*arrow*)

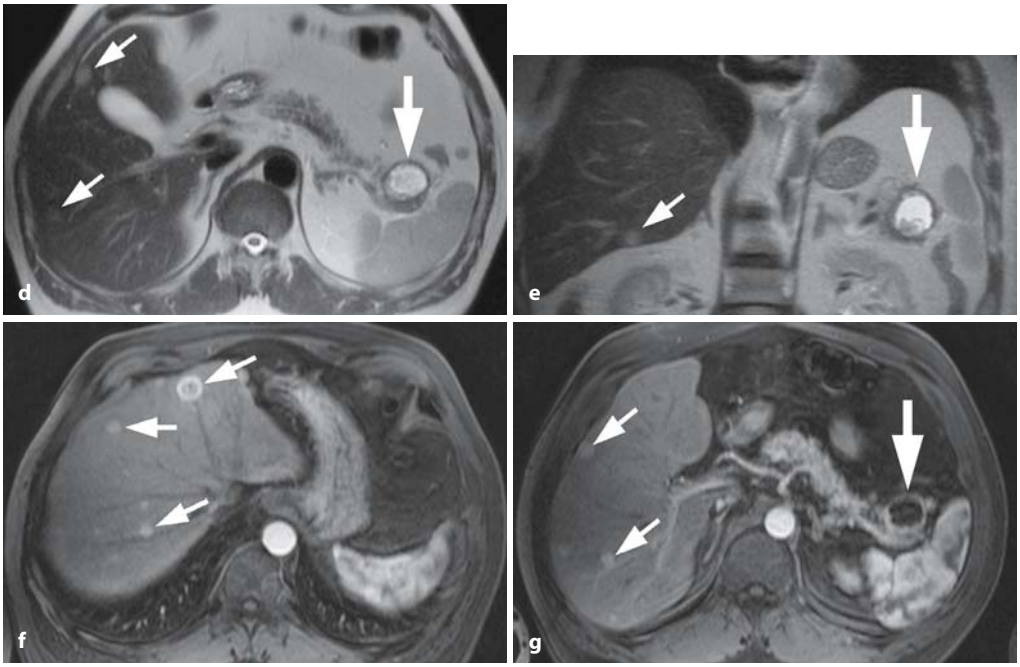

Fig. 197 d–g. Patient with a malignant cystic neuroendocrine tumor with hypervascular liver metastases. **d, e** Axial and coronal T2-weighted HASTE images showing a hyperintense cystic mass in the pancreatic tail with a thick irregular wall (*large arrow*), and multiple T2-hyperintense liver lesions (*small arrows*). **f, g** Axial contrast-enhanced T1-weighted VIBE images obtained in the arterial phase showing strong uptake of contrast medium in these lesions (*small arrows*). Note the nonenhancing cystic neuroendocrine tumor in the pancreatic tail [*large arrow* in (**g**)]

#198 Mucinous Pancreatic Neoplasm (Peripheral Type)

Related topics: #175, 176 (serous cystadenoma), #199 (intraductal neoplasm)

KEY FACTS: DISEASE

- Synonyms:
  - Macrocystic pancreatic neoplasm
  - Mucinous cystadenoma/cystadenocarcinoma
- Cystic lesions lined by columnar, mucin-producing cells
- Macroscopic appearance:
  - Unilocular or multilocular
  - Cystic components usually greater than 2 cm in diameter
  - Papillary protrusions may be seen
  - Sometimes peripheral calcifications
- To be distinguished from intraductal mucinous neoplasms (see #199)
- Mean age: 50 years
- Ratio of women to men: 6:1–9:1
- Location: 85% in the pancreatic tail
- Usually large
- All tumors are malignant or have malignant potential
- Local recurrence is common

KEY FACTS: MRI (FIG. 198)

- Unilocular or multilocular cystic lesion
- Cysts greater than 2 cm in diameter
- Signal intensity of contents of cystic spaces: reflects varying concentrations of mucin
  - Usually like fluid
  - Sometimes T1-hyperintense (high concentration of mucin)
  - Sometimes lower signal intensity in dependent portions on T2 ("layering")
  - The intensities may vary in different loculi
- No enhancing components
- Malignant tumors have a propensity for invasion of local organs and vessels

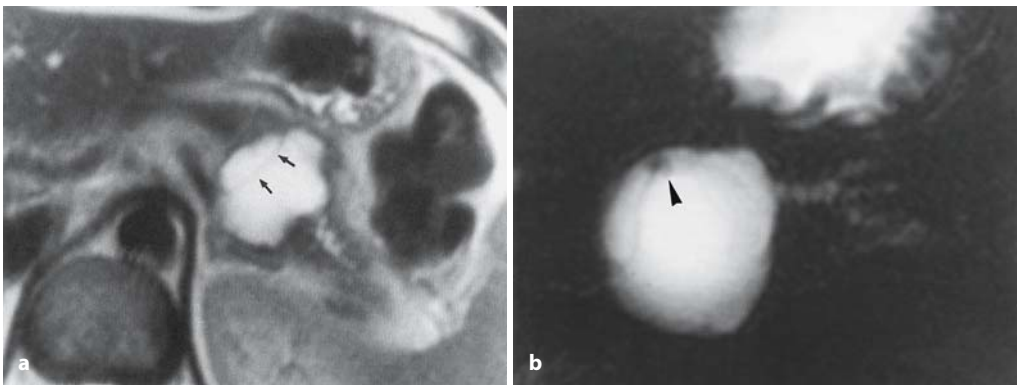

Fig. 198 a, b. **a** Axial T2-weighted image showing a cystic lesion in the pancreatic body/tail, containing a septum (*arrows*). **b** Projective image showing a septum and small mural nodule (*arrowhead*), which would be unusual for a (pseudo-)cyst.

References

Compagno J, Oertel JE (1978) Mucinous cystic neoplasms of the pancreas with overt and latent malignancy (cystadenocarcinoma and cystadenoma): a clinicopathologic study of 41 cases. Am J Clin Pathol 69 : 573 – 580

Kim YH, Saini S, Sahani D, Hahn PF, Mueller P, Auh Y (2005) Imaging diagnosis of cystic pancreatic lesions: pseudocyst versus nonpseudocyst. RadioGraphics 25 : 671 – 685

Minami M, Itai Y, Ohtono K, Yoshida H, Yoshikawa K, Lio M (1989) Cystic neoplasms of the pancreas: comparison of MR imaging with CT. Radiology 171 : 53 – 56

Sahani D, Prasad S, Saini S, Mueller P (2002) Cystic pancreatic neoplasms: evaluation by CT and magnetic resonance cholangiopancreatography. Gastrointest Endoscopy Clin N Am 12 : 657 – 672

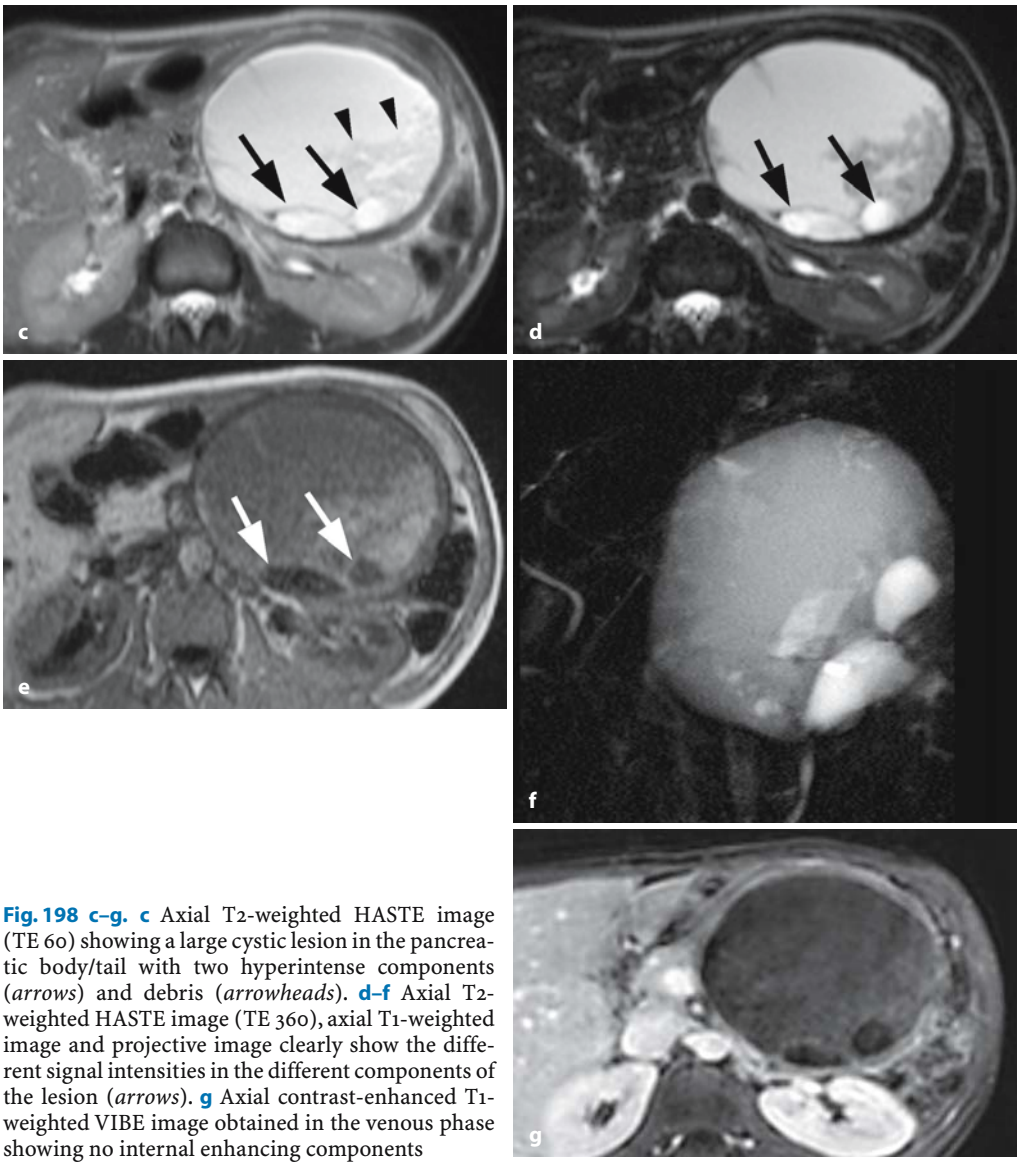

Fig. 198 c–g. **c** Axial T2-weighted HASTE image (TE 60) showing a large cystic lesion in the pancreatic body/tail with two hyperintense components (*arrows*) and debris (*arrowheads*). **d–f** Axial T2-weighted HASTE image (TE 360), axial T1-weighted image and projective image clearly show the different signal intensities in the different components of the lesion (*arrows*). **g** Axial contrast-enhanced T1-weighted VIBE image obtained in the venous phase showing no internal enhancing components

#199 Intraductal Papillary Mucinous Tumor (IPMT)

Related topic: #198 (mucinous pancreatic neoplasm, peripheral type)

KEY FACTS: DISEASE

- Mucin-producing tumor of intraductal origin
- No preponderance for men or women
- Belongs to the group of mucinous pancreatic tumors. Classification (Itai and Ohtomo 1996):
  - *Branch duct type:* mucin-secreting intraductal tumor usually located in the uncinate process and causing localized dilation of a side branch
  - *Main duct type:* mucin-secreting intraductal tumor characterized by dilation of the main pancreatic duct
- Like tumors of the peripheral type, these tumors have malignant potential
- The prognosis depends on the presence or absence of local invasion

KEY FACTS: MRI

- General remarks:
  - The mucin-secreting tumor is often too small to be visualized; the hallmark of the disease is marked focal or diffuse ductal dilation
  - Mucin has a very high signal intensity on T2-weighted images and cannot usually be differentiated from fluid
- Typical appearance of the *branch duct type* (Fig. 199):
  - "Polycystic" mass in the uncinate process, actually representing focally dilated side branches filled with mucin
  - Differential diagnosis: pseudocyst(s)
- Typical appearance of the *main duct type:*
  - Usually marked global dilation of the main pancreatic duct without a demonstrable cause of obstruction
  - Clue to diagnosis on ERCP: endoscopic visualization of a protruding gelatinous substance (mucin)
  - Differential diagnosis: other diseases causing ductal dilation (ductal or orificial stenosis, lithiasis)
- Signs of malignancy (Irie et al. 2000)
  - Branch duct type: filling defects visible at MRI; main pancreatic duct dilation
  - Main duct type: filling defects visible at MRI; diffuse main pancreatic duct dilatation greater than 15 mm

References

Irie H, Honda H, Aibe H et al. (2000) MR cholangiopancreatographic differentiation of benign and malignant intraductal mucin-producing tumors of the pancreas. AJR Am J Roentgenol 174:1403–1408

Irie H, Yoshimitsu K, Aibe H et al. (2004) Natural history of pancreatic intraductal papillary mucinous tumor of branch duct type: follow-up study by magnetic resonance cholangiopancreatography. J Comput Assist Tomogr 28:117–122

Itai Y, Ohtomo K (1996) Cystic tumors of the pancreas. Eur Radiol 6:844–850

Itai Y, Ohhashi K, Nagai H et al. (1986) 'Ductectatic' mucinous cystadenoma and cystadenocarcinoma of the pancreas. Radiology 161:697–700

Lim JH (2003) Cholangiocarcinoma: morphologic classification according to growth pattern and imaging findings. AJR Am J Roentgenol 181:819–827

Procacci C, Graziani R, Bicego E et al. (1996) Intraductal mucin-producing tumors of the pancreas: imaging findings. Radiology 198:249–257

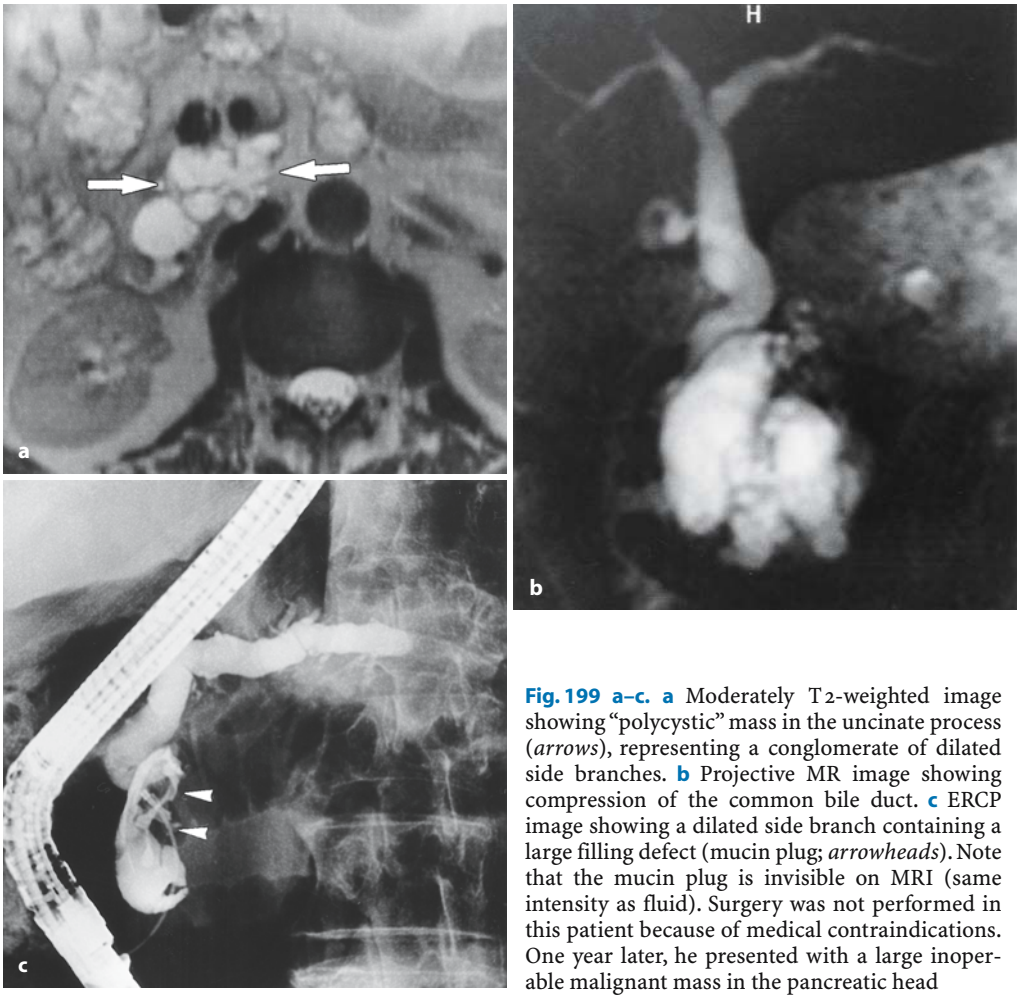

Fig. 199 a–c. **a** Moderately T2-weighted image showing "polycystic" mass in the uncinate process (*arrows*), representing a conglomerate of dilated side branches. **b** Projective MR image showing compression of the common bile duct. **c** ERCP image showing a dilated side branch containing a large filling defect (mucin plug; *arrowheads*). Note that the mucin plug is invisible on MRI (same intensity as fluid). Surgery was not performed in this patient because of medical contraindications. One year later, he presented with a large inoperable malignant mass in the pancreatic head

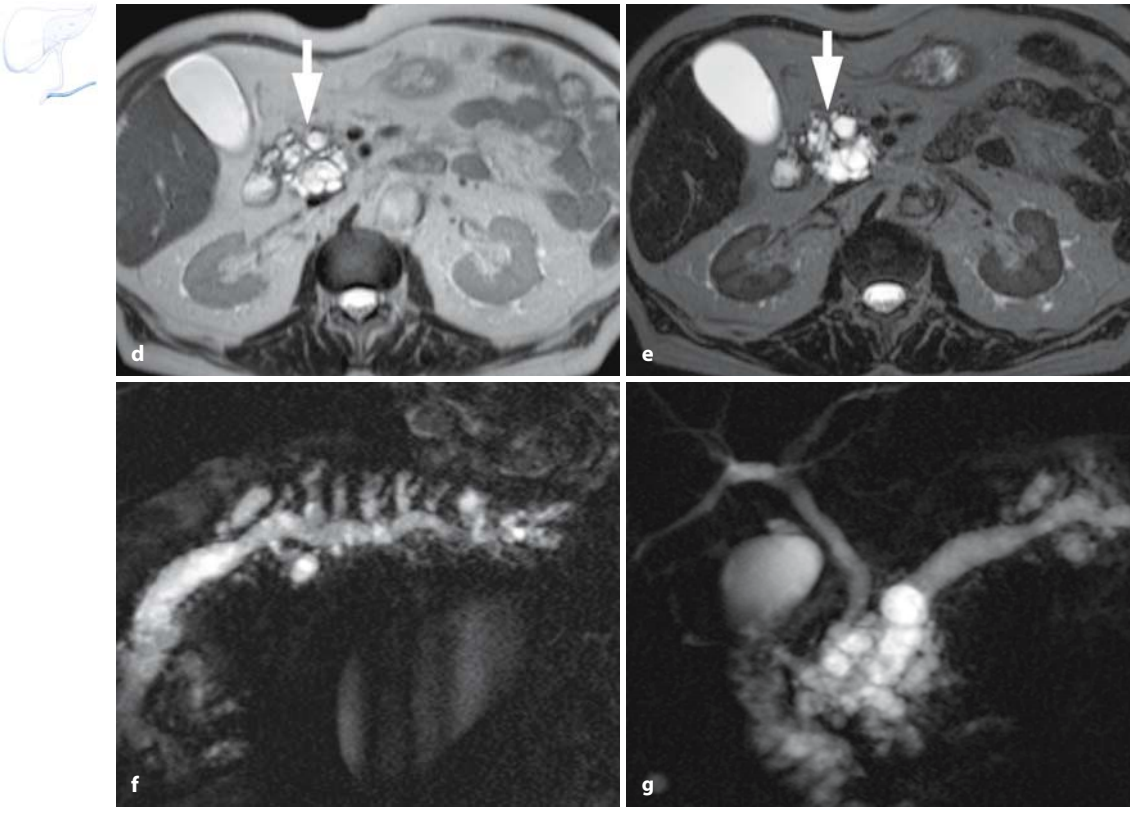

Fig. 199 d–g. IPMT branch duct type with associated dilatation of main duct. (**d, e**) Axial T2-weighted HASTE image (TE 60 and 360) showing a "polycystic" mass in the pancreatic head (*arrow*), representing a conglomerate of dilated side branches. **f, g** Projective images showing marked global dilatation of the main pancreatic duct and all of the side branches without a demonstrable cause of obstruction

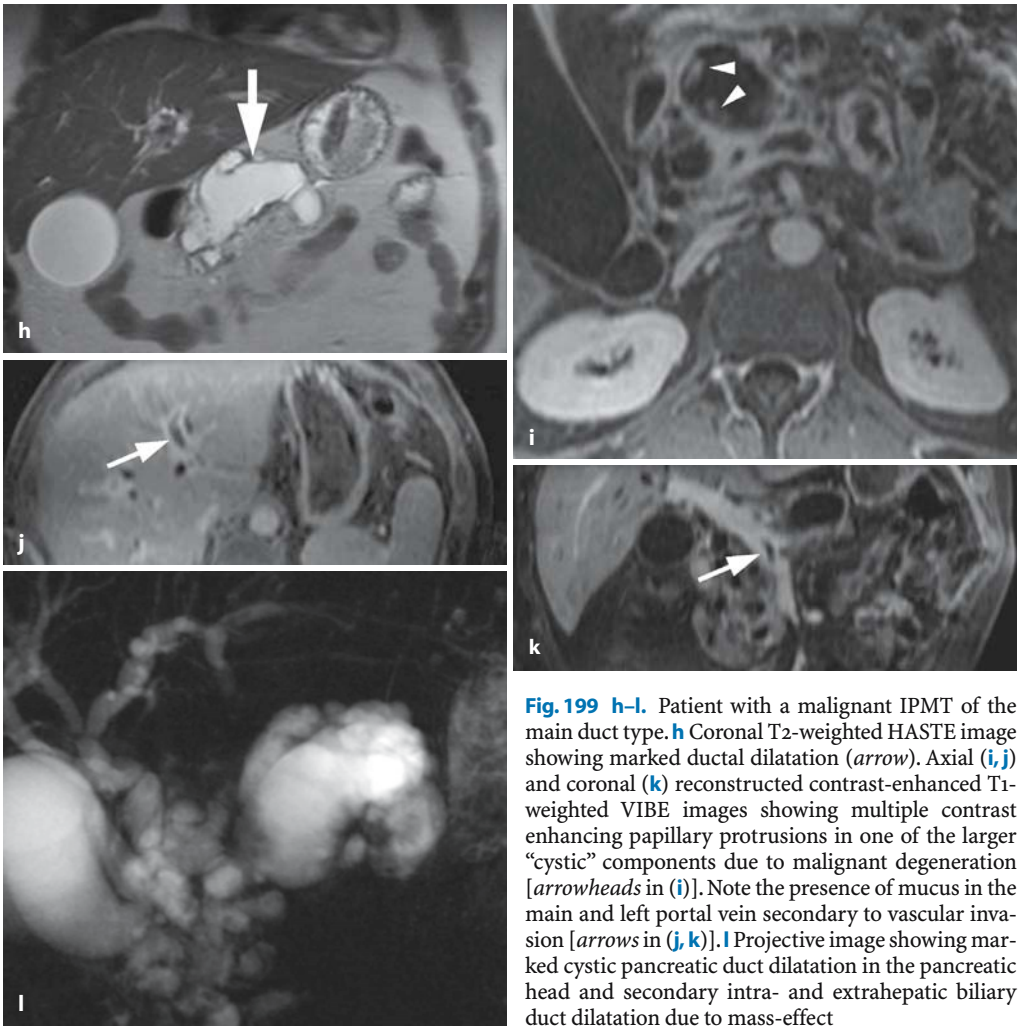

Fig. 199 h–l. Patient with a malignant IPMT of the main duct type. **h** Coronal T2-weighted HASTE image showing marked ductal dilatation (*arrow*). Axial (**i, j**) and coronal (**k**) reconstructed contrast-enhanced T1-weighted VIBE images showing multiple contrast enhancing papillary protrusions in one of the larger "cystic" components due to malignant degeneration [*arrowheads* in (**i**)]. Note the presence of mucus in the main and left portal vein secondary to vascular invasion [*arrows* in (**j, k**)]. **l** Projective image showing marked cystic pancreatic duct dilatation in the pancreatic head and secondary intra- and extrahepatic biliary duct dilatation due to mass-effect

Subject Index

E

F

G

H

I

K

L

M

N

O

P

R

S

T

U

V

W

X